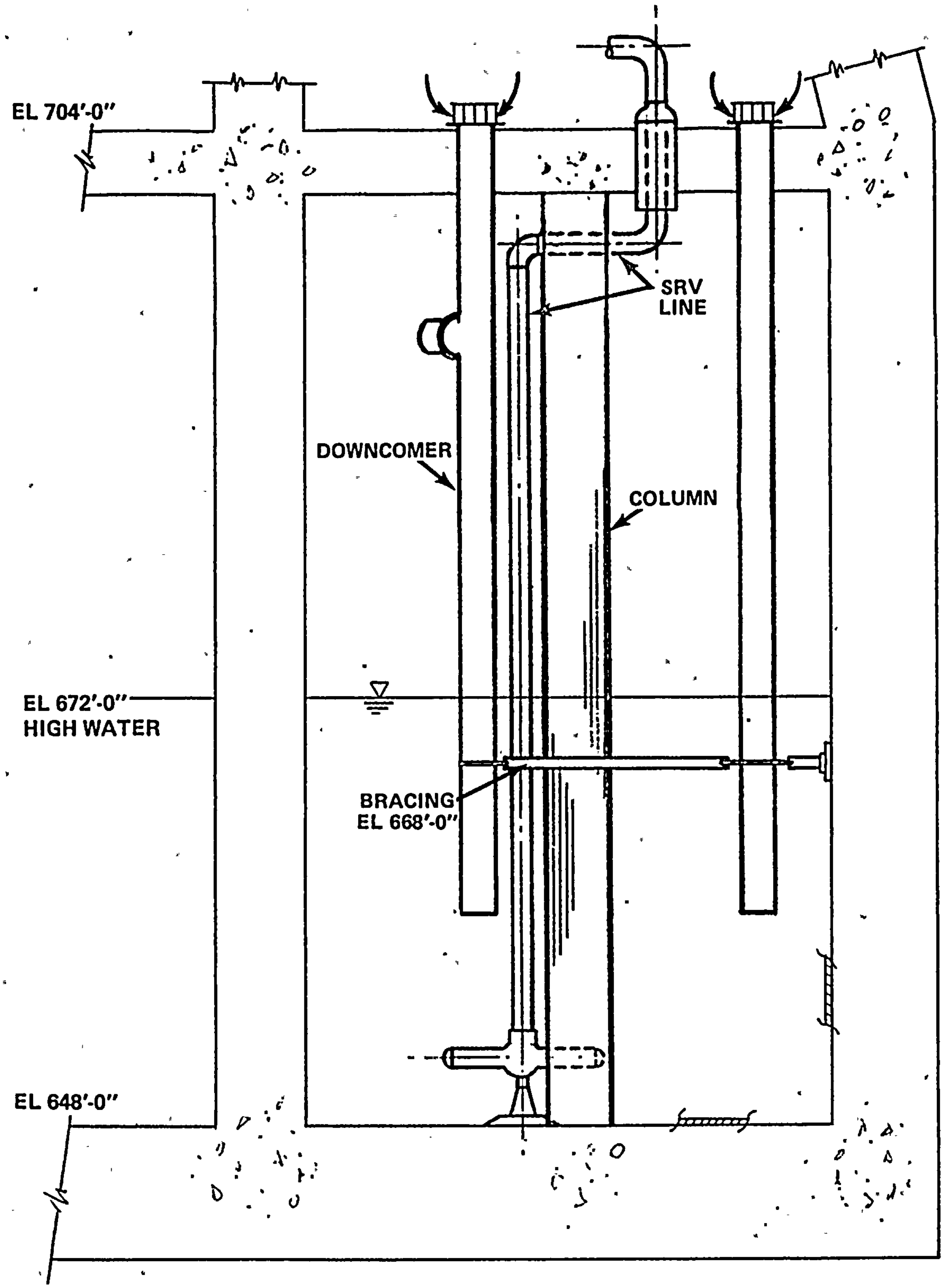

Rev. 3, 7/80

SUSQUEHANNA STEAM ELECTRIC STATION UNITS 1 AND 2 DESIGN ASSESSMENT REPORT
SUPPRESSION CHAMBER— SECTION VIEW
FIGURE 1-3

8008250416

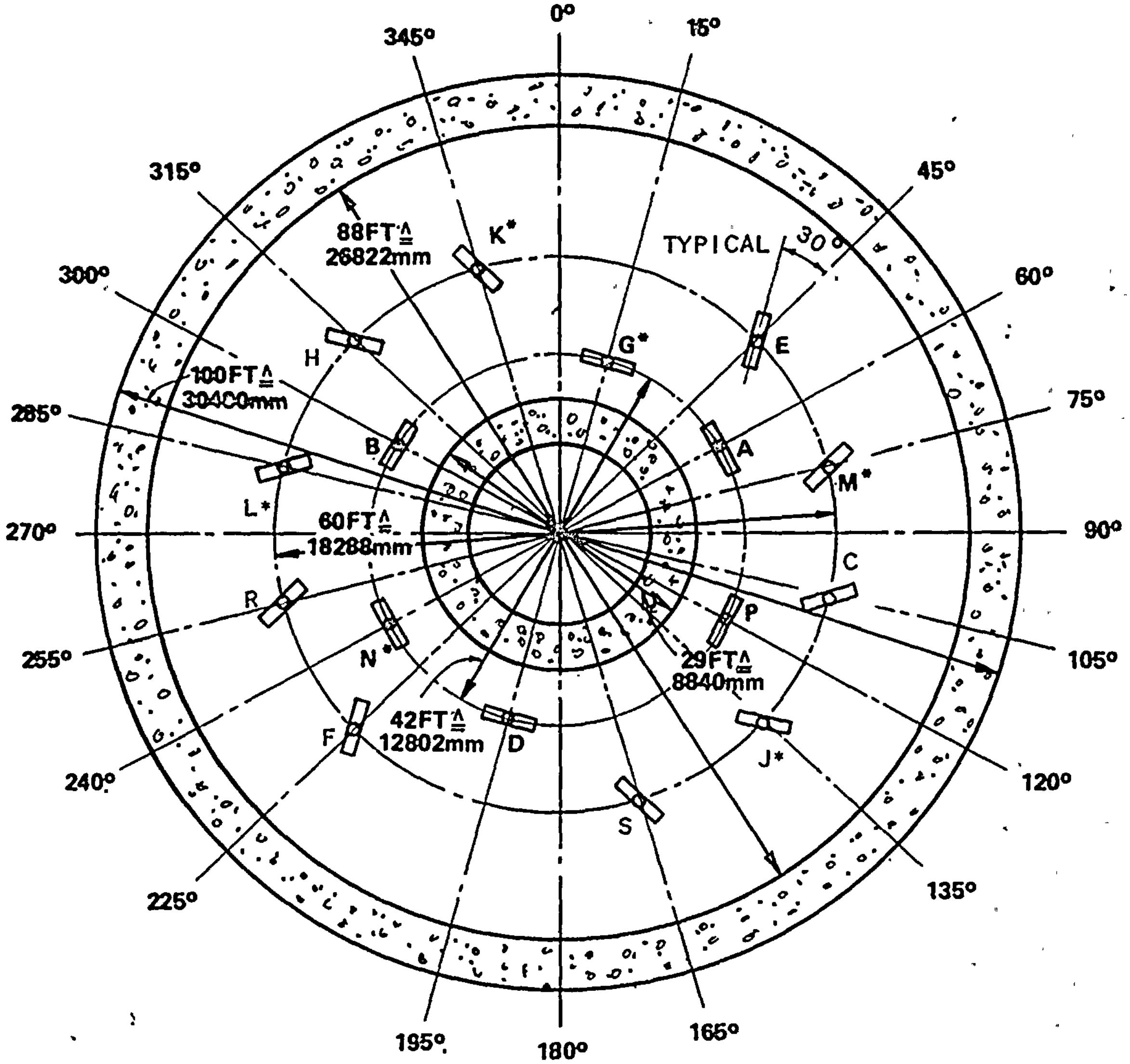

NOTE: * INDICATES ADS-ASSOCIATED QUENCHER

Rev. 2, 5/80

SUSQUEHANNA STEAM ELECTRIC STATION UNITS 1 AND 2 DESIGN ASSESSMENT REPORT
QUENCHER DISTRIBUTION
FIGURE 1-4

TABLE 1-1

SSES LICENSING BASIS

I. Mark II Containment - Supporting Program

A. LOCA - Related Tasks

Task Number	Activity	Activity Type	Target Completion	Documentation	Used for SSES Licensing
A.1	"4T" Test Program	Phase I Test Report	Completed	NEDO/NEDE 13442-P-01	Yes
		Phase I Appl Memo	Completed	Application Memo	Yes
		Phase II & III Test Rept	Completed	NEDO/NEDE 13468-P	Yes
		Application Memorandum	Completed	NEDO/NEDE 23678-P	Yes
A.2	Pool Swell Model Report	Model Report	Completed	NEDO/NEDE 21544-P	Yes
A.3	Impact Tests	PSTF 1/3 Scale Tests	Completed	NEDO/NEDE 13426-P	Yes
		Mark I 1/12 Scale Tests	Completed	NEDO/NEDC 20989-2P	Yes
A.4	Impact Model	PSTF 1/3 Scale Tests	Completed	NEDO/NEDE 13426-P	Yes
		Mark I 1/12 Scale Tests	Completed	NEDO/NEDC 20989-2P	No
A.5	Loads on Submerged Structures	LOCA/RH Air Bubble Model	Completed	NEDO/NEDE 21471-P	Yes (Partial)
		LOCA/RH Water Jet Model	Completed	NEDO/NEDE 21472-P	Yes (Partial)
		Ring Vortex Model	Completed	Letter Report	No
			4Q 79	Topical Report	No
		Applications Methods	Completed	NEDO/NEDE 21730-P	No
		Quenc. Air Bubble Model	3Q 79	NEDO 21471 Supplement	No
		Appl. Memo. Supplement	3Q 79	NEDE 21730 Supplement	No
		Quencher Air Bubble 1/4 Scaling Tests	Complete	NEDE 23817-P	No
		Data Eval.	4Q 79	Report	No
		Steam Condensation Methods	-	Plant DAR's	___
A.6	Chugging Analysis and Testing	Single Cell Report	Completed	NEDO/NEDE 23703-P	Yes
		Multivent Model	Completed	NEDO/NEDE 21669-P	No
		4T FSI Report	Completed	NEDO/NEDE 23710-P	Yes
A.7.	Chugging Single Vent	CREARE Report	Completed	NEDO/NEDE 21851-P	No
A.9	EPRI Test Evaluation	EPRI - 4T Comparison	Completed	NEDO 21667	Yes
-	EPRI 1/13 Scale Tests	3D Tests	Completed	EPRI NP-441	Yes
-	EPRI Single Cell Tests	Unit Cell Tests	3Q 79	EPRI Report	Yes

Task Number	Activity	Activity Type	Target Completion	Documentation	Used for SSES Licensing
A.11	Multivent Subscale Testing and Analysis	Preliminary MV Prog Plan	Completed	NEDO 23697	Yes
		MV Test Program Plan & Proc. - Phase I	Completed	NEDO 23697 Rev 1	Yes
		Phase I Test Report	3Q 79	Report	Yes
		MV Test Prog Plan & Proc - Phase II	3Q 79	NEDO 23697, Rev. 1, Supp. 1	Yes
		Phase II Test Report	2Q 80	Report	Yes
		CONMAP Tests	3Q 79	Report	Yes
		MBM Verification 1/10 Scale	Completed	NEDE 25116-P	Yes
A.13	Single Vent Lateral Loads	Dynamic Analysis	Completed	NEDO 24106-P	Yes
		Summary Report	Completed	NEDE 23806-P	Yes
		Summary Report (Extension)	3Q 79	Report	Yes
A.16	Improved Chugging Load Definition	Impulse Evaluation	Completed	Letter Report	No
		Improved Chug Load Defn.	3Q 79	Report	No
A.17	Steam Condensation Oscill.	4T C.O. Test	2Q 80	Report	Undecided

B. SRV Related Tasks

Task Number	Activity	Activity Type	Target Completion	Documentation	Used for SSES Licensing
B.1	Quencher Empirical Model	DFFR Model	Completed	NEDO/NEDE 21061-P	No
		Supporting Data	Completed	NEDO/NEDE 21078-P	No
B.2	Ramshead Model	DFFR Model	Completed	NEDO/NEDE 21061-P	No
		Supporting Data	Completed	NEDO/NEDE 21062-P	No
		Analysis	Completed	NEDO/NEDE 20942-P	No
B.3	Monticello In-Plant S/RV Tests	Preliminary Test Report	Completed	NEDO/NEDC 21465-P	No
		Hydrodynamic Report	Completed	NEDO/NEDC 21581-P	No
B.5	S/RV Quencher In-Plant Caorso Tests	Test Plan	Completed	NEDM 20988 Rev. 2	No
		Test Plan Addendum 1	Completed	NEDM 20988 Rev. 2, Add 1	No
		Test Plan Addendum 2	Completed	NEDM 20988 Rev. 2, Add 2	No
		Test Summary	Completed	Letter Report	No
	Phase I	Test Report	Completed	NEDE-25100-P	No
	Phase II	Test Report	1Q 80	Report	No
B.6	Thermal Mixing Model	Analytical Model	Completed	NEDO/NEDC 23689-P	No
B.10	Monticello FSI	Analysis of FSI	Completed	NEDO 23834	No
B.11	DFFR Ramshead Model To Monticello Data	Data/Model Comparison	Completed	NSC-GEN 0394	No
B.12	Ramshead SRV Methodology Summary	Analytical Methods	Completed	NEDO 24070	No
B.14	Quencher Empirical Model Update	Model Confirmation	1Q 80	Report	No

C. Miscellaneous Tasks

Task Number	Activity	Activity Type	Target Completion	Documentation	Used for SSES Licensing
C.0	Supporting Program	Supp Prog Rpt	Completed	NEDO 21297	
		Supp Prog Rpt Rev.	Completed	NEDO 21297 - Rev. 1	
		Supp Prog Rpt Rev.	4Q 70	NEDO 21297 - Rev. 2	
C.1	DFFR Revisions	Revision 1	Completed	NEDO/NEDE 21061-P Rev. 1	-
		Revision 2	Completed	NEDO/NEDE 21061-P Rev. 2	-
		Revision 3	Completed	NEDO/NEDE 21061-P Rev. 3	Yes (Partial)
C.3	NRC Round 1 Questions	DFFR Rev. 2	Completed	NEDO/NEDE 21061-P Rev. 2	Yes
		DFFR Rev. 2 Amendment 1	Completed	NEDO/NEDE 21061-P Rev. 2 Amend. 1	Yes
		DFFR Rev. 3. Appendix A	Completed	NEDO/NEDE 21061-P Rev. 3 Appendix A	Yes
C.5	SRSS Justification	Interim Report	Completed	(NEDE 24010)	Yes
		SRSS Report	Completed	NEDO/NEDE 24010-P	Yes
		SRSS Exec. Report	Completed	Summary Report	Yes
		SRSS Criteria Appl.	Completed	NEDO/NEDE 24010-P Suppl. 1	Yes
		SRSS Bases	Completed	NEDO/NEDE 24010-P Suppl. 2	Yes
		SRSS Justification Suppl.	3Q 79	Report	Yes
C.6	NRC Round 2 Questions	DFFR Amendment 2	Completed	NEDO/NEDE 21061-P Rev. 2 Amend. 2	Yes
		DFFR Amend 2, Suppl 1	Completed	NEDO/NEDE 21061-P Rev. 2 Amend. 2 Supp. 1	Yes
		DFFR Amend 2, Suppl 2	Completed	NEDO/NEDE 21061-P Rev. 2 Amend. 2 Supp. 2	Yes
		DFFR Rev. 3, Appendix A	Completed	NEDO/NEDE 21061-P Rev. 3 Appendix A	Yes
C.7	Justification of "4T" Bounding Loads	Chugging Loads Justification	Complete	NEDO/NEDE 23617-P	Yes
			Complete	NEDO/NEDE 24013-P	Yes
			Complete	NEDO/NEDE 24014-P	Yes
			Complete	NEDO/NEDE 24015-P	Yes
			Complete	NEDO/NEDE 24016-P	Yes
			Complete	NEDO/NEDE 24017-P	Yes
			Complete	NEDO/NEDE 23627-P	Yes
C.8	S/RV and Chugging FSI	Prestressed Concrete Reinforced Concrete Steel	Completed	NEDO/NEDE 21936-P	Yes
C.9	Monitor World Tests	Monitor Tests	End of Program	None	No
C.13	Load Combinations & Functional Capability Criteria	Criteria Justification	Completed	NEDO 21985	Yes
C.14	NRC Round 3 Questions	Letter Report	Completed	Letter Report	Yes
		DFFR, Rev. 3, Appendix A		NECO/NEDE 21061-P Rev. 3 Appendix A	Yes
C.15	Submerged Structure Criteria	NRC Question Responses	3Q 79	Letter Report	Yes

II. KWU Tests and Reports (supplied to PP&L)

Document Number	Title	Status	Documentation	Used for SSES Licensing
1.	Formation and oscillation of a spherical gas bubble	Completed	AEG - Report 2241	Yes
2.	Analytical model for clarification of pressure pulsation in the wetwell after vent cleaning	Completed	AEG - Report 2208	Yes
3.	Tests on mixed condensation with model quenchers	Completed	KWV - Report 2593	Yes
4.	Condensation and vent cleaning tests at GKM with quenchers	Completed	KWV - Report 2594	Yes
5.	Concept and design of the pressure relief system with quenchers	Completed	KWV - Report 2703	Yes
6.	KKB vent clearing with quencher	Completed	KWV - Report 2796	Yes
7.	Tests on condensation with quenchers when submergence of quencher arms is shallow	Completed	KWV - Report 2840	Yes
8.	KKB - Concept and task of pressure relief system	Completed	KWV - Report 2871	Yes
9.	Experimental approach to vent clearing in a model tank	Completed	KWV - Report 3129	Yes
10.	KKB - Specification of blowdown tests during non-nuclear hot functional test - Rev. I dated October 4, 1974	Completed	KWU/V 822 Report	Yes
11.	Anticipated data for blowdown tests with pressure relief system during the non-nuclear hot functional test at nuclear power station Brunsbuttel (KKB)	Completed	KWU - Report 3141	Yes
12.	Results of the non-nuclear hot functional tests with the pressure relief system in the nuclear power station Brunsbuttel	Completed	KWU - Report 3267	Yes
13.	Analysis of the loads measured on the pressure relief system during the non-nuclear hot functional test at KKB	Completed	KWU - Report 3346	Yes
14.	KKB - Listing of test parameters and important test data of the non-nuclear hot functional tests with the pressure relief system	Completed	KWU - Working Report R 521/40/77	Yes
15.	KKB - Specification of additional tests for testing of the pressure relief valves during the nuclear start-up, Rev. 1.	Completed	KWU/V 822 TA	Yes

Document Number	Title	Status	Documentation	Used for SSES Licensing
16.	KKB - Results from nuclear start-up testing of pressure relief system	Completed	KWU - Working Report R 142-136/76	Yes
17.	Nuclear Power Station Phillipsburg - Unit 1 Hot Functional Test: Specification of pressure relief valve tests as well as emergency cooling and wetwell cooling systems	Completed	KWU/V 822/RF 13	Yes
18.	Results of the non-nuclear hot functional tests with the pressure relief system in the nuclear power station Phillipsburg	Completed	KWU - Working Report R 142-38/77	Yes
19.	KKPI - Listing of test parameters and important test data of the non-nuclear hot functional tests with the pressure relief system	Completed	KWU - Working Report R 521/41/77	Yes
20.	Air oscillations during vent clearing with single and double pipes	Completed	AEG - Report 2327	Yes

TABLE 1-2

SSES CONTAINMENT DESIGN DIMENSIONS

A. Suppression Chamber	
Inside Diameter	88 ft 0 in
Height	52 ft 6 in
B. Drywell	
Inside Diameter of Base	86 ft 3 in
Inside Diameter of Top	36 ft 4.5 in
Height	87 ft 9 in
C. Reactor Pedestal	
Inside Diameter Below Diaphragm Slab	19 ft 7 in
Inside Diameter Above Diaphragm Slab	20 ft 3 in
Wall Thickness Below Diaphragm Slab	5 ft 1 in
Wall Thickness Above Diaphragm Slab	4 ft 5 in
Height	81 ft 9.6 in
D. Reinforced Concrete Thickness	
Base Foundation Slab	7 ft 9 in
Containment Wall	6 ft 0 in
Diaphragm Slab	3 ft 6 in

Table 1-2 (Cont'd)

E.	Steel Line Plate Thickness for Base Foundation, Containment Wall, and Diaphragm Slab	0.25 in
F.	Suppression Chamber Columns	
	Outside Diameter	3 ft 6 in
	Wall Thickness	1.25 in
	Height	52 ft 6 in

TABLE 1-3

SSES CONTAINMENT DESIGN PARAMETERS

A.	Drywell and Suppression Chamber		Drywell		Suppression Chamber
1.(a)	Internal Design Pressure		53 psig		53 psig 6
1.(b)	Internal Design Pressure in Combination with other Loads		44 psig		29 psig
2.	External Design Pressure		5 psid		5 psid
3.	Drywell Floor Design				
	Differential Pressure				
	Upward			28 psid	
	Downward			28 psid	
4.	Design Temperature		340°F		220°F
5.	Drywell Free Volume (including vents)	(Minimum)	239,337 ft^3		
		(Normal)	239,593 ft^3		
		(Maximum)	239,850 ft^3		
6.	Suppression Chamber Free Volume	(Minimum)			148,590 ft^3
		(Normal)			153,860 ft^3
		(Maximum)			159,130 ft^3
7.	Suppression Chamber Water Volume	(Minimum)			122,410 ft^3
		(Normal)			126,980 ft^3
		(Maximum)			131,550 ft^3
8.	Pool Cross-Section Area				
	Gross (Outside Pedestal)				5379 ft^2
	Total Gross (Including Pedestal Water Area)				5679 ft^2
	Free (Outside Pedestal)				5065 ft^2
	Total Free				5277 ft^2

Table 1-3 (Cont'd)

	Drywell	Supression Chamber
9. Pool Depth (Minimum)		22 ft.
(Normal)		23 ft.
(Maximum)		24 ft.
B. Vent System		
1. Number of Downcomers		82 (Five capped: see Appendix K) 6
2. Downcomer Outer Diameter		2 ft.
3. Total Downcomer Vent Area		257 $ft.^2$
4. Downcomer Submergence (Minimum)		10 ft.
(Normal)		11 ft.
(Maximum)		12 ft.
5. Downcomer Loss Factor		2.5
C. Safety Relief Valves		
1. Opening Time		
a. Delay Time (between trip and motion)		0.10 sec.
b. Response Time (close to open)		0.15 sec.

Table 1-3 (Cont'd)

2. Safety and Relief Setpoints for the 16 valves.

Valves	Spring Set* Pressure, psig	Pressure Switch** Set Pressure, psig	ASME Rated Capacity at 103% of Spring Set Pressure lb./hr.
(See Figure 1-4)			
B,E	1146	1076	862,400
A,C,D	1175	1086	883,950
P,R,S	1185	1096	891,380
J,L,N	1195	1106	898,800
G,K,M	1205	1116	906,250
H	1175	1096	883,950
F	1185	1086	891,380

* Will open if switch fails
** Reset pressure 55 to 100 psi below pressure switch set point

3. Reaction Forces (vertical, Fv, and horizontal, Fh) on valve supports during Valve Opening and Closing at 1250 psig.

a. No Flow Established

Fv = 60,300 lb.

Fh = 23,600 lb.

b. At Full Flow

Fv = 56,200 lb.

Fh = 24,200 lb.

Table 1-3 (Cont'd)

4. Maximum Steam Flow Rate at 70 bar (1000 psig)* Reactor Pressure (conservative value for design calculation) — 390.93 metric tons/hr (862,400 lb/hr)

   * When a value is given in two sets of units, the first value is the original one; the second is an approximation provided for convenience.

D. Safety Relief Valve Discharge Pipes

1. Outer Diameter — 12 in

2. Distance of Quencher Middle Plane to Basemat — 3 ft 6 in

3. Quencher Submergence (Minimum) — 18.5 ft
   (Normal) — 19.5 ft
   (Maximum) — 20.5 ft

4. Length, Number of Bends, and Air Volume for each SRV Pipe

	Pipe Length, ft			Number of Bends			
Quencher Position	Inside Drywell	Inside Wetwell	Total	Inside Drywell	Inside Wetwell	Total	Air Volume, ft^3
(See Figure 1-4)							
A	67.67	73.11	140.78	12	3	15	92.38
B	66.4	73.23	139.63	9	4	13	91.48
C	67.71	54.47	122.18	10	0	10	78.12
D	69.95	75.16	145.11	7	3	10	95.79
E	93.06	54.47	147.53	16	-	16	98.03
F	61.96	54.47	116.43	7	0	7	73.6
G	70.40	75.04	145.44	9	3	12	96.05
H	73.09	78.22	151.31	12	4	16	100.66

Table 1-3 (Cont'd)

Quencher Position	Pipe Length, ft: Inside Drywell	Inside Wetwell	Total	Number of Bends: Inside Drywell	Inside Wetwell	Total	Air Volume, ft^3
J	73.34	74.85	148.19	12	3	15	98.2
K	80.82	72.53	153.35	13	3	16	102.34
L	67.44	54.47	121.91	11	0	11	77.91
M	59.84	54.47	114.35	9	0	9	71.97
N	75.09	81.60	156.69	12	5	17	105.15
P	71.77	83.91	155.68	10	4	14	104.1
R	72.59	54.47	127.06	12	0	12	81.95
S	67.23	72.11	139.34	13	3	16	91.25

TABLE 1-4

- Review of Susquehanna SES Units 1 & 2 Pool Dynamic Loadings -

-Comparison with NUREG 0487, NUREG 0487-Supplement No. 1, Lead Plant and Generic Long Term Program-

NRC Acceptance Criteria NUREG 0487	NRC Acceptance Criteria Supplement No. 1	Lead Plant Position (Zimmer DAR, Amendment 13)	Generic Long Term Program Position	Susquehanna Position	Remarks
I. LOCA RELATED HYDRODYNAMIC LOADS					
A. Submerged Boundary Loads During Vent Clearing. 33 psi overpressure added to local hydrostatic below vent exit (walls and basemat)-linear attenuation to pool surface.	24 PSI overpressure statically applied with hydrostatic pressure to surfaces below vent exit (attenuate to 0 psi at pool surface) for period of vent clearing for plants with $(\dot{m}hL)/[(A_p/A_v)V_{DW}] \leq 55$. where: $\dot{m}$ = mass flow in vents – lb/sec V_{DW} = drywell volume – ft^3 h = enthalpy of air in vent– Btu/lb L = submergence – ft A_p/A_v = pool area to vent area For plants where $(\dot{m}hL)/[(A_p/A_v)V_{DW}] > 55$, the loading increase over hydrostatic pressure on basemat and submerged walls below vent exit is $p = 24 + 0.27\ (\dot{m}hL)/[(A_p/A_v)V_{DW}] - 55$ (attenuate to 0 psi at pool surface).	March 20, 1979 letter. 24 psi statically applied to surfaces below vent exit (attenuate to 0 psi at pool surface) for period of vent clearing. Zimmer and LaSalle meet NUREG 0487.	Evaluating impact.	Evaluation indicates 24 PSI overpressure is conservative (see Subsection 4.2.1.2)	6
B. Pool Swell Loads.					
1. Pool Swell Analytical Model (PSAM)					
a. Air bubble pressure-use PSAM described in NEDE-21544-P.	(a) No change from NUREG 0487.	(a) Accept NUREG 0487.	(a) Accept NUREG 0487.	(a) Accept NUREG 0487.	5
b. Pool swell elevation-Use PSAM des-	(b) Use PSAM with polytropic exponent of 1.2 to a maximum swell height	(b) Accept NUREG 0487.	(b) Accept NUREG 0487 -Supplement No. 1	(b) Accept NUREG 0487 -Supplement No. 1	

TABLE 1-4

NRC Acceptance Criteria NUREG 0487	Supplement No. 1	Lead Plant Position (Zimmer DAR, Amendment 13)	Generic Long Term Program Position	Susquehanna Position	Remarks
cribed in NEDE-24544-P with a polytropic exponent of 1.2 for wetwell air compression.	which is the greater of 1.5 vent submergence or the elevation corresponding to the drywell floor uplift Δ P used for design assessment per response to Question 020.68 and February 16, 1979 letter from Shoreham provided the drywell pressure response used for the swell height is calculated according to NEDM-10320.				
c. Pool swell velocity-use PSAM described in NEDE-24544-P multiplied by a factor of 1.1.	(c) No change from NUREG 0487.	(c) Accept NUREG 0487 with velocity vs elevation obtained from PSAM.	(c) Accept NUREG 0487 with velocity vs elevation obtained from PSAM.	(c) Following lead plant/long term position.	
d. Pool swell acceleration-use PSAM described in NEDE-24544-P.	(d) No change from NUREG 0487.	(d) Accept NUREG 0487.	(d) Accept NUREG 0487.	(d) Accept NUREG 0487.	
e. Wetwell air compression-use PSAM described in NEDE-24544-P.	(e) No change from NUREG 0487.	(e) Accept NUREG 0487.	(e) Accept NUREG 0487.	(3) Accept NUREG 0487.	
f. Drywell pressure history-unique based on NEDM-10320.	(f) No change from NUREG 0487.	(f) Accept NUREG 0487.	(f) Accept NUREG 0487.	(f) Accept NUREG 0487.	
2. Loads on Submerged Boundaries. Maximum bubble pressure predicted by PSAM is to be added uniformly to	No change from NUREG 0487.	Accept NUREG 0487.	Accept NUREG 0487.	Accept NUREG 0487.	

TABLE 1-4

NRC Acceptance Criteria: NUREG 0487	NRC Acceptance Criteria: Supplement No. 1	Lead Plant Position (Zimmer DAR, Amendment 13)	Generic Long Term Program Position	Susquehanna Position	Remarks
local hydrostatic below vent exit (walls and basemat) and linear attenuation to pool surface. Apply to walls up to maximum pool swell elevation.					
3. Impact Loads					
a. Small structures-(For horizontal pipes, I-beams, and other similar structures having one dimension $\leq$ 20 in.). The loading function shall have the versed sine shape: $p(t)=0.5\ p_{max}(1-\cos 2\pi \frac{t}{\tau})$	(a) No change from NUREG 0487.	(a) Accept NUREG 0487.	(a) Accept NUREG 0487.	(a) Accept NUREG 0487.	
b. Large structures-not applicable, no large structures are impacted by pool swell.	(b) No change from NUREG 0487.	(b) Not applicable (no large structures).	(b) Not applicable (no large structures).	(b) Not applicable (no large structures).	
c. Grating-The static drag load, F_{ss}, is to be calculated by forming the product of ΔP from Figure 4-40 of NEDO-21060, Rev.	(c) No change from NUREG 0487.	(c) Not applicable (no grating).	(c) Accept NUREG 0487 with velocity vs elevation obtained from PSAM.	(c) Not applicable (no grating in pool swell zone).	

TABLE 1-4

NRC Acceptance Criteria NUREG 0487	NRC Acceptance Criteria Supplement No. 1	Lead Plant Position (Zimmer DAR, Amendment 13)	Generic Long Term Program Position	Susquehanna Position	Remarks
2, and the total area of the grating. To account for the dynamic nature of the initial loading, the static drag load is increased by a multiplier given by: $F_{SP}/D = 1+ \quad 1+(0.064Wf)^2$ for $Wf < 2000$ in/sec					
4. Wetwell Air Compression					
a. Wall loads-directly apply the PSAM calculated pressure due to wetwell compression.	(a) No change from NUREG 0487.	(a) Accept 0487.	(a) Accept NUREG 0487.	(a) Accept NUREG 0487.	5
b. Diaphragm upward load-calculate Δ PUP using the correlation: $\Delta PUP = 8.2 - 44F$, for $0 \leq F \leq 0.13$ $\Delta PUP = 2.5$ psi, for $F > 0.13$ where: $F = \frac{AB \cdot AP \cdot VS}{VD\,(AV)^2}$ AB = break area AP = net pool area AV = total vent area	(b) No change from NUREG 0487.	(b) Use Δ PUP = 5.5 PSID.	(b) Same as lead plant.	(b) Same as lead plant.	6

TABLE 1-4

NRC Acceptance Criteria NUREG 0487	Supplement No. 1	Lead Plant Position (Zimmer DAR, Amendment 13)	Generic Long Term Program Position	Susquehanna Position	Remarks	
VS = initial wetwell air space volume VD = drywell volume						
5. Asymmetric Load. Apply the maximum air bubble pressure calculated from PSAM and a minimum air bubble pressure (zero increase) in a worst case distribution to the wetwell wall.	Use twice the 10% of maximum bubble pressure statically applied to 1/2 of the submerged boundary (with hydrostatic pressure) proposed in March 16, 1979 letter from GE.	Accept NUREG 0487-Supplement No. 1.	Accept NUREG 0487-Supplement No. 1	Accept NUREG 4087-Supplement No. 1.		5
C. Steam Condensation and Chugging Loads.						
1. Downcomer Lateral Loads.						
a. Single vent loads: -A static equivalent load of 8.8 KIPs shall be used provided: (i) the downcomer is 24" in diameter. (ii) the downcomer dominant natural frequency is $\leq$ 7 Hz, submerged. (iii) the downcomer is unbraced or braced at or above approx. 8' from the exit.	(a) No change from NUREG 0487.	(a) Accept NUREG 0487.	(a) Use single vent dynamic lateral load developed under Task A-13 (NEDE-24106-P). However, extrapolate the 30 Kip and 3 msec impulse to 65 Kips and 3 msec.	(a) Following long term program. Confirmation through plant unique GKM-IIM test data on lateral bracing loads.	See DAR, Subsection 9.6.3 for verification of lateral tip load.	6

TABLE 1-4

NRC Acceptance Criteria NUREG 0487	Supplement No. 1	Lead Plant Position (Zimmer DAR, Amendment 13)	Generic Long Term Program Position	Susquehanna Position	Remarks
-A static equivalent load of 8.8 KIPs multiplied by the ratio of the natural frequency and 7 Hz for dominant natural frequencies between 7 and 14 Hz. Other restrictions in (i) and (iii) apply. -If the natural frequency of the downcomer is > 14 Hz or if bracing is closer than 8' above the exit, a plant specific dynamic structural calculation shall be performed using a dynamic load defined by: $F(t) = F_0 \sin \frac{\P t}{\tau}$; $0 < t < \tau$ $=$ for $t < 0$ and $t > \tau$ where: 2 msec $< \tau <$ 10 msec, and the impulse $I = 2 F_0 (\tau/\P)$ is 200 lbf-sec. Restriction (i) also applies.					

TABLE 1-4

NRC Acceptance Criteria: NUREG 0487	NRC Acceptance Criteria: Supplement No. 1	Lead Plant Position (Zimmer DAR, Amendment 13)	Generic Long Term Program Position	Susquehanna Position	Remarks
b. Multiple vent loads - Use the load specified in Figure 4-10b of NEDE-21061-P, Rev. 2, multiplied by a factor of 1.26 for downcomers with natural frequencies less than 7 Hz. For natural frequencies greater than 7 Hz, apply an additional multiplier equal to the ratio of its frequency and 7 Hz.	(b) No change.	(b) Accept NUREG 0487.	(b) Use multivent lateral load methodology documented in letter report "Method of Applying Mark II Single Vent Dynamic Lateral Load to Mark II Plants with Multiple Vents", transmitted to the NRC on April 9, 1980 under Task A.13.	(b) Following long term program.	
2. Submerged Boundary Loads					
a. High Steam Flux Loads Sinusoidal pressure fluctuation added to local hydrostatic. Amplitude uniform below vent exit, linear attenuation to pool surface. 4.4 psi peak-to-peak amplitude. 2-7 Hz frequencies. NEDE-21061-P, Rev 2.	(a) No change from NUREG 0487.	(a) Accept NUREG 0487 with additional plant unique empirical load specification.	(a) • Use Condensation Oscillation load specification based on NEDE-24288-P.	(a) Use IWEGS/MARS acoustic model documented in NEDE-24822-P with sources derived from GKM II-M steam condensation tests.	(a) Application procedure documented in SSES DAR, Section 9.5.

TABLE 1-4

NRC Acceptance Criteria NUREG 0487	Supplement No. 1	Lead Plant Position (Zimmer DAR, Amendment 13)	Generic Long Term Program Position	Susquehanna Position	Remarks
b. Medium Steam Flux Loads. Sinusoidal pressure fluctuation added to local hydrostatic. Amplitude uniform below vent exit, linear attenuation to pool surface. 7.5 psi peak-to-peak amplitude. 2-7 Hz frequencies. NEDE-21061-P, Rev. 2	(b) No change from NUREG 0487.	(b) Accept NUREG 0487 with additional plant unique empirical load specification.	(b) Use Condensation Oscillation load specification based on NEDE-24288-P.	(b) Same as (a).	5
c. Chugging. -Uniform loading condition - Maximum amplitude uniform below vent exit, linear attenuation to pool surface. +4.8 psi max overpressure, -4.0 psi max underpressure. (Pending resolution of FSI concerns) NEDE-21061-P, Rev. 2. -Asymmetric loading condition - Maxi-	(c) No change from NUREG 0487.	(c) Accept NUREG 0487 with additional plant unique empirical load specification.	(c) Use IWEGS/MARS acoustic model presented in NEDE-24822-P with sources derived from 4T-CO. Application methodology documented in NEDE-24302-P.	(c) Same as (a).	6

TABLE 1-4

NRC Acceptance Criteria NUREG 0487	Supplement No. 1	Lead Plant Position (Zimmer DAR, Amendment 13)	Generic Long Term Program Position	Susquehanna Position	Remarks
mum amplitude uniform below vent exit - linear attenuation to pool surface. +20 psi max overpressure, -14 psi max underpressure. 20-30 Hz frequency, peripheral variation of amplitude follows observed statistical distribution with maximum and minimum diametrically opposed. NEDE-21061-P, Rev. 2.					

TABLE 1-4

NRC Acceptance Criteria: NUREG 0487	NRC Acceptance Criteria: Supplement No. 1	Lead Plant Position (Zimmer DAR, Amendment 13)	Generic Long Term Program Position	Susquehanna Position	Remarks
II. SRV-RELATED HYDRODYNAMIC LOADS					
A. Pool Temperature Limits					
All Mark II facilities shall use quencher type devices. The suppression pool local temperature shall not exceed 200°F for all plant transients involving SRV operations. Measurements from temperature sensors located on the containment wall in the sector containing the discharge device at the same elevation as the device can be used as local indication.	No change from NUREG 0487.	Accept NUREG 0487.	Accept NUREG 0487.	Accept NUREG 0487. Mass & Energy analysis documented in SSES DAR Appendix I.	
B. Air Clearing Loads.					
a. Methodology for bubble load prediction T-quencher - use ramshead methodology described in Sec. 3.2 of NEDO-21061-P, Rev. 2. x-quencher - Use Sec. 3.3 of NEDO-21061-P, Rev. 2.	(a) Accept "Interim T-Quencher Load Definition" with the following modifications: -Bubble frequenncy-3 to 11 Hz -Peak Pressure Multiplier for Subsequent Actuation - 1.5 -Vertical Pressure Profile - maximum amplitude from basemat to 2.5' above quencher center line, linear attenuation to zero at pool surface. -Multiple SRV Actuations - 1) linear ABSS superposition of peak single values with all bubbles in phase. 2) if the combined peak pressure exceeds local single value peak use the lower value	(a) T-Quencher load specification presented in Susquehanna DAR, Subsection 4.1.3. Accept NUREG 0487 - Supplement No. 1 modifications except use bubble frequency in SSES DAR and a peak pressure multiplier of 1.5 for all actuations.	(a) T-Quencher load-Same as lead plant. X-Quencher load-Plant unique load definition.	(a) Same as lead plant.	

TABLE 1-4

NRC Acceptance Criteria NUREG 0487	NRC Acceptance Criteria Supplement No. 1	Lead Plant Position (Zimmer DAR, Amendment 13)	Generic Long Term Program Position	Susquehanna Position	Remarks
b. SRV Discharge Load Cases. The following load cases shall be considered for design evaluation of containment structures and equipment inside the containment: 1. Single valve, first and subsequent actuation. 2. ADS valve actuation. 3. Two adjacent valve first actuation. 4. All valves discharged sequentially by setpoint. 5. All valves discharged simultaneously by assuming all bubbles are oscillating in phase.	(b) Same as NUREG 0487 but load case 4 is not included.	(b) Accept NUREG 0487-Supplement No. 1.	(b) Accept NUREG 0487-Supplement No. 1.	(b) Accept NUREG 0487-Supplement No. 1.	

TABLE 1-4

NRC Acceptance Criteria NUREG 0487	NRC Acceptance Criteria Supplement No. 1	Lead Plant Position (Zimmer DAR, Amendment 13)	Generic Long Term Program Position	Susquehanna Position	Remarks	
c. Bubble Frequency. T-quencher - a range of bubble frequency of 4-12 Hz is the minimum range that shall be increased if required to include the frequency predicted by the ramshead methodology together with ± 50% margin.	(c) 3-11 Hz.	(c) Plant unique frequency range based on Susquehanna DAR.	(c) Same as lead plant.	(c) Following frequency range documented in Susquehanna DAR.	Additional study performed confirming conservatism of frequency range in Susquehanna DAR (see Subsection 10.2.3).	6
X-quencher - a range of bubble frequency of 4-12 Hz shall be evaluated.			X-quencher bubble frequency being developed by Burns & Roe based largely on Caorso test data.			
c. Quencher Arm and Tie Down Loads.						5
1. Quencher Arm Loads. Vertical and lateral arm loads are to be developed on the basis of bounding assumptions for air/water discharge from the quencher and conservative combinations of maximum/minimum bubble pressures acting on the quencher per NEDE-21061-P, Rev. 2.	No change from NUREG 0487.	Accept NUREG 0487. Load Specification in SSES DAR Subsection 4.1.2.5 used to verify the conservatism of this approach.	T-quencher arm loads are presented in Susquehanna DAR, Section 4.1.2.5. X-quencher-Accept NUREG 0487.	Following long term program.		

TABLE 1-4

NRC Acceptance Criteria NUREG 0487	Supplement No. 1	Lead Plant Position (Zimmer DAR, Amendment 13)	Generic Long Term Program Position	Susquehanna Position	Remarks
2. Quencher Tie-down Loads. The vertical and lateral arm load transmitted to the basemat via the tie-down plus vertical transient wave and thrust loads calculated from a standard momentum balance are to be calculated based on conservative clearing assumptions per NEDE-21061-P, Rev. 2.	No change from NUREG 0487.	Accept NUREG 0487. Load specification in SSES DAR Subsection 4.1.2.6 used to verify conservatism.	T-quencher tie-down loads are defined in Susquehanna DAR, Subsection 4.1.2.6. X-Quencher-Accept NUREG 0487.	Following long term program.	

TABLE 1-4

NRC Acceptance Criteria NUREG 0487	NRC Acceptance Criteria Supplement No. 1	Lead Plant Position (Zimmer DAR, Amendment 13)	Generic Long Term Program Position	Susquehanna Position	Remarks
III. LOCA/SRV SUBMERGED STRUCTURE LOADS					
A. LOCA/SRV Jet Loads.					
1. LOCA Downcomer Jet Load Calculate based on methods described in NEDE-21730 and the following constraints and modifications: (a) Standard drag at the time the jet first encounters the structure must be multiplied by the factor: $1 + \frac{6 \cdot V_a}{C_D \cdot A_X \cdot R_i}$ where: V_a=acceleration volume as defined in NEDE-21730. C_D=drag coefficient as defined in NEDE-21730. A_X=projected area as defined in NEDE-21730. R_i=vent exit radius.	Accepts alternative methodology presented in Zimmer DAR dealing with LOCA jet load.	The LOCA downcomer jet load is calculated by the methodology presented in the Zimmer DAR, Subsection 5.3.2.1.	Ring matex model developed by Burns & Roe used for WPPSS Unit #2. Remaining plants following lead plant methodology.	Following lead plant position.	

TABLE 1-4

NRC Acceptance Criteria NUREG 0487	Supplement No. 1	Lead Plant Position (Zimmer DAR, Amendment 13)	Generic Long Term Program Position	Susquehanna Position	Remarks
(b) Forces in the vicinity of the jet front shall be computed on the basis of Formula 2-12 and 2-13 of NEDE-21730. The local velocity, U_∞ , . and acceleration, U_∞, are to be conservatively calculated by the methods of NEDE-21471 from the potential function: $\phi = \frac{-3}{8\pi} \cdot U_j \cdot V_w \frac{\text{Cos } \theta}{r^2}$ where: r & θ = spherical coordinates from jet front. U_j = jet velocity from NEDE-21730. V_w = initial volume of water in the vent. (c) After the last fluid particle has reached the jet front a spherical vortex					

TABLE 1-4

NRC Acceptance Criteria NUREG 0487	Supplement No. 1	Lead Plant Position (Zimmer DAR, Amendment 13)	Generic Long Term Program Position	Susquehanna Position	Remarks
continues propagating. The drag on structures in its vicinity can be bounded by using the flow field from the formula for ϕ above with U_j as the jet front velocity from NEDE-21730 at time $t = t_f$.					
2. SRV Quencher Jet Loads					
This load may be neglected for those structures located outside a zone of influence which is a sphere circumscribed around the quencher arms. If there are holes in the end caps; the radius of the sphere should be increased by 10 holes diameters. (Confirmation during long term program required).	SRV quencher jet loads may be neglected beyond a 5' cylindrical zone of influence.	Accept NUREG 0487 - Supplement No. 1.	Accept NUREG 0487-Supplement No. 1 X-quencher - Accept NUREG 0487.	Accept NUREG 0487-Supplement No. 1.	
B. LOCA/SRV Air Bubble Drag Loads.					

TABLE 1-4

NRC Acceptance Criteria NUREG 0487	Supplement No. 1	Lead Plant Position (Zimmer DAR, Amendment 13)	Generic Long Term Program Position	Susquehanna Position	Remarks	
1. LOCA Air Bubble Loads Calculate based on the analytical model of the bubble charging process and drag calculations of NEDE-21471 until the bubbles coalesce. After bubble contact, the pool swell analytical model, together with the drag computation procedure NEDE-21471 shall be used. Use of this methodology shall be subject to the following constraints and modifications:	No change from NUREG 0487.	Documented in plant unique DAR's.	Documented in plant unique DAR's.	Documented in Subsection 4.2.1.7 of SSES DAR.		6
a. A conservative estimate of bubble asymmetry shall be added by increasing accelerations and velocities computed in step 12 of Section 2.2 of NEDE-21730 by 10%. If the alternate steps 5A, 12A and 13A are used the acceleration drag shall be directly	(a) No change	(a) Position documented on page 5.4-8 of of Zimmer DAR.	(a) Accept NUREG-0487.	(a) Following the Long Term Program.	Documented in Subsection 4.2.3.2 of SSES DAR.	5

TABLE 1-4

NRC Acceptance Criteria NUREG 0487	Supplement No. 1	Lead Plant Position (Zimmer DAR, Amendment 13)	Generic Long Term Program Position	Susquehanna Position	Remarks
increased by 10% while the standard drag shall be increased by 20%.					
b. Modified coefficients C_D' from accelerating flows as presented in Kenlegan & Carpenter and Sarpkaya references shall be used with transverse forces included, or an upper bound of a factor of three times the standard drag coefficients shall be used for structures with no sharp corners or with streamwise dimensions at least twice the width.	(b) Accept lead plant position documented in Attachment 1.k of the Zimmer FSAR with the following modifications: (1) Use $C_H = C_M - 1$ in the F_A formula. (2) For non-cylindrical structures use lift coefficients for appropriate shape of $C_L = 1.6$. (3) The standard drag coefficient for pool swell and SRV oscillating bubbles should be based on data for structures with with sharp edges.	(b) Position documented on page 5.4-8 of Zimmer DAR.	(b) Following Lead Plant Position and evaluating NUREG 0487-Supplement No. 1 modifications.	(b) Following Lead Plant Program.	(b) Addressed in Subsection 4.2.3.3 of SSES DAR.
c. The equivalent uniform flow velocity and acceleration for any structure or structural segment shall be taken as the maximum values "seen" by that structure not the value at the geometric center.	(c) Accepts lead plant position.	(c) Position documented on page 5.4-8 of Zimmer DAR.	(c) Following Lead Plant Position.	(c) Following Long Term Program.	(c) Addressed in Subsection 4.2.3.4 of SSES DAR.

TABLE 1-4

NRC Acceptance Criteria NUREG 0487	Supplement No. 1	Lead Plant Position (Zimmer DAR, Amendment 13)	Generic Long Term Program Position	Susquehanna Position	Remarks
d. For structures that are closer together than three characteristic dimensions of the larger one, either a detailed analysis of the interference effects must be performed or a conservative multiplication of acceleration and drag forces by a factor of four must be performed.	(d) Accepts Lead Plant position.	(d) Position documented on page 5.4-8 of Zimmer DAR.	(d) Following Lead Plant Program.	(d) Following Long Term Program.	(d) Addressed in Subsec-section 4.2.3.5 of SSES DAR.
e. If significant blockage from downcomer bracing exists relative to the net pool area, the standard drag coefficients shall be modified by conventional methods (Pankhurst & Holder reference).	(e) No change from NUREG 0487.	(e) Position documented on page 5.4-9 of Zimmer DAR.	(e) Following lead Plant Program.	(e) Following Long Term Program.	(e) Addressed in Subsection 4.2.3.6 of SSES DAR.
f. Formula 2-23 of NEDE-21730 shall be modified by replacing M_H by $P_{FB}V_A$ where V_A is obtained from Tables 2-1 and 2-2.	(f) No change since NUREG 0487.	(f) Accept NUREG 0487.	(f) Accept NUREG 0487.	(f) Accept NUREG 0487.	(f) Documented in DAR, Subsection 4.2.3.7.

TABLE 1-4

NRC Acceptance Criteria NUREG 0487	Supplement No. 1	Lead Plant Position (Zimmer DAR, Amendment 13)	Generic Long Term Program Position	Susquehanna Position	Remarks
2. a. SRV ramshead air bubble loads.	(a) No change since NUREG 0487.	(a) Documented on Page 5.4-9 of Zimmer DAR.	(a) N/A	(a) N/A	
b. SRV quencher air bubble loads. T-quencher - loads may be computed on the basis of the above ramshead bubble pressure and assuming the bubble to be located at the center of the quencher device having a bubble radius equal to the quencher radius.	(b) No change since NUREG 0487.	(b) Documented on Page 5.4-9 of Zimmer DAR.	(b) T-quencher submerged structure methodology is presented in Susquehanna DAR, Section 4.1.3.	(b) Following Long Term Program	5
X-quencher - loads may be computed on the basis of the above ramshead methodology using bubble pressure calculated by the methods of NEDE-21061-P, Rev. 2 for the X-quencher.			X-quencher methodology being developed by Burns & Roe.		
C. Steam Condensation Drag Loads.					
Review will be conducted on a plant unique basis.	No change since NUREG 0487.	Documented on Page 5.4-9 of Zimmer DAR.	Plant unique method being developed.	Plant unique methodology documented in DAR Subsection 4.2.2.5.	6

PAF:cvc
34P-B

CHAPTER 2

SUMMARY

TABLE OF CONTENTS

2.0 SUMMARY

This Design Assessment Report contains the SSES adequacy evaluation for dynamic loads due to LOCA and SRV discharge.

2.1 LOAD DEFINITION SUMMARY

2.1.1 SRV Load Definition Summary

Hydrodynamic loads resulting from SRV actuation fall into two distinct categories: loads on the SRV system itself (the discharge line and the discharge quencher device), and the air clearing loads on the suppression pool walls and submerged structures.

Loads on the SRV system during SRV actuation include loads on the SRV piping due to effects of steady backpressure, transient water slug clearing and SRV line temperature. Determination of loading on the quencher body, arms, and support is based on transients resulting from valve opening (water clearing and air clearing), valve closing and operation of an adjacent quencher.

Air clearing loads are examined for four loading cases: symmetric (all valve) SRV actuation, asymmetric adjacent SRV actuation, single SRV actuation, and Automatic Depressurization System (ADS-six valves) actuation. Dynamic forcing functions for loading of the containment walls, pedestal, basemat, and submerged structures are developed using techniques developed in Section 4.1. Loads on the SRV system due to SRV actuation are discussed in Subsection 4.1.2, and loads on suppression pool structures due to SRV actuation are discussed in Subsection 4.1.3. A full scale, unit cell test program was employed to verify SSES unique SRV loading as described in Chapter 8.

2.1.2 LOCA Load Definition Summary

The spectrum of LOCA-induced loads on the SSES containment structure is characterized by LOCA loads associated with poolswell, condensation oscillation and chugging loads, as well as long term LOCA loads.

The LOCA loads associated with poolswell result from short duration transients and include downcomer clearing loads, water jet loads, poolswell impact and drag loads, pool fallback drag loads, poolswell air bubble loads, and loads due to drywell and wetwell temperature and pressure transients. Techniques used to evaluate these loads are described in Subsection 4.2.1.

Condensation oscillations result from mixed flow (air/steam) and pure steam flow effects in the suppression pool. Chugging loads result from low mass flux pure steam condensation. The load definitions for these phenomena are contained in Subsection 4.2.2.

Long term LOCA loads result from those wetwell and drywell pressure and temperature transients which are associated with design basis accidents (DBA), intermediate accidents (IBA), and small break accidents (SBA). Their load definitions are contained in Subsection 4.2.5.

Structures directly affected by LOCA loads include the drywell walls and floor, wetwell walls, RPV pedestal, basemat, liner plate, columns, downcomers, downcomer bracing system, quenchers, and wetwell piping. Their loading conditions are described in Subsection 4.2.6.

2.2 DESIGN ASSESSMENT SUMMARY

Design assessment of the SSES structures and components is achieved by analyzing the response of the structures and components to the load combinations explained in Chapter 5. In Chapter 7 predicted stresses and responses (from the loads defined in Chapter 4 and combined as described in Chapter 5) are compared with the applicable code allowable values identified in Chapter 6 and the SSES design will be assessed as adequate by virtue that the design capabilities exceed the stresses or responses resulting from SRV discharge and/or LOCA loads.

2.2.1 Containment Structure and Reactor Building Assessment Summary

2.2.1.1 Containment Structure Assessment Summary

The primary containment walls, base slab, diaphragm slab, reactor pedestal and reactor shield are analyzed for the effects of SRV and LOCA in accordance with Table 5-1. The ANSYS finite element program is used for the dynamic analysis of structures.

Response spectra curves are developed at various locations within the containment structure to assess the adequacy of components. Stress resultants due to dynamic loads are combined with other loads in accordance with Table 5-1 to evaluate rebar and concrete stresses. Design safety margins are defined by comparing the actual concrete and rebar stresses at critical sections with the code allowable values. The assessment methodology of the containment structure is presented in Subsection 7.1.1.1.

The results of the structural assessment of the containment structure are summarized in Appendix A. The results show that the reinforcing bar design stresses and the concrete design stresses are below the allowable stresses.

2.2.1.2 Reactor Building Assessment Summary

The reactor building is assessed for the effects of SRV and LOCA loads in accordance with Table 5-1.

Containment basemat acceleration time histories are used to investigate the reactor building response to the SRV and LOCA loads. Response spectra curves at various reactor building elevations are used to assess the adequacy of components in the reactor building. The assessment methodology of the reactor building is presented in Subsection 7.1.1.2.

The results of the structural assessment of the reactor building are summarized in Appendix E. The results show that the reinforcing bars and concrete design stresses as well as the structural steel design stresses are below the allowable stresses.

2.2.2 Containment Submerged Structures Assessment Summary

Design assessment of the suppression chamber columns includes non-hydrodynamic as well as hydrodynamic loads. Subsection 7.1.2.2 describes the methodology used to evaluate the columns. The results are presented in Figure A-59 and indicate a minimum design margin of 11.4%.

6 The downcomers are dynamically analyzed per Subsection 7.1.4 for the load combinations given in Table 5-3. A summary of the stresses under various load combinations are given in Figure A-66 and indicates that the minimum design margin is 14% when the loads are combined by ABS and 50% when the loads are combined by SRSS.

Results from the analysis of the suppression pool liner plate
2 indicate that no structural modifications are required (see Subsection 7.1.3 and 7.2.1.5).

The original downcomer and SRV bracing system has been redesigned so that the downcomers and SRV discharge lines are now supported by separate bracing systems. The SRV discharge lines are supported by bracing connected to the columns, while the downcomers are braced together by a truss system, but no connections exist at the containment or pedestal wall. Subsections 7.1.2.1 and 7.1.2.2 document the evaluation of the downcomer and SRV discharge line bracing systems, respectively.

Figure A-67 presents the SRV support system's maximum stresses and design margins, while Figures A-60 and A-61 show the design margins for the downcomer bracing system members and connections, respectively. All stresses are acceptable.

2.2.3 BOP and NSSS Piping System Assessment Summary

6 All Seismic Category I BOP and NSSS piping are analyzed for the LOCA and SRV hydrodynamic loads and non-hydrodynamic loads per Subsections 7.1.5 and 7.1.6.1.1, respectively. Appendix F gives the stresses and design margins for selected BOP piping systems.

The stress reports for the above evaluation are available for NRC review.

2.2.4 BOP and NSSS Equipment Assessment Summary

All Seismic Category I BOP and NSSS equipment are evaluated for the hydrodynamic and non-hydrodynamic loads per the SSES Seismic Qualification Review Team (SQRT) Program. For each equipment Purchase Order, 4-page SQRT summary forms are prepared documenting the qualification results.

These SQRT summary forms are available for NRC review.

2.2.5 Electrical Raceway System Assessment Summary

Seismic Category I electrical raceway systems in the containment, reactor systems and control building are assessed by the methods contained in Subsection 7.1.8. Loads are combined as shown in Table 5-6. As a result of static and dynamic analysis, it was determined that high stresses resulted in certain members of a few support types. These structural members were strengthened or replaced by stronger members to reduce the stresses below the 6 allowables.

2.2.6 HVAC Duct System Assessment Summary

Seismic Category I HVAC duct system in the containment, reactor building and control building are assessed by the methods contained in Subsection 7.1.9. Loads are combined as shown in Table 5-2. As a result of structural analysis, it was found that a few structural members had high stresses but most of the members had adequate margin of safety. The overstressed members were strengthened or replaced by stronger members to ensure an adequate margin of safety.

CHAPTER 3

SRV DISCHARGE AND LOCA TRANSIENT DESCRIPTION

TABLE OF CONTENTS

3.0 SRV DISCHARGE AND LOCA TRANSIENT DESCRIPTION

The purpose of this section is to provide a description of the SRV discharge and LOCA events.

A quantitative description of specific SRV and LOCA related loads for SSES is presented in Sections 4.1 and 4.2 respectively.

3.1 DESCRIPTION OF SAFETY RELIEF VALVE DISCHARGE

Susquehanna Unit 1 (and 2) is equipped with a safety relief system which condenses reactor steam in a suppression chamber pool. By this arrangement, reactor steam is conducted to the wetwell via fast acting safety relief valves and quencher equipped discharge lines. This section discusses the causes of SRV discharge, describes the SRV discharge process, and identifies the resultant SRV discharge actuation cases.

3.1.1 Causes of SRV Discharge

During certain reactor operating transients, the SRVs may be actuated (by pressure, by electrical signal, or by operator action) for rapid relief of pressure in the reactor pressure vessel. The following reactor operating transients have been identified as those which may result in SRV actuation:

a. Turbine generator trip (with bypass or without)

b. Main steam line isolation valve (MSIV) closure

c. Loss of condenser vacuum

d. Feedwater controller failure

e. Pressure regulator failure - closed

f. Generator load rejection (with and without bypass)

g. Loss of ac or auxiliary power

h. Loss of feedwater flow

i. Trip of two recirculation pumps

j. Recirculation flow control failure - decreasing flow

k. Inadvertent safety relief valve opening

l. Control Rod withdrawal error

m. Anticipated Transient Without Scram (ATWS)

A detailed description of these transients is provided in Section 15.2 of the FSAR.

3.1.2 Description of the SRV Discharge Phenomena and SRV Loading Cases

Before an individual safety relief valve opens, the water level in the discharge line is approximately equal to the water level in the pool. As a valve opens, steam flows into the discharge line air space between the valve and the water column and mixes with the air (see detailed evaluation in Chapter 3 of Reference 1, pages 6-12 through 6-14). Since the downstream portion of the discharge line contains a water slug and does not allow an immediate steam discharge into the pool, the pressure inside the line increases. The increased pressure expels the water slug from the SRV discharge line and quencher. The magnitude of the water clearing pressure is primarily influenced by the steam flow rate through the valve, the degree to which entering steam is condensed along the discharge line walls, the volume of the discharge line airspace, and the volume of the water slug to be accelerated.

The clearing of water is followed by an expulsion of the enclosed air-steam volume. The exhausted gas forms an oscillating system with the surrounding water, where the gas acts as the spring and the water acts as the mass. This oscillating system is the source of short term air clearing loads.

As the air-steam mixture oscillates in the pool it also rises because of buoyancy and eventually breaks through the pool water surface at which time air clearing loads cease. When all the air leaves the safety relief system, steam flows into the suppression pool through the quencher holes and condenses. The SSES quencher design assures stable condensation even with elevated pool water temperature.

The SRV actuation cases resulting from the transients listed in Subsection 3.1.1 are classified, as being one of the following cases:

a. Symmetric (all valve, or AOT) discharge

b. Asymmetric discharge, including single valve discharge

c. Automatic Depressurization System (ADS) discharge

Also considered in the containment design is the effect of subsequent SRV actuations (second-pop), discussed in Subsection 4.1.3.6.

The symmetric discharge case [otherwise termed the all-valve, or abnormal operating transient (AOT) case] is classified as the type of SRV discharge that would follow rapid isolation of the vessel from the turbine such as turbine trip, closure of all MSIVs, loss of condenser vacuum, etc. As pressure builds up following isolation of the vessel, the SRVs actuate sequentially according to the pressure set points of the valves. This may or may not result in actuation of all the SRVs, but for conservatism in loading considerations all valves are assumed to actuate. Refer to Subsection 4.1.3.1 for discussion of the loads resulting from this all-valve case.

Asymmetric discharge is defined as the firing of the SRVs for the three adjacent quencher devices which results in the greatest asymmetric pressure loading on the containment. This situation is hypothesized when, following a reactor scram and isolation of the vessel, decay heat raises vessel pressure so that low set point valves actuate. If, during this time of discharge of decay heat energy, manual actuation of the two other adjacent SRVs that comprise the asymmetric case is assumed, this actuation would result in the maximum asymmetric pressure load on the containment. Subsection 4.1.3.2 gives a discussion of the loads resulting from the asymmetric discharge case.

The single valve discharge case is classified as the firing of the SRV which gives the single largest hydrodynamic load. Transients that could potentially initiate such a case are an inadvertent SRV discharge or Design Basis Accident (DBA). Refer to Subsection 3.2.3 for a discussion of the latter possibility. Subsection 4.1.3.2.1 provides a discussion of the loads resulting from the single valve case.

The ADS discharge is defined as the simultaneous actuation of the six SRVs associated with the ADS. See Figure 1-4 for the location of the quencher devices associated with the ADS valves. The ADS is assumed to actuate during an Intermediate Break Accident (IBA) or Small Break Accident (SBA). If an ADS discharge is hypothesized coincident to an IBA or SBA (described in Subsections 3.2.2 and 3.2.1, respectively), the effects of an increased suppression pool temperature (resulting from steam condensation during the LOCA transient) and increased suppression chamber pressure (resulting from clearing of the drywell air into the pool during the transient) are considered in the calculation of pressure loadings for the ADS discharge case. See Subsection 4.1.3.3 for further discussion of the loads resulting from the ADS case.

3.2 DESCRIPTION OF LOSS-OF-COOLANT ACCIDENT

This event involves the postulation of a spectrum of piping breaks inside the containment varying in size, type, and location of the break. For the analysis of hydrodynamic loadings on the containment, the postulated LOCA event is identified as a Small Break Accident (SBA), an Intermediate Break Accident (IBA), or aDesign Basis Accident (DBA).

3.2.1 Small Break Accident (SBA)

This subsection discusses the containment transient associated with small primary system blowdowns. The primary system ruptures in this category are those ruptures that will not result in reactor depressurization from either loss of reactor coolant or automatic operation of the ECCS equipment, ie, those ruptures with a break size less than 0.1 sq ft.

The following sequence of events is assumed to occur. With the reactor and containment operating at the maximum normal conditions, a small break occurs that allows blowdown of reactor steam or water to the drywell. The resulting pressure increase in the drywell leads to a high drywell pressure signal that scrams the reactor and activates the containment isolation system. The drywell pressure continues to increase at a rate dependent upon the size of the steam leak. The pressure increase lowers the water level in the downcomers. At this time, air and steam enter the suppression pool at a rate dependent upon the size of the leak. Once all the drywell air is carried over to the suppression chamber, pressurization of the suppression chamber ceases and the system reaches an equilibrium condition. The drywell contains only superheated steam, and continued blowdown of reactor steam condenses in the suppression pool. The principal loading condition in this case is the gradually increasing pressure in the drywell and suppression pool chamber and the loads related to the condensation of steam at the end of the vents.

3.2.2 Intermediate Break Accident (IBA)

This subsection discusses the containment transient associated with intermediate primary system blowdowns. This classification covers breaks for which the blowdown will result in limited reactor depressurization and operation of the ECCS, ie, the break size is equal to or slightly greater than 0.1 sq ft.

Following the break, the drywell pressure increases at approximately 1.0 psi/sec. This drywell pressure transient is sufficiently slow so that the dynamic effect of the water in the vents is negligible and the vents will clear when the drywell-to-suppression chamber differential pressure is equal to the hydrostatic pressure corresponding to the vent submergence. The resulting pressure increase in the drywell will lead to a high drywell pressure signal that will scram the reactor and activate the containment isolation system. Approximately 5 seconds after the 0.1 sq ft break occurs, air, steam, and water will start to flow from the drywell to the suppression pool; the steam will be condensed, and the air will rise to the suppression chamber free space. The continual purging of drywell air to the suppression chamber will result in a gradual pressurization of both the wetwell and drywell. The ECCS will be initiated by the break and will provide emergency cooling of the core. The operation of these systems is such that the reactor will be depressurized in approximately 600 seconds. This will terminate the blowdown phase of the transient. The principal loading condition in this case will be the gradually increasing pressure in the drywell and suppression chamber and the loads related to the condensation of steam at the end of the vents.

3.2.3 Design Basis Accident (DBA)

An occurrence of events which could result in a DBA (instantaneous rupture of a main steam or recirculation line) is a remote possibility. Since such an accident provides an upper limit estimate to the resultant effects for this category of pipe breaks, it is evaluated without the causes being identified. For Susquehanna, an assumed instantaneous double-ended rupture of a recirculation line causes the maximum drywell pressure and therefore the governing LOCA hydrodynamic loads.

The sequence of events immediately following the rupture of a recirculation line has been determined. A drywell high pressure signal is almost instantaneously sensed, initiating a scram and containment isolation and signaling the HPCI, CS and LPCI to start. The flow in both sides of the break will accelerate to the maximum allowed by the critical flow considerations. In the side adjacent to the suction nozzle, the flow will correspond to critical flow in the pipe cross-section. In the side adjacent to the injection nozzle, the flow will correspond to critical flow at the 10 jet pump nozzles associated with the broken loop. In addition, the cleanup line cross-tie will add to the critical flow area. This high rate of flow out of the ruptured recirculation line results in a drywell pressure rise of approximately 44 psig in 14.5 seconds (refer to FSAR Table 6.2-5 and FSAR Figure 6.2-2).

This rapid increase in drywell pressure accelerates the water initially in the containment vent system out through the vents. Immediately following vent water clearing, an air/steam bubbles start to form at the downcomer exits. Initially, the bubble pressure is essentially equal to the current drywell pressure. As the flow of air/steam from the drywell becomes established in the vent system, the initial vent exit bubble expands, thus accelerating upward the suppression pool water above the vent exits. The steam fraction of the flow is condensed, but continued injection of drywell air and expansion of the air bubble results in a rapid rise in the suppression pool surface known as pool swell.

Following the pool swell and fallback, there is a period of high-steam flow rate through the containment vent system. For large primary system ruptures, reactor blowdown and, therefore, vent steam condensation last for approximately 60 seconds.

Shortly after a DBA, the ECCS pumps (HPCI, CS, and LPCI) automatically start pumping condensate storage tank water or suppression pool water into the reactor pressure vessel. Within 40 seconds all the ECCS pumps are at rated flow. This floods the reactor core until water starts to cascade into the drywell from the break. The time at which this occurs would depend upon break size and location. Because the drywell would be full of steam at the time of vessel flooding, the sudden introduction of cold water causes steam condensation and drywell depressurization. When the drywell pressure falls below the suppression chamber pressure, the drywell vacuum relief system is actuated and air from the suppression chamber enters the drywell. Eventually, sufficient air returns to the drywell to equalize the pressures. Similarly, small differential pressures between the drywell and the suppression chamber can be produced if the containment spray system is actuated, condensing steam in the drywell.

Following the vessel flooding and drywell/suppression chamber pressure equalization phase of the accident, suppression pool water will be continuously recirculated through the core by the ECCS pumps. The energy associated with the core decay heat will result in a slow heatup of the suppression pool. The suppression pool temperature is controlled by the RHR heat exchangers. The capacity of these heat exchangers is such that the maximum suppression pool temperature increase is reached after several hours. The suppression pool can experience a peak temperature of approximately 200°F under worst case conditions. The post LOCA containment heatup and pressurization transient is terminated when the RHR heat exchangers reduce the pool temperature and containment pressure to nominal values.

The primary loads on the containment generated by a DBA are the pressure build-ups in the drywell and suppression chamber, and the loads resulting from the various modes of steam condensation at the vent ends. The high rate of system depressurization resulting from a DBA militates against the firing of an SRV; however, for conservatism a single SRV discharge is considered coincident with the DBA for containment structural loading purposes.

CHAPTER 4

LOAD DEFINITION

TABLE OF CONTENTS

FIGURES

FIGURES (Cont.)

CHAPTER 4

TABLES

4.0 LOAD DEFINITION

4.1 SAFETY RELIEF VALVE (SRV) DISCHARGE LOAD DEFINITION

See the Proprietary Supplement for this section.

4.2. LOCA LOAD DEFINITION

Subsections 4.2.1, 4.2.2 and 4.2.3 discuss the numerical 1
definition of loads resulting from a LOCA in the SSES
containment. The LOCA loads are divided into five groups. 2

(1) Short term LOCA loads associated with poolswell (Subsection 4.2.1). 1

(2) Condensation oscillations and chugging loads (Subsection 4.2.2).

(3) Submerged Structures Loads (Subsection 4.2.3)

(4) Secondary Loads (Subsection 4.2.4). 2

(5) Long term LOCA loads (Subsection 4.2.5).

The application of these loads to the various components and 1
structures in the SSES containment is discussed in
Subsection 4.2.6. 2

4.2.1 LOCA LOADS ASSOCIATED WITH POOLSWELL

A description of the LOCA/Poolswell transient is given in
Section 3.2.3 of this Design Assessment Report. The LOCA loads 2
associated with poolswell are listed in Table 4-16. A discussion
of these loads and their SSES unique values follows.

4.2.1.1 Wetwell/Drywell Pressures during Poolswell

The drywell pressure transient used for the poolswell portion of
the LOCA transient ($\leq$ 2.0 sec) is given in Table IV-D-3 of 1
Reference 7. A portion of this table is reproduced herein as
Table 4-17. This drywell pressure transient includes the
blowdown effects of pipe inventory and reactor subcooling and is
the highest possible drywell pressure case for poolswell. This
drywell pressure transient is calculated using the method 2
documented in Reference 56.

The short term poolswell wetwell pressure transient resulting
from this drywell pressure transient is calculated by applying
the poolswell model contained in Reference 8. The equations and 1
assumptions in the poolswell model were coded into a Bechtel
computer program and verified against the Class 1, 2 and 3 test
cases contained in Reference 9. This verification is documented
in Appendix D to this report. Inputs used for the calculation of
the SSES plant unique poolswell transient are shown in Table 4-18. The short term wetwell pressure transient calculated with
the poolswell code is shown in Figure 4-39. The short term
wetwell pressure peak is 56.1 psia (41.4 psig).

Reference 46, Subsection III.B.3.d.2 formulates a methodology for 2
determining the maximum diaphragm uplift P to be used for design
assessment. This ΔP is based on following relation:

$$\Delta PUP = 8.2 - 44 \cdot F \text{ (PSI)} \qquad 0<F\leq 0.13$$

$$\Delta PUP = 2.5 \text{ (PSI)} \qquad F>0.13$$

Rev. 2, 5/80

$$F = \frac{AB \cdot AP \cdot VS}{VD \cdot (AV)^2}$$

where: AB = break area;
AP = net pool area;
AV = total vent area
VS = initial wetwell air space volume; and
VD = drywell volume

For SSES (see Tables 4-18 and 4-19):

AB = 3.53 ft^2
AP = 5065.03 ft^2
AV = 257.52 ft^2
VS = 149,000 ft^3
VD = 239,600 ft^3

2 Inserting into the above equation yields:

$$F = 0.168 > 0.13$$

This gives a maximum uplift ΔP of 2.5 PSID. However, as required by NUREG 0808, a more conservative uplift ΔP of 5.5 PSID will be used for design.

4.2.1.2 Submerged Boundary Loads During Vent Clearing

The submerged jet formed by the expulsion of the water leg in the downcomers creates a vent clearing load on the basemat and on the submerged wetwell walls. This loading is defined by Reference 57 as a 24 PSI overpressure statically applied with hydrostatic pressure to surfaces below vent exit with a linear attentuation to zero at pool surface (see Figure 4-41). This load is applied during the vent clearing.

The NRC, in Supplement No. 1 to NUREG-0487, accepts the above 24 PSI overpressure for the vent clearing load for those plants where

$$(\dot{m}hL)/[(A_P/A_V)V_{DW}] \leq 55$$

with: $\dot{m}$ = mass flow in vents -lb/sec
V_{DW} = drywell volume - ft^3
h = enthalpy of air in vents - btu/lb
L = submergence - ft
A_P/A_V = pool area to vent area ratio

6 For SSES, the various parameters are:

$\dot{m}$ = 17,900 lb/sec
V_{DW} = 239,850 ft^3
h = 194 btu/lb
L = 12 ft
A_P/A_V = 5065/257

Substituting into the above gives:

$$[(17,900)(194)(12)(257)]/[(5065)(239,850)] = 8.8$$

Thus, for SSES, the 24 PSI overpressure specified for the air clearing load is acceptable. 6

4.2.1.3 LOCA-Jet-Loads

During the vent clearing stage induced velocity and acceleration fields are created in the suppression pool producing drag forces on submerged strctures. The original methodology employed to predict the drag forces is contained in Reference 12 (often called the Moody jet model) and is an analytical representation of an unsteady water jet discharging into a suppression pool. The jet is made up of constant velocity fluid particles traveling at the speed at which they exited the discharge pipe. The jet front is described as the locus of points which a particle overtakes the one exiting immediately before it. No velocities or accelerations are defined in the fluid external to the jet.

Reference 46, subsection III.D.1.a proposed that velocity and acceleration be predicted throughout the pool using the potential function of a sphere at the jet front. A modification of the load calculated at jet impingement was also required. The Acceptance Criteria was a simple method to determine a bounding jet load for all structures below the downcomer exits.

The Moody jet model was clearly derived for jets with constant or linearly increasing acceleration. However, the vent clearing transients predicted for Mark II plants typically have an acceleration increase greater than linear. Strict applicaton of 2
Reference 12 leads to unrealistic mathematicl results. Two interpretations of the results are possible depending upon the time base employed. Examining the jet in "real time" (t in Reference 12) a jet can be seen with two independent fronts traveling at different speeds at different locations which coincide only at the point of jet dissipation. On the other hand, if we use the "exit time" (τ) as a basis the jet reverses and moves backward in both space and "real time" before dissipation. Clearly neither of these observations is of much use in calculating loads on structures.

To overcome the difficulties of using this model, an alternative methodology has been formulated. The jet front will be described by the motion of the particle having travelled the farthest at any instant in time. This will be identical to the Moody jet motion for jets with linearly increasing acceleration but will yield a single continuous velocity and acceleration time history even if the acceleration increases more rapidly.

A sphere is then placed at the jet front generating a potential flow described by the following function:

$$\phi = \frac{-3}{8\pi} U_j V_w \frac{\cos\theta}{r^2}$$

where r and θ are the spherical coordinates from the sphere center to some position in the suppression pool with θ measured from the jet direction, U_j is the velocity of the sphere determined by the velocity of the particle having traveled the farthest at the instant in time the drag forces are being computed and V_w is the initial volume of water in the vent.

The local velocity U_∞, and acceleration, $\dot{U}_\infty$ are then calculated from the above relation by the methods of Reference 14. Once the local velocity and acceleration are known the drag forces are computed from Reference 13 as follows:

$$F_A = \frac{\dot{U}_{\infty n} \nu \rho}{g_c}$$

$$F_S = \frac{C_D A_x U_{\infty n}^2 \rho}{2 g_c}$$

where F_A is the acceleration drag, $\dot{U}_{\infty n}$ is the local acceleration field normal to the structure, ν is the acceleration drag volume for flow normal to the structure, ρ is the fluid density, F_S is the standard drag, C_D is the drag coefficient for flow normal to the structure, A_x is the projected structure area normal to $U_{\infty n}$, and $U_{\infty n}$ is the local velocity field normal to the structure.

When the jet is predicted to dissipate the sphere is traveling at the final jet velocity at the point of maximum jet penetration. This condition is used as the final load calculation point. The final jet velocity is that of the jet front just before the last particle leaving the vent reaches the jet front. The velocity of the last particle is disregarded.

4.2.1.4 Boundary Loads During Poolswell

During the poolswell transient, the high pressure air bubble which forms in the vicintiy of the vent exit creates an increase in pressure on all suppression pool boundaries below the vent exit as well as those walls which it is in direct contact. Boundaries which are above the bubble location and up to the point of maximum pool elevation also experience increased pressure loads corresponding to the increased pressure in the wetwell airspace as well as the hydrostatic contribution of the water slag.

Reference 46, Subsection III.B.3.b methodology for specification of these loads uses the Poolswell Analytical Model to determine the maximum values of bubble pressure and wetwell airspace pressure. The analysis takes the maximum pool elevation as 1.5 times the initial submergence. Using this data, a static loading is applied to the containment structure as follows:

1. for the basemat - uniform pressure equal to the maximum bubble pressure superimposed on the hydrostatic load corresponding to a submergence from vent exit to the basemat;

2. for the containment walls below vent exit - maximum bubble pressure plus hydrostatic head corresponding to vertical distance from vent exit;

3. for the containment walls between vent exit and maximum pool elevation-linear variation between maximum bubble pressure and maximum wetwell airspace pressure;

4. for the containment walls above maximum pool elevation - maximum wetwell airspace pressure.

The pressure distribution used for the SSES analysis is shown in Figure 4-44.

4.2.1.5 Poolswell Asymmetric Air Bubble Load

The methodology used in the proceeding subsection assumes that the air flow rate in each downcomer is equal leading to a symmetric loading of the containment boundary. Reference 46 has expressed concern that circumferential variations in the downcomer air flow rate can occur due to dyrwell air/steam mixture variation that would result in variations in the bubble pressure load on the wetwell wall. 2

This loading condition is calculated by statically applying the maximum air bubble pressure obtained from the PSAM to 1/2 of the submerged boundary and statically applying 120% of the maximum bubble pressure to the other 1/2 of the submerged boundary. The pressure load on the basemat and wetwell walls below the vent exit is the sum of the air pressure and the hydrostatic pressure. For the portion of the wall above the vent exit, the pressure increase due to the air bubble is linearly attenuated from the bubble pressure at the vent exit to zero at the pool surface. This increase is then added to the local hydrostatic pressure to obtain the total pressure. The time period of application of the load is from the termination of vent clearing until the maximum swell height is reached.

4.2.1.6 Poolswell Impact Load

Any structure located between the initial suppression pool surface (El. 672') and the peak poolswell height (El. 690'-2", see Figure 4-38) is subject to the pool swell impact load. As documented in the response to NRC Question 020.68, the poolswell maximum elevation is determined by the poolswell Analytical Model with a polytropic exponent of 1.2 for wetwell air compression to a maximum swell height which is the greater of 1.5 vent submergence or the elevation corresponding to the drywell floor uplift ΔP determined from the equation documented in Subsection 4.2.1.1 (2.5 PSID). For SSES, using the design drywell floor 6
uplift ΔP=2.5 PSID leads to the greatest poolswell height and yields 1.51 times the initial vent submergence. Since all grating is removable only "small" structures as defined in Reference 10a, Subsection 4.2.5.1 are subject to poolswell impact 2
loads.

Poolswell impact loads of "small" structures are determined as specified in Reference 46, Subsection III.B.3.c.1. An SSES plant-unique velocity vs. elevation curve has been generated with the poolswell model (see Figure 4-40). The velocity curve is conservatively increased by a 1.1 multiplier and used to calculate the impulse per unit area, pulse duration and maximum impact pressure at the component's elevation. The peak pressure is then used to define a versed sine shaped hydrodynamic loading function

$$P(t) = \frac{P_{max}(1-\cos 2\pi t/\tau)}{2}$$

2

where: P = pressure acting on the projected area of the structure;
P_{max} = the temporal maximum of pressure acting on the projected area of the structure;

t = time;

τ = duration of impact

The loading function corresponds to impact on rigid structures. In actuality, the structures being analyzed may be more flexible, resulting in the pressure pulses, during impact, being modified by the motion of the structure. To account for this, the hydrodynamic mass of impact is added to the mass of the impacted structure when performing the structural dynamic analysis.

4.2.1.7 LOCA Air Bubble Submerged Structure Load

During the drywell air purge phase of a LOCA, an expanding bubble is created at the downcomer exits. These rapidly expanding bubbles eventually coalesce into a "blanket" of air which leads to the pool swell phenomena. The bubble charging process creates fluid motion in the suppression pool which causes drag loads on the submerged structures.

6

The submerged structure drag loads due to air clearing, prior to pool swell, are calculated in the same manner as the drag loads due to CO and chugging presented in Subsection 4.2.2.5. However, the chugging and CO sources are replaced with a source representing the bubble growth prior to pool swell. This source is derived from the original 4T data. All sources are assumed in-phase (87 sources).

4.2.1.8 Poolswell Drag Load

Subsequent to bubble contact all bubbles are assumed to coalesce
into a blanket of air and the poolswell drag loads are due the
rapidly accelerating upward slug of water and acts in the
2 vertical direction only (except for lift forces which act in the
traverse direction to flow). The one dimensional pool swell
model is used to predict the vertical flow field. Once the flow
field is known the drag forces are calculated by the methods of
Reference 13 modified by the methodology presented in Subsection

4.2.3. This load applies to any structure located between the elevation of the vent exit and the peak poolswell height. The duration of the drag load begins when the vent clears except for structures which are originally not submerged. For structures which are not submerged, the drag load duration is based on the slug transient time (Reference 10a, page 4-78, step 3).

4.2.1.9. Poolswell Fallback Load

After the termination of poolswell the slug of water falls under the influence of gravity causing drag forces on structures lcoated between the peak poolswell height and the vent exit. The motion of the water is described by the following equations:

$$H(t) = H_{max} - gt^2/2$$

$$V_{FB}(t) = gt$$

$$\dot{V}_{FB}(t) = g$$

where g is the acceleration constant, H(t) is the height above initial water level at time t, H_{max} is the maximum swell height, and t is time starting with t = 0 at maximum swell height = H_{max}. The drag load is then calculated from the methods of Reference 13 modified by Subsection 4.2.3 of the DAR. The loading stops when H(t) has fallen below the structure or when H(t) has returned to normal water level - whichever is calculated to occur first.

4.2.2 Condensation Oscillations and Chugging Loads

Condensation oscillation and chugging loads follow the poolswell loads in time. There are basically three loads in this secondary time period, i.e., from about 4 to 60 seconds after the break. "Condensation oscillation" is broken down into two phenomena, a mixed flow regime and a steam flow regime. The mixed flow regime is a relatively high mass flux phenomenon which occurs during the final period of air purging from the drywell to the wetwell when the mixed flow through the downcomer vents contains some air as well as steam. The steam flow portion of the condensation oscillation phenomena occurs after all the air has been carried over to the wetwell and a relatively high intermediate mass flux of pure steam flow is established. 2

"Chugging" is a pulsating condensation phenomenon which can occur either following the intermediate mass flux phase of a LOCA, or during the class of smaller postulated pipe breaks that result in steam flow through the vent system into the suppression pool. A necessary condition for chugging to occur is that only pure steam flows from the LOCA vents. Chugging imparts a loading condition to the suppression pool boundary and all submerged structures.

In Revision 2 of the DAR, we stated that the DFFR CO and chugging steam condensation boundary load definition (see Appendix A to Reference 21 and Reference 16) would be compared with the LOCA steam condensation load definition derived from the GKM II-M test data to evaluate the conservatism of the DFFR load. Subsections 9.6.1.1 and 9.6.1.2 document this comparison. 6

As a result of this comparison and the possible schedule delays associated with licensing SSES based on the DFFR load, PP&L decided on April 1, 1982 to terminate the re-evaluation of SSES based on the DFFR load and re-assess SSES with the GKM II-M load definition. Subsection 9.5.3 documents the GKM II-M load definition. For chugging, both a symmetric and asymmetric load case are considered, while for CO, only a symmetric load case is considered.

For plant evaluation, PP&L does not define a separate CO and chugging load definition, as with the Mark II Owners. Instead, the acceleration response spectra (ARS) generated for the LOCA steam condensation phenomena for combination with the other
6 dynamic loads (i.e., SRV (ADS), seismic, etc.) is the so-called LOCA load, which represents an envelope of the ARS curves generated for both the GKM-IIM CO and chugging load definition, and symmetric and asymmetric load cases (see Subsection 9.6.1.1).

Subsection 7.0 provides the results of the re-evaluation of the SSES plant to the LOCA steam condensation load derived from the GKM-IIM test data.

4.2.2.1 Containment Boundary Loads Due To Condensation Oscillations

This subsection has been deleted.

4.2.2.2 Pool Boundary Loads Due to Chugging

This subsection has been deleted.

4.2.2.3 Downcomer Lateral Loads

2

The chugging load imparted to the downcomer is taken from Reference 47. This reference specifies two sinusoidal dynamic loads used when evaluating downcomer lateral bracing systems.
5 The durations and amplitudes specified are 3ms, 30 kip and 6 ms, 10 kip (as shown in Figures 4-62G & H).

However, in response to the NRC's concerns with the Mark II single vent lateral load, SSES is re-evaluating the downcomers with an extrapolated single vent lateral load of 65 Kips and 3 msec time duration for faulted conditions. Subsection 9.6.3 verifies the conservatism of this load based on a statistical analysis of the GKM II-M bracing force data at 10^{-5} exceedance
6 probability.

4.2.2.4 Multivent Lateral Loads Due to Chugging

Multivent lateral loads due to chugging are presently being evaluated by the methodology documented in letter report "Method of Applying Mark II Single Vent Dynamic Lateral Load to Mark II Plants with Multiple Vents," transmitted to the NRC on April 9, 1980 under Task A.13.

4.2.2.5 Submerged Structure Loads Due to Condensation Oscillations and Chugging

Condensation Oscillation and chugging induce flows fields in the suppression pool causing drag loads on the submerged structures (i.e., SRV lines, downcomers, etc.). The methodology for calculating these drag loads to be combined with the other design basis loads is presented below.

The force on a submerged structure is the sum of an acceleration force F_A and an unsteady drag force F_D .

$$F_T = F_A + F_D$$

Under certain conditions the pressure gradient is of sufficient magnitude so that the submerged structure force is essentially the acceleration drag force. In order for this to be true, the Stroughal Number must be sufficiently large.

For the SSES submerged structures and the flow fields induced by chugging and CO, the Stroughal Number is sufficiently high that negligible error will be incurred by ignoring the unsteady drag force.

The submerged structure drag force can be approximated by the integral of the pressure field P_Φ over the structure surface:

$$\vec{F} = \oint_S p_\Phi d\vec{S} \cdot K$$

where: P_Φ = determined by the equations for potential flow 6
K = hydrodynamic mass factor

For a linear isentropic fluid where the velocity is everywhere small compared to the sonic speed c, the equations for potential flow reduce to the acoustic wave equation (Reference 65). Thus, the pressure field also satisfies the acoustic wave equation.

Thus, for calculating the SSES submerged structure drag load due to CO and chugging, the above expression is used, with the pressure P_Φ , as a function of time and position, calculated by the IWEGS/MARS acoustic model of the SSES suppression pool. The pressure P_Φ is calculated in an analagous manner as the symmetric wall loads (see Subsection 9.5.3.4.1) for each source, except that the pressures are calculated at the submerged structure surface locations instead of the containment boundary.

For each structure being analyzed (i.e., column) a pressure time history (PTH) is calculated for every 60° increment circumferential around the structure at each elevation corresponding to a nodal point of the structural model. Thus, for each node point elevation, six pressure time histories are calculated. This is repeated for each source. These sets of PTHs, calculated for each source, are then integrated across the structure's surface to give resultant force time histories for structural analysis.

The force time histories are then multiplied by a hydrodynamic
6 mass factor, K, of 2 to account for the modification of the flow field due to structure's presence.

4.2.3 Response to NRC Criteria for Loads On Submerged Structure

4.2.3.1 Introduction

In October 1978 the NRC published NUREG-0487, Mark II Containment Lead Plant Program Load Evaluation and Acceptance Criteria. It addresses the load methodologies proposed by the Mark II Lead Plant Program for determining LOCA and SRV hydrodynamic loads. NUREG-0487 was highly critical of the lead plant position for determining submerged structure loads and stipulated very conservative alternative loading criteria. The following subsections will present the NRC submerged structures acceptance criteria and the corresponding Mark II response.

4.2.3.2 NRC Criteria III.D.2.a.1: Bubble Asymmetry

A conservative estimate of asymmetry should be added by increasing acceleration and velocities computed in Step 12 of Section 2.2 of Reference 13 by 10%. If the alternative steps 5A, 12A, and 13A are used, the acceleration drag shall be directly increased by 10% while the standard drag shall be increased by 20%.

Response: These criteria are acceptable.

2 #### 4.2.3.3 NRC Criteria III.D.2.a.2: Standard Drag In Accelerating Flow

The drag coefficients C_D for the standard drag contribution in steps 13, or 13A, 15 of section 2.2 and step 3 of section 2.3 of Reference 13 may not be taken directly from the steady state coefficients of Table 2-3. Modified coefficients C_D from accelerating flow as presented in References 49 and 50 shall be used with transverse forces included, or an upper bound of a factor of three times the standard drag coefficients shall be used for structures with no sharp corners or with streamwise dimensions at least twice the width.

Response:

The three references show that in oscillating flows the standard drag coefficient for cylinders can exceed the steady flow value. Values of C_D in excess of 2.0 were observed while steady state values (for cylinders) never exceed 1.2. The NRC's position is interpreted to mean that neglecting the unsteady effect on standard drag coefficients will be nonconservative in some cases.

A method is presented in Reference 51, Appendix A to account for unsteady effects on standard and acceleration drag during various phases of the LOCA and SRV transients. Also included are methods to estimate transverse forces due to vortex shedding.

Subsequent to reviewing the methodology contained in Appendix A of Reference 51, the NRC in Supplement No. 1 of NUREG-0487, 2 required several modifications to the methodology for determining the unsteady drag coefficients.

A review of the SSES pool swell and fallback drag load calculations indicates that SSES has incorporated these modifications into their calculations. Drag coefficients are not required for calculating the submerged structure drag loads due 6 to air bubble charging prior to pool swell, and the drag loads due to chugging and CO, since these loads are calculated using the pressure time histories at the structure locations (see Subsection 4.2.1.7 and 4.2.2.5).

4.2.3.4 NRC Criteria III.D.2.a.3: Segmentation of Structures

The equivalent uniform flow velocity and acceleration for any structure or structural segment shall be taken as the maximum values "seen" by that structure, not the value at the geometric center.

Response:

For structures submerged in a non-uniform flow field, the velocity and acceleration will be a function of position along the structure. The NRC's criterion is interpreted to mean that the velocity and acceleration should be taken at the end of the segment closest to the disturbing source instead of the geometric center. For certain restrictions on segment length, the error in the calculation of drag using the velocity and acceleration at the geometric center is very small. This is demonstrated for 2 acceleration drag in Reference 51, Appendix B and for standard drag Reference 51, Appendix C. Appendix B also contains a discussion that shows that neglecting end effects in drag calculations is conservative.

4.2.3.5 NRC Criteria III.D.2.a.4: Interference Effects

The computation of drag forces on submerged structures independent of each other (as presented in Reference 13) is adequate for structures sufficiently far from each other so that interference effects are negligible. Interference effects can be expected to be insignificant when two structures are separated by more than three characteristic dimensions of the larger one. For structures closer together than this separation, either detailed analysis of interference effects shall be performed or a conservative multiplication of both the acceleration and standard drag forces by four shall be performed.

Response:

Interference effects can have a significant effect on drag forces. A modification to the calculational procedure is proposed to account for interference. Reference 51, Appendix D describes the proposed method for standard drag with the exception that the free stream velocity used will be that at the structures geometric center in all cases. Reference 51, Appendix
2 E presents the proposed method for acceleration drag.

4.2.3.6 NRC Criteria III.D.2.a.5: Blockage In Downcomer Bracing

A specific example of interference which must be accounted for is the blockage presented to the motion of the water slug during pool swell due to the presence of downcomer bracing systems. If significant blockage relative to the net pool area exists, the standard drag coefficients shall be modified for this effect by conventional methods (Reference 52).

Response:

6 Blockage effects on the pool swell drag loads produced on the downcomer bracing system were accounted for by using the methods in Reference 87.

4.2.3.7 NRC Criteria III.D.2.a.6: Formula 2-23 of Reference 13

Formula 2-23 of Reference 13 shall be modified by replacing M_H with $\rho_{FB} V_A$ where V_A is obtained from Table 2-1 and 2-2. This is then consistent with the analysis of Reference 14.

Response:

This criteria is acceptable.

4.2.4 Secondary Load

The previous subsections have identified and specified loading methodologies that result in significant containment dynamic
2 loads. In addition, several pool dynamic loads can occur which are considered secondary when compared to the previous loads or because the containment and related equipment response is small when subjected to them. The following subsections identify the secondary loads and the load criteria to be applied to the SSES containment.

4.2.4.1 Downcomer Friction Drag Loads

Friction Drag loads are experienced internally by the downcomers during vent clearing and subsequent air/or steam flow. In addition, the downcomers experience an external drag load during poolswell. Using standard drag force calculation procedures these loads are determined to be 0.6 and .3 KIPS per downcomer, respectively and are not considered in the structural evaluation of the containment.

4.2.4.2 Sonic Waves

Immediately following the postulated instantaneous rupture of a large primary system pipe, a sonic wave front is created at the break location and propagates through the drywell to the vent system. This load has been determined to be negligible and none is specified.

4.2.4.3 Compressive Wave

The compression of the air in the drywell and vent system causes a compressive wave to be generated in the downcomer water legs. This compressive wave then propagates through the pool and causes a differential pressure loading on the submerged structures and on the wetwell wall. This load has been evaluated and is considered negligible.

4.2.4.4 Fallback Loads on Submerged Boundaries 2

During fallback "water hammer" type loads could exist if the water slug remained intact during this phase. However available test data indicates that this does not occur and the fallback process consists of a relatively gradual settling of the pool water to its initial level as the air bubble "percolates" upward. This is based on visual observations during the EPRI tests (Reference 32) as well as indirect evidence provided by a careful examination of pool bottom pressure forces from the 4T, EPRI, foreign licensee and Marviken tests. Thus these loads are small and will not be considered.

4.2.4.5 Vent Clearing Loads on the Downcomers

The expulsion of the water leg in the downcomers at vent clearing creates a transient water jet in the suppression pool. This jet formation may occur asymmetrically leading to lateral reaction loads on the downcomer. However, this load is bounded by the load specification during chugging and will not be considered for containment analysis.

4.2.4.6 Post Poolswell Waves

Reference 46 indicates the potential for containment loading due to post poolswell waves impinging on the wetwell wall and internal components. Per the response to Question M020.8 documented in Appendix A to Reference 10a, this load is considered negligible when compared to the other design basis 6
loads.

4.2.4.7 Seismic Slosh

Seismic slosh loads are defined as those hydrodynamic loads exerted on the suppression pool walls by water in the suppression pool during a seismic event. Although these loads are expected to be small in comparison with other hydrodynamic loads such as those associated with air/steam SRV discharge and LOCA poolswell and steam condensation loads, they have been calculated for the SSES containment evaluation, as requested by the NRC in NUREG-0487.

The methodology used to calculate seismic slosh loads for the SSES containment is the SOLA-3D computer code, developed at Los Alamos Scientific Laboratory for multi-dimensional fluid flow analyses, including seismic slosh (Reference 71 and 72). The code has been used for seismic slosh analysis previously, where a toroidal MK I BWR suppression pool was approximated by an annular geometry, and excited by a simulated sinusoidal seismic event. Results of this analysis are reported in Reference 73. It was demonstrated that SOLA-3D could be used to describe suppression pool water motion for a seismic excitation applied to the containment structure.

The seismic slosh analysis for SSES suppression pool has been patterned after the annular suppression pool analysis described in Reference 73, with appropriate SSES suppression pool and
6 containment parameters used. The results of calculations are pressure-time histories, caused by water wave motion, to be applied to suppression pool boundaries in manner and location similar to the method used for SRV and LOCA hydrodynamic loads.

Generally, water motion above the quiescent suppression pool surface causes "wave loads" and water motion below causes "inertial loads." The inertia loads will always appear to be larger than the wave loads because the normal hydrostatic load would be included below the water surface. (For example, at 24 ft. submergence in cold water, the hydrostatic head would be slightly more than 10 psi, giving a 10 psi bias to the inertia loads at pool bottom.)

Some numerical results of the calculations are shown in Table 4-22 for the selected locations in the suppression pool. As can be observed, these pressures are small relative to those calculated for the other hydrodynamic loads. Figures 4-62 i, j, k, and m show typical wave motion at the four containment locations in Table 4-22.

4.2.4.8 Thrust Loads

Thrust loads are associated with the rapid venting of air and/or steam through the downcomers. To determine this load a momentum balance for the control volume consisting of the drywell, diaphragm floor and vents is taken. Results of the analysis
2 indicates that the load reduces the downward pressure differential on the diaphragm.

4.2.5 Long Term LOCA Load Definition

1 The loss-of-coolant accident causes pressure and temperature transients in the drywell and wetwell due to mass and energy released from the line break. The drywell and wetwell pressure and temperature time histories are required to establish the

structural loading conditions in the containment because they are the basis for other containment hydrodynamic phenomena. The response must be determined for a range of parameters such as leak size, reactor pressure and containment initial conditions. The results of this analysis are containment initial conditions. The results of this analysis are documented in Reference 7.

4.2.5.1 Design Basis Accident (DBA) Transients

The DBA LOCA for SSES is conservatively estimated to be a 3.53 ft^2 break of the recirculation line (Reference 7). The SSES plant unique inputs for this analysis are shown in Table 4-19. Drywell and wetwell pressure responses are shown in Figures 4-46 and 4-47 (extracted from Reference 7). These transient descriptions do not, however, contain the effects of reactor subcooling. Suppression pool temperature response is shown in Figure 4-48 (Reference 7). This transient description also does not contain the effect of reactor subcooling. Drywell temperature response is shown in Figure 4-49 and similarly does not contain the effects of pipe inventory or reactor subcooling.

4.2.5.2 Intermediate Break Accident (IBA) Transients

The worst-case intermediate break for the Mark II plants is a main steam line break on the order of 0.05 to 0.1 ft^2. Suppression pool temperature response is shown in Figure 4-50. Drywell temperature and wetwell and drywell pressures for the SSES IBA are shown in Figure 4-51.

4.2.5.3 Small Break Accident (SBA) Transients

At this time plant-unique SBA data for SSES is not available. The wetwell and drywell pressure and temperature transients for a typical Mark II containment are used to estimate SSES containment response to these accidents. These curves are shown in Figure 4-17 (extracted from Reference 10).

4.2.6 LOCA Loading Histories For SSES Containment Components

The various components directly affected by LOCA loads are shown schematically in Figures 4-53 and 4-54. These components may in turn load other components as they respond to the LOCA loads. For example, lateral loads on the downcomer vents produce minor reaction loads in the drywell floor from which the downcomers are supported. The reaction load in the drywell floor is an indirect load resulting from the LOCA and is defined by the appropriate structural model of the downcomer/drywell floor system. Only the direct loading situations are described explicitly here. Table 4-20 is a LOCA load chart for SSES. This chart shows which LOCA loads directly affect the various structures in the SSES containment design. Details of the loading time histories are discussed in the following subsections.

4.2.6.1 LOCA Loads on the Containment Wall and Pedestal

Figure 4-55 shows the LOCA loading history for the SSES containment wall and the RPV pedestal. The wetwell pressure loads apply to the unwetted elevations in the wetwell; and addition of the appropriate hydrostatic pressure is made for loads on the wetted elevations. Condensation oscillation and chugging loads are applied to the wetted elevations in the wetwell only. The poolswell air bubble load applies to the wetwell boundaries as shown in Figure 4.44.

4.2.6.2 LOCA Loads on the Basemat and Liner Plate

Figure 4-56 shows the LOCA loading history for the SSES basemat and liner plate. Wetwell pressures are applied to the wetted and unwetted portions of the liner plate as discussed in Subsection 4.2.6.1. The downcomer water jet impacts the basemat liner plate as does the poolswell air bubble load. Chugging and condensation oscillation loads are applied to the wetted portion of the liner plate.

4.2.6.3 LOCA Loads on the Drywell and Drywell Floor

Figure 4-57 shows the LOCA loading history for the SSES drywell and drywell floor. The drywell floor undergoes a vertically applied, continuously varying differential pressure, the upward component of which is especially prominent during poolswell when the wetwell air space is highly compressed.

4.2.6.4 LOCA Loads on the Columns

Figure 4-58 shows the LOCA loading history for the SSES columns. Poolswell drag and fallback loads are very minor since the column surface is oriented parallel to the pool swell and fallback velocities. The poolswell air bubble, condensation oscillations and chugging will provide loads on the submerged (wetted) portion of the columns.

4.2.6.5 LOCA Loads on the Downcomers

Figure 4-59 shows the LOCA loading history for the SSES downcomers. The downcomer clearing load is a lateral load applied at the downcomer exit (in the same manner as the chugging lateral load) plus a vertical thrust load. Poolswell drag and fallback loads are very minor since the downcomer surfaces are oriented parallel to the pool swell and fallback velocities. The poolswell air bubble load is applied to the submerged portion of the downcomer as are the chugging and condensation oscillation loads.

4.2.6.6 LOCA Loads on the Downcomer Bracing

Figure 4-60 shows the LOCA loading history for the SSES downcomer bracing system. This system is not subject to impact loads since it is submerged at elevation 668'. As a submerged structure it is subject to poolswell drag, fallback and air bubble loads. Condensation oscillations and chugging at the vent exit will also load the bracing system both through downcomer reaction (indirect load) and directly through the hydrodynamic loading in the suppression pool.

4.2.6.7 LOCA Loads on Wetwell Piping

Figure 4-61 shows the LOCA loading history for piping in the SSES wetwell. Since the wetwell piping occurs at a variety of elevations in the SSES wetwell, sections may be completely submerged, partially submerged, or initially uncovered. Piping may occur parallel to poolswell and fallback velocities as with the main steam safety relief piping. For these reasons there are a number of potential loading situations which arise as shown in Table 4-21. In addition, the poolswell air bubble load applies to the submerged portion of the wetwell piping as do the condensation oscillation and chugging loads.

4.3 ANNULUS PRESSURIZATION

The RPV shield annulus has the recirculation pumps suction lines passing through it (for location in containment see Figure 1-1). The mass and energy release rates from a postualted recirculation line break constitute the most severe transient in the reactor shield annulus. Therefore, this pipe break is selected for analyzing loading of the shield wall and the reactor pressure vessel support skirt for pipe breaks inside the annulus. The reactor shield annulus differential pressure analysis and analytical techniques are presented in Appendices 6A and 6B of the SSES Final Safety Analysis Report (FSAR).

Figures 4-1 through 4-37 and Figure 4-62 are proprietary and are found in the proprietary supplement to this DAR.

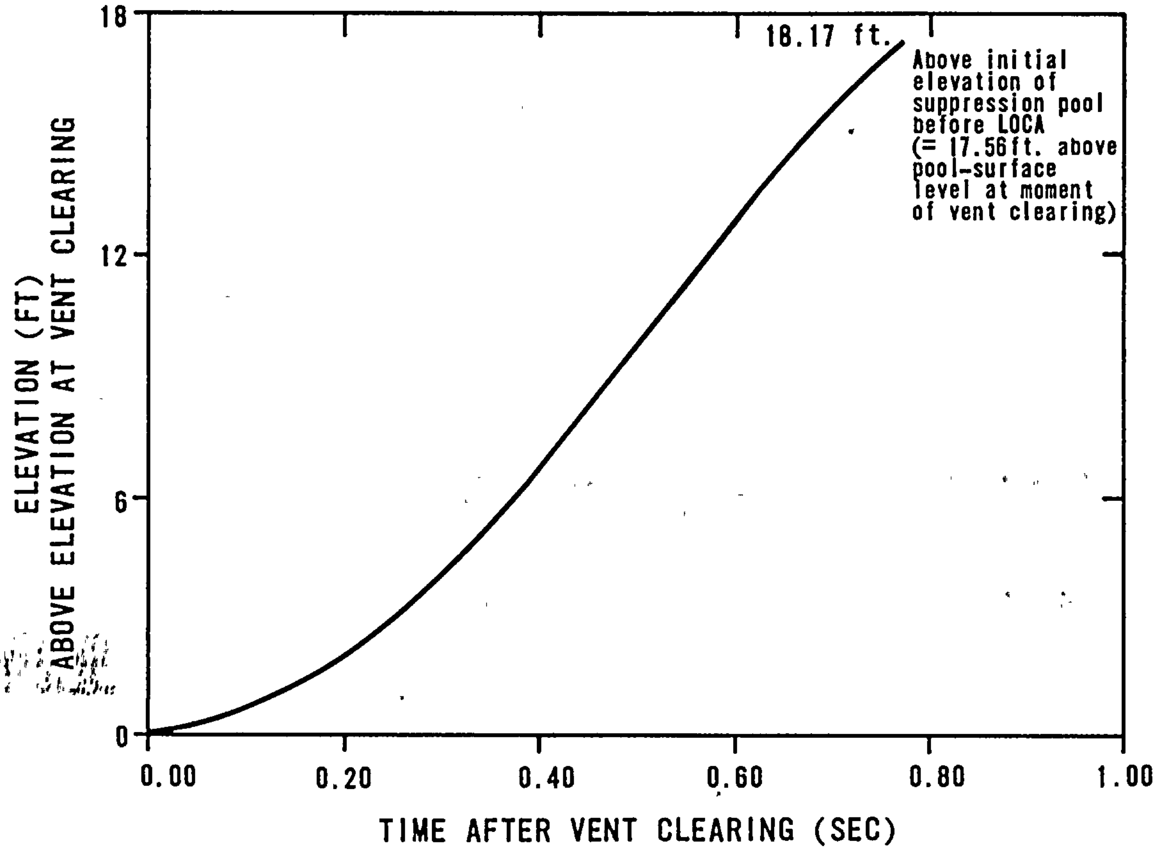

Rev. 2, 5/80

SUSQUEHANNA STEAM ELECTRIC STATION
UNITS 1 AND 2
DESIGN ASSESSMENT REPORT

SSES SHORT TERM SUPPRESSION POOL SURFACE HEIGHT

FIGURE 4-38

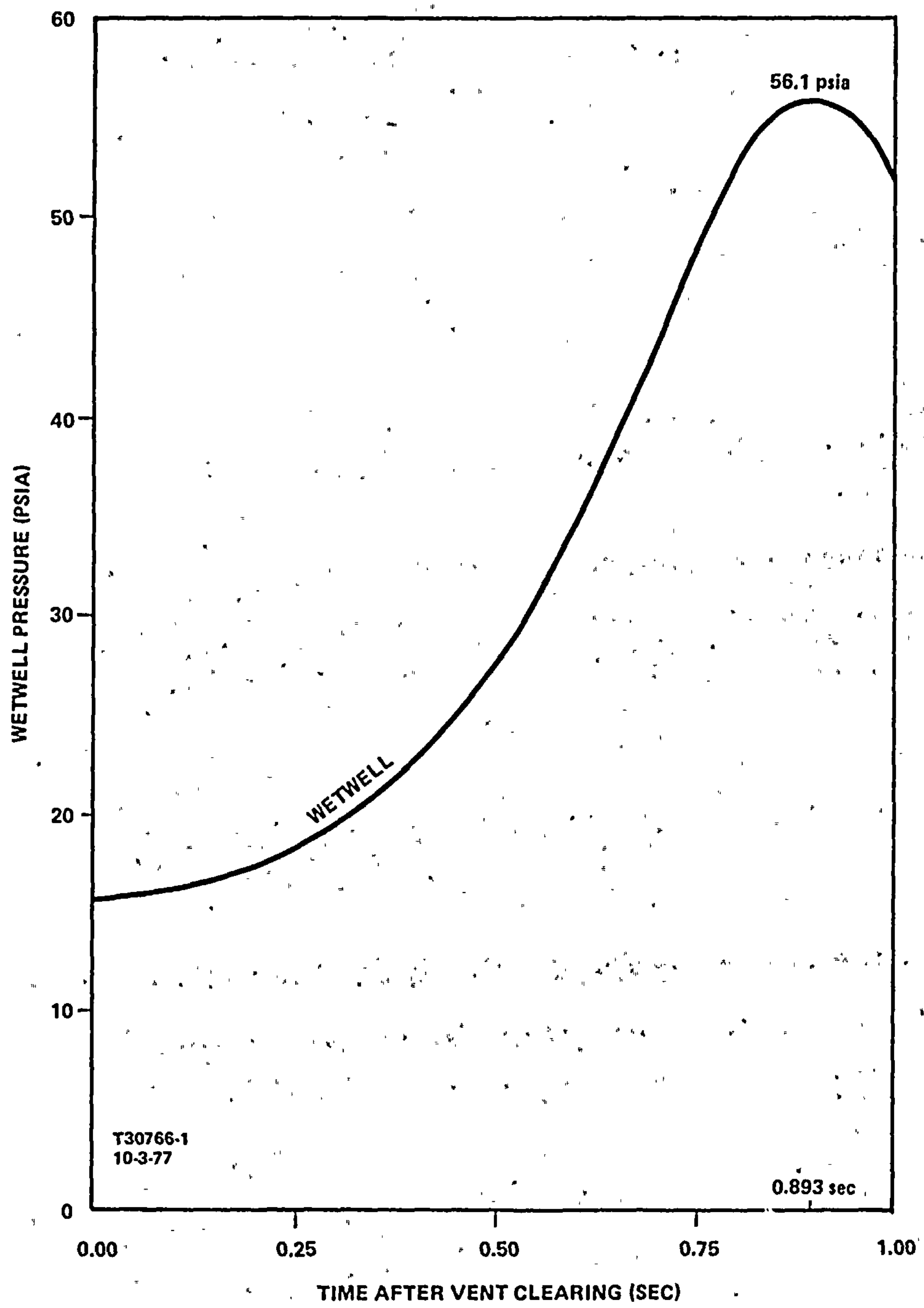

Rev. 2, 5/80

SUSQUEHANNA STEAM ELECTRIC STATION
UNITS 1 AND 2
DESIGN ASSESSMENT REPORT

SSES SHORT TERM
WETWELL PRESSURE

FIGURE 4-39

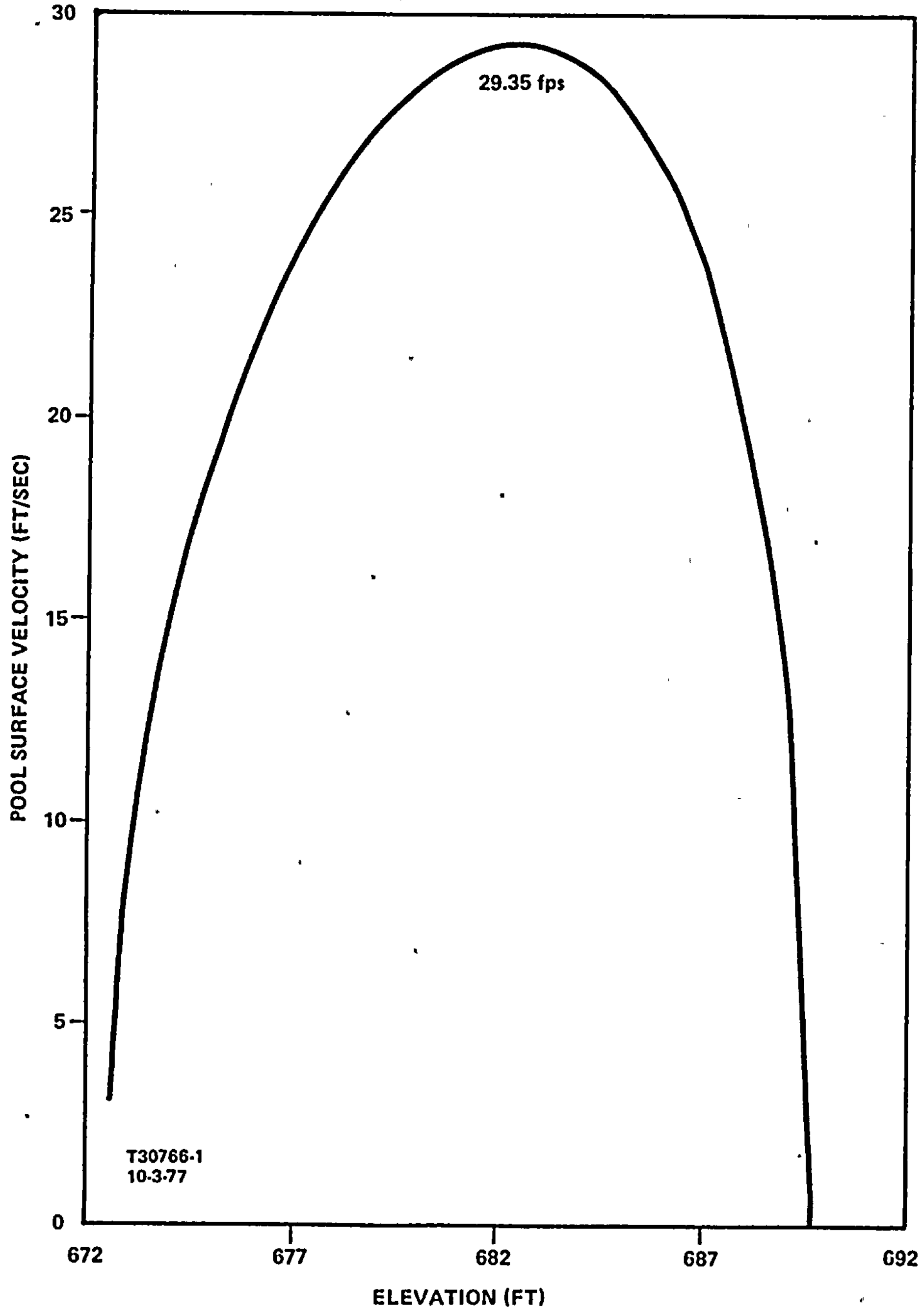

SUSQUEHANNA STEAM ELECTRIC STATION
UNITS 1 AND 2
DESIGN ASSESSMENT REPORT

SSES POOL SURFACE VELOCITY vs ELEVATION

FIGURE 4-40

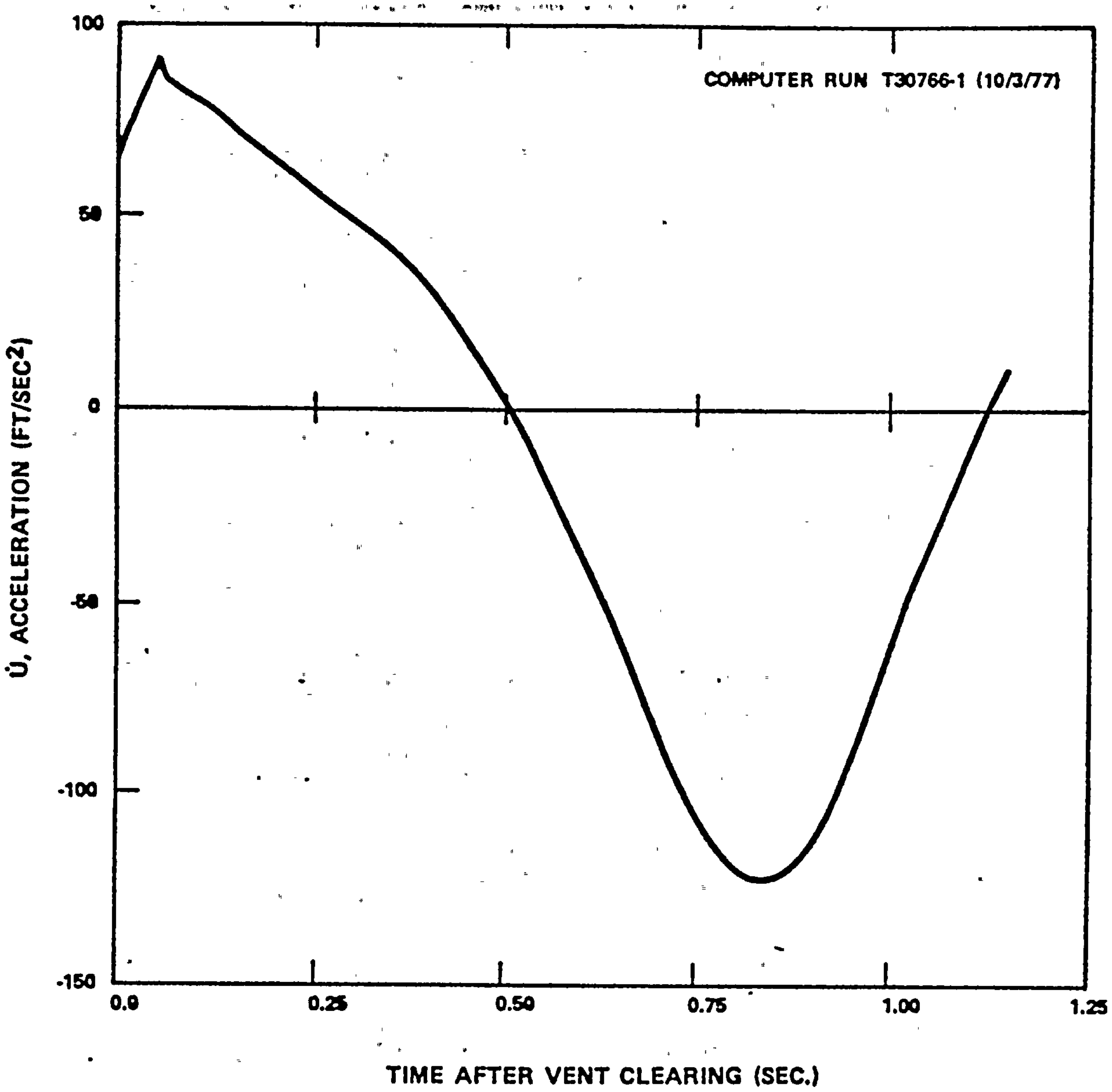

Rev. 2, 5/80

SUSQUEHANNA STEAM ELECTRIC STATION
UNITS 1 AND 2
DESIGN ASSESSMENT REPORT

POOLSWELL ACCELERATION
TIME HISTORY

FIGURE 4-40a

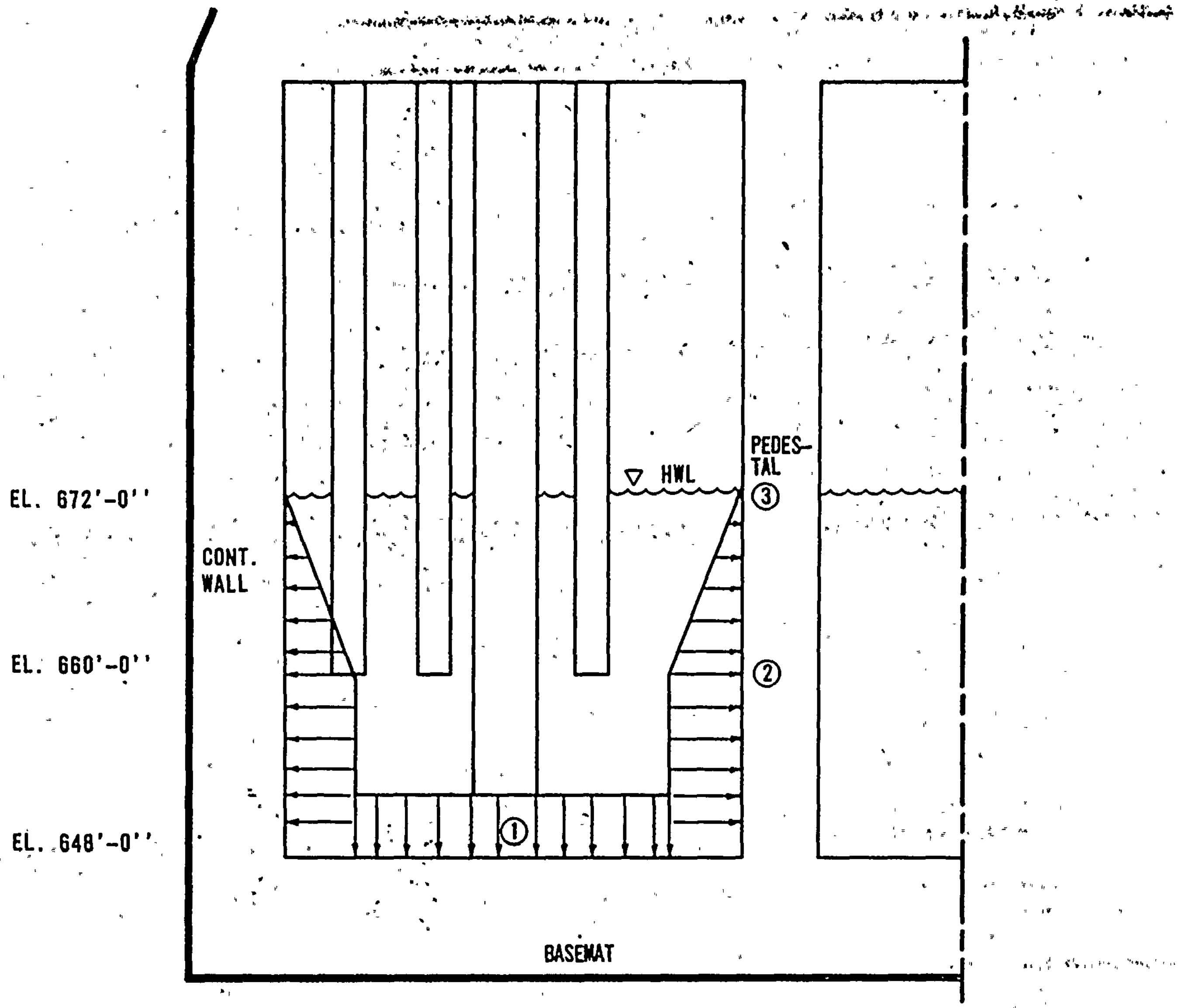

① 24 + 14.7 + 10.4 = 49.1 psia

② 24 + 14.7 + 5.2 = 43.9 psia

③ 0 + 14.7 + 0 = 14.7 psia

Rev. 2, 5/80

SUSQUEHANNA STEAM ELECTRIC STATION
UNITS 1 AND 2
DESIGN ASSESSMENT REPORT

SSES VENT CLEARING

PRESSURE DISTRIBUTION

FIGURE 4-41

THIS FIGURE HAS BEEN DELETED

Rev. 2, 5/80

SUSQUEHANNA STEAM ELECTRIC STATION
UNITS 1 AND 2
DESIGN ASSESSMENT REPORT

SSES JET IMPINGEMENT AREA
(WATER CLEARING)

FIGURE 4-42

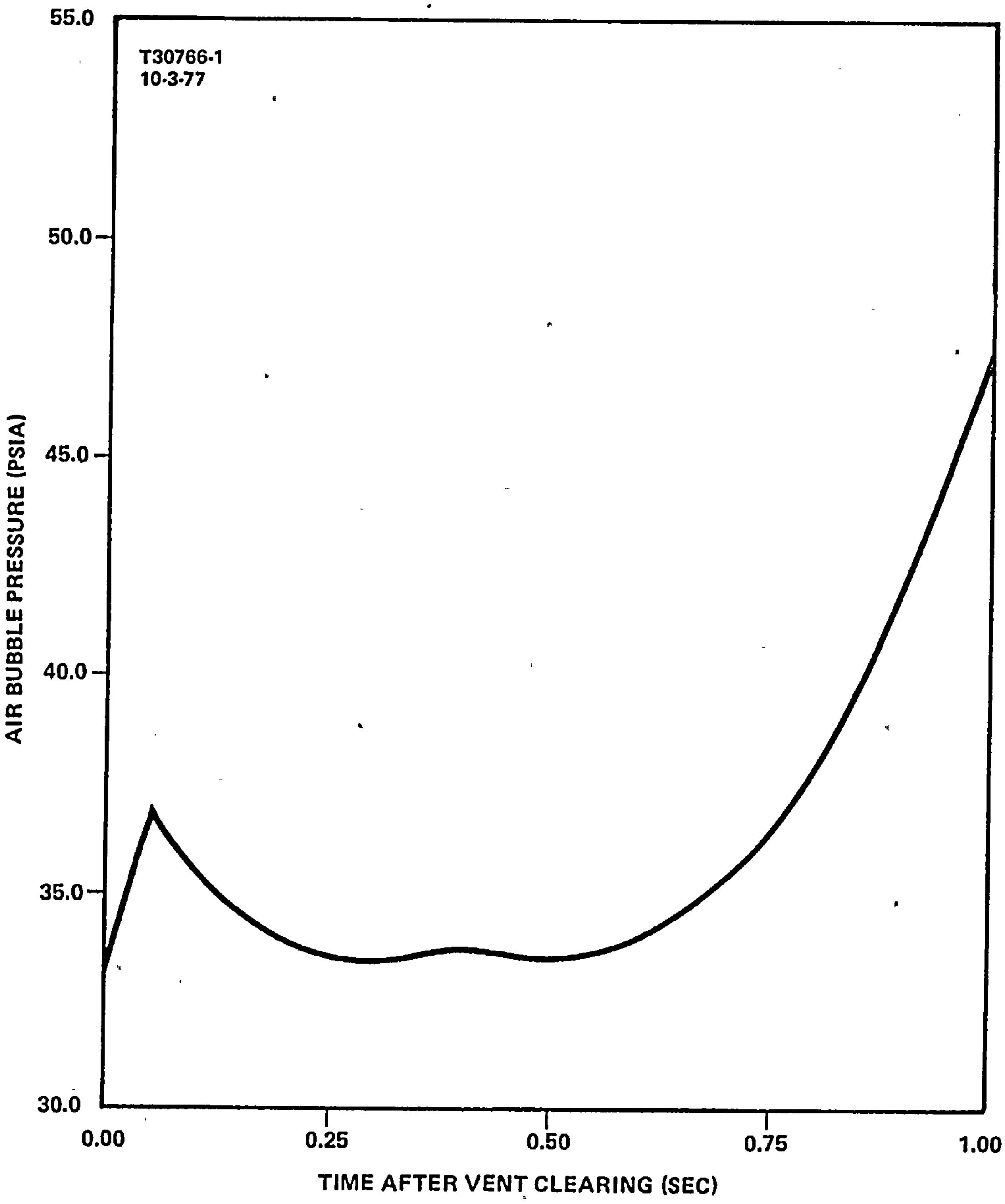

SUSQUEHANNA STEAM ELECTRIC STATION
UNITS 1 AND 2
DESIGN ASSESSMENT REPORT

SSES POOLSWELL
AIR BUBBLE PRESSURE

FIGURE 4-43

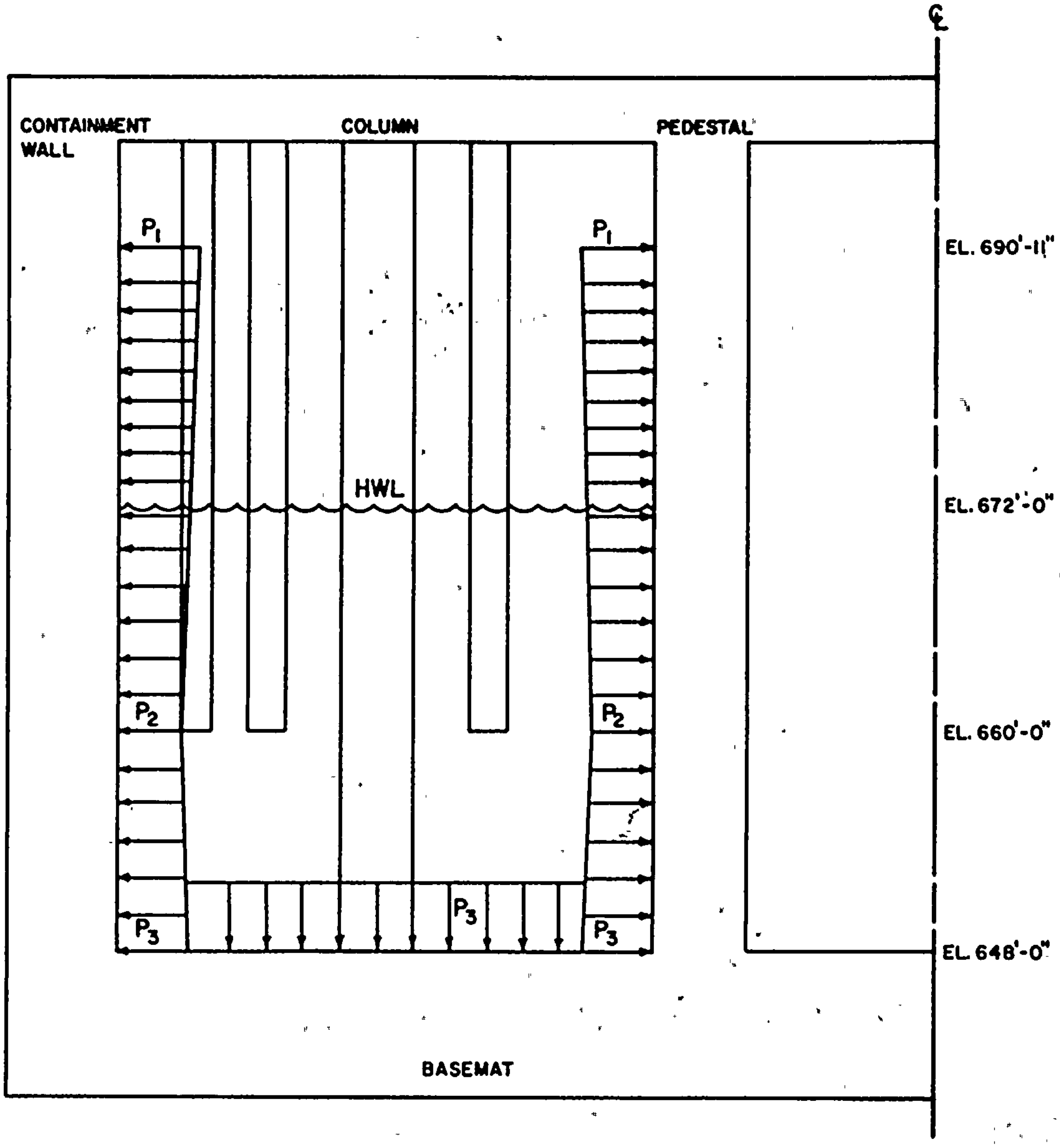

P_1 = 56.67 PSIA

P_2 = 41.96 PSIA

P_3 = 52.36 PSIA

Rev. 2, 5/80

SUSQUEHANNA STEAM ELECTRIC STATION
UNITS 1 AND 2
DESIGN ASSESSMENT REPORT

AIR BUBBLE PRESSURE ON SUPPRESSION POOL WALLS

FIGURE 4-44

This figure has been deleted

REV. 6, 4/82

SUSQUEHANNA STEAM ELECTRIC STATION
UNITS 1 AND 2
DESIGN ASSESSMENT REPORT

CONDENSATION PRESSURE FORCING FUNCTIONS

FIGURE 4-44 A

This figure has been deleted

REV. 6, 4/82

SUSQUEHANNA STEAM ELECTRIC STATION
UNITS 1 AND 2
DESIGN ASSESSMENT REPORT

SYMMETRIC AND ASSYMMETRIC
SPATIAL LOADING SPECIFICATION

FIGURE 4-45

SUSQUEHANNA STEAM ELECTRIC STATION
UNITS 1 AND 2
DESIGN ASSESSMENT REPORT

SSES DRYWELL PRESSURE
RESPONSE TO DBA LOCA

FIGURE 4-46

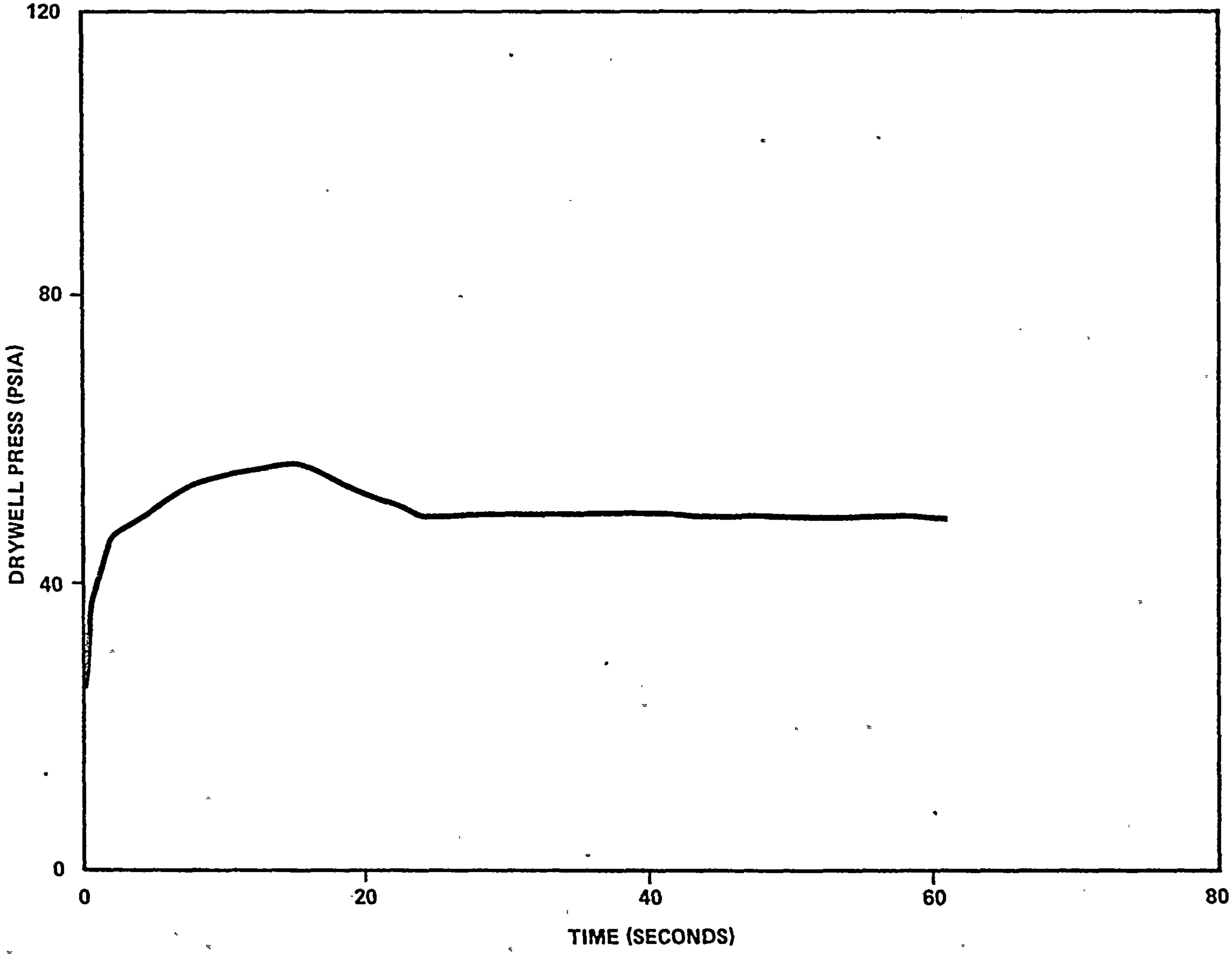

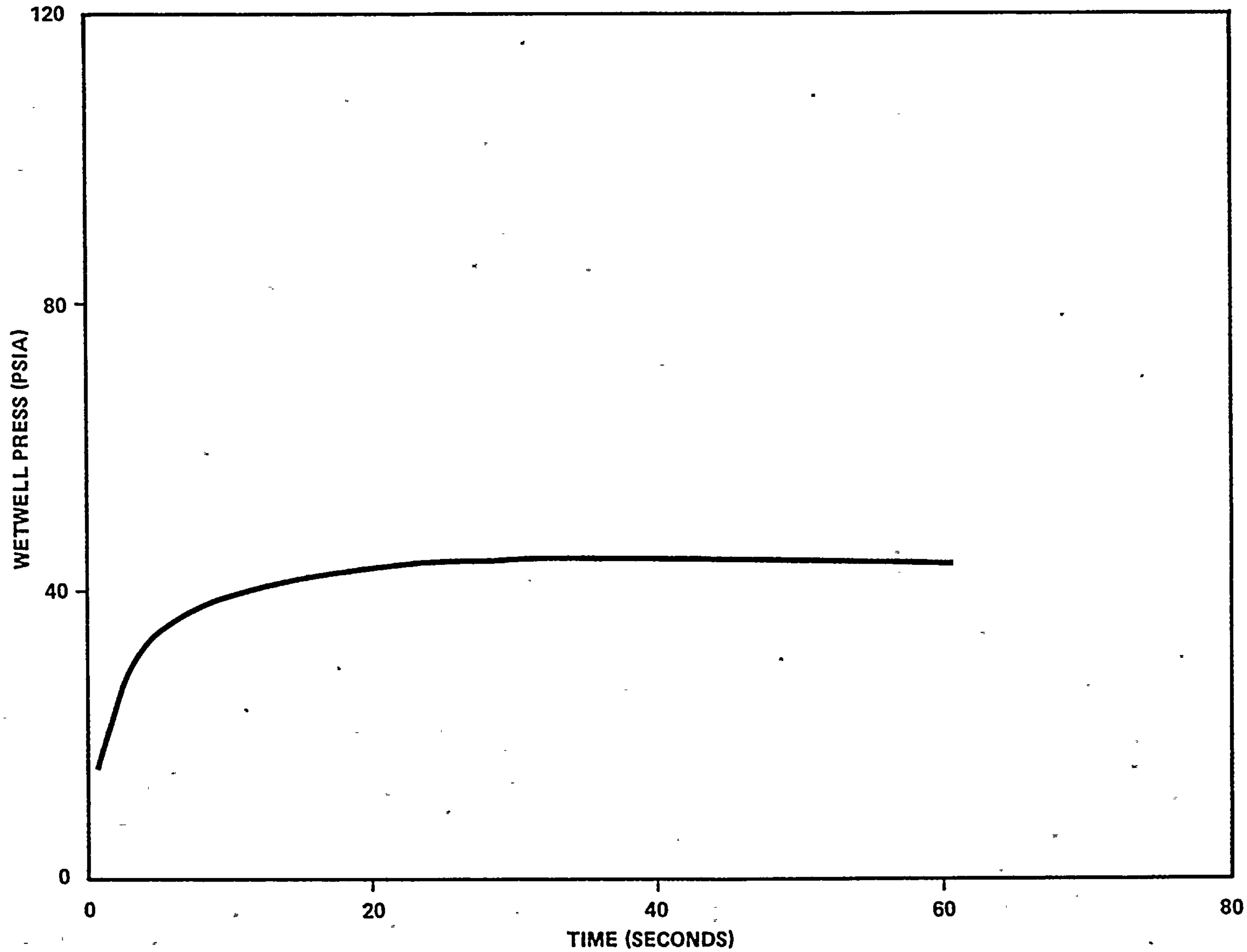

SUSQUEHANNA STEAM ELECTRIC STATION
UNITS 1 AND 2
DESIGN ASSESSMENT REPORT

SSES WETWELL PRESSURE
RESPONSE TO DBA LOCA

FIGURE 4-47

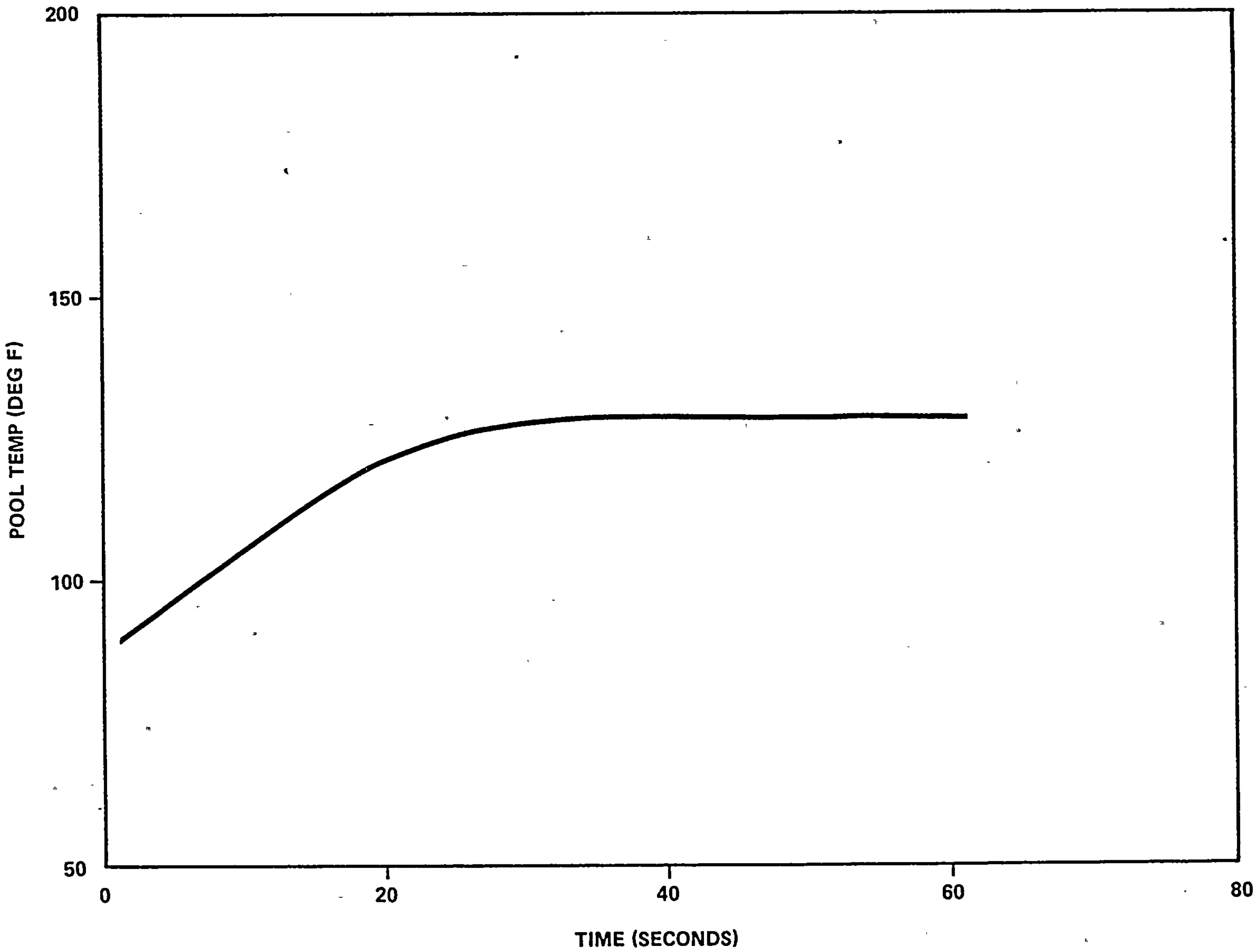

SUSQUEHANNA STEAM ELECTRIC STATION
UNITS 1 AND 2
DESIGN ASSESSMENT REPORT

SSES SUPPRESSION POOL TEMPERATURE RESPONSE TO DBA LOCA

FIGURE 4-48

REFER TO FIGURE 6.2-3 OF THE FSAR (DRYWELL CURVE)

SUSQUEHANNA STEAM ELECTRIC STATION
UNITS 1 AND 2
DESIGN ASSESSMENT REPORT

DRYWELL TEMPERATURE RESPONSE FOR DBA LOCA

FIGURE 4-49

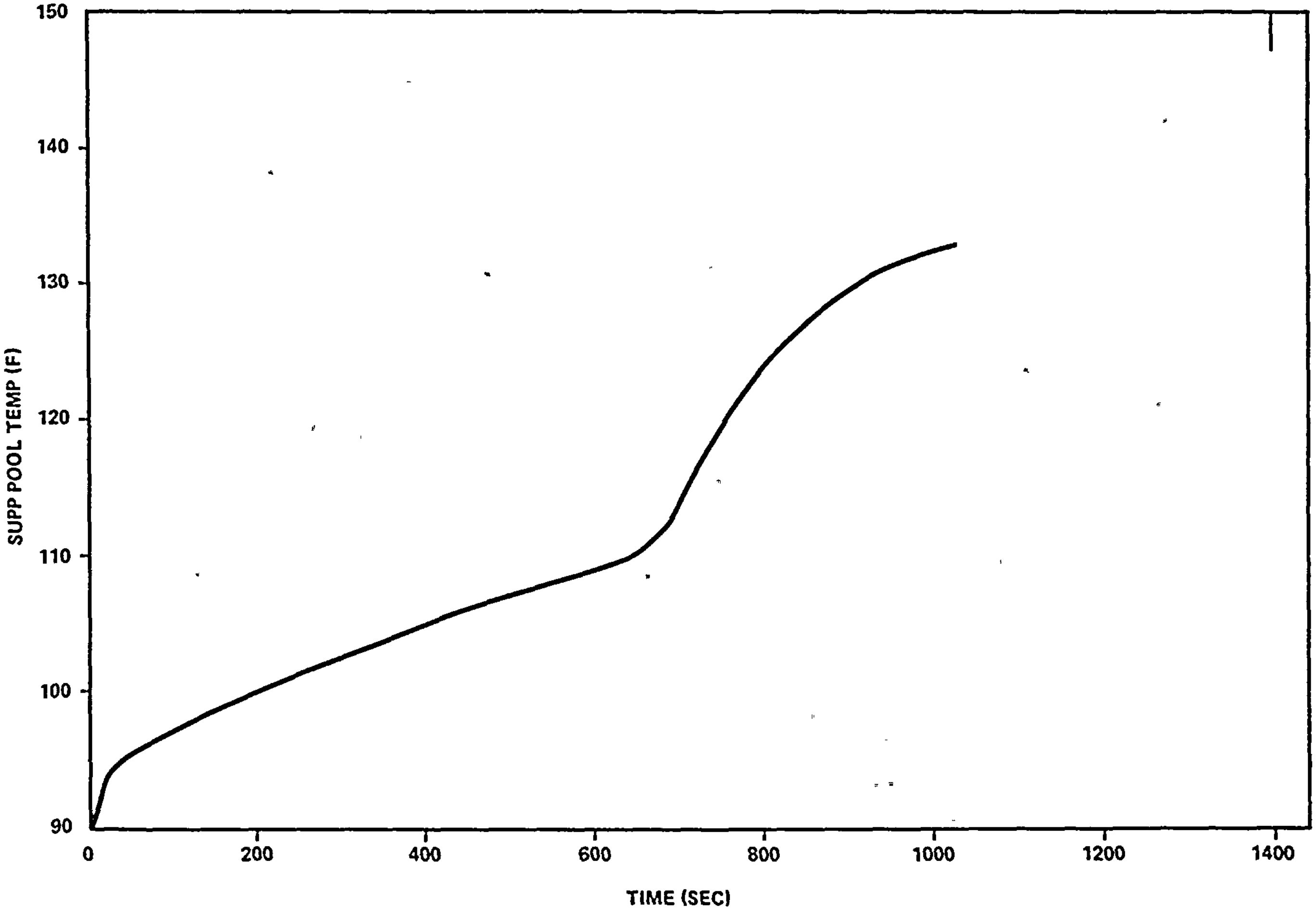

SUSQUEHANNA STEAM ELECTRIC STATION
UNITS 1 AND 2
DESIGN ASSESSMENT REPORT

SSES SUPPRESSION POOL
TEMPERATURE RESPONSE TO IBA

FIGURE 4-50

SEE FSAR FIGURE 6.2-14

(a) CONTAINMENT PRESSURE RESPONSE FOR INTERMEDIATE BREAK AREA

SEE FSAR FIGURE 6.2-15

(b) DRYWELL TEMPERATURE RESPONSE FOR INTERMEDIATE BREAK AREA

Rev. 2, 5/80

SUSQUEHANNA STEAM ELECTRIC STATION
UNITS 1 AND 2
DESIGN ASSESSMENT REPORT

SSES PLANT UNIQUE CONTAINMENT RESPONSE TO THE IBA

FIGURE 4-51

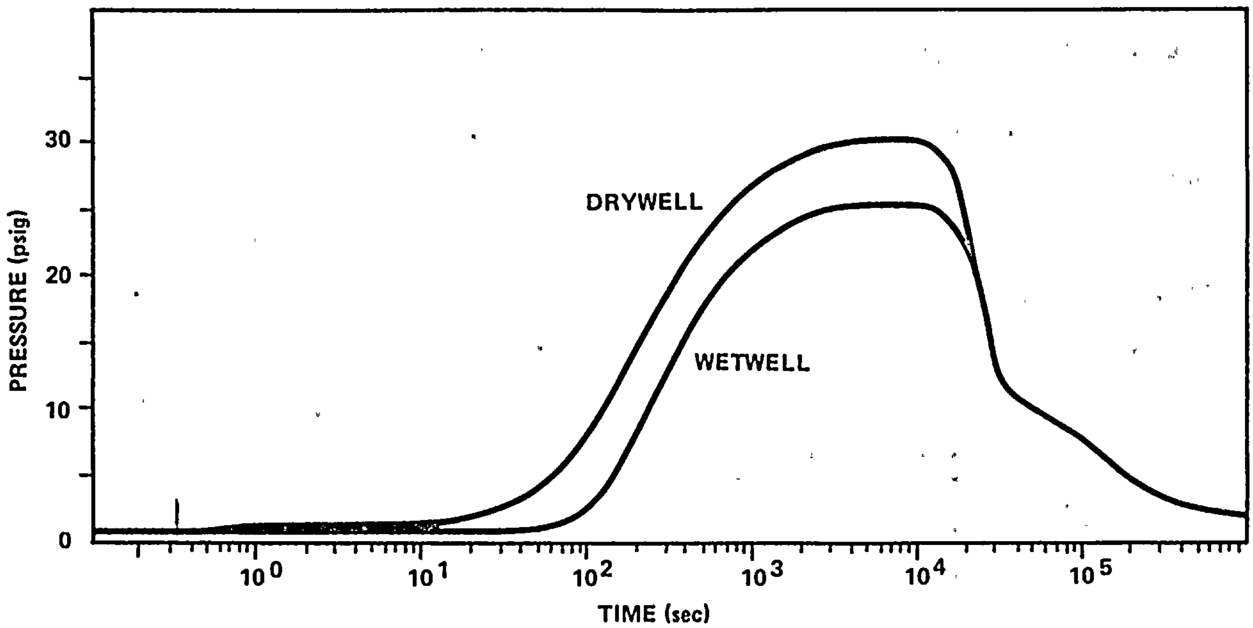

(a) CONTAINMENT PRESSURE RESPONSE FOLLOWING SMALL BREAK

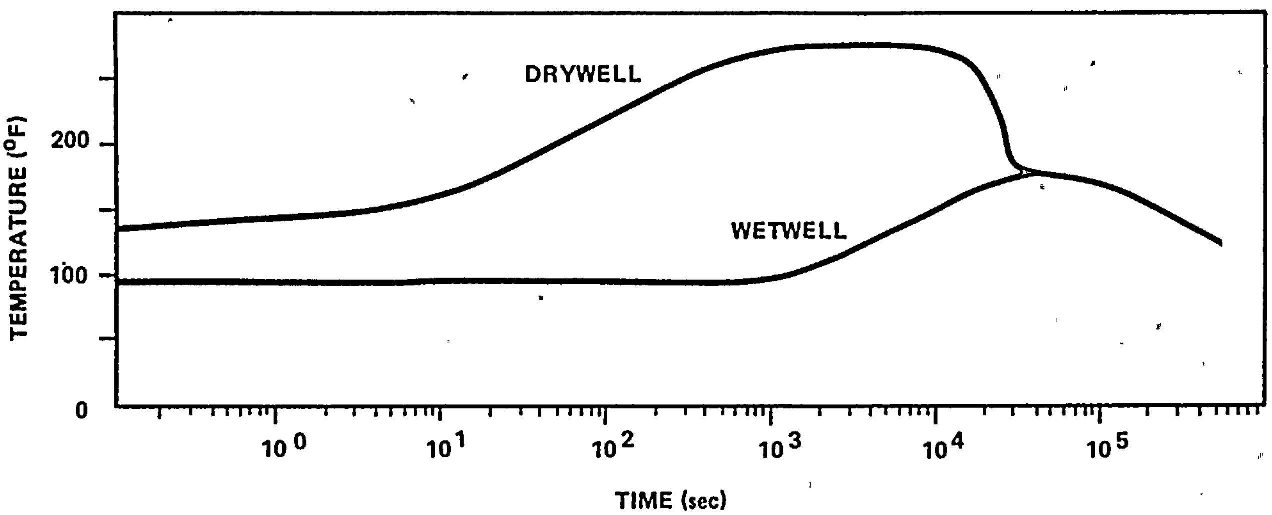

(b) CONTAINMENT TEMPERATURE RESPONSE FOLLOWING SMALL BREAK (LIQUID BREAK)

SUSQUEHANNA STEAM ELECTRIC STATION
UNITS 1 AND 2
DESIGN ASSESSMENT REPORT

TYPICAL MARK II CONTAINMENT RESPONSE TO THE SBA

FIGURE 4-52

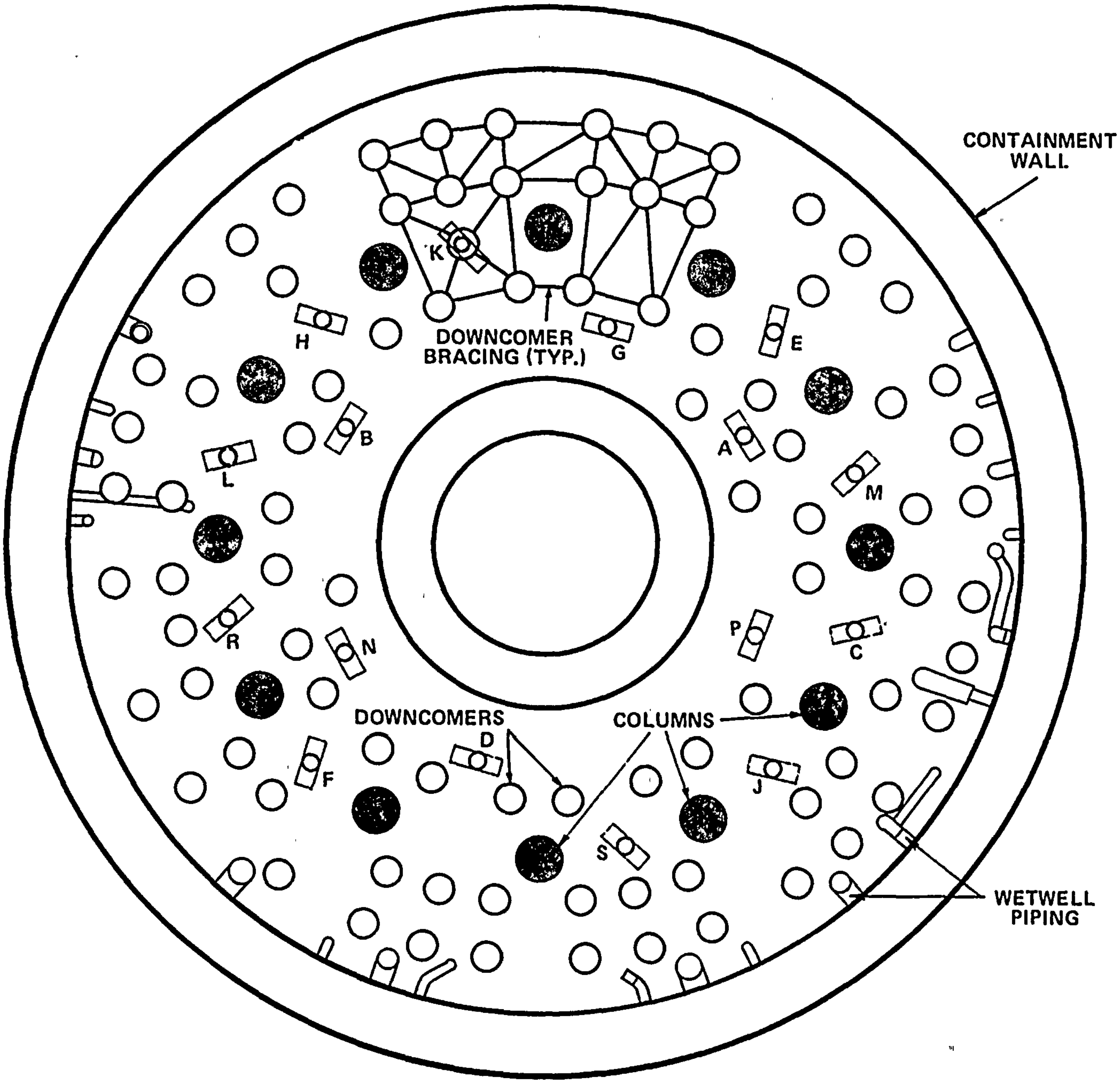

NOTE:
DOWNCOMER BRACING IS ONLY PARTIALLY SHOWN IN THE INTEREST OF CLARITY.
LETTERS INDICATE SRV QUENCHERS

REV. 6, 4/82

SUSQUEHANNA STEAM ELECTRIC STATION
UNITS 1 AND 2
DESIGN ASSESSMENT REPORT

SSES COMPONENTS AFFECTED BY LOCA LOADS

FIGURE 4-53

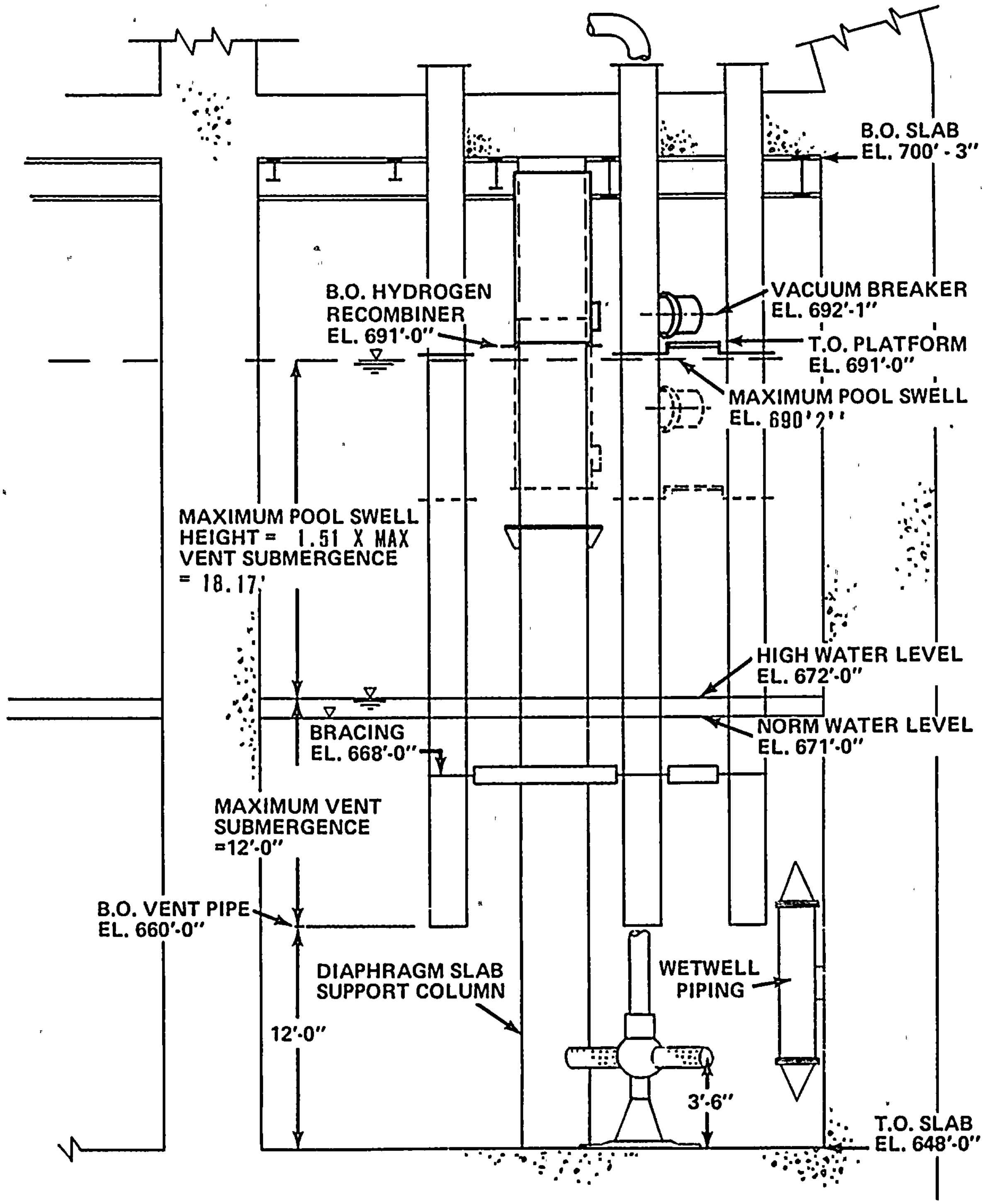

REV. 6, 4/82

SUSQUEHANNA STEAM ELECTRIC STATION
UNITS 1 AND 2
DESIGN ASSESSMENT REPORT

SSES COMPONENTS
AFFECTED BY LOCA LOADS

FIGURE 4-54

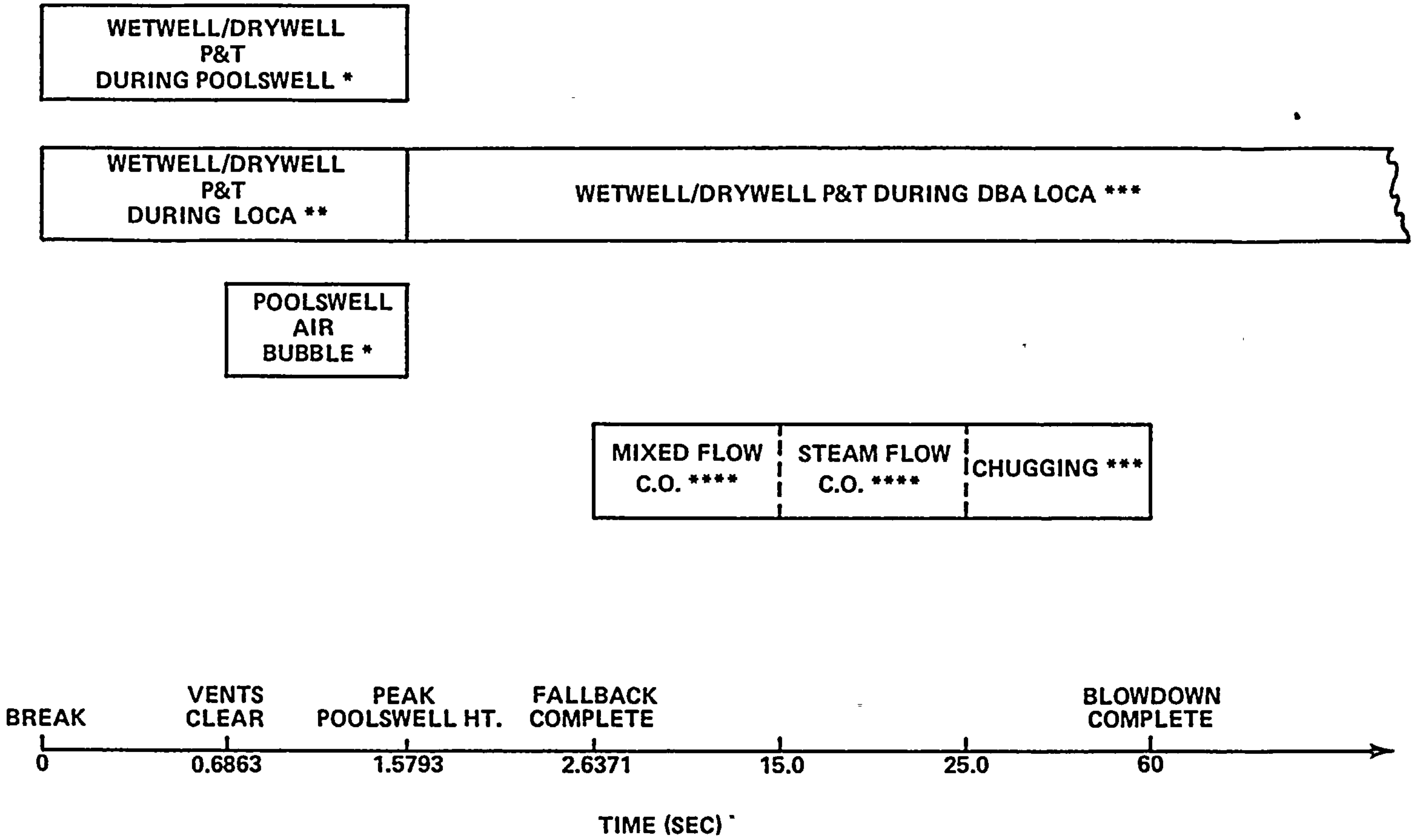

* DBA ONLY
** IBA OR SBA
*** EITHER DBA, IBA OR SBA
**** DBA AND IBA ONLY

SUSQUEHANNA STEAM ELECTRIC STATION
UNITS 1 AND 2
DESIGN ASSESSMENT REPORT

LOCA LOADING HISTORY FOR THE SSES CONTAINMENT WALL AND PEDESTAL

FIGURE 4-55

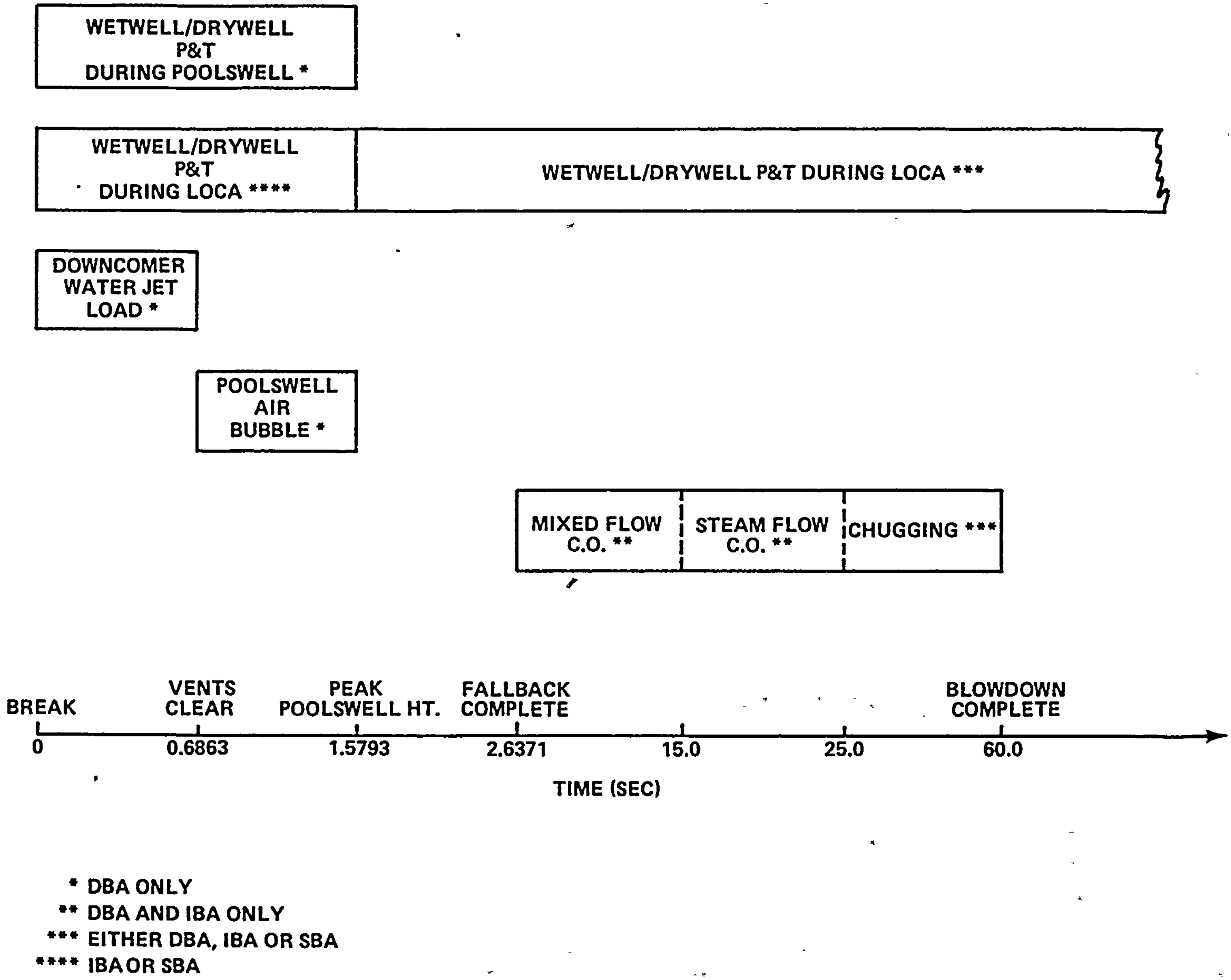

SUSQUEHANNA STEAM ELECTRIC STATION
UNITS 1 AND 2
DESIGN ASSESSMENT REPORT

LOCA LOADING HISTORY FOR THE SSES BASEMAT AND LINER PLATE

FIGURE 4-56

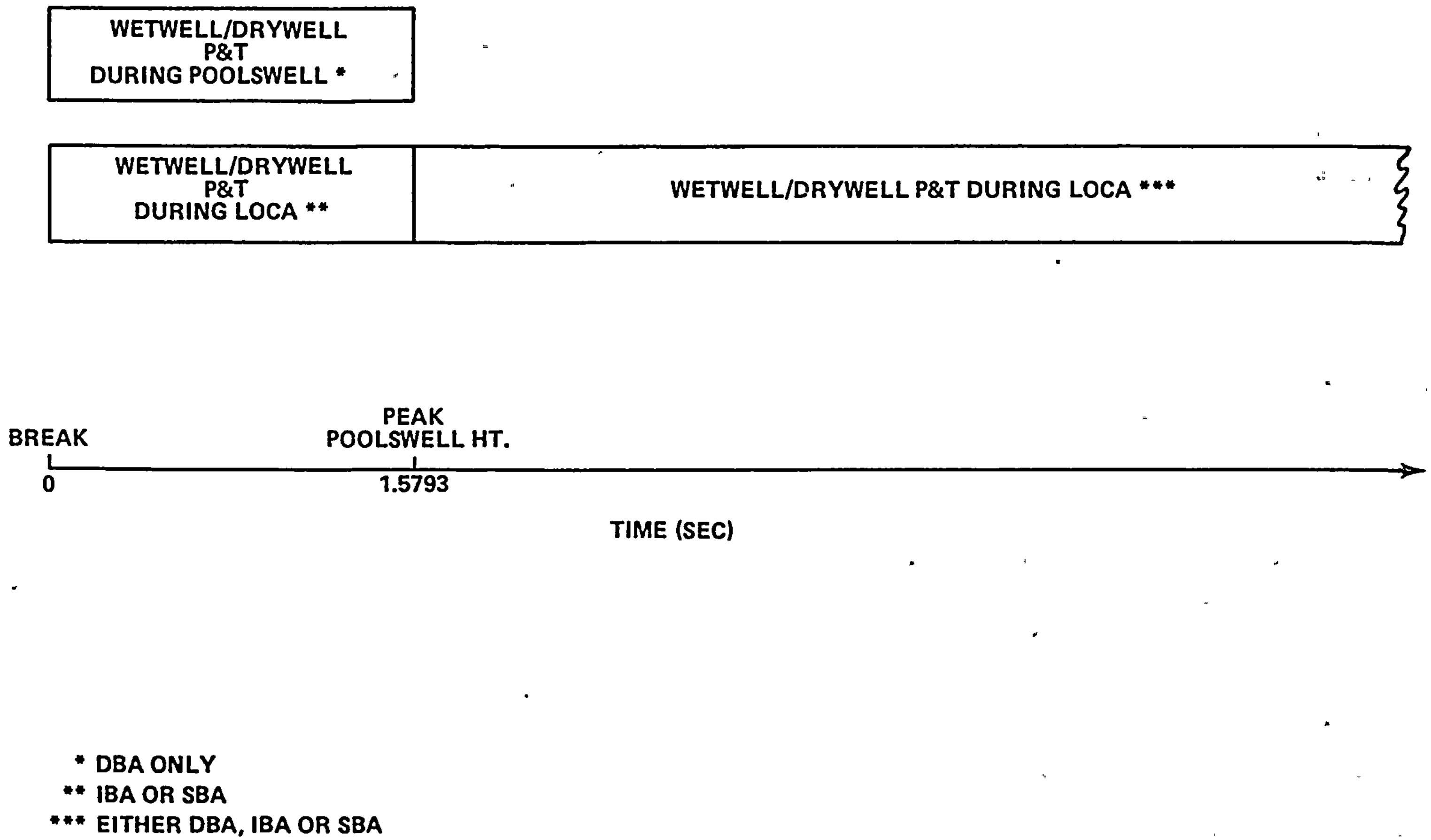

SUSQUEHANNA STEAM ELECTRIC STATION
UNITS 1 AND 2
DESIGN ASSESSMENT REPORT

LOCA LOADING HISTORY
FOR THE SSES DRYWELL
AND DRYWELL FLOOR

FIGURE 4-57

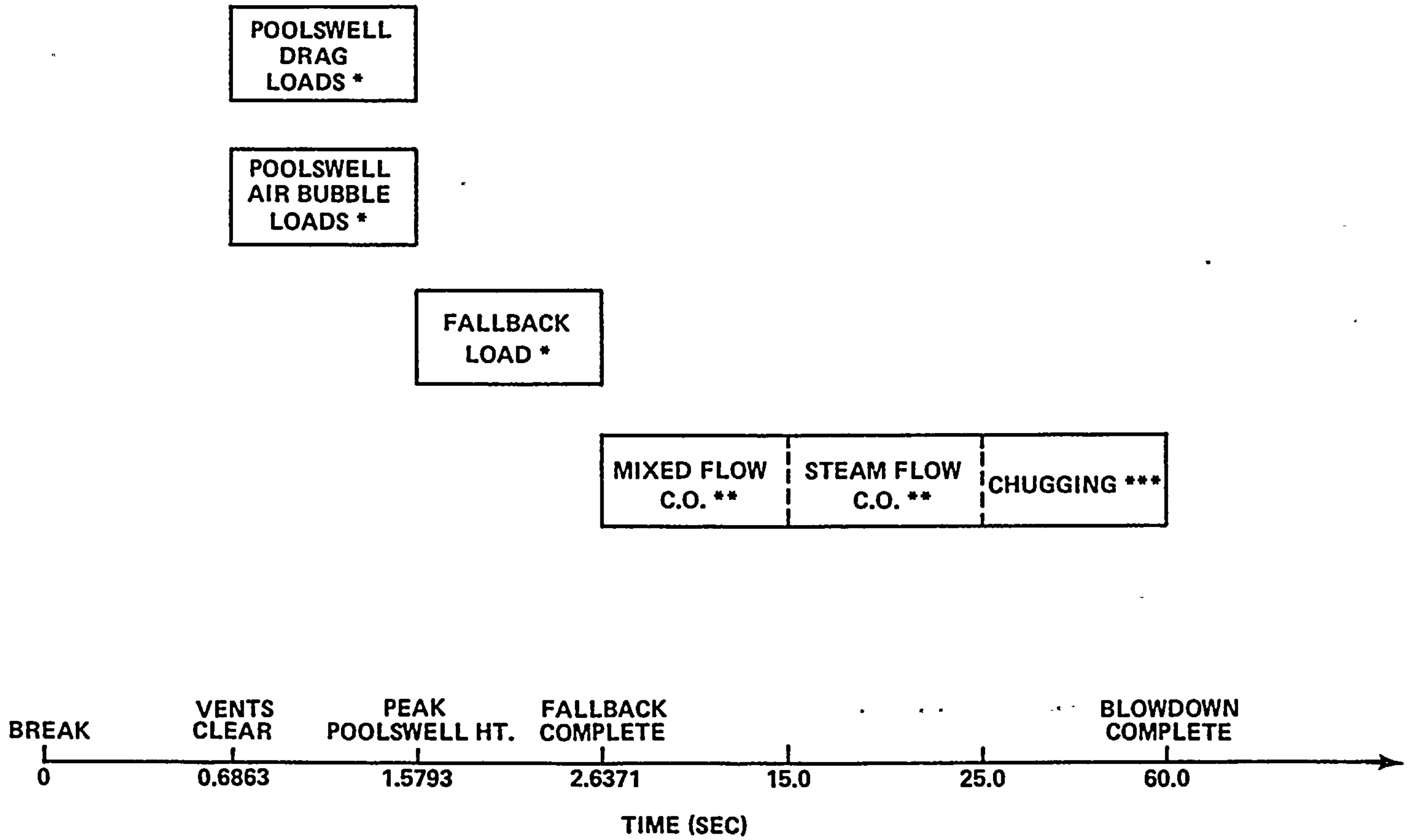

* DBA ONLY
** DBA AND IBA ONLY
*** DBA, IBA AND SBA

SUSQUEHANNA STEAM ELECTRIC STATION
UNITS 1 AND 2
DESIGN ASSESSMENT REPORT

LOCAL LOADING HISTORY FOR THE SSES COLUMNS
LOCA LOADING HISTORY FOR THE SSES COLUMNS

FIGURE 4-58

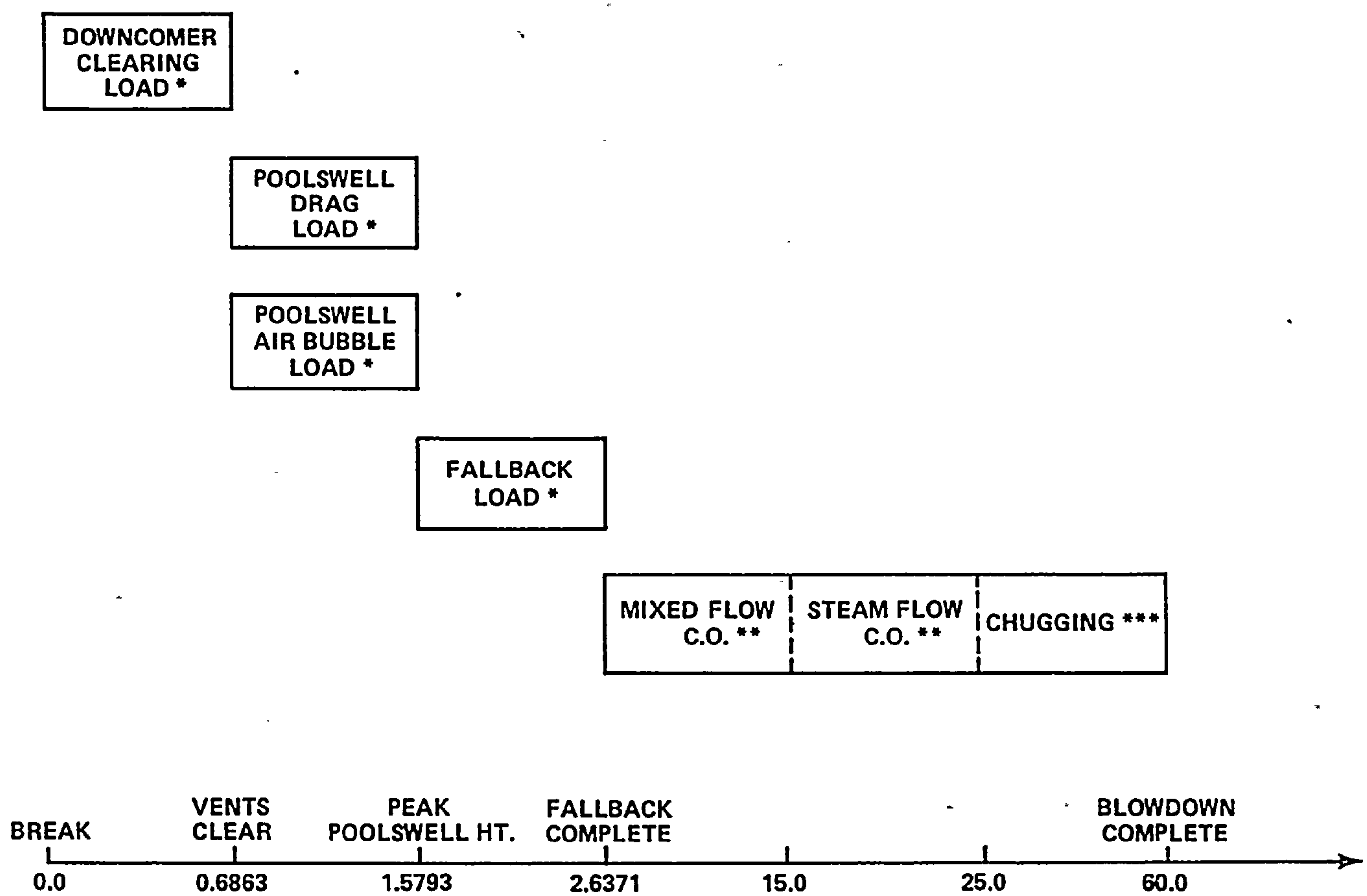

* DBA ONLY
** DBA AND IBA ONLY
*** DBA, IBA AND SBA

SUSQUEHANNA STEAM ELECTRIC STATION
UNITS 1 AND 2
DESIGN ASSESSMENT REPORT

LOCA LOADING HISTORY
FOR THE SSES DOWNCOMERS

FIGURE 4-59

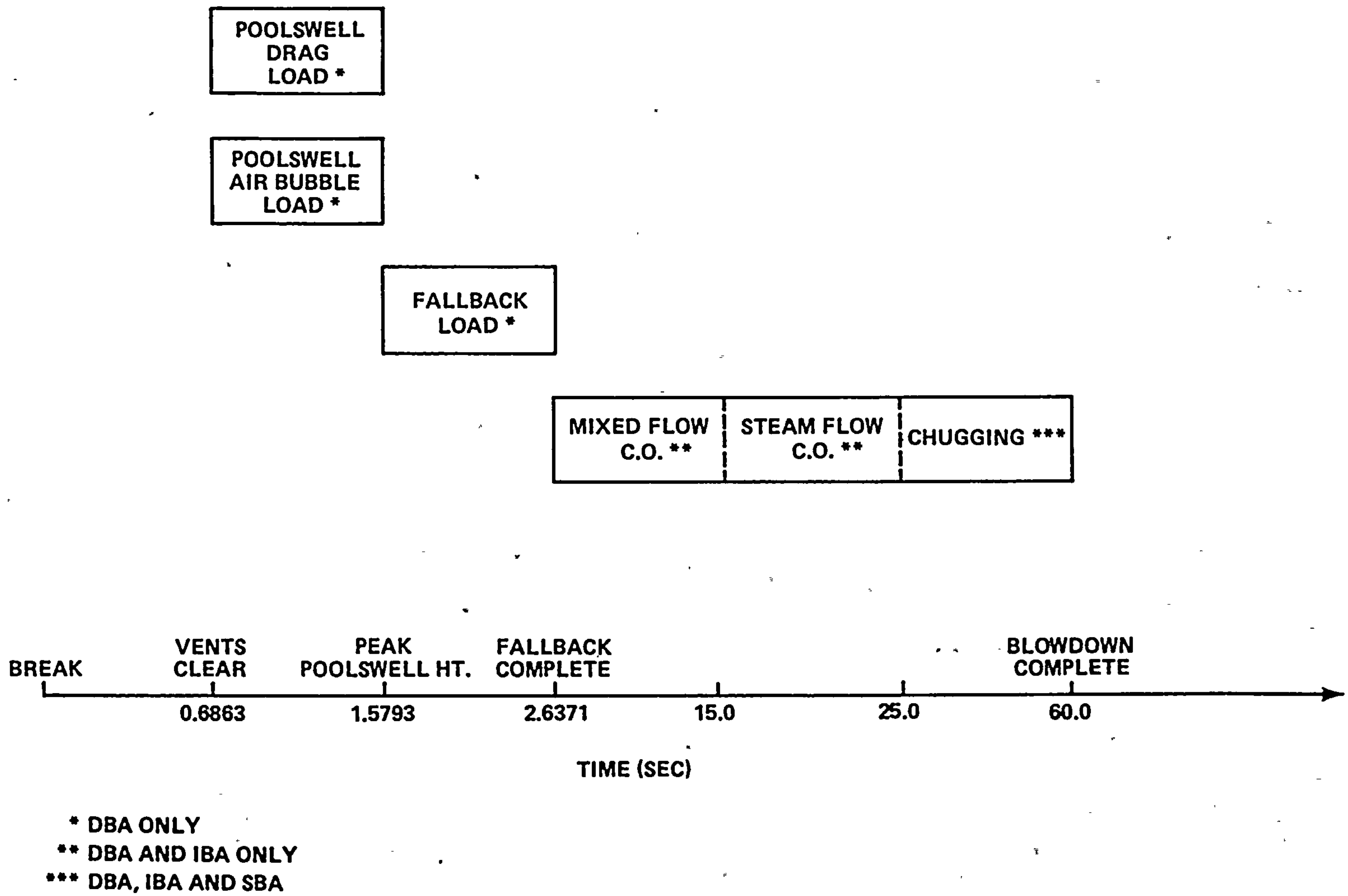

SUSQUEHANNA STEAM ELECTRIC STATION
UNITS 1 AND 2
DESIGN ASSESSMENT REPORT

LOCA LOADING HISTORY
FOR THE SSES DOWNCOMER
BRACING SYSTEM

FIGURE 4-60

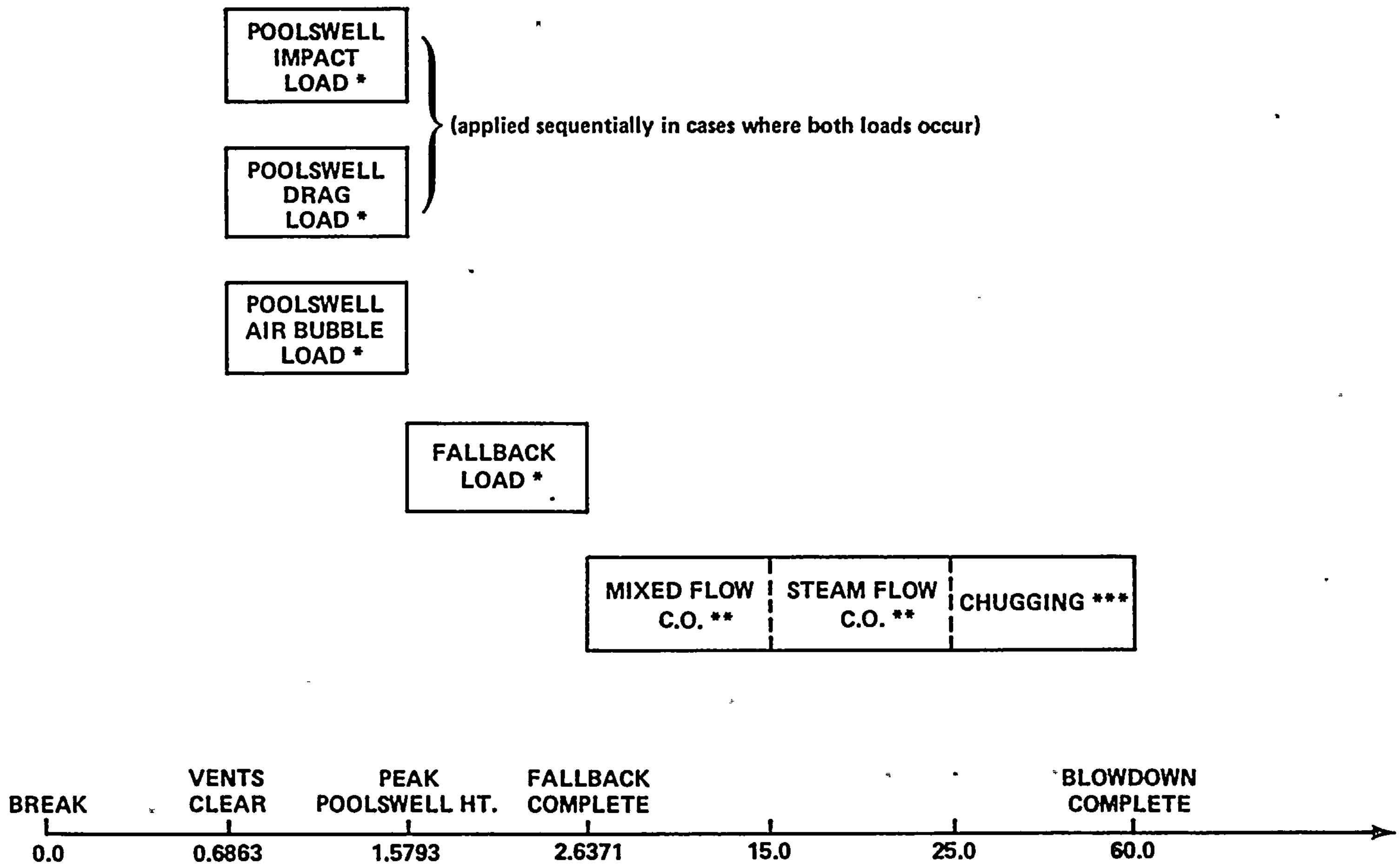

* DBA ONLY
** DBA AND IBA ONLY
*** DBA, IBA AND SBA

SUSQUEHANNA STEAM ELECTRIC STATION
UNITS 1 AND 2
DESIGN ASSESSMENT REPORT

LOCA LOADING HISTORY FOR THE SSES WETWELL PIPING

FIGURE 4-61

This figure has been deleted

REV. 6, 4/82

SUSQUEHANNA STEAM ELECTRIC STATION
UNITS 1 AND 2
DESIGN ASSESSMENT REPORT

CHUGGING POOL BOUNDARY LOADS

FIGURE 4-62 A & B

This figure has been deleted

REV. 6, 4/82

SUSQUEHANNA STEAM ELECTRIC STATION
UNITS 1 AND 2
DESIGN ASSESSMENT REPORT

CHUGGING POOL BOUNDARY LOADS

FIGURE 4-62 C & D

This figure has been deleted

REV. 6, 4/82

SUSQUEHANNA STEAM ELECTRIC STATION
UNITS 1 AND 2
DESIGN ASSESSMENT REPORT

CHUGGING POOL BOUNDARY LOADS

FIGURE 4-62 E & F

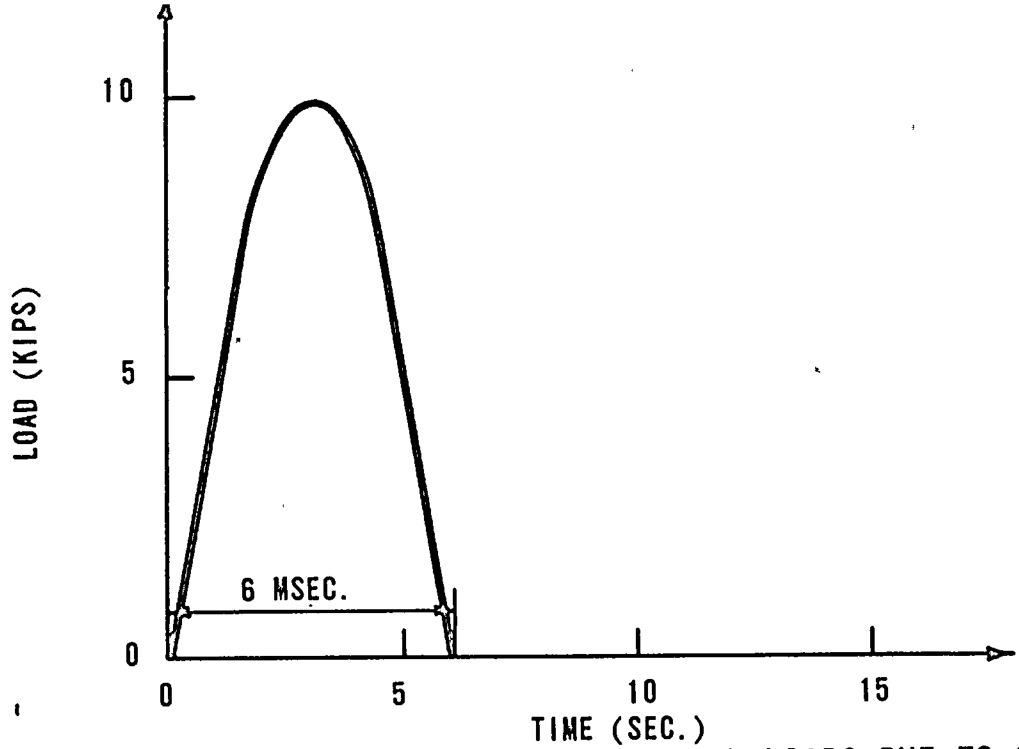

FIGURE 4-62g DYNAMIC DOWNCOMER LATERAL LOADS DUE TO CHUGGING

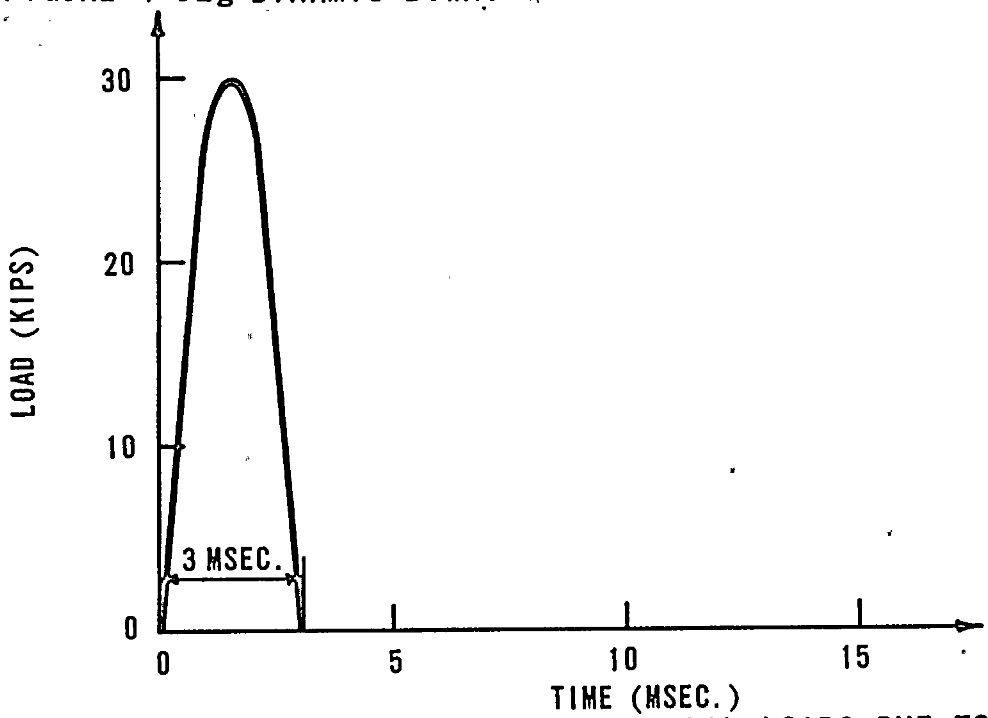

FIGURE 4-62h DYNAMIC DOWNCOMER LATERAL LOADS DUE TO CHUGGING

Rev. 5, 3/81

SUSQUEHANNA STEAM ELECTRIC STATION UNITS 1 AND 2 DESIGN ASSESSMENT REPORT
DYNAMIC DOWNCOMER LATERAL LOAD DUE TO CHUGGING FIGURE 4-62 G & H

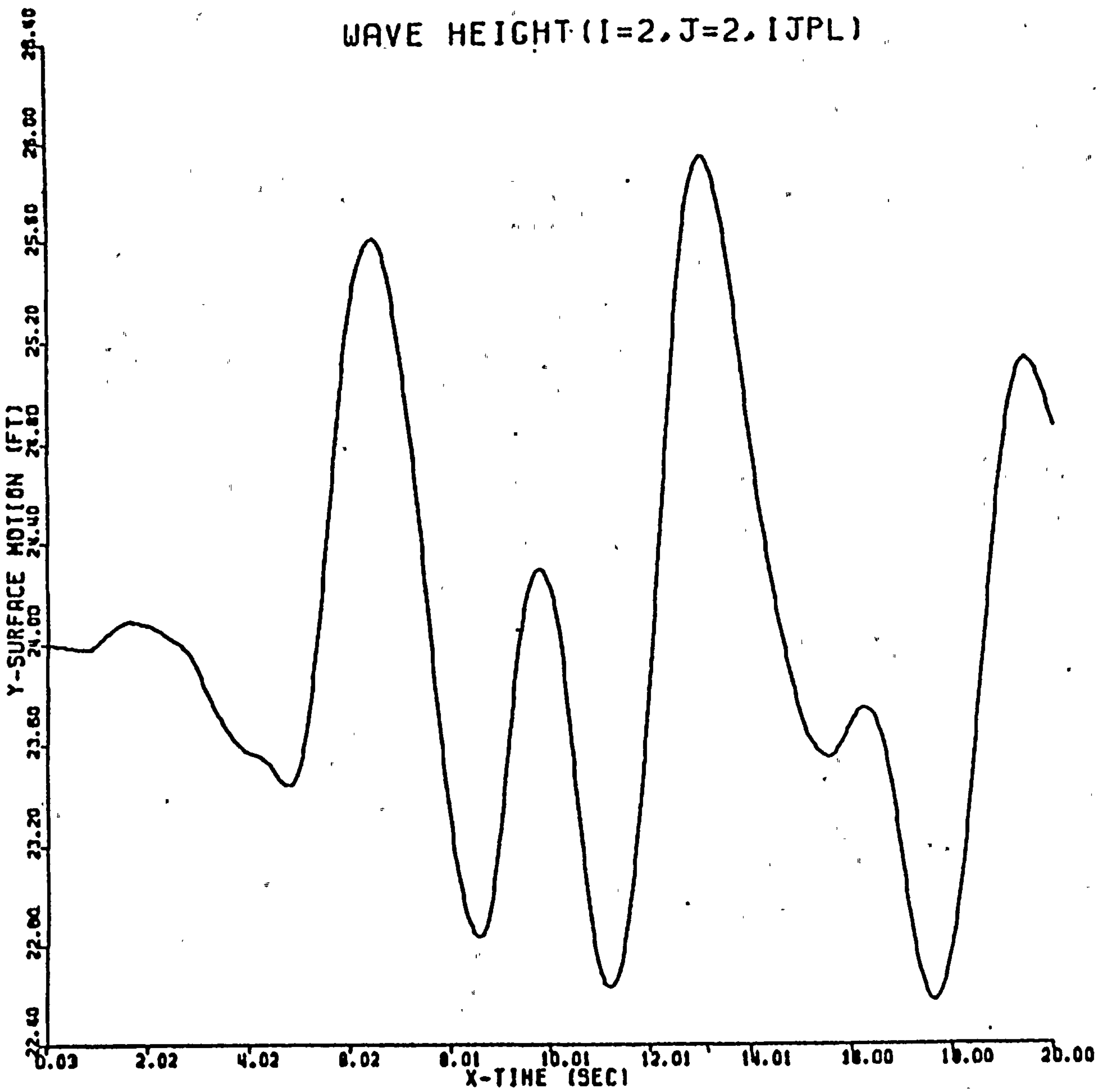

REV. 6, 4/82

SUSQUEHANNA STEAM ELECTRIC STATION
UNITS 1 AND 2
DESIGN ASSESSMENT REPORT

TYPICAL WAVE MOTION DUE TO SEISMIC SLOSH

FIGURE 4-62I

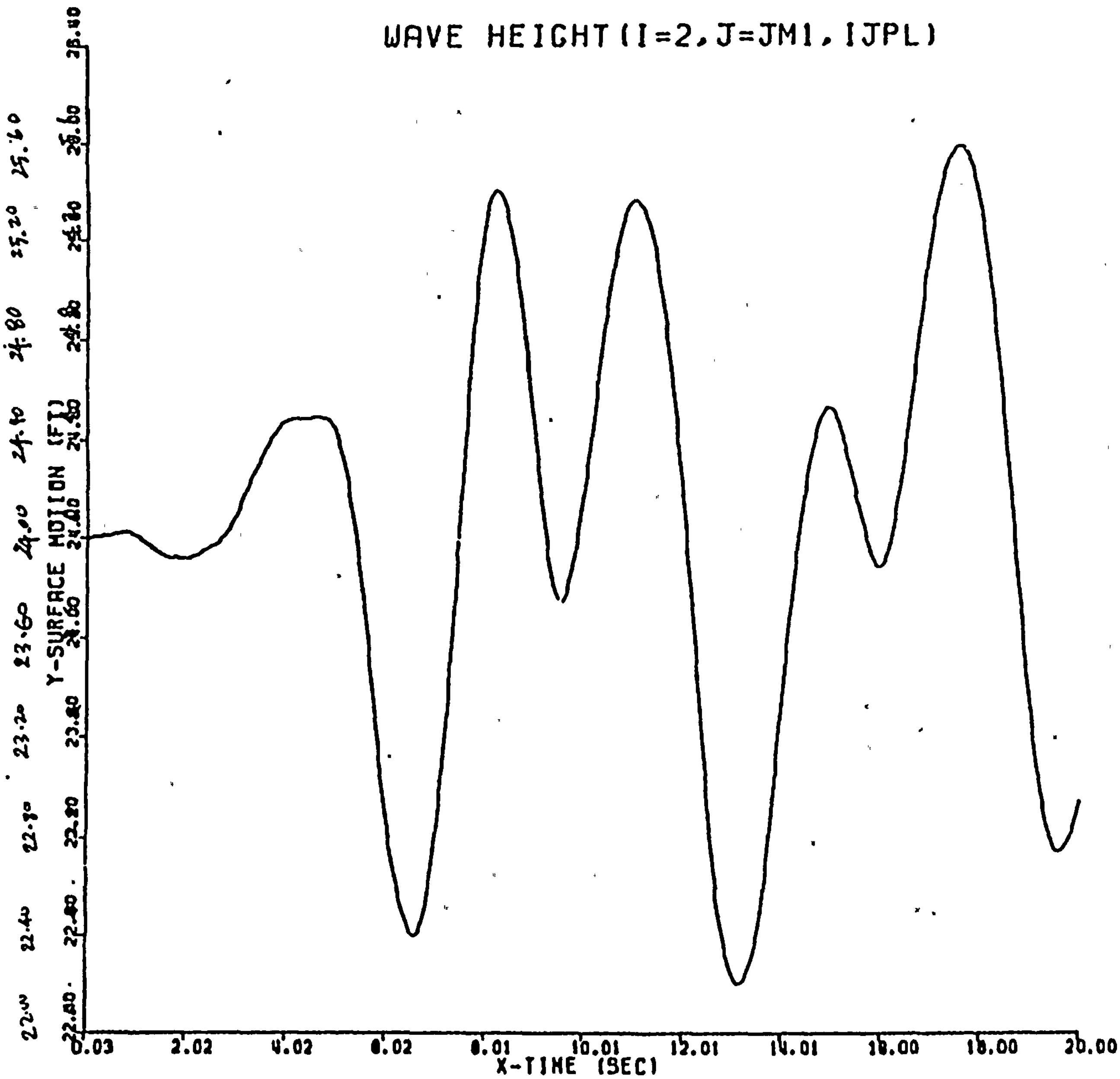

REV. 6, 4/82

SUSQUEHANNA STEAM ELECTRIC STATION
UNITS 1 AND 2
DESIGN ASSESSMENT REPORT

TYPICAL WAVE MOTION
DUE TO SEISMIC SLOSH

FIGURE 4-62J

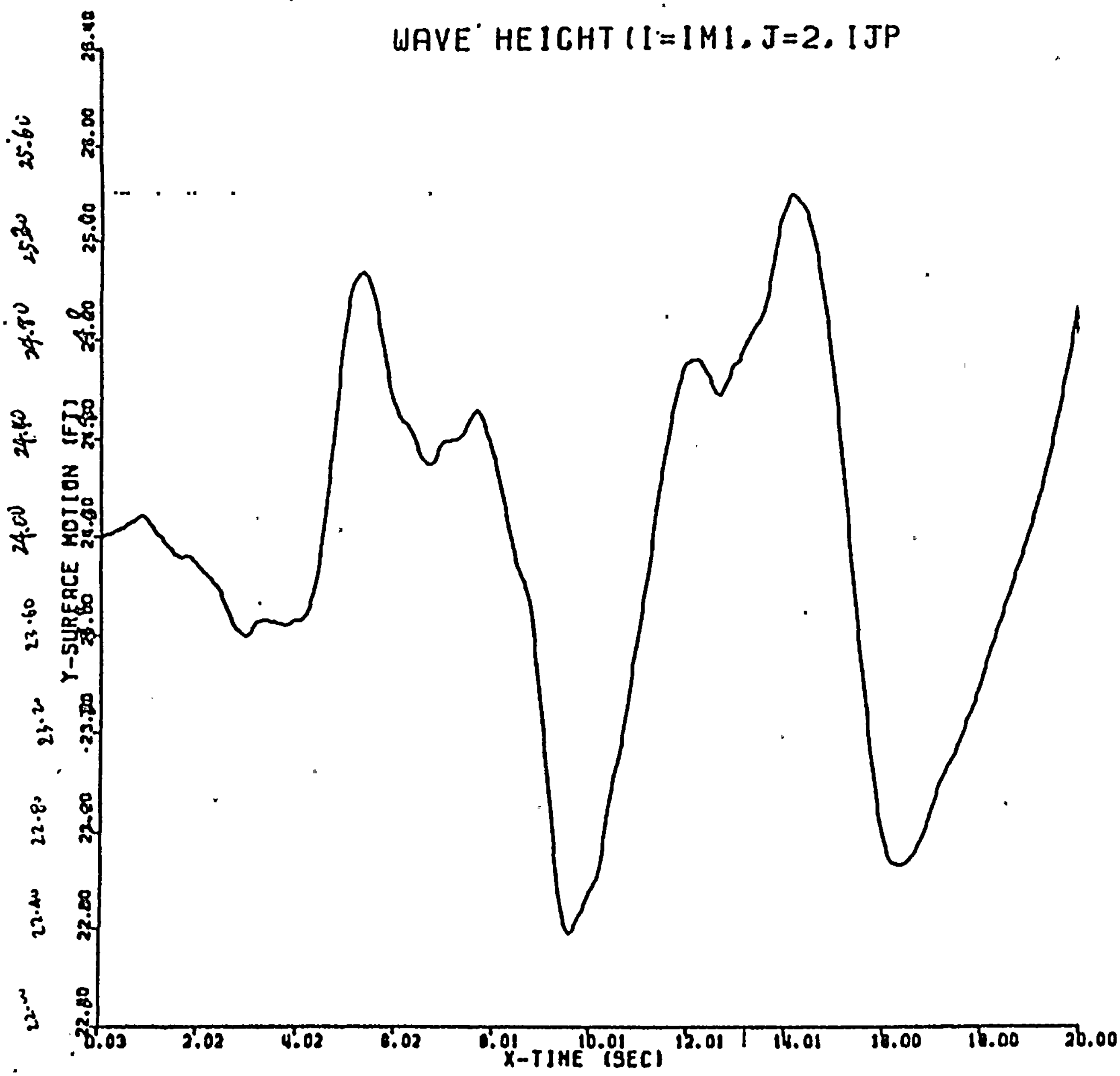

REV. 6, 4/82

SUSQUEHANNA STEAM ELECTRIC STATION
UNITS 1 AND 2
DESIGN ASSESSMENT REPORT

TYICAL WAVE MOTION
DUE TO SEISMIC SLOSH

FIGURE 4-62K

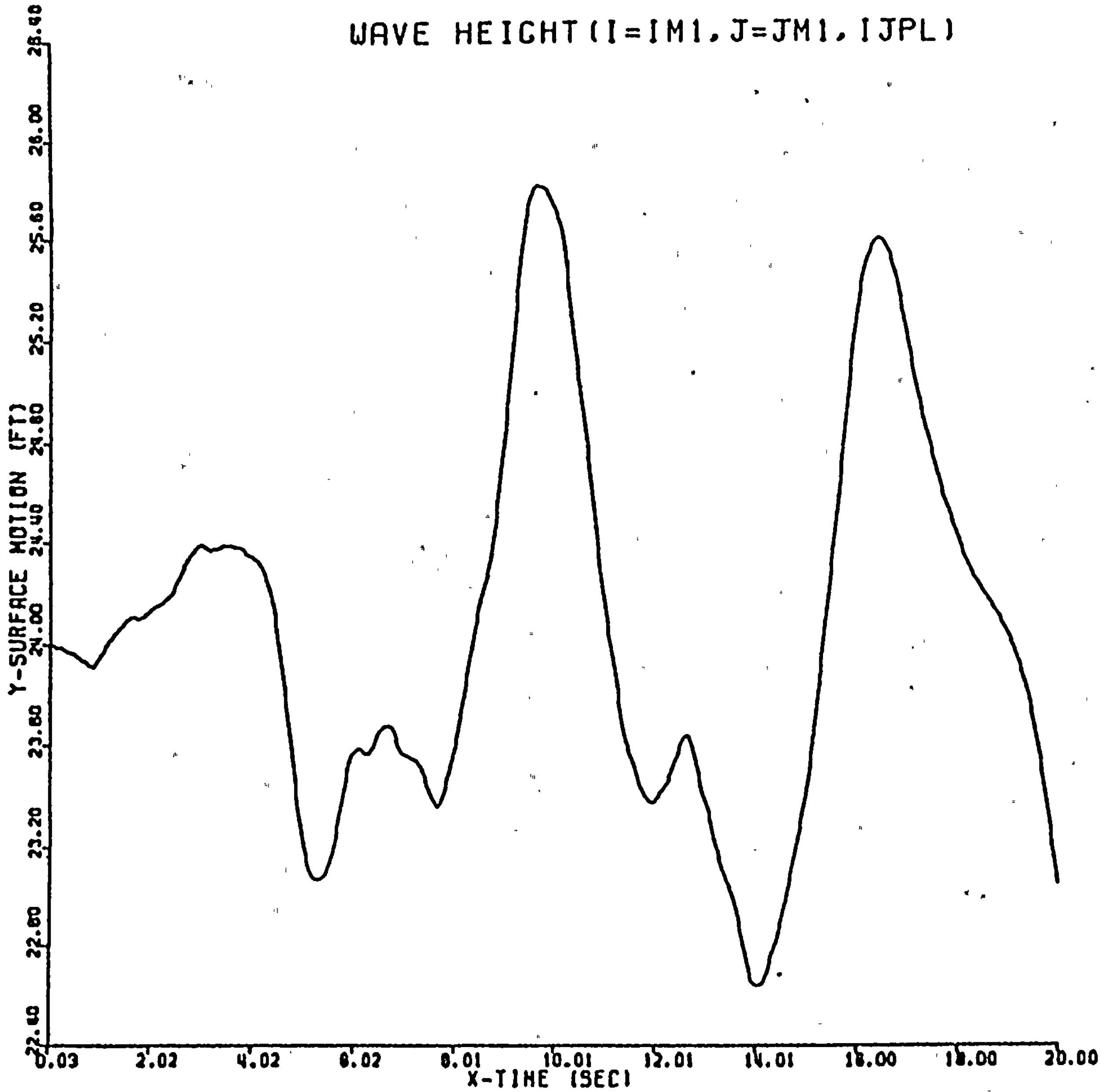

SUSQUEHANNA STEAM ELECTRIC STATION
UNITS 1 AND 2
DESIGN ASSESSMENT REPORT

TYPICAL WAVE MOTION
DUE TO SEISMIC SLOSH

FIGURE 4-62M

Tables 4-1 through 4-15 are proprietary and are found in the proprietary supplement to this DAR.

TABLE 4-16

LOCA LOADS ASSOCIATED WITH POOLSWELL

Load

1. Wetwell/Drywell Pressures during Poolswell
2. Poolswell Impact Loads
3. Poolswell Drag Loads
4. Downcomer Clearing Loads
5. Downcomer Water Jet Load
6. Poolswell Air Bubble Load
7. Poolswell Fallback Load

TABLE 4-17

SSES DRYWELL PRESSURE

Time (seconds)	Pressure (psia)
0.00000	15.46
0.00195	15.18
0.00208	15.21
0.00586	14.79
0.0645	18.17
0.127	21.16
0.252	26.61
0.502	36.52
0.627	38.26
0.658	37.71
1.057	42.09
1.867	48.43
1.900	48.54
2.119	48.73

TABLE 4-18

SSES PLANT UNIQUE POOLSWELL CODE INPUT DATA

Downcomer Area (each)	2.96 ft^2
Suppression Pool Free Surface Area	5065 ft^2
Maximum Downcomer Submergence	12.00 ft
Downcomer Overall Loss Coefficient	2.5
Number of Downcomers	87
Initial Wetwell Pressure	15.45 psia
Wetwell Free Air Volume	149,000 ft^3
Vent Clearing Time	0.6863 sec
Pool Velocity at Vent Clearing	3.0 ft/sec
Initial Drywell Temperature	135°F
Initial Drywell Relative Humidity	0.20

TABLE 4-19

INPUT DATA FOR SSES LOCA TRANSIENTS

Drywell free air volume (including vents)	239,600 ft^3
Wetwell free air volume	149,000 ft^3
Maximum downcomer submergence	12.0 ft
Downcomer flow area (total)	256.7 ft
Downcomer loss coefficient	2.5
Initial drywell pressure	15.45 psia
Initial wetwell pressure	15.45 psia
Initial drywell humidity	40% -55%
Initial pool temperature	90°F
Estimated DBA break size	3.53 ft^2
Number of vents	87
Initial mass of steam in vessel	24,500 lbm
Initial mass of saturated water in vessel	674,000 lbm
Minimum suppression pool mass	7.6×10^6 lbm
Initial vessel pressure	1,055 psia
Vessel & internals mass	2,940,300 lbm
Vessel & internals overall heat transfer coefficient	484.9 Btu/sec°F
Vessel and internals specific heat	0.123 Btu/lbm °F
Initial control rod drive flow	10.83 lbm/sec
Initial steam flow to main turbine	3931.5 lbm/sec
RCIC & HPCI (HPCS) flow initiation level, distance from vessel "0"	489.5 in

Table 4-19 (Continued)

RCIC & HPCI (HPCS) flow shutoff level (normal water level), distance from vessel "O"	581.5 in
Rated RCIC flow rate to vessel	83.4 lbm/sec
Rated HPCI (HPCS) flow rate to vessel	695 lbm/sec
RCIC shutoff pressure	165 psia
HPCI (HPCS) shutoff pressure	165 psia
Condensate storage tank enthalpy	48 Btu/lbm
CRD enthalpy	48 Btu/lbm
Initial power level	3.23×10^6 Btu/sec
Feedwater enthalpy	78 Btu/lbm
Cleanup system flow	36.94 lbm/sec
Cleanup system return enthalpy	413.2 Btu/lbm
Initial vessel fluid enthalpy	573.1 Btu/lbm
RHR heat exchanger "K" in pool cooling mode	306 Btu/sec °F
RHR heat exchanger steam flow in condensing mode	25 lbs/sec
RHR heat exchanger flow in pool cooling mode	1390 lbs/sec
RHR heat exchanger outlet enthalpy in condensing mode	108 Btu/lbm
Service water temperature	90 °F

TABLE 4-20

COMPONENT LOCA LOAD CHART FOR SSES

STRUCTURE DIRECTLY AFFECTED	LOAD 1	2	3	4	5	6	7	8	9	10	11	12	13
Containment Wall	X					X		X	X	X	X	X	X
Pedestal (incl. interior)	X					X		X	X	X	X	X	X
Basemat	X				X	X		X	X	X	X	X	X
Liner Plate	X				X	X		X	X	X	X	X	X
Drywell Floor	X										X	X	X
Drywell	X										X	X	X
Columns			X			X	X	X	X	X			
Downcomers			X	X		X	X	X	X	X			
Downcomer Bracing			X			X	X	X	X	X			
Wetwell Piping		X	X		X	X	X	X	X	X			

LOAD LEGEND

1 Wetwell/Drywell pressure during poolswell
2 Poolswell impact load
3 Poolswell drag load
4 Downcomer clearing load
5 Downcomer water jet load
6 Poolswell air bubble load
7 Fallback load
8 High mass flux condensation load
9 Medium mass flux condensation load
10 Chugging load
11 Wetwell/Drywell P&T during DBA
12 Wetwell/Drywell P&T during IBA
13 Wetwell/Drywell P&T during SBA

TABLE 4-21

WETWELL PIPING LOCA LOADING SITUTATIONS

Piping Configuration	LOCA Load to be Applied
1 Completely Submerged	
(a) vertical	skin drag load only (C_f)
(b) horizontal	drag load (C_D)
2 Partially Submerged	
(a) vertical	skin drag load only (C_f)
3 Initially Uncovered	
(a) vertical	skin drag load only (C_f)
(b) horizontal	impact load, then drag load (C_D)

Table 4-22

Sloshing Wave Height

Time of Max. Height sec.	HF2, (2,2) I = 2, J = 2 ft.	HF3, (2,17) I = 2, J = 17 ft.	HBK2, (7,2) I = 7, J = 2 ft.	HBK3, (7,17) I = 7, J = 17 ft
14.0			25.40 (1.40)	
9.90				25.80 (1.80)
17.50		25.60 (1.60)		
12.90	25.95 (1.95)			
	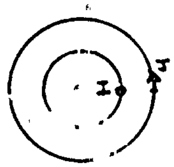 Fig. 4-62i	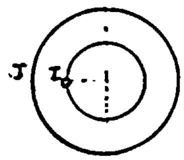 Fig. 4-62j	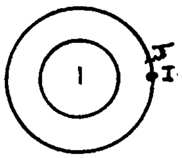 Fig. 4-62k	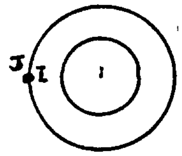 Fig. 4-62m

Note: ● = Shows Location

() = Inside bracket is the net wave height from the initial position 24 ft. from the bottom of tank.

I = Mesh numbers on the radius from inside to outside.

J = Circumferential division numbers.

CHAPTER 5

LOAD COMBINATIONS FOR STRUCTURES, PIPING,
AND EQUIPMENT

TABLE OF CONTENTS

CHAPTER 5

FIGURES

CHAPTER 5

TABLES

5.0 LOAD COMBINATIONS FOR STRUCTURES, PIPING, AND EQUIPMENT

To verify the adequacy of mechanical and structural design, it is necessary first to define the load combinations to which structures, piping, and equipment may be subjected. In addition to the loads due to pressure, weight, thermal expansion, seismic, and fluid transients, hydrodynamic loads resulting from LOCA and SRV discharge are considered in the design of structures, piping, and equipment in the drywell and suppression pool. This chapter specifies how the LOCA and SRV discharge hydrodynamic loads will be combined with the other loading conditions. For the load combinations discussed in this chapter, seismic and hydrodynamic responses are combined by the methods specified in Reference 10 Subsection 5.2.2 and Reference 10 Section 6.3.

5.1 CONCRETE CONTAINMENT AND REACTOR BUILDING LOAD COMBINATIONS

The loads on the containment, internal and reactor building concrete structures are combined to assess the structural integrity in accordance with the design load combinations given in Table 5-1. The factored load approach is used in the design and analysis of the structural components. The load factors adopted are based upon the degree of certainty and probability of occurrence for the individual loads as discussed in Ref 10, Subsection 5.2.2. The time sequences of occurrence of the various time dependent loads (as presented in Figures 4-55 through 4-61, for example) are taken into account to determine the most critical loading conditions.

5.2 STRUCTURAL STEEL LOAD COMBINATIONS

The load combinations for structural steel in the containment and the reactor building are given in Table 5-2. These combinations apply to the suppression chamber steel columns, the downcomer bracing, and the reactor building structural steel.

5.3 LINER PLATE LOAD COMBINATIONS

The liner plate and anchorage system are designed for the load combinations listed in Table 5-1 except that all load factors are taken as unity.

5.4 DOWNCOMER LOAD COMBINATIONS

Load combinations for the downcomers are given in Table 5-3. These load combinations are based on the load combinations given in Table 6-1 of Reference 10.

5.5 PIPING, QUENCHER, AND QUENCHER SUPPORT LOAD COMBINATIONS

LOCA loads considered on piping systems include poolswell impact loads, poolswell drag loads, downcomer water jet loads, poolswell air bubble loads, fallback drag loads, condensation oscillation loads, chugging loads, and inertial loading due to acceleration of the containment structure produced by LOCA loads. Loads due to SRV discharge on piping systems include water clearing loads, air clearing loads, fluid transient loads on SRV discharge piping, reaction forces at the quencher, and inertial loading due to the acceleration of the containment structure produced by SRV discharge loads.

The load combinations and the acceptance criteria for piping systems are given in Table 6-1 of Reference 10.

5.5.1 Load Considerations for Piping Inside the Drywell

Piping systems inside the drywell are subjected to inertial loading due to the acceleration of the containment produced by LOCA and SRV discharge loads in the wetwell. The SRV discharge piping in the drywell is also subjected to fluid transient forces due to SRV discharge.

5.5.2 Load Considerations for Piping Inside the Wetwell

All piping in the wetwell is subject to the inertial loading due to LOCA and SRV discharge.

Drag and impact loads due to LOCA and SRV discharge on individual pipes in the wetwell depend on the physical location of the piping. Other SRV discharge and LOCA loads applicable to piping in the wetwell are discussed in the paragraphs that follow.

Piping systems located below the suppression chamber water level are shown on Figures 5-1 and 5-2. These lines are located outside of the jet impingement cone of the downcomer. In addition to the inertial loads, these piping systems are subject to air bubble loads, condensation oscillation loads, and chugging loads due to LOCA and SRV operation. The SRV piping, quencher, and quencher support are also subject to fluid transient forces due to SRV discharge.

Piping systems within the poolswell volume are shown on Figures 5-2, 5-3 and 5-4. All horizontal runs of these pipes are above the suppression chamber water level. The following loads, in addition to inertial loads, act on these systems:

a. The horizontal runs of pipe below elevation 690'-2", experience poolswell impact , poolswell drag, and fallback drag loads.

b. The vertical portions of pipe in the water below elevation 690'-2" experience poolswell drag and fallback drag loads.

5.5.3 Quencher and Quencher Support Load Considerations

The quencher and quencher supports are subjected to the following hydrodynamic loads in addition to the pressure, weight, thermal, and seismic loads:

a. Unbalanced loads on the quencher due to SRV water clearing and air clearing transients, irregular condensation, and steady state blowdown

b. Drag loads due to SRV discharge and LOCA

c. SRV piping end loads

d. Inertial loading due to the acceleration of the containment produced by SRV discharge and LOCA.

5.5.4 Load Considerations for Piping in the the Reactor Building

The effects of the inertial loading due to acceleration of the containment produced by SRV discharge and LOCA loads will be evaluated for this piping.

5.6 NSSS LOAD COMBINATIONS

The load combinations used for the evaluation of the NSSS piping and equipment are contained in Table 5-5.

6 5.7 BOP EQUIPMENT LOAD COMBINATIONS

Load combinations for seismic category I equipment located within
2 the Containment, reactor and control buildings are assessed for
the load combinations shown in Table 5-4.

5.8 ELECTRICAL RACEWAY SYSTEM LOAD COMBINATIONS

The load combinations for evaluating the Electrical Raceway System are given in Table 5-6. 6

5.9 HVAC DUCT SYSTEM LOAD COMBINATIONS

7 The load combination for the HVAC duct system are given in Table 5-7.

FIG. NO.	LINE NO.	QTY	SYSTEM	PENET NO.	ELEVATION			DIM. X	REST. EL
					A	B	C		
A	24"–HBB–110	4	RHR	X–203A,B,C & D	660'-0"	658'-1"	656'-2"	23"	–
A	16"–HBB–104	2	CORE SPRAY	X–206A & B	659'-6"	658'-1"	656'-8"	18"	–
B	6"–HBB–102	1	RCIC	X–214	654'-10-1/8"	654'-1"	652'-1"	13-7/8"	654'-1"
C	16"–HBB–109	1	HPCI	X–209	655'-6"	654'-1"	652'-8"	2'-1-1/2"	654'-1"

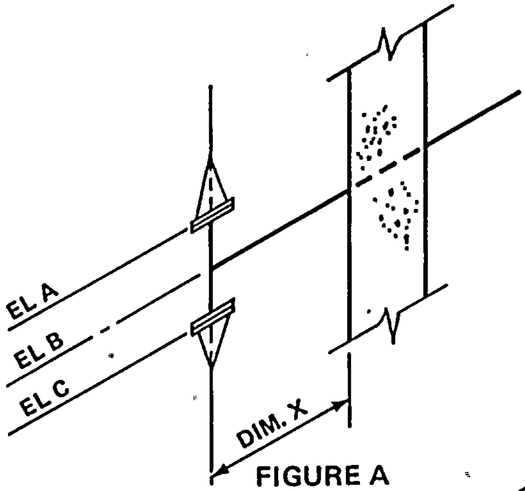

FIGURE A

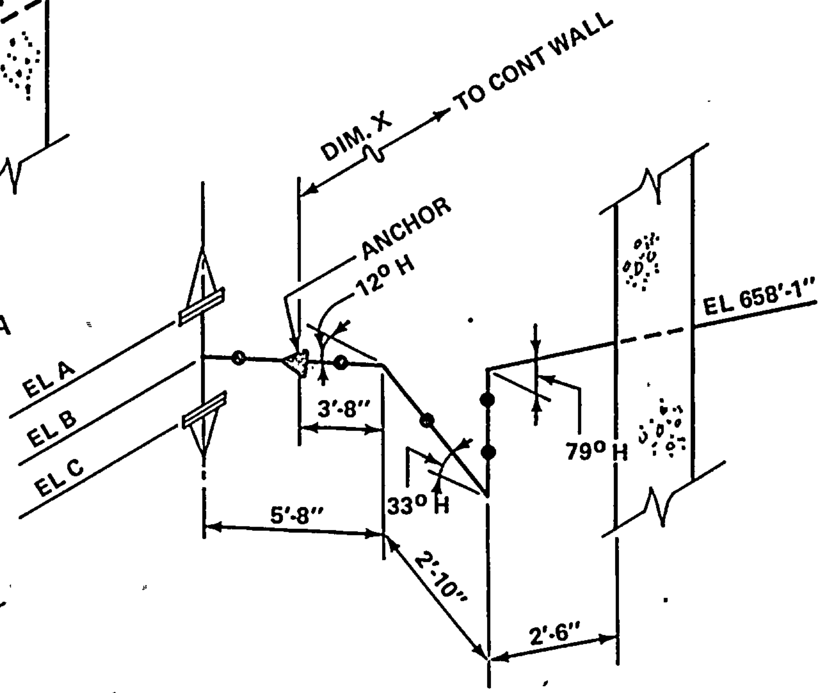

FIGURE C

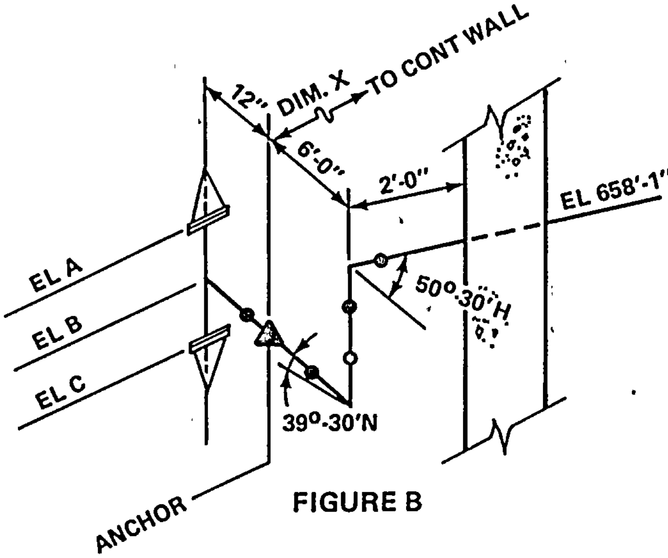

FIGURE B

SUSQUEHANNA STEAM ELECTRIC STATION
UNITS 1 AND 2
DESIGN ASSESSMENT REPORT

PIPING STRESS
DIAGRAMS AND TABLES

FIGURE 5-1

FIG. NO.	LINE NO.	QTY	SYSTEM	PENET NO.	TYPE OF PENET	ELEVATION		DIM. X	REST. EL
						A	B		
A	12"–HBB–101	1	RCIC	X–215	SLEEVE	674'-3"	659'-0"	2'-9"	668'-0" 659'-9"
A	24"–HBB–108	1	HPCI	X–210	SLEEVE	674'-1"	657'-4"	6'-9"	668'-0" 658'-1"
B	10"–HBB–120	2	RHR	X–246A & B	SLEEVE	674'-0"	666'-6"	3'-3 1/8" / 3'-6 5/8"	667'-0"
C	6"–HBD–186	2	RHR	X–226A & B	SLEEVE	673'-3"	665'-0"	1'-6"	673'-3" 668'-0"
LATER	2"–HBB–114	1	RCIC	X–216	EMBEDDED	667'-3"	LATER	LATER	LATER
D	4"–EBB–102	1	HPCI	X–211	EMBEDDED	677'-0"	665'-0"	1'-0"	668'-0"
D	4"–HBD–183	2	CORE SPRAY	X–208A & B	EMBEDDED	673'-3"	665'-0"	1'-0"	668'-0"
E	10"–HBD–183	2	CORE SPRAY	X–207A & B	EMBEDDED	685'-1"	665'-0"	1'-9"	676'-6" 677'-0" 668'-0"
C	18"–HBD–185	2	RHR	X–204A & B	SLEEVE	685'-1"	666'-0"	2'-3"	685'-1" 670'-0" 673'-10"
LATER	3"–HBB–108	1	HPCI	X–244	EMBEDDED	670'-0"	LATER	LATER	LATER
LATER	2"–HBB–101	1	RCIC	X–245	EMBEDDED	673'-0"	LATER	LATER	LATER
LATER	2"–HBB–101	1	RCIC	X–217	EMBEDDED	673'-0"	LATER	LATER	LATER

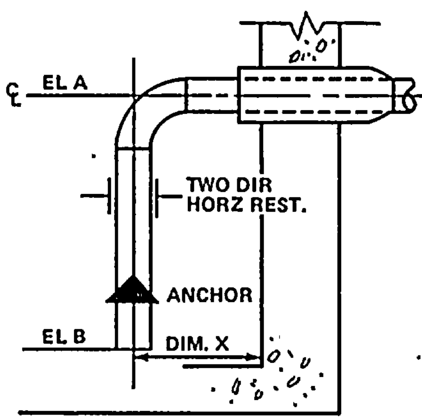

FIGURE A

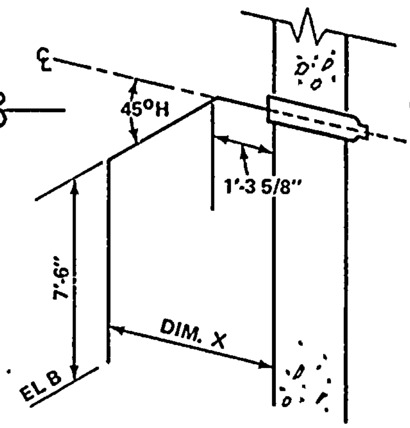

FIGURE B

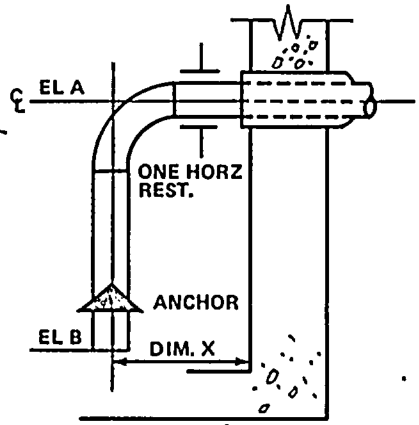

FIGURE C

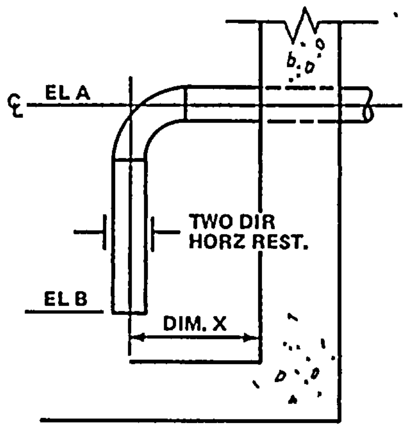

FIGURE D

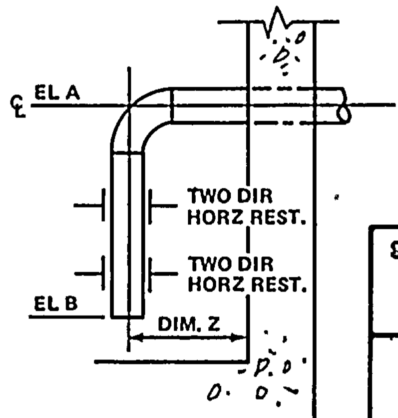

FIGURE E

SUSQUEHANNA STEAM ELECTRIC STATION
UNITS 1 AND 2
DESIGN ASSESSMENT REPORT

PIPING STRESS
DIAGRAMS AND TABLES

FIGURE 6-8

FIG. NO.	LINE NO.	QTY	SYSTEM	EL A
A	12"-GBC-101	6	M.S.R.V. DISCHARGE PIPING R.F.C.M.E.L.	651'-6"
B	12"-GBC-101	10	S.J.B.D.P.N.G.K.A.H.	651'-6"

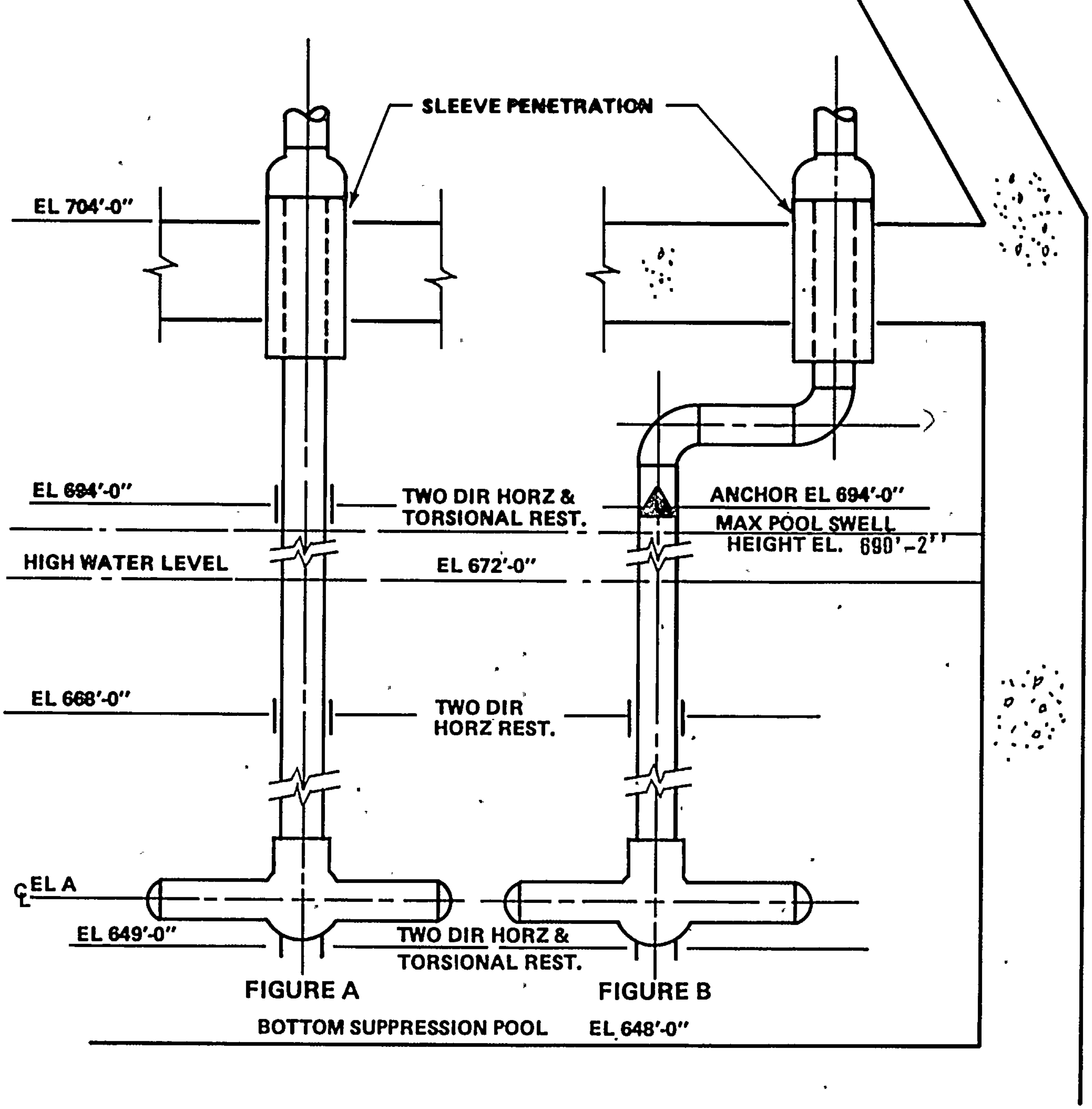

Rev. 2, 5/80

SUSQUEHANNA STEAM ELECTRIC STATION
UNITS 1 AND 2
DESIGN ASSESSMENT REPORT

PIPING STRESS DIAGRAMS AND TABLES

FIGURE 5-3

FIG. NO.	QTY	LINE NO.	SYSTEM	EL A	EL B	EL C	RAD Y	DIM. X	REST. EL
		6"-GBB-120	RHR	668'-5 1/2"	685'-0"	697'-6"	42'-8 3/8"	15 5/8"	697'-6" 685'-6"

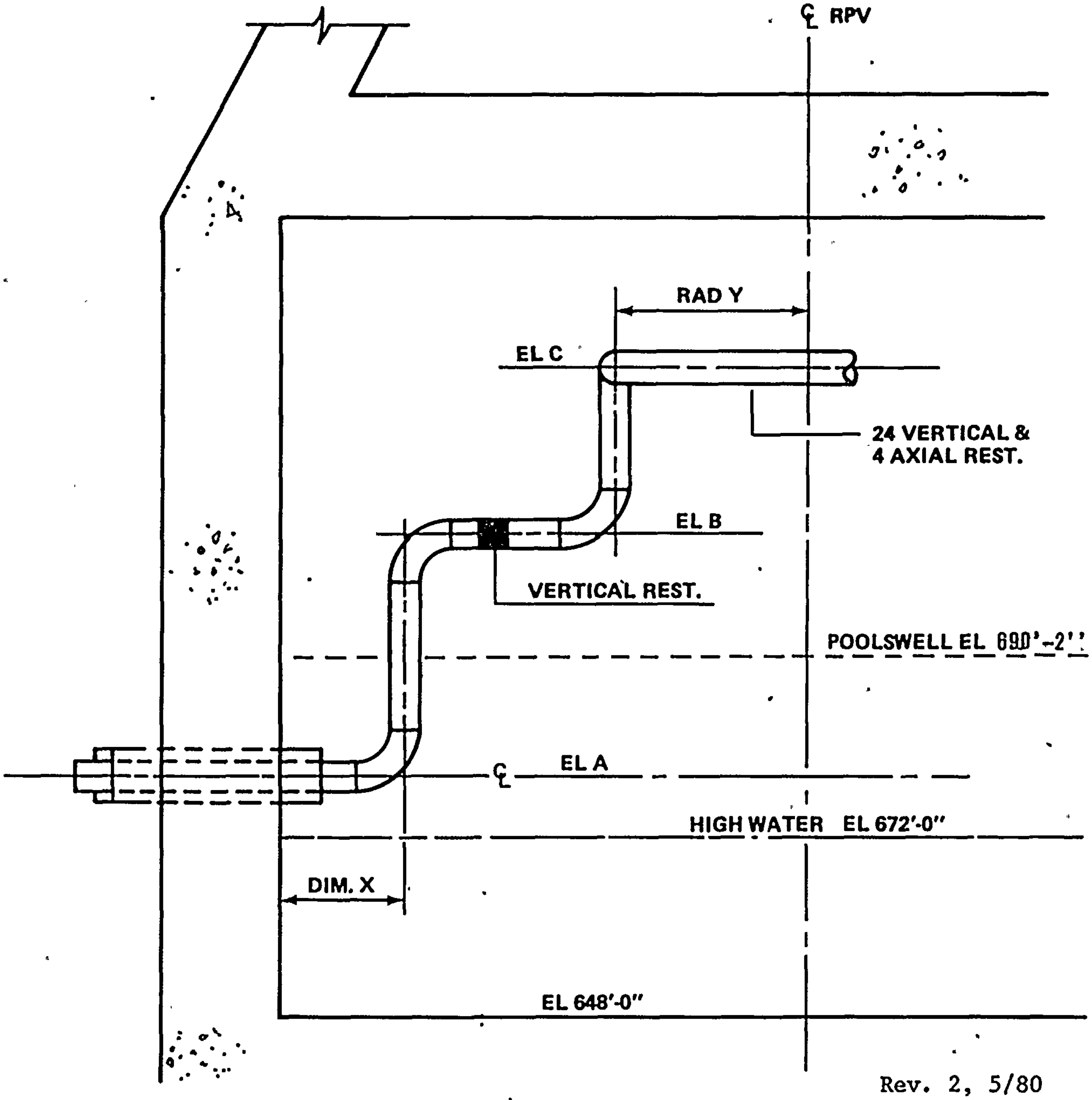

Rev. 2, 5/80

SUSQUEHANNA STEAM ELECTRIC STATION
UNITS 1 AND 2
DESIGN ASSESSMENT REPORT

PIPING STRESS
DIAGRAMS AND TABLES.

FIGURE 5-4

TABLE 5-1

LOAD COMBINATIONS FOR CONTAINMENT AND REACTOR BUILDING CONCRETE STRUCTURES AND *CONTAINMENT LINER PLATE (CONSIDERING HYDRODYNAMIC) LOADS

Equation	Load Condition	D	L	P_o	T_o	R_o	E_o	E_{ss}	P_B	P_A	T_A	R_A	R_V	SRV(2)	AOT	ADS	ASYM	Single Valve	LOCA(3)
1	Normal w/o Temp.	1.4	1.7	1.0	-	-	-	-	-	-	-	-	-	1.5	X(1)	-	X	-	
2	Normal w/Temp.	1.0	1.3	1.0	1.0	1.0	-	-	-	-	-	-	-	1.3	X	-	X	-	
3	Normal Sev. Env.	1.0	1.0	1.0	1.0	1.0	1.25	-	-	-	-	-	-	1.25	X	-	X	-	
4	Abnormal	1.0	1.0	-	-	-	-	-	1.25	-	1.0	1.0	-	1.25	-	X	X	-	X
4a	Abnormal	1.0	1.0	-	-	-	-	-	-	1.25	1.0	1.0	-	1.0	-	-	-	X	X
5	Abnormal Sev. Env.	1.0	1.0	-	-	-	1.1	-	1.1	-	1.0	1.0	-	1.1	-	X	X	-	X
5a	Abnormal Sev. Env.	1.0	1.0	-	-	-	1.1	-	-	1.1	1.0	1.0	-	1.0	-	-	-	X	X
6	Normal Ext. Env.	1.0	1.0	1.0	1.0	1.0	-	1.0	-	-	-	-	-	1.0	X	-	X	-	-
7	Abnormal Ext. Env.	1.0	1.0	-	-	-	-	1.0	1.0	-	1.0	1.0	1.0	1.0	-	X	X	-	X
7a	Abnormal Ext. Env.	1.0	1.0	-	-	-	-	1.0	-	1.0	1.0	1.0	1.0	1.0	-	-	-	X	X

* For liner plate the coefficients are unity.

Load Description

D = Dead Loads	E_o = Operating-Basis Earthquake
L = Live Loads	E_{SS} = Safe Shutdown Earthquake
	P_B = SBA or IBA (LOCA) Pressure Load
P_o = Operating Pressure Loads	R_A = Pipe Break Temperatures Reaction Loads
T_o = Operating Temperature Loads	P_A = DBA (LOCA) Pressure Load
R_o = Operating Pipe Reactions	T_A = Pipe Break Temperature Load
SRV = Safety Relief Valve Loads	R_y = Reaction and jet forces associated with the pipe break

Notes:

1) X indicates applicability for the designated load combination.

2) For the columns designated AOT, ADS, ASYM, and Single Valve, only one of the four possible columns may be included in the load combination for any one equation. For example, in Equation 1 either AOT or ASYM may be considered with the other loads but not both AOT and ASYM simultaneously.

3) LOCA includes chugging, condensation oscillation, and large air bubble loads.

Table 5-2

LOAD COMBINATIONS AND ALLOWABLE STRESSES FOR STEEL STRUCTURAL COMPONENTS (Suppression Chamber Columns, Downcomer Bracing, and Reactor Building Structural Steel. 7

Equation	Condition	Load Combination	Stress Limit	
1	Normal w/o Temp.	D+L+SRV	F_s	
2	Normal w/Temp.	$D+L+T_o+SRV$	F_s	
3	Normal/ Severe	$D+L+T_o+E+SRV$	$1.5\ F_s$	
4	Normal/ Extreme	$D+L+T_o+E'+SRV$	$1.5\ F_s$	
5	Abnormal	$D+L+P+(T_o+T_a)+R$ $+SRV+LOCA$	(Note 1)	2
6	Abnormal Severe	$D+L+P+(T_o+T_a)+R+E$ $+SRV+LOCA$	(Note 1)	2
7	Abnormal/ Extreme	$D+L+P+(T_o+T_a)+R+E'$ $+SRV+LOCA$	(Note 1)	2

Note 1: In no case shall the allowable stress exceed $0.90F_y$ in bending, $0.85F_y$ in axial tension or compression. and $0.50F_y$ in shear. Where the design is governed by requirements of stability (local or lateral buckling), the actual stress shall not exceed $1.5F_s$.

<u>Table 5-2</u> (Cont'd)
Notations

Notations:

F_s	=	Allowable stress according to the AISC, "Specification for the Design, Fabrication, and Erection of Structural Steel for Buildings," dated 1969, Part 1.
D	=	Dead Load
L	=	Live Load
T_o	=	Thermal effects during normal operating conditions including temperature gradients and equipment and pipe reactions.
T_a	=	Added thermal effects (over and above operating thermal effects) which occur during a design accident.
P	=	Design basis accident pressure load
R	=	Local force or pressure on structure due to postulated pipe rupture including the effects of steam/water jet impingement, pipe whip, and pipe reaction.
E	=	Load due to Operating Basis Earthquake.
E'	=	Load due to Safe Shutdown Earthquake.
SRV	=	Safety relief valve loads.
LOCA	=	Loads due to Loss of Coolant Accident conditions (chugging, condensation oscillation, or large air bubble loads).
F_y	=	Minimum specified yield strength

Table 5-3

LOAD COMBINATIONS AND ALLOWABLE STRESSES FOR DOWNCOMERS

Equation	Condition	Load Combination	Primary Stress Limit
1	Upset	$D+P_o+SRV_{ALL}$	$1.5\ S_m$
2	Emergency	$D+P_o+SRV_{ALL}+E$	$2.25\ S_m$
3	Emergency	$D+P_{SBA}+SRV_{ADS}+E+LOCA(SBA)$	$2.25\ S_m$
4	Faulted	$D+P_o+SRV_{ALL}+E'$	$3\ S_m$
5	Faulted	$D+P_{IBA}+SRV_{ADS}+E+LOCA(IBA)$	$3\ S_m$
6	Faulted	$D+P_{SBA}$ (or P_{IBA}) $+SRV_{ADS}+E'+LOCA$(SBA or IBA)	$3\ S_m$
7	Faulted	$D+P_A+E'+LOCA(DBA)$	$3\ S_m$

Notations:

S_m = Maximum allowable stress according to Table I-10.1, Ref. 29.

D = Dead weight of the downcomer

P_o = Pressure differential between drywell and suppression chamber during normal operating condition.

P_{SBA} = Pressure differential between drywell and suppression chamber during SBA.

P_{IBA} = Pressure differential between drywell and suppression chamber during IBA.

P_A = Pressure differential between drywell and suppression chamber during DBA.

SRV_{ALL} = Dynamic lateral pressure and inertia load due to the discharge of all 16 safety relief valves simultaneously.

SRV_{ADS} = Dynamic lateral pressure and inertia load due to the discharge of all 6 ADS safety relief valves simultaneously.

E = Load due to Operating Basis Earthquake

E' = Load due to Safe Shutdown Earthquake

LOCA = Loads due to chugging, condensation, oscillation, or air bubble loads. The governing applicable loading case should be considered. The loads should include:

1. Lateral load at the tip of the downcomer
2. Horizontal and vertical inertial loads
3. Submerged structures loads

TABLE 5-4

LOAD COMBINATIONS AND ALLOWABLE STRESSES FOR BALANCE OF PLANT (BOP) EQUIPMENT 6

Equation	Condition	Load Combination	Stress Limit
1	Normal w/o Temp & pr.	D+L+SRV	F_s
2	Normal w/Temp & pr.	D+L+T+P+SRV	F_s
3	Abnormal/Severe	D+L+T+P+E+SRV+LOCA	$1.5F_s$
4	Abnormal/Extreme	D+L+T+P+E'+SRV+LOCA	$1.5F_s$

where

F_s = Allowable stress for normal conditions

D = Dead Load

L = Live Load 2

P = Pressure loads during operating conditions including pressure gradients and equpment and pipe reactions.

T = Thermal effects during normal operating conditions including temperature gradients and equipment and pipe reactions.

E = Loads due to operating basis earthquake

E' = Loads due to Safe Shutdown earthquake

SRV = Loads due to Main Steam Safety relief valve operation

LOCA = Loads due to Loss-of-Coolant Accident occurrence.

TABLE 5-5

LOAD COMBINATION AND ACCEPTANCE CRITERIA FOR ASME CODE CLASS 1, 2 AND 3 NSSS PIPING AND EQUIPMENT

Load Combination	Design Basis	Evaluation Basis	(Service Level)
N + SRV	Upset	Upset	(B)
N + OBE	Upset	Upset	(B)
N + OBE + SRV	Emergency	Upset	(B)
N + SSE + SRV	Faulted	Faulted*	(D)
N + SBA + SRV	Emergency	Emergency*	(C)
N + IBA + SRV	Faulted	Faulted*	(D)
N + SBA + SRV	Emergency	Emergency*	(C)
N + SBA + OBE + SRV	Faulted	Faulted*	(D)
N + IBA + OBE + SRV	Faulted	Faulted*	(D)
N + SBA/IBA + SSE + SRV	Faulted	Faulted*	(D)
N + LOCA** + SSE	Faulted	Faulted*	(D)

LOAD DEFINITION LEGEND

Normal (N)	-	Normal and/or abnormal loads depending on acceptance criteria.
OBE	-	Operational basis earthquake loads.
SSE	-	Safe Shutdown earthquake loads.
SRV	-	Loads associated with Safety Relief Valve actuation.

LOAD COMBINATION TABLE (Cont.)

$LOCA_1$	-	The loss of coolant accident associated with the postulated pipe rupture of large pipes (e.g., main steam, feedwater, recirculation piping).
$LOCA_2$	-	Pool swell drag/fallback loads on piping and componentslocated between the main vent discharge outlet and the suppression pool water upper surface.
$LOCA_3$	-	Pool swell impact loads on piping and components located above the suppression pool water upper surface.
$LOCA_4$	-	Oscillating pressure induced loads on submerged piping and components during condensation oscillations.
$LOCA_5$	-	Building motion induced loads from chugging.
$LOCA_6$	-	Vertical and horizontal loads on main vent piping.
$LOCA_7$	-	Annulus pressurization loads.
SBA	-	The abnormal transients associated with a Small Break Accident.
IBA	-	The abnormal transients associated with an Intermediate Break Accident.

* All ASME Code Class 1, 2, and 3 piping systems which are required to function for safe shutdown under the postulated events shall meet the requirements of NRC's "Interim Technical Position - Functional Capability of Passive Components" - by MEB.

** The most limiting case of load combination among $LOCA_1$ through $LOCA_7$.

TABLE 5-6

LOAD COMBINATIONS AND ALLOWABLE STRESSES FOR THE ELECTRICAL RACEWAY SYSTEM

Load Combination		Allowable Stresses
1.	D+L+SRV	F
2.	D+L+E	Note 2
3.	D+E'+SRV+LOCA	Note 2

NOTES:

1. For notations, see Table 5-2.
2. For detailed discussion, see Subsection 3.7b.3.1.6.1 of the SSES FSAR.

TABLE 5-7

LOAD COMBINATIONS AND ALLOWABLE STRESSES FOR HVAC DUCTS AND SUPPORTS

Ducts

Load Combination		Allowable Stresses
1.	$D+L+SRV$	F_S
2.	$D+P_M+SRV$	F_S
3.	$D+P_T$	$1.25F_S$
4.	$D+P_M+E$	$1.25F_S$ *
5.	$D+P_M+E+SRV$	Note 1
6.	$D+P_M+E'+SRV$	Note 1
7.	$D+P_M+P_A+E'+SRV+LOCA$	Note 1
8.	When protection against tornado depressurization is required.	
	$D+P_O+W_D+SRV+LOCA$	Note 1
9.	For ducts inside drywell of containment, the following additional load combination is also appliable:	
	$D+H_A+P_O+P_A+E'+SRV+LOCA$	Note 1

Duct Supports

1.	$D+L+SRV$	F_S
2.	$D+E$	$1.25F_S$ *
3.	$D+E+SRV$	Note 1
4.	$D+E'+SRV+LOCA$	Note 1

* This value shall be F_S for transverse and longitudinal bracing and their connections.

Note 1: In no case shall the allowable stress exceed $0.90F_Y$ in bending, $0.85F_Y$ in axial tension or compression, and $0.50F_Y$ in shear. Where the design is governed by requirements of stability (local or lateral buckling), the actual stress shall not exceed $1.5F_S$.

TABLE 5-7 (Cont.)

Notations

D	=	Dead Load
L	=	Live Load
P_O	=	Duct Normal Operating Pressure Load
P_T	=	Duct Test Pressure Load
P_A	=	Design Basis Accident Pressure Load
P_M	=	Duct Maximum Operating Pressure Load, excluding P_A & P_T, e.g., Fan Cutoff Pressure Load
E	=	"Operating Basis Earthquake" (OBE) load
E'	=	"Safe Shutdown Earthquake" (SSE) load
W_D	=	Tornado Depressurization Load
H_A	=	Forces due to thermal expansion of HVAC ducts under accident conditions
SRV	=	Safety Relief Valve Loads (Hydrydynamic Loads)
LOCA	=	Loss of Coolant Accident Loads (Hydrodynamic Loads)
F_S	=	Allowable Stress for Steel, governed by AISI or AISC Codes, as Applicable
F_S	=	Yield Strength for Steel (ASTM specification minimum)

CHAPTER 6

DESIGN CAPABILITY ASSESSMENT CRITERIA

TABLE OF CONTENTS

6.0 DESIGN CAPABILITY ASSESSMENT CRITERIA

The criteria by which the design capability is determined are discussed in this chapter. Design of the SSES is assessed as adequate when the design capability of the structures, piping, and equipment is greater than the loads (including LOCA and SRV discharge) to which the structures, piping, and equipment are subjected. Loading combinations are discussed in Chapter 5. The margins by which design capabilities exceed these loadings are discussed in Chapter 7, Design Assessment.

6.1 CONCRETE CONTAINMENT AND REACTOR BUILDING CAPABILITY ASSESSMENT CRITERIA

6.1.1 Containment Structure Capability Assessment Criteria

The acceptance criteria detailed in the SSES FSAR Section 3.8.1.5 have been used to assess the structural integrity of the containment and internal structures. No changes are made in these acceptance criteria when the effects of the dynamic SRV discharge and LOCA loads are included.

6.1.2 Reactor Building Capability Assessment Criteria

The acceptance criteria for Seismic Category I structures presented in the SSES FSAR Subsection 3.8.4.5 have been used to assess the structural integrity of the reactor building and its components. No change is made in these acceptance criteria when the effects of the dynamic SRV discharge and LOCA loads are included.

6.2 STRUCTURAL STEEL CAPABILITY ASSESSMENT CRITERIA

The allowable stresses for structural steel in the containment and the reactor building are given in Table 5-2. These criteria apply to the suppression chamber steel columns, the downcomer bracing, and the reactor building structural steel.

6.3 LINER PLATE CAPABILITY ASSESSMENT CRITERIA

The strains in the liner plate and anchorage system (welds and anchors) from self-limiting loads such as dead load, creep, shrinkage, and thermal effects are limited to the allowable values specified in Table CC-3720-1 of Reference 30, and the displacements of the liner anchorage are limited to the displacement values of Table CC-3730-1 of Reference 30.

Primary membrane stresses in the liner plate and anchorage system (welds and anchors) from mechanical loads such as SRV discharge and chugging are checked according to Subsection NE-3221.1 of Reference 29. Primary plus secondary membrane plus bending stresses are checked according to Subsection NE-3222.2 of the same code. Fatigue strength evaluation is based on Subsection NE-3222.4. Allowable design stress intensity values, design fatigue curves, and material properties used conform to Subsection NA, Appendix I of Reference 29.

The capacity of the liner plate anchorage is limited by concrete pull-out to the service load allowables of concrete as specified in Reference 31.

6.4 DOWNCOMER CAPABILITY ASSESSMENT CRITERIA

The allowable stresses for the downcomers are given in Table 5-3. These allowable stresses are in accordance with Reference 29; Subsection NE. As permitted by Subsection NE-1120 for MC components, the downcomers are analyzed in accordance with Subsection NB-3650 of Reference 29; however, the lower allowable stresses, S_m, from Table I-10.1 for MC components are used when performing the analysis.

6.5 PIPING, QUENCHER, AND QUENCHER SUPPORT CAPABILITY ASSESSMENT CRITERIA

Piping in the containment and reactor building is analyzed in accordance with Reference 29 Subsections NB3600, NC3600, and ND3600 for the loading described in Subsection 5.5.

The quencher is designed in accordance with Reference 29, Subsection NC3200, for loading discussed in Subsection 5.5.3. The quencher support is designed in accordance with Subsection NF3000 of Reference 29.

6.6 NSSS CAPABILITY ASSESSMENT CRITERIA

The capability assessment criteria used for the analysis of NSSS piping systems, reactor pressure vessel (RPV), RPV supports, RPV internal components and floor structure mounted equipment are shown in Table 5-5, Load Combinations and Acceptance Criteria. Table 5-5 is in agreement with a conservative general interpretation of the NRC technical position, "Stress Limits for ASME Class 1, 2 and 3 Components and Component Supports of Safety-Related Systems and Class CS Core Support Structures Under Specific Service Loading Combinations."

Peak response due to related dynamic loads postulated to occur in the same time frame but from different events are combined by the square-root-of-the-sum-of-the-squares method (SRSS). A detailed discussion of this load combination technique is presented in Reference 80.

6.7 BALANCE OF PLANT (BOP) EQUIPMENT CAPABILITY ASSESSMENT CRITERIA

6.7.1.1 Seismic Category I BOP equipment located within the containment, reactor and control building are assessed for load combinations shown in Table 5-4. In these load combinations, seismic and hydrodynamic loads are generally combined using the absolute sum method. 6

6.7.1.2 However, for the "marginal" cases the responses of the "dynamic" events (Seismic, SRV, LOCA) are combined by the square root of the sum of the squares (SRSS) method before adding these values to the other loads by the absolute sum (ABS) method. The maximum loading effects of both the horizontal and vertical directions are considered as arising from simultaneous excitation in all three principal directions for all combinations involving dynamic loads as detailed in Subsection 7.1.7.4.1.3.

6.7.2 Testing

6.7.2.1 When equipment is qualified by testing, the test motions have simulated the combinations and damping. The equipment have remained operational and functional, before, during and after such tests. 2

(a)	OBE	alone	-	1/2% damping
(b)	SSE	alone	-	1% damping
(c)	SRV	alone	-	2% damping
(d)	LOCA	alone	-	2% damping
(e)	OBE+SRV+LOCA		-	2% damping
(f)	SSE+SRV+LOCA		-	2% damping

6.7.2.2 Cases (a) and (b) are covered in the FSAR. Cases (c) and (d) are covered in the test evaluation for (e) and (f). Test requirements are depicted by tests response spectrum (TRS) for a given damping value. Equipment is deemed to be qualified if the equipment did not fail or malfunction during the test and the TRS envelope the required response Spectrum (RRS). The RRS for cases (e) and (f) are obtained by combining the response spectrum of the individual components of each event by adding the larger of the horizontal responses to the vertical responses on an absolute sum basis. However, for marginal cases the square root of sum of the squares (SRSS) method is allowed for the individual dynamic events and components. 6

6.8 ELECTRICAL RACEWAY SYSTEM CAPABILITY ASSESSMENT CRITERIA

The allowable stresses for the Electricl Raceway System are contained in Table 5-6.

6.9 DUCT SYSTEM CAPABILITY ASSESSMENT CRITERIA

The allowable stresses for the miscellaneous steel for the HVAC duct system are given in Table 5-7. 7

CHAPTER 7

DESIGN ASSESSMENT

TABLE OF CONTENTS

CHAPTER 7

FIGURES

FIGURES (Cont.)

6

CHAPTER 7

TABLES

7.0 DESIGN ASSESSMENT

Loads on SSES structures, piping, and equipment are defined in Chapter 4. The methods by which these loads are combined are discussed in Chapter 5. The criteria for establishing design capability are stated in Chapter 6.

This chapter describes the assessment of the adequacy of the SSES design by comparing design capabilities with the loadings to which structures, piping, and components are subjected and demonstrating the extent of the design margin. The first section of this chapter discusses the methodology by which design capability and loads are compared. The second section summarizes the results of these comparisons.

7.1 ASSESSMENT METHODOLOGY

7.1.1 Containment and Reactor Building Assessment Methodology

7.1.1.1 Containment Structure

7.1.1.1.1 Hydrodynamic Loads

7.1.1.1.1.1 Structural Models

2 The dynamic analysis for the structural response of the containment and internal structures due to the SRV discharge loads and LOCA loads is performed using the finite element
6 method. The ANSYS (see Reference 75 and 76) finite element computer program was chosen for the transient dynamic analysis. Figure 7-1 shows the ANSYS finite element model. Beam elements and spar elements are used for the stabilizer truss. Lumped mass elements are used for the RPV internals and suppression pool fluid. Spring-damper elements are used to model the rock foundation. The ANSYS model includes a total of 761 elements and 200 dynamic degrees of freedom.

The soil structure interaction is taken into consideration by modelling the soil using a series of discrete springs and dampers in three directions as shown in Figure 7-1. The properties of the discrete springs and dampers are calculated based on the formulae for lumped parameter foundations found in Reference 33. The validity of this soil model is proven by comparing the results with those of an independent model which represents the soil by finite elements.

7.1.1.1.1.2 Damping

a. Structural Damping

The equations of motion for a discretized structure must include a term to account for viscous damping that is
2 linearly proportional to the velocity. The equations of motion for a damped system are:

$$[M]\{\ddot{r}\} + [C]\{\dot{r}\} + [K]\{r\} = \{R(t)\}$$

where [C] is the viscous damping matrix.

A viscous damping matrix of the form

$[C] = \alpha [M] + \beta [K]$ was used (Reference 53).

Where α and β are proportionality constants which relate damping to the velocity of the nodes and the strain rates respectively. This damping matrix leads to the following relation between α and β and the damping ratio of the ith mode C_i:

$$C_i = \alpha / 2w_i + \beta w_i / 2$$

where ω_i is the natural frequency of the ith mode. For the usual case of only structural damping, $\alpha = 0$ and therefore $\beta = 2C_i / \omega_i$.

Since only a single value of β is permitted in the ANSYS input, the most dominant natural frequency of the structure is selected for the computation of β (See Reference 54).

A value of β equal to 0.00063 is used in the ANSYS model which corresponds to structural modal damping of approximately 4 percent of critical at 20 Hz which is the most dominant natural frequency of the structure.

Figure 7-2 shows modal damping ratio versus modal frequency for structural stiffness-proportional-damping.

b. Soil Springs and Radiation Damping

The elastic half-space theory as described by Reference 33 (BC-TOP-4A Rev. 3) were used to compute the values of the Spring Constants and dampers in the horizontal and vertical directions (K_H, K_V, C_H & C_V). The following parameters are used to represent the rock foundation:

G = Shear Modulus of foundation medium

= 1.154×10^3 KSI

ν = Poisson's ratio of foundation medium

= 0.3

V_s = Shear wave velocity

= 6180 ft/sec

From which we get the following:

K_H = 3.37×10^6 K/in

C_H = 1.57×10^4 K-sec/in

K_v = 3.96×10^6 K/in

C_V = 2.72×10^4 K-sec/in

The above lumped foundation springs and dampers were then distributed to every node on the basemat according to the tributary area.

7.1.1.1.1.3 Fluid-Structure Interaction

For the application of SRV loads described in Section 4.1, a finite element model of the containment was developed in which the suppression pool water was included. The water mass constitutes only one seventh of the total mass of the reinforced concrete structure. The model used considers fluid-structure coupling by lumping the water mass in the suppression pool at each nodal point of the wetted surface. The weighted area
6 approach is considered to determine the fluid mass at each node of the suppression pool.

For the application of the LOCA steam condensation loads, based on the containment wall pressure time histories calculated by the acoustic methodology (see Subsection 9.5.3.4.1 and 9.5.3.4.2), the water mass was excluded. The exclusion of the water-mass is due to the fact that fluid structure interaction was already considered during the pressure time history calculations (Reference 65).

7.1.1.1.1.4 Supplementary Computer Programs

Supplementary computer programs were used for preprocessing and postprocessing of data generated for or by the ANSYS computer program.

A preprocessing program called CHUG was developed to convert the pressure time history forcing functions into concentrated force time - history forcing functions acting at the associated nodes of the ANSYS model. The program writes the nodal forces onto a file for processing by ANSYS.

A postprocessor program was developed to calculate the acceleration time history. This program is called DISQ. It
2 reads the structural response displacement time histories generated from ANSYS displacements, scans the maximum displacements and generates the acceleration time histories using the Fast Fourier Transformation method.

Bechtel inhouse computer program MSPEC was used to compute the acceleration response spectrum obtained from DISQ. The program also performs plotting and broadening of the spectrum.

A computer program ENVLP was developed to generate envelopes of a number of spectrum obtained from MSPEC.

Computer program FORCE was developed to scan the maximum absolute stresses generated by ANSYS stress pass. A further explanation of FORCE is found in Subsection 7.1.1.1.1.6.2.

Verification of CHUG, DISQ, ENVLP and FORCE are available for review.

7.1.1.1.1.5 Load Application

7.1.1.1.1.5.1 SRV Discharge Loads

The SRV loads have been defined in Section 4.1 based on KWU SRV 6
Traces #76, 82 and 35.

To obtain the maximum response of the containment due to bubble
oscillation, a wide range of frequency content of the forcing
function is considered.

The range of frequencies specified by KWU is between 55% and 110%
of the frequencies of the three original traces as present in
Subsection 4.1.3.5. 2

Based on the natural frequencies and the mode shapes of the
primary containment as shown in Appendix B-1, five different
frequencies in the range specified are selected in order to
obtain the maximum structural response. The five frequency
values are considered for each of the three original KWU
pressure-time history traces which result in fifteen pressure-
time histories to be considered.

As described in Subsection 4.1.3, four pressure distributions
depending upon the number of valves actuated are considered;
i.e., "All valve, ADS, asymmetric, and single valve". However,
the azimuth distribution on the periphery indicates that the all 6
valve case governs the ADS case for the symmetric loading and the
asymmetric case governs the single valve case for the asymmetric
loading. Therefore, the design assessment is based on only two
cases, i.e., "symmetric and asymmetric".

7.1.1.1.1.5.2 LOCA Related Loads

The LOCA loads are based on LOCA steam condensation tests
performed by Kraftwek Union AG (KWU) at their GKM-II-M test 2
facility. Section 9.0 describes the test facility, test matrix,
test results and the GKM-II-M LOCA load definition developed to
re-evaluate SSES for chugging and condensation oscillation.

7.1.1.1.1.6 Analyses

7.1.1.1.1.6.1 Time History Analysis 6

The structural finite element model of containment as outlined in
Subsection 7.1.1.1.1.1 is solved by "Reduced Linear Transient
Dynamic Analysis" of the ANSYS computer program. The description 8
of the analysis and the data input are contained in References 75
and 76, respectively.

For each set of pressure time histories, based on the analytical
procedure in Figure 7-4, acceleration response spectra were
generated at 52 dynamic degrees of freedom in the containment. 6
Nodal point response spectra generated from several load

8 conditions/traces were enveloped into one set of floor response spectra curves which represent SRV and LOCA.

The response spectra were generated in two pairs of damping values, the low and the high dampings. The low damping values are 0.5, 1, 2 and 5 percent of critical, and the high damping values are 7, 10, 15 and 20 percent of critical. The peak
6 frequencies of the spectra are broadened by 15% and 20% for low and high damping values, respectively.

Appendix B contains the above response spectra for low damping values at 9 locations.

7.1.1.1.1.6.2 Stress Analysis

The ANSYS computer program (stress pass) is used to compute the force and moment resultants due to SRV and LOCA related loads. A postprocessor program called "FORCE" is developed and used to scan for the maximum absolute values of forces and moments in the azimuth direction.

A multiplier factor for the force and moment resultants due to SRV loads has been established to cover for all the range of
3 frequencies as specified in Subsection 7.1.1.1.1.5.1. The following procedure is used to establish the multiplier.

A statistical analysis of all the forces and moments obtained from the three traces with varying frequencies in the range specified is performed. Trace number 82 is taken as the base to establish a multiplier factor to cover the other 2 traces and the variation of frequencies since it is observed to develop the highest stresses at most cross-sections. A multiplication factor of 1.7 is established to be applied to the resultant forces and moments from Trace #82 SRV discharge loading.

The forces and moments due to Chugging and Condensation Oscillation (CO) loads are considered. From the response spectra plots of Chugging and CO loads, it was found that KWU Sources 306 and 303 were the controlling cases. Therefore, these two load cases have been analyzed for stresses in containment. The displacement-time histories obtained from the GKM-II-M load
6 definition (see Subsection 9.5.3) are inputted to ANSYS computer model. A post processor program called SCALE was used to scan for the maximum values of forces and moments in the azimuth direction for each load case. For the containment sections shown in Figure A-2, the envelope of force resultants for all the load cases was inputted to the CECAP computer analysis (Refer to Flow Chart, Fig. 7-5, for further information).

7.1.1.1.2 Seismic Loads

Seismic loads constitute a significant loading in the strucutral
2 assessment. The same seismic loads as those used in the initial building design are used. In that design, a dynamic analysis was made using discrete mathematical idealization of the entire

structure using lumped masses. The resulting axial forces, moments, and shear at various levels due to the Operating Basis Earthquake and the Safe Shutdown Earthquake are used (see section 3.7 of FSAR). The effects of the seismic overturning moment and vertical accelerations are converted into forces at the elements. 2

As required by NUREG 0487, the effect of sloshing on the containment due to horizontal and vertical SSE is invetigated by performing a time-history analysis. As described in Subsection 4.2.4.7, pressure time histories due to seismic slosh were generated for input to the ANSYS model shown in Figure 7-1. 6

The response spectra generated from the seismic slosh load are presented in Figures B-51 to B-58. By inspection, the peaks are small.

7.1.1.1.3 Static and Thermal Loads

The loads under consideration are the static loads (dead load and accident pressure) and temperature loads (operating and accident temperature) which are all axisymmetrical.

a. To analyze the above static loads, an inhouse computer program FINEL is used. Moments, axial and shear forces are computed by FINEL in an uncracked axisymmetric finite element containment model.

b. The operating and accident temperature gradients are computed using ME 620 computer program (Bechtel program). This procedure is discussed in Subsection 3.8.4.1 of the FSAR. 2

c. The results from a, b and the dynamic/seismic analysis are combined and applied to a containment element. The element contains data relative to rebar location, direction and quantity and concrete properties. Within that wall element an equilibrium of forces and strains compatibility is established by allowing the concrete to crack in tension. In this way the stresses in the rebar and concrete are determined. The program used for this analysis is called CECAP. For further explanation, see Figure 7-5. 6

7.1.1.1.4 Load Combinations

All load combinations from 1 through 7a as presented on Table 5-1 have been analyzed. This was done under step c of Subsection 7.1.1.1.3 above. If all the SRV actuation cases and chugging-symmetric and asymmetric-loading along with other loads are to be considered, 41 loading combinations would have to be assessed. 2

Some of these load combinations have been eliminated by inspection since they are not governing. The five basic load combinations which have been assessed and presented in this report are 1, 4, 4a, 5a and 7a.

The reversible nature of the structural responses due to the pool dynamic loads and seismic loads is taken into account by considering the peak positive and negative magnitudes of the response forces and maximizing the total positive and negative forces and moments governing the design.

Seismic and pool dynamic load effects are combined by summing the peak responses of each load by the absolute sum (ABS) method. This is conservative and the square root sum of squares (SRSS) method is more appropriate since the peak effects of all loads may not occur simultaneously. However, the conservative ABS method is used in the design assessment of the containment and internal concrete structures in order to expedite licensing.

7.1.1.1.5 Design Assessment

2 Material stresses at the critical sections in the primary containment and internal concrete structure are analyzed using the CECAP computer program. Critical sections for bending moment, axial force and shear in three directions are located throughout the containment structure. The liner plate is not considered as a structural element. The CECAP program considers concrete cracking in the analysis of reinforced concrete sections. CECAP uses an iterative technique to obtain stresses considering the redistribution of forces due to cracking and in the process it reduces the thermal stresses due to the relieving effect of concrete cracking. The program is also capable of describing the spiral and transverse reinforcement stresses directly. The input data for the program consists of the uncracked forces, moments and shears calculated by FINEL, ANSYS, and seismic analysis. The loads are then combined in accordance with Table 5-1 with appropriate load factors.

7.1.1.1.6 Equipment Hatch

There are two equipment hatch openings in the containment drywell wall at approximately El. 723 ft. The openings are 180° apart and have a diameter of approximately 12 ft. Concrete and rebar stresses around the local hatch area were assessed.

7.1.1.1.6.1 Structural Model

6 Figure 7-6 shows the STARDYNE finite element model that was developed for analysis of the drywell wall around the hatch opening. The model consists of a section of the drywell wall, diaphragm slab, and wetwell wall with all boundaries at least two hole diameters away from the edge of the opening. All loads can be considered as symmetric about the opening centerline, thus only one half of the opening was modeled. The model uses quadrilateral plate elements with both membrane and bending stiffnesses. Uncracked sections with concrete material properties were used. Loads were applied statically and boundary conditions were chosen to be consistent with the type of loading applied (Ref. BC Topical Report #5).

7.1.1.1.6.2 Loads and Load Combinations

Load combinations are as per Table 5-1. Hydrodynamic loads applied to the model boundaries were taken from the force and moment results of the ANSYS containment model described in Section 7.1.1.1.1. Seismic loads were taken from force and moment results of the containment model as given in Section 7.1.1.1.2. Temperature was considered for the worst case wall gradient.

7.1.1.1.6.3 Design Assessment 6

Four critical sections around the hatch opening were used for assessment. Moment and force resultants from the STARDYNE model were input to computer program CECAP (CE987) to determine stresses in the concrete and rebar.

7.1.1.2 Reactor and Control Buildings

7.1.1.2.1 Hydrodynamic Loads

7.1.1.2.1.1 Structural Model

The construction of the SSES reactor building is such that no direct coupling with the containment occurs. A 2 in. separation joint is kept between the containment structure and the reactor building at all levels where the two structures abut, except at the base slab where a cold joint exists. This arrangement 1
minimizes the transfer of any direct dynamic response to the reactor building from the containment, where the SRV discharge and LOCA related hydrodynamic loads originate.

The horizontal motions of the containment are considered to be fully transferred to the reactor building through the cold joint at base slab; but the vertical motions are attenuated to account for the transfer through the rock under the two structures. The 2
attenuation has been accounted for by using the weighted average acceleration time histories at different points away from the containment and to the end of the reactor building boundary. The weighted average acceleration is defined as:

$$\bar{\ddot{a}} = \frac{\sum_{i=1}^{n} A_i \ddot{a}_i}{\sum_{i=1}^{n} A_i} = \sum_{i=1}^{n} C_i \ddot{a}_i$$

in which $\ddot{a}_i$ is the individual acceleration. A_i is the free 3
field area on which the acceleration acts and C_i is the weighted average coefficient.

This average time history is applied as an input motion to the reactor building dynamic model. The finite element soil-structure interaction model used for the attenuation study is shown in Figure 7-3.

The mathematical models of the reactor and control buldings
consist of lumped masses connected by the linear elastic members.
Using the elastic properties of the structural members, the
representative stiffness values for the models are determined.
2 The models used for design and hydrodynamic load assessment
programs prior to January 1, 1983, forNorth-South, East-West, and
Vertical directions are shown in Figures C-1, C-2, and C-3
respectively in Appendix 'C'. (These models are the same as
those used for the seismic analysis prior to January 1, 1983.)
Subsequently, revised reactor and control building dynamic models
for the North-South, East-West and Vertical directions have been
utilized in designs, qualifications and assessment programs. In
the months preceeding January 1, 1983, the models were revised as
a result of discrepancies in some of the original modeling
8 assumptions and representations. Using the revised models, a new
set of response spectra was generated. Safety related
structures, systems and components that were designed/qualified
to response spectra from the previous models were assessed to the
revised response spectra. Appendix L provides a discussion of
the modeling changes, revised response spectra and a description
of the assessment program.

7.1.1.2.1.2 Load Application

7.1.1.2.1.2.1 SRV Discharge Loads

The axisymmetric and asymmetric SRV discharge loadings used in
2 the reactor building assessment are described in the chapter 4.1
of this report. During the axisymmetric loading, only the gross
vertical motion of the base slab is transferred to the reactor
building. Therefore, the broadened response spectra curves for
axisymmetric loading given in Appendices 'C' and 'L' are for
vertical direction only. However, during the asymmetric loading,
gross vertical motion as well as the gross horizontal motion of
8 the base slab are considered in developing the vertical and
horizontal response spectra curves for the reactor building. The
vertical motions are attenuated and the horizontal motions are
directly transmitted to the Reactor/Control Building foundation,
refer to 7.1.1.2.1.1. The broadened response spectra curves for
asymmetric loading given in the Appendices 'C' and 'L' are for
both vertical and horizontal directions.

Three different pressure-time history traces (Figures 4-28
through 4-30 of Chapter 4) are used for generating response
2 spectra curves at the base of reactor building over a wide range
of frequencies, i.e., 55% to 110% of the original.

7.1.1.2.1.2.2 LOCA Related Loads

Loadings associated with Loss of Coolant Accident (LOCA) are
6 briefly described in 7.1.1.1.1.5.2. The gross vertical and
horizontal motions of the Containment base slab due to symmetric
and asymmetric load conditions are transferred to the
Reactor/Control Building. The vertical motions are attenuated

and the horizontal motions are directly transmitted to the Reactor/Control Building foundation, refer to 7.1.1.2.1.1.

7.1.1.2.1.3 Analyses

7.1.1.2.1.3.1 Time History Analysis

To develop floor response spectra, a time history analysis of Reactor/Control Building was performed using three separate lumped mass models which simulate the E-W, N-S, and vertical responses. The models are shown on Figures C-1/L-1, C-2/L-2, and C-3/L-3. The analytical procedure is presented in the flow chart in Figure 7-7.

The structural or modal damping used in the transient analysis of 8
the Reactor/Control Building for hydrodynamic loads due to SRV and LOCA is 4 percent of critical damping. Based on Regulatory Guide 1.61, this is the damping value recommended for reinforced concrete structures for OBE condition. As this value is used for both Upset condition (load combinations including OBE) and Faulted condition (load combinations including SSE) it is considered to be conservative.

Like in the containment, nodal point response spectra generated from several load conditions/traces were enveloped into one set of floor response spectra curves which represented SRV and LOCA.

For analyses utilizing the models presented in Appendix C, the damping values included in generating the floor response spectra and broadening of the peak frequencies of the spectra are the same as in the containment structure.

Appendix C contains the floor response spectra based on original 6
models for low damping values for SRV and LOCA. Appendix L
contains the floor response spectra based on the revised models 8
for low damping values for SRV and LOCA.

7.1.1.2.1.3.2 Stress Analysis

The largest responses at the reactor building base due to all the hydrodynamic loadings are used to obtain forces and moments in the members of the reactor building. The damping values are 2% and 5% for load combinations involving OBE and SSE/LOCA respectively. For the first part of the analysis, the Bechtel Program CE 917 is used to do the modal analysis for the vertical,
the East-West and the North-South directions. The results of 6
these analyses are used for input to the Bechtel Program CE 918. Another input to program CE 918, is the envelope of the acceleration response spectra of the gross motion time-histories due to KWU Sources 303, 305, 306, 309 and 314, symmetric and asymmetric load cases. These are obtained from steps 12 and 15 of Figure 7-4. The analysis determines member axial forces, shear forces, and bending moments. The analytical procedure is presented in the flow chart in Figure 7-8. The following load cases are considered.

1. Condensation-Oscillation vertical for 2% and 5% dampings.

2a. SRV vertical symmetric and asymmetric for 2% and 5% dampings.

2b. SRV North-South asymmetric for 2% and 5% dampings.

2c. SRV East-West asymmetric for 2% and 5% dampings. Case 2c
2 involved four separate conditions depending on the positions
of the Reactor Building crane.

3a. LOCA vertical symmetric and asymmetric for 2% and 5% dampings.

3b. LOCA North-South symmetric and asymmetric for 2% and 5% dampings.

3c. LOCA East-West symmetric and asymmetric for 2% and 5% dampings.

The combined forces and moments in the members of the models
presented in Appendix 'C' due to LOCA, SRV, and seismic loads for
both 2% and 5% damping values in each of the vertical, East-West,
8 and North-South directions were determined (see Figures E-23 thru
E-32). The stress analysis for the revised models is discussed
in Appendix L.

The reactor building superstructure steel was analyzed separately
using a 3-D finite element lumped mass model. The model is shown
in Figure E-21. The bridge crane and crane girders were also
modeled. The dynamic analysis was done using the time-history
method for seismic loads and response spectrum method for
hydrodynamic loads with Bechtel computer program BSAP. Member
2 forces and moments were generated for several different crane and
trolley positions. In general, the members experienced their
highest stresses when the bridge cranes were positioned such that
the maximum possible tributary load is distributed to the
columns. The critical case is when bridge crane bumper strikes
on one side of the superstructure during SSE or OBE. The results
are described in Subsection 7.2.1.2.

The refueling pools and girders were analyzed separately using a
3-D finite element model. The structure contains the surge tanks
vault, fuel shipping cask storage pool, spent fuel storage pool,
reactor well, and the steam dryer and separator storage pool.
For refuelling conditions, all compartments are considered full
of water with the exception of the surge tanks vault, which is
6 empty. For operating condition, only the spent fuel storage pool
and the fuel shipping cask storage pool are full of water while
the remaining compartments are empty. Water mass was lumped at
the compartment floors for the dynamic analysis.

The dynamic analysis was done using the response spectrum method with the computer program STARDYNE. Static and thermal analyses were also performed on STARDYNE program.

The analysis was performed for critical load combinations which were established by inspection. The results are described in subsection 7.2.1.2.

The box section columns supporting the refueling pool girders were included in the finite element model of the refueling pool analyzed above. The displacements and reactions obtained from the above model were used to assess the structural strength and stability of the columns. 6

7.1.1.2.2 Seismic Loads

The seismic analysis methodology is discussed in the subsection 3.7b.2.1 of the FSAR.

7.1.1.2.3 Static and Thermal Loads

The static loads are discussed in the subsection 3.8.4.4 of the FSAR.

7.1.1.2.4 Load Combinations

All individual loads are combined with the appropriate load factors as shown in Table 5-1. 2

Steel structures are checked for the load combination listed in Table 5-2.

7.1.1.2.5 Design Assessment

Critical sections for bending moment, axial force and shear in all three directions are located throughout the reactor building. Design capability at the critical sections is determined and then the design capability is compared with the actual forces and moments acting on the sections under all the load combinations. This comparison yields design margins. The design margins are discussed in Section 7.2.1.2

7.1.2 Structural Steel Assessment Methodology

7.1.2.1 Downcomer Bracing

7.1.2.1.1 Bracing System Description

There are 87 downcomers which extend vertically from the diaphragm slab to El. 660'-0" in the wetwell, which is approximately 12 feet below normal water level. The five vacuum breaker downcomers have been capped (see Figure 7-25), however, with regards to the bracing system, these five downcomers still provide vertical and lateral support, since they were capped at the downcomer exits. Downcomers are 24" O.D. pipes with 3/8 inch wall thickness, and are embedded in the diaphragm slab. Downcomers are separated into four independent quadrants. At El. 668'-0" all downcomers within a quadrant are tied together laterally with a bracing system consisting of 6 inch O.D. XX-strong pipes. The bracing members are not connected to either the wetwell wall or pedestal, thus eliminating stresses due to thermal expansion and wetwell wall displacement during hydrodynamic loads. The downcomers support the bracing vertically. The bracing connections consist of 1/2" ring plates and vertical stiffeners. The SRVD lines are not connected to the bracing. Figures 7-9 and 7-10 Sheets 1-3 show a plan view of the bracing system and the bracing connection details, respectively.

7.1.2.1.2 Structural Models

A 3-D STARDYNE finite element model of both the bracing and downcomers was developed for analysis of both the downcomers and bracing. The worst case quadrant of the four was chosen for modeling (3 ADS lines in the vicinity of the quadrant). The chosen quadrant extends from containment radial of 345° to radial of 66.7°. This quadrant consists of 23 downcomers modeled as pipes and having fixed boundary conditions at the diaphragm slab. Bracing members are modeled as pipe elements between downcomers using the actual brace member lengths. Beam connector elements extend from the node at the center line of each downcomer to the end of the brace member. Connector elements have equivalent section properties chosen so as to match stiffnesses determined analytically from the finite element model of the bracing connections described later. A lumped water mass consisting of two times the downcomer or bracing pipe volume (one time for the virtual mass effect and one time for the contained fluid) is used for nodes below the water level to account for the effect due to fluid-structure interaction. The model consists of 323 nodes, 251 pipe elements, 88 beam elements, and 276 dynamic degrees of freedom for reduced eigenvalue solution (STARDYNE HQR). Total weight considered in the model is 214.5 kips. Figure 7-11 (Sheets 1 & 2) shows the model.

A separate BSAP finite element model was developed for assessment of the bracing connection and downcomer in the vicinity of the connection. Figure 7-11, Sheet 3 shows the model. A section of the downcomer at the brace level is modelled with plate elements.

Boundaries of the downcomer were taken sufficiently far away from the connection to eliminate their influence. The connector plates, top partial plates, main ring plates, vertical stiffeners, and top ring plates were modeled with plate elements. (see Figure 7-11, Sheet 3). Brace member forces from the STARDYNE downcomer and bracing analysis were used as input loads for the assessment of the connection shown in Figure 7-10, Sheet 3. The BSAP finite element model was also used to determine the stiffnesses of the connector elements used in STARDYNE.

7.1.2.1.3 Loads

The basis for all hydrodynamic loads considered, is given in Sections 4 and 9.

7.1.2.1.3.1 SRV Discharge Loads

SRV actuation results in fluid pressure loads acting on the containment, downcomers, and bracing. All loads are based on KWU Traces 76, 82, and 35. With respect to the downcomers and bracing, two different types of loads can be defined. One type consists of inertia loading. This is movement of the containment structure due to SRV fluid pressures acting directly on the containment. The response spectrum method is used for analysis of this loading by applying the diaphragm slab spectra (El. 702'-3", see Appendix B) due to SRV to the STARDYNE model.

The second type of loads are described as submerged structure loads. These loads are due to the direct fluid pressures acting on the downcomers and bracing. As described in Subsection 4.1.3.7.3, potential flow theory and the method-of-images were used to calculate the load time histories for each downcomer in the model. These were applied to the STARDYNE model and a linear transient dynamic analysis was performed.

7.1.2.1.3.2 LOCA Related Loads

During a LOCA several types of loads act on the downcomers and bracing. Two of these are inertia and submerged structure loads. These have the same definition as for the SRV case and the analysis is performed in the same manner. This consists of the response spectra method for inertia load analysis and linear transient dynamic analysis for submerged structure loads.

Subsection 4.2.2.5 describe the methodology for determining the downcomer drag loads due to CO and chugging.

The containment response spectra generated for CO and chugging were determined by the methodology documented in Subsection 9.5.3.

In addition to the above loads, a dynamic lateral load due to chugging at the downcomer tip also occurs. For analyzing multiple downcomers in a quadrant, the generic multi-vent lateral load definition documented in Subsection 4.2.2.4 is used.

In addition, as required by the NRC, a single vent impulse with a 65 kip amplitude and 3 msec duration is applied one time per LOCA event to any single downcomer. This is a low probability event and is only used to show that the downcomer would not fail for one such loading.

For both types of tip loads, several linear transient dynamic analyses were performed. Loads were applied in directions, so as to maximize forces and moments in the downcomers and braces.

Air clearing in the downcomers during a LOCA also produces poolswell drag and fallback loads on the bracing. This load occurs before Chugging and CO and need not be considered in combination with those LOCA loads. Bechtel Nuclear Staff defined the pressure time history loads on the braces and they were analysed locally for these loads (see Subsection 4.2.1.7). An overall equivalent static load on the bracing system was applied to the STARDYNE model.

7.1.2.1.3.3 Seismic Loads

The diaphragm slab response spectra developed for OBE and SSE as described in Subsection 3.8.1.4.1 of the FSAR were used as input to the STARDYNE model to obtain resultant forces in the downcomers and bracing.

In addition to the inertia loading, seismic sloshing in the suppression pool imparts loads on the downcomers and bracing (see Subsection 4.2.4.7). The sloshing frequency is very low and static loads based on the sloshing fluid pressures were applied to the STARDYNE model.

7.1.2.1.3.4 Static and Thermal Loads

The dead load of the downcomers and bracing is considered. The LOCA condition results in the worst temperature loading (Ref. Figure 4-52, Section 4). A maximum temperature of 180°F is used with 65° being taken as the stress free condition.

7.1.2.1.4 Load Combinations

Load combinations and allowable stresses are in accordance with Subsection 5.2. The stochastic loads, i.e., seismic inertia, and the inertia and submerged pressure loads of SRV and chugging are combined by SRSS method. The chugging lateral load is defined as a single impulse and is added by absolute sum method. The seismic sloshing loads are added by absolute sum method due to their low frequency wave. All the static loads are combined by absolute sum method. Poolswell is not combined with other LOCA loads since it preceeds them (see Subsection 4.2.1).

7.1.2.1.5 Design Assessment

The results from the three dimensional STARDYNE model of the bracing and downcomers are combined to determine the total stress due to both axial forces and moments. A comparison between the calculated combined stresses and allowables is made and the stress margins are given in Appendix A.

7.1.2.2 SRV Support and Column

7.1.2.2.1 Description of SRV Support Assemblies and Suppression Chamber Columns

In the suppression pool, there are three types of support configurations to laterally brace the SRV discharge lines; two are at El. 666' and the third is at El. 667'. Each type of support assembly consists of two horizontal bracing members and at least one knee brace member. The support assemblies are connected from the SRV discharge lines to the adjacent column (or columns) with 4-inch diameter double extra strong pipes.

The support assemblies restrain the SRV discharge lines in a horizontal direction but not in vertical direction. The general plan of these support assemblies is shown in Figure 7-12 and member connection and the details are shown in Figure 7-13.

The suppression chamber columns are 42 inch diameter pipes with 1-1/4 inch wall thickness. The columns are attached at the diaphragm slab at El. 700' and at the basemat at El. 648'.

7.1.2.2.2 Structural Models

a. The columns were independently analyzed for static and dynamic loads. The analytical methods used for non-hydrodynamic loads such as dead, live, pressure, temperature, seismic and pipe rupture loads are described in the FSAR, Section 3.8.3.4.5.

b. For the hydrodynamic SRV loads, the ANSYS computer program was used. For the hydrodynamic LOCA related loads NASTRAN computer program was used. A typical column model is shown in Figure 7-14. The total length of the column is divided into beam elements which are joined at node points. An effective water mass due to submergence was also considered. Dynamic horizontal forces were applied to the column at the node points below the water. Time-varying forces and moments in the column were calculated for each element.

c. Another finite element model was developed in which the SRV lines, the SRV support assembly and the column were included. SRV and LOCA related submerged structure loads as well as the inertia effects from the dynamic loads were considered. From this analysis, the SRV discharge pipe's reactions at the support locations were obtained.

The assessment of the columns is based on the combination of loads obtained from a, b, and c above. The assessment of the SRV support assembly is based on loads obtained in paragraph c above. Each of the support types is analyzed separately.

In order to determine the local stresses in the vicinity of the support assembly on the column wall, the column was modeled withthe NASTRAN computer program using plate finite elements. The model is shown in Figure 7-15.

7.1.2.2.3 Loads

The support assemblies of the SRV discharge lines are submerged structures. They are subjected to direct pressure loads from air bubble etc., the reactions from the SRV lines due to SRV discharge loads, and the inertia loads due to the building response from dynamic loads. Thermal loads are due to increase in pool temperature during LOCA.

7.1.2.2.3.1 SRV Discharge Loads

The horizontal SRV discharge pressure-time histories are considered as acting on the columns, the SRV discharge pipe and the support assemblies. The vertical SRV discharge pressures are considered as acting on the support assemblies alone.

The reactions from the SRV lines obtained from Subsection 7.1.2.2.2.c are applied to the end of the SRV support members for computation of longitudinal member forces. The direct hydrodynamic pressures due to SRV actuations are applied statically perpendicular to the SRV support members, with a dynamic magnification factors. The SRV hydrodynamic pressures are determined as defined in Subsection 4.1.3.7. This is done for the computation of moments and shear forces in the members.

The inertia forces from building responses due to SRV discharge load are also included by using the response spectra results shown in Appendix B.

Member forces and moments obtained from direct application of SRV discharge pressures, reaction forces of SRV pipe line, and the inertia building responses are combined by absolute sum.

The SRV submerged structure load definition is based on Subsection 4.1.3.7.

7.1.2.2.3.2 LOCA Related Loads

During a LOCA, several phenomena cause hydrodynamic loads on the SRV support assemblies. The manner in which the LOCA related loads are applied to the SRV support assemblies is exactly the same as described for the SRV loads in Subsection 7.1.2.2.3.1. The LOCA related loads used for the bracing are used for the SRV support assemblies, except the lateral tip load due to chugging is eliminated.

Among the LOCA related loads, poolswell load and fallback load occur before Chugging and CO and need not be considered in combination with those LOCA loads. The pressure time history loads, due to pool swell, for the SRV assembly supports, were determined by linearly reducing the pressure time history, due to poolswell, for the downcomer bracing, by the ratio of the diameters.

7.1.2.2.3.3 Seismic Load

The seismic loads on the coupled structure of SRV lines, support assemblies, and columns were obtained by dynamic analysis using the response spectra developed for OBE and SSE as described in Subsection 3.8.1.4.1 of the FSAR.

7.1.2.2.3.4 Static Load

The dead load, thermal load and bouyancy of the support assemblies were considered.

7.1.2.2.3.5 Load Combinations

The load combinations and allowable stresses are in accordance with Subsection 5.2. Although the loads on the bracing system under consideration act in a random horizontal directions, each individual load is applied to the system in the worst possible direction to find the maximum resultant forces.

7.1.2.2.3.6 Design Assessment

The combined stresses due to axial forces and bending moments were determined for all bracing members. Comparison between the resulting calculated stresses and the allowable stresses has been made. Resulting stress margins for the bracing members and their connections are tabulated in Appendix A.

7.1.2.3 Openings In Containment Liner

7.1.2.3.1 Equipment Hatch-Personnel Air Lock

The portion of the equipment hatch-personnel air lock not backed by concrete was reevaluated for additional loads due to hydrodynamic effects (SRV and LOCA). This reevaluation was performed by Chicago Bridge and Iron Company (CBI) under subcontract from Bechtel. The general arrangement of the personnel lock is shown in Figure 7-16.

The personnel air lock doors are designed to withstand a pressure of 55 psig in the containment vessel. The door mechanism is designed to seal the door against an internal pressure of 5 psig.

For reevaluation, CBI used their computer program E781 for static analysis of shells. The program is based on Reference 77. Equivalent static loads were considered for seismic and hydrodynamic cases using peak spectral accelerations. CBI used the hydrodynamic spectra as given in Appendix C. Design Load combinations given in Table 5-2 were used with modifications for forces on the structure due to thermal expansion of pipes under accident conditions. Stress limits specified in the ASME code were used.

CBI's model was divided into 2 parts:

The first model comprised the 1" thick cylinder and the 3" thick flange extending to the parting joint. An axissymmetrical configuration was used since the shape of the containment vessel at its intersection with the equipment hatch is conical. No restraints at the junction with the containment vessel were considered.

The second model included the 3" thick flange beyond the parting joint, the conical head and a portion of the personnel lock extending from the interior bulk head to an appropriate distance beyond. .

At the flange interface, the seismic, SRV, LOCA, jet and pressure loads have a tendency of prying open the door. A meridional force is, therefore, required to permit relatively small radial deflections and rotations at the interface. This force was applied as a restoring force at the parting joint in the form of a meridional force and a transverse shear. Relative displacements were evaluated to assure leaktightness.

The major dead load contribution is in the airlock. Therefore, dead loads and loads from seismic accelerations were applied to the second model as discontinuous loads at the center of gravity of the air lock.

Loads due to SRV, Seismic and LOCA cases were combined by SRSS.

7.1.2.3.2 CRD Removal Hatch, Suppression Chamber Access Hatch And Equipment Hatch

These hatches were subcontracted to CBI for design and analysis for additional SRV and LOCA loads. Designs were performed manually in accordance with Bechtel specifications and appropriate design codes. Details of the CRD removal hatch and equipment hatch are given in Figures 7-17 and 7-18.

7.1.2.3.3 Refuelling Head and Support Skirt

Reevaluation of the refuelling head and support skirt was performed by CBI under subcontract from Bechtel. Figure 7-19 shows the refuelling head.

CBI's program E 781 was used for the static analysis. For dynamic analysis, equivalent pressures from the peak response spectra at El. 778.8 ft. were used. The static and dynamic stresses were then combined as per Table 5-2 of this report. Leak tightness of the flanged joint was investigated for the various loads and suitable pre-stress was recommended to prevent separation of the flange joint components.

7.1.3 Liner Plate Assessment Methodology

FSAR Subsection 3.8.1 provides a description of the liner plate and anchorage system for the containment.

The analysis of the liner plate and anchorages for nonhydrodynamic loads is in accordance with Reference 18.

For the analysis of the liner plate and anchorage for hydrodynamic suction loads, the contributing load on the liner is that due to the net "negative" pressure.

The loads considered for this assessment are KWU Chugging, KWU SRV, hydrostatic pressure and wetwell air pressure.

Figure 7-20 presents the maximum negative pressure due to KWU chugging which were scanned from the symmetric and asymmetric load conditions of Sources 303, 305, 306 and 309. As can be noted from Figure 7-20, Trace 306 gives the maximum negative pressure on all locations.

The maximum negative pressure due to the actuation of all SRV's is -7.8 psi.

The hydrostatic pressure of 24' water gives 10.4 psi pressure on the base slab liner plate.

The wetwell air pressure is 25 psi due to a small break LOCA.

For normal condition the combination of hydrostatic pressure and the actuation of all the SRV's is considered. The distribution of this pressure is shown in Figure 7-21.

For abnormal condition, the combination of KWU chugging, SRV, hydrostatic pressure and wetwell air pressure is considered. The phasing of SRV and chugging events is obtained by aligning the maximum suction peaks. These events are combined by direct addition of pressures as demonstrated in Figure 7-22. The total net peak pressures for the abnormal condition are tabulated in Figure 7-23. Point 1 in this figure does not lie on pressure boundary and thus, is not critical.

The assessment of liner plate is found in Subsection 7.2.1.5.

7.1.4 Downcomer Assessment Methodology

7.1.4.1 Downcomer System Description

In the wetwell, there are 87 downcomers, 82 of which function as dry well vents during a LOCA. The other 5 provide wetwell to drywell pressure relief through the two vacuum breakers in series mounted on each of them. These five downcomers are capped at the bottom end to protect the vacuum breakers from the cycling due to chugging. Appendix K provides the assessment of capping five of the eighty-seven downcomers as a fix for VB cycling during chugging.

Downcomer layout, location of vacuum breakers and the cap arrangement are shown on Figures 7-9, 7-24 and 7-25, respectively.

7.1.4.2 Structural Model

The downcomers are modeled with the bracing system as described in Subsection 7.1.2.1.2.

The downcomers with the vacuum breakers are included in the STARDYNE model.

6 An additional 3-D model was developed in which not only the bracing system and downcomers as described in subsection 7.1.2.1.1 were included, but also the vacuum breaker, the vacuum breaker support and a column. This was done in the same quadrant as described in Subsection 7.1.2.1.1.

7.1.4.3 Loads and Load Combinations

Loads affecting the downcomers are the same as those described in Subsection 7.1.2.1.3. Load combinations are given in Table 5-3. The SRSS sum is used for the dynamic loads, except for the chugging lateral and seismic sloshing loads which are added by absolute sums as described in Subsection 7.1.2.1.4.

7.1.4.4 Design Assessment

Reference 30 is used for checking the downcomer stresses due to the load combinations given in Table 5-3.

7.1.4.5 Fatigue Evaluation of Downcomers In Wetwell Air Volume

In an effort to evaluate the steam bypass potential arising from a failure of the downcomers in the wetwell air space, a complete fatigue analysis of the same has been performed. Specifically, the analysis was performed where the downcomers penetrate the diaphram slab as shown in Figure 7-26. This analysis considered all the cyclic loading acting on the downcomers and is in accordance with the applicable portions of ASME Code. This evaluation is considered supplemental and does not displace the
5 original design basis for these lines as set forth in the appropriate FSAR/DAR sections.

7.1.4.5.1 Loads and Load Combinations used for Assessment

The downcomers are subject to numerous dynamic and hydrodynamic loads from normal, upset, and LOCA-related plant operating conditions. For purposes of fatigue evaluation, the following loads are include: (1) All significant thermal and pressure transients. (2) All cyclic effects due to the hydrodynamic loads including SRV actuations, CO and chugging. (3) Seismic effects. A description of each of these loads is provided in the appropriate DAR sections. The determination of load combinations as well as number and duraction of each event is obtained from the applicable sections of DFFR, and FSAR.

7.1.4.5.2 Acceptance Criteria

The design rules, as set forth in the ASME Boiler and Pressure Vessel Code, Section III, Subsection NB were utilized for the fatigue assessment. When required, allowables for fatigue stress evaluation were based on Mill certification reports for downcomers. 5

7.1.4.5.3 Methods of Analysis

The SRV discharge lines and downcomers in the wetwell air volume, were analyzed for the appropriate load combinations and their associated number of cycles. The combined stresses and corresponding equivalent stress cycles were computed to obtain the fatigue usage factors in accordance with the equations of Subsection NB-3600 of the ASME Code.

7.1.4.5.4 Results and Design Margins

The cumulative usage factors for the various loading conditions for the downcomer (see Figure 7-26) are summarized in Table 7-3.

7.1.5 BOP Piping and SRV Systems Assessment Methodology

The BOP piping and SRV systems were analyzed for the loads discussed in Section 5.5 using Bechtel computer programs ME101 and ME632. These programs are described in FSAR Section 3.9. Static and dynamic analysis of the piping and SRV systems are performed as described in the paragraphs below. 6

Static analysis techniques are used to determine the stresses due to steady state loads and/or dynamic loads having equivalent static loads. The drag and impact loads are applied as equivalent static loads.

Response spectra at the piping anchors are obtained from the dynamic analysis of the containment subjected to LOCA and SRV loading. Piping systems are then analyzed for these response spectra following the method described in Reference 19. 1

Time history dynamic analysis of the SRV discharge piping subjected to fluid transient forces in the pipe due to relief valve opening is performed using Bechtel computer code ME632.

7.1.5.1 Fatigue Evaluation of SRV Discharge Lines in Wetwell Air Volume

In an effort to evaluate the steam bypass potential arising from a failure of the SRV discharge line in the wetwell air space, a complete fatigue analysis of the same has been performed. 6

Specifically, structural analyses of all the SRV discharge lines from the diaphragm slab penetration to the quencher was performed. Fatigue evaluation of fluedhead penetration, elbows and 3-way restrainst attachment to pipe was done. This analysis considered all the cyclic loading acting on the SRV discharge lines and is in accordance with the applicable portions of ASME Code. This evaluation is considered supplemental and does not displace the original design basis for these lines as set forth in the appropriate FSAR/DAR sections.

7.1.5.1.1 Loads and Load Combinations Used for Assessment

The SRV discharge lines are subject to numerous dynamic and hydrodynamic loads from normal, upset, and LOCA-related plant operating conditions. For purposes of fatigue evaluation, the following loads are included: (1) All significant thermal and pressure transients. (2) All cyclic efforts due to the hydrodynamic loads including SRV actuations, CO and chugging and (3) Seismic effects. A description of each of these loads is provided in the appropriate DAR sections. The determination of load combinations as well as number and duration of each event is obtained from the applicable sections of DFFR and FSAR.

7.1.5.1.2 Acceptance Criteria

The design rules, as set forth in the ASME Boiler and Pressure Vessel Code, Section III, Subsection NB were utilized for the fatigue assessment. When required, allowables for fatigue stress evaluation were based on Mill certification reports for SRV discharge lines.

7.1.5.1.3 Methods of Analysis

The SRV discharge lines, in the wetwell air volume, were analyzed for the appropriate load combinations and their associated number of cycles. The combined stresses and corresponding equivalent stress cycles were computed to obtain the fatigue usage factors in accordance with the equations of Subsection NB-3600 of the ASME Code.

7.1.5.1.4 Results and Design Margins

The cumulative usage factors for fluedhead, 3-way restraint attachment to pipe and elbow are summarized in Table 7-4.

7.1.6 NSSS Assessment Methodology

"Safety related" General Electric Company supplied NSSS piping and equipment located within the containment and the reactor and control buildings are subjected to hydrodynamic loads due to SRV and LOCA discharge effects principally originating in the suppression pool of the containment structure. Section 4.1 and 4.2 describe the methodologies used to define these SRV and LOCA loads, respectively. The NSSS piping and equipment are assessed to verify their adequacy to withstand these hydrodynamic loads in combination with seismic and all other applicable loads in accordance with the load combinations given in Table 5-5.

The structural system responses for the SRV and LOCA suppression pool hydrodynamic phenomena are generated by Bechtel Power Corporation using defined forcing functions. These structural system responses are transmitted to General Electric in the form of (1) broadened response spectra and (2) acceleration time-histories at the pedestal to diaphram floor intersection and the stabilizer elevation.

The response spectra for piping attachment points on the reactor pressure vessel, shield wall and pedestal complex (above the pool area) are generated by General Electric, based upon the acceleration time-histories supplied by Bechtel Power Corporation, using a detailed lumped mass beam model for the reactor pressure vessel internals, including a representation of the structure. For the assessment of the NSSS primary piping (main steam and recirculation) a combination of General Electric and Bechtel developed response spectra are used as input responses for all attachment points of each piping system. For the assessment of the NSSS floor mounted equipment, except the reactor pressure vessel, the broadened response spectra supplied directly by Bechtel are used.

The acceleration time-histories and the detailed reactor pressure vessel and structure lumped mass beam model are used to generate the forces and moments acting on the reactor pressure vessel supports and internal components. These forces and moments are used for the GE assessment of reactor pressure vessel supports and internals.

The structural system response for the LOCA induced annulus pressurization transient asymmetric pressure build up in the annular region between the biological shield wall and the reactor pressure vessel is based on pressure time-histories supplied by Bechtel. These pressure time-histories are combined with jet reaction, jet impingement and pipe whip restraint loads for the assessment. A time-history analysis is performed resulting in accelerations, forces and moment time-histories as well as response spectra at the piping attachment points on the reactor pressure vessel, shield wall, pedestal, pressure vessel supports and external components (see FSAR Appendices 6A and 6B).

7.1.6.1 NSSS Qualification Methods

7.1.6.1.1 NSSS Piping

The NSSS piping stress analyses are conducted to consider the secondary dynamic responses from: (1) the original design-basis loads including seismic vibratory motions, (2) the structural system feedback loads from the suppression pool hydrodynamic events, and (3) the structural system loads from the LOCA induced annulus pressurization from postulated feedwater, recirculation and main steam pipe breaks.

Lumped mass models are developed by General Electric for the NSSS primary piping systems, main steam and recirculation lines. These lumped mass models include the snubbers, hangers and pipe mounted valves, and represent the major balance of the plant branch piping connected to the main steam and recirculation systems. Amplified response spectrum for all attachment points within the piping system are applied; i.e., distinct acceleration excitations are specified at each piping support and anchor point. The detailed models are analyzed independently to determine the piping system resulting loads (shears and moments) for:

1) each design-basis load which includes pressure, temperature, weight, seismic events, etc.,

2) the bounding suppression pool hydrodynamic event; and

3) the annulus pressurization dynamic effects on the unbroken piping system.

Additionally, the end reaction forces and/or accelerations for the pipe mounted/connected equipment (valves and nozzles) are simultaniously calculated.

The piping stresses from the resulting loads (shears and moments) for each load event are determined and combined in accordance with the load combinations delineated in Table 5-5. These stresses are calculated at geometrical discontinuities and compared to ASME code allowable determined stresses (ASME Boiler and Pressure Vessel Code, Section III-NB-3650) for the appropriate loading condition in order to assure design adequacy. Computer codes used to perform the NSSS piping stress analysis are described in FSAR Section 3.9.1.2.

7.1.6.1.2 Valves

The reaction forces and/or accelerations acting on the pipe mounted equipment when combined in accordance with the required load combinations are compared to the valve allowables to assure design adequacy. The reactor core pressure boundary valves are qualified for operability during seismic and hydrodynamic loading events by both analysis and test. This qualification is unique for each valve.

7.1.6.1.3 Reactor Pressure Vessel, Supports and Internal Components

The bounding load combinations for seismic, hydrodynamic and annulus pressurization forces are established within each acceptance criteria range (upset, emergency and faulted). At the initial analysis step, the loads are conservatively combined using the maximum vertical forces with the maximum horizontal shears and moments from all combinations within each acceptance criteria range. These conservative maximum loads are then compared to generic bounding forces originally used to establish the component design. When the combined calculated forces are less than the design forces, then the component is deemed adequate. When the calculated forces are greater than the design forces, then the increased stresses are compared to the material allowables. When the calculated stresses are below the material allowables, then the design is deemed adequate. If the increased stresses are above the material allowables, then the specific load combination is identified and another stress analysis is conducted using refined methods, if required, to demonstrate the component adequacy.

In certain cases, component test results are combined with analyses to assess component adequacy. Fatigue evaluations of the Reactor Pressure Vessel, supports and internal components are also conducted for SRV cyclic duty loads. The equipment is analyzed for fatigue usage due to SRV load cycles based upon the loading during the SRV events. SRV fatigue usage factors are calculated and combined with all other upset condition usage factors to obtain a cumulative fatigue usage factor.

Computer programs used to conduct RPV component analyses are described in FSAR Section 3.9.1.2.

7.1.6.1.4 Floor Structure Mounted Equipment

7.1.6.1.4.1 Qualification Methods

The adequacy of the design of the equipment is assessed by one of the following:

a. Dynamic analysis
b. Testing
c. Combination of testing and analysis

The choice is based on the practicality of the method depending upon function, type, size, shape, and complexity of the equipment and the reliability of the qualification method.

In general, the requirements outlined in IEEE-344-75, Reference 55, are followed for the qualification of equipment.

7.1.6.1.4.1.1 Dynamic Analysis

7.1.6.1.4.1.1.1 Methods and Procedures

The dynamic analysis of various equipment is classified into three groups according to the relative rigidity of the equipment based on the magnitude of the fundamental natural frequency described below.

(a) Structurally simple equipment - comprises that equipment which can be adequately represented by a one degree of freedom system

(b) Structurally rigid equipment - Comprises that equipment whose fundamental frequency is:

(i) greater than 33 Hz for the consideration of seismic loads, and,

(ii) greater than the high frequency asymptate (ZPA) of the required response spectra (RRS) for the consideration of hydrodynamic loads

(c) Structurally Complex equipment - Comprises that equipment which cannot be classified as structurally simple or structurally rigid.

The appropriate response spectra for specific equipment are obtained from the response spectra for the floor at which the equipment is located in a building for OBE, SSE and hydrodynamic loads. This includes the vertical as well as both the N-S and E-W horizontal directions. For equipment which is structurally simple, the dynamic loading (either seismic or hydrodynamic) consists of a static load corresponsing to the equipment weight times the acceleration selected from the appropriate response spectrum. The acceleration selected corresponds to the equipment's natural frequency, if the equipment's natural frequency is known. If the equipment's natural frequency is not known, the acceleration selected corresponds to the maximum value of the response spectra.

For equipment which is structurally rigid, the seismic load consists of a static load corresponding to the equipment weight times the acceleration at 33 Hz, selected from the appropriate response spectrum and the hydrodynamic loading consist of a static load corresponding to the equipment weight times the accelerations at the ZPA, selected from the appropriate response spectrum.

For the analysis of structurally complex equipment, the equipment is idealized by a mathematical model which adequately predicts the dynamic properties of the equipment and a dynamic analysis is performed using any standard analysis procedure. An acceptable alternative method of analysis is by static coefficient analysis for verifying structural integrity of frame type structures that can be represented by a simple model. No determination of natural frequencies is made and the response of the equipment is assumed to be the peak of the response spectrum. This response is then multiplied by a static coefficient of 1.5 to take into account the effects of both multifrequency excitation and multimode response.

7.1.6.1.4.1.2 Testing

In lieu of performing dynamic analysis, dynamic adequacy is established by providing dynamic test data. Such data must conform to one of the following:

1. Performance data of equipment which has been subjected to equal or greater dynamic loads (considering appropriate frequency range) than those to be experienced under the specified dynamic loading conditions.

2. Test data from comparable equipment previously tested under similar conditions, which has been subjected to equal or greater dynamic loads than those specified.

3. Actual testing of equipment in operating conditions simulating, as closely as possible, the actual installation, the required loadings and load combinations.

A continuous sinusoidal test, sine beat test, or decaying sinusoidal test is used when the applicable floor acceleration spectrum is a narrow band response spectrum. Otherwise, random motion test (or equivalent) with broad frequency content is used.

The equipment to be tested is mounted in a manner that simulates the actual service mounting. Sufficient monitoring devices are used to evaluate the performance of the equipment. With the appropriate test method selected, the equipment is considered to be qualififed when the test response spectra (TRS) envelopes the required response spectra (RRS) and the equipment did not malfunction or fail. A new test does not need to be conducted if equipment requires only a very minor modification such as additional bracings or change in switch model, etc., and proper justification is given to show that the modifications do not jeopardize the strength and function of the equipment.

7.1.6.1.4.1.3 Combined Analysis and Testing

There are several instances where the qualification of equipment by analysis alone or testing alone is not practical or adequate because of its size, or its complexity, or large number of similar configurations. In these instances a combination of analysis and testing is the most practical. The following are general approaches:

(a) An analysis is conducted on the overall assembly to determine its stress level and the transmissibility of motion from the base of the equipment to the critical components. The critical components are removed from the assembly and subjected to a simulation of the environment on a test table.

(b) Experimental methods are used to aid in the formulation of the mathematical model for any piece of equipment. Mode shapes and frequencies are determined experimentally and incorporated into a mathematical model of the equipment.

7.1.6.1.4.2 Computer Programs

Computer programs used to conduct equipment analyses are described in FSAR Section 3.9.1.2.

7.1.7 Balance of Plant (BOP) Equipment Assessment Methodology

6 Seismic Category I BOP equipment located within the containment and the reactor and control buildings are subjected to hydrodynamic loads due to SRV LOCA discharge affects principally originating in the suppression pool of the containment structure. The equipment and equipment support are assessed to verify their adequacy to withstand these hydrodynamic loads in combination with seismic and all other applicable loads in accordance with the load combinations given in Section 5.7.

7.1.7.1 Hydrodynamic loads

2 7.1.7.1.1 SRV Discharge Loads

Loadings associated with the axisymmetric and asymmetric SRV discharges are described in Chapter 3 and 4 of this report. Acceleration response spectra at the various elevations where the equipment are located have been generated for all appropriate pressure history traces (Figures 4-28 thru 4-30 of Chapter 4) for damping values of 1/2%, 1%, 2%, and 5%. These have been enveloped into a single curve for each of the above damping values. Such enveloped curves are generated for each of the N-S, E-W and vertical directions. These curves form the basis for the SRV loads for equipment assessment.

7.1.7.1.2 LOCA Related Loads

6 Loadings associated with loss-of-coolant accident (LOCA) are described in Section 4.2. Acceleration response spectra at various elevations where the equipment are located have been generated for the LOCA loads for damping values of 1/2%, 1%, 2% and 5%. These have been enveloped into a single curve for each of the above damping values. Such enveloped curves are generated for each of the N-S, E-W and vertical directions.

These curves form the basis for the LOCA loads for equipment assessment.

7.1.7.2 Seismic Loads

2 The details of seismic input and seismic loads are discussed in Section 3.7 of FSAR. The effects of both operating basis earthquake (OBE) and safe shutdown earthquake (SSE) are considered. These loads are provided in the form of Acceleration response spectra at each floor for damping values of 1/2%, 1%, 2% and 5% for each of N-S, E-W and vertical directions.

7.1.7.3 Other Loads

In addition to hydrodynamic and seismic loads, other loads such as dead loads, live loads, operating loads, pressure loads, thermal loads, nozzle loads and equipment piping interaction loads, as applicable, are also considered.

7.1.7.4 Qualification Methods

The adequacy of the design of the equipment is assessed by one of the folowing:

a. Dynamic analysis

b. Testing under simulated conditions

c. Combination of testing and analysis.

The choice is based on the practicality of the method depending upon function, type, size, shape, and complexity of the equipment and the reliability of the qualification method.

In general the requirements outlined in IEEE-344-75, Reference 55, are followed for the qualification of equipment.

7.1.7.4.1 Dynamic Analysis

7.1.7.4.1.1 Methods and Procedures

The dynamic analysis of various equipment is classified into three groups according to the relative rigidity of the equipment based on the magnitude of the fundamental natural frequency described below.

(a) Structurally simple equipment - comprises of that equipment which can be adequately represented by one degree of freedom system.

(b) Structurally rigid equipment - Comprises of that equipment whose fundamental frequency is:

  (i) greater than 33 Hz for the consideration of seismic loads, and,

  (ii) greater than 80 Hz for the consideration of hydrodynamic loads.

(c) Structurally Complex equipment - Comprises of that equipment which cannot be classified as structurally simple or structurally rigid.

When the equipment is structurally simple or rigid in one direction but complex in the other, each direction may be classified separately to determine the dynamic loads.

The appropriate response spectra for specific equipment are obtained from the response spectra for the floor at which the equipment is located in a building for OBE, SSE and hydrodynamic loads. This includes the vertical as well as both the N-S and E-W horizontal directions.

For equipment which is structurally simple, the dynamic loading (either seismic or hydrodynamic) consists of a static load corresponding to the equipment weight times the acceleration selected from the appropriate response spectrum. The acceleration selected corresponds to the equipment's natural frequency, if the equipment's natural frequency is known. If the equipment's natural frequency is not known, the acceleration selected corresponds to the maximum value of the response spectra.

For equipment which is structurally rigid the seismic load consists of a static load corresponding to the equipment weight times the acceleration at 33 Hz, selected from the appropriate response spectrum and the hydrodynamic loading consist of a static load corresponding to the equipment weight times the acceleration at 80 Hz., selected from the appropriate response spectrum.

For the analysis of structurally complex equipment, the equipment is idealized by a mathematical model which adequately predicts the dynamic properties of the equipment and a dynamic analysis is performed using any standard analysis procedure. An acceptable alternative method of analysis is by static coefficient analysis for verifying structural integrity of frame type structures such as members physically similar to beams and columns that can be represented by a simple model. No determination of natural frequencies is made and the response of the equipment is assumed to be the peak of the response spectrum at damping values as per Section 7.1.7.4.1.2. This response is then multiplied by a static coefficient of 1.5 to take into account the effects of both multifrequency excitation and multimode response.

7.1.7.4.1.2 Appropriate Damping Values

The following damping values are used for the design assessment:

1) Load Combinations involving OBE but not hydrodynamic loads - 1/2%

2) Load Combinatiosn involving SSE but not hydrodynamic loads - 1%

3) Load Combinations involving hydrodynamic loads, or seismic and hydrodynamic loads - 2%

If the actual damping value of the equipment is different (from test results) then these actual values are used.

7.1.7.4.1.3 Three Components of Dynamic Motions

The responses such as internal forces, stresses and deformations at any point from the three principal orthogonal directions of the dynamic loads are combined as follows:

The response value used is the maximum value obtained by adding the response due to vertical dynamic load with the larger value of the responses due to one of the horizontal corresponding dynamic load by the absolute sum method.

7.1.7.4.2 Testing

In lieu of performing dynamic analysis, dynamic adequacy is established by providing dynamic test data. Such data must 2
conform to one of the following:

1. Performance data of equipment which has been subjected to equal or greater dynamic loads (considering appropriate frequency range) than those to be experienced under the specified dynamic loading conditions.

2. Test data from comparable equipment previously tested under similar conditions, which has been subjected to equal or grater dynamic loads than those specified.

3. Actual testing of equipment to the required load 6
combinations while simulating the actual field installation.

A continuous sinusoidal test, sine beat test, or decaying sinusoidal test is used when the applicable floor acceleration spectrum is a narrow band response spectrum. Otherwise, random motion test (or equivalent) with broad frequency content is used.

The equipment to be tested is mounted in a manner that simulates the actual service mounting. Sufficient monitoring devices are used to evaluate the performance of the equipment. With the appropriate test method selected, the equipment is considered to be qualified when the test response spectra (TRS) envelopes the required response spectra (RRS) and the equipment did not malfunction or fail. A new test does not need to be conducted if equipment requires only a very minor modifications such as additional bracings or change in switch model etc. and proper 2
justification is given to show that the modifications do not jeopardize the strength and function of the equipment.

7.1.7.4.3 Combined Analysis and Testing

There are several instances where the qualification of equipment by analysis alone or testing alone is not practical or adequate because of its size, or its complexity, or large number of similar configurations. In these instances a combination of analysis and testing is the most practical. The following are general approaches:

(a) An analysis is conducted on the overall assembly to determine its stress level and the transmissibility of motion from the base of the equipment to the critical components. The critical components are removed from the assembly and subjected to a simulation of the environment on a test table.

(b) Experimental methods are used to aid in the formulation of the mathematical model for any piece of equipment. Mode
2 shapes and frequencies are determined experimentally and incorporated into a mathematical model of the equipment.

7.1.8 Electrical Raceway System Assessment Methodology

7.1.8.1 General

The FSAR Subsection 3.7b.3.1.6 provides a detailed description of the electrical raceway system design methodology. The analysis and design of supports or Electrical Raceway Systems for non-hydrodynamic loads are in accordance with Reference 3.7b-7 of the FSAR. SRV discharge and LOCA loads are considered similar to seismic loads by using appropriate floor response spectra for the hydrodynamic loads. A damping value of 7% of critical is used for all raceway systems for abnormal/extreme load condition and a damping value of 3% of critical is used for normal load condition involving SRV discharge loading only.

7.1.8.2 Loads

6 7.1.8.2.1 Static Loads

The static loads are the dead loads and live loads. For cable trays, the weight of the cable is considered to be 45 lbs/ft and a concentrated live load of 200 lb. applicable at any point or cable tray span is used.

7.1.8.2.2 Seismic Loads

The details of the seismic motion input are discussed in Section 3.7 of the FSAR. The effects of the operating basis earthquake (OBE) and the Safe Shutdown earthquake (SSE) are considered.

7.1.8.2.3 Hydrydynamic Loads

The details of the axisymmetric and asymmetric SRV discharge loads, as well as LOCA loads including condensation-oscillation and chugging are discussed Section 4.0

The enveloped acceleration response spectra at each floor for N-S, E-W, and vertical directions have been generated and widened.
8 These curves form the basis for the hydrodynamic load assessment of the electrical raceway system. Examples of the response spectrum curves for the containment and Reactor and Control buildings are presented in Appendices B, C and L.

7.1.8.3 Analytical Methods

Cable tray systems are modeled as three dimensional dynamic
6 system consisting of several consecutive supports complete with cable trays and longitudinal and transverse bracing. The cable tray properties are determined from the load deflection tests.

Member joints are modeled as spring elements having rotational stiffness with known spring values as determined from the test results. 6

Composite spectra are developed by enveloping the broadened floor response spectra for critical floors for seismic, SRV and LOCA loading conditions. The design spectrum is obtained by adding these response spectra curves by the square root sum of the squares method. The composite response spectra curves are obtained for vertical and two horizontal directions. Acceleration values utilized in the design are determined from the composite response spectra with the consideration of a ± 20% frequency variation at the fundamental frequency of the cable 8 tray system.

Modal and response spectrum analyses are performed utilizing "Bechtel Structural Analysis Program" (BSAP) which is a general purpose finite-element computer program. The seismic and hydrodynamic responses are combined by the square root sum of the squares method. The total response due to the dynamic loads is calculated by determining absolute sum of vertical response and only the larger response of the two horizontal responses.

Dead and live load stresses are determined from a static analysis of a plane frame model using BSAP computer program and these results are combined with those from the response spectrum analysis. For normal load condition, SRV discharge stresses are proportioned from the response spectrum analysis of SSE plus SRV discharge plus LOCA loads according to their spectral acceleration ratios at the fundamental frequencies. Several different support types which are widely used have been analyzed by these methods.

An alternative method for analyzing other support types which occur less frequently, uses long hand calculations by a response spectrum analysis technique. The support may be idealized as a single degree of freedom system. In general, the maximum peak spectral accelerations were used in the analysis. In some cases where the stresses are critical, a more refined value for the 6 acceleration response was used corresponding to the computed system fundamental frequency and considering a frequency variation as explained earlier in this section. The vertical and horizontal seismic responses are combined according to Subsection 3.7b.2.6 of the FSAR. The member stresses are kept within the elastic limit.

7.1.9 HVAC Duct System Assessment Methodology

The SRV discharge and LOCA are considered similar to seismic loads by using appropriate floor response spectra generated for the CO, chugging, and SRV loads described in Section 4.0.

A damping value of 5% of critical is used for load combinations involving SSE, SRV discharge and LOCA loads. While a damping value of 3% of critical is used for load combinations involving

OBE and/or SRV discharge loads. For a discussion of the seismic
and hydrodynamic loads input for HVAC duct system assessment,
refer to Subsections 7.1.8.2.2 and 7.1.8.2.3, respectively. The
HVAC duct system had been analyzed by the alternative method
8 described in the Subsection 7.1.8.3 by determining the
fundamental frequencies of the system in three directions. The
inertia forces are determined from the composite spectra
described in Subsection 7.1.8.3 to establish member forces and
moments due to hydrodynamic as well as seismic loads.

7.2 DESIGN CAPABILTY MARGINS

7.2.1 Stress Margins

Stresses at the critical sections for all of the structures described in Section 7.1, piping and equipment are evaluated for all the loading combinations presented in Section 5.0. The stress margin is defined as

$$(1 - \text{stress ratio}) \times 100$$

$$\text{stress ratio} = \Sigma\, C_n \cdot \frac{fn}{Fn}$$

Where, f_n = Actual Stress
f_n = Allowable Stress

C_n = Amplification Coefficient

7.2.1.1 Containment Structure

The results from the structural assessment of the containment structure are summarized in Appendix A. Figure A-2 shows the design sections in the basemat, containment walls, reactor pedestal, and the diaphragm slab which were considered in the structural assessment. The tables in Appendix A give the calculated design stresses and margins for load combination Equations 1, 4, 4a, 5, 5a, and 7 (as listed in Table 5-1).

The following observations are made from a review of the structural stresses. The calculated stress level is very low for load combination equation No. 1 (an upset condition) i.e., reinforcing bar stresses are less than 20 ksi. In general, among all the applicable load combinations, the most critical load combination is No. 7a. The maximum reinforcing bar design stress is predicted as 47.24 ksi, which occurs in a wetwell section on the outside face helical bars when using the absolute sum (ABS) method. This given a minimum stress margin of 12.5% (see Figure A-29).

However, the calculated maximum reinforcing bar design stresses are relatively low in the reactor pressure vessel pedestal, diaphragm slab, and the base slab, as they are less than 18 ksi, 34 ksi, and 45 ksi respectively. The maximum principal concrete compressive stress occurs at the base slab and is calculated as 4280 psi. Thus, all the reinforcing bar design stresses are below the allowble stresses. It should be noted that the allowable stresses on which the margins are based, are related to the minimum specified strength. The actual quality control test results for the reinforcing bars and concrete show the material strengths to be higher than the minimum specified and therefore, the margins are actually greater than calculated.

In general, the concrete stresses were found to be low except at section 27 in the containment basemat (see Figure A-2), where the concrete stress in compression exceeded the maximum allowable stress in five load combinations out of six that were considered in this report. However, under each load combination the concrete is in triaxial compression at Section 27. Under the worst load case, the "hydrostatic" component of the stress is 2830 psi and the "deviatoric" component is only 1392 psi. Because of this large hydrostatic component, the concrete
6 compressive strain is much smaller than the value of 0.003 in/in permitted by the codes. The concrete, therefore, has a very large strain margin before failure will commence. It must also be emphasized that not only the actual strength of the placed concrete is higher than the minimum specified, as indicated in the paragraph above, but that the concrete continues to gain strength after placement. The increase in strength at the end of five years could be as much as 20% over the 90 days strength. Therefore, the locally high compressive stresses in the concrete at Section 27 are deemed acceptable.

7.2.1.2 Reactor and Control Building

The results of the structural assessment of the Reactor and Control Building are summarized in Appendices E and L. The
8 analytical results presented herein and in Appendix "E" are based on analyses performed using the structural models shown in Appendix "C". The assessment results based on analyses performed using the revised structural models (as discussed in Subsection 7.1.1.2.1.1) are presented in Appendix "L". Figures E-1 through E-22 show the design sections in the basemat and the concrete structure composed of floor slabs, shear walls, blockwalls, refueling pool girders, as well as floor structural steel and superstructure steel, which were considered in the structural assessment. The sections selected for assessment were considered to be most critical based on previous seismic calculations. The
6 tables in Appendix E give the calculated design stresses and margins for the critical load combinations equations 1 and 7a of Table 5-1 and equations 1 and 7 Table 5-2. The other load combinations do not govern.

In the case of floor slabs, the calculated stress levels, in general, are very low for slabs above El. 683.0 ft. The governing load combination is equation 1 of Table 5-1 (normal condition) and the reinforcing steel stresses are significantly less than 20 ksi. For slabs below El. 683.0 ft. also, the governing load combination is equation 1 of Table 5-1. The maximum reinforcing steel stress was 49.79 ksi, which occurs in
6 the reactor building slab at El. 645.0 ft. (see Figure E-33). The selected floor sections for the review and assessment are given in Figures E-1 through E-6.

In the case of shear walls, the maximum rebar stress was 43.25 ksi, and the minimum stress margin is 20% (see Figure E-34). The assessed elements are given in Figures E-1, E-3, E-4, E-7, and E-8.

In the blockwalls the calculated maximum reinforcing bar design stress is 30.6 ksi for load combination equation 7a (see Figure E-35). The minimum stress margin for compressive stress in the concrete is 22%. The blockwall elements reviewed for assessment are shown in Figures E-9 through E-16.

In the case of Reactor Building structural steel (see Figure E-36), load combination Eq. 7 of Table 5-2 generally governs. The maximum bending stress was found to be 31.9 ksi which is less than the allowable value. This stress occurs in a beam at El. 719.1 ft. In the other cases the stress margins are 29% or more. The structural steel elements selected for assessment are given in Figures E-17 through E-20.

A three-dimentsional lumped mass model was generated for determining the dynamic response of the Reactor Building Crane Support Structure. This model is shown in Figure E-21. Equation 7, Table 5-2 serves as the governing loading combination. Selected members as given in the model were assessed for structural integrity and stability. The design margins for structure and crane girder are 0% (see Figure E-37). This condition is reached by letting the rails deform in such a way that the crane bumper strikes against one of the rail girders.

The assessment of the Refueling Pool Girder shows that the maximum rebar stress was 51.7 ksi and the design margin is 4% (see Figure E-38). The elements selected for assessment are shown in Figure E-22.

As shown in Figure E-38a, the box section columns supporting the refueling pool were found to have adequate strength for resisting dead, live, and dynamic loads including seismic (OBE, SSE), SRV, and LOCA loads imposed by the refueling girders. Equation 6 was found to be the governing euqation for columns. The strength of the box section columns is summarized under elements 41 and 42. The minimum design margin is 38%.

7.2.1.3 SRV Support Assemblies and Suppression Chamber Columns

The stresses at critical sections of the SRV support assemblies and the suppression chamber columns were calculated separately for the load combinations in Table 5.2. The maximum stresses are governed by load combination 7a for both the SRV support assemblies and columns. The results of the SRV support assembly analysis are shown in Figure A-67. The lowest stress margin of SRV support system which includes all bracing members and connections is 21.7%. On the other hand, the maximum stresses in column (42 inch diameter pipe), at the top and bottom bolt anchorages are shown in Figure A-59. The lowest stress margin in the column structure is 11.4%.

7.2.1.4 Downcomer Bracing

Stresses in the bracing members and connections were checked using the load combinations and allowable stresses as given in

Table 5-2. Dynamic loads were combined on the basis of the SRSS method. Combined axial and bending stresses were investigated for the most highly loaded members. Equations 1, 3, 4 and 7 govern for the brace members with the design margins as indicated in Figure A-60. For the connections, equations 2 and 7 are critical and the resulting design margins are shown in Figure A-61. All bracing members and connections are adequate.

7.2.1.5 Liner Plate

For the normal load condition, the liner plates do not experience any net negative pressure as can be observed from Figure 7-21.

For the abnormal load condition, the maximum net negative pressure on the pressure boundary portion of the liner plates occurs on the containment wall, at point 8 of Figure 7-23, and is -6.39 psi. Since this is an impulse load of .004 seconds duration and the liner plate is supported every 2 feet, the stress in the liner plate is 12.5 ksi, well below the allowable. There is a margin of 51% for pullout of the embedded T steel sections that support the liner plate.

The liner plates on the base slab are supported by embedded W4x13 structural steel members every 10 feet. The maximum negative net pressure on the base slab occurs at the corner. The magnitude is
6 -5.12 psi. However, due to liner plate connection on the corner between base slab and containment wall, the negative net pressure does not cause a bending problem in the liner plate and no pullout problem on W4x13 sections. The liner plate located away from the corner described above, do not experience negative pressure.

7.2.1.6 Downcomers

A list of downcomer and bracing system modal frequencies and participation factors is given in Table 7-5. The fundamental system mode is at a frequency of 1.8 Hz, which is a cantiliever type of mode for all downcomers moving together. Downcomer stresses were checked according to ASME Code Section NB3652 using load combinations in Table 5-3. Stresses and design margins are given in Figure A-66.

7.2.1.7 Electrical Raceway System

It is apparent from the analysis that high stresses are a result of responses due to horizontal inertia loads. During the normal load condition, stresses under SRV discharge are generally low. However, for the abnormal/extreme load condition, certain members required strengthening to relieve high stresses. After implementing these modifications, the resultant stresses do not exceed the allowable stresses in any member of the electrical raceway system supports. The modifications to electrical raceway systems are a result of the assessments performed using the
8 structural models shown in Appendix "C". The assessment results based on analyses performed using the revised structural models

(as discussed in Subsection 7.1.1.2.1.1) are presented in 8
Appendix "L".

7.2.1.8 HVAC Duct System

Similar to the analysis of the electrical raceway system, the
analysis of the HVAC duct system demonstrated that most of the 6
support members have actual stresses lower than the allowable
stresses. However, certain structural members required
strengthening to relieve high stresses under the abnormal/extreme
load conditions. The strengthening of HVAC duct supports are a
result of the assessments performed using the structural models
shown in Appendix "C". The assessment results based on the
analyses performed using the revised structural models (as 8
discussed in Subsection 7.1.1.2.1.1) are presented in Appendix
"L".

7.2.1.9 BOP Equipment

All Seismic Category I BOP equipment are re-evaluated for the
hydrodynamic and non-hydrodynamic loads (see Subsection 7.1.7)
via the SSES Seismic Qualification Review Team (SQRT) program.
For each BOP equipment, 4-page SQRT summary forms have been 6
prepared documenting the re-evaluation of that equipment. In
some cases, modifications were required to reduce the stresses
below the allowables. The modifications to BOP equipment are a
result of the assessments performed using the structural models
shown in Appendix "C". The assessment results based on analyses
performed using the revised structural models (as discussed in 8
Subsection 7.1.1.2.1.1) are presented in Appendix "L".

In response to SER Open Item #11, the BOP SQRT summary forms
requested by the NRC were formally submitted on February 25, 1982
(Reference: PLA-1024). The remaining BOP SQRT summary forms are 6
available for review.

7.2.1.10 NSSS Equipment 8

All Seismic Category I NSSS equipment are re-evaluated for the
load combinations given in Table 5-5 via the SSES SQRT program. 6
For each NSSS equipment, SQRT summary forms are prepared
documenting the re-evaluation of that particular equipment. The
assessment results based on analyses performed using the revised
structural models (as discussed in Subsection 7.1.1.2.1.1) are 8
presented in Appendix "L".

The NSSS SQRT summary forms requested by the NRC will be formally
submitted to the NRC under the SSES SQRT program. All NSSS SQRT 6
summary forms are available for review.

7.2.1.11 NSSS and BOP Piping 8

As documented in Subsection 7.1.5 and 7.1.6.1.1, all Seismic
Category I BOP and NSSS piping have been analyzed for 6
hydrodynamic and non-hydrodynamic loads per the load combinations

given in Subsections 5.5 and 5.6, respectively. As a result of this evaluation, many modifications were required to maintain the
6 stresses below the allowable values. Appendix F provides a summary of the stresses and design margins for selected BOP piping systems based on analysis results for the structural models shown in Appendix "C". The above required modifications are a result of analyses performed using the Appendix "C"
8 structural models. The assessment results based on analyses performed using the revised structural models (as discussed in Subsection 7.1.1.2.1.1) are presented in Appendix "L".

The results of the above evaluation are documented in stress reports, which are available for NRC review.

7.2.2 Acceleration Response Spectra

6

7.2.2.1 Containment Structure

The method of analysis and load description for the acceleration response spectra generation are outlined in Subsection 7.1.1.1.1.6.1. Appendix B contains example acceleration response spectra for SRV, condensation oscilation and chugging, and seismic sloshing load cases. From a review of the SRV and LOCA
8 acceleration response spectra curves the maximum spectral accelerations are tabulated in Table 7-1 for 1% of critical damping.

7.2.2.2 Reactor and Control Building

6 The methods of analysis and load application for the computation of the acceleration response spectrum in the reactor and control building are described in Subsections 7.1.1.2.1.1 and 7.1.1.2.1.2. Appendix "C" contains the acceleration response spectra for low damping values for SRV and LOCA load cases based on analyses performed using the structural models shown in Figures C-1, C-2 and C-3. Appendix "L" contains example response spectra generated using the revised structural models, as
8 discussed in Subsection 7.1.1.2.1.1. From a review of the SRV and LOCA acceleration response spectra curves based on the models presented in Appendix "C", the maximum spectral accelerations are tabulated in Table 7-2 for 4% of critical damping.

7.2.3 Containment Liner Openings

7.2.3.1 Equipment Hatch-Personnel Air Lock

Stresses in the equipment hatch-personnel air lock were all within allowable limits. However, as a result of the new loads,
6 bolt pre-load had to be increased from 65 to 72 kips to maintain acceptable levels of displacement at the flanged joint. The resultant equivalent radial load applied at the bearing on the hinge support results in a minimum safety factor of 3 at ultimate for the roller and race.

7.2.3.2 CRD Removal Hatch, Suppression Chamber Access Hatch

and Equipment Hatch

CBI's analysis indicated no stresses in excess of the specified allowable limits for the additional loadings considered.

7.2.3.3 Refueling Head and Support Skirt

The refueling head and flange were found to have no stresses exceeding allowable limits. The only effect of the new loads applied was to increase bolt pre-stress from 161 to 200 kips to maintain leaktightness at the flanged joint. Figure A-33.1 gives the stress margins in the refueling head and the flange.

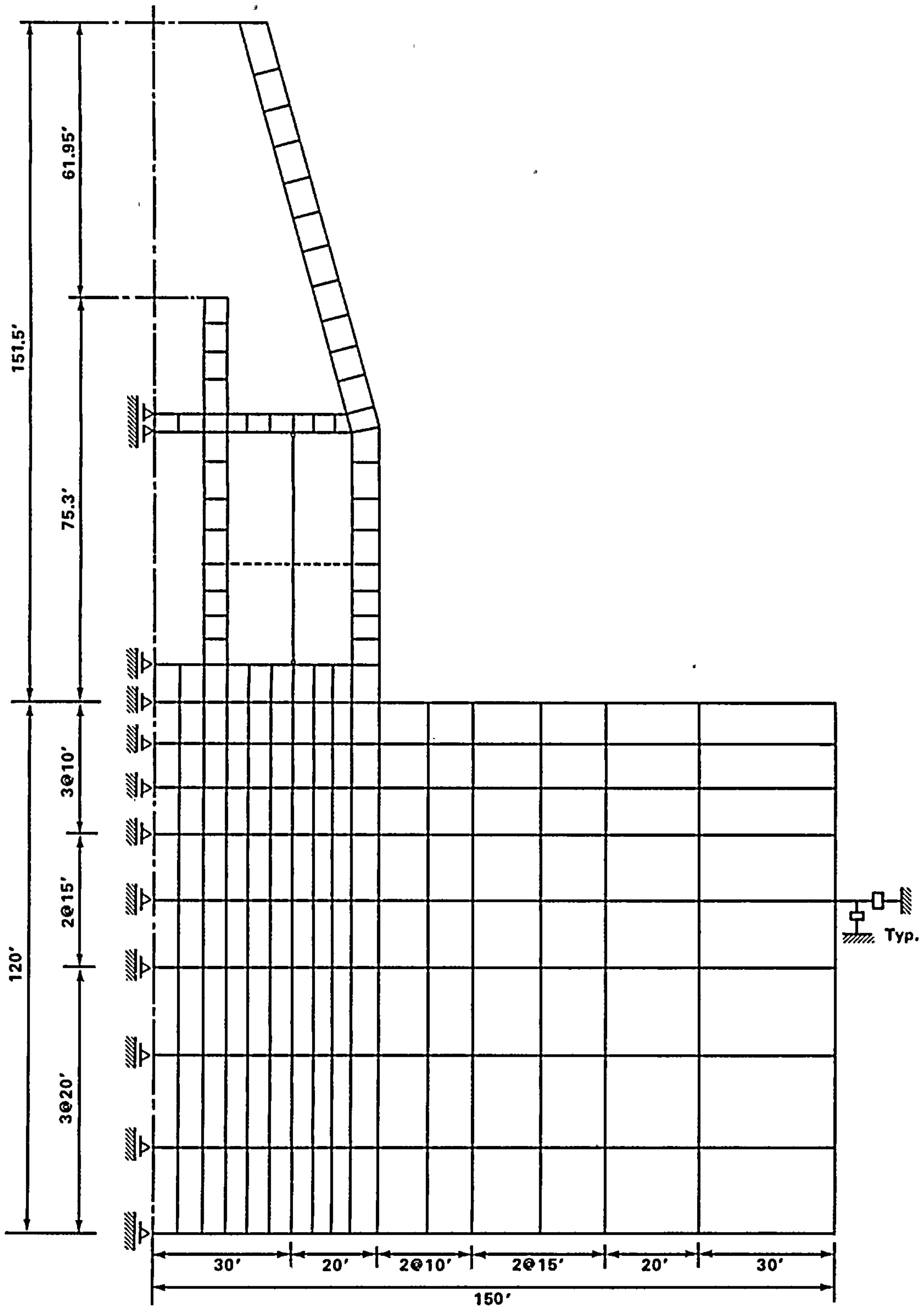

Rev. 2, 5/80

SUSQUEHANNA STEAM ELECTRIC STATION
UNITS 1 AND 2
DESIGN ASSESSMENT REPORT

FINITE ELEMENT
SOIL-STRUCTURE
INTERACTION MODEL

FIGURE 7-3

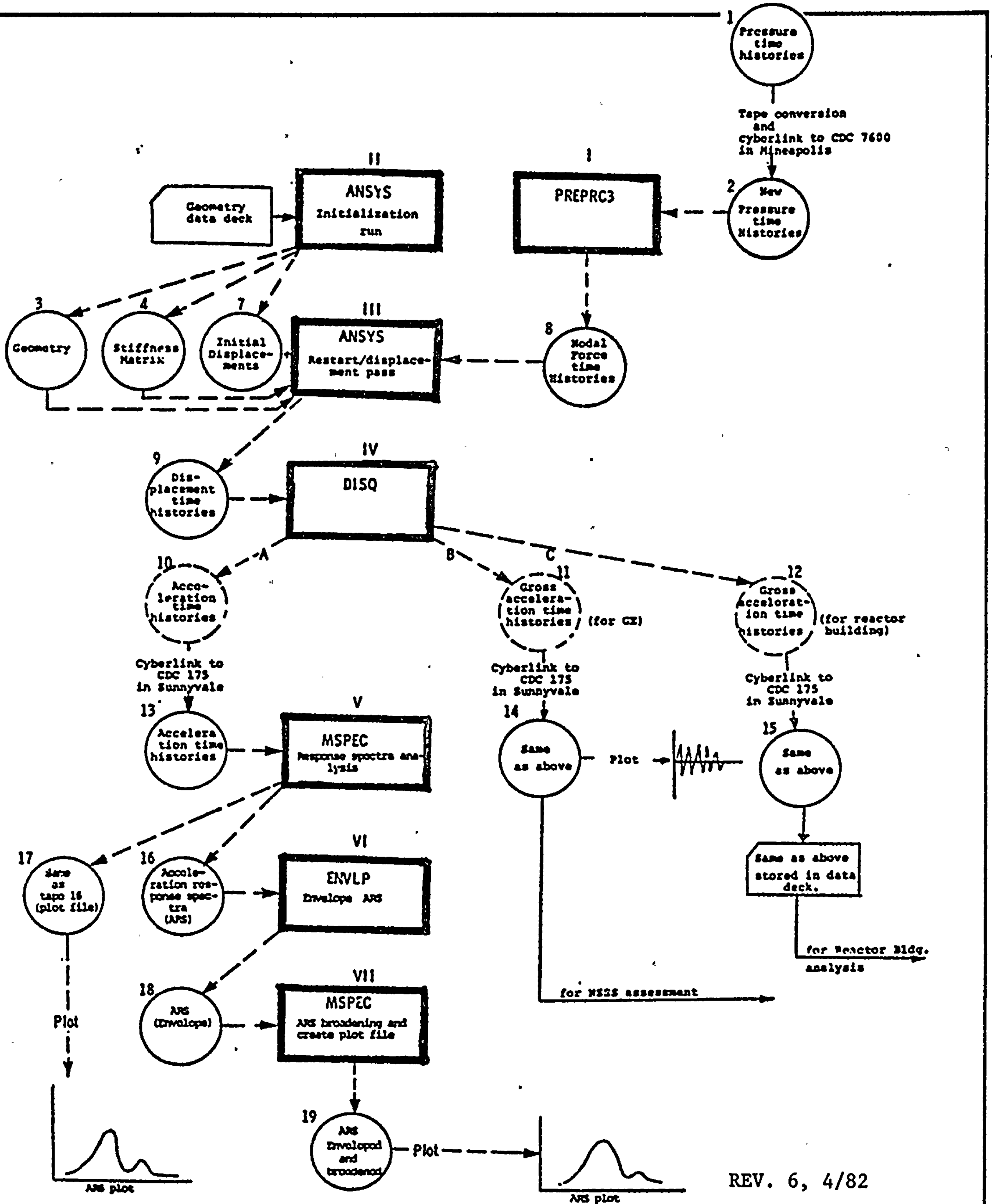

REV. 6, 4/82

SUSQUEHANNA STEAM ELECTRIC STATION
UNITS 1 AND 2
DESIGN ASSESSMENT REPORT

CONTAINMENT RESPONSE ANALYSIS

FIGURE 7-4

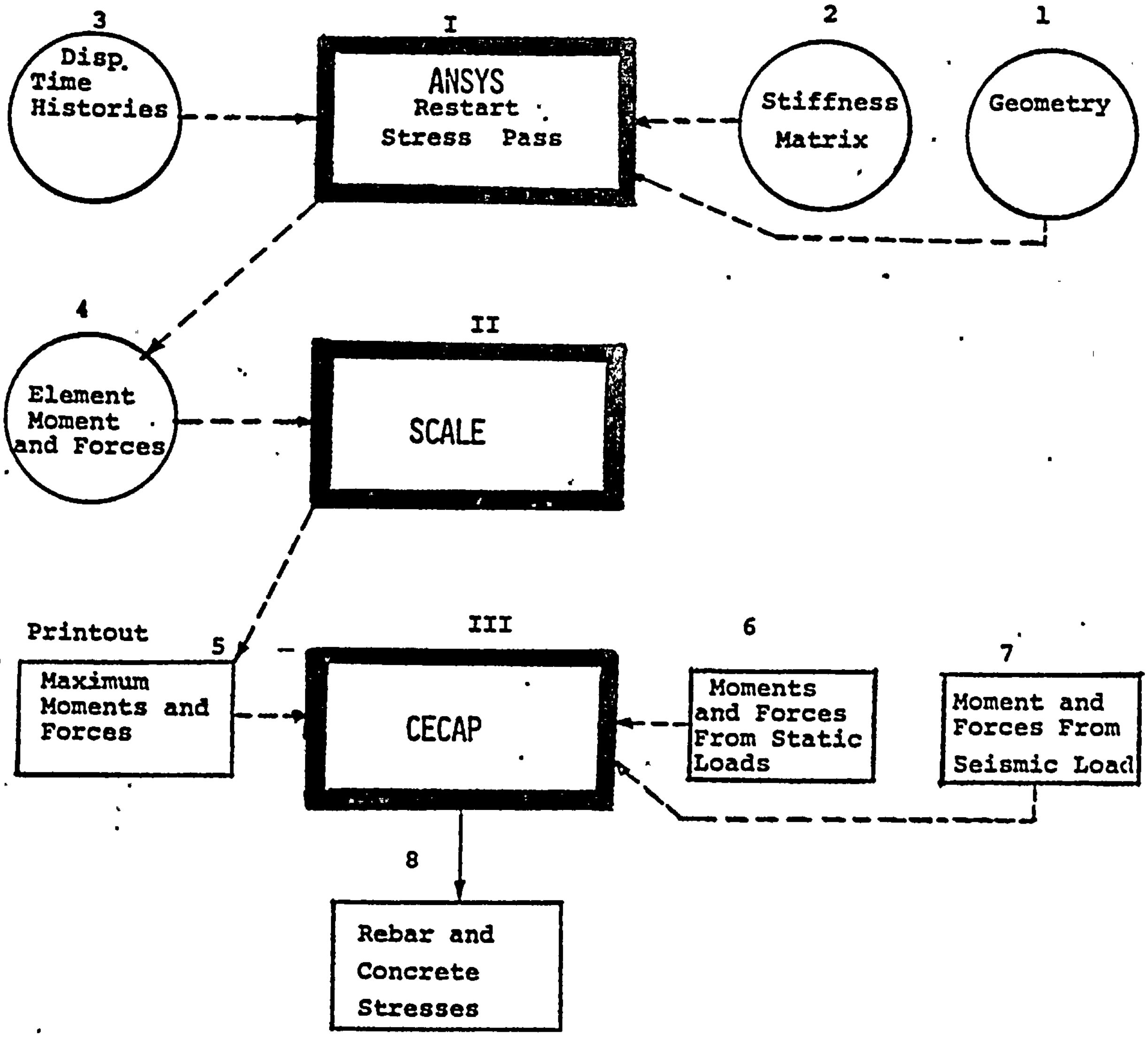

REV. 6, 4/82

SUSQUEHANNA STEAM ELECTRIC STATION
UNITS 1 AND 2
DESIGN ASSESSMENT REPORT

CONTAINMENT STRESS ANALYSIS

FIGURE 7-5

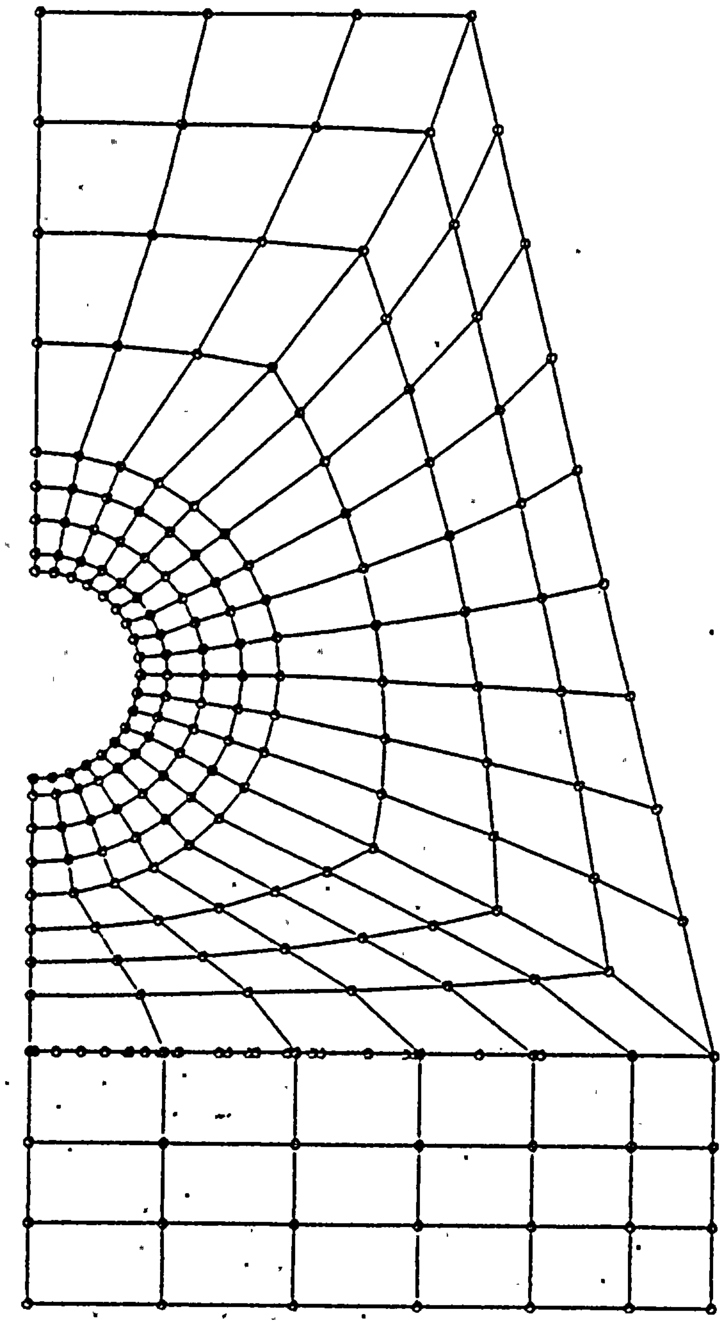

REV. 6, 4/82

SUSQUEHANNA STEAM ELECTRIC STATION
UNITS 1 AND 2
DESIGN ASSESSMENT REPORT

FINITE ELEMENT CONTAINMENT EQUIPMENT HATCH MODEL

FIGURE 7-6

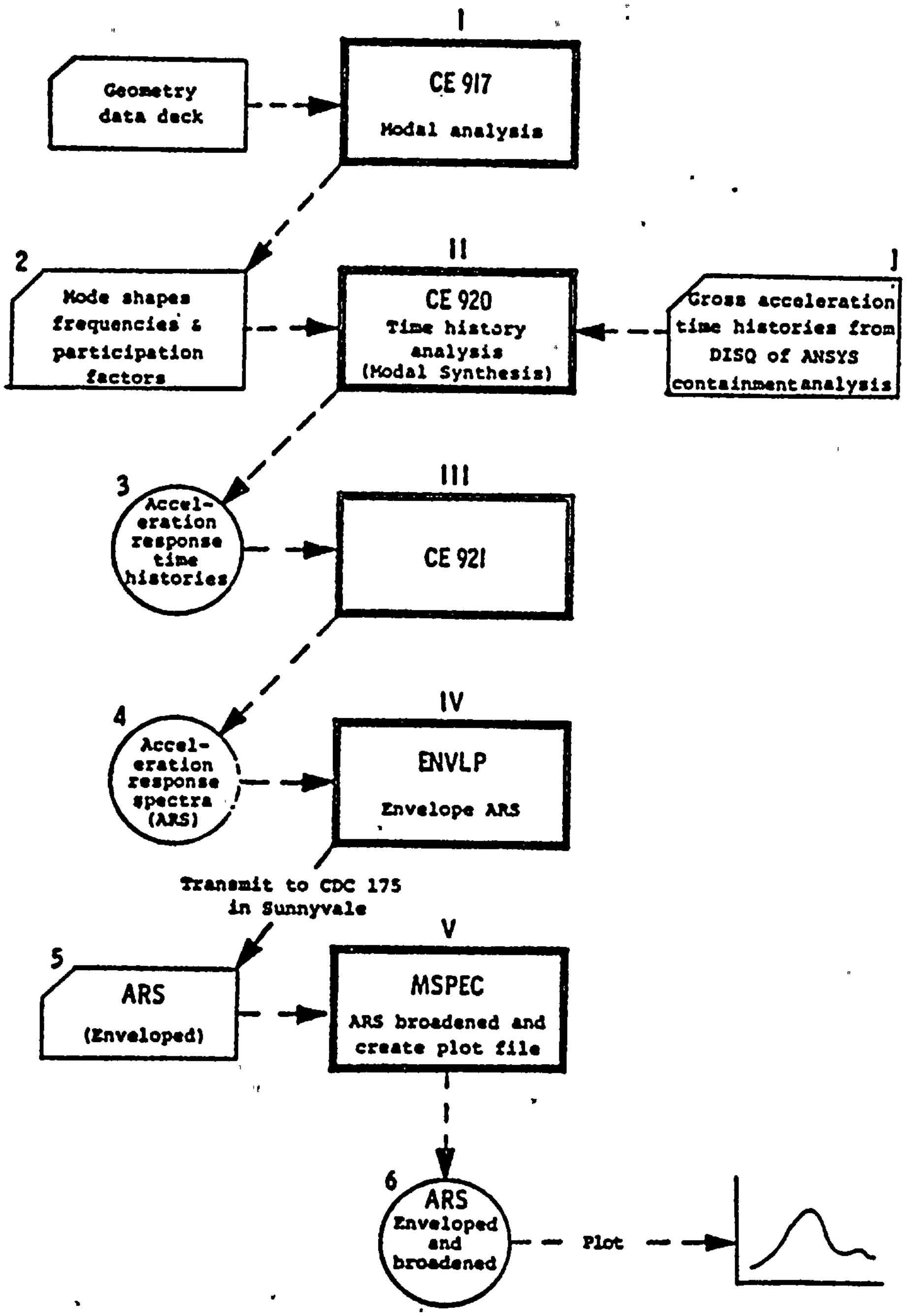

REV. 6, 4/82

SUSQUEHANNA STEAM ELECTRIC STATION
UNITS 1 AND 2
DESIGN ASSESSMENT REPORT

REACTOR BUILDING RESPONSE ANALYSIS

FIGURE 7-7

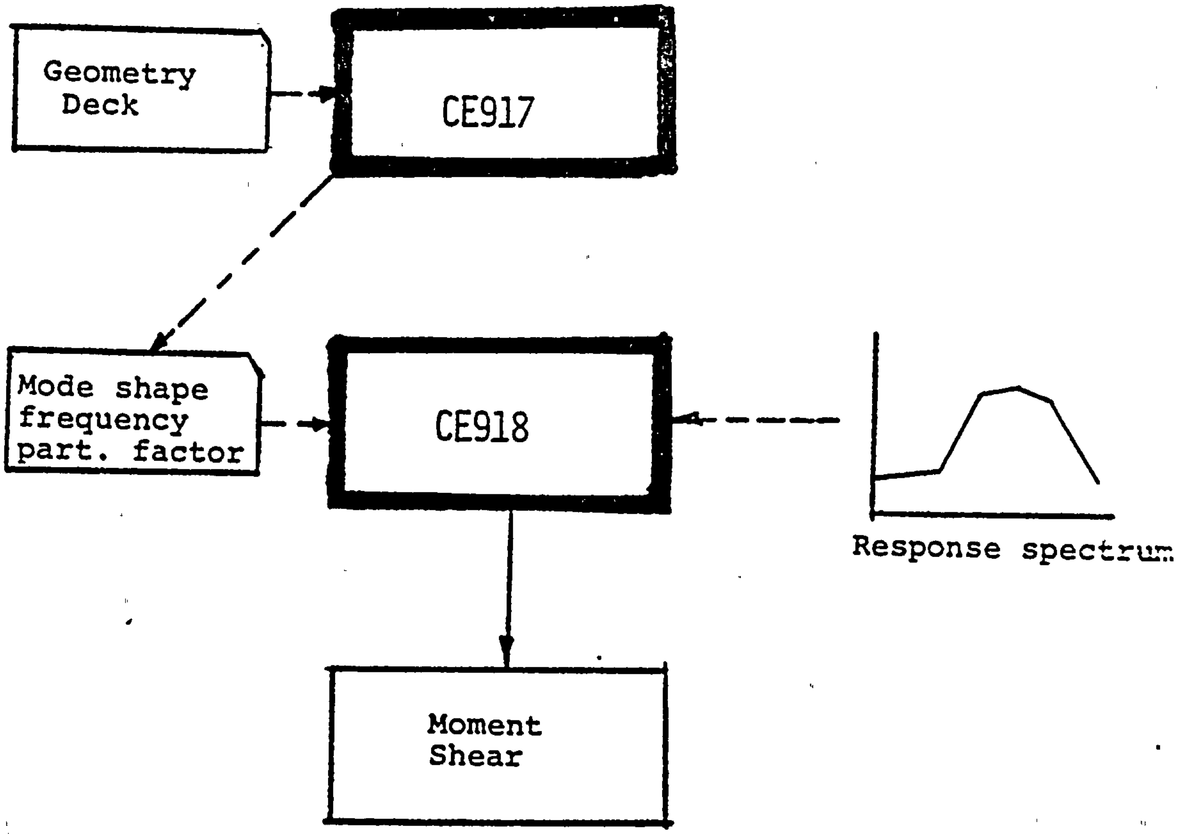

REV. 6, 4/82

SUSQUEHANNA STEAM ELECTRIC STATION
UNITS 1 AND 2
DESIGN ASSESSMENT REPORT

REACTOR BUILDING
STRESS ANALYSIS

FIGURE 7-8

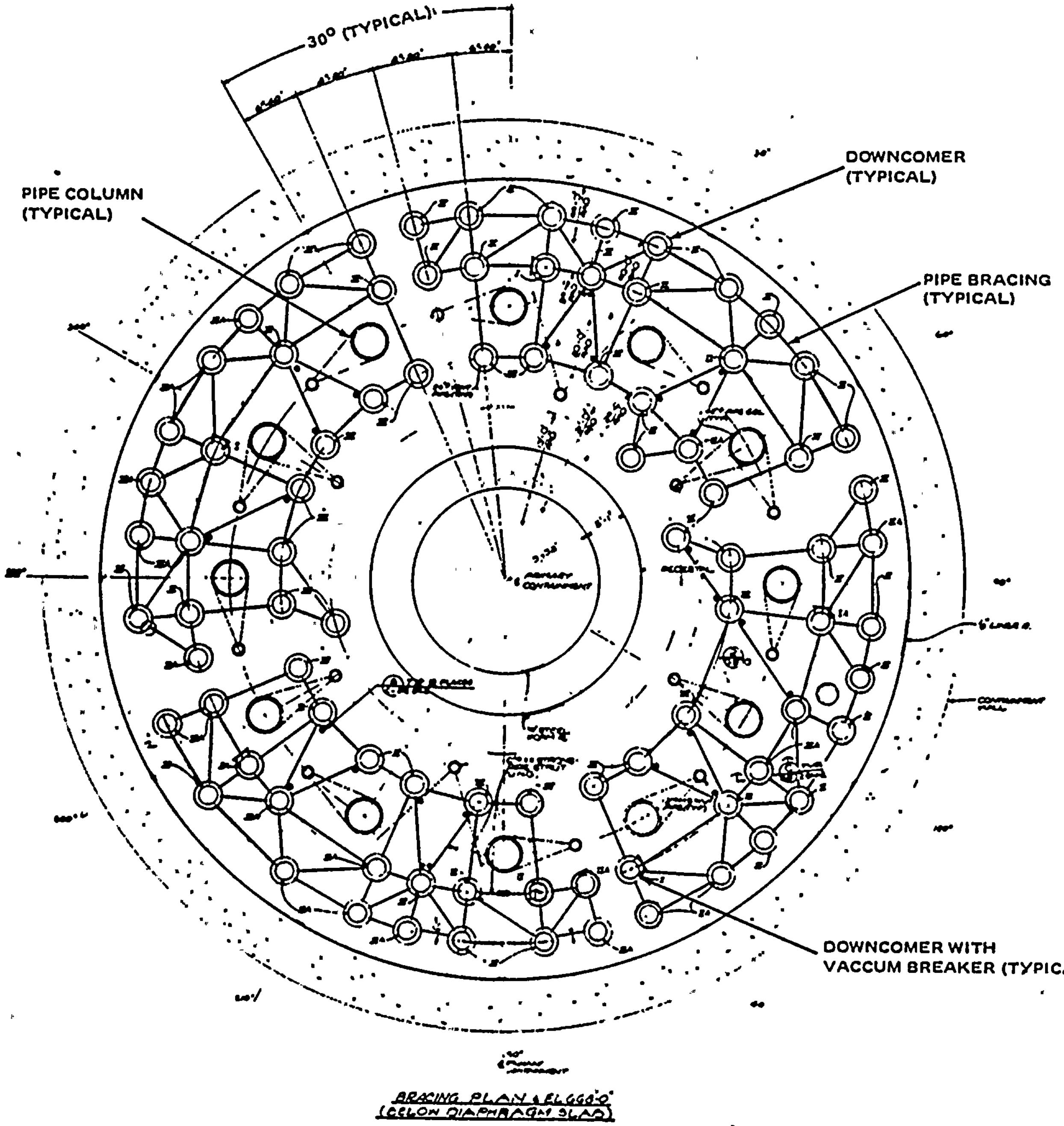

REV. 6, 4/82

SUSQUEHANNA STEAM ELECTRIC STATION
UNITS 1 AND 2
DESIGN ASSESSMENT REPORT

DOWNCOMER BRACING SYSTEM
PLAN

FIGURE 7-9

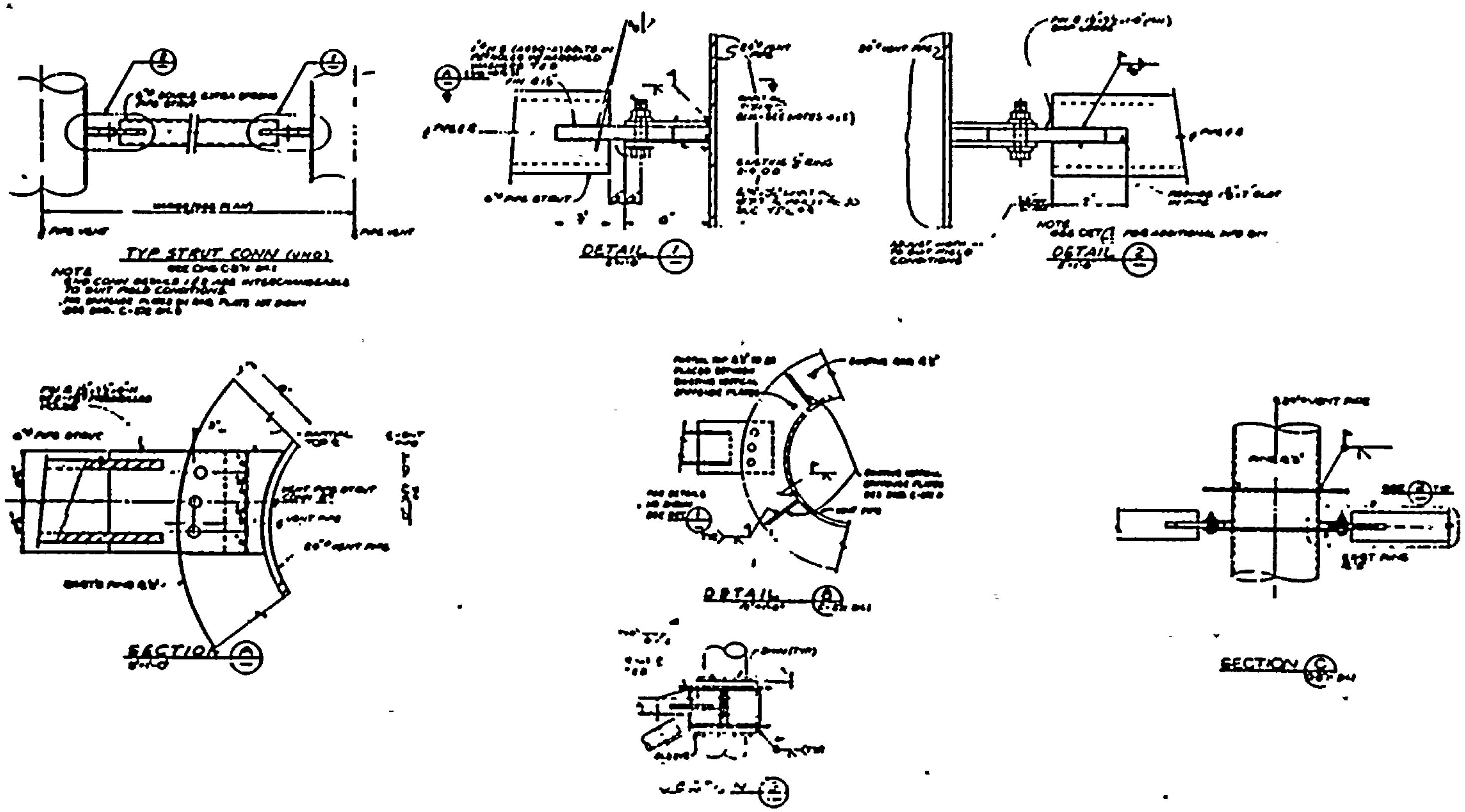

REV. 6, 4/82

SUSQUEHANNA STEAM ELECTRIC STATION
UNITS 1 AND 2
DESIGN ASSESSMENT REPORT

DOWNCOMER BRACING SYSTEM
CONNECTION DETAILS

FIGURE 7–10 (Sheet 1)

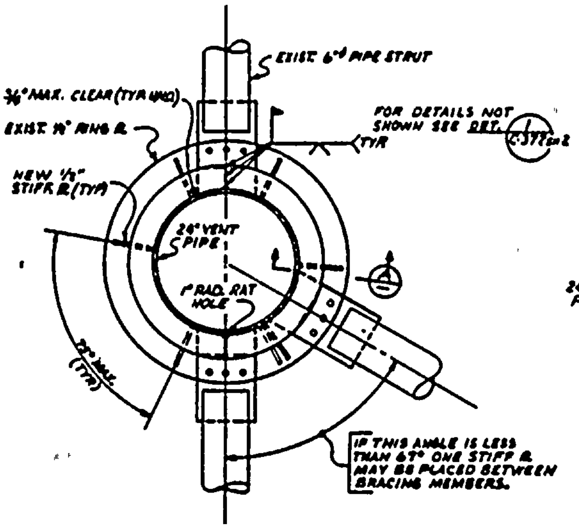

SINGLE RING PLATE
STIFFENER DETAIL

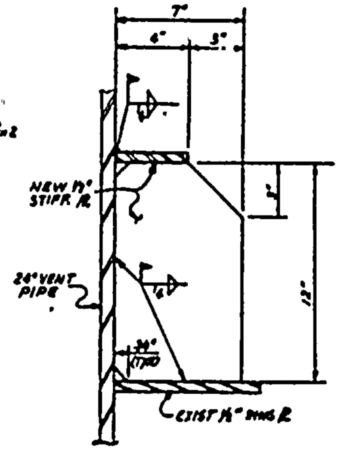

SECTION A
3" = 1'-0"

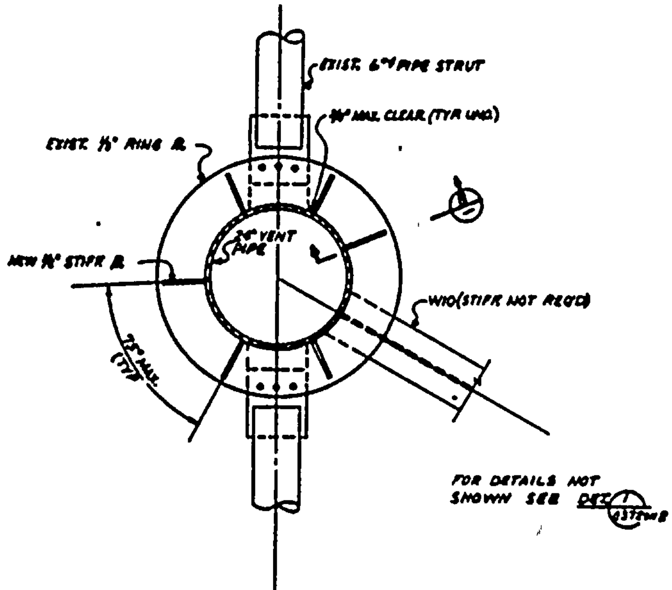

DOUBLE RING PLATE
STIFFENER DETAIL

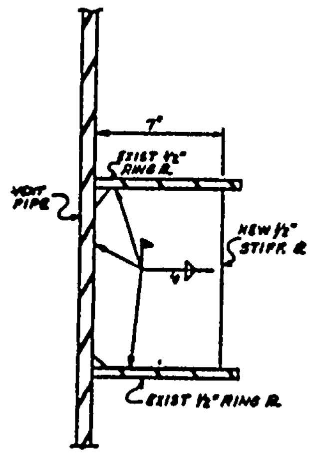

SECTION B

REV. 6, 4/82

SUSQUEHANNA STEAM ELECTRIC STATION
UNITS 1 AND 2
DESIGN ASSESSMENT REPORT

DOWNCOMER BRACING SYSTEM
CONNECTION DETAILS

FIGURE 7-10 (Sheet 2)

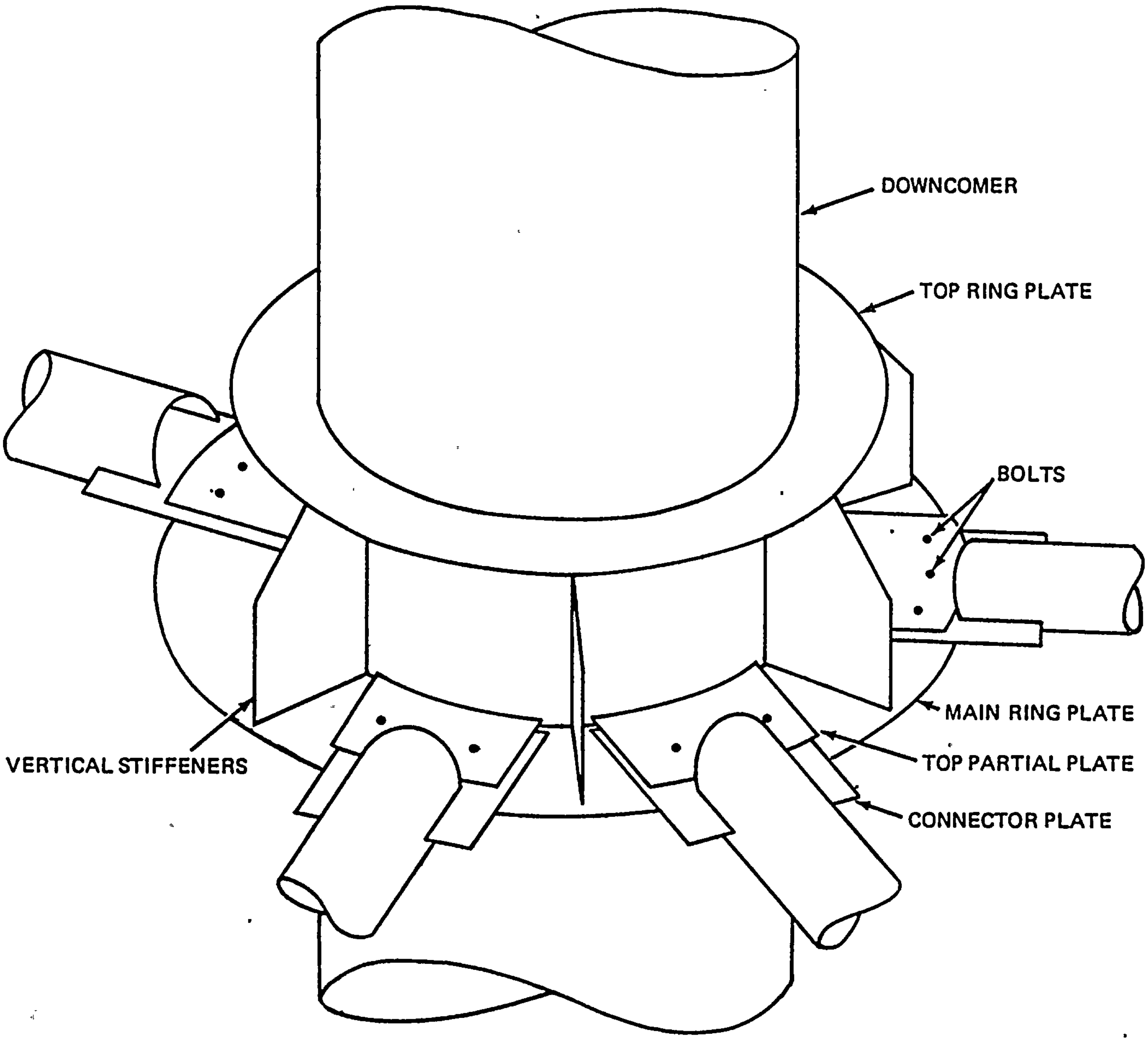

REV. 6, 4/82

SUSQUEHANNA STEAM ELECTRIC STATION
UNITS 1 AND 2
DESIGN ASSESSMENT REPORT

DOWNCOMER BRACING SYSTEM CONNECTION

FIGURE 7–10 (Sheet 3)

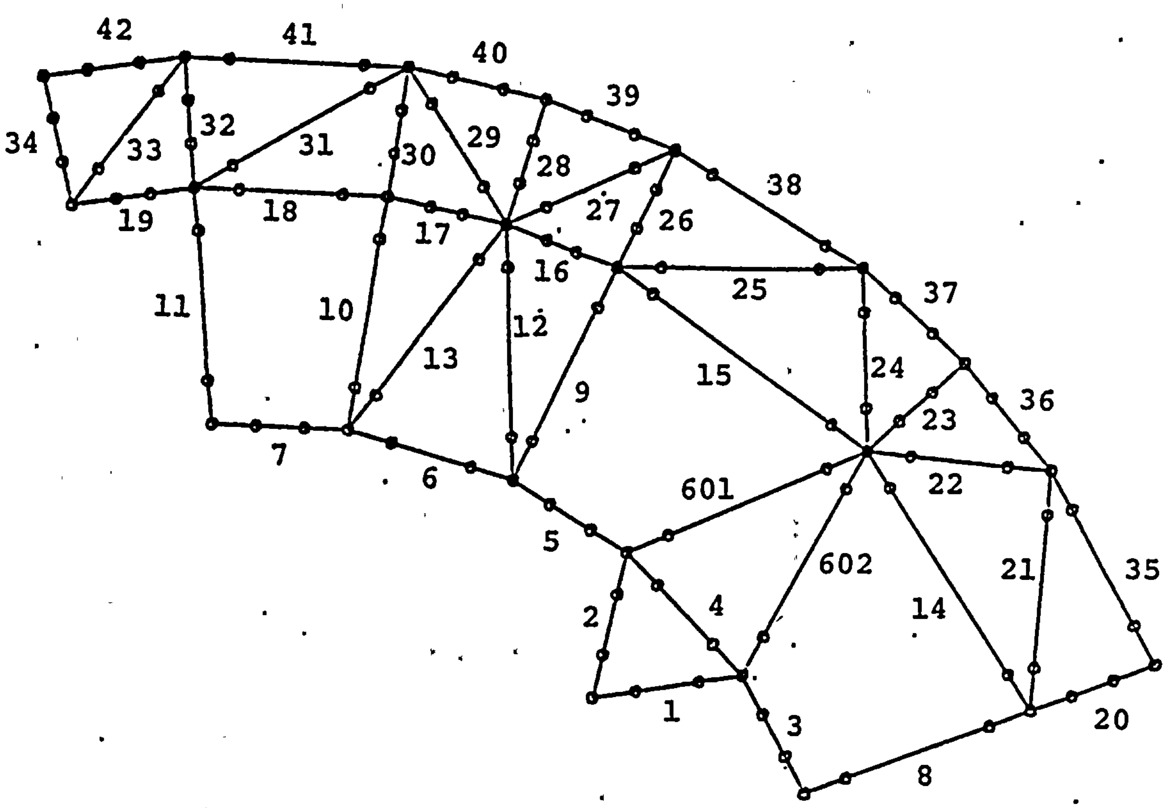

REV. 6, 4/82

SUSQUEHANNA STEAM ELECTRIC STATION
UNITS 1 AND 2
DESIGN ASSESSMENT REPORT

DOWNCOMER BRACING SYSTEM
COMPUTER MODEL

FIGURE 7-11 (Sheet 1)

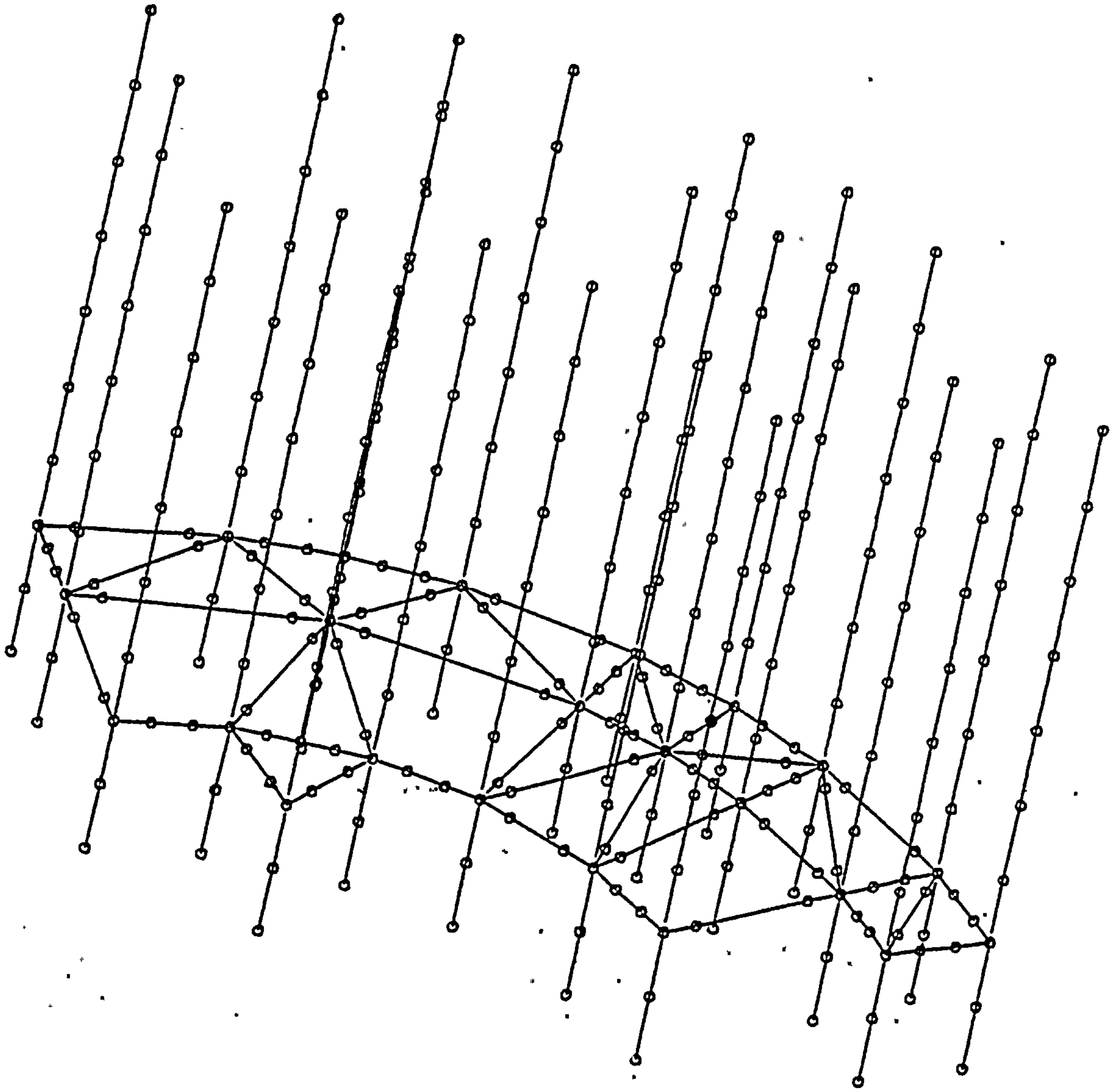

REV. 6, 4/82

SUSQUEHANNA STEAM ELECTRIC STATION
UNITS 1 AND 2
DESIGN ASSESSMENT REPORT

DOWNCOMER BRACING SYSTEM
COMPUTER MODEL

FIGURE 7-11 (Sheet 2)

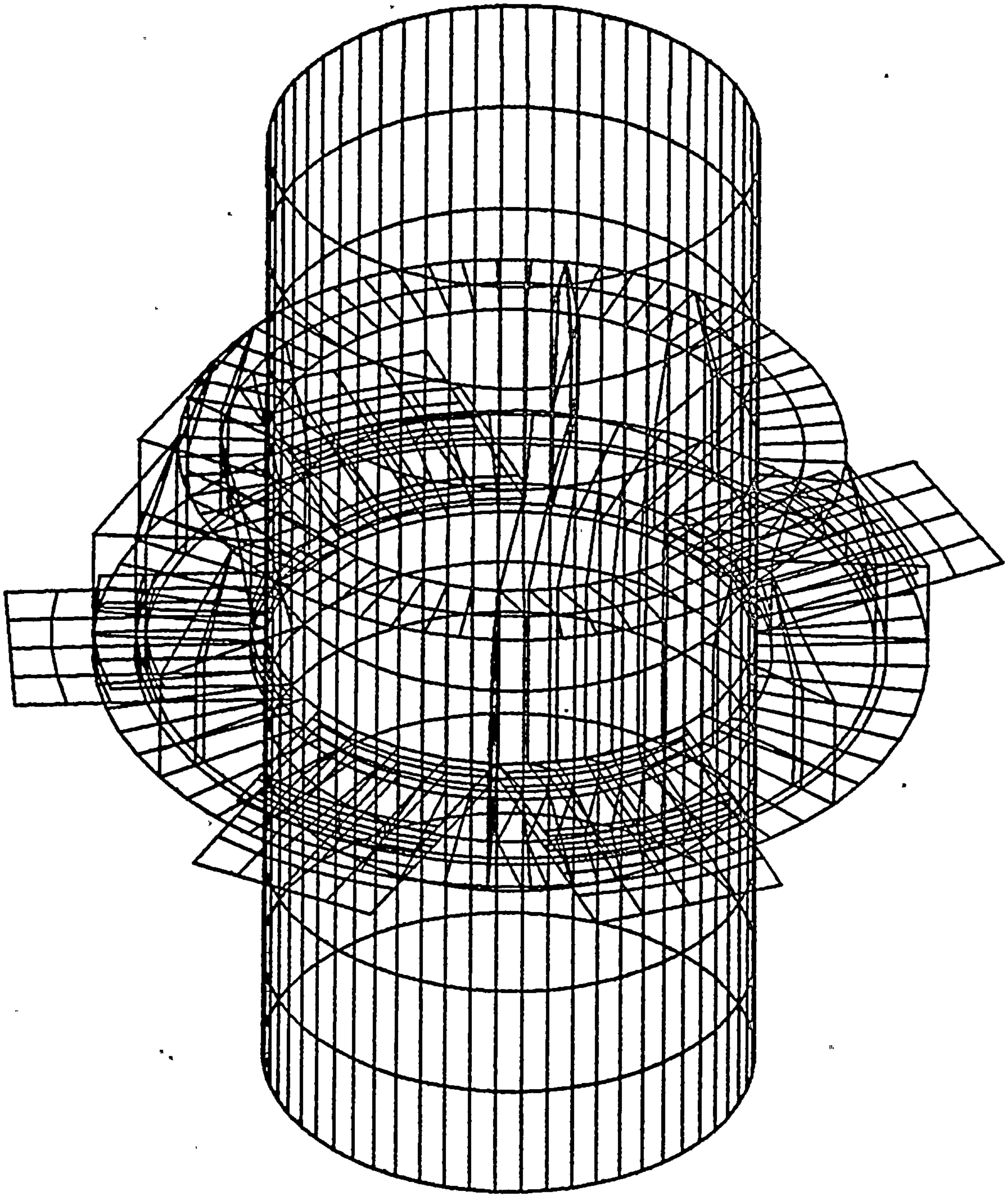

REV. 6, 4/82

SUSQUEHANNA STEAM ELECTRIC STATION
UNITS 1 AND 2
DESIGN ASSESSMENT REPORT

DOWNCOMER BRACING SYSTEM
CONNECTION COMPUTER MODEL

FIGURE 7-11 (Sheet 3)

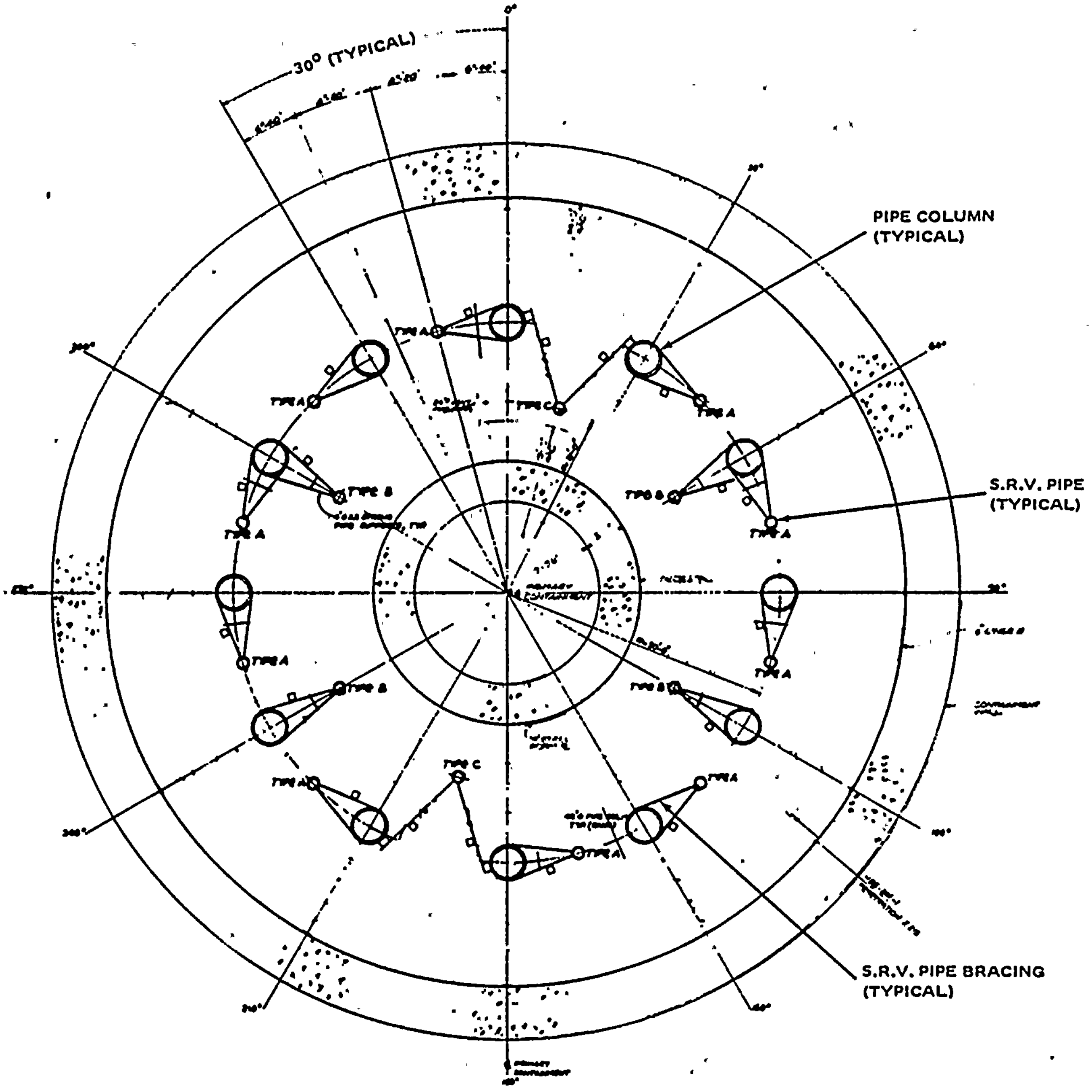

REV. 6, 4/82

NOTE:
☐ INDICATES KNEE BRACING ON THIS SIDE
TYPES A, B, & C, FOR DETAILS SEE DWG C-372 SH. 4
TYPES A & C ℄ PIPES EL. 667'-0"
TYPE B ℄ EL. 66'-0"

SUSQUEHANNA STEAM ELECTRIC STATION
UNITS 1 AND 2
DESIGN ASSESSMENT REPORT

SRV SUPPORT SYSTEM
PLAN

FIGURE 7-12

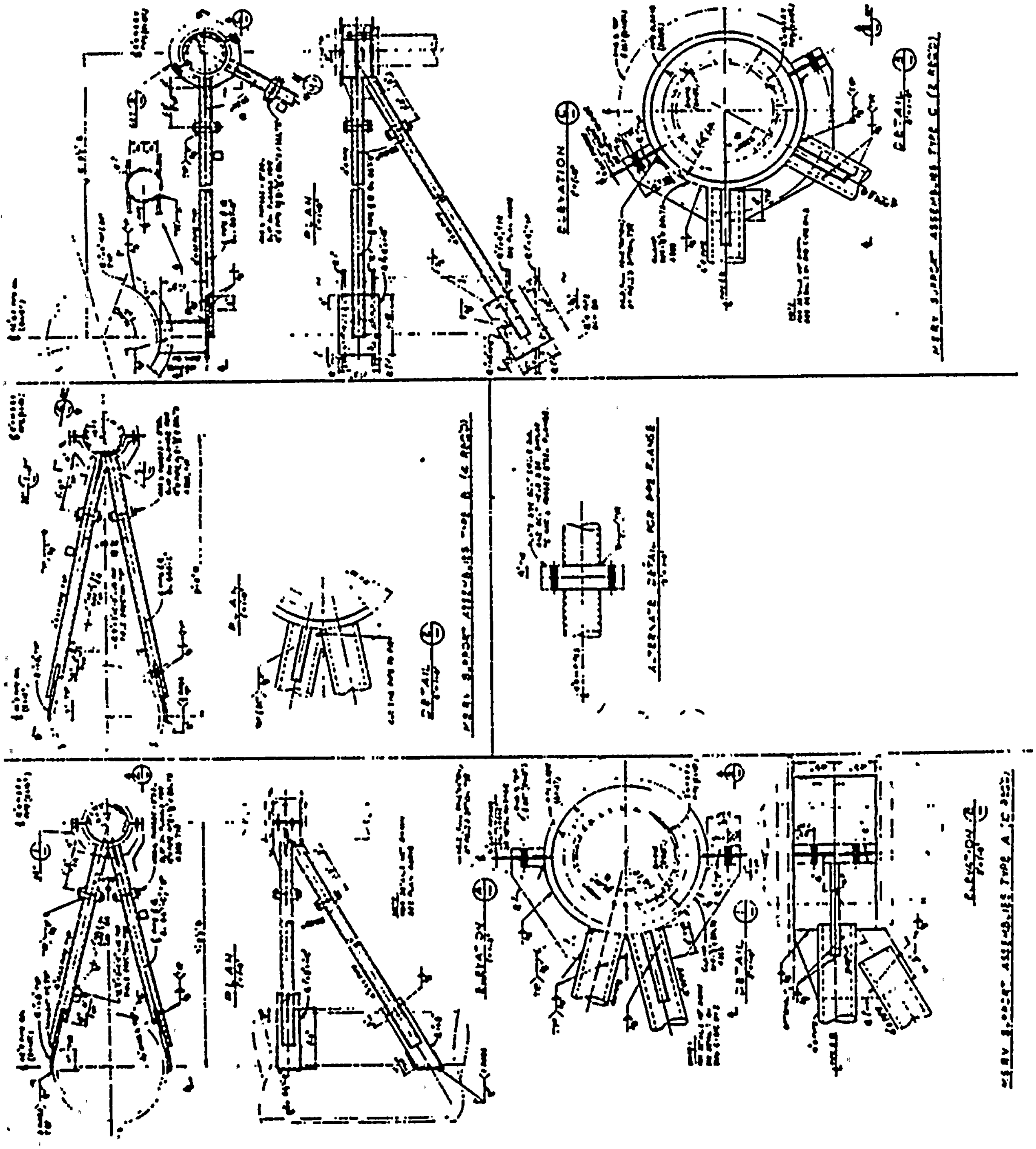

REV. 6, 4/82

SUSQUEHANNA STEAM ELECTRIC STATION
UNITS 1 AND 2
DESIGN ASSESSMENT REPORT

SRV SUPPORT SYSTEM DETAILS

FIGURE 7-13

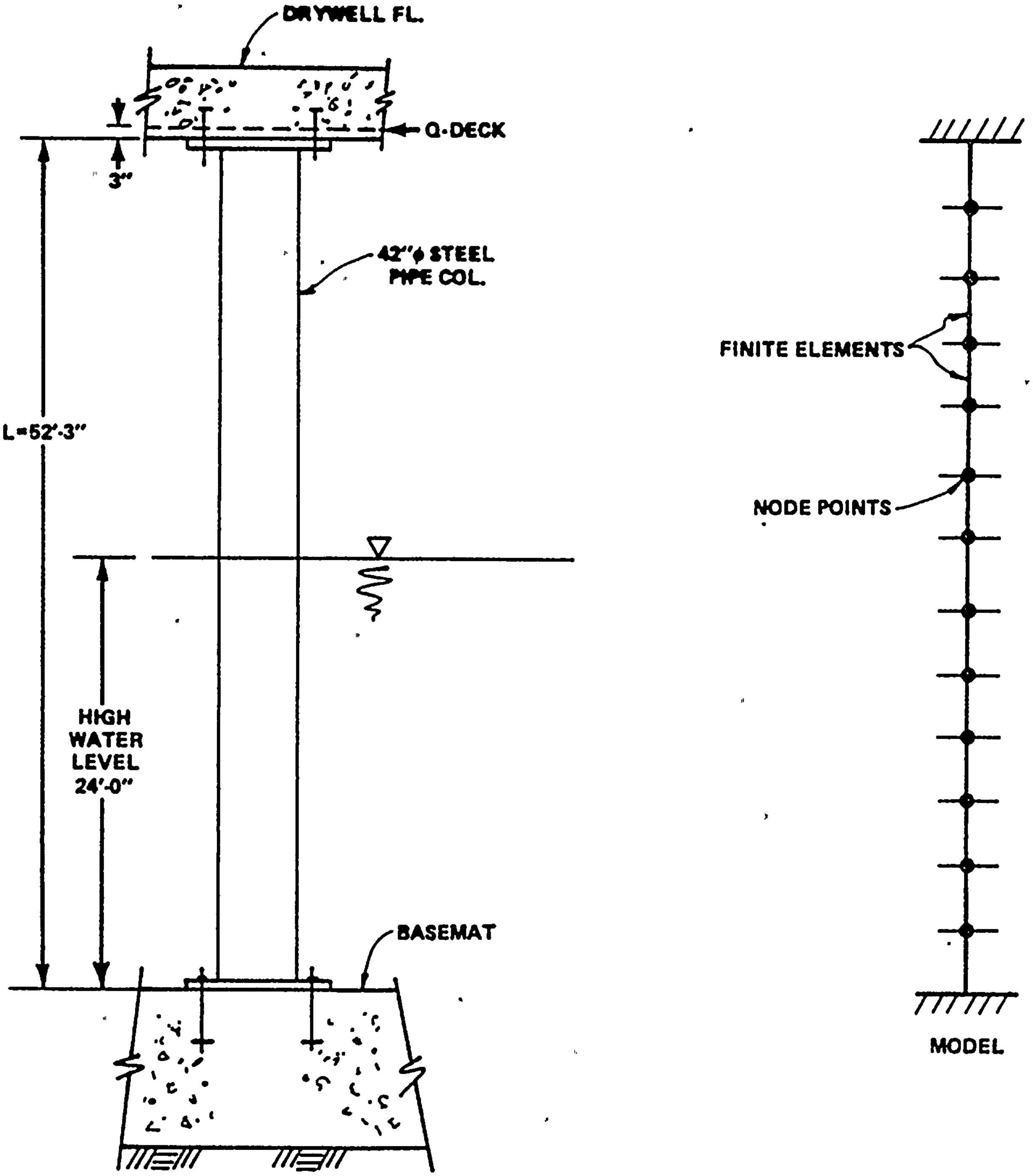

REV. 6, 4/82

SUSQUEHANNA STEAM ELECTRIC STATION
UNITS 1 AND 2
DESIGN ASSESSMENT REPORT

FINITE ELEMENT MODEL OF COLUMN

FIGURE 7-14

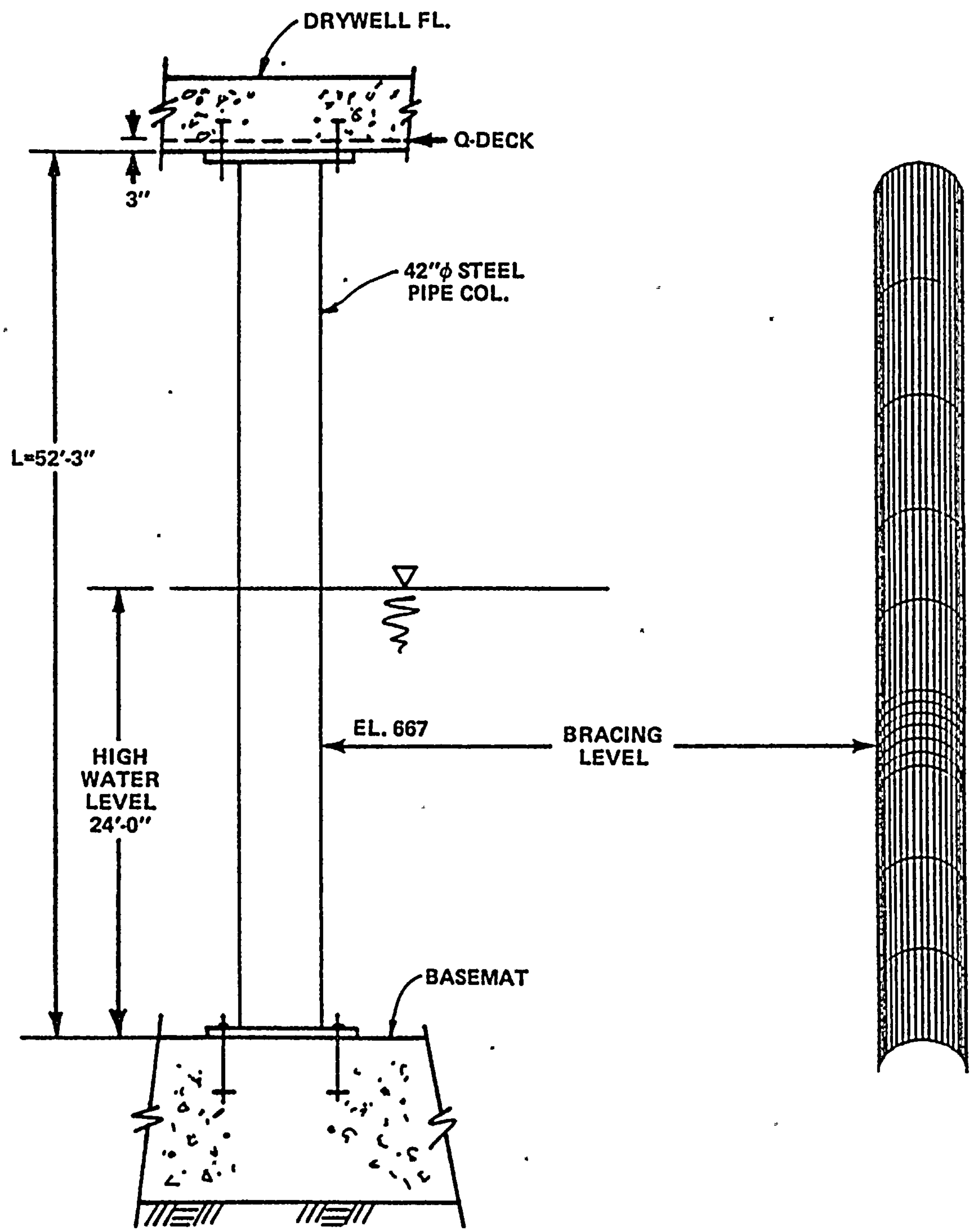

REV. 6, 4/82

SUSQUEHANNA STEAM ELECTRIC STATION
UNITS 1 AND 2
DESIGN ASSESSMENT REPORT

FINITE ELEMENT MODEL OF COLUMN

FIGURE 7-15

ITEM NO.	BASE	QTY	DESCRIPTION			SPEC	
1	100-A		LOCK SHIPPING ASSY				
	101-A	1	LOCK FINAL ASSY				
	153-A	2	MEDALLION ASS'Y				
	160-A	12	TIE DOWN BOLT ASSY.				
	166-2	1	5100-A NAMEPLATE			SS	
	100-1	4	DRIVE SCREWS #10 U-TYPE	D	D	SS	
	162-B	1	EQUIPT. DOOR NECK ASSY				

[illegible]

LOCK TEST PRESSURE - 63.25 PSIG

THE LOCKING MECHANISM IS DESIGNED TO SEAL THE DOOR AGAINST A PRESSURE OF 5 PSIG. THE DOORS AND LOCK ARE DESIGNED FOR A PRESSURE OF 55 PSIG EXISTING IN THE CONTAINMENT VESSEL OR THE CONTAINMENT VESSEL AND LOCK SIMULTANEOUSLY. BOTH DOORS AND VALVES CAN BE [illegible] OPERATED FROM EITHER SIDE OF EITHER DOOR AND ARE MECHANICALLY INTERLOCKED TO PREVENT OPENING BOTH DOORS AND VALVES AT THE SAME TIME. ONE DOOR AND VALVE CANNOT BE OPENED UNLESS THE OPPOSITE DOOR AND VALVE IS SEALED. THE OPERATING AND MAINTENANCE [illegible] [illegible] THE [illegible] OF [illegible] VIOLATING THE INTERLOCK.

THE OPERATION OF THE HANDWHEEL WILL PERFORM THE FOLLOWING FUNCTIONS: (1) ACTUATE THE MECHANICAL INTERLOCK TO BLOCK OPERATION OF THE OPPOSITE MECHANISM. (2) OPEN THE PRESSURE EQUALIZING VALVE. (3) UNLOCK THE DOOR. (4) SWING THE DOOR OPEN ON IT'S HINGE. THESE OPERATIONS ARE IN THE SEQUENCE AS DESCRIBED FOR OPENING A DOOR AND ARE REVERSED FOR CLOSING A DOOR. THE REMOTE OPERATOR ON THE OUTSIDE OF THE LOCK AT EACH DOOR WILL PERFORM THE ABOVE FUNCTIONS ON THE OPPOSITE DOOR.

LIMIT SWITCHES ARE SUPPLIED AT THE VALVE AND LATCH OPERATORS FOR EACH DOOR TO FACILITATE REMOTE INDICATION OF EACH DOOR AND VALVE POSITION. POSITION INDICATORS AT EACH HANDWHEEL INDICATE THE POSITION OF ITS RELATED VALVE, LATCH AND DOOR.

TIE DOWNS ARE REQUIRED ON THE INTERIOR DOOR FOR LOCK TESTS GREATER THAN 5 PSIG OVER CONTAINMENT PRESSURE. SEE DWG. [illegible]

SEE VESSEL GENERAL PLAN FOR ADDITIONAL INFORMATION.

HANDWHEEL ROTATION	OPERATION	HANDLE EFFORT
0 - 1½ TURNS	VALVE OPEN	10 LBS.
1½ - 5½ TURNS	DOOR UNLOCK	40 LBS.
5½ - 9½ TURNS	DOOR SWINGS	15 LBS.

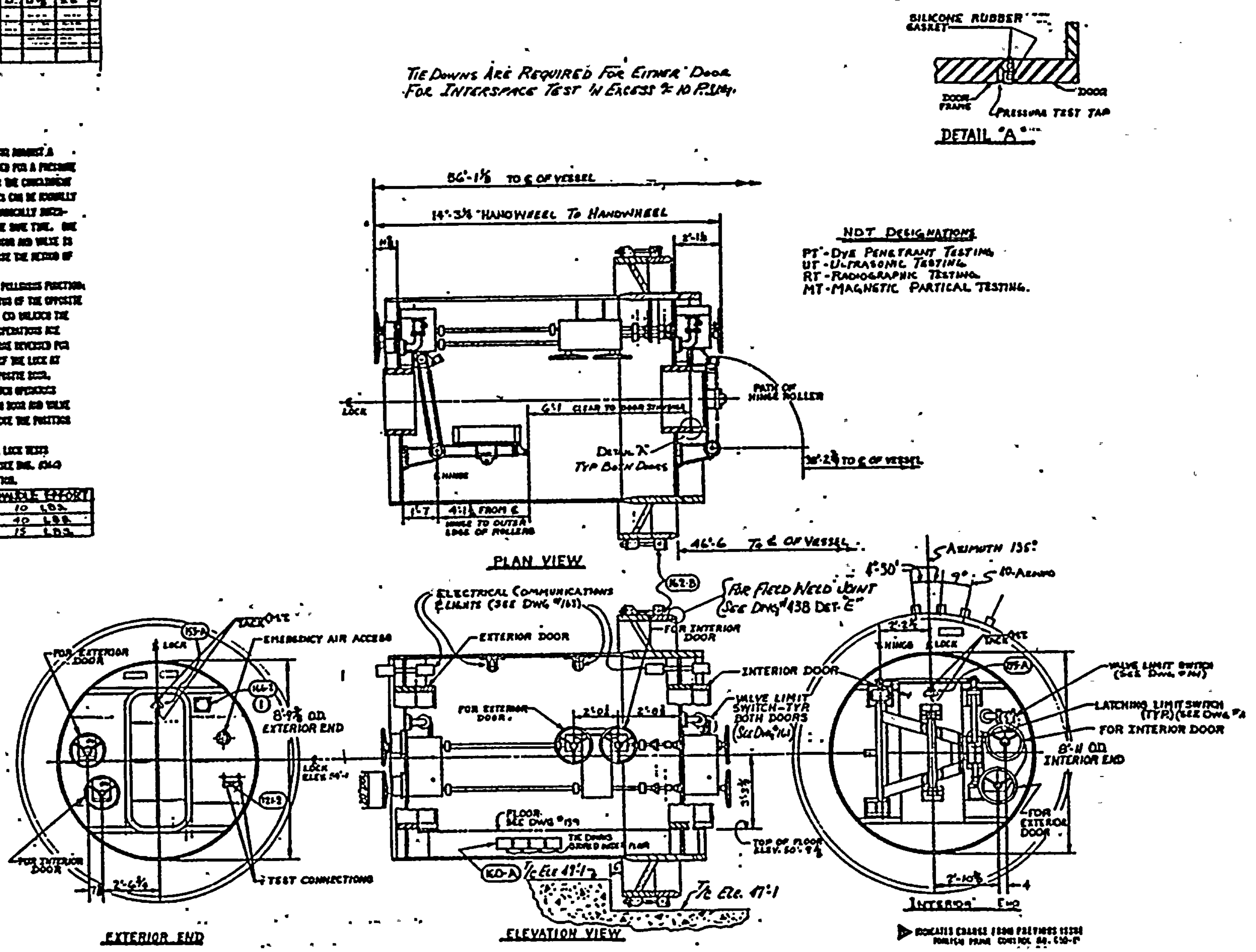

REV. 6, 4/82

SUSQUEHANNA STEAM ELECTRIC STATION
UNITS 1 AND 2
DESIGN ASSESSMENT REPORT

GENERAL ARRANGEMENT
PERSONNEL LOCK

FIGURE 7-16

1	532-A		EQUIPMENT DOOR NECK ASSY.					
	532-1	1	INNER GASKET-[illegible] WIDE x [illegible]	38	1[illegible]	[illegible]	D	[illegible]
	532-2	1	OUTER GASKET-[illegible] WIDE x [illegible]	38	7[illegible]	[illegible]	D	[illegible]
	532-3	2	PL 26½ x 3 x (½ 57 x 19'-5⅝)	19	2½	[illegible]	A	[illegible]
	532-4	1	PL 72" x 1" (PL 73" x 38'-7)	38	5½	[illegible]	A	[illegible]
	532-5	32	PL 5" x ¾ ([illegible])	0	5½	[illegible]	A	[illegible]
	533-4	64	PL SK x ¾ (PL 5 x 0'-8⅝) (C-22)			[illegible]	A	[illegible]
	432-6	3	PL 4 x 1 (S/W 432-6)	19	10½	A36	D	[illegible]
1	532-B		EQUIPMENT DOOR HEAD ASSY					
	532-3	2	PL 26½ x 3 S/W 532-3 ABOVE	19	2½	[illegible]	A	[illegible]
	533-3	64	PL SK x ¾ (PL 5½ x 1'-1⅝) (C-22)			[illegible]	A	[illegible]
	533-1	32	PL SK x ¾ (PL 5 x 0'-5⅝) (C-22)			[illegible]	A	[illegible]
	533-7	2	PL SK x 1 (C/F PL 79" x 25'-0⅝)	[illegible]		[illegible]	A	[illegible]
	533-5	2	PL SK x ¾ (PL 6" x 0'-11⅝) (C-22)			[illegible]	B	[illegible]
	533-9	2	PL 10"Ø x ¾ [illegible] (C-22)			[illegible]	B	[illegible]
	533-8	3	PL SK x 1 ([illegible] PL 2⅜ x 0'-7⅝)			[illegible]	B	[illegible]
1	533-10		PL SK x ⅜ ([illegible] PL 11⅝ x 1'-0⅜) [illegible] 533-1			A36	D	[illegible]
32	533-6		2"Ø PIN x SK	0	4½	[illegible]	A	[illegible]
64	532-7		⅜"Ø STD. COTTER PINS	0	2½	STEEL	D	
32	532-8		1¾-8UN EXT. HEX. NUTS			[illegible]	A	[illegible]
32	532-9		SPHERICAL WASHER FOR 1¾ BOLT			*	D	[illegible]
32	532-10		1¾"Ø EYEBOLTS x 1'-4½ LG C/C E.			[illegible]	A	[illegible]
			4"Ø x 1½ THK x 2[illegible]Ø HOLE IN [illegible]					
			THD. END TO [illegible] x 1¾-8UN					

* AISI 4145 HEAT TREAT TO BRINELL OF 249 TO 352
SA 516 GR 70 (MS 6006) & SA 516 GR 70 (MS 6008)
SA 193 B7 (MS 860)
SA 194 GR 7 (MS 862)
SA 516 GR 70 (MS 6017)
SILICONE RUBBER (MS 570)

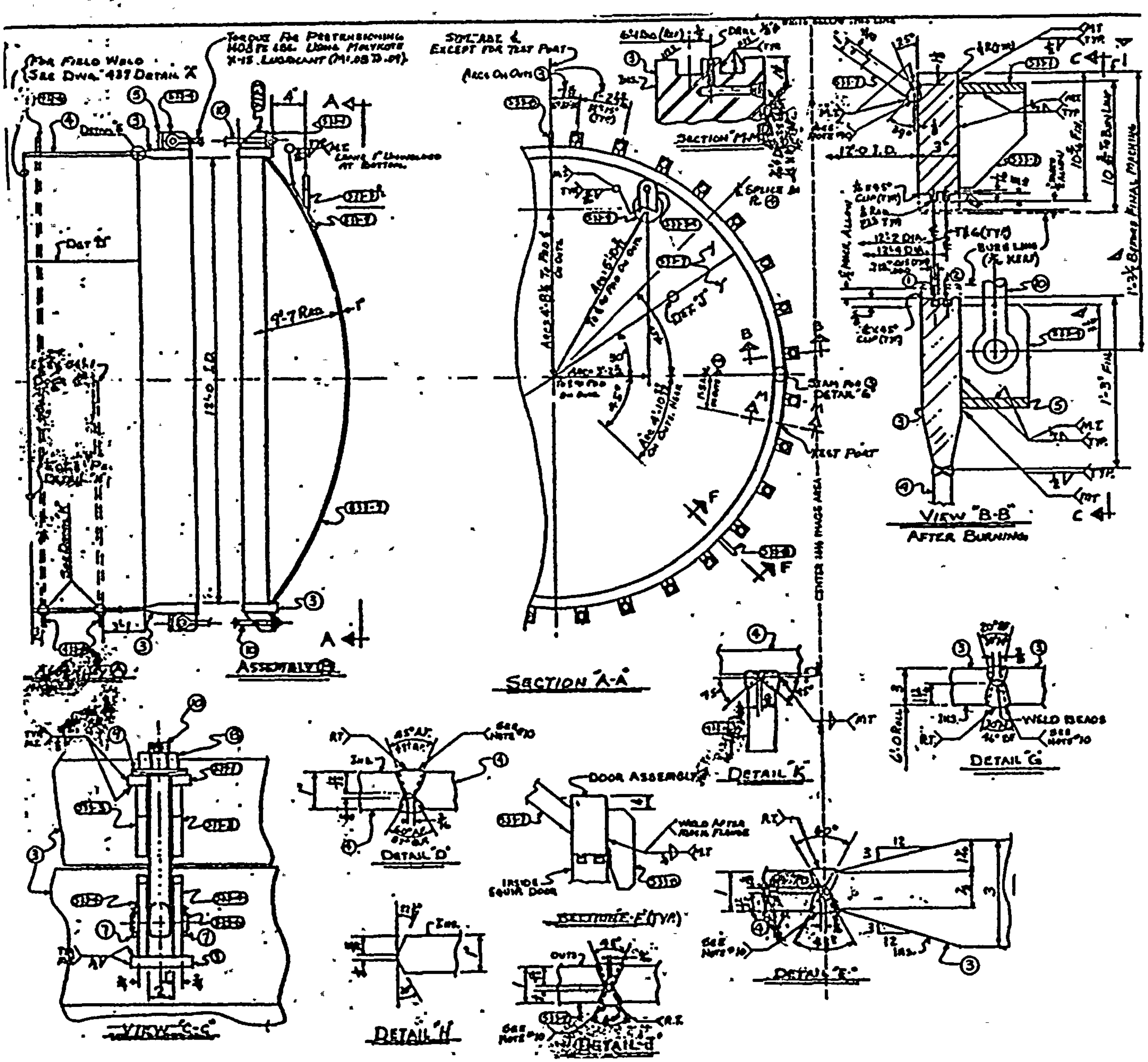

REV. 6, 4/82

SUSQUEHANNA STEAM ELECTRIC STATION
UNITS 1 AND 2
DESIGN ASSESSMENT REPORT

EQUIPMENT DOOR DETAILS

FIGURE 7-17

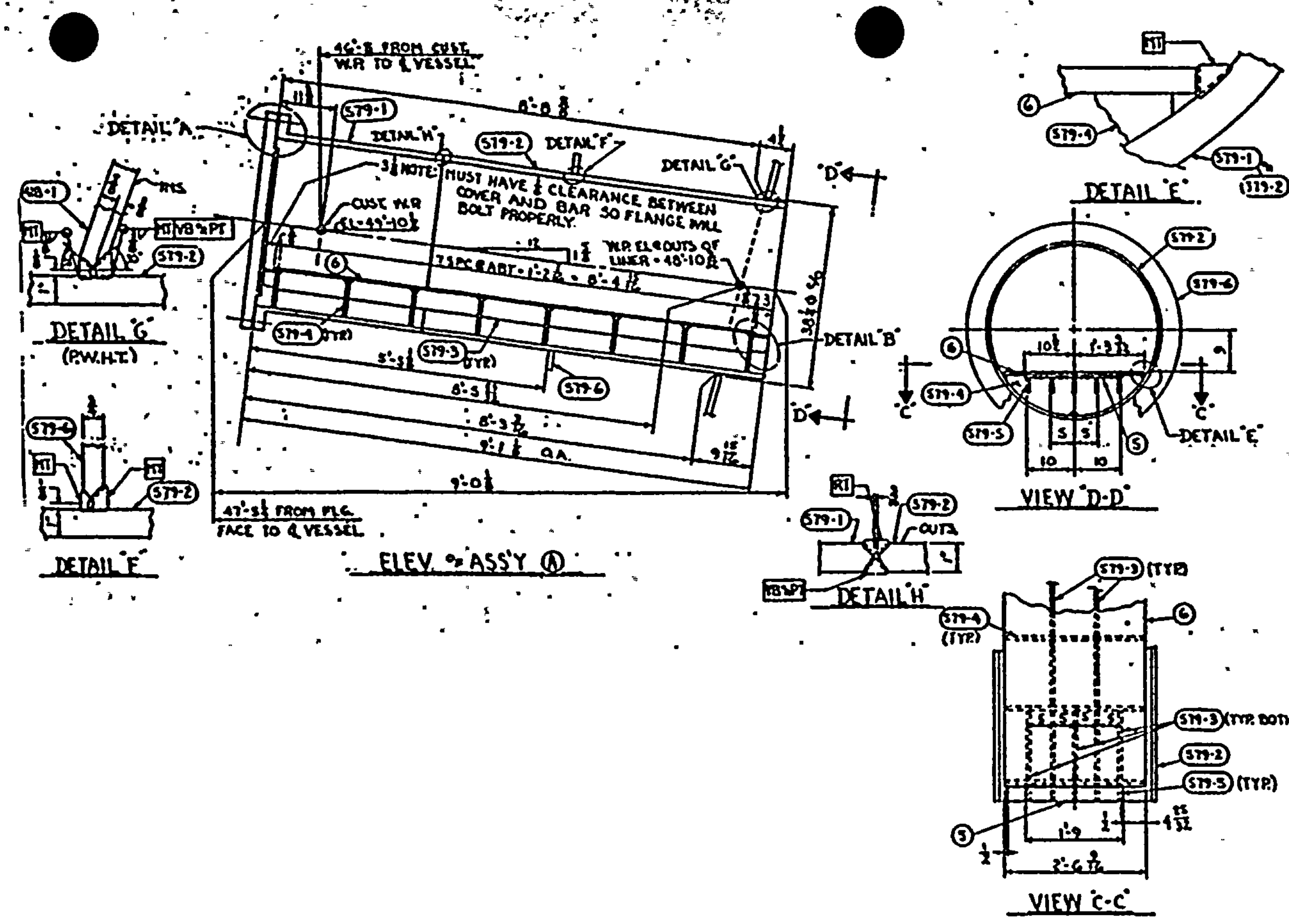

S78-A		PENETRATION ASS'Y (1-REQ'D)						
		SHOP ATTACH TO ASS'Y (410-A)						
S78-1	1	COVER R-46" Ø x 3 (MACH.)					A	1304
		(¼ R-40 x 8'-0)						
S78-2	1	FLG R-46" O.D.-2 (MACH.)					A	503
		(¼ R-40 x 3 x 8'-2)						
S78-3	1	OUTS. GASKET-Ø IN ONE CONT.					D	
		LENGTH OF 10'-2 W/ONE BUTT						
		SPLICE OF CONSTANT CROSS SECT.						
S78-4	1	INS. GASKET-Ø IN ONE CONT.					D	
		LENGTH OF 9'-9 W/ONE BUTT						
		SPLICE OF CONSTANT CROSS SECT.						
S78-5	2	R-3 x (¼ 302-3) SEE CUT SK C-1	1	9	A36	D		10
S78-6	1	R-30 x (¼ 301-0) SEE CUT SK C-1	8	6		C		442
S78-7	32	1⅛ Ø STUDS-8-UN-2A	0	9		A		144
S78-8	64	1⅛ Ø ASHSF HEX NUT-8-UN-2B				A		95
S79-1	1	R-36 x 1	9	8		A		1137
		(¼ R-100 x 9'-9 73-5519)						
S79-2	1	R-73 x 1	9	8		A		2453
		(¼ R-100 x 9'-9) SEE CUT SK C-2						
S79-3	10	R-4 x (¼ 302-3) SEE CUT SK C-1	1	1	A36	D		161
S79-4	8	R-5 x (¼ 302-3) SEE CUT SK C-1			A36	D		205
S79-5	10	R-3 x (¼ 302-3) SEE CUT SK C-1	0	8	A36	D		14
S79-6	1	R-5 x (¼ 523-1) SEE CUT SK C-1			A36	D		109

NOTE:
SEE DWG# 607 FOR DETAIL OF DAVIT ASS'Y

MS-6017 — SA 516 Gr 70
MS-572 — SILICONE RUBBER
MS-850 — SA193 B7
MS-852 — SA194 Gr 7
MS-691 — SA516 Gr 60

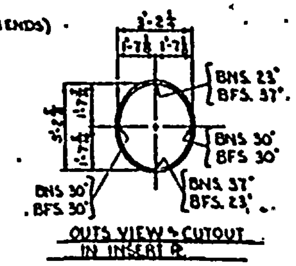

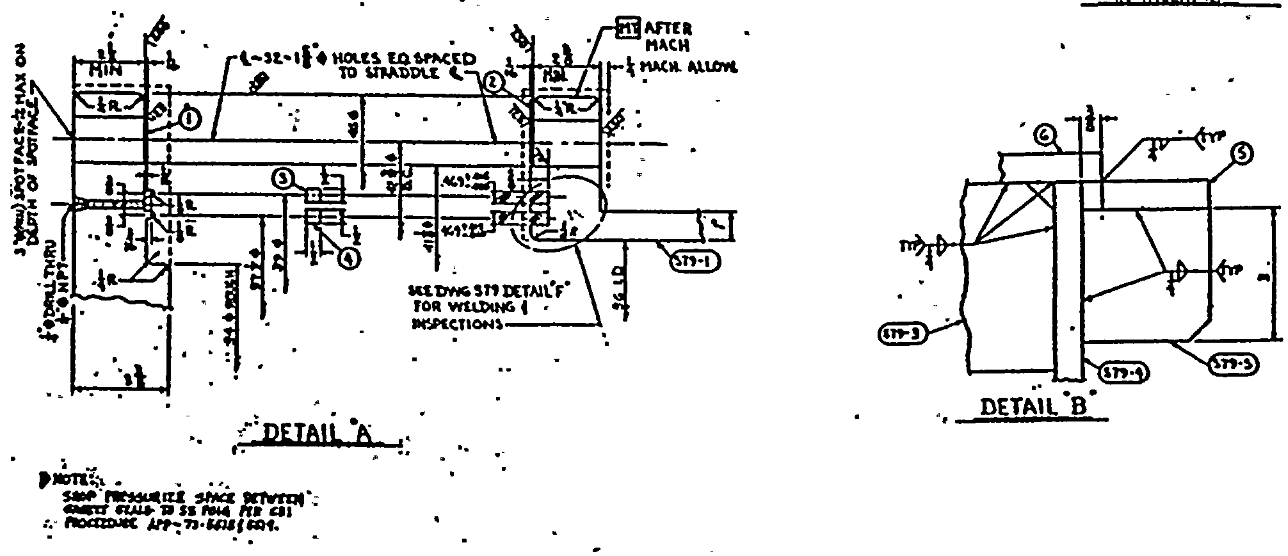

REV. 6, 4/82

SUSQUEHANNA STEAM ELECTRIC STATION
UNITS 1 AND 2
DESIGN ASSESSMENT REPORT

CRD HATCH DETAILS

FIGURE 7-18

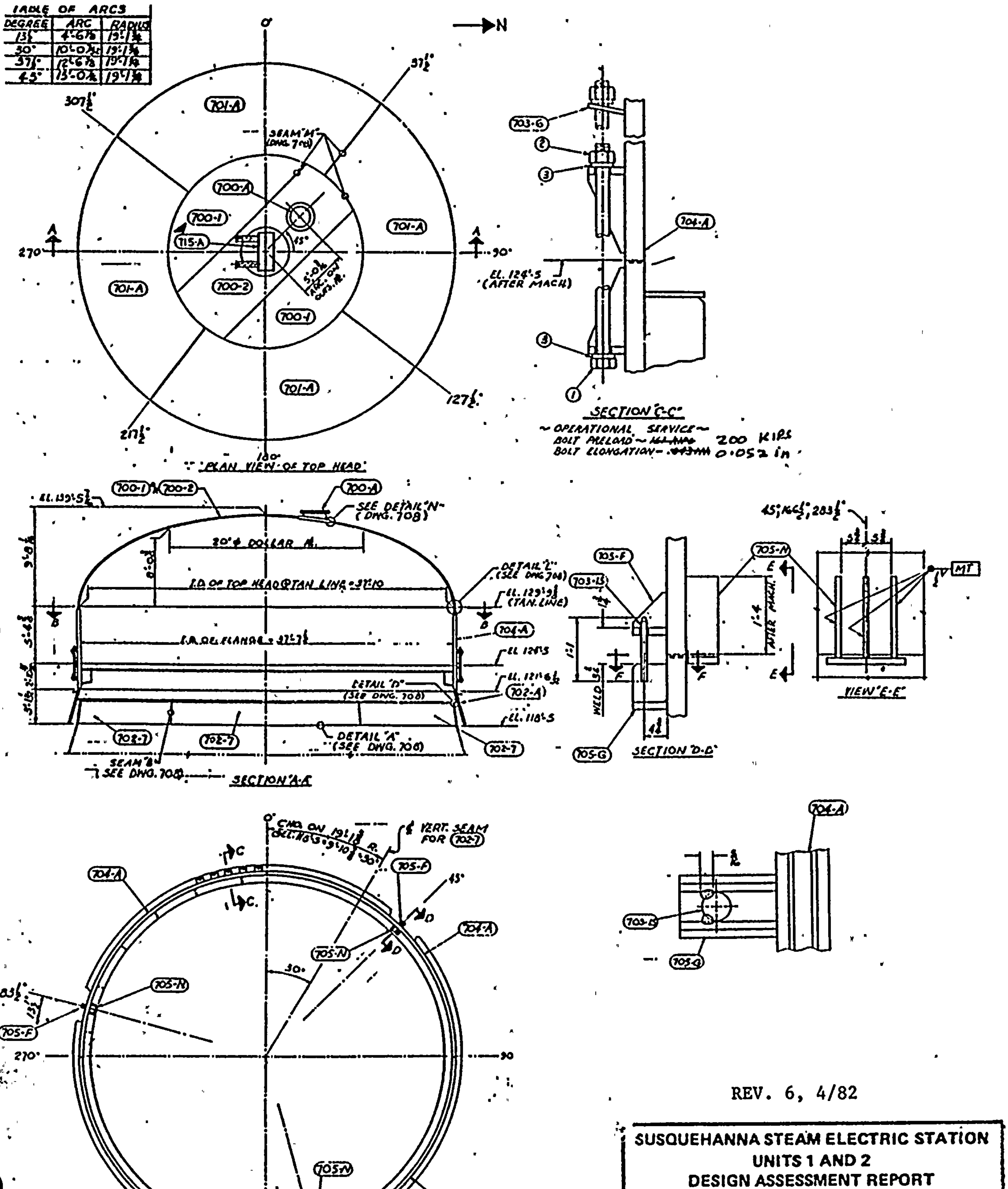

REV. 6, 4/82

SUSQUEHANNA STEAM ELECTRIC STATION
UNITS 1 AND 2
DESIGN ASSESSMENT REPORT

REFUELING HEAD DETAILS

FIGURE 7-19

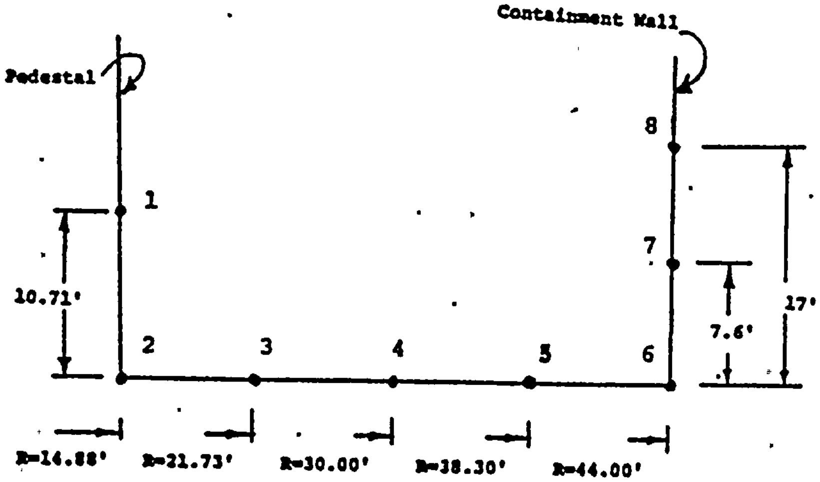

MAXIMUM NEGATIVE PRESSURE FROM KWU 300 SERIES CHUGGING

Point No.	Maximum Negative Pressure psi.	Trace No.
1	-62.16	KWU 306
2	-26.42	KWU 306
3	-24.74	KWU 306
4	-26.85	KWU 306
5	-26.69	KWU 306
6	-32.72	kwu 306
7	-28.40	KWU 306
8	-31.39	KWU 306

REV. 6, 4/82

SUSQUEHANNA STEAM ELECTRIC STATION
UNITS 1 AND 2
DESIGN ASSESSMENT REPORT

LINER PLATE HYDRODYNAMIC PRESSURE DUE TO CHUGGING

FIGURE 7-20

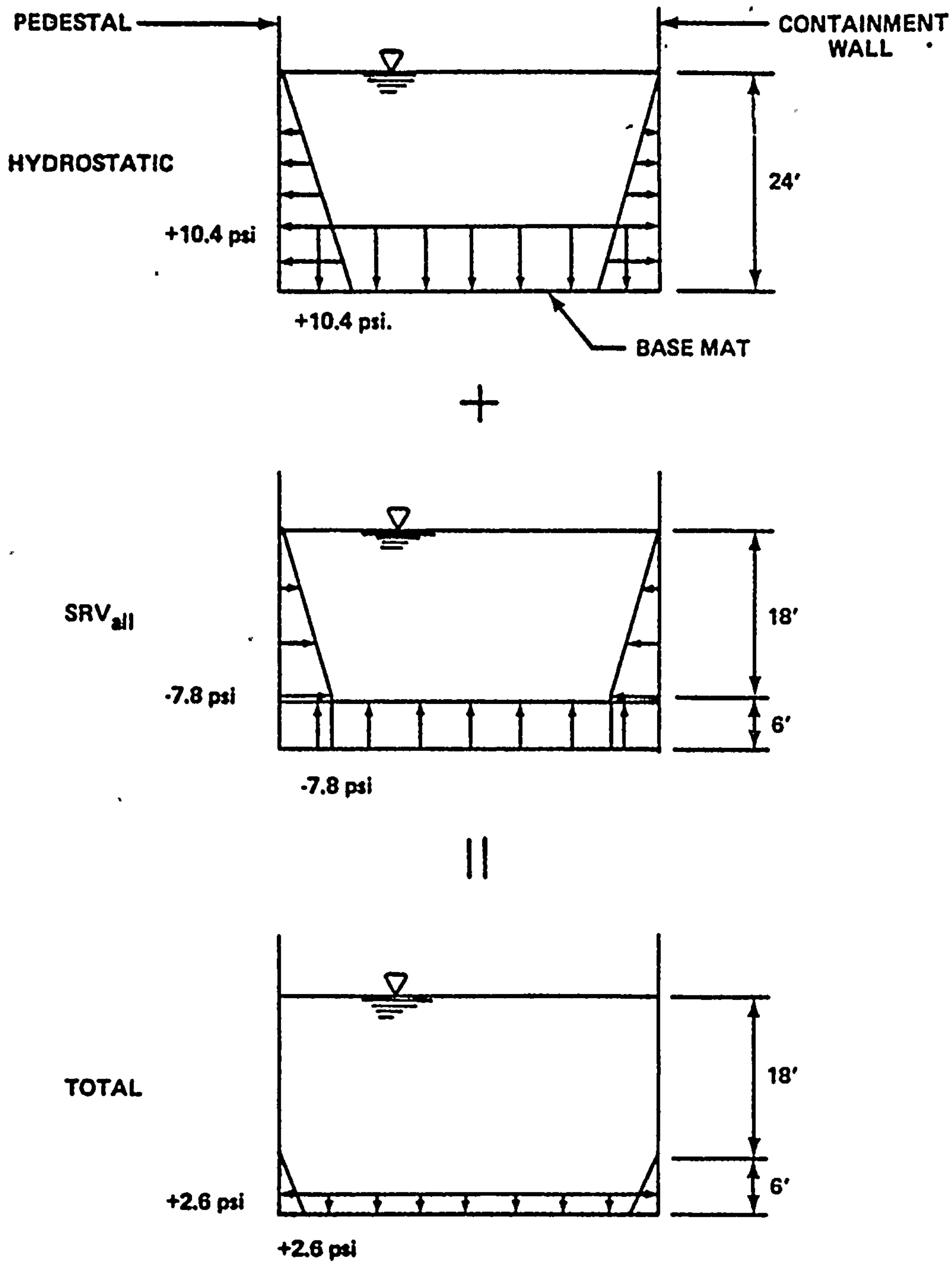

REV. 6, 4/82

SUSQUEHANNA STEAM ELECTRIC STATION
UNITS 1 AND 2
DESIGN ASSESSMENT REPORT

LINER PLATE PRESSURES
NORMAL CONDITION

FIGURE 7–21

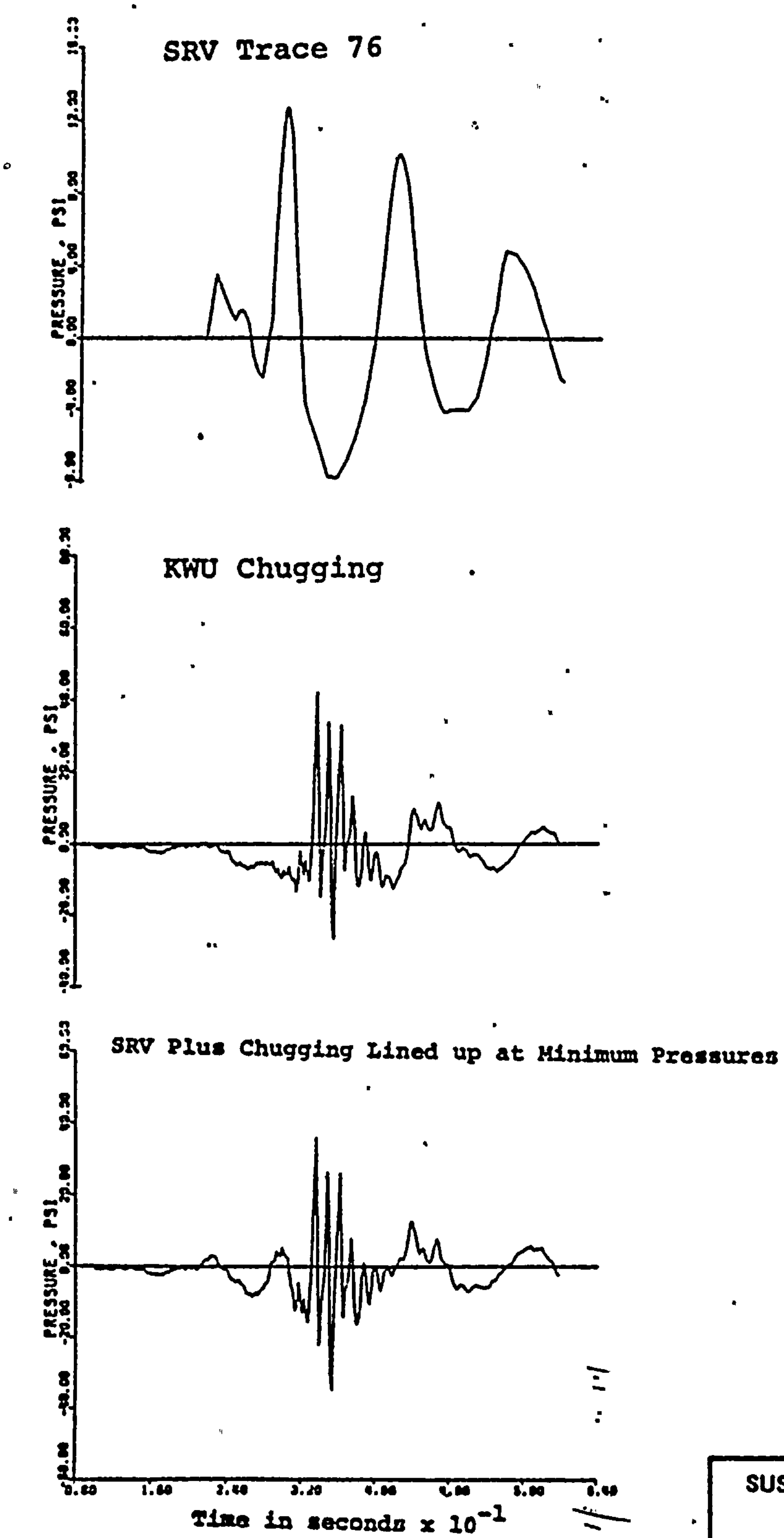

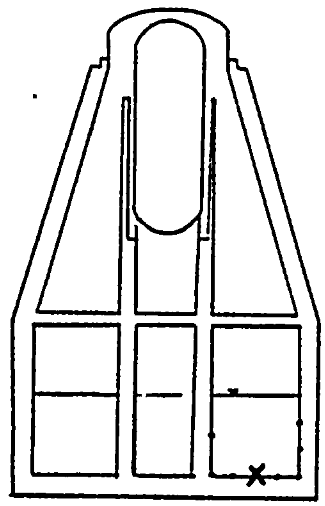

REV. 6, 4/82

SUSQUEHANNA STEAM ELECTRIC STATION
UNITS 1 AND 2
DESIGN ASSESSMENT REPORT

LINER PLATE HYDRODYNAMIC PRESSURE DUE TO CHUGGING AND SRV

FIGURE 7–22

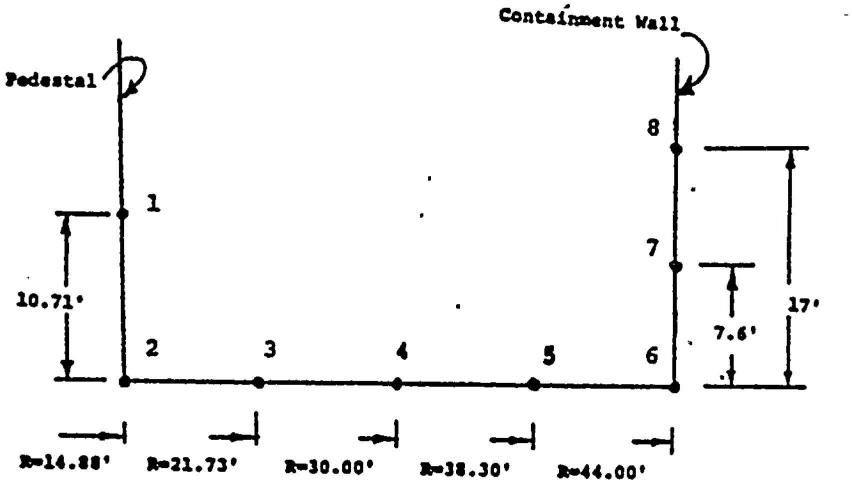

LOAD CASE	POINT IN FIGURE							
	1	2	3	4	5	6	7	8
CHUGGING	-62.16	-26.42	-24.74	-26.85	-26.69	-32.72	-28.40	-31.39
SRV Trace 76	- 5.76	- 7.80	- 7.80	-7.80	- 7.80	- 7.80	- 7.09	- 3.05
Hydrostatic	5.76	10.40	10.40	10.40	10.40	10.40	6.82	3.05
Wetwell pressure due to SBA or IBA*	25.00	25.00	25.00	25.00	25.00	25.00	25.00	25.00
NET PRESSURE	-37.16	1.18	2.86	0.75	0.91	-5.12	-3.69	-6.39

*Wetwell pressure due to DBA is 34 psi.

REV. 6, 4/82

SUSQUEHANNA STEAM ELECTRIC STATION
UNITS 1 AND 2
DESIGN ASSESSMENT REPORT

LINER PLATE PRESSURE
ABNORMAL CONDITION

FIGURE 7-23

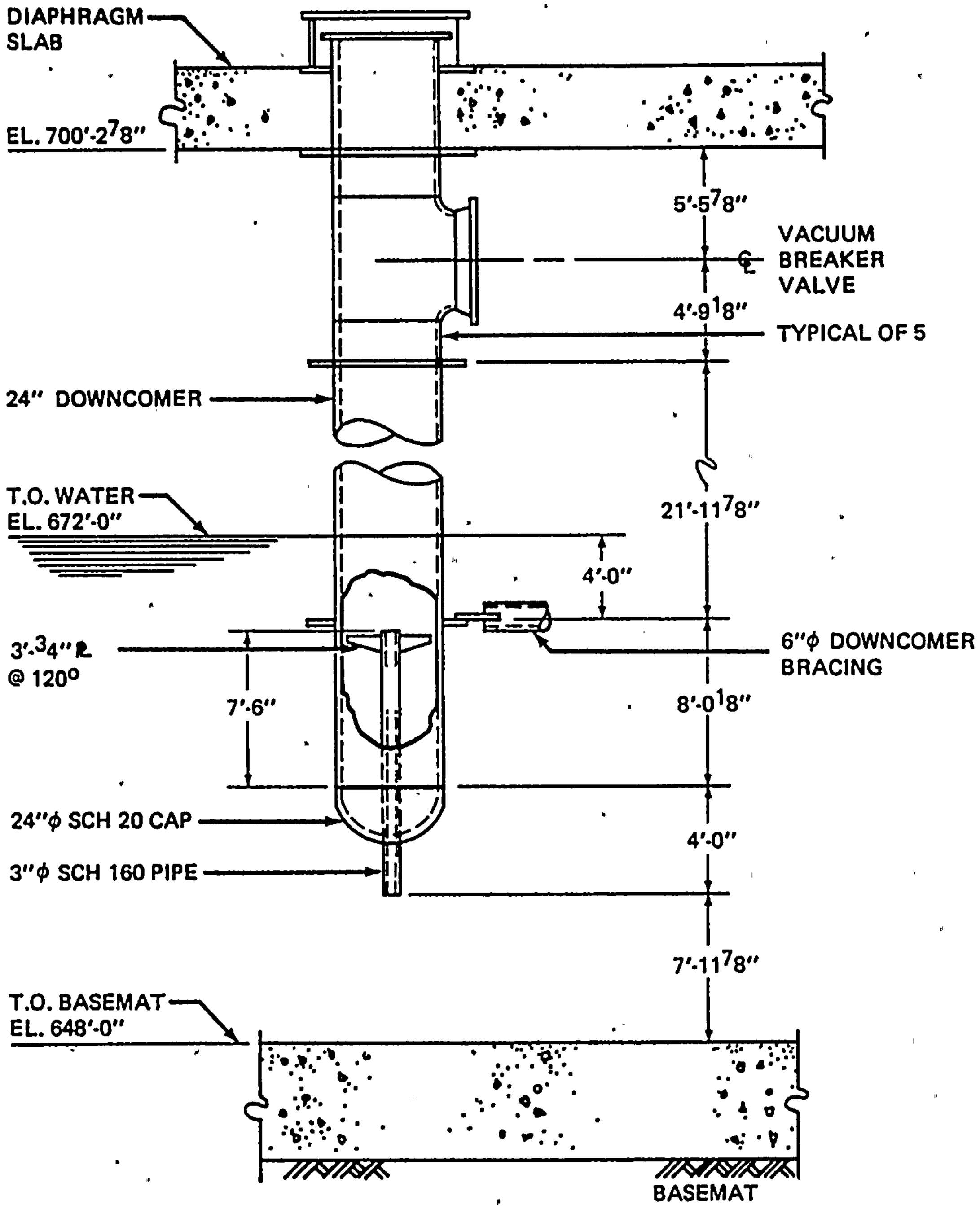

REV. 6, 4/82

SUSQUEHANNA STEAM ELECTRIC STATION
UNITS 1 AND 2
DESIGN ASSESSMENT REPORT

DOWNCOMER WITH
VACUUM BREAKER AND
DETAIL OF CAP

FIGURE 7–24

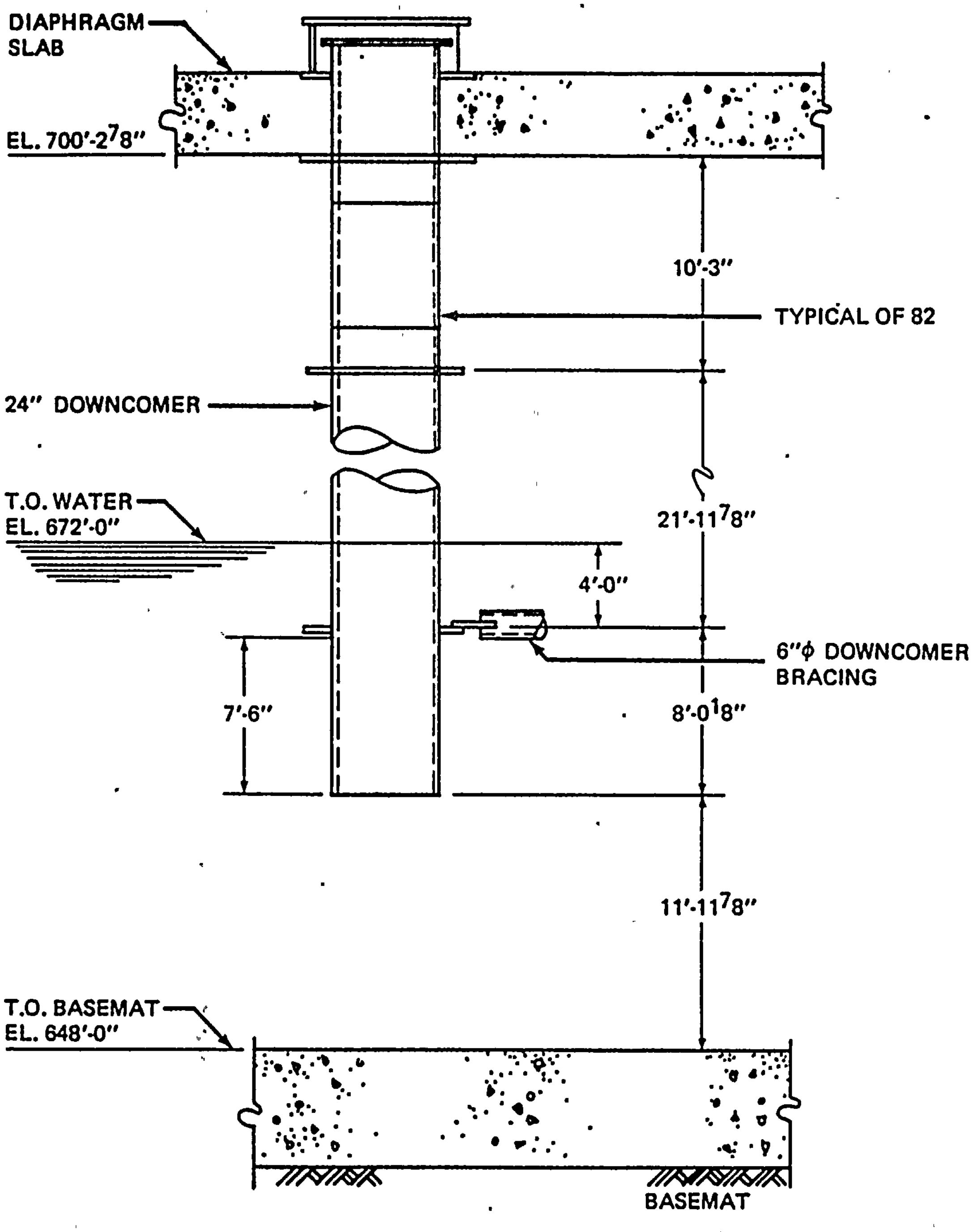

REV. 6, 4/82

SUSQUEHANNA STEAM ELECTRIC STATION UNITS 1 AND 2 DESIGN ASSESSMENT REPORT
DOWNCOMER WITHOUT VACUUM BREAKER
FIGURE 7-25

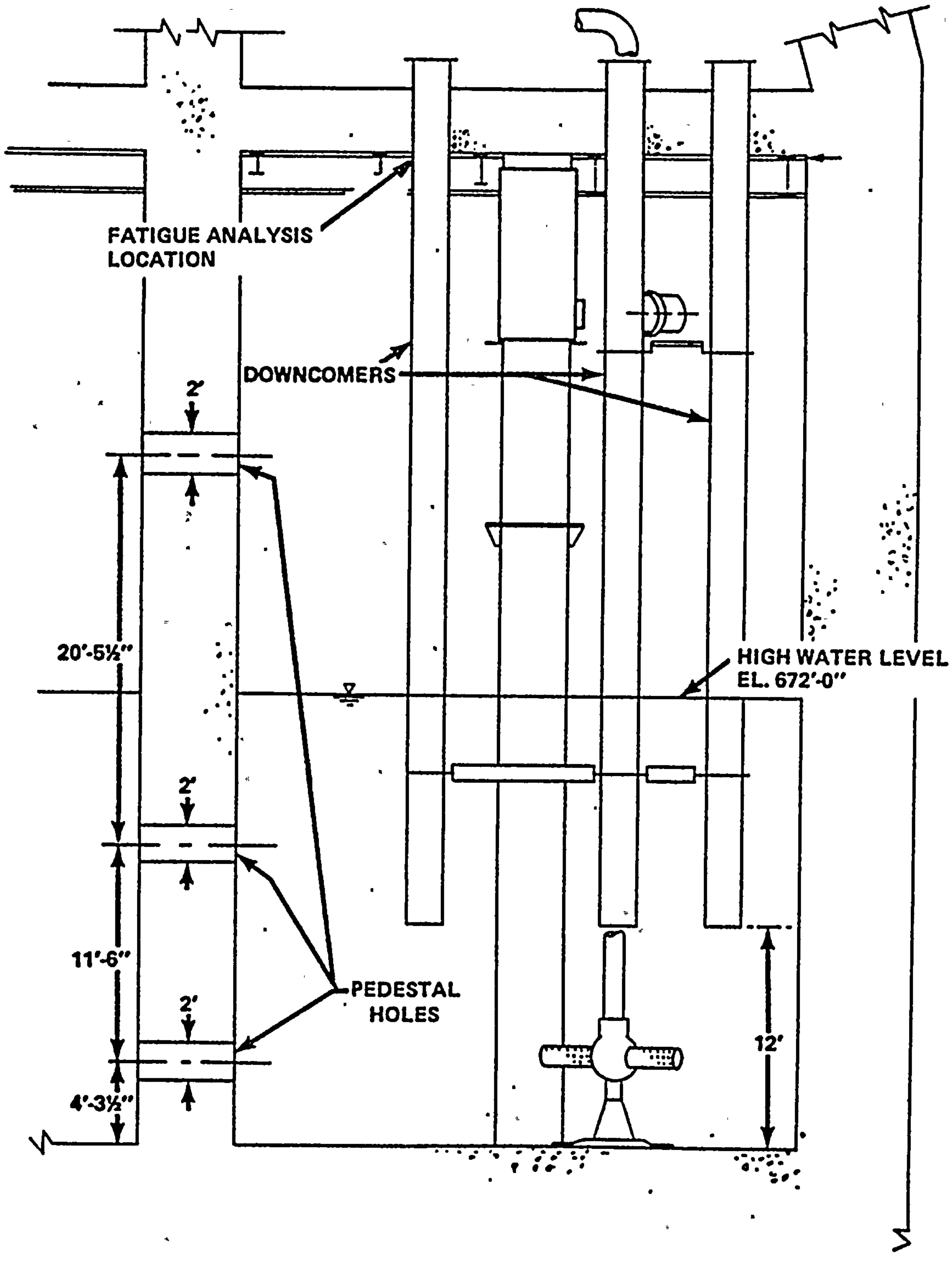

REV. 6, 4/82

SUSQUEHANNA STEAM ELECTRIC STATION
UNITS 1 AND 2
DESIGN ASSESSMENT REPORT

LOCATION WHERE DOWNCOMER FATIGUE ANALYSIS WAS PERFORMED

FIGURE 7–26

Table 7-1

MAXIMUM SPECTRAL ACCELERATIONS OF CONTAINMENT DUE TO SRV AND LOCA

LOADS AT 1% DAMPING

TYPE OF LOAD		LOAD CASE	DIRECTION	NODE NUMBER	ELEVATION	MAXIMUM SPECTRAL ACCELERATION (g)	STRUCTURAL FREQUENCY Hz
SRV		Axisymmetric	Vertical	841	778'-9-3/4"	1.088	15
			Horizontal	135	672'-0"	1.58	38
		Asymmetric	Vertical	252	702'-3"	0.83	40
			Horizontal	131	672'-0"	0.875	38
LOCA	CHUGGING	Axisymmetric	Vertical	235	702'-3"	1.80	54
			Horizontal	131	672'-0"	8.5	30
		Asymmetric	Vertical	235	702'-3"	1.56	54
			Horizontal	131	672'0"	7.1	30
	(CO)	Axisymmetric	Vertical	850	731'-3-1/4"	1.0	11
			Horizontal	131	672'-0"	1.97	30

Table 7-2

MAXIMUM SPECTRAL ACCELERATIONS* OF REACTOR AND CONTROL BUILDINGS
FOR 4% OF CRITICAL DAMPING

TYPE OF LOAD		LOAD CASE	DIRECTION	NODE NUMBER	ELEVATION	MAXIMUM SPECTRAL ACCELERATION (g)	STRUCTURAL FREQUENCY Hz
SRV		Axisymmetric	Vertical	25	697'-0"	1.7	15
			Horizontal	NA	NA	NA	NA
		Asymmetric	Vertical	25	697'-0"	0.35	15
			Horizontal (E-W)	37	683'-0"	0.35	25
LOCA	CHUGGING	Axisymmetric	Vertical	25	697'-0"	3.5	15
			Horizontal (E-W)	37	683'-0"	3.0	25
		Asymmetric	Vertical	25	697'-0"	2.7	15
			Horizontal (E-W)	36	670'-0"	2.1	75
	(CO)	Axisymmetric	Vertical	23	870'-0"	1.85	11
			Horizontal (E-W)	37	683'-0"	1.0	25

*These accelerations are based on a review of the acceleration response spectra presented in Appendix C.

Table 7-3

USAGE FACTOR SUMMARY OF DOWNCOMERS

	NORMAL/UPSET CONDITION			EMERGENCY/FAULTED CONDITION		
LOADS	± OBE ± SRV1 ± SRV2	± SRV1 ± SRV2 ± CHUG	± SRV1 ± SRV2	SBA •Pressure •Thermal Transient •Steam Flow ± CHUG ± SRV*	IBA or SBA •Pressure •Thermal Transient •Steam Flow ± CHUG ± SRV* ± SSE	DBA •Pressure •Thermal Transient •Steam Flow ± CHUG ± SSE
At diaphragm location	0.0083	0.608	0.774	0.774	0.791	.782

Notes: 1) SRV* is a combination of direct loads and building response loads.

2) CHUG is the maximum chugging load (direct load and building response).

3) The calculation is based on ASME, Section III, 1979 Summer Addendum.

4) The combination of ± CHUG, ± SRV* and SSE or OBE is by SRSS.

5) Thermal and pressure loads are combined with 4) by absolute sum.

6) SRV1 is submerged structure load.

7) SRV2 is building response load.

TABLE 7-4 MAXIMUM CUMULATIVE USAGE FACTORS
FOR SRV DISCHARGE LINE

COMPONENT	CALCULATED CUMULATIVE USAGE FACTORS	CODE ALLOWABLE CUMULATIVE USAGE FACTORS
Flued Head	0.46	1.0
3-Way Restraint	0.51	1.0
Elbow (Line P)	0.56	1.0

Table 7-5

DOWNCOMERS AND BRACING SYSTEM

MODAL FREQUENCIES

MODE	FREQ. (HZ)	WEIGHT PARTICIPATION FACTORS HORIZ-X	HORIZ-Y	VERTICAL
1	1.84	0.320	1.274	---
2	1.84	-1.278	0.321	---
3	2.53	0.001	-0.013	---
4	6.58	---	0.001	---
5	8.64	0.001	-0.002	---
6	9.95	-0.001	0.001	---
7	13.27	0.004	-0.002	-0.002
8	14.05	-0.001	0.004	-0.002
9	14.55	0.001	-0.001	0.004
10	15.12	0.003	0.002	-0.001
11	15.17	-0.007	---	0.006
12	15.27	0.002	0.001	---
13	15.38	---	0.003	-0.008
14	15.44	-0.001	0.003	-0.007
15	15.46	-0.003	-0.001	0.002
45	15.75	---	0.002	-0.012
46	15.76	-0.004	0.001	0.004
47	17.44	0.010	0.521	---
48	17.44	-0.504	0.006	---
49	17.50	0.023	-0.116	---
50	17.78	0.015	0.126	---
93	45.05	-0.072	0.460	---
94	45.14	-0.416	-0.059	---
95	45.33	-0.005	-0.027	---
96	45.82	0.007	0.256	---

CHAPTER 8

SSES QUENCHER VERIFICATION TEST

Chapter 8 is proprietary and is found in the proprietary supplement to this DAR.

CHAPTER 9

SSES LOCA STEAM CONDENSATION VERIFICATION TEST GKM-IIM

TABLE OF CONTENTS 2

CHAPTER 9

FIGURES

2 **Number** **Title**

Figures 9-15 thru 9-151 are contained in the Proprietary Supplement.

CHAPTER 9

TABLES

Tables 9-6 thru 9-11 are contained in the Proprietary Supplement.

9.0 GKM IIM TESTS

9.1 INTRODUCTION

The NRC in NUREG 0487, "Mark II Containment Lead Plant Program Load Evaluation and Acceptance Criteria", accepted the Mark II Owners load definition for condensation oscillation but with regards to the specified frequency range cautioned that: "Some modification may be required to correct for the difference in
3 vent configuration between the 4T (Temporary Tall Test Tank) facility and the prototypical Mk II Containment." The Mark II Owners then proceeded to run several series of small scale tests to investigate the effect of vent length on the condensation oscillation load. Results from these tests proved inconclusive. It was then decided that the most expedient way to resolve the questions associated with vent length effects was to run a series of full-scale tests in a facility with a prototypical vent configuration.

2 The Mark II Owners Group selected the GE 4T facility to run this new series of full-scale tests. In addition, it was decided by PP&L to conduct a series of transient steam blowdown tests in a modified GKM II test tank in Mannheim, Germany. This chapter presents a description of this test program, the results from these tests and a comparison of the results with the design specification used on the SSES containment.

9.1.1 Purpose of Test

The load specification for the LOCA steam condensation events for the SSES is based on the results of the tests performed in the first quarter of 1976 at the 4T test tank in the GE Pressure Suppression Test Facility. These load definitions are provided in Section 4.2 of the SSES DAR. In order to resolve NRC concerns regarding the differences in vent length between the 4T tank and the prototypical MK II containment and to verify the LOCA steam condensation load specification used on SSES, it was decided by PP&L to conduct this series of tests.

9.1.2 Test Concept

The concepts used to design and perform the tests were:

1) Use of a conservatively defined single cell

3 2) The close prototypical simulation of the downcomer system parameters

9.1.2.1 Unit Cell Approach

9.1.2.1.1 Single Cell Theory

For a gas bubble oscillating in a free water space, the water mass coupled to the bubble is alternately accelerated and decelerated. During this process the overpressure and underpressure amplitudes decrease with increasing distance from the bubble. When a solid wall is placed near the oscillating bubble, the water acceleration is restricted in the direction of the wall and the decrease in pressure amplitude in the direction of the wall is less. This effect can be expressed mathematically by replacing the bubble by a potential source and accounting for the wall by the method of images. The effects of the real source and the image source are added for each point of the flow field. 2

For the case in which a bubble is enclosed in a narrow water space, closely surrounded by solid walls and a solid bottom with a free water surface at the top, the water space below the bubble is for all practical purposes unmoved. Only the water volume above the bubble is free to oscillate. Consequently, the pressure gradient in the lower water space is nearly zero, while the pressure amplitude above the bubble decreases with increasing proximity to the water surface, until it is zero at the water surface. 3

Analytically, the case in which a planar field of uniform strength sources are all acting in phase is the same as the case in which solid walls exist between each of the individual sources. The single cell test configuration used at GKM-IIM simulates this extremely conservative case of parallel sources acting in phase with the same strength.

9.1.2.2 Simulation of SSES Parameters

The following section provides a description of those parameters that were simulated in the GKM-IIM test facility. A single cell corresponding to the SSES is simulated at actual scale in the GKM-IIM test stand. The single cell consists of a vent pipe with proportionate drywell and suppression chamber. A comparison of the plant and test parameters is given in Table 9-1.

9.1.2.2.1 Drywell

The volume of the drywell part of the test tank corresponds to the proportionate volume of the drywell in the plant. The drywell walls are preheated to temperatures of about 143 °C (corresponding to 4 bar saturated steam) in order to avoid significant steam condensation. As a result, the mass flow values in the test are higher than in the plant, where greater condensation on the dry well internals and walls is possible. Since the drywell of the test stand consists of a volume without any major internals, the air is flushed over just as fast, and probably even somewhat faster than in the plant. 3

9.1.2.2.2 Suppression Chamber (Wetwell)

Like the drywell volume, the free air volume of the suppression chamber also corresponds to the proportionate value in the plant. As a result, the pressure build-ups in the test tank and in the SSES containment are equal.

The ratio of surrounding water surface to the cross-sectional area of the vent pipe varies in the plant as a function of the pipe's position. Theoretical and experimental investigations show that the condensation loads decrease with increasing area ratio. Therefore, the single cell with the smallest area ratio at the containment wall was simulated in the test stand. Its
3 area of 3.77 m^2 (40.7 $ft.^2$) is clearly less than the mean value in the SSES (5.64 m^2); 60.7 $ft.^2$. This adds considerable conservatism to loads measured in the test stand.

Due to the decreased volume of water relative to the mean value in the plant, there is a greater heating of the water in the suppression chamber during the tests than would be expected in
2 the plant.

The volume flexibility of the suppression chamber walls is less than or equal to the plant value of 0.6×10^{-3} m^3/bar (37.2 in^3/bar) relative to the single cell.

9.1.2.2.3 Vent Pipe

The vent pipe has practically the same dimensions and the same distance from the bottom as in the plant. Previous test series and also theoretical considerations have shown that the condensation loads vary somewhat with the submergence depth of the pipe.

For small submergence depths, the loads first increase rapidly with increasing depth and then approach a limiting value asymptotically. Therefore, the tests are performed at the highest value of submergence depth, 3.66 m (12 ft), occurring in the plant.

The vent pipe braces have a stiffness greater than or equal to the maximum value of 770×10^6 N/m (4386 kips/in) occurring in the plant and are located at the same position as in the plant.

9.1.2.2.4 Pool Internals

To be able to determine the load on a perforated-pipe quencher of the depressurization system located near the vent pipe in the suppression chamber during the condensation processes, a quencher arm having the actual dimensions is installed in the test tank. The quencher arm with central member is welded to the inner cylinder in the pool at a distance of 1.1 m from the bottom.

To determine the vertical loads produced by the condensation on steel structures in the water region, an I-beam (ASCI W 10 x 45) is arranged horizontally between the vent pipe outlet and the pool surface (6.3 m from the bottom).

9.2 TEST FACILITY AND INSTRUMENTATION

9.2.1 Physical Configuration

The test configuration as constructed is typically illustrated diagrammatically in Figure 9-1. The entire test system consists of:

- The steam accumulator (GKM Designation: Condensate Accumulator S 6),

2 - The arrangement for steam buffering of the steam accumulator (GKM Designation: Feedwater Tank B202), and

- The actual Test Tank (GKM Designation: Condensate Accumulator S 3).

The test set-up simulates the pressure suppression system of the reactor plant in a so-called single cell (one vent pipe with proportionate drywell and suppression chamber) at actual scale.

3 From a tank (S 6) which is filled partially with saturated steam (simulating the reactor pressure vessel), steam flows via a discharge line and flow orifice into the actual test tank (S 3) which is subdivided into a drywell and a suppression chamber.

3 9.2.1.1 Steam Accumulator and Discharge Line (Main Steam Line Break)

The Condensate Accumulator S 6 in Shop I of GKM, with a capacity of about 120 m^3, is used to simulate the reactor pressure vessel in the test stand; see Figures 9-1 to 9-5. Before test start, this accumulator is filled with water and steam in a saturated condition. The pressure is 20 bar or less, depending on the requirement of the relevant tests.

Between the accumulator S 6 and the actual test tank there is mounted an ND 400 pipe as a discharge line; cf. Figures 9.1 - 9.5. Located in this line is an isolating slide valve, quick-opening valve and a standard orifice for flow-rate limitation in accordance with the simulated break size. By using orifices of different diameter and by specifying the pressure and water filling of the condensate accumulator, the blowdown transient is set. Besides flow-rate limitation, the standard orifice is also used for flow-rate measurements.

Before test start, the discharge line is sealed at the entrance into the test tank (S 3) by a rupture disk combination ND 400 with support pressure (nitrogen). The rupture disks expose the flow cross-section in a few milliseconds at test start.

9.2.1.2 Steam Buffering of the Steam Accumulator (Recirculation Line Break)

The blowdown from an assumed pipe break inside the containment (RCL break) results in a relatively high level, short term constant mass flow rate. However, using the test stand as set-up in Subsection 9.2.1.1 leads to a steadily decreasing mass flow rate.

In order to simulate this situation under the given conditions of the test stand, the assignments of the individual tanks was changed so that tank B 202 was used as the actual accumulator. The tank S 6 was then used as a buffer tank which is continually connected to the GKM superheated-steam network. At the beginning of the test, this tank is connected directly to the discharge line to the test tank. Within 10 to 20 seconds after test start, this connection is broken by means of a quick-closing valve in accordance with the prescribed mass flow rate variation and the 2
test proceeds as described previously until pressure equalization is achieved in tank B 202 and test tank S 3.

9.2.1.3 Test Tank

The condensate accumulator S 3 is used to simulate the SSES containment and is constructed as shown in Figures 9-1 to 9-5. The upper portion of the tank is the drywell and the lower portion is a partially waterfilled suppression chamber. The following volume subdivisions result:

- Drywell S 3 (with pipe portion of the suppression chamber at high water level in the inner tank) 75.6 m^3 3
- Suppression chamber air space with completely filled annular gap and high water level in the inner tank 47 m^3 3
- Water filling of the inner tank in the S 3 at high water level 26 m^3 3

This subdivision conservatively simulates the SSES "single cell."

The bottom of the drywell serves as the diaphragm floor where the vent pipe is attached. The vent pipe is identical in length, diameter and wall thickness to the plant version.

In the lower part of the test tank, the simulated suppression pool, a thick-walled inner cylinder made of steel, was installed. The installation of this inner cylinder satisfies two requirements resulting from the specified similarity to the plant. First, the water volume is reduced to simulate the smallest plant single cell and second, the wall thickness of 100 mm results in a stiffness which corresponds to that of the concrete walls in the plant. The vent pipe bracing stiffness and location is very closely prototypical of the actual SSES as built arrangement. 3

The partition wall between drywell and suppression chamber is provided with swing-check valves for protection of the test stand. The steam inflow at the upper end of the vent pipe is simulated in a representative manner by the installation of the correct vent riser and jet deflector plate.

The drywell region of the test tank is provided with an electrical heating system on the outside wall. The initial temperature of the wall and thus the condensation of steam inside
3 the drywell can thereby be controlled.

Besides comprehensive instrumentation, viewing ports are mounted on the test tank in the air region and water region of the suppression pool, making it possible to observe the processes with a television camera and high-speed cameras. To permit good film quality, demineralized water is used to fill the suppression pool.

9.2.2 Instrumentation

Instrumentation is provided for controlling the test sequence, determining the prescribed measurement quantities, and recording them.

9.2.2.1 General Description

2

The instrumentation used in the GKM-IIM test facility consists of operating instrumentation and test instrumentation. The purpose of the operating instrumentation is to control the test sequence and monitor the test stand. The test instrumentation ensures the recording of all data of significance for evaluation of the phenomena which occur during steam condensation.

Details on the operating instrumentation are given in Subsection 9.2.2.3. A detailed description of the test instrumentation can be found in Subsection 9.2.2.4.

9.2.2.2 Instrumentation Identification

The measurement transducers are identified by a system of letters and numbers. Each identification starts with a letter or letters describing the type of transducer:

P	for Pressure Transducer
T	for Temperature Sensor (Thermocouple)
L	for Water Level Measurement
DG	for Displacement Gage
SG	for Strain Gage
I	for Electrical Impulse Signal
LP	for Level Probe
LC	for Load Cell
AF	for Air Fraction
OR	for Oxygen Rate

Following these letters is a number which characterizes the mounting location or measurement location in the test stand. For that purpose, the test stand is divided into different System Groups as follows (see Fig. 9-1): 3

System Group 1	steam lines to the accumulator S6 and to the feedwater tank B 202 and in the feedwater tank B 203 3
System Group 2	feedwater tank B 202
System Group 3	steam accumulator S6 3
System Group 4	steam supply to the test stand
System Group 5	instrumentation of the proportionate drywell with the vent pipe
System Group 6	suppression chamber 3

The System Groups 1-4 contain the operating instrumentation, while groups 5 and 6 designate the test instrumentation. 3

After this identification number there is a decimal point which separates this number from the running numbers of the transducers.

9.2.2.3 Operating Instrumentation

The purpose of the operating instrumentation (see Table 9-2, Figures 9-1, 9-3, and 9-4) is to monitor the steam accumulator, feedwater tank and steam lines. The signals from the measurement 2 transducers are read by a process control computer and recorded. This computer is a part of the operating instrumentation. All data are stored on magnetic tape and can be printed out or plotted after each test. Before test start, the process control computer compares the recorded measurement signals with prescribed setpoint valves and prints them out. If the measurement value differs from the setpoint value by a prescribed percentage, that measured value is identified in the printout.

The operating instrumentation concentrates on the measurement of pressures, temperatures and water levels in the steam accumulator, steam lines and feedwater tanks.

9.2.2.4 Test Instrumentation

The test instrumentation (see Table 9-3 and Figures 9-3 to 9-8) 3 records all the data needed to evaluate the phenomena occurring during steam condensation and the resulting loads in the pool, and also the data needed to determine the steam flow rate in the discharge line. The dynamic pressure loads and accelerations are measured at several points in the pool. The forces occurring at the vent pipe bracing and on submerged structures in the suppression pool are recorded by strain gauges. The pressure build-up in the vent pipe is measured at several points. In addition, level probes are installed on the vent pipe so as to be 3

able to record the dynamic behavior of the water surface. The
strains on the pipe are measured at two places on the vent pipe:
100 mm below the bracing (see Figure 9-5) and approximately 100
3 mm below the gusset plate bracing arrangement simulating the
diaphragm slab (see Figure 9-3). Pressure and temperature
measuring points in the air space of the suppression chamber and
in the proportionate accumulator provide information about the
variation of pressure and temperature during the tests. Two
differential-pressure measuring points in the water region of the
suppression chamber record the air bubble fraction in the pool.
At the upper end of the vent pipe there was a measuring point for
3 the continuous sampling of the steam to determine the air
content. The measurement system for continuous sampling is
provided by SRI International.

The data is recorded on magnetic tape in analog form by means of
carrier-frequency amplifiers and dc amplifiers. This ensures
that high-frequency measurement signals are recorded with proper
frequency and amplitude. The data is reduced later by a
computer. Simultaneously with the recording on magnetic tape,
3 most of the measurement points are also recorded on Visicorders.
That type of recording makes it possible to get a quick look at
important measurement variables shortly after each test. At the
same time, a few selected transducer channels of the test
instrumentation are recorded additionally at the process control
computer. This procedure makes it possible to perform a quick
and simple summary evaluation of that data after each test.

Each measurement chain consists of a transducer, connection
cable, amplifier (carrier-frequency or dc amplifier), balancing
3 unit and recording unit (see Figure 9-10).

The utilized pressure transducers have a measuring diaphragm and a foil strain gage system which is directly connected to the diaphragm. All pressure transducers in the water region of the suppression chamber have an exposed measuring diaphragm with direct contact to the surrounding water. Earlier studies by KWU have shown that this type of transducer is best suited for recording higher-frequency pressure oscillations with correct frequency and amplitude.

The measuring diaphragm for pressure transducers P4.1, P5.1, P5.5
and P6.9 required protection from the hot steam. This was
3 accomplished by means of a short water-filled pipe which connects
the transducers to the measurement site. The remaining pressure
transducers did not require protection.

9.2.2.5 Visual Recording

The processes in the water region of the suppression chamber are recorded optically on film by a high-speed camera and on video tape by a television camera.

The cameras are mounted outside the tank and observe the processes by means of bull's eyes. Several underwater searchlights are installed in order to ensure satisfactory lighting of the end of the vent pipe.

A uniform electrical reference signal ensures time correlation between all the data acquisition systems.

9.2.2.6 Inspection and Calibration of the Measuring Instrumentation

The calibration and the electrical and physical checking of all sensors before, during and after the tests were performed in accordance with the Test and Calibration Specifications.

Figure 9-11 shows diagrammatically the physical calibration of the transducers, the setting and calibration of the amplifiers and recorders, and the quality inspection of the transducers. The time intervals stipulated for these inspections and calibrations per the Inspection and Calibration Procedures are given in Figure 9-12. Figure 9-13 shows the chain of the calibration system from the National Standards of the Physikalisch Technische Bundesanstalt (PTB) to the measuring instruments.

An additional physical inspection of the pressure transducers in the water region was performed by incrementally lowering the water level and comparing the measured pressure to the known hydrostatic pressure at the transducer location.

With a few exceptions, the 88 sensors used in the tests were fully operational for the duration of the tests. On December 10, 1979, the pressure transducer P 5.4 failed. It was replaced by a new transducer for the subsequent tests. After initial difficulties with the continuous O measuring device, a modification of the sampling arrangement resulted in satisfactory performance. At a few level probes, the insulators were damaged by parts of the rupture-disk diaphragms being carried along by the steam flow. Those level probes were replaced. The strain gauges of measuring point SG 5.1 had to be replaced on November 14, 1979 due to too low insulation resistance.

The final inspection of the sensors after the completion of the test project showed a fully operable instrumentation system.

9.2.2.7 Analysis of Measurement Errors

Based on the information from the manufacturers of the measurement instruments, KWU's own investigations, and taking into consideration the experience gathered in similar test projects, the maximum measurement errors for the individual transducers are as follows:

Pressure transducers P 6.1 ... P 6.8

Linearity error and hysteresis error of the transducer 0.5% of 10 bar ≅ 1.25% of 3 bar	1.25%
Sensitivity error relative to 40 K temperature difference	0.75%
Error of the measuring amplifier	0.5%

Error of the balancing unit and the recorder	0.5%

Maximum total error ± 3% of the measured value

Pressure transducer P 4.1

Linearity error of the transducer 0.3% of 50 bar ≅ 0.75% of 20 bar	0.75%
Reproduction error of the transducer 0.1% of 50 bar	0.05 bar
Sensitivity error relative to 10 K temperature difference	0.1%
Error of the measuring amplifier	0.5%
Error of the balancing unit and the recorder	0.5%

Maximum total error |± 0.05 bar + 1.85% of the measured value|

Pressure Transducers P 5.1, P 5.5, P 6.9

Linearity error of the transducer 0.3% of 20 bar ≅ 1.5% of 4 bar	1.5%
Reproduction error of the transducer 0.1% of 20 bar	0.02 bar
Sensitivity error relative to 40 K temperature difference	0.4%
Error of the measuring amplifier	0.5%
Error of the balancing unit and the recorder	0.5%

Maximum total error ±0.02 bar + 2.9% of the measured value

Pressure transduers P 5.2, P5.3, P 5.4

Linearity error of the transducer 1% of 10 bar ≅ 2.5% of 4 bar	2.5%
Sensitivity error relative to 40 K temperature difference	2 %
Error of the measuring amplifier	0.5%
Error of the balancing unit and the recorder	0.5%

Maximum total error	±5.5% of the measured value

<u>Differential-pressure transducers P 4.2, P 5.6, AF 6.1, AF 6.2</u>

Linearity error of the transducer	0.5%
Sensitivity error relative to 10 K temperature difference	0.2%
Error of the measuring amplifier	0.5%
Error of the balancing unit and the recorder	0.5%

Maximum total error	±2% of the measured value

<u>Displacement transducers DG 6.1 ... 6.5</u>

Error of the transducer	1 %
Error of the measuring amplifier	0.5%
Error of the balancing unit and the recorder	0.5%

Maximum total error	±2% of the measured value

<u>Acceleration transducers AG 6.1, AG 6.2</u>

Linearity error of the transducer	0.75%
Sensitivity error relative to 10 K temperature difference	0.2%
Error of the measuring amplifier	0.5%
Error of the balancing unit and the recorder	0.5%

Maximum total error	± 2% of the measured value

<u>Strain gauges SG, LC</u>

Tolerance of the k-factor	3 %
Influence of temperature on the k-factor	1 %
Error of the measuring amplifier	0.5%

Error of the balancing unit and the recorder	0.5%

Maximum total error	$\pm$ 5% of the measured value

<u>Temperature measuring points</u>

Error of the transducer	1 K
Error of the measuring amplifier	0.5%
Error of the balancing unit and the recorder	0.5%

Maximum total error	$\pm$ 1 K + 1% of the measured value

Repeated recalibrations yielded far better results than indicated by the list of errors.

An overall inspection of the pressure transducers in the water 3
region by incremental lowering of the water level (see Subsection 9.2.2.6) yielded maximum deviations of approximately +0.005 bar and -0.003 bar from the nominal value.

The deviations are illustrated as a frequency distribution in Figure 9-14. They are characterized by a Gaussian distribution.

In order to record the high frequency process with correct frequency and amplitude, the measurement chains were designed for the dynamic range anticipated during the tests. The dynamic range was limited by the carrier-frequency measuring amplifier to approximately 1.4 kHZ, which was substantially less than the 10 kHZ eigenfrequency of the pressure transducers. The magnetic tape recorders did not impose any limitation with a frequency cut-off of 2.5 kHz.

The frequency cut-off of the Visicorders was determined by the utilized galvanometers. They were at 1 kHz for all the high-frequency measuring points. The frequency characteristics of the individual galvanometers was inspected before the tests.

9.3 TEST PARAMETERS AND MATRIX

The test matrix provided for twenty-two tests with eleven 2
different parameter combinations (see Table 9-4). Earlier test series indicate that the strength of the condensation events is very highly stochastic and can differ for tests with identical boundary conditions. In order to largely rule out any erroneous correlation of measurement values with the parameters, each test is repeated once.

Four different line breaks were investigated:

2 - the complete break-off of a recirculation loop (RCL break)

3 - the complete break-off of a main-steam line (full MSL break)

- two other steam-line breaks corresponding to 1/3 and 1/6 of
3 the full MSL break area.

For the RCL break, the break flow consists of both liquid and steam flow. A portion of the liquid flashes into steam and together with the steam from the break gives the total steam flow into the suppression pool. FSAR Table 6.2-9 presents the break steam flow and break liquid flow, together with their associated enthalpies at various times during the RCL break. FSAR Figure 6.2-2 shows the drywell pressure response for the RCL break. This data was used to calculate the fraction of liquid break flow that flashes into steam (assuming thermodynamic equilibrium), and the corresponding total vent steam flow. Figure 9-14a shows the SSES calculated vent steam mass flux vs. time for the RCL break. The RCL tests were run to match this curve as closely as possible (see Subsection 9.4.1.1.1).

3

For the full MSL break, the break flow is also comprised of both liquid and steam flow. Again, a portion of the liquid flashes into steam and combines with the steam from the break to give the total vent steam flow. FSAR Table 6.2-10 gives the break steam flow and break liquid flow, as well as their associated enthalpies at various times during the full MSL break. FSAR Figure 6.2-11 shows the drywell pressure response for the full MSL break. This data was used to calculate the fraction of liquid break flow that flashes into steam (assuming thermodynamic equilibrium), and the corresponding total vent steam flow. Figure 9-14b plots the SSES calculated vent steam mass flux vs. time for the full MSL break. The full MSL tests were run to match this curve as accurately as possible (see Subsecton 9.4.1.1).

3 For these larger break transients the range of low mass flow
densities is passed through very rapidly. In the event of
smaller breaks the blowdown times are distinctly longer. The 1/3
3 and 1/6 MSL breaks were chosen to investigate longer blowdown
transients. Their break sizes were selected so that, if
required, it is possible to compare the results with data known
from earlier tests series.

The test matrix provides for tests at initial water temperatures
2 of 24°C, 32°C and 55°C (75°F, 90°F and 130°F). The value of 32°C
corresponds to the mean temperature which is maintained by the
cooling system of the suppression pool during normal plant
operation. The emphasis on the tests at 32°C is explained by the
fact that no clear dependence of the condensation loads on the
water temperature was observed in previous test series. The
temperatures 24°C and 55°C were taken from the limits of the
operation field of the pressure relief system of the plants.

The amount of air flushed over from the drywell influences the backpressure in the suppression chamber and also the composition of the air-steam mixture flowing through the vent pipe.

Most of the tests are performed with the same (proportionate) amount of air as in the plant. The steam is introduced in such a manner that it can mix in a mostly homogeneous manner with the air. By introducing cool air to the drywell just before the beginning of the test, the air temperature is brought to a 2
temperature corresponding to that in the plant. To investigate the effect of a possible incomplete steam-air mixing, individual tests are performed with reduced air content in the drywell. In those tests, cool air is not introduced into the drywell. The air temperature is then raised by means of the drywell wall heating system mentioned previously in Section 9.2. Thus, the mass of air is decreased by about 15%.

A detailed listing of the test parameters and operating conditions measured before and after each test is contained in Table 9-5. The following parameters are compiled in this table:

- Test duration
- Bottom clearance and submergence
- Water temperature in the test tank
- Temperature of wall and air in the drywell
- Water volume in the accumulator S 6
- Pressure in the accumulators S 6 and B 202 3
- Pressure in the drywell and in the air space of the suppression chamber
- Air content in the drywell
- Diameter of the flow limiter.

The initial and final values were obtained from the computer listings (see Subsection 9.2.2.4). The air temperature in the drywell was not read from the listings "before test," but rather they were obtained from a listing just after the shutdown of the ventilator connected to the drywell some time before the beginning of the test.

For the water temperature and the air temperature in the drywell, the mean value was formed from the corresponding measuring points.

At the end of the test, the water temperature after the mixing of the pool was indicated.

9.4 TEST RESULTS

See the Proprietary Supplement for this section.

9.5 DATA ANALYSIS AND LOAD SPECIFICATION

See the Proprietary Supplement for this Section.

9.6 VERIFICATION OF THE DESIGN SPECIFICATION

See the Proprietary Supplement for this Section.

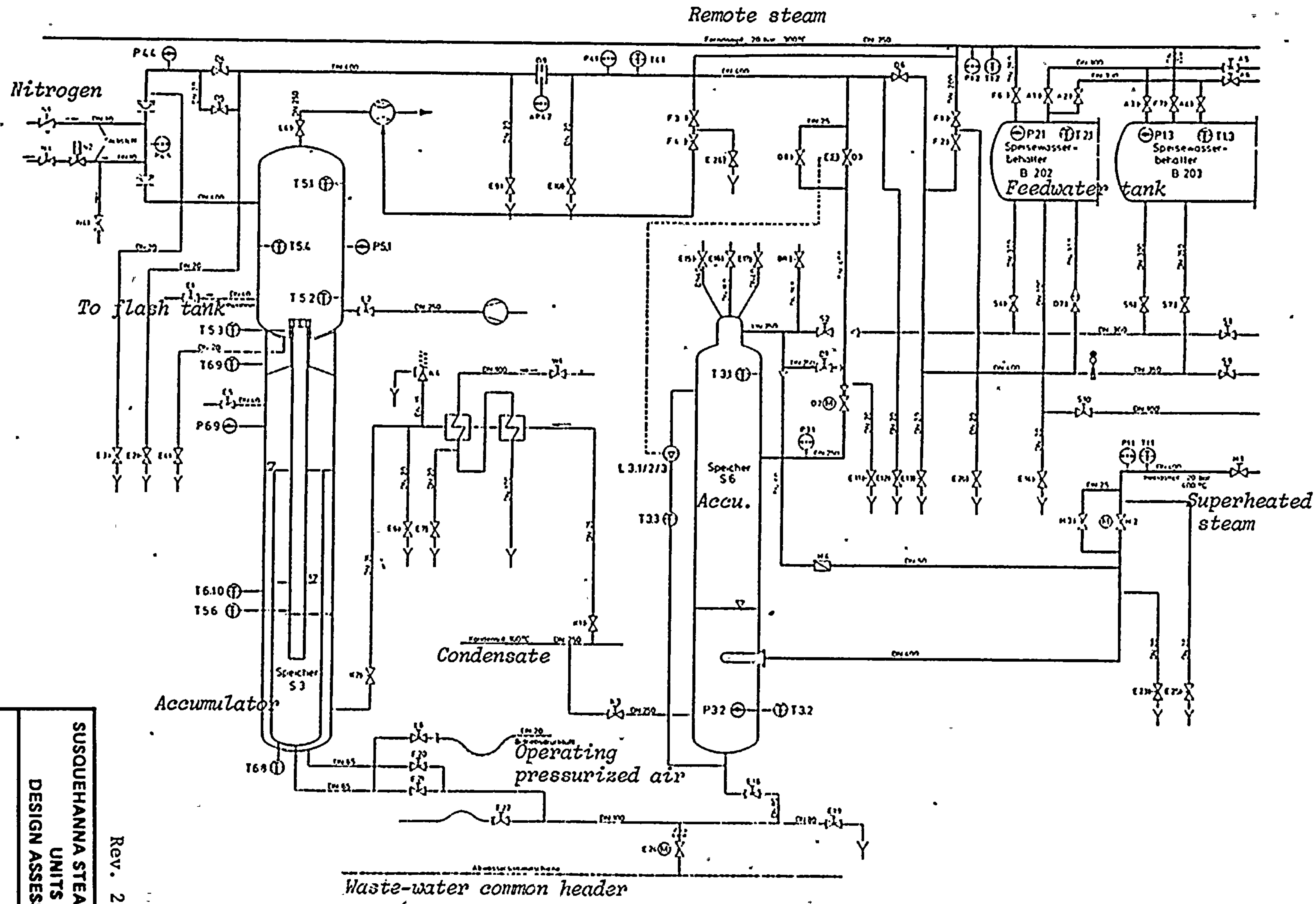

Rev. 2, 5/80

SUSQUEHANNA STEAM ELECTRIC STATION
UNITS 1 AND 2
DESIGN ASSESSMENT REPORT

GKM-IIM CONDENSATION TESTS
TEST STAND SCHEMATIC DIAGRAM

FIGURE 9-1

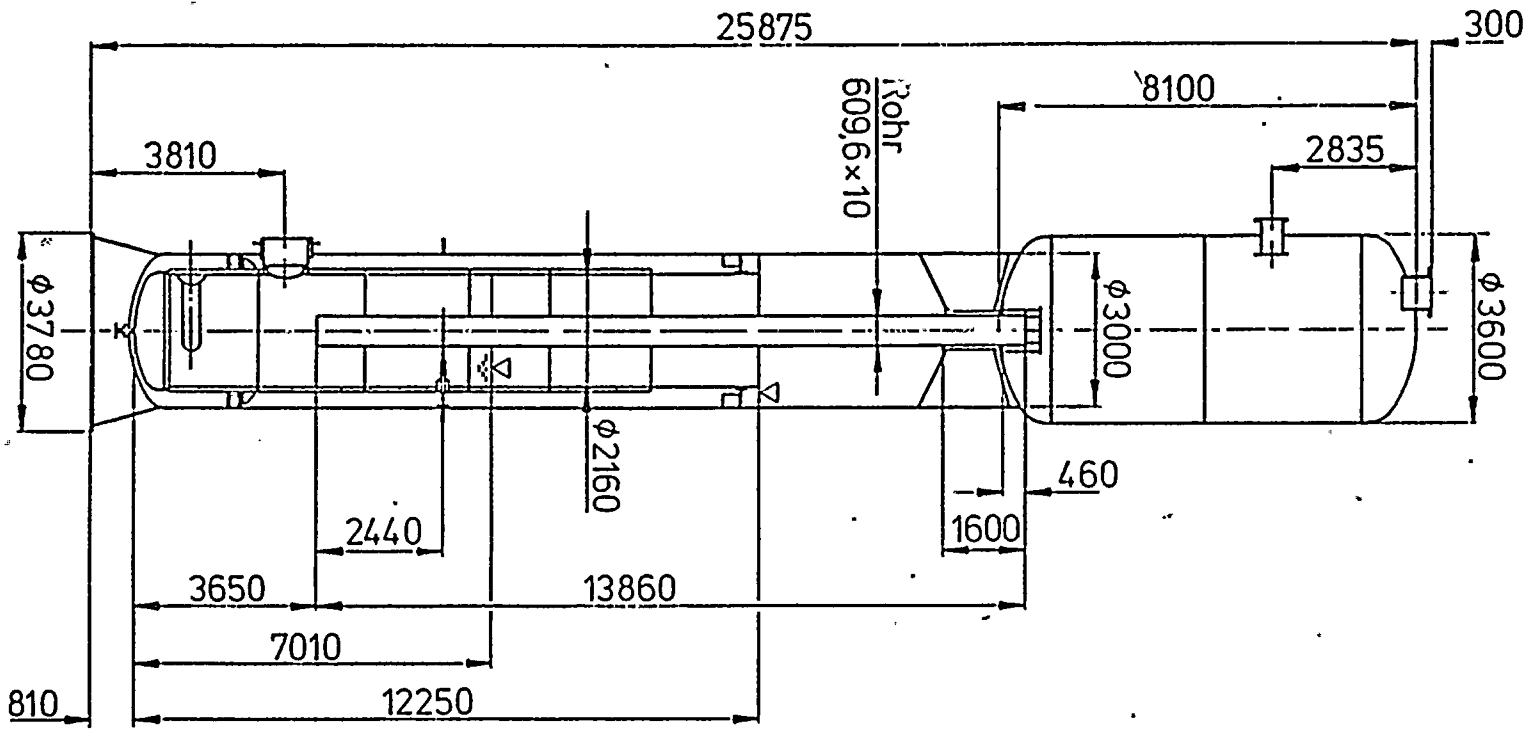

Rev. 2, 5/80

SUSQUEHANNA STEAM ELECTRIC STATION
UNITS 1 AND 2
DESIGN ASSESSMENT REPORT

GKM-IIM CONDENSATION TESTS
TEST TANK

FIGURE 9-2

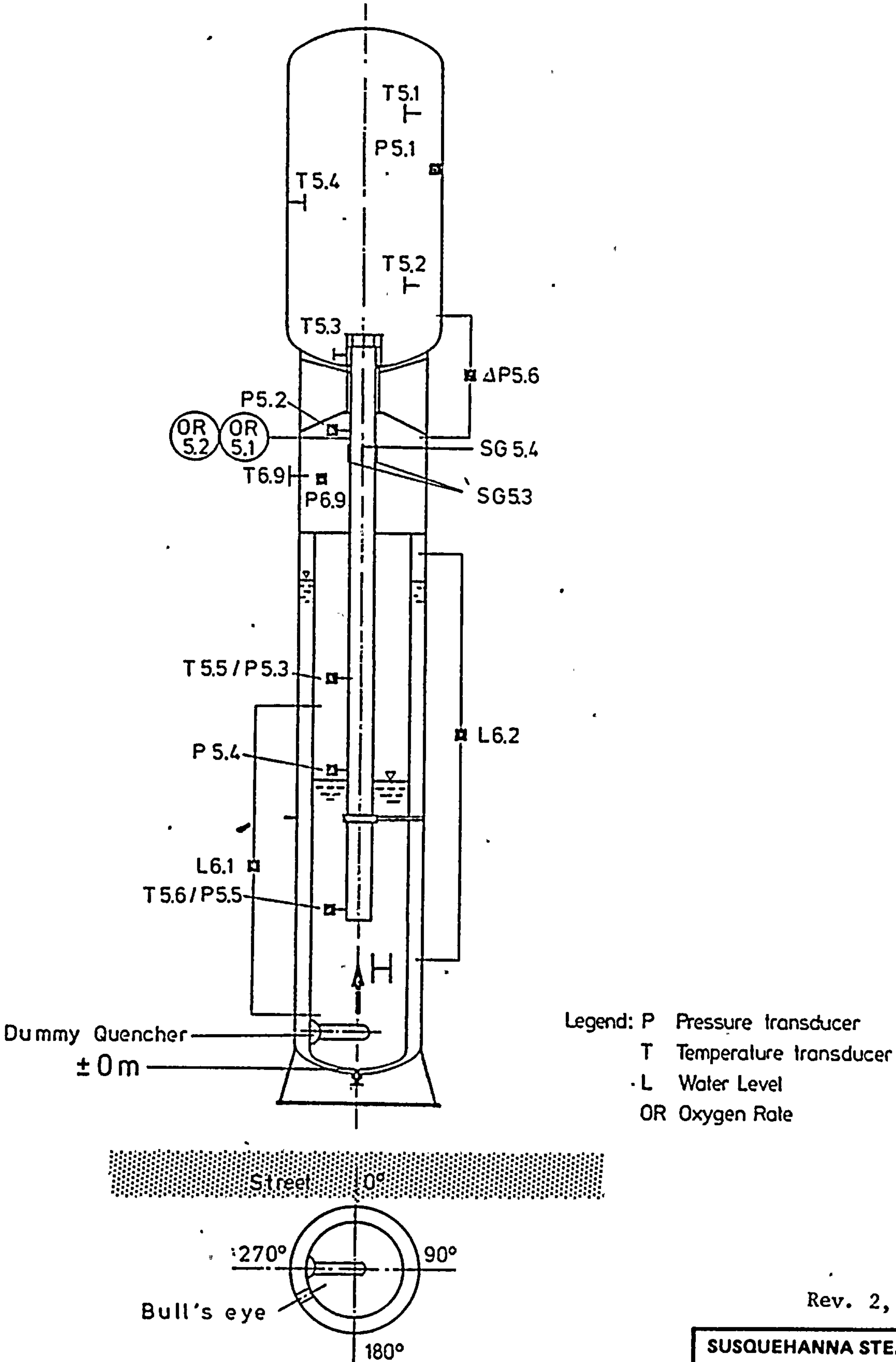

Rev. 2, 5/80

SUSQUEHANNA STEAM ELECTRIC STATION
UNITS 1 AND 2
DESIGN ASSESSMENT REPORT

GKM-IIM CONDENSATION TESTS
COORDINATE SYSTEM AND TEST
INSTRUMENTATION

FIGURE 9-3

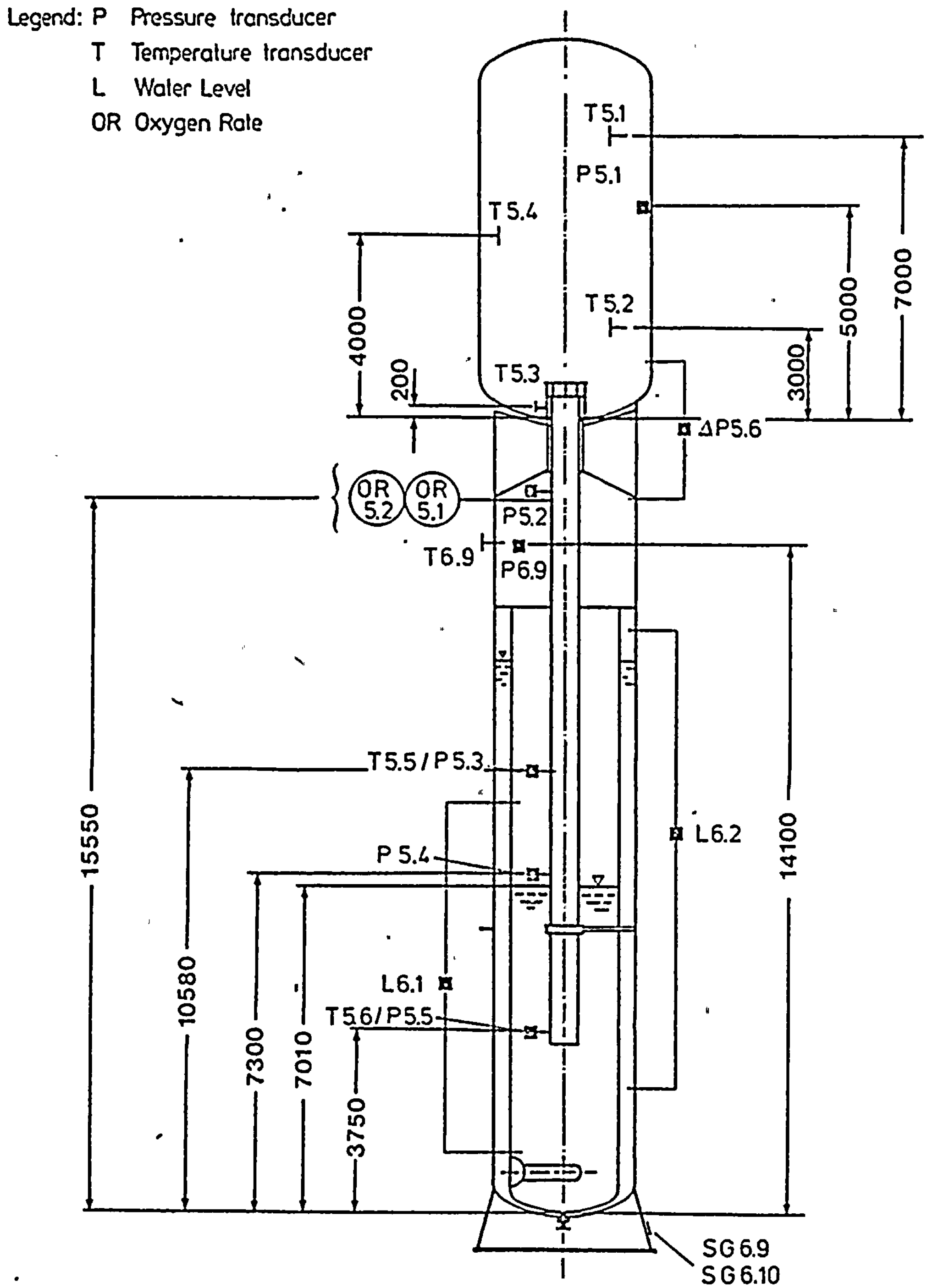

Rev. 2, 5/80

SUSQUEHANNA STEAM ELECTRIC STATION
UNITS 1 AND 2
DESIGN ASSESSMENT REPORT

GKM-IIM CONDENSATION TESTS
TEST INSTRUMENTATION

FIGURE 9-4

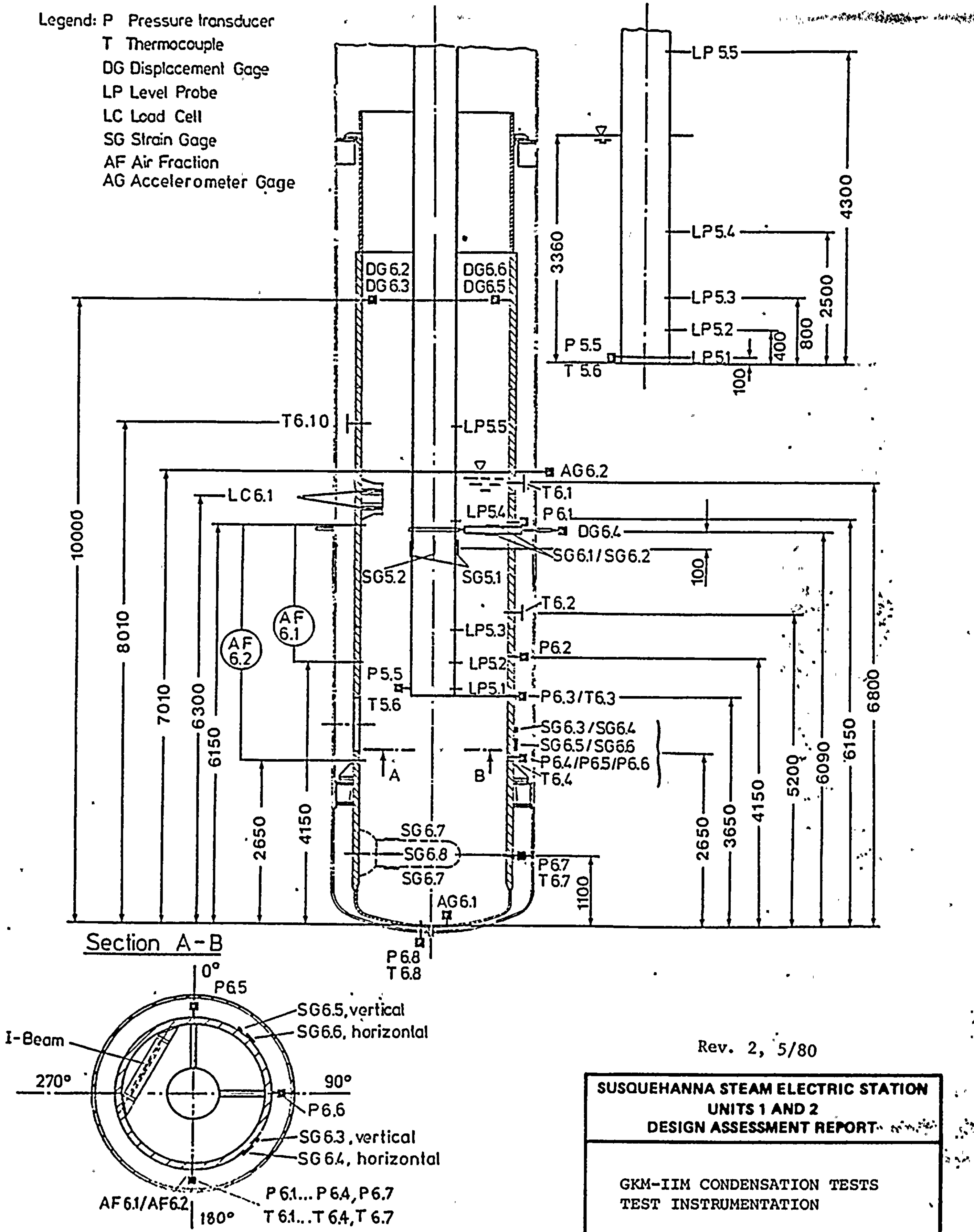

Rev. 2, 5/80

SUSQUEHANNA STEAM ELECTRIC STATION
UNITS 1 AND 2
DESIGN ASSESSMENT REPORT

GKM-IIM CONDENSATION TESTS
TEST INSTRUMENTATION

FIGURE 9-5

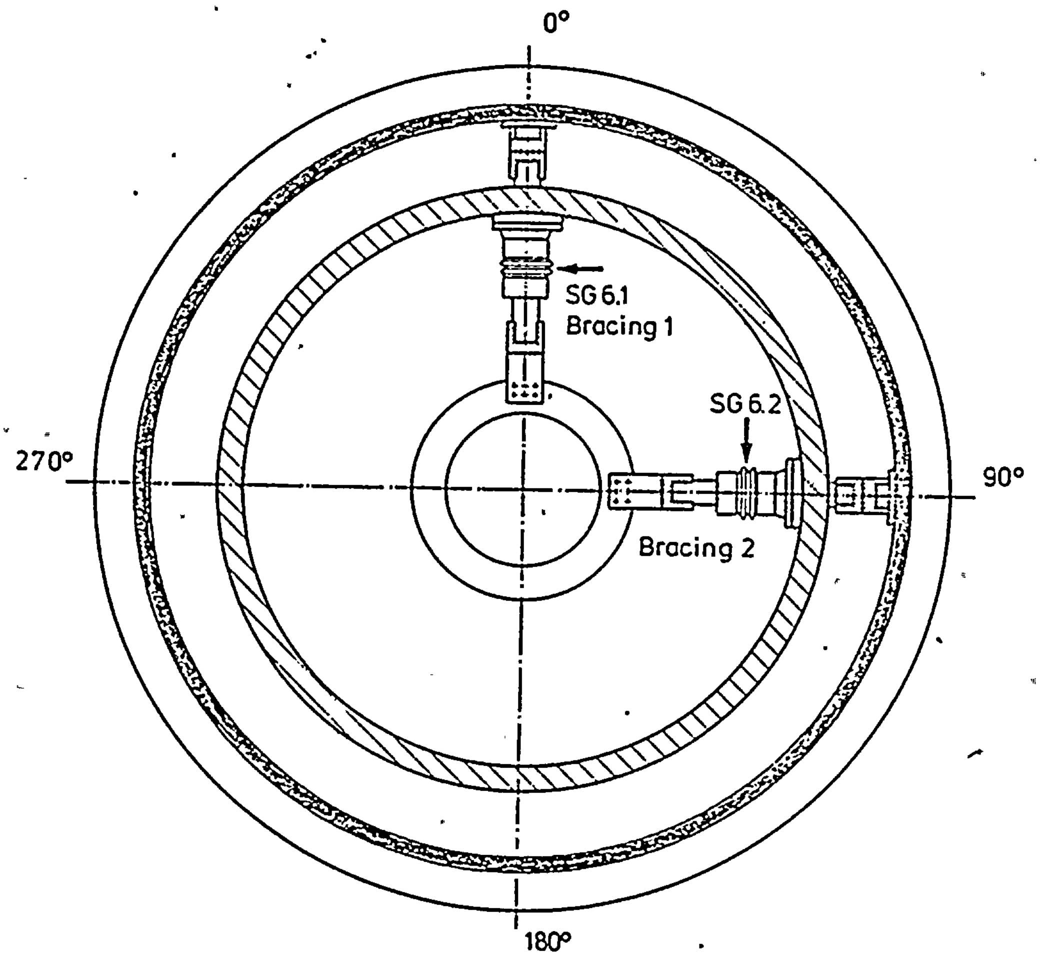

Rev. 2, 5/80

SUSQUEHANNA STEAM ELECTRIC STATION
UNITS 1 AND 2
DESIGN ASSESSMENT REPORT

GKM-IIM CONDENSATION TESTS
BRACING CONFIGURATION

FIGURE 9-6

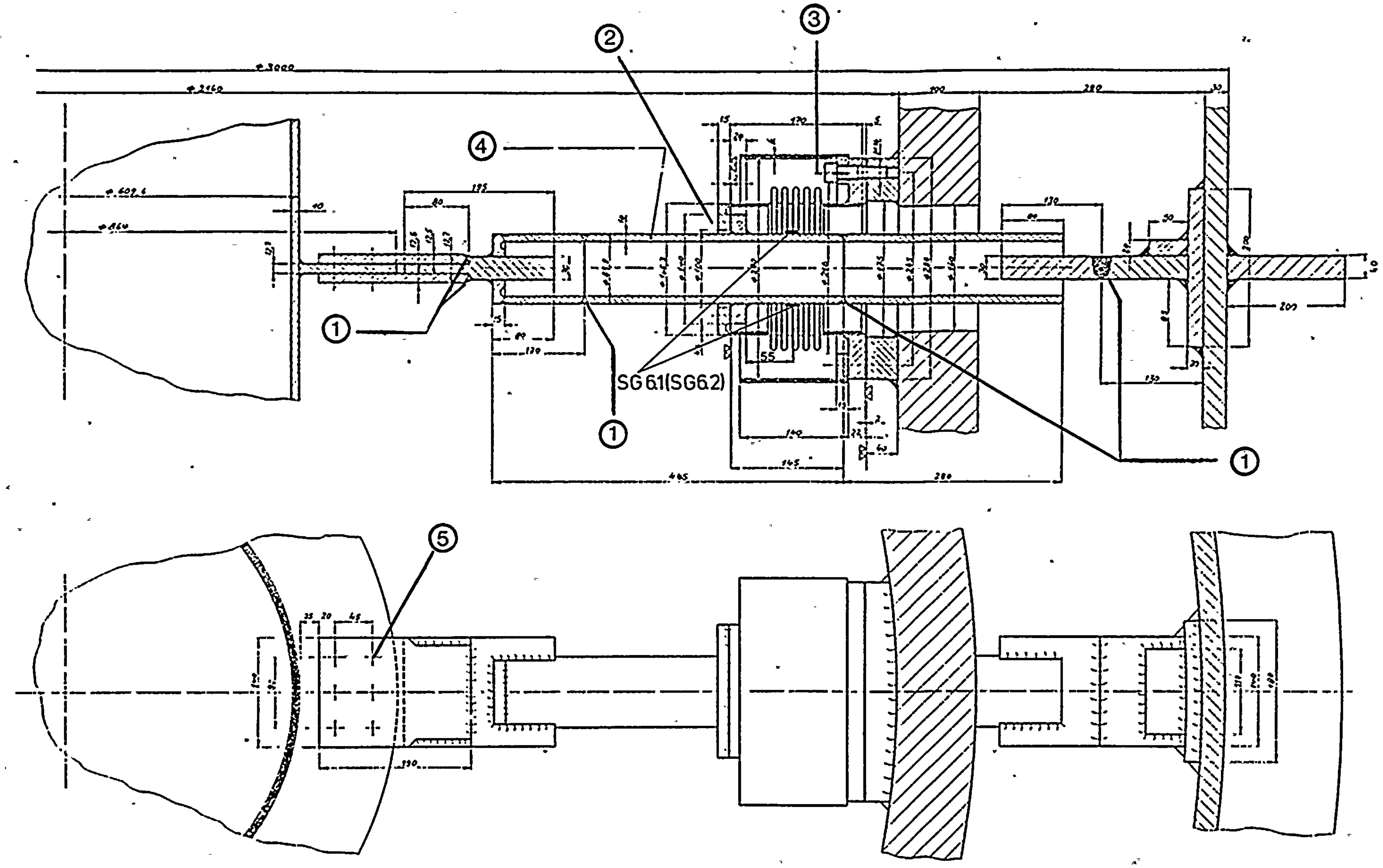

KEY:
1. Assembly welds
2. 8 socket-head cap screws, M8x30 DIN 912
3. 8 socket-head cap screws, M16x65 DIN 912
4. Pipe material St 358
   Elastic modulus 212 kN/mm^2 (20°C)
   206 kN/mm^2 (100°C)
5. 6 hexagon bolts, M20x70 DIN 931 with nuts and washers

Rev. 3, 7/80

SUSQUEHANNA STEAM ELECTRIC STATION
UNITS 1 AND 2
DESIGN ASSESSMENT REPORT

BRACING DESIGN

FIGURE 9-7

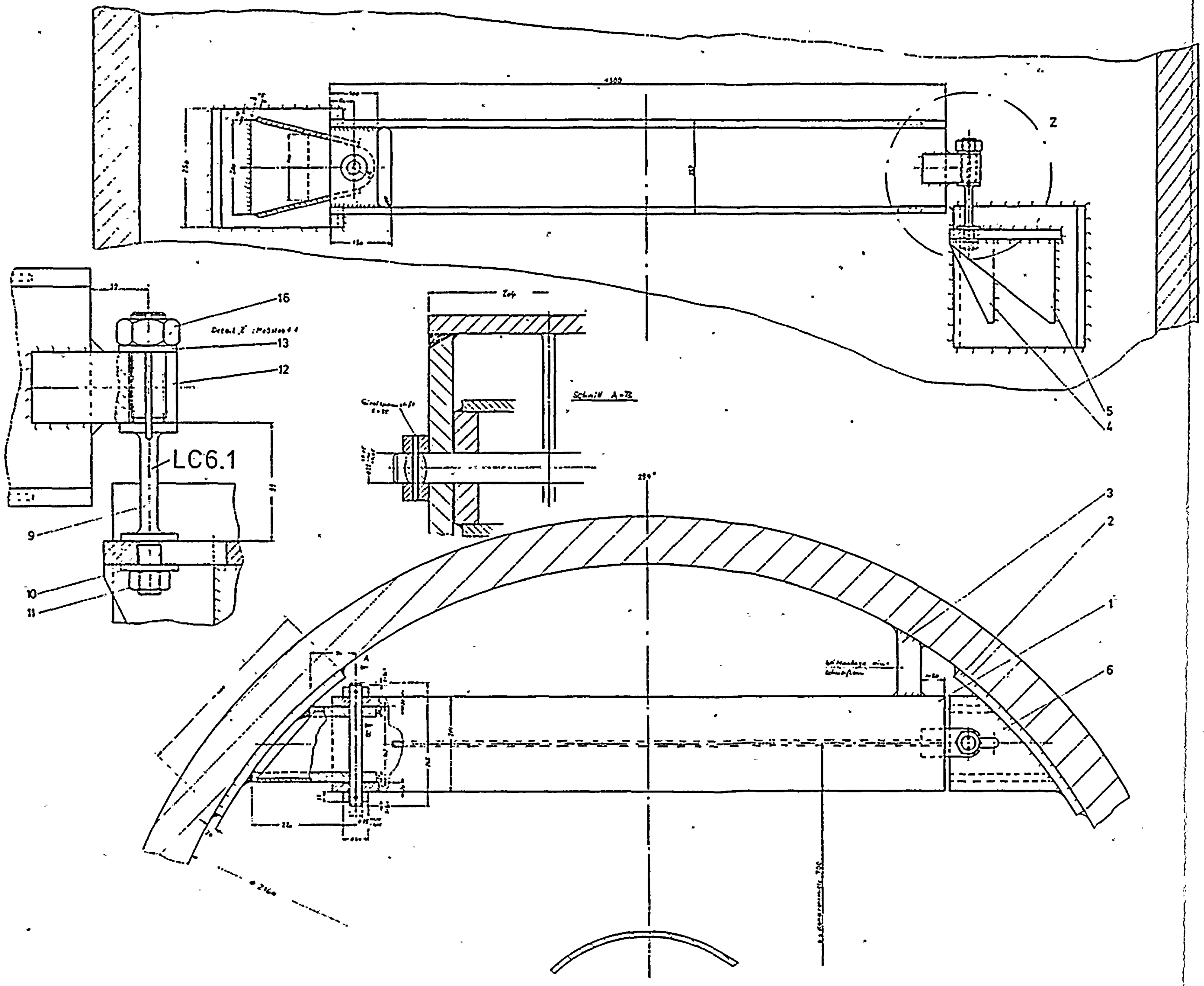

Rev. 3, 7/80

SUSQUEHANNA STEAM ELECTRIC STATION
UNITS 1 AND 2
DESIGN ASSESSMENT REPORT

I-BEAM DESIGN

FIGURE 9-9

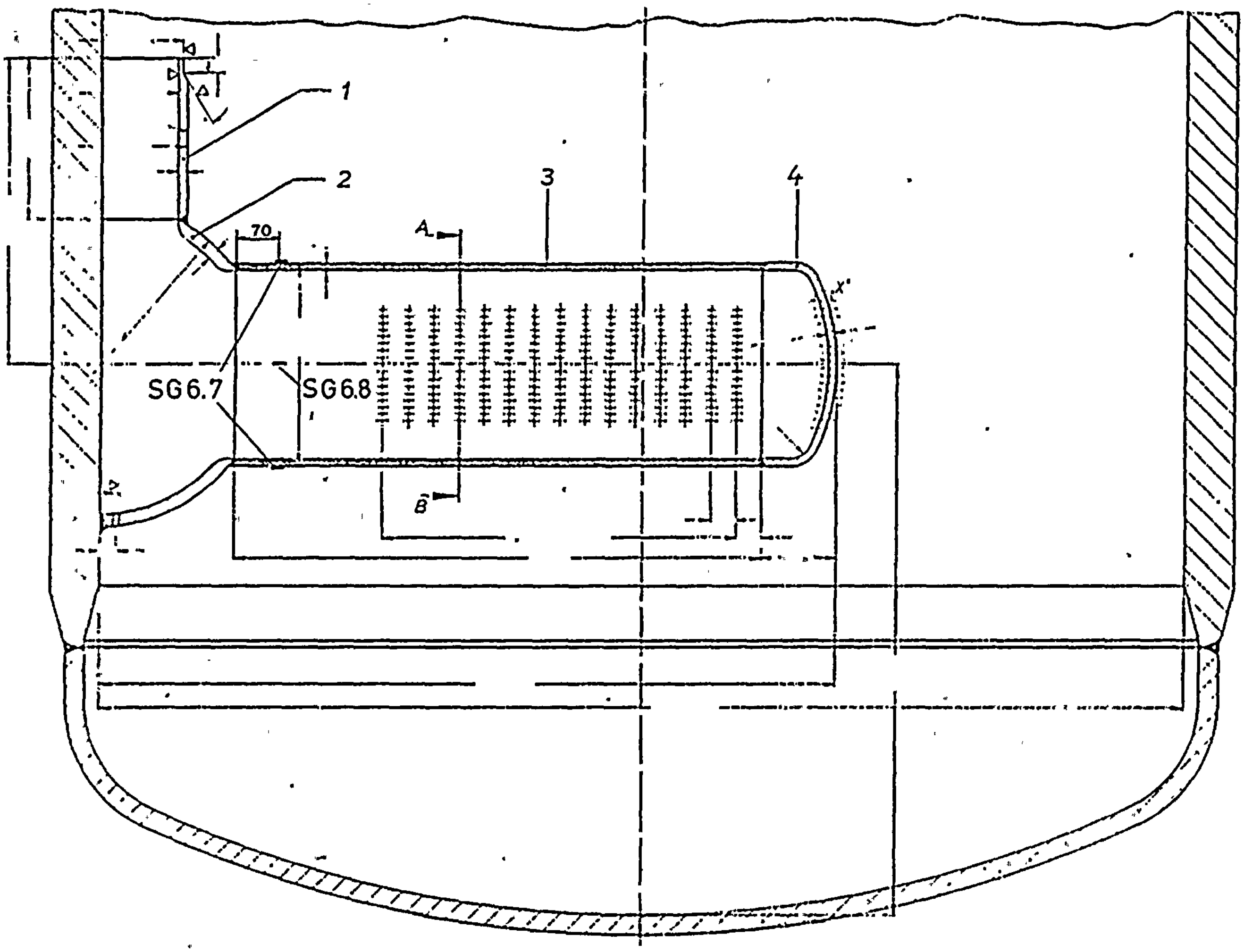

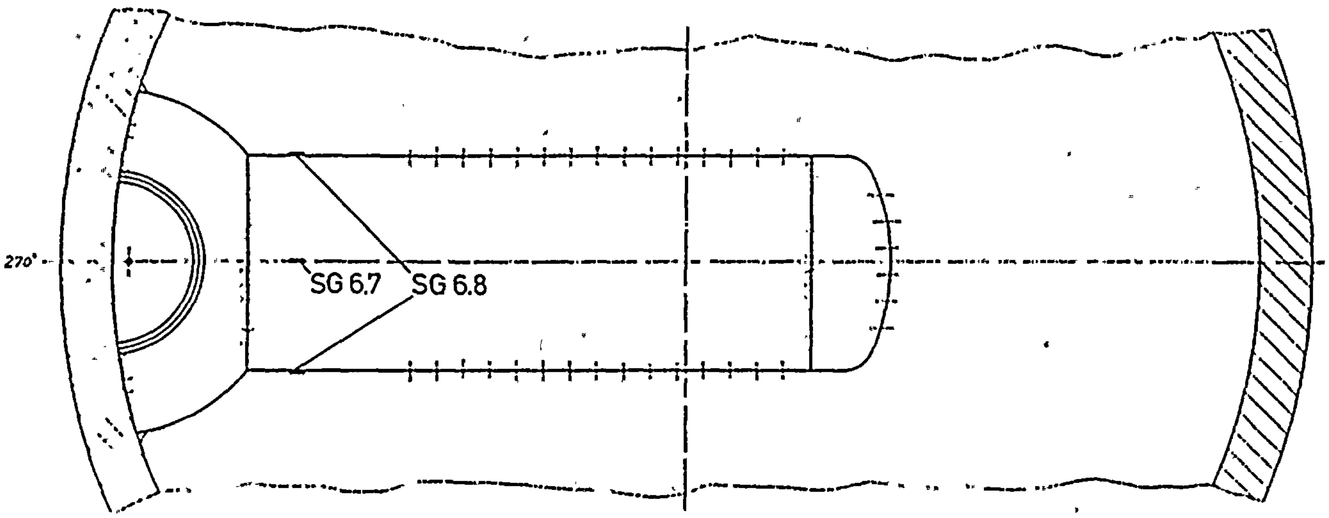

Rev. 3, 7/80

SUSQUEHANNA STEAM ELECTRIC STATION
UNITS 1 AND 2
DESIGN ASSESSMENT REPORT

DUMMY QUENCHER

FIGURE 9-8

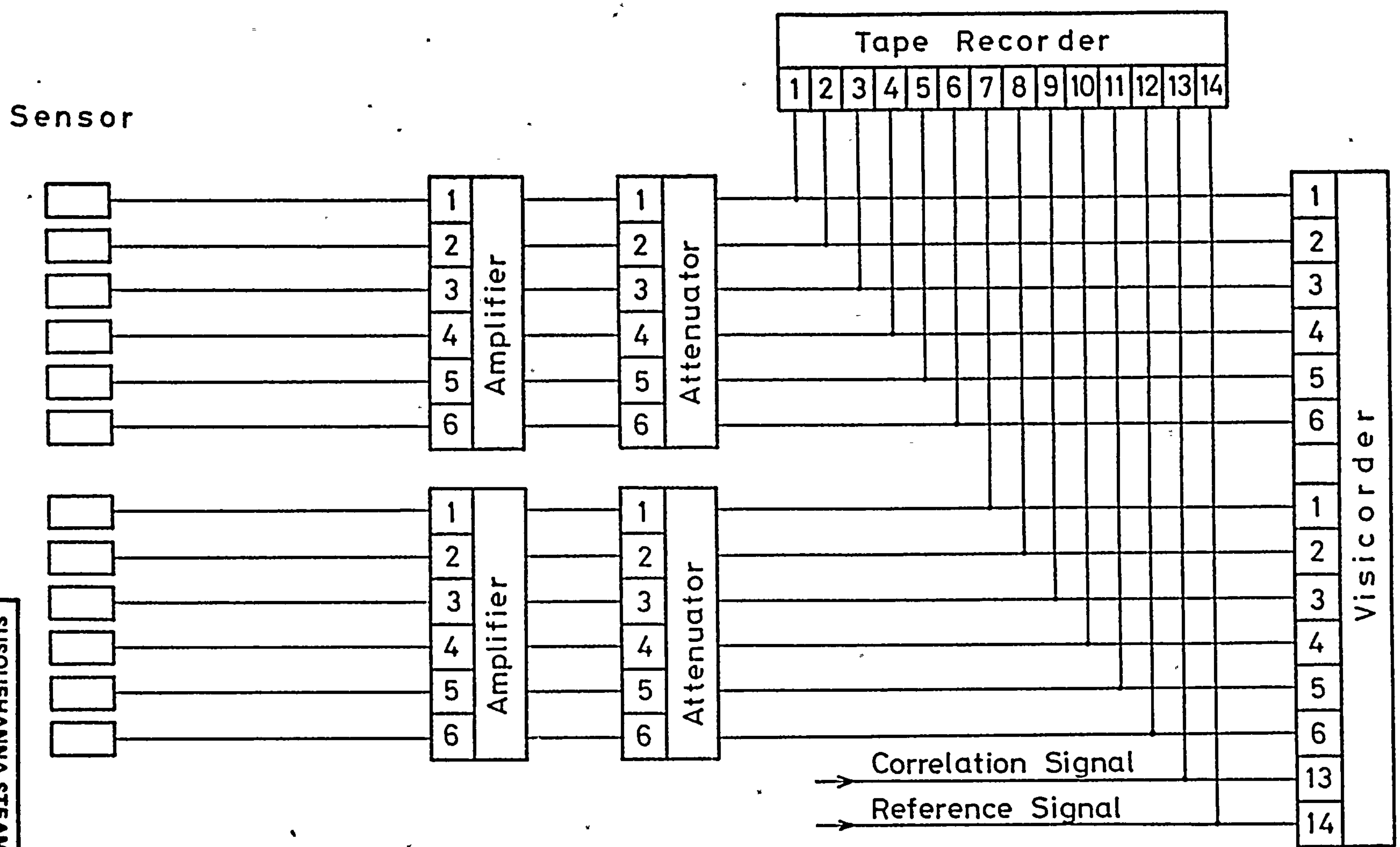

Rev. 3, 7/80

SUSQUEHANNA STEAM ELECTRIC STATION
UNITS 1 AND 2
DESIGN ASSESSMENT REPORT

DATA RECORDING: SCHEMATIC
BLOCK DIAGRAM

FIGURE 9-10

Physical Calibration of the Sensors

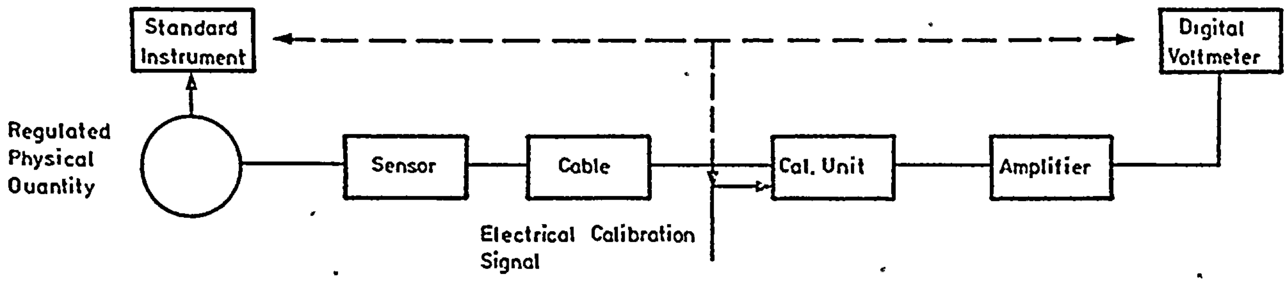

Adjustment and Calibration of the Registration Instruments

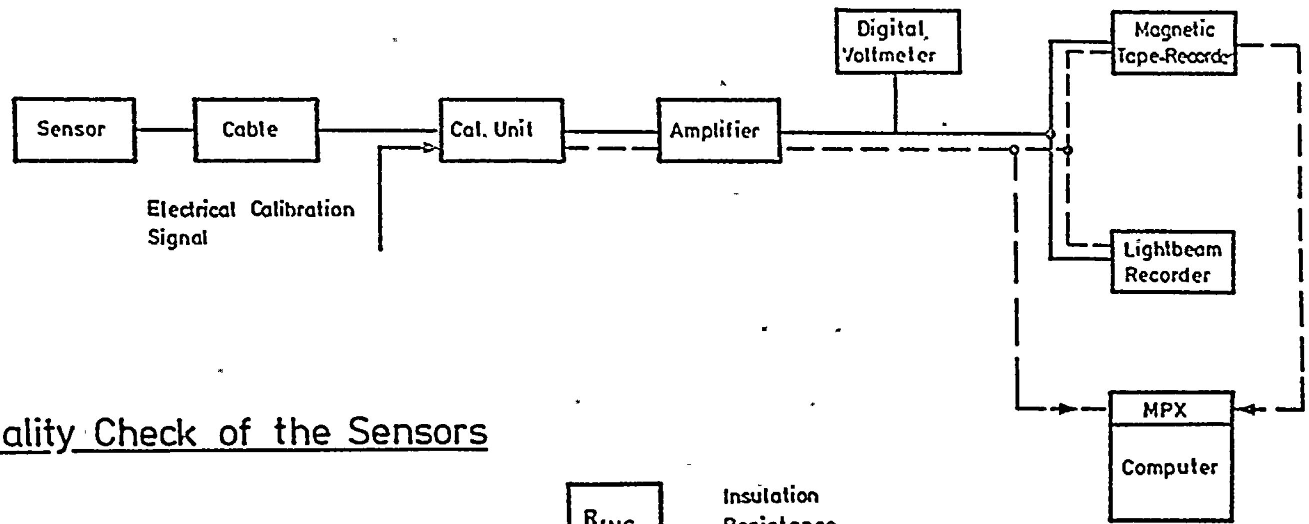

Quality Check of the Sensors

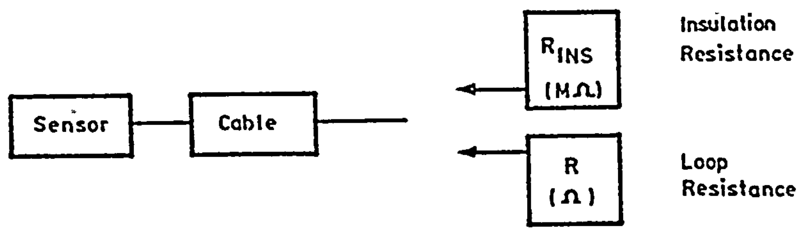

computer checks cal.-step,
computer compares the cal.-step on reproduce channels with input cal.-step

Rev. 3, 7/80

SUSQUEHANNA STEAM ELECTRIC STATION
UNITS 1 AND 2
DESIGN ASSESSMENT REPORT

CALIBRATION OF THE SENSORS AND REGISTRATION INSTRUMENTS

FIGURE 9-11

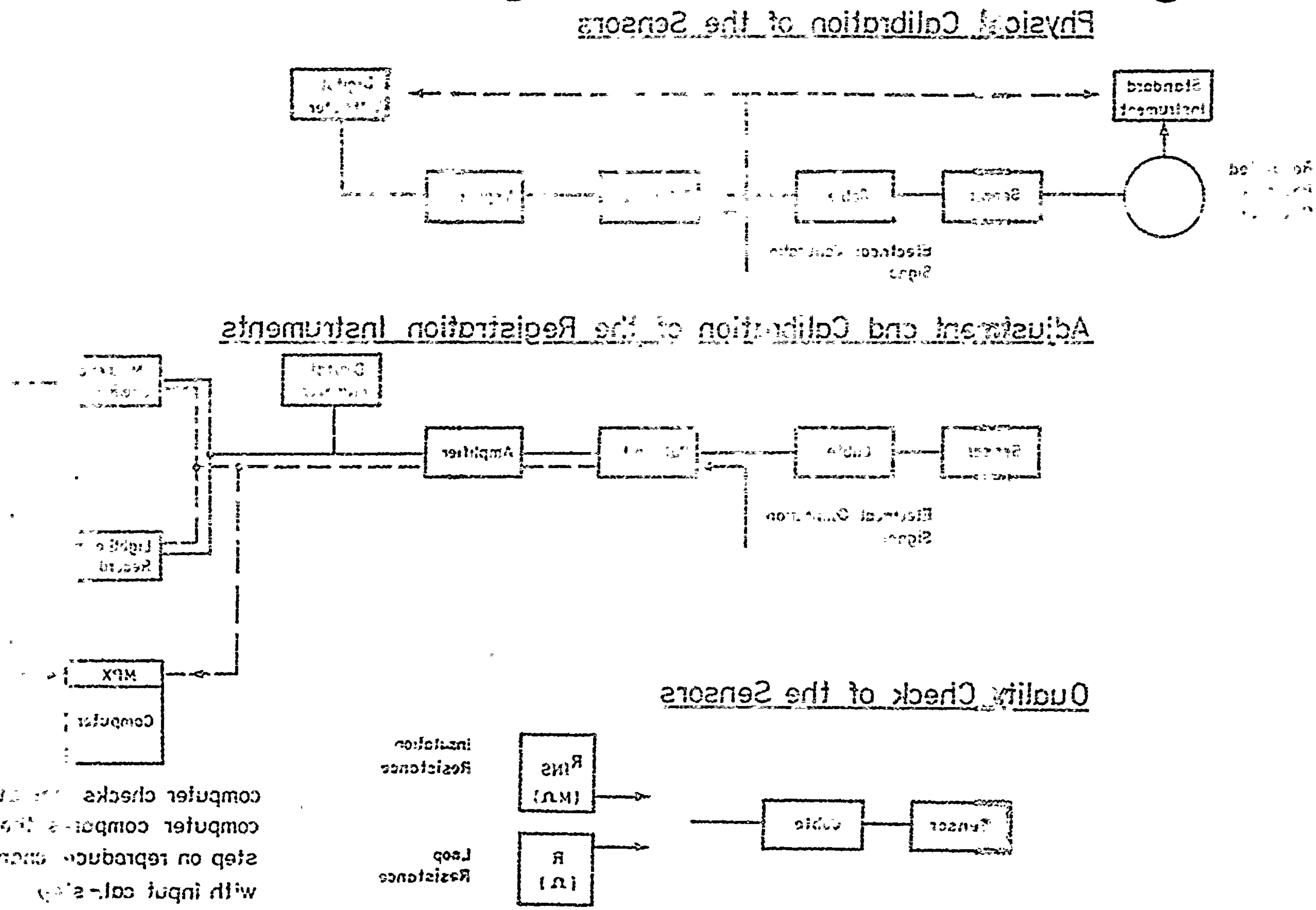

Rev. 3, 7/80

SUSQUEHANNA STEAM ELECTRIC STATION
UNITS 1 AND 2
DESIGN ASSESSMENT REPORT

CALIBRATION OF THE SENSORS AND REGISTRATION INSTRUMENTS

FIGURE 9-11

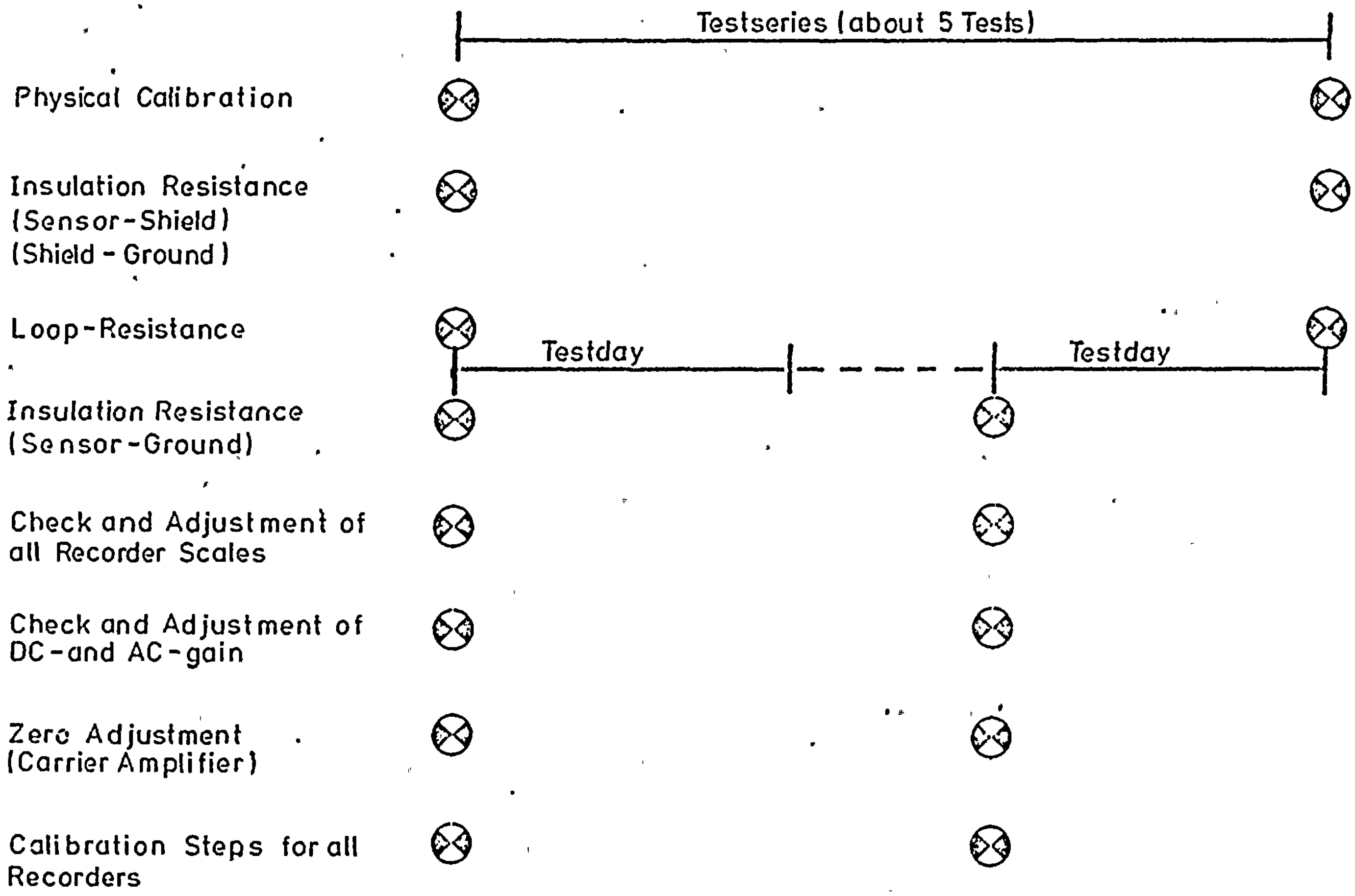

Rev. 3, 7/80

SUSQUEHANNA STEAM ELECTRIC STATION
UNITS 1 AND 2
DESIGN ASSESSMENT REPORT

INTERVALS FOR CALIBRATIONS,
CHECKS AND ADJUSTMENTS

FIGURE 9-12

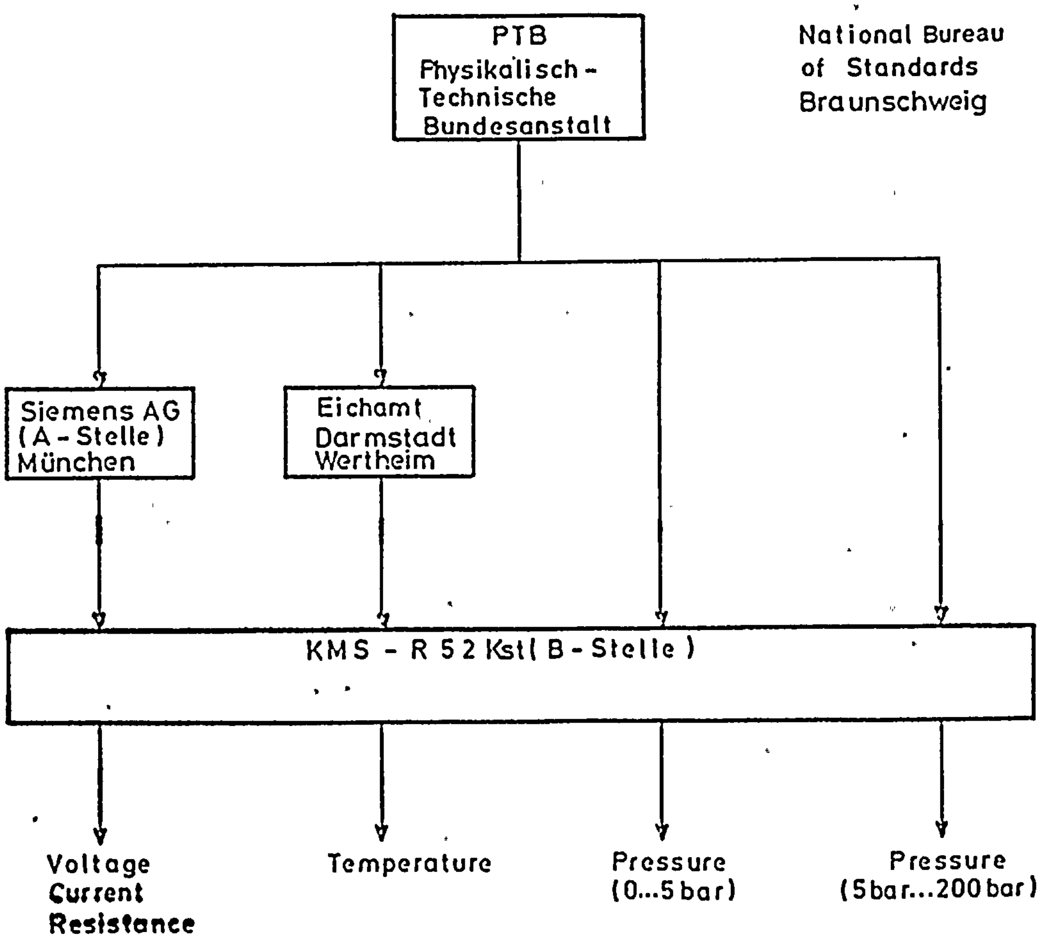

Rev. 3, 7/80

SUSQUEHANNA STEAM ELECTRIC STATION
UNITS 1 AND 2
DESIGN ASSESSMENT REPORT

CALIBRATION SYSTEM

FIGURE 9-13

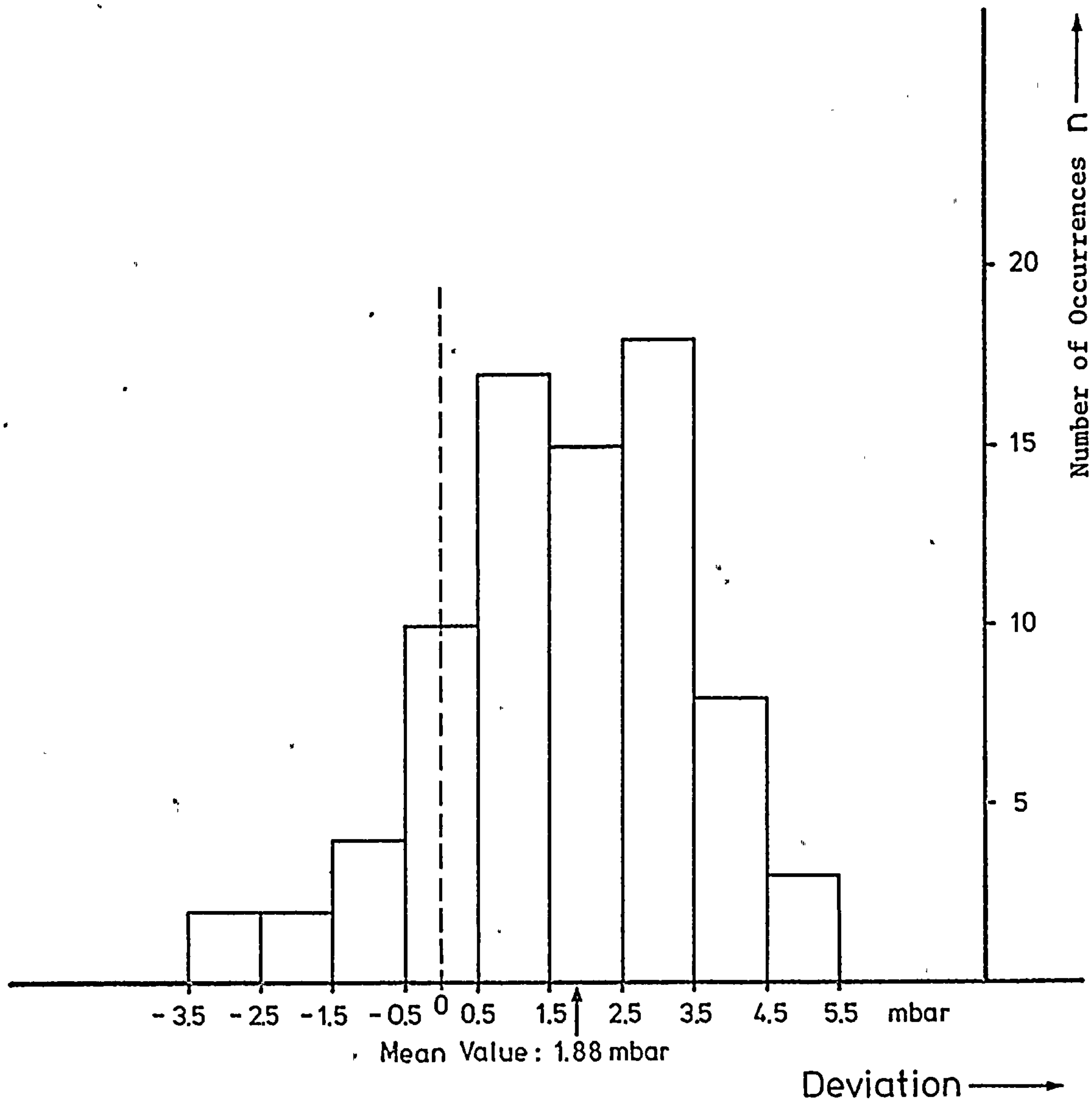

Rev. 3, 7/80

SUSQUEHANNA STEAM ELECTRIC STATION
UNITS 1 AND 2
DESIGN ASSESSMENT REPORT

PHYSICAL CALIBRATION OF THE PRESSURE TRANSDUCERS P6.1... P6.8 BY LOWERING OF THE WATER LEVEL

FIGURE 9-14

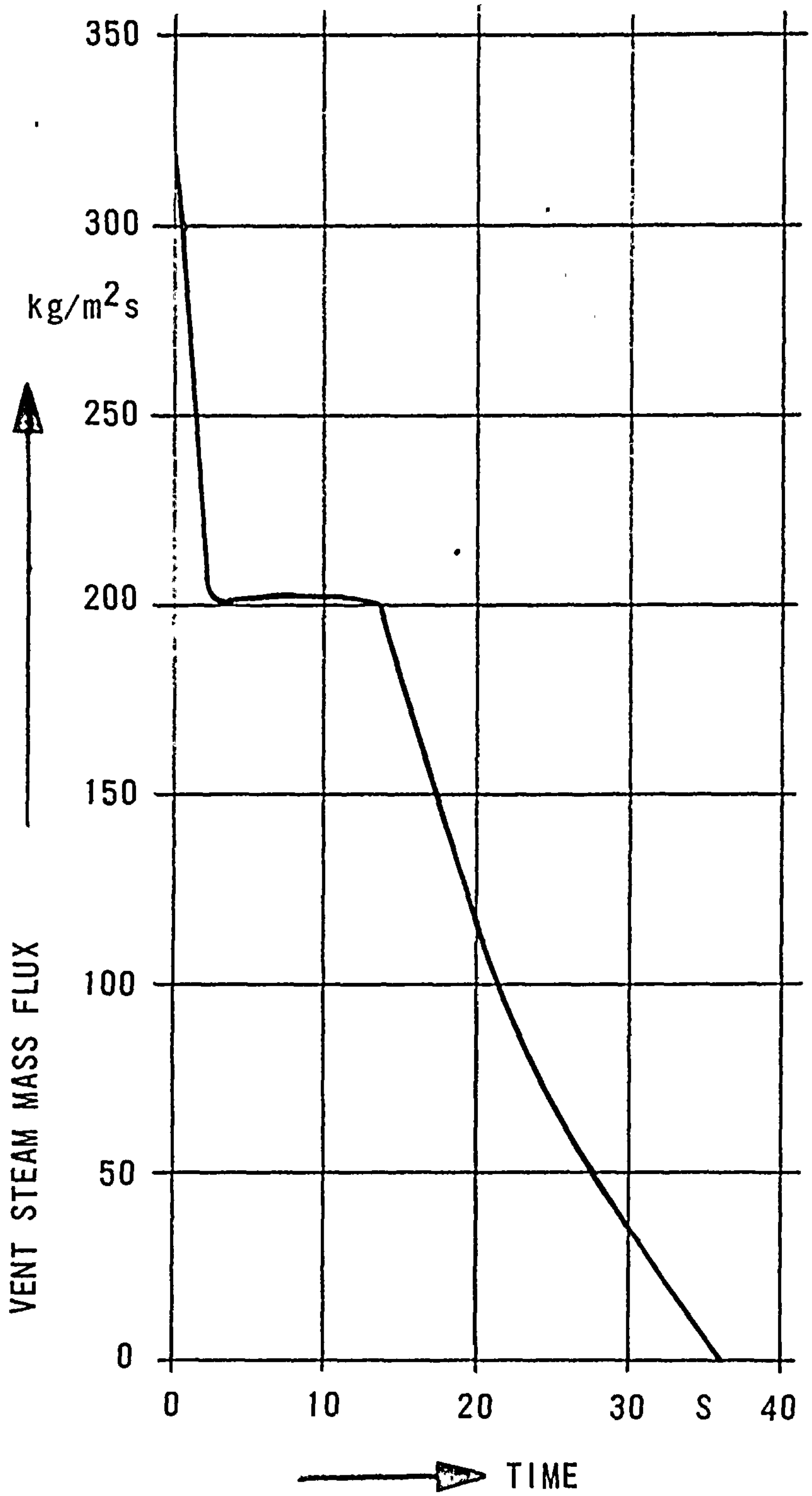

Rev. 3, 7/80

SUSQUEHANNA STEAM ELECTRIC STATION
UNITS 1 AND 2
DESIGN ASSESSMENT REPORT

CALCULATED SSES VENT
STEAM MASS FLUX VS. TIME-
RCL BREAK

FIGURE 9-14a

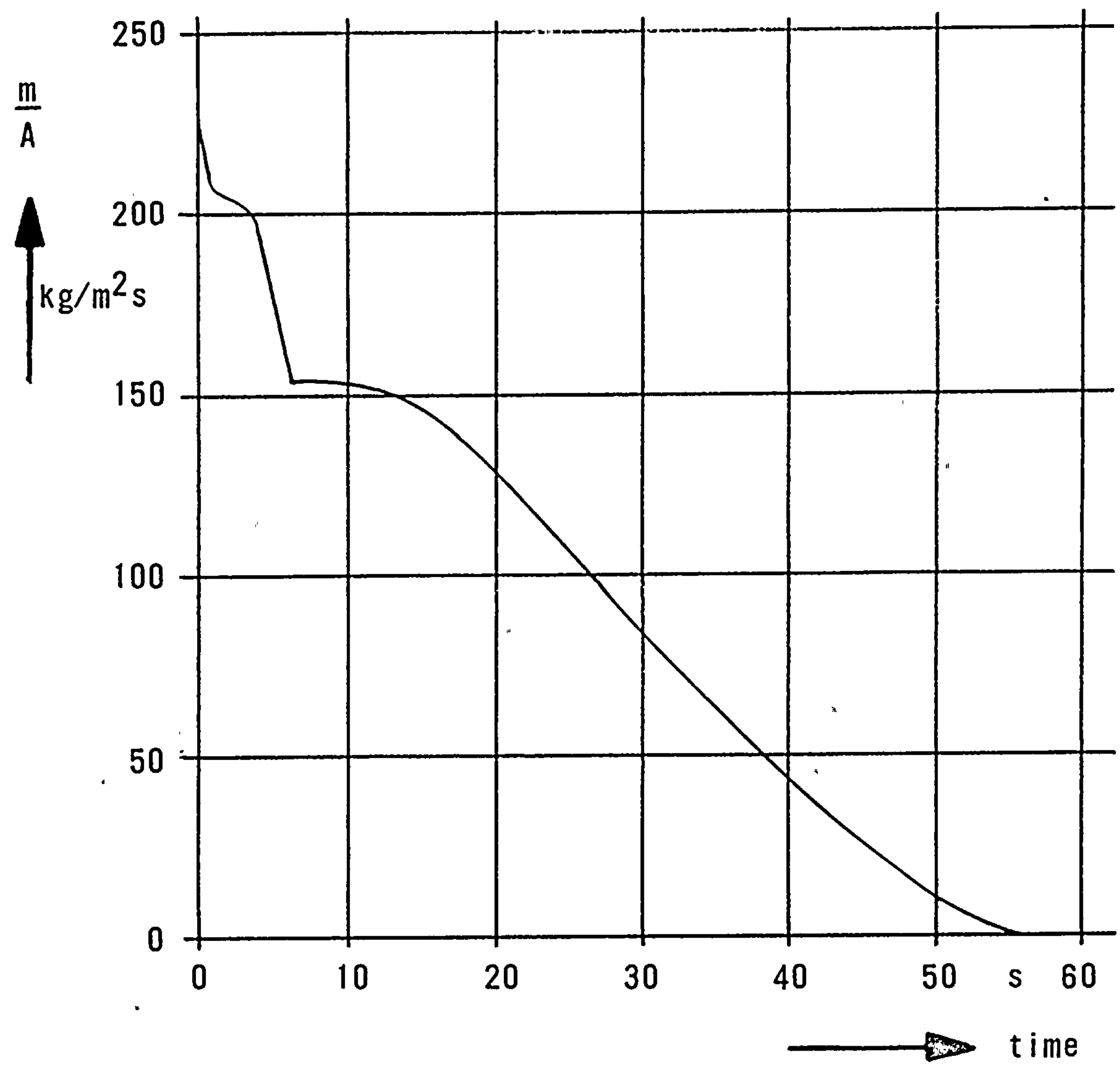

Rev. 3, 7/80

SUSQUEHANNA STEAM ELECTRIC STATION
UNITS 1 AND 2
DESIGN ASSESSMENT REPORT

CALCULATED SSES VENT STEAM MASS FLUX VS. TIME-FULL MSL BREAK

FIGURE 9-14b

TABLE 9.1
COMPARISON OF FIXED PARAMETERS

	SSES Single Cell	GKM II M Test Vessel (As Built Values)	
Drywell Free Volume, m^3 (Including Vent Pipe at High Water Level)	77.9	75.6	
Wetwell Free Air Volume, m^3 (High Water Level)	48.4	47	
Drywell/Wetwell Air Volume Ratio (High Water Level)	1.61	1.61	5
Free Pool Area, M^2			
Small Cell at Containment Wall	3.7	3.77	
Mean Value	5.8		
Vent Pipe Dimensions			
Length, m	13.86	13.76	
Outer Diameter, mm	610	610	
Wall Thickness, mm	9.5	10.0	
Vent Pipe Submergence, m (High Water Level)	3.66	3.66	2
Vent Pipe Clearance, m (Exit to Pool Bottom)	3.35 to 3.54	3.63*	5
Distance Between Bracing and Vent Opening, m	2.44	2.44	
Volume Flexibility of Wet Containment Walls, dm^3/bar	0.6	0.6	

* At the Deepest Point 5

Table 9-2, (1 of 2)

OPERATING INSTRUMENTATION

Transducer	Measuring - Point Marking	Measuring - Location *	Transducer Data			Measuring Amplifier	Recording Place		
			Type	Measuring Range	Stock-No.		DPS Channel	Control Station	Test Facility
P 1.1	Pressure in the superheated steam line	steam line to the steam accumulator	PG with remote sensor	25 bar		20 mA	2/0	x	x
P 1.2	"	main steam line	"	"		"	2/1	x	x
P 1.3	Pressure in the feedwater tank	feedwater tank B 203	"	"		"		x	x
P 2.1	"	feedwater tank B 202	"	"		"	2/2	x	x
P 3.1	Pressure in the steam accumulator, steam zone		"	"		"	2/3	x	x
L 3.1	Water level in the steam accumulator		Barton cell	1.565 bar		20 mA	2/6	x	
L 3.2	"		"	0.1825 bar		20 mA	2/7	x	
L 3.3	"		Water gage	-		-			x
P 4.1	Pressure in the blowdown line before throttle nozzle		PG with remote sensor	25 bar		20 mA		x	
P 4.4	Pressure in the blowdown line before the rupture discs		PG with remote sensor	25 bar		20 mA	2/4	x	
P 4.5	Pressure between the two rupture discs		"	"		"	2/5	x	
T 1.1	Temperature in the superheated steam line	steam line to the steam accumulator	RTD	550°c		D C A	2/8	x	
T 1.2	"	main steam line	RTD	400°c		"	2/9	x	

3

* A more exact position indication for these sensors is not mecessary for the usability of the measurement signals and for the test execution

Rev. 3, 7/80

Table 9-2, (2 of 2)

OPERATING INSTRUMENTATION

Transducer	Measuring - Point Marking	Measuring - Location *	Transducer Data Type	Measuring Range	Stock-No.	Measuring Amplifier	Recording Place DPS Channel	Control Station	Test Facility
T 1.3	Temperature in the feedwater tank	feedwater tank B 203	RTD	300 °C		D C A	4/13	X	
T 2.1	"	feedwater tank B 202	"	"		"	2/10	X	
T 3.1	Temperature in the steam accumulator, steam zone		"	"		"	2/11	X	
T 3.2	Temperature in the steam accumulator, water zone		"	"		"	2/12	X	
T 3.3	Temperature for the correction of the water level measurement in the steam accumulator		"	"		"	2/13	X	
T 4.1	Temperature in the blowdown line before the throttle nozzle		CTC	250 °C		"	2/14	X	
T 5.4	Temperature in the drywell, at the wall		"	250 °C		"	3/11	X	
L 6.1	Water level in the suppression pool		Barton cell	1235 bar		0...20mA	5/6	X	
L 6.2	Water level in the annulus gap		"	1235 bar		"	2/15	X	

3

* A more exact position indication for these sensors is not necessary for the usability of the measurement signals and for the test execution

Rev. 3, 7/80

Table 9-3, (1 of 5)

TEST INSTRUMENTATION

Transducer	Measuring-Point Marking	Measuring Location Level H (mm)	Angle ∢ (°)	Transducer Data Type	Measuring Range	Stock-No.	Measuring Amplifier	Data Recording DPS Channel	Visi-corder	Magnetic Tape
SG 6.3	Strain in the tank wall, outside, vertical	2650	135	SG semi bridge	6000 μm/m		C F A		x	x
SG 6.4	Strain in the tank wall, outside, horizontal	2650	135	"	"		"		x	x
SG 6.5	Strain in the tank wall, outside, vertical	2650	45	"	"		"		x	x
SG 6.6	Strain in the tank wall, outside, horizontal	2650	45	"	"		"		x	x
SG 6.7	Vertical bending strain at the quencher dummy	1093	*	"	"		"	5/7	x	x
SG 6.8	Horizontal bending strain at the quencher dummy	1093	*	"	"		"	5/8	x	x
SG 6.9	Vertical bending strain at the legs of the test vessel	**	0	"	"		"		x	x
SG 6.10	Vertical bending strain at the legs of the test vessel	**	90	"	"		"		x	x
DG 6.2 DG 6.6	Displacement of the inner cylinder at the crossing place	10000	270 90	"	± 2 mm		"		x x	x x
DG 6.3 DG 6.5	Displacement of the inner cylinder at the crossing place	10000	0 180	"	"		"		x x	x x
DG 6.4	Displacement at the stiffening ring	6107	90	"	"		"	4/10	x	x
T 6.1	Temperature in the suppression pool, water zone	6800	180	C T C	150 °C		D C A	3/0	x	x
T 6.2	"	5200	180	"	"		"	3/1	x	x

* 70 mm from the middle of the weld seam/quencher arm

** 100 mm below the weld seam at the leg of the vessel

3

Rev. 3, 7/80

Table 9-3, (2 of 5)

TEST INSTRUMENTATION

3

Transducer	Measuring-Point Marking	Measuring Location Level H (mm)	Angle ∢ (°)	Transducer Data Type	Measuring Range	Stock-No.	Measuring Amplifier	Data Recording DPS Channel	Visi-corder	Magnetic Tape
T 6.3	Temperature in the suppression pool, water zone	3651	180	C T C	150°C		D C A	3/2	X	X
T 6.4	"	2653	180	"	"		"	3/3		
T 6.7	"	1097	180	"	"		"	3/4		
T 6.8	"	0	**	"	"		"	3/5		
T 6.9	Temperature in the suppression pool, air zone, top	14000	270	"	"		"	3/6		
T 6.10	Temperature in the suppression pool, air zone, below	8010	270	"	"		"	3/7		
*P 4.1	Pressure in the blowdown line before throttle nozzle	-	-	SG complete bridge	50 bar		C F A	5/1	X	X
*ΔP 4.2	Differential pressure at the throttle nozzle	-	-	"	35 bar		"	5/2	X	X
*ΔP 4.3	"	-	-	Barton cell	4 bar		20 mA	5/0	X	X
*T 4.1	Temperature in the blowdown line before throttle nozzle	-	-	C T C.	250°C		D C A	2/14		
P 3.2	Dynamic pressure in the steam accumulator, water zone	***	-	Piezo-electric transducer	20 bar		Charge amplifier		X	X
P 5.1	Pressure in the drywell	-	-	SG complete bridge	20 bar		C F A	5/4	X	X
P 5.2	Pressure in the downcomer pipe, top	15550	225	"	10 bar		"		X	X
P 5.3	Pressure in the downcomer pipe, middle	10580	270	"	"		"		X	X

* The arrangement of the sensors required for the steam flow measurement is according to DIN 1952

** 200 mm out of center

*** The sensor was instralled according to the drawing R 523 G - 22 - 1986

Rev. 3, 7/80

Table 9-3, (3 of 5)

TEST INSTRUMENTATION

Transducer	Measuring-Point Marking	Measuring Location		Transducer Data			Measuring Amplifier	Data Recording		
		Level H (mm)	Angle ∢ (°)	Type	Measuring Range	Stock-No.		DPS Channel	Visi-corder	Magnetic Tape
P 5.4	Pressure in the downcomer pipe,below	7320	270	SG complete bridge	10 bar		C F A		x	x
P 5.5	Pressure in the downcomer pipe,exit	3750	270	"	20 bar		"		x	x
ΔP 5.6	Pressure differential between dry-well and suppression chamber	-	-	"	3,5 bar		"		x	x
OR 5.1	Oxigene rate in the downcomer pipe	15290	180		-			5/3	x	x
DG 5.1	Indication of the swing check valve between drywell and suppression chamber	-	-		-		C F A	3/14		
DG 5.2	"	-	-		-		"	3/15		
T 5.1.	Temperature in the drywell,top	-	-	C T C	250°C		D C A	3/8		
T 5.2	Temperature in the drywell,below	-	-	"	"		"	3/9		
T 5.3	Temperature in the drywell,sump	-	-	"	"		"	3/10		
T 5.5	Temperature in the downcomer pipe,middle	10580	260	"	"		"	3/12		
T 5.6	Temperature in the downcomer,exit	3750	260	"	"		"	3/13	x	x
P 6.1	Pressure at the suppression pool wall,water zone	6156	180	SG complete bridge	10 bar		C F A	4/0	x	x
P 6.2	"	4155	180	"	"		"	4/1	x	x

3

Table 9-3, (4 of 5)

TEST INSTRUMENTATION

Transducer	Measuring-Point Marking	Measuring Location Level H (mm)	Angle ∢ (°)	Transducer Data Type	Measuring Range	Stock-No.	Measuring Amplifier	Data Recording DPS Channel	Visi-corder	Magnetic Tape
P 6.3	Pressure at the suppression pool wall, water zone	3651	180	SG complete bridge	10 bar		C F A	4/2	X	X
P 6.4	"	2653	180	"	"		"	4/3	X	X
P 6.5	"	2653	0	"	"		"	4/4	X	X
P 6.6	"	2653	90	"	"		"	4/5	X	X
P 6.7	"	1097	180	"	"		"	4/6	X	X
P 6.8	"	0	*	"	"		"	4/7	X	X
P 6.9	Pressure in the suppression chamber, air zone	16770	300	"	20 bar		"	5/5	X	X
AF 6.1	Air fraction in the suppression chamber, water zone	4155/6156	180	"	3.5 bar		"	4/11	X	X
AF 6.2	"	2653/6156	180	"	"		"	4/12	X	X
LP 5.1	Water level in the downcomer pipe	3750	90	spark plug	-		D C A		X	X
LP 5.2	"	4050	90	"	-		"		X	X
LP 5.3	"	4450	90	"	-		"		X	X
LP 5.4	"	5950	90	"	-		"		X	X
LP 5.5	"	7950	90	"	-		"		X	X

3

* 200 mm out of center

TEST INSTRUMENTATION

Transducer	Measuring-Point Marking	Measuring Location		Transducer Data			Measuring Amplifier	Data Recording		
		Level H (mm)	Angle ∢ (°)	Type	Measuring Range	Stock-No.		DPS Channel	Visi-corder	Magnetic Tape
SG 6.1	Longitudinal strain, Bracing 1	6107	0	SG complete bridge	6000 µm/m		C F A	4/8	x	x
SG 6.2	Longitudinal strain, Bracing 2	6107	90	"	"		"	4/9	x	x
LC 6.1	Loads on the I-Beam	6322	270	"	"		"	5/9	x	x
SG 5.1	Bending strain in the downcomer	6007	90/270	"	"		"		x	x
SG 5.2	"	6007	0/180	"	"		"		x	x
SG 5.4	"	15700	90/270	SG semi bridge	"		"		x	x
SG 5.3	"	15700	0/180	"	"		"		x	x
AG 6.1	Acceleration of the inner cylinder	0	center	SG complete bridge	±25g		"		x	x
AG 6.2	"	7010	90	"	"		"		x	x
L 6.1	Water level in the suppression pool			Barton cell	1.235bar		0...20 mA	5/6	X	X

3

Rev. 3, 7/80

Table 9-4

GKM II-M TEST MATRIX

Test Number		1	2	3	4	5	6	7	8	9	10	11	12	13	14	15	16	17	18	19	20	33	34
Break Size (mm)	Ø 210 (RCL)	*	*																			*	*
	Ø 190 (MSL)			*	*	*	*	*	*	*	*												
	Ø 110 (1/3 MSL)											*	*										
	Ø 80 (1/6 MSL)													*	*	*	*	*	*	*	*		
Pool Temperature	24°C (75 F)			*	*									*	*								
	32°C (90 F)	*	*			*	*	*	*			*	*			*	*	*	*				
	55°C (130 F)									*	*									*	*	*	*
Drywell Air Content	100 %	*	*	*	*	*	*			*	*	*	*	*	*	*	*			*	*	*	*
	85 % (approx.)							*	*									*	*				
Repeat Test			*		*		*		*		*		*		*		*		*		*		*

3

Rev. 3, 7/80

Table 9-5, (1 of 3)

TEST PARAMETER

Test	Test Duration	DB	Sub	Water temperature Start	Water temperature End*	Temp. at the Drywell, Wall Start	Temp. in the Drywell Air Space Start	Water Volume in S6 Start	Pressure in S6 Start	Drywell Pressure Start	Drywell Pressure End	Cond. Chamber Pressure Start	Cond. Chamber Pressure End	Drywell Air Content Start	Diameter at the Flow Restrictor
No.	s	m	m	°C	°C	°C	°C	m^3	bar	bar	bar	bar	bar	%	mm
1	37	3.6	3.7	34	65	180	56	31.0	**19.8	1.0	3.2	1.0	2.8	100	210
2	37	3.6	3.7	33	66	177	58	29.2	**19.6	1.0	3.2	1.0	2.8	100	210
3	72	3.6	3.8	24.5	57	140	65	7.1	19.7	1.0	3.1	1.0	2.7	100	190
4	73	3.6	3.7	25	59	142	61	7.6	19.8	1.0	3.2	1.0	2.8	100	190
5	72	3.6	3.6	32	64	141	61	7.8	19.8	1.0	3.2	1.0	2.8	100	190
6	73	3.6	3.6	33	65	144	62	7.6	19.8	1.0	3.3	1.0	2.8	100	190
7	81	3.6	3.7	33	70	170	146	7.8	17.3	1.0	3.0	1.0	2.5	≈85	190
8	80	3.6	3.7	34	68	160	136	7.3	17.0	1.0	3.0	1.0	2.5	≈85	190
9	74	3.6	3.6	56	87	143	62	7.6	19.8	1.0	3.3	1.0	2.9	100	190
10	71	3.6	3.7	55	84	144	55	7.7	18.6	1.1	3.4	1.0	2.9	100	190

DB = Distance from the Bottom
Sub = Submergence
* = After Mixing of the Pool

** the same pressure in the B 202

Table 9-5, (2 of 3)

TEST PARAMETER

Test	Test Duration	DB	Sub	Water temperature Start	End*	Temp. at the Drywell Wall Start	Temp. in the Drywell Air Space Start	Water Volume in S6 Start	Pressure in S6 Start	Drywell Pressure Start	End	Cond.Chamber Pressure Start	End	Drywell Air Content Start	Diameter at the Flow Restrictor
No.	s	m	m	°C	°C	°C	°C	m³	bar	bar	bar	bar	bar	%	mm
11	224	3.6	3.8	34	68	143	54	8.7	17.2	1.1	3.3	1.0	2.8	100	110
12	216	3.6	3.8	35	67	143	57	8.5	17.1	1.1	3.3	1.0	2.9	100	110
13	428	3.6	3.8	25	60	143	63	9.5	17.2	1.1	3.3	1.0	2.8	100	80
14	413	3.6	3.8	25	60	141	62	8.5	17.9	1.1	3.2	1.0	2.8	100	80
15	413	3.6	3.8	33	63	143	67	8.7	17.1	1.1	3.2	1.0	2.8	100	80
16	403	3.6	3.8	33	65	139	64	8.5	17.2	1.1	3.2	1.1	2.8	100	80
17	438	3.6	3.7	34	68	170	142	8.7	17.2	1.0	2.8	1.0	2.4	≈85	80
18	432	3.6	3.7	33	69	173	145	8.7	17.1	1.0	2.8	1.0	2.4	≈85	80
19	420	3.6	3.8	52	84	137	70	8.8	17.2	1.0	3.1	1.0	2.7	100	80
20	403	3.6	3.6	55	85	137	63	8.5	17.1	1.0	3.0	1.0	2.8	100	80

DB = Distance from the Bottom
Sub = Submergence
* = After Mixing of the Pool

3

Rev. 3, 7/80

Table 9-5, (3 of 3)

TEST PARAMETER

Test	Test Duration	DB	Sub	Water Temperature Start	Water Temperature End*	Temp. at the Drywell Wall Start	Temp. in the Drywell Air Space Start	Water Volume in S6 Start	Pressure in S6 Start	Drywell Pressure Start	Drywell Pressure End	Cond.Chamber Pressure Start	Cond.Chamber Pressure End	Drywell Air Content Start	Diameter at the Flow Restrictor
No.	s	m	m	°C	C	C	C	m	bar	bar	bar	bar	bar	%	mm
33	36	3,6	3,6	54	85	172	62	29,8	**19,9	1,1	3,3	1,1	2,9	100	210
34	36	3,6	3,6	54	85	182	59	30,4	**19,8	1,1	3,4	1,1	3,0	100	210

DB - Distance from the Bottom
Sub = Submergence
* = After Mixing of the Pool

**the same pressure in the B 202

3

CHAPTER 10

RESPONSES TO NRC QUESTIONS

TABLE OF CONTENTS

CHAPTER 10

FIGURES

Figures (Cont.)

FIGURES (Cont.)

CHAPTER 10

TABLES

10.0 RESPONSES TO NRC QUESTIONS

This chapter will provide responses to those Nuclear Regulatory Commission (NRC) questions which have been designated by 1 Reference 10 (as amended) to be found in the plant-unique Design Assessment Report, to those questions for which the response in Reference 10 is inapplicable, to those questions generated from 2 previous NRC reviews of the plant unique DAR, and those questions received during preparation of the SER. The NRC questions for which responses will be provided are identified in Subsections 6 10.1.1, 10.1.2, and 10.1.3, and detailed resposes to these questions are found in Subsections 10.2.1, 10.2.2 and 10.2.3.

6 ## 10.1.1 IDENTIFICATION OF QUESTIONS UNIQUE TO SSES

The below listed questions address concerns unique to SSES.
2 These questions are answered in detail in Subsection 10.2.1

NRC Question Number	Question Topic
M020.26	Primary and Secondary LOCA Loads
M020.27	Inventory Effects on Blowdown
M020.44	Poolswell Waves and Seismic Slosh
M020.55	SRV Loads on Submerged Structures
M020.58(1),(2),(3)	Plant Unique Poolswell Calculations
M020.59(1),(3),(4)	Downcomer Lateral Braces
M020.60	Wetwell Pressure History
M020.61	Poolswell Inside Pedestal
M130.1	Pressure Loading Due to SRV Discharge
M130.2	Load Combination History
M130.4	Soil Modeling
M130.5	Liner and Anchorage Mathematical Model
M130.6	Containment Structural Model-Asymmetric Loads
M130.12	SRV Structural Response

10.1.2 IDENTIFICATION OF QUESTIONS PERTAINING TO THE NRC's REVIEW OF THE DAR 6

The below listed questions address concerns generated as a result 2
of the NRC's review of the DAR. These questions are answered in
detail in Subsection 10.2.2 6

Question Number	Question Topic
1	NUREG-0487 Acceptance Criteria
2	Drywell Pressurization
3	Chugging Loads on Submerged Structures
4	IBA and SBA for Typical Mark II Containment 2
5	Poolswell Waves and Seismic Slash
6	List of Piping, Equipment, etc., Subject to Pool Dynamic Loads
7	Applicability of the Generic Programs, Tests and Analysis to the SSES Design
8	Time History of Plant Specific Loads
9	Mass and Energy Release
10	"Local" and "Bulk" Pool Temperature
11	Suppression Pool Temperature Monitoring System

10.1.3 QUESTIONS RECEIVED DURING THE PREPARATION OF THE SAFETY EVALUATION REPORT (SER)

The below listed questions were informally received during the NRC's preparation of the SER. These questions are answered in detail in Subsection 10.2.3.

Question Number	Question Topic
1	SSES LOCA Steam Condensation Load Definition (SER Item #27)
2	T-Quencher Frequency Range (SER Item #28)
3	SSES ADS Load Case (SER Item #28)
4	Quencher Bottom Support at Karlstein (SER Item #28)
5	Bending Moment in the Quencher Arm Recorded at Karlstein (SER Item #28)
6	Suppression Pool Temperature Response (SER Item #30)
7	Local to Bulk Temperature Difference for SSES (SER Item #30)
8	Quencher Steam Mass Flux (SER Item #30)

10.2 RESPONSES

10.2.1 QUESTIONS UNIQUE TO SSES AND RESPONSES THERETO

QUESTION M020.26

The DFFR presents a description of a number of LOCA related hydrodynamic loads without differentiating between primary and secondary loads. Provide this differentiation between the primary and secondary LOCA-related hydrodynamic loads. We recognize that this differentiation may vary from plant to plant. We would designate as a primary load any load that has or will result in a design modification in any Mark II containment since the pool dynamic concerns were identified in our April 1975 generic letters.

RESPONSE M020.26

The table below shows the LOCA-related hydrodynamic loads on the SSES containment. Those loads which have resulted in containment design modifications are designated as "Primary Loads." These primary loads result from the poolswell transient.

Drywell floor uplift pressures during the wetwell compression phase of poolswell lead to the decision to increase the SSES drywell floor design safety margin for uplift pressures by relocating drywell floor shear ties.

Poolswell impact, drag, and fallback loads resulted in the relocation of equipment in the SSES wetwell to a position above the peak poolswell height. Furthermore, the downcomer bracing system was redesigned.

All other LOCA-related hydrodynamic loads are designated as "Secondary Loads" since no design modification has resulted from their presence.

LOCA Load	"Primary Load"	"Secondary Load"
1. Wetwell/Drywell Pressures (During Poolswell)	X(1)	
2. Poolswell Impact Load	X(2)	
3. Poolswell Drag Load	X(3)	
4. Downcomer Clearing Load		X
5. Downcomer Jet Load		X
6. Poolswell Air Bubble Load		X
7. Poolswell Fallback Load	X(4)	

LOCA Load	"Primary Load"	"Secondary Load"
8. Mixed Flow Condensation Oscillation Load		X
9. Pure Steam Condensation Oscillation Load		X
10. Chugging		X
11. Wetwell/Drywell Pressure and Temperature during DBA LOCA (Long Term)		X
12. Wetwell/Drywell Pressure and Temperature during IBA LOCA (Long Term)		X
13. Wetwell/Drywell Pressure and Temperature during SBA LOCA (Long Term)		X

Footnotes:

(1) Shear ties changed in drywell floor.

(2) Equipment moved in wetwell.

(3) Equipment moved in wetwell. Bracing system redesign.

(4) Equipment moved in wetwell.

QUESTION M020.27

The calculated drywell pressure transient typically assumes that the mass flow rate from the recirculation system or steamline is equal to the steady-state critical flow rate based on the critical flow area of the jet pump nozzle or steamline orifice. However, for approximately the first second after the break opening, the rate of mass flow from the break will be greater than the steady-state value. It has been estimated that for a Mark I containment this effect results in a temporary increase in the drywell pressurization rate of about 20 percent above the value based solely on the steady-state critical flow rate. The drywell pressure transient used for the LOCA pool dynamic load evaluation, for each Mark II plant, should include this initially higher blowdown rate due to the additional fluid inventory in the recirculation line.

RESPONSE M020.27

The drywell pressure transients have been recalculated by GE (Reference 7) with the additional blowdown flow rate produced by the inventory effects included in the analysis. The LOCA loads presented in Section 4.2 have been calculated using these recalculated drywell pressure transients. Specifically, the drywell pressure transient resulting from the DBA LOCA including the effects of pipe inventory has been used as input to the poolswell model.

QUESTION M020.44 2

Table 5-1 and Figures 5-1 through 5-16 in the DFFR provide a listing of the loads and the load combinations to be included in the assessment of specific Mark II plants. This table and these figures do not include loads resulting from pool swell waves following the pool swell process or seismic slosh. We require that an evaluation of these loads be provided for the Mark II containment design.

RESPONSE M020.44

Subsections 4.2.4.6 and 4.2.4.7 provide our response. 6

QUESTION M020.55

The computational method described in DFFR Section 3.4 for calculating SRV loads on submerged structures is not acceptable. It is our position that the Mark II containment applications should commit to one of the following two approaches:

(1) Design the submerged structures for the full SRV pressure loads acting on one side of the structures; the pressure attenuation law described in Section 3.4.1 of NEDO-21061 for the ramshead and Section A10.3.1 of NEDO-11314-08 for the quencher can be applied for calculating the pressure loads.

(2) Follow the resolution of GESSAR-238 NI on this issue.
The applicant for GESSAR-238 NI has proposed a method 2
presented in the GE report, "Unsteady Drag on Submerged Structures," which is attached to the letter dated March 24, 1976 from G.L. Gyorey to R.L. Tedesco. This report is actively under review.

RESPONSE M020.55

Loads on submerged structures due to SRV actuation are discussed in Subsection 4.1.3.7.

QUESTION M020.58

Relating to the pool swell calculations, we require the following information for each Mark II plant:

(1) Provide a description of and justify all deviations from the DFFR pool swell model. Identify the party responsible for conducting the pool swell calculations (i.e., GE or the A&E). Provide the program input and

results of bench mark calculations to qualify the pool swell computer program.

(2) Provide the pool swell model input including all initial and boundary conditions. Show that the model input represents conservative values with respect to obtaining maximum pool swell loads. In the case of calculated input, (i.e., drywell pressure response, vent clearing time), the calculational methods should be described and justified. In addition, the party responsible for the calculation (i.e., GE or the A&E) should be identified.

(3) Pool swell calculations should be conducted for each Mark II plant. The following pool swell results should be provided in graphic form for each plant:

   (a) Pool surface position versus time

   (b) Pool surface velocity versus time

   (c) Pool surface velocity versus position

   (d) Pressure of the suppression pool air slug and the wetwell air versus time.

RESPONSE M020.58

(1) A specific response to this question can be found in Subsection 4.2.1.1. Verification of the SSES poolswell model is provided in Appendix Section D.1.

(2) Input and discussion of the poolswell model input can be found in Tables 4-17, 4-18, and Section 4.2.1.1.

(3) The requested graphic results of the SSES poolswell calculation can be found in Figures 4-38, 4-39, 4-40, and 4-43.

QUESTION M020.59

In the 4T test report NEDE-13442P-01 Section 3.3 the statement is made that for the various Mark II plants a wide diversity exists in the type and location of lateral bracing between downcomers and that the bracing in the 4T tests was designed to minimize the interference with upward flow. Provide the following information for each Mark II plant:

(1) A description of the downcomer lateral bracing system. This description should include the bracing dimensions, method of attachment to the downcomers and walls, elevation and location relative to the pool surface. A sketch of the bracing system should be provided.

(2) The basis for calculating the impact or drag load on the bracing system or downcomer flanges. The magnitude and

duration of impact or drag forces on the bracing system or downcomer flanges should also be provided.

(3) An assessment of the effect of downcomer flanges on vent lateral loads. 2

RESPONSE M020.59

(1) Subsection 7.1.2.1 describes the SSES bracing system and the methodology for assessing the adequacy of bracing system. 6

(2) The basis for calculating the impact or drag loads on the downcomer bracing system (El. 668') and downcomer stiffener rings (El. 668' and El. 682') is given in Section 4.2. The magnitude and duration of impact or drag forces on the bracing system and downcomer stiffener rings is also given in Section 4.2 .

(3) This item is not applicable to the SSES design.

QUESTION M020.60

In the 4T test report NEDE-13442P-01 Section 5.4.3.2 the statement is made that an underpressure does occur with respect to the hydrostatic pressure prior to the chug. However, the pressurization of the air space above the pool is such that the overall pressure is still positive at all times during the chug. We require that each Mark II plant provide sufficient information regarding the boundary underpressure, the hydrostatic pressure, the air space and the SRV load pressure to confirm this statement or alternatively provide a bounding calculation applicable to all Mark II plants. 2

RESPONSE M020.60

This information is provided in Subsection 7.1.3 of the DAR.

QUESTION M020.61

Significant variations exist in the Mark II plants with regard to the design of the wetwell structures in the region enclosed by the reactor pedestal. These variations occur in the areas of (1) concrete backfill of the pedestal, (2) placement of downcomers, (3) wetwell air space volumes, and (4) location of the diaphragm relative to the pool surface. In addition to variation between plants, for a given plant, variations exist in some of these areas within a given plant. As a result, for a given plant, significant differences in the pool swell phenomena can occur in these two regions. We will require that each plant provide a separate evaluation of pool swell phenomena and loads inside of the reactor pedestal.

RESPONSE M020.61

The SSES pedestal and wetwell area is shown on Figures 1-1 and 10.3. Due to the absence of downcomers in the pedestal interior, no pool swell would be expected in this region. There are 12 holes in the pedestal, however, eight of which would allow the flow of water from the suppression pool to the pedestal during a LOCA. Some downcomers are near the pedestal flow holes, leading to the possibility that air could be blown through the pedestal holes, which would lead to a greater pedestal pool swell than would be experienced by incompressible water flow alone. One would expect the pedestal pool swell to be much reduced from the suppression pool swell due to its relative separation from the suppression pool and the lack of direct charging from downcomer vents. Indeed, 1/13.3 scale model tests of the SSES pedestal design conducted at the Stanford Research Institute under the sponsorship of EPRI show that the pedestal pool swell is less than 20 percent of the pool swell in the suppression pool (Reference 32). There is no piping or equipment inside the SSES pedestal and, since the pedestal pool swell is very small, the only load involved due to pedestal pool swell would be a small •P across the pedestal due to different water levels between the suppression pool and the pedestal interior. This load is considered in the design of the SSES pedestal.

QUESTION M130.1

Provide in Section 5 a description of the pressure loadings on the containment wall, pedestal wall, base mat, and other structural elements in the suppression pool, due to the various combinations of SRV discharges, including the time function and profile for each combination. If this information is not generic, each affected utility should submit the information as described above.

RESPONSE M130.1

Chapter 4 describes the pressure loadings and time histories due to SRV discharge and other hydrodynamic loads.

QUESTION M130.2

In DFFR Section 5.2 it is stated that the load combination histories are presented in the form of bar charts as shown on Figures 5-1 through 5-16. It is not indicated how these load combination histories are used. In particular, it is not clear whether only loads represented by concurrent bars will be combined, and it should be noted that depending on the dynamic properties of the structures and the rise time and duration of the loads, a structure may respond to two or more given loads at the same time even though these loads occur at different times. Also, although condensation oscillations are depicted as bars on the bar charts, the procedure for the analysis of structures due to these loads has not been presented. Accordingly, the description of the method should include consideration of such conditions. Also, for condensation oscillation loads and for SRV oscillatory loads, include low cycle fatigue analysis.

RESPONSE M130.2 2

The loads will be combined according to Section 5.0. Section 7.0 describes the assessment methodology and results for the re- 6
assessment of SSES for the hydrodynamic and non-hydrodynamic loads.

QUESTION M130.4

Through the use of figures, describe in detail the soil modelling as indicated in DFFR Subsection 5.4.3 and describe the solid finite elements which you intend to use for the soil.

RESPONSE M130.4

Soil modelling is explained in Subsection 7.1.1.1.

QUESTION M130.5

Describe the mathematical model which you will use for the liner and the anchorage system in the analysis as described in DFFR Subsection 5.6.3.

RESPONSE M130.5

The mathematical model which will be used for analysis of the liner and the anchorage for hydrodynamic suction pressures is described in Subsection 7.1.3. 2

QUESTION M130.6

In DFFR Subsection 5.1.1.1 it was stated that the SRV discharge could cause axisymmetric or asymmetric loads on the containment. In Subsection 5.4.1 an axisymmetric finite element computer program is recommended for dynamic analysis of structures due to SRV loads, and no mention is made of the analysis for asymmetric loads. Describe the structural analysis procedure used to consider asymmetric pool dynamic loads on structures and through the use of figures, describe in more detail the structural model which you intend to use.

RESPONSE M130.6

The dynamic analyses and models used are explained in Chapter 7 .

QUESTION M130.12

Reference is made in DFFR Subsection 5.4.3 to studies of structural response to SRV load. Provide citations for this reference and where such studies are not readily available, copies are requested.

RESPONSE M130.12

Studies mentioned in DFFR Subsection 5.4.3 are the results of analysis completed for a specific plant at the time of writing of the DFFR. Reference to the studies was intended to indicate the need for considering strain dependent soil properties. For the SSES analysis, Reference 33 is used to determine the soil constants in the analysis.

10.2.2 QUESTIONS PERTAINING TO THE NRC'S REVIEW OF THE DAR AND RESPONSE THERETO 6

QUESTION 1

The LOCA and SRV related pool dynamic loads that are currently acceptable to us are discussed in NUREG-0487. Table IV-1 of NUREG-0487 summarizes these Mark II pool dynamic loads. By letter, dated February 2, 1979, you indicated on Table IV-1 the LOCA related dynamic loads acceptable to the staff that will be adopted for SSES. Revise the DAR to incorporate this information and provide the same information for the SRV related pool dynamic loads. For both the SRV and LOCA loads indicate the alternative criteria that will be used for each item for which an exemption is proposed and provide references that discuss these alternative criteria.

RESPONSE

See response to Question 021.69 contained in Volume 16 of the SSES FSAR and Table 1-4 of the DAR. 2

QUESTION 2

Subsection 4.2.1.1 of the DAR state that the drywell pressure transient used for the pool swell portion of LOCA is based on the methodology described in NEDO-21061. Subsection III.B.3.a.6 of NUREG-0487 requires that a comparison similar to those presented in reference 1* be made if the model used is different from the model described in NEDM-10320. We require the model prior to completion of review of the pool swell calculations.

*Reference (1) Letter "Response to NRC Request for Additional Information (Round 3 Questions," to J. F. Stolz (NRC-DPM) from L. J. Sobon (GE), dated June 30, 1978.

RESPONSE

See response to Question 021.70 contained in the SSES FSAR.

QUESTION 3

Subsection 4.2.2.2 of the DAR states that the chugging loads on submerged structures and imparted on the downcomers will be evaluated later. Provide the present status of these evaluations and the schedule for your submission of the completed evaluation. 6

RESPONSE

See response to Question 021.71 in the SSES FSAR.

QUESTION 4 2

Statements are made in Subsections 4.2.3.2 and 4.2.3.3 of the DAR that plant unique data of the Susquehanna SES intermediate break accident (IBA) and small break accident (SBA) are estimated from curves for a typical Mark II containment. Discuss the applicability of these analyses (e.g., power level, initial conditions, downcomer configuration, etc.) to Susquehanna SES.

RESPONSE

See response to Question 021.72 contained in the SSES FSAR.

QUESTION 5

Provide the information previously requested in 020.44 regarding loads resulting from pool swell waves following the pool swell process or seismic slosh. Discuss the analytical model and assumptions used to perform these analyses.

RESPONSE

See response to Question 021.73 contained in the SSES FSAR.

QUESTION 6

Provide a list and drawing to identify all piping, equipment instrumentation and structures in containment that may be subjected to pool dynamic loads. In addition, provide drawings to show the location of access galleys in the wetwell, the vent vacuum breaker configuration, wetwell grating, vent bracing configuration, vent configuration in the pedestal region of wetwell and large horizontal structures in the pool swell zone.

RESPONSE

See response to Question 021.74 contained in the SSES FSAR.

QUESTION 7

Discuss the applicability of the generic supporting programs, tests and analyses to Susquehanna SES design (i.e., FSI concerns, downcomer stiffners, downcomer diameter, etc.).

RESPONSE

See response to Question 021.75 contained in the SSES FSAR.

QUESTION 8

Provide the time history of plant specific loads and assessment of responses of plant structures, piping, equipment and components to pool dynamic loads. Identify any significant plant modifications resulting from pool dynamic loads considerations.

RESPONSE

See response to Question 021.76 contained in the SSES FSAR.

QUESTION 9

Provide figures showing reactor pressure, quencher mass flux and suppression pool temperature versus time for the following events:

(1) a stuck-open SRV during power operation assuming reactor scram at 10 minutes after pool temperature reaches 110°F and all RHR systems operable;

(2) same as event (1) above except that only one RHR train available;

(3) a stuck-open SRV during hot standby condition assuming 120°F pool temperature initially and only one RHR train available;

(4) the Automatic Depressurization System (ADS) activated following a small line break assuming an initial pool temperature of 120°F and only one RHR train available; and

(5) the primary system is isolated and depressurizing at a rate of 100°F per hour with an initial pool temperture of 120°F and only one RHR train available.

Provide parameters such as service water temperature, RHR heat exchanger capability, and initial pool mass for the analysis.

RESPONSE

See response to Question 021.77 contained in the SSES FSAR.

QUESTION 10

With regard to the pool temperature limit, provide the following additional information:

(1) Definition of the "local" and "bulk" pool temperature and their application to the actual containment and to the scaled test facilities, if any; and

(2) The data base that support any assumed difference between the local and the bulk temperatures.

RESPONSE

See response to Question 021.78 contained in the SSES FSAR.

QUESTION 11

For the suppression pool temperature monitoring system, provide the following additional information:

(1) Type, number and location of temperature instrumentation that will be installed in the pool; and

(2) Discussion and justification of the sampling or averaging technique that will be applied to arrive at a definitive pool temperature.

RESPONSE

See response to Question 021.79 contained in the SSES FSAR.

10.2.3 Questions Received During the Preparation of the Safety Evaluation Report and Response Thereto

QUESTION 1

With regard to the SSES LOCA steam condensation load definition, provide the following additional information:

(1) Justification for the interchangeability of the GKM II-M temporal chug strength probability distribution with the spacial variation of chug strengths at SSES.

(2) Justification for not considering CO & SRV(ADS).

(3) Comparison of the CO measured at 4T-CO with the CO absenved at GKM II-M.

RESPONSE 1

(1) The SSES LOCA steam condensation load definition assumes that the chugs occurring simultaneously at different vent pipes of SSES have different intensities and follow the same distribution of chug amplitudes in time as in the GKM II-M single vent facility. This assumption forms the basis for two key elements of the LOCA load definition.

The first element assumes that the average of simultaneously occurring chugs at different vents in SSES is equivalent to the average of consecutive GKM II-M chugs. Thus, as documented in Subsection 9.5.3.1.2, the random amplitude chugs at SSES were replaced with the same chug at every vent which represents the average of consecutive GKM II-M chugs or "mean value" chug.

The second element assumes that the chug amplitude or strength at the individual SSES vents are random variables which have the same probability distribution as the distribution of chug amplitudes at GKM II-M. The GKM II-M probability distribution was then applied statistically to an analytical model of the SSES suppression pool to calculate the symmetric and asymmetric amplitude factors. These factors were then applied to the selected mean value chugs to achieve the desired exceedance probability prior to transportation to SSES for containment analysis (see Subsections 9.5.3.4.1 and 9.5.3.4.2).

These two elements infer that the multi-vent facility is composed of many "single cells" whose chug strengths vary stochastically and independently of each other. The random nature of chugging is explained qualitatively by looking at the actual bubble collapsing mechanism. The most plausible mechanism for bubble collapse at the individual vents appears to be the convection in the pool. This means that bubble collapses at indivdual vents are triggered by the local turbulent convection at each vent. Thus due to the stochastic nature of turbulence, the time at which rapid condensation and hence bubble collapse is triggered varies from vent to vent. This implies that the size of the bubble formed before collapse starts, will also vary from vent to vent. Therefore, the chug strength will vary from vent to vent. Since, the GKM II-M tests were designed to be prototypical of SSES (i.e., same initial pool temperature, same steam flow, etc.), this random variation is expected to be similar for both the GKM II-M single vent facility and the SSES plant.

Additional qualitative data verifying the random nature of chugging is provided by numerous multi-vent test programs. Specifically, the KWU multi-vent concrete cell tests in Karlstein, Creare subscale multi-vent tests and JAERI full scale multi-vent tests provide multi-vent data of the chugging phenomena.

The Karlstein facility investigated the chugging phenomena for 2, 6, and 10 vents at subscale. Each vent in the concrete cell was instrumented with a pressure transducer in such a way that it was indicative of the chug strength for its respective vent. Figures 10-4, 10-5, and 10-6 illustrate these vent transducers and the remaining transducers for the 10, 6, and 2 vent facilities, respectively.

Figures 10-7 and 10-8 show typical pressure time histories for the pressure transducers mounted near the vent pipes for the six vent configuration. These pressure transducers were all exposed to a steam environment and clearly indicate that the chug strengths differ by up to a factor of 10.

In addition, Figure 10-9 shows that the distribution of relative frequencies of the measured wall pressures becomes narrower as the number of vent pipes increases from 2 to 6 to 10. Again, the variation in chug strengths results in a lower global pressure amplitude with increasing number of vents.

This variation in chug strengths was also observed in the Creare subscale multi-vent test program. This observation was obtained by examining the pool wall pressures measured at the three different circumferential locations at the vent exit. All test geometries had three transducers located 120° apart circumferentially at the vent exit elevation. In the multi-vent geometrics, each of these pressure transducers was located close to a particular vent. Therefore, the amplitude of the POP measured at each circumferential location reflects to a large extent the chug strength at the vent closest to it (since pressure amplitude varies inversely with the distance between the vent and wall pressure measurement location). For example, only if the chug strengths at all vents were identical, would the peak over-pressure (POP) measured at each of these three circumferential locations be identical.

Figure 10-10 shows the pool wall pressures at the three circumferential vent exit locations in the 1/6 scale 3 vent geometry. The steam mass flux was 8 lbm/sec ft^2 and as determined from the vent static pressures over 80% of the chugs shown had all three vents participating. This figure shows that the POP's at the three locations are different for individual chugs. Therefore, it can be concluded that the chug strength varies from vent to vent.

Similar data from the 1/10 scale 19 vent geometry at a steam mass flux of 8 lbm/sec ft^2 are shown in Figure 10-11. Again, from vent static pressure data for vents closest to each circumferential wall pressure measurement location, it was determined that all three vents participated in the chugs shown. The POP's at the three different circumferential locations are seen as being different for individual chugs. Note that the variation of chug strength from vent to vent is expected to be stochastic to a large extent. Therefore, it is expected that for some chugs, the chug strength at the three vents would be similar.

Additional proof that the chug strengths in a multi-vent facility behave stochastically is given by the JAERI multi-vent test data. There are several pool wall pressure transducers that are located near the exits of different vents in the JAERI facility. Specifically, transudcers WWPF-202, 302, 602, and 702 are located at the vent exit elevation next to vents 2, 3, 4, and 7, respectively (see Figure 10-12 and 10-13). The pressure amplitudes measured by these transducers reflect the chug strengths at vents closest to them.

The variation of chug strengths at individual vents is shown in Figure 10-14. The pool wall pressures at the vent exit elevation for a chug occur at 62.5 seconds in JAERI test 0002. In this chug event, a high amplitude chug occurred at vent 7 as indicated by the large pressure spike at WWPF702. The other vents had relatively smaller chugs. Keep in mind that the variation of chug strengths from vent to vent is stochastic in nature and that not all pool chugs will exhibit the large variation seen in Figure 10-14. Nonetheless, varying degrees of variation in chug strengths from vent to vent were found in all the chugs from Tests 0002, 2101, and 3102 for which expanded time traces are available.

So far, we have stated that chugging is stochastic in nature, and as such the chug strengths are expected to vary, even though the same thermodynamic conditions exist at each vent (i.e., steam air content, mass flux, bulk pool termperature, etc.). As presented above, this phenomena has been observed in numerous multi-vent test facilities. However, we have not quantitatively verified our assumption of the interchangeability of the temporal chug strength variations at GKM II-M with the spacially varying chug strengths at SSES. Again, the Creare subscale multi-vent test data and

JAERI test data provide information verifying the conservatism of this assumption. Each will be presented below.

As previously stated, one element of our LOCA load definition replaces the random amplitude chugs at SSES with the same chug at every vent, which is representative of the mean value data at GKM II-M. The Creare test data coupled with the accepted acoustic methodology provides verification of this assumption. Creare has acoustically modeled the 1/10-scale single and multi-vent geometries and they have derived a source which represents the mean value chug in the 1/10-scale single vent geometry.

They then placed this mean value chug source at each vent location of their acoustic model for the 1/10-scale 3, 7, and 19 vent geometries. For each of the three multi-vent geometries, the pressure time histroy at the pool bottom elevation (same as the transducer location at this elevation in the test geometries) was computed for 20 chug events. Each chug event involved selecting start times for individual vents randomly within a 20 msec time window. The multi-vent multiplier was then computed based on the mean POP at the pool bottom elevation for the 20 computed chugs. The predicted multi-vent multipliers compared quite favorably with the measured values. Subsection A 5.2.2 of Reference 66 gives a detailed description of the analysis and results. Thus, for subscale multi-vent geometries, the first element of our LOCA load definition is verified.

Final quantitative justification for our key assumption is provided by comparing the available JAERI full-scale multi-vent data with the GKM II-M single vent data.

There are two sets of JAERI data available that can be used to infer chug strengths at individual vents in a given multi-vent chug event. The first set is the pool wall pressure data from the pool wall transducers located at the vent exit elevation. In the JAERI test geometry, there were four pool wall pressure transducers-WWPF 202, 302, 602, and 702-located such that each of these transducers is very near the exits of four individual vents. Therefore, the pressure data from a given transducer reflects the chug strength at the vent closest to that transducer.

As previously stated, the data from these wall pressure transducers were used to qualitatively show that the chug strengths vary significantly from vent to vent in a JAERI multi-vent chug event. Unfortunately, since a pool transducer "sees" pressures due to chugs at all vents to varying extents, the data from such transducers are not suitable for quantitative evaluation of vent to vent chug strength variations.

The other set of JAERI data that provides a measure of chug strengths at the individual vents are the vent static pressure measurements. Five of the seven vents in the JAERI test facility are instrumented with vent exit static pressure transducers.

The vent static pressure is a direct measure of the "vent component" of the chug-induced pool wall pressure. Further, due to desynchronization in a multi-vent geometry, the "vent component" is the dominant component of the chug induced pool pressures observed in multi-vent chugging. Therefore, the spatial (vent to vent) variation of the vent static pressures in the JAERI multi-vent geometry should provide a reliable estimate of the vent to vent chug strength variation in a multi-vent geometry.

Individual vent exit static pressures of 1.125 sec periods are available for 38 chug events from six JAERI tests, eight chugs from Test 0002, seven chugs from Test 0003, six chugs from Test 0004, five chugs from Test 1101, five chugs from Test 1201, and seven chugs from Test 2101. These chugs were selected from periods of high amplitude chugging in each test. Therefore, this data base covers the worst chugging regions observed in these JAERI tests.

The indivdual vent exit static pressures for a given pool chug event were processed in the following manner. First, the rms pressure P_i was computed for each vent static pressure trace. Next, the average rms pressure P was computed. For example, if vent static pressures were available for all the five instrumented vents, the average rms vent static pressure for that chug is:

$$\bar{p} = \frac{P_1 + P_2 + P_3 + P_4 + P_5}{5}$$

Since we are interested in the relative variation in chug strengths between individual vents, the individual rms vent static pressures were normalized by the average rms pressure $\bar{P}$.

The normalized indivdual rms vent static pressure $\bar{P}_i$ for the 38 chugs analyzed are given in Table 10-1. Also shown are the values of the normalized variances for the individual vent rms pressures for individual chug events. Note that due to instrumentation malfunctions, for all except one JAERI test, vent exit static pressure data are not available for all five instrumented vents.

Due to small number of vents (at most five) for which vent static pressure data are available, it is difficult to draw meaningful statistical inferences for vent to vent chug strength variations from any one individual pool chug event.

Therefore, it is necessary to make an assumption that allows the use of the data from all 38 chug events such that meaningful statistical inferences can be drawn. This assumption is that the normalized statistical distribution of chug strengths from vent to vent is independent of blowdown conditions. That is, the normalized vent to vent chug strength for all 38 chug events are samples selected from the same statistical population. Note that this is precisely the same assumption made in analyzing the temporal statistical properties of the GKM II-M single vent data (see Subsection 9.5.3.2.1).

The GKM II-M data that provides a direct measure of the vent component of the chug strength are the pool wall pressure data band pass filtered between 0.5-13 Hz. In this frequency range, the pool wall pressures measured are due to the vent pressure oscillations produced by the chug (see Subsection 9.4.2.1.2).

As described in Subsection 9.5.3.2.1, the pressure amplitudes of individual chugs were normalized by the sliding mean value over a given time interval. In this way, a normalized data base reflecting the temporal variations of chug strengths was obtained for all the GKM II-M tests. Note that again implicit in this procedure is the assumption that the statistics of the variation of the normalized chug strengths is independent of system conditions. As previously mentioned, this assumption was also used for combining the JAERI data for 38 pool chug events into a single statistical data base.

The histograms of the normalized chug strengths for the various GKM II-M tests are given in Figures 9-181, 9-182, and 9-183.

At this point, we now have a normalized vent to vent chug strength variation data base from the JAERI multi-vent tests and a corresponding normalized chug to chug strength variation data base from the GKM II-M single vent tests. Table 10-2 shows the variance for the JAERI and GKM II-M data bases. The variance for the JAERI data base is the average value of the individual variances shown in Table 10-1 for each of the 38 chug events. The variance of the GKM II-M data was calculated for the 0.5-13 Hz band passed data plotted in Figures 9-181, 9-182, and 9-183. It is seen that the average variance from the JAERI tests is virtually identical to the variance from the GKM II-M Full MSL tests* and is somewhat greater than the variances from the 1/3 and 1/6 MSL GKM II-M tests. This implies that the variation of vent to vent chug strengths in the JAERI multi-vent tests is equal to or greater than the chug to chug strength variation observed in the GKM II-M single vent tests.

Figures 10-15 through 10-17 show the comparison of the probability density histograms of the JAERI data and the low

---

* The full MSL break chug strength statistics were used to develop the SSES probabilistic amplitude factors.

band passed GKM II-M Full MSL, 1/3 MSL and 1/6 MSL data, respectively. Again, the JAERI and GKM II-M data histograms are quite similar.

From the above comparisons it can be again concluded that the assumption that the vent to vent variation in chug strengths in a single vent geometry is equivalent to the vent to vent chug strength variation in a multi-vent geometry, used in developing the SSES chugging load definition from the GKM II-M single vent test data is quite reasonable.

Additional verification of the conservatism of the SSES LOCA load definition is provided by comparing the wall loads at JAERI calculated with the SSES LOCA load definition with the available JAERI wall load data (see Subsection 9.5.3.5.1). Figures 9-268 and 9-269 show that the SSES LOCA load definition bounds the available JAERI data by a substantial margin. Please note that the wall loads calculated by the SSES LOCA load definition do not include the symmetric amplitude factor and thus represent "mean value" chugs.

(2) The Mark II Owners have specified two different CO loads for containment analysis. The first CO load (CO 1) corresponds to the CO occurring at the beginning of a postulated LOCA and the second CO load (CO 2) corresponds to the reduced CO load occurring later in the blowdown. For containment analysis, the Owners combine the reduced CO 2 load with loads due to SRV (ADS), on the basis that ADS occurs later in a LOCA justifying a reduced CO load for the combination CO & SRV (ADS).

However, SSES combines the so-called LOCA loads with SRV (ADS) for containment analysis. The LOCA load comprises the envelop of the responses due to both chugging and CO. Thus, the SSES load combination LOCA & SRV (ADS) considers both CO and chugging and is more conservative than the Owner's combination of a reduced CO load (CO 2) with SRV (ADS).

(3) The SSES LOCA laod definition selected one CO pressure time history (PTH No. 14) from GKM II-M as representative and bounding of the CO at GKM II-M (see Figure 9-177a & b). Subsequently, this CO PTH was sourced and applied in-phase to the IWEGS/MARS acoustic model for containment analysis.

Figure 9-264 represents the enveloping PSD of PTH No. 14. Figure 2-1 of Reference 70 presents the envelop for PSD values observed for CO in the 4T-CO tests. These two figures indicate that the PSD of PTH No. 14 from GKM II-M compares favorably with the enveloping PSD of the CO in 4T-CO.

QUESTION 2

The dominant frequency for the Karlstein T-Quencher Test 21.2 appears to be 8.0 Hz instead of the 6.8 Hz reported in Table 8-10 of the DAR. Using the multipliers from Figure 8-174 and this 8.0

Hz frequency, we get a transposed frequency of 10.6 Hz. This value falls outside of the specified frequency range. A Fourier analysis indicates an exceedance of approximately 70% at this 10.6 Hz frequency. Please provide justification for the existing load specification frequency range.

RESPONSE 2

As can be seen in Figure 8-188, Test 21.2 does not show a clearly predominant frequency. We have interpreted 6.5 Hz as the predominant frequency because of the maximum peak occurring in the PSD at that frequency; however, a second peak, only slightly lower than the 6.5 Hz peak, can be seen in that PSD at approximately 8.0 Hz.

To investigate further the significant of Test 21.2 to the acceptability of the Susquehanna T-Quencher load specification, KWU performed a pressure response spectra comparison of the load specification and Test 21.2.

The method of "weighted traces" presented to the NRC in the June 13, 1980 Lead Plant Meeting and documented in the KWU Report R - 141/141/79 is used for this comparison. Figure 10-18 shows that the Susquehanna load specification bounds the measured pressure time history of Karlstein Test 21.2 representing the all valve case.

Assuming a maximum predominant frequency in Test 21.2 of 8 Hz and transferring the measured data of Test 21.2 to the all-valve and single-valve load case we get the comparison shown in Figure 10-19. The pressure response spectra of the Susquehanna load specifications is slightly exceeded by the pressure spectra from Test 21.2 in the frequency range between 10 Hz and 11 Hz. This slight exceedance is only related to the single-valve load case and is considered insignificant to the total load specification and in relation to the total data base from Karlstein.

In addition, the term "dominant frequency" is highly subjective and sensitive to the method chosen for determining the dominant frequency. Originially, KWU determined the dominant frequency range for the three SSES design traces (KKB Traces #35, 76 and 82) to be <u>6.5 to 8.0 Hz</u> (see SSES DAR, page 8P-101). This frequency range was based on a PSD analysis of the three traces. However, for these non-stationary SRV traces, the PSD analysis is sensitive to the time segment chosen for analysis. Using a particular time duration may give one dominant frequency while another may give a slightly different dominant frequency.

Subsequently, Bechtel has taken the design traces and performed their own analysis to determine the dominant frequency. They calculated a dominant frequency range of <u>6.45 to 8.69 Hz</u> for the three traces. This frequency range was based on the inverse of the peak-to-peak oscillation time period for the first two peaks. This was done for both negative and positive peak-to-peak periods.

Furthermore, Sargent & Lundy have determined the dominant frequency range of the three traces to be 6.8 to 8.9 Hz. As can be seen, the dominant frequency varies according to who performs the analysis and the methodology selected.

For containment analysis, the KWU methodology requires that time scale multipliers be applied to the three design traces. They range from 0.9 (time contraction or frequency expansion) to 1.8 (time expansion or frequency contraction). When these multipliers are applied to the three design traces, specified frequency ranges of 3.3 to 8.9 Hz, 3.6 to 9.7 Hz and 3.8 to 9.9 Hz are obtained by using the above dominant frequency ranges from the original traces. Thus, the specified frequency range varies depending on the interpretation of the "dominant frequency".

However, regardless of the interpreted dominant frequency range, the same three traces and time expansion and contration factors are used for containment analysis. Thus, ones opinion of what the dominant frequency range is for the three traces is not as important as the time factors chosen for actually applying the traces to the containment boundary.

With this in mind, Figures 10-20 thru 10-41 illustrate the response spectra generated by KWU Trace #76 for SSES. The trace was frequency expanded and contracted by 110% and 55%, respectively, to give a specified frequency ranges of 3.3 to 8.9 Hz, 3.6 to 9.7 Hz or 3.8 to 9.9 Hz, again, depending on the interpretation of the "dominant frequency".

Figures 10-42 thru 10-63 show the response spectra generated by KWU Trace #76 for the Limerick Generating Station (LGS). The LGS structural model is essentially identical to the SSES model. However, these spectra reflect the use of frequency expansion and contraction factors of 125% and 55%, respectively. This gives specified frequency ranges of 3.3 to 10 Hz, 3.6 to 10.9 Hz or 3.8 to 11 Hz. Thus, depending on the dominant frequency, these spectra reflect the use of the NRC's upper bound dominant frequency of 11 Hz, as required by Supplement No. 1 to NUREG-0487.

A node by node comparison of the two spectra shows that the expanded spectral input used for LGS has negligible effect on the total response contributed by all modes. Thus, this supports the conclusion that an extention of the upper frequency multiplier would have no significant impact on the SSES response spectra analysis.

QUESTION 3

The Karlstein tests run with depressed water legs to simulate the ADS load case utilized the longest discharge line length for SSES. Is this line length prototypical of the SSES ADS line lengths? If not, what is the magnitude of the difference between the SSES ADS line lengths and the test line length? If not prototypical, is the data from the ADS tests acceptable for transportation to SSES with regards to frequency content?

RESPONSE 3

Tests 10.3, 11.1, 12.1, and 13.1 are considered representative for the ADS actuation load case. These tests were all performed with the long discharge line. No tests with a short discharge line and a depressed initial water level (representing ADS conditions) were performed. These long line tests represent a bounding condition, in that the longest discharge line with depressed initial water level contains the largest possible initial air mass and will therefore produce the lowest possible pressure oscillation frequency.

To check whether the frequencies expected from short line ADS actuation fall within our specified frequency range we will transpose the test results from Test 11.1 to short line conditions.

Table 8B on page 8P-105 of the Susquehanna DAR shows the average frequencies measured during the Karlstein tests. A portion of that table is shown below:

		Measured Frequencies (Hz)
Long	Clean Conditions	(3.5) *-4
Line	Real Conditions	5
Short	Clean Conditions	5
Line	Real Conditions	6.5

*Tests with low amplitude

This data indicates a ratio of approximately 1.3 exists between the frequencies measured in long line tests and short line tests.

Subsection 8.5.3.3.4.6 of the Susquehanna DAR provides the comparison of the T-Quencher ADS load specification with the Karlstein test results. When the measured frequency for Test 11.1 was adjusted to account for back pressure and water surface area effects the measured 3 Hz frequency was raised to 5.7 Hz. To check the short line ADS load case we will adjust this 5.7 Hz by the 1.3 ratio obtained above. This produces a predominant frequency for the ADS - short line conditions of

$$V = 5.7 \times 1.3 = 7.4 \text{ Hz}$$

This frequency lies within the specified frequency range.

QUESTION 4

Was the quencher bottom support used at Karlstein prototypical of the supports at Susquehanna SES?

RESPONSE 4

The bottom support used in Karlstein is protopical but not identical of those used at Susquehanna. The T-Quencher installed in the Karltsein test tank had the same distance between the bottom of the support and the quencher mid-plane as those quenchers installed at Susquehanna. Therefore, the thermo-hydraulic loading on the quencher supports are the same for the Karlstein test tank and Susquehanna. From a structural point of view, the bottom support used at Karlstein is not identical to those used at Susquehanna in that the supports in the plant are stiffer.

QUESTION 5

In three instances, the bending moment in the quencher arm recorded at Karlstein exceeds the specified bending moment. Is the specified bending moment in the quencher arm conservative? Why?

RESPONSE 5

As shown in Figure 8-153 the measured bending moments transposed to the weld of the quencher arm exceed the specified moment in 3 out of a total of 99 cases during vent cleaning. The total load specification for the quencher arm is made up of three components:

a) internal pressure

b) bending moment

c) temperature gradient

The following table lists the specified and maximum measured values for each of the load components.

Condition	Specified Value	Maximum Measured Value
Steady State. Pressure	22 bars	13 bars
Internal Temperature	219° C	191.6° C
Bending Moment	65 kNm	85 kNm

As can be seen, the specified values exceed the measured maximum values except for the referenced bending moments noted above.

As a result of this exceedance, a stress analysis, identical to the one performed for the specified values, was completed using the above maximum measured values. This analysis shows that the total stress due to the specified loads bounds the total stress due to the maximum measured loads. In addition, a fatigue evaluation of the arm weld was performed using the maximum measured data. The results indicate the weld has a usage factor less than unity, and thus is acceptable.

QUESTION 6

Explain why a single failure will not disable both the RHR shutdown cooling function and one RHR loop in the suppression pool cooling mode.

RESPONSE 6

A single failure can indeed disable the RHR shutdown cooling function and one RHR loop in the suppression pool cooling mode under the following assumptions. Both units are operating at full power when a complete long-term loss of offsite power (LOOP) occurs. This leads to main steam line isolation and reactor scram. Following the LOOP all four (4) diesel generators should start to supply power to the ESS busses, however, it is assumed that the diesel generator 0G501C does not start (single failure). 0G501C supplies power to the ESS busses 1A203 and 2A203*, to the RHR pumps 1C and 2C*, and to the RHR service water pump 1A. Loss of 0G501C means that the inboard shutdown cooling isolation valves on both units, 1F009 and 2F009*, loose power to their operators, thus disabling the RHR shutdown cooling mode. Since these valves are located inside the primary containment, it is conservativey assumed that they will not be manually reopened. Only the "B" loop and the corresponding RHRSW loop of the RHR system (in both units) would be readily available for suppression pool cooling, using e.g., RHR pumps 1B and 2D*. The "A" loop of one unit could be made available by manually operating four (4) valves (close F048A, open F024A, HV-1210A and HV-1215A) and using RHRSW pump 2A* and either RHR pump 1A or 2A*. However, a simultaneous operation of RHR pumps 1A and 2A* is prohibited by electrical interlocks. Thus one of the units would have only one RHR loop available in the suppression pool cooling mode without the possibility to switch to shutdown cooling.

This case has not been considered in the transients submitted as part of Appendix I of the DAR and may be more limiting. However, a similar but more conservative case was analyzed as part of a sensitivity study and resulted in a maximum pool temperature of 203°F. The assumptions for this case are indentical to case 2.a (Appendix I, DAR) except that shutdown cooling is not initiated. For this case, the curves for reactor pressure vs. time and suppression pool temperature vs. time are found in Figures 10-64 and 10-65, respectively.

---

* Indicates Unit #2 component.

As mentioned above, this case is similar, but more conservative than the case under consideration. The major difference is that reactor water make-up would not be from the feedwater/condensate system but from HPCI (at reactor pressures above approximately 300 psia) and core spray (at reactor pressures below approximately 300 psia), which both take suction from the condensate storage tank and/or the suppression pool. Thus, water much colder than feedwater would be used for make-up.

This contributes to the reactor depressurization and leads to less steam being dumped into the suppression pool. The peak suppression pool temperature for this case will therefore be lower than that shown in Figures 10-65.

To confirm a temperature of less than 203°F we have initiated an additional analysis case, whose results are contained in Appendix I (Figures I-14 and I-15).

QUESTION 7

How will PP&L use the LaSalle in-plant test data to establish the local to bulk ΔT for Susquehanna SES?

RESPONSE 7

The following table gives a comparison of suppression pool geometries for LaSalle and Susquehanna SES:

	LaSalle	Susquehanna
Suppression Pool I.D.	86'-8"	88'
Pedestal O.D.	30'	29'-9"
Suppression Pool Volume (Normal Water Level)	142,160 ft^3	126,980 ft^3
No. of Quenchers	18	16
Pool Volume/Quencher	7898 ft^3	7936 ft^3
Quencher Submergence (Normal Water Level)	21.5 ft	19.5 ft
Height of Quencher Center-Line Above Base Mat	5 ft	3.5 ft

Based on the similarity between Susquehanna and LaSalle the local to bulk ΔT established from LaSalle inplant tests is also applicable to Susquehanna. In addition, PP&L is continuing to fund the development of computer codes (like Bechtel's KFIX) for the prediction of SRV discharge induced suppression pool mixing processes. The calculated temperature distributions will be compared to existing (Caorso) and future (LaSalle or Zimmer) in-plant test data.

Following satisfactory qualification of the computer codes they can then be used to establish local to bulk temperature differences without test.

QUESTION 8

What are the reactor pressures that correspond to quencher steam mass fluxes of 42 lbm/ft^2s and 94 lbm/ft^2s?

RESPONSE 8

The reactor pressures are 163 psia and 369 psia respectively.

This figure has been deleted.

REV. 6, 4/82

SUSQUEHANNA STEAM ELECTRIC STATION
UNITS 1 AND 2
DESIGN ASSESSMENT REPORT

DOWNCOMER
BRACING SYSTEM

FIGURE 10-1

This figure has been deleted.

REV. 6, 4/82

SUSQUEHANNA STEAM ELECTRIC STATION
UNITS 1 AND 2
DESIGN ASSESSMENT REPORT

DOWNCOMER
BRACING DETAILS

FIGURE 10-2

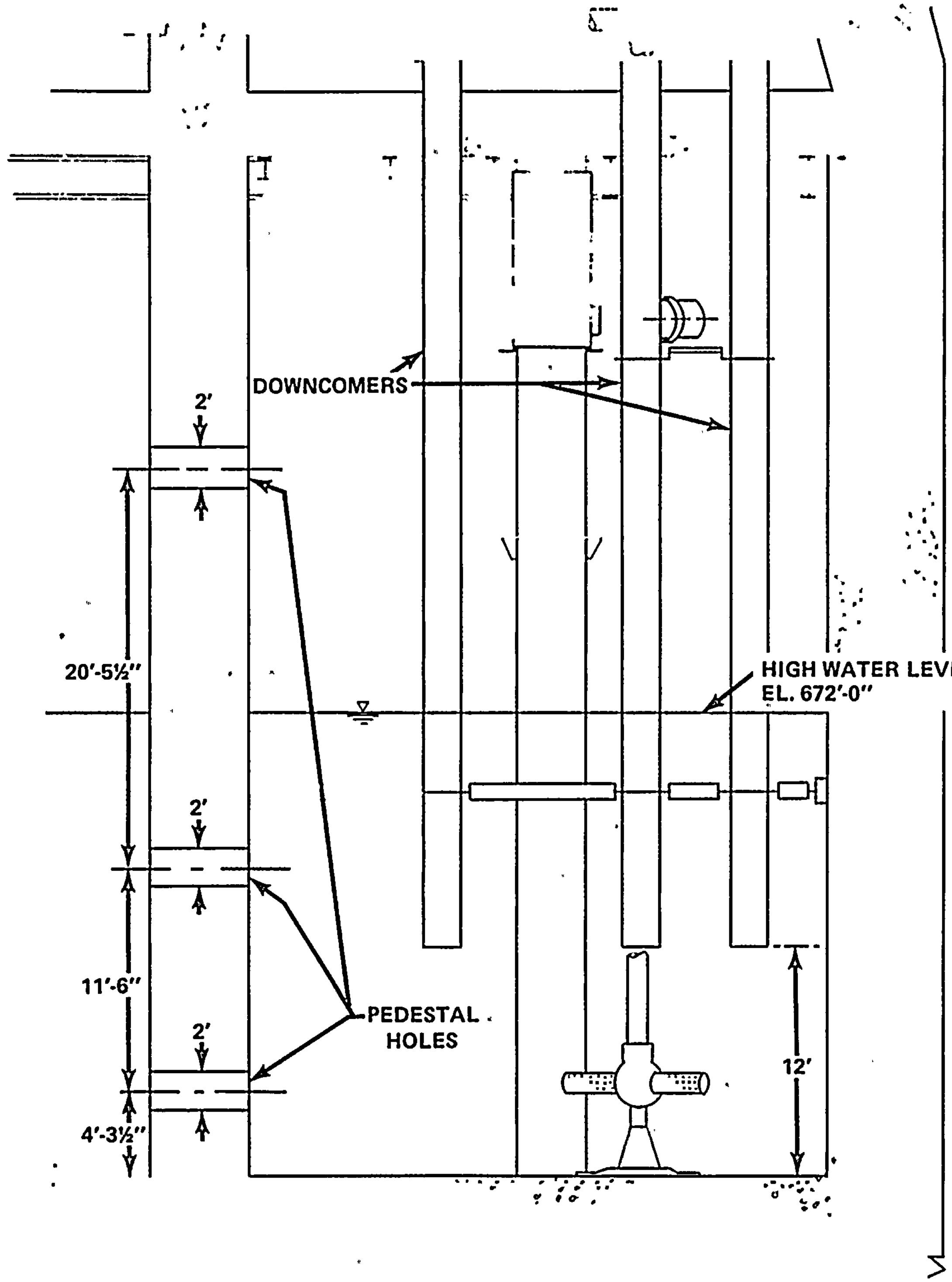

Rev. 5, 3/81

SUSQUEHANNA STEAM ELECTRIC STATION
UNITS 1 AND 2
DESIGN ASSESSMENT REPORT

SPATIAL RELATIONSHIP
OF DOWNCOMERS
AND PEDESTAL HOLES

FIGURE 10-3

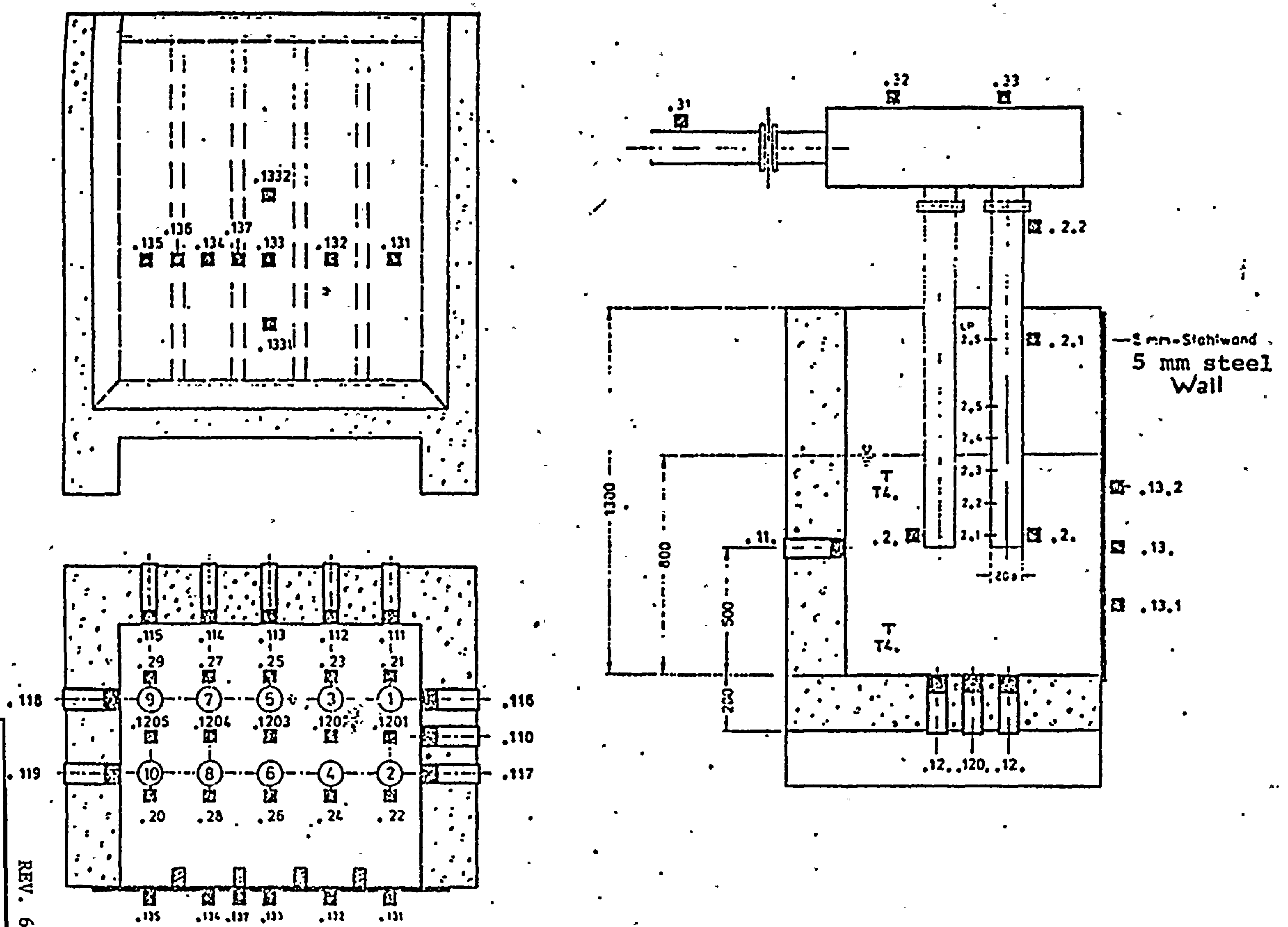

Concrete-cell test stand

Concrete cells 3 and 4

Diagram of measuring points

REV. 6, 4/82

SUSQUEHANNA STEAM ELECTRIC STATION
UNITS 1 AND 2
DESIGN ASSESSMENT REPORT

TRANSDUCER LOCATIONS
FOR THE TEN VENT PIPE
CONFIGURATION

FIGURE 10-4

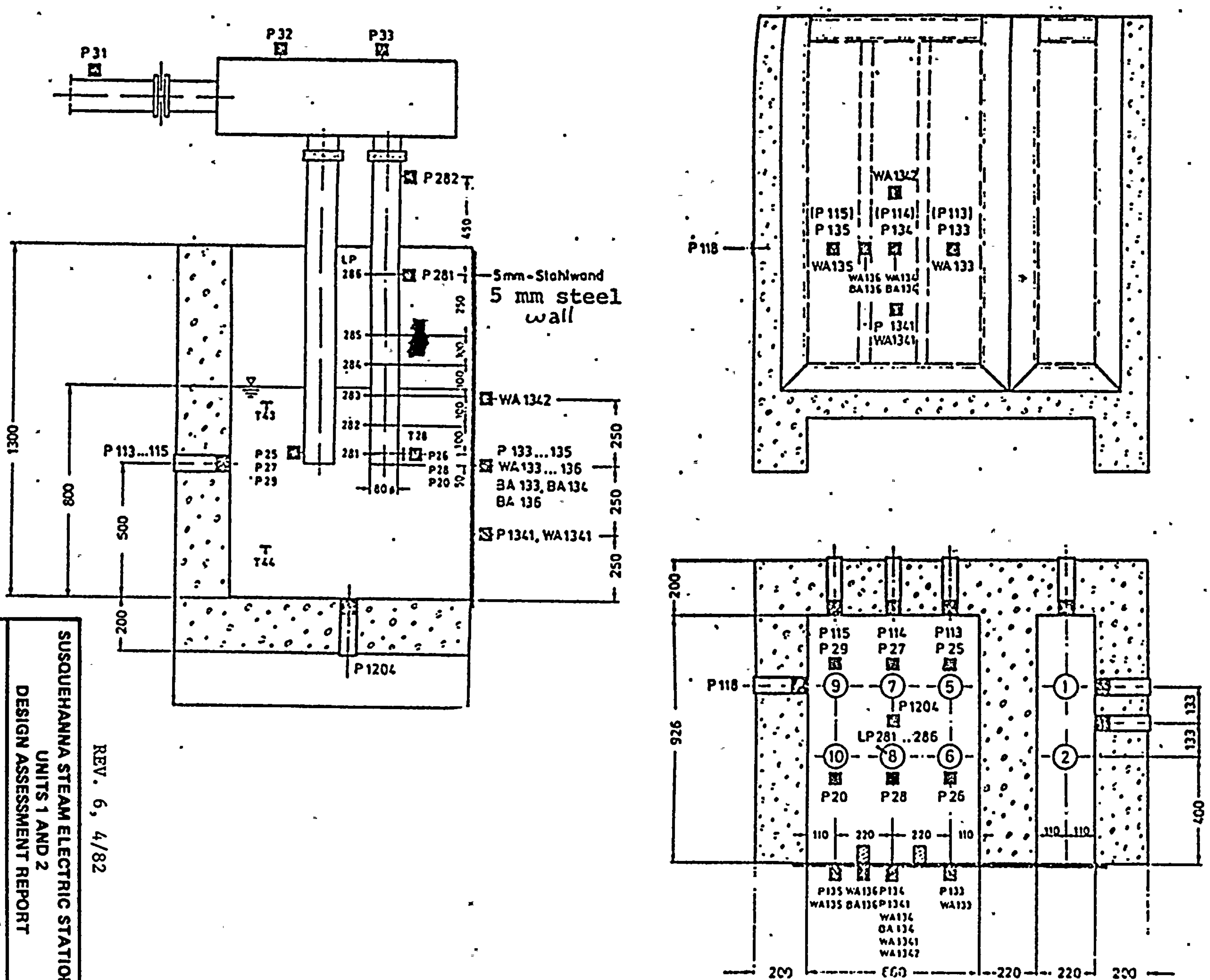

REV. 6, 4/82

SUSQUEHANNA STEAM ELECTRIC STATION
UNITS 1 AND 2
DESIGN ASSESSMENT REPORT

TRANSDUCER LOCATIONS
FOR THE SIX VENT PIPE
CONFIGURATION

FIGURE 10-5

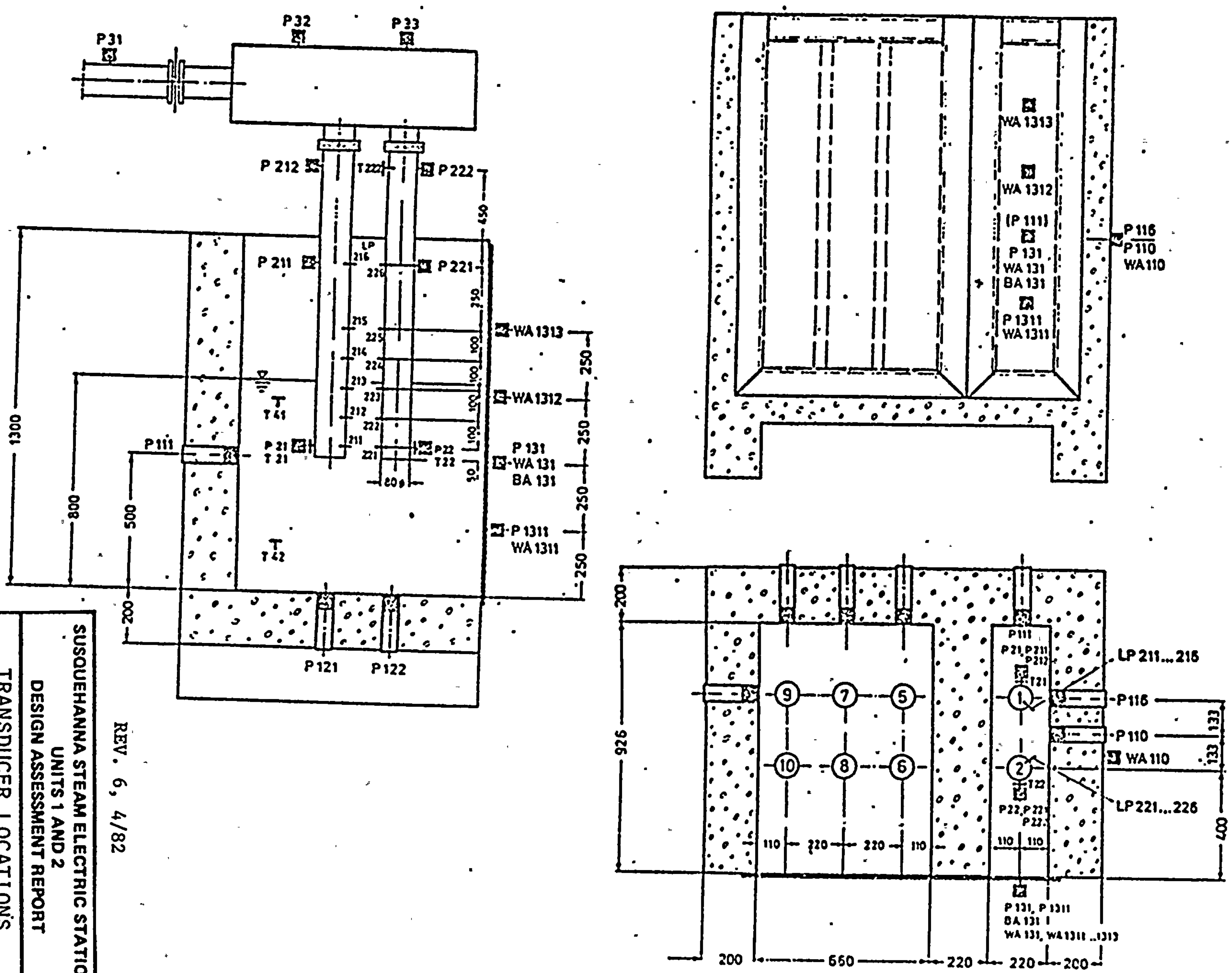

REV. 6, 4/82

SUSQUEHANNA STEAM ELECTRIC STATION
UNITS 1 AND 2
DESIGN ASSESSMENT REPORT

TRANSDUCER LOCATIONS
FOR THE TWO VENT PIPE
CONFIGURATION

FIGURE 10-6

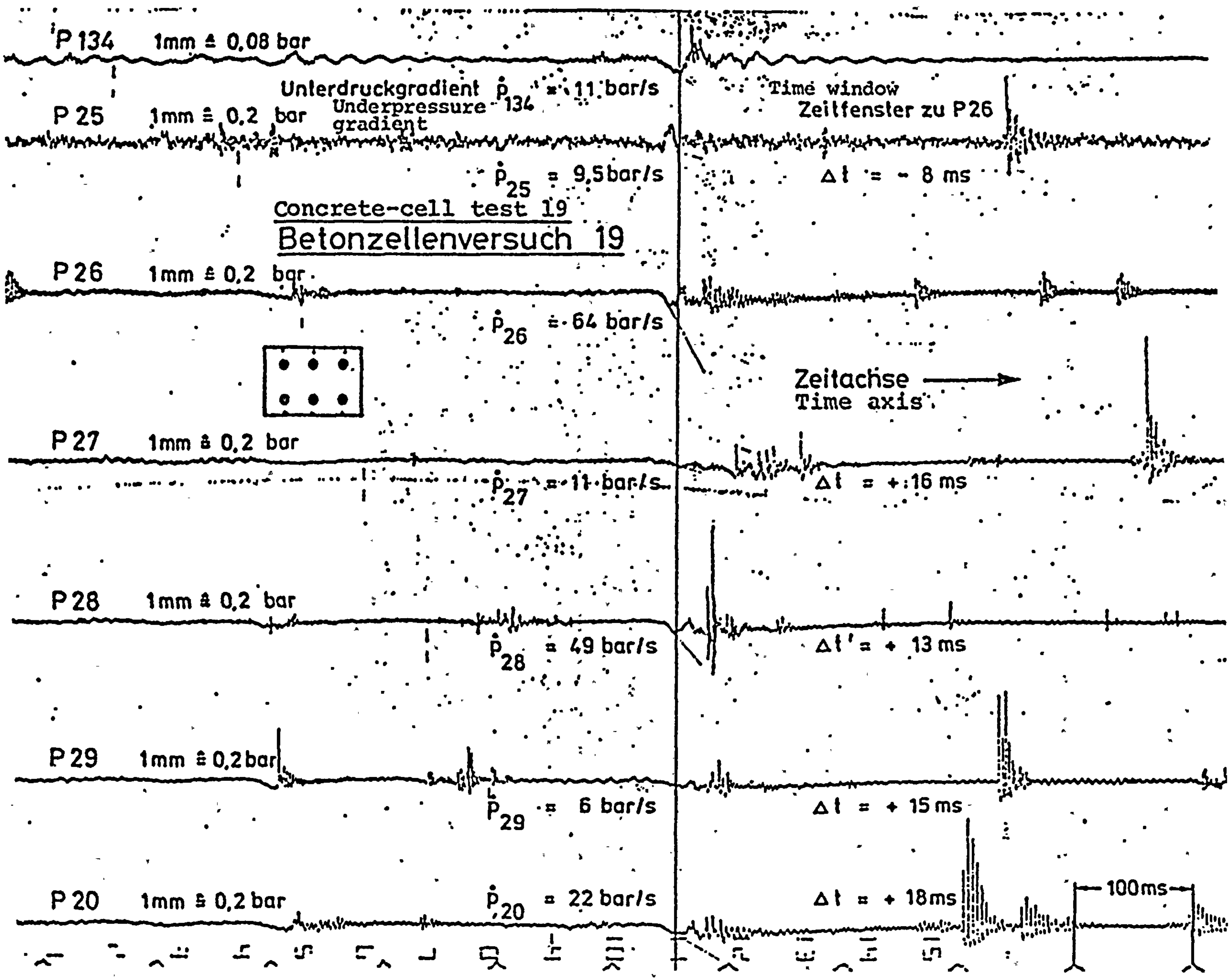

REV. 6, 4/82

SUSQUEHANNA STEAM ELECTRIC STATION
UNITS 1 AND 2
DESIGN ASSESSMENT REPORT

TYPICAL PRESSURE TIME HISTORIES FROM PRESSURE TRANSDUCERS P20,P25,.29 &P134

FIGURE 10-7

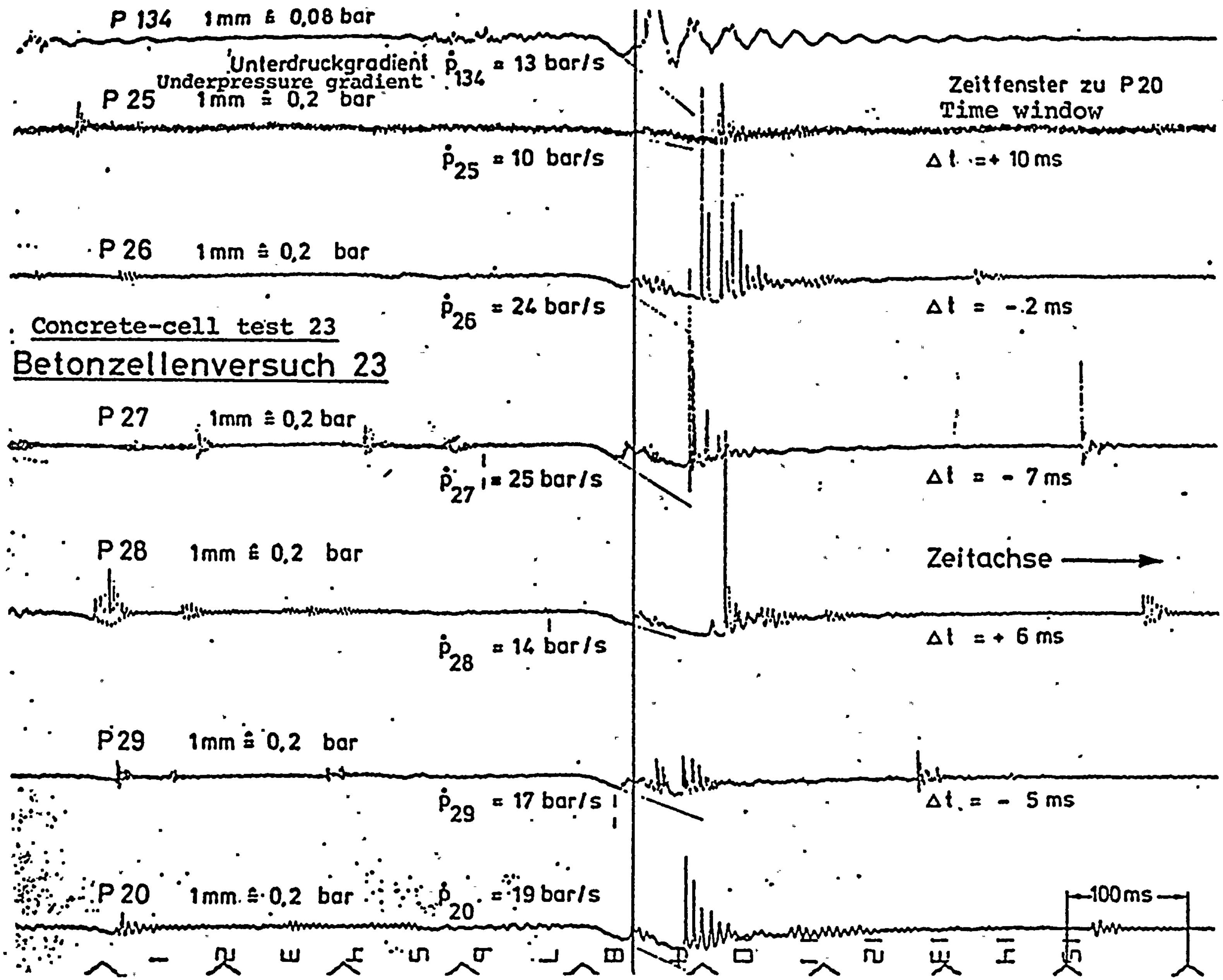

REV. 6, 4/82

SUSQUEHANNA STEAM ELECTRIC STATION
UNITS 1 AND 2
DESIGN ASSESSMENT REPORT

TYPICAL PRESSURE TIME HISTORIES FROM PRESSURE TRANSDUCERS P20,P25..29,P134

FIGURE 10-8

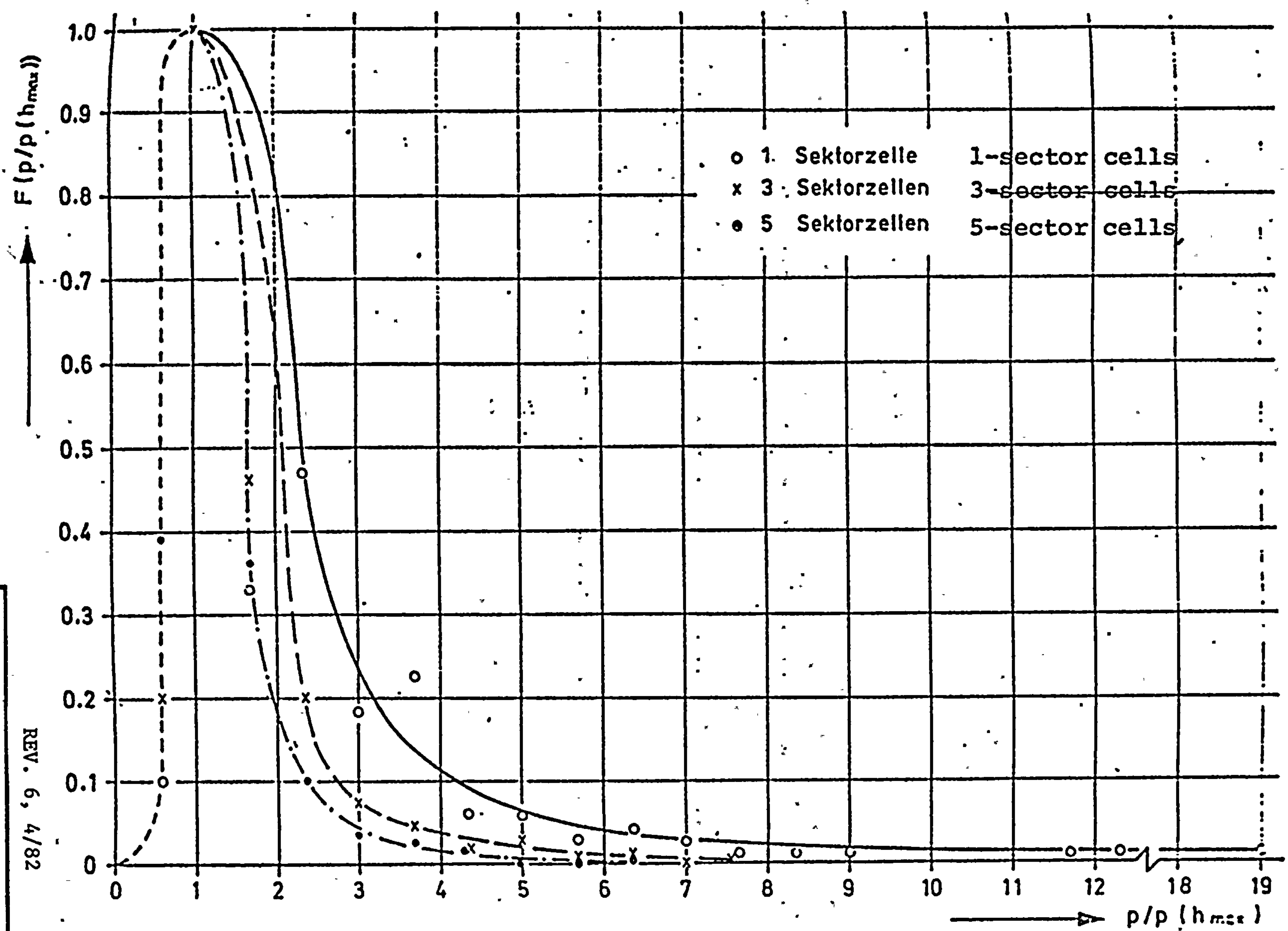

REV. 6, 4/82

SUSQUEHANNA STEAM ELECTRIC STATION
UNITS 1 AND 2
DESIGN ASSESSMENT REPORT

FREQUENCY DISTRIBUTION OF MEASURED NORMALIZED WALL PRESSURES

FIGURE 10-9

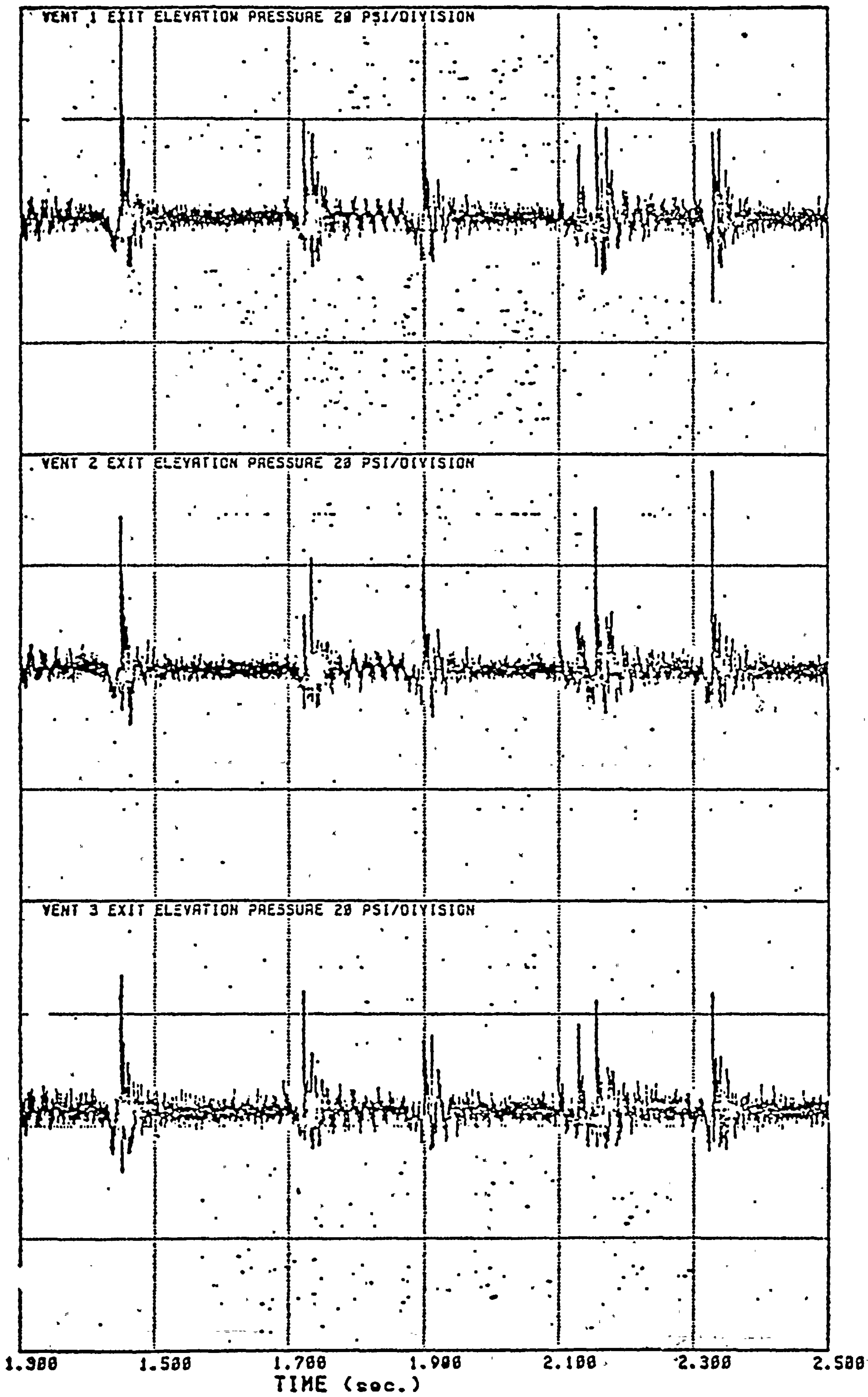

REV. 6, 4/82

SUSQUEHANNA STEAM ELECTRIC STATION
UNITS 1 AND 2
DESIGN ASSESSMENT REPORT

POOL WALL PRESSURES AT THREE CIRCUMFERENTIAL VENT EXIT LOCATIONS-1/4 SCALE 3 VENT GEOMETRY

FIGURE 10-10

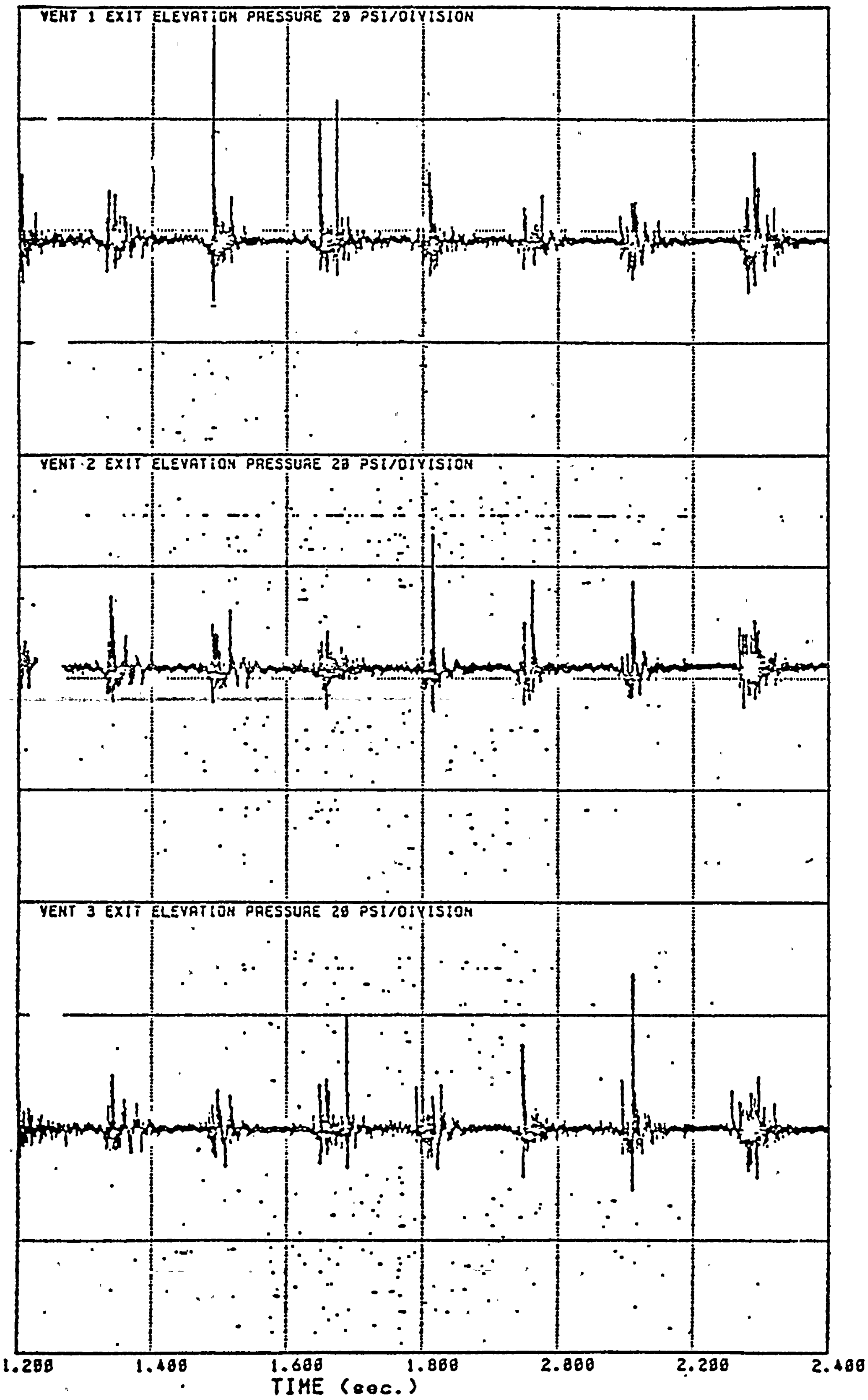

REV. 6, 4/82

SUSQUEHANNA STEAM ELECTRIC STATION
UNITS 1 AND 2
DESIGN ASSESSMENT REPORT

POOL WALL PRESSURES AT THREE CIRCUMFERENTIAL VENT EXIT LOCATIONS-1/10 SCALE 1D VENT GEOMETRY

FIGURE 10-11

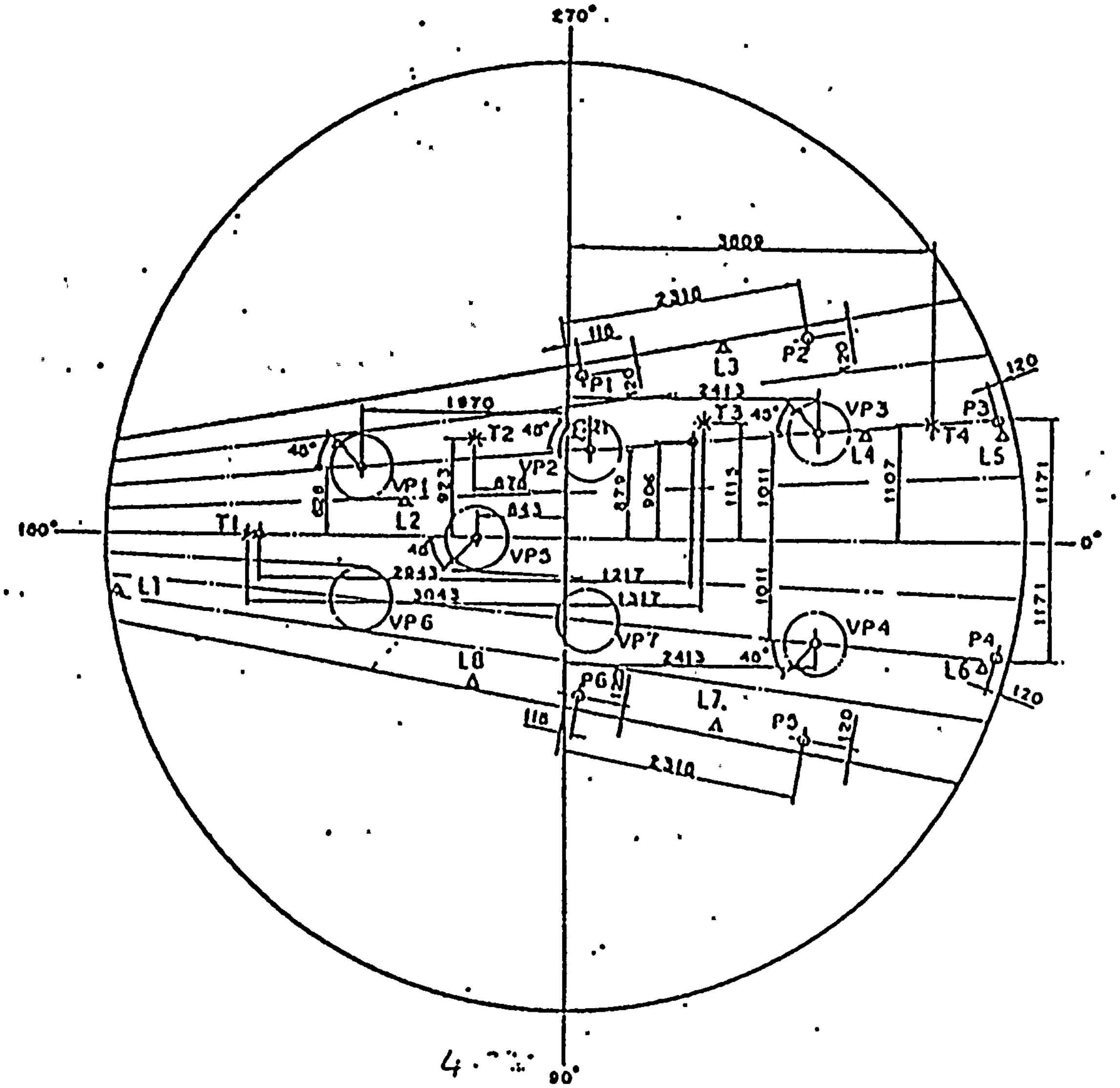

Δ : Water level
O : Pressure
O : Pressure on wetwell bottom floor
X : Temperature
VP : Vent pipe

REV. 6, 4/82

SUSQUEHANNA STEAM ELECTRIC STATION
UNITS 1 AND 2
DESIGN ASSESSMENT REPORT

PLAN LOCATIONS OF TRANSDUCERS FOR WETWELL

FIGURE 10-12

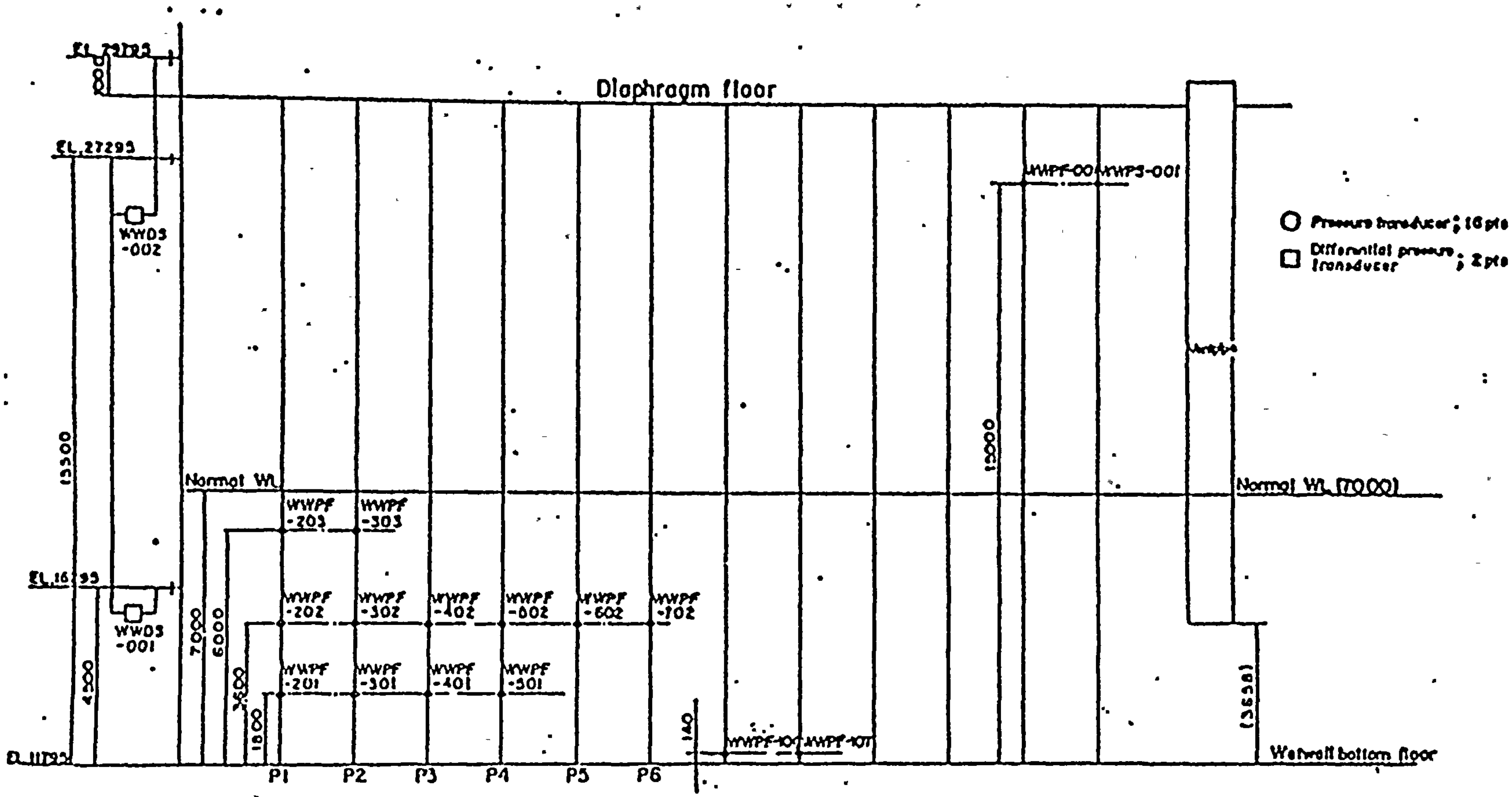

REV. 6, 4/82

SUSQUEHANNA STEAM ELECTRIC STATION
UNITS 1 AND 2
DESIGN ASSESSMENT REPORT

LOCATIONS OF PRESSURE TRANSDUCERS FOR WETWELL

FIGURE 10-13

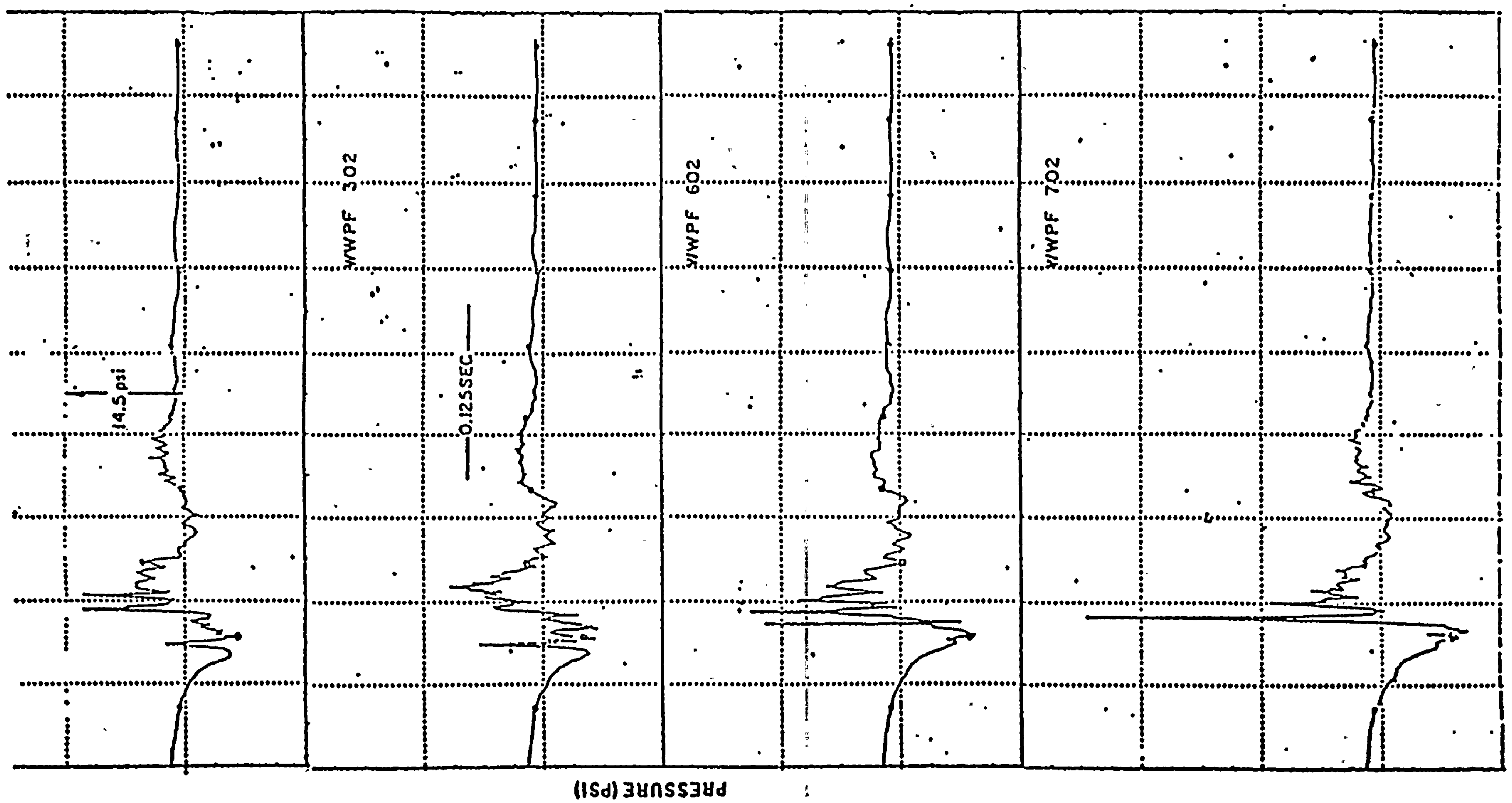

REV. 6, 4/82

SUSQUEHANNA STEAM ELECTRIC STATION
UNITS 1 AND 2
DESIGN ASSESSMENT REPORT

VENT EXIT ELEVATION POOL WALL PRESSURES FOR A CHUG FROM JAERI TEST 0002

FIGURE 10-14

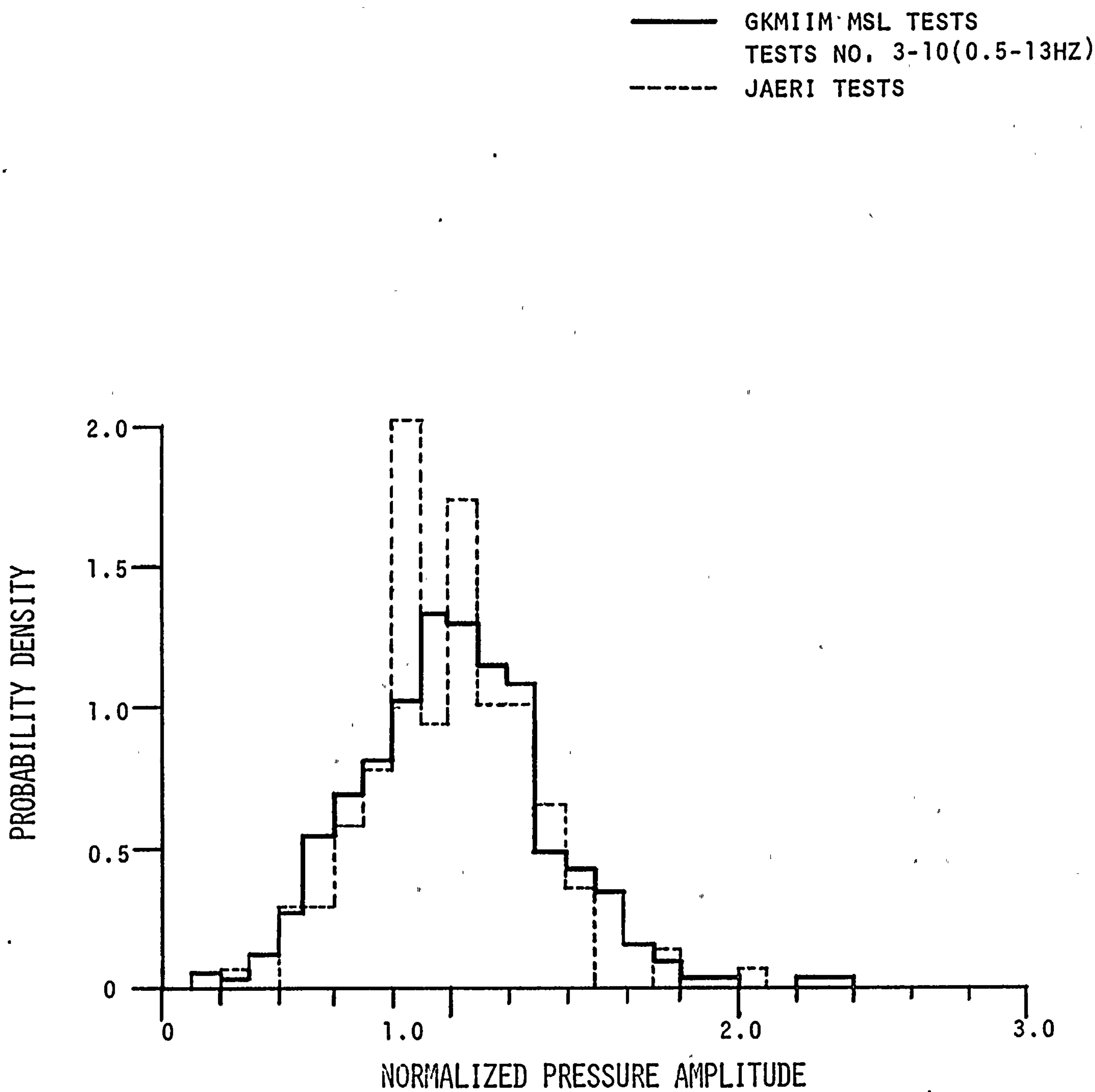

REV. 6, 4/82

SUSQUEHANNA STEAM ELECTRIC STATION
UNITS 1 AND 2
DESIGN ASSESSMENT REPORT

COMPARISON OF PROBABILITY DENSITY OF THE NORMALIZED PRESSURE AMPLITUDES FROM GKM II-M TESTS 3..10 & JAERI

FIGURE 10-15

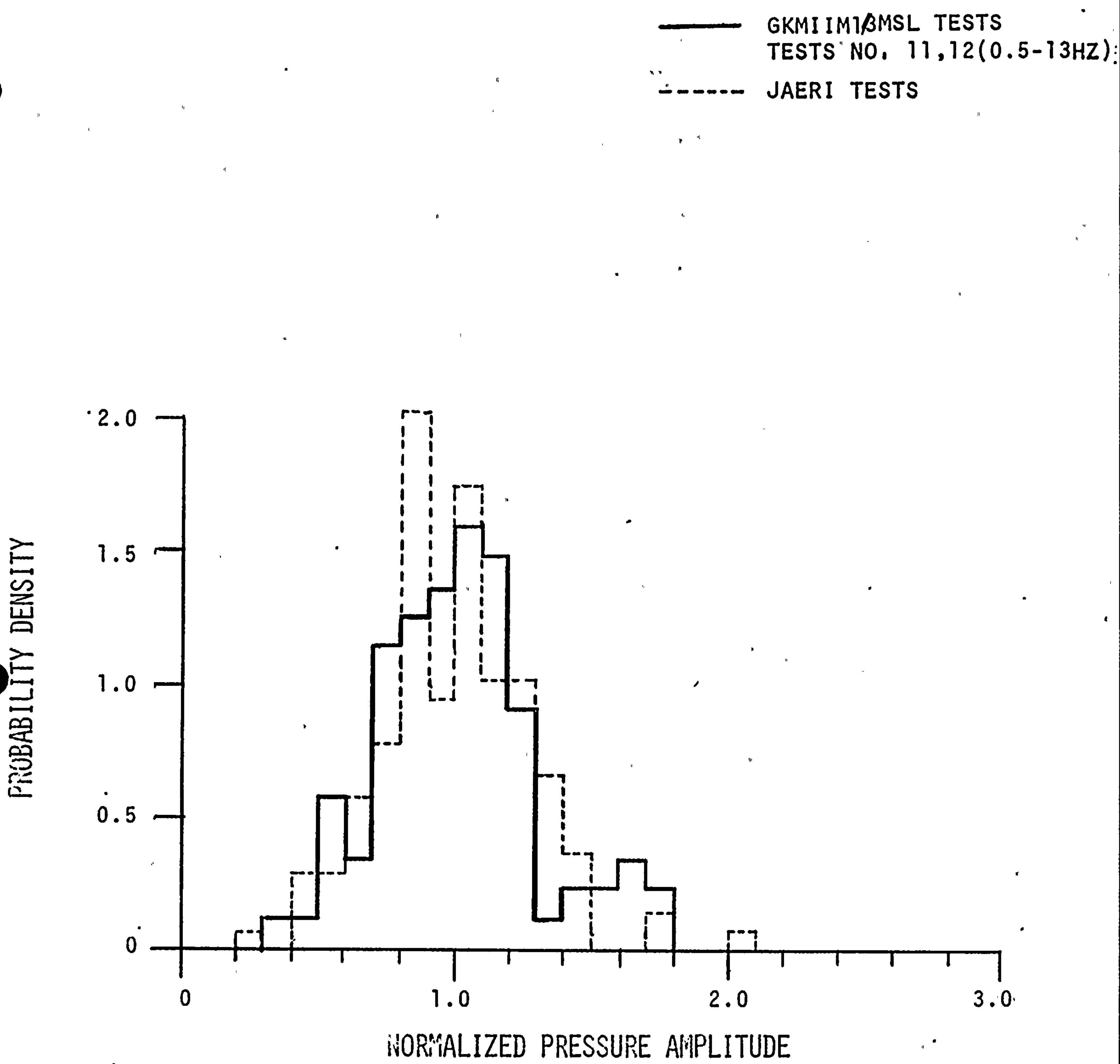

REV. 6, 4/82

SUSQUEHANNA STEAM ELECTRIC STATION UNITS 1 AND 2 DESIGN ASSESSMENT REPORT
COMPARISON OF PROBABILITY DENSITY OF THE NORMALIZED PRESSURE AMPLITUDES FROM GKMII-M TESTS 11 & 12 & JAERI
FIGURE 10-16

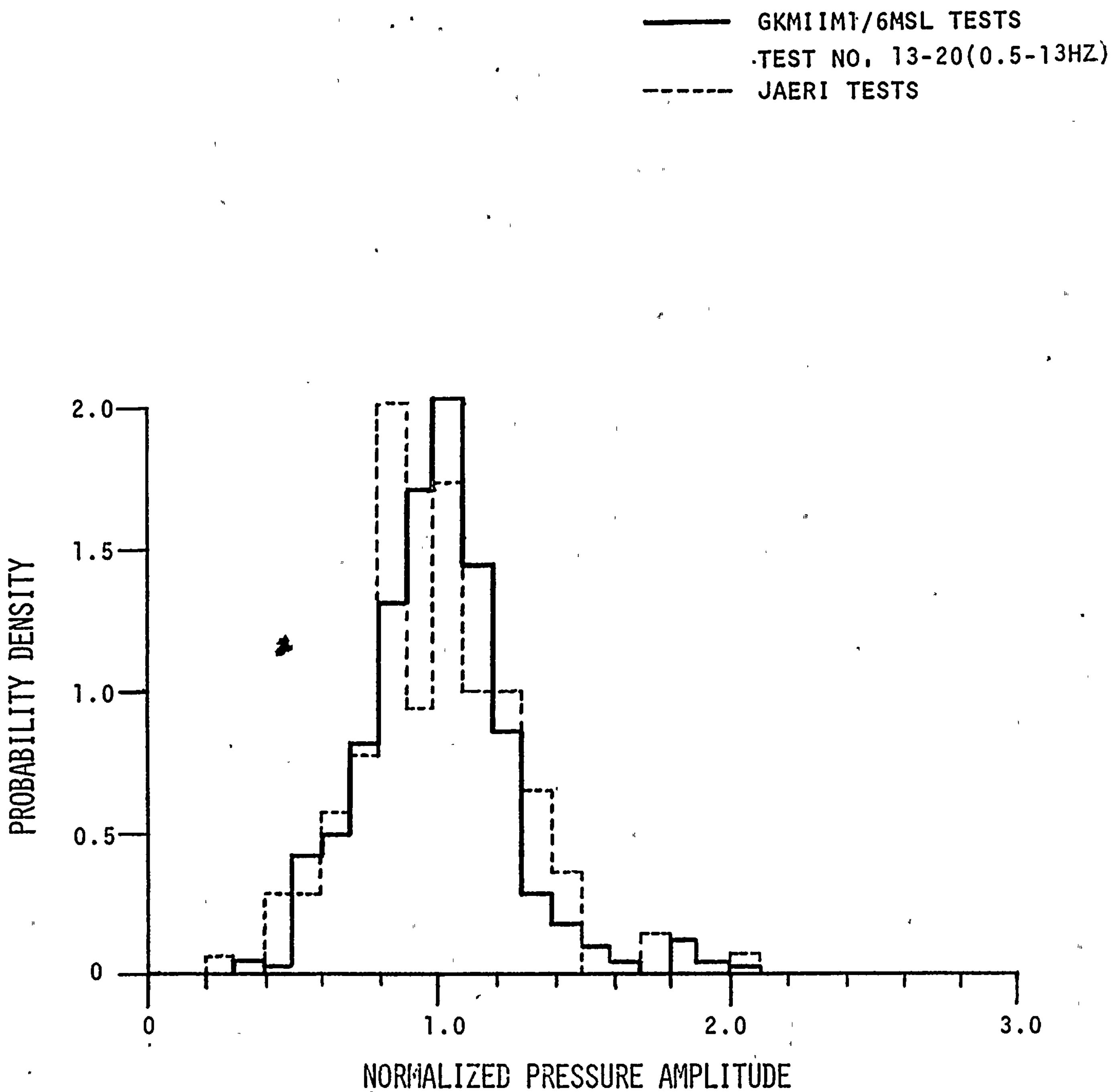

REV. 6, 4/82

SUSQUEHANNA STEAM ELECTRIC STATION
UNITS 1 AND 2
DESIGN ASSESSMENT REPORT

COMPARISON OF PROBABILITY DENSITY OF THE NORMALIZED PRESSURE AMPLITUDES FORM GKMII-M TESTS 13..20 &JAERI

FIGURE 10-17

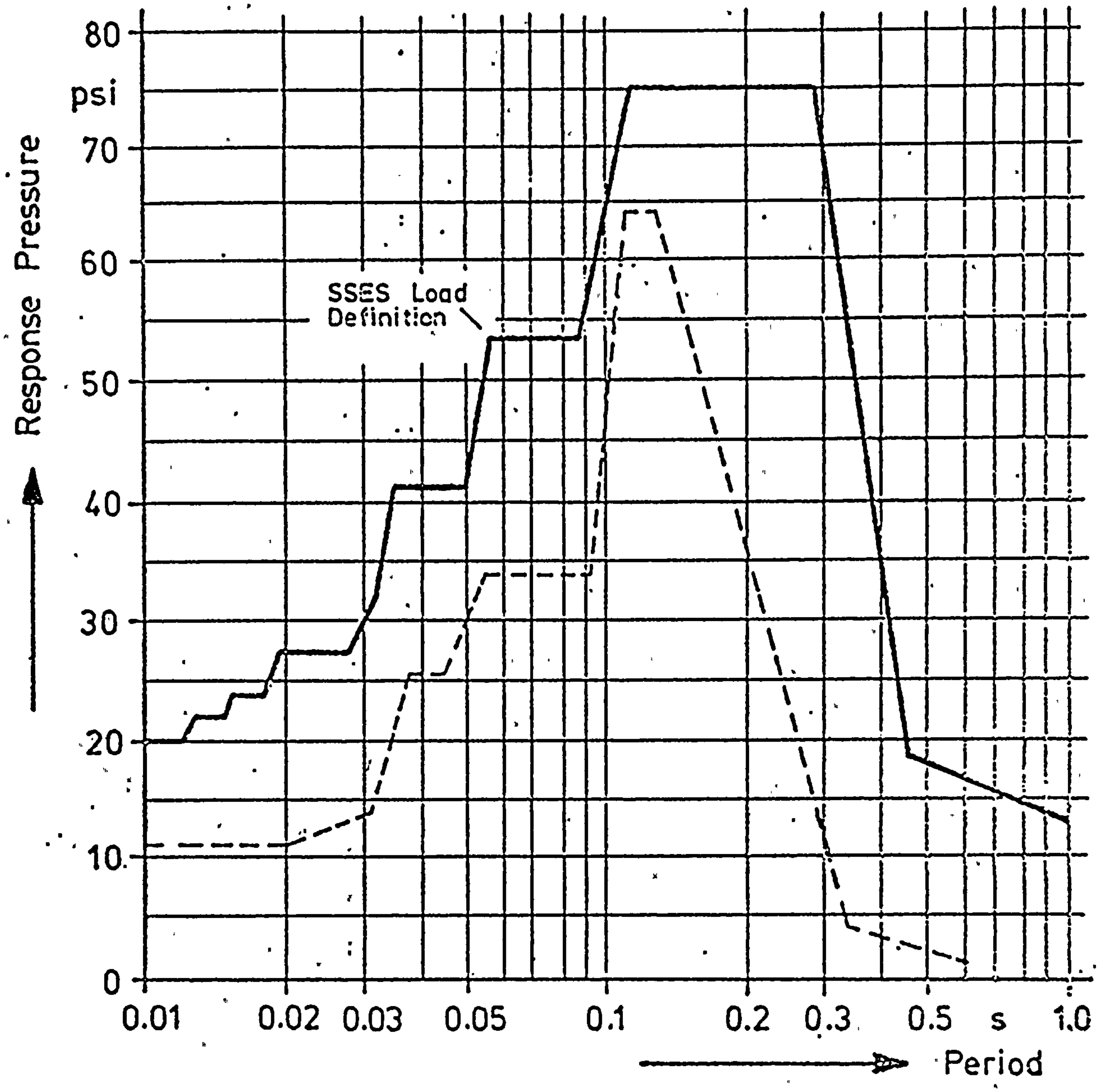

REV. 6, 4/82

SUSQUEHANNA STEAM ELECTRIC STATION
UNITS 1 AND 2
DESIGN ASSESSMENT REPORT

COMPARISON OF PRESSURE RESPONSE SPECTRA OF TEST 21.2 -ALL VALVE CASE-AND THE SSES LOAD DEFINITION

FIGURE 10-18

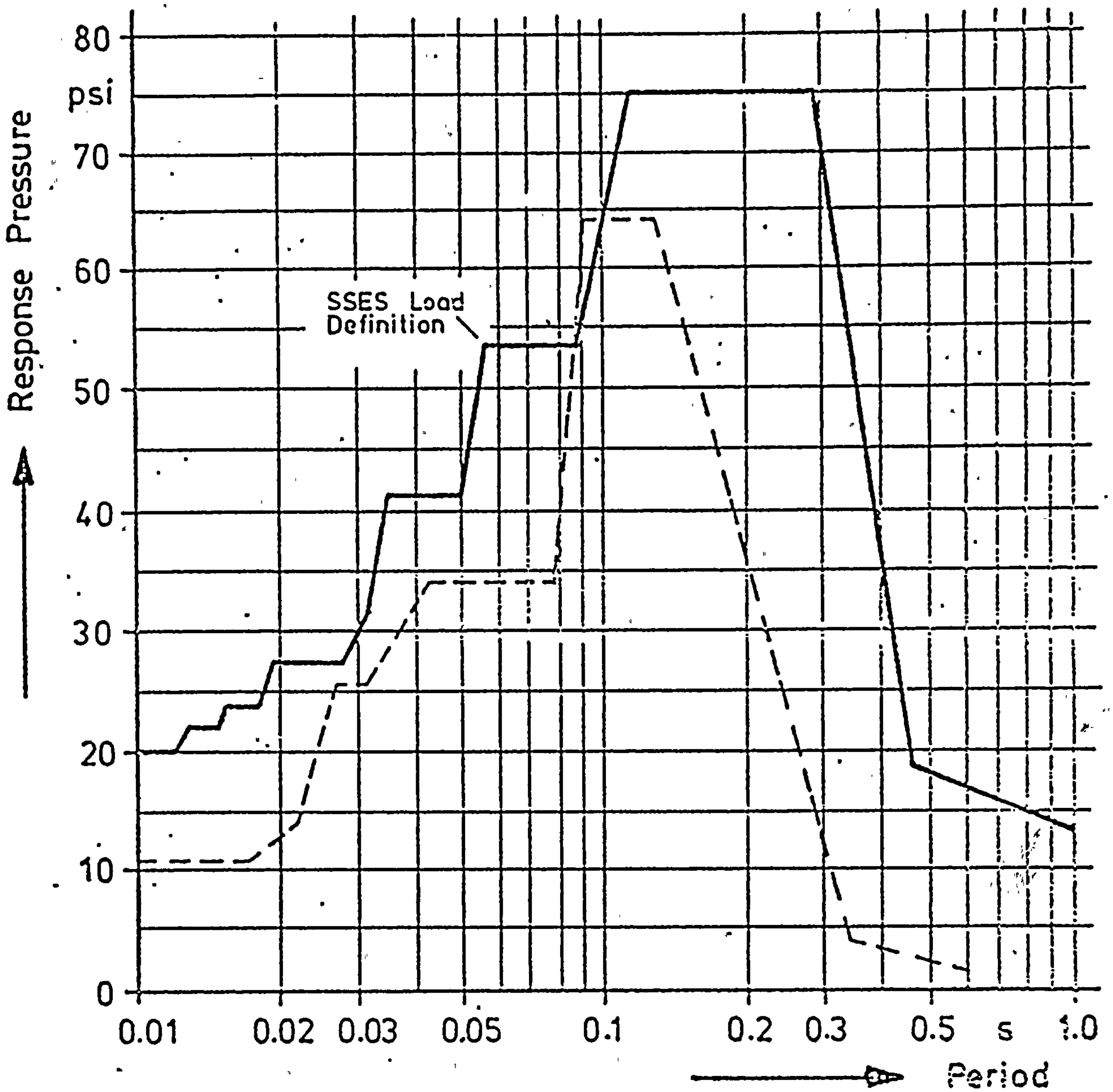

REV. 6, 4/82

SUSQUEHANNA STEAM ELECTRIC STATION
UNITS 1 AND 2
DESIGN ASSESSMENT REPORT

COMPARISON OF PRESSURE RESPONSE SPECTRE OF TEST 21.2 ALL VALVE CASE AND ONE VALVE CASE AND THE SSES LOAD DEFINITION

FIGURE 10-19

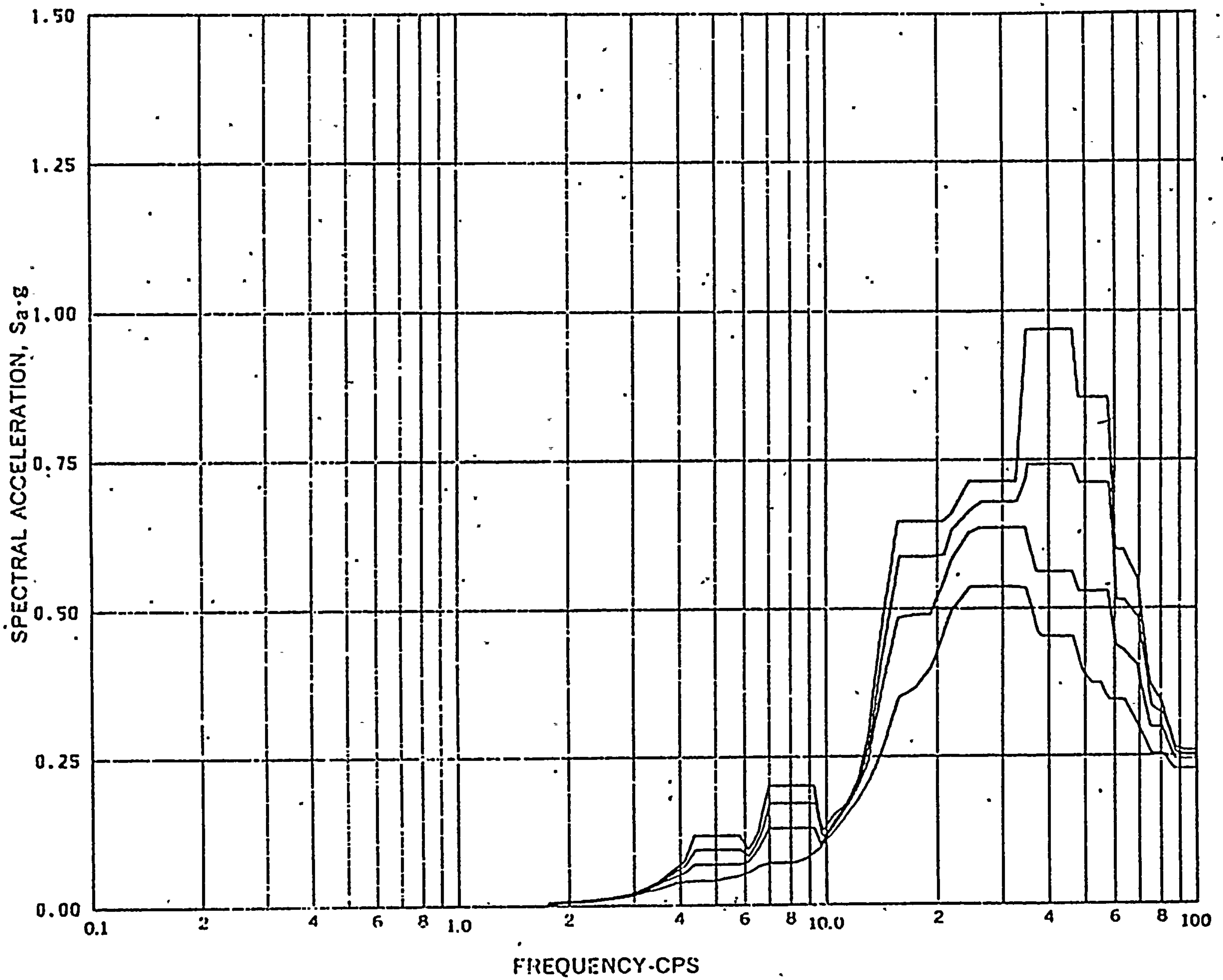

Acceleration Spectra for CONTAINMENT SHELL

Load Case: Susquehanna KWU-SRV #76 ASYMM.

Node 131, Direction X, Elev 672'-0"

Damping: 0.005, 0.01, 0.02, 0.05

REV. 6, 4/82

SUSQUEHANNA STEAM ELECTRIC STATION
UNITS 1 AND 2
DESIGN ASSESSMENT REPORT

SSES CONTAINMENT RESPONSE SPECTRA KWU SRV # 76 ASYMMETRIC - DIRECTION HORIZONTAL

FIGURE 10-20

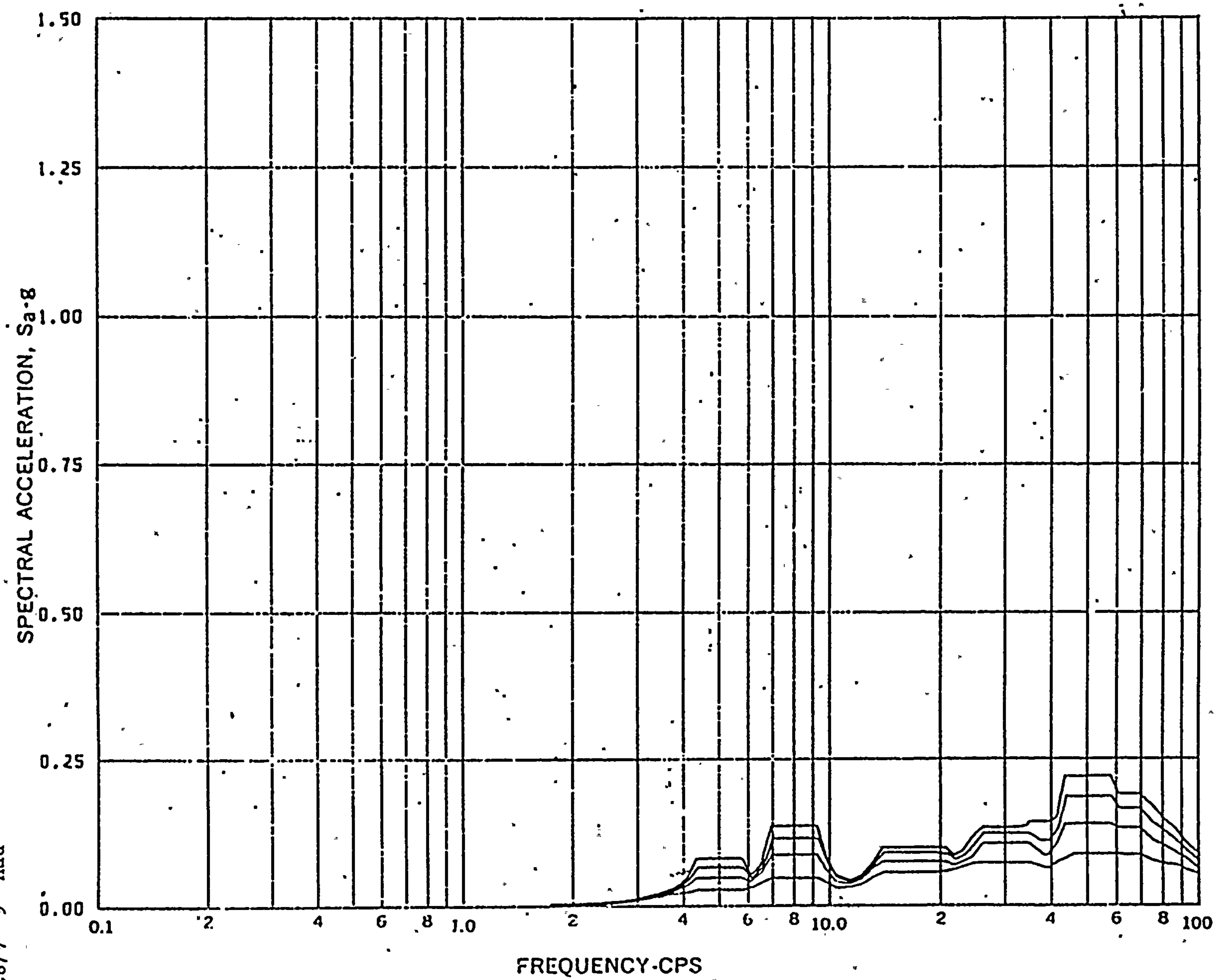

Acceleration Spectra for CONTAINMENT SHELL

Load Case: Susquehanna KWU-SRV #76 ASYMM.

Node 131, Direction Z, Elev 672'-0"

Damping: 0.005, 0.01, 0.02, 0.05

REV. 6, 4/82

SUSQUEHANNA STEAM ELECTRIC STATION
UNITS 1 AND 2
DESIGN ASSESSMENT REPORT

SSES CONTAINMENT RESPONSE
SPECTRA KWU SRV #76 -
ASYMMETRIC- DIRECTION
VERTICAL

FIGURE 10-21

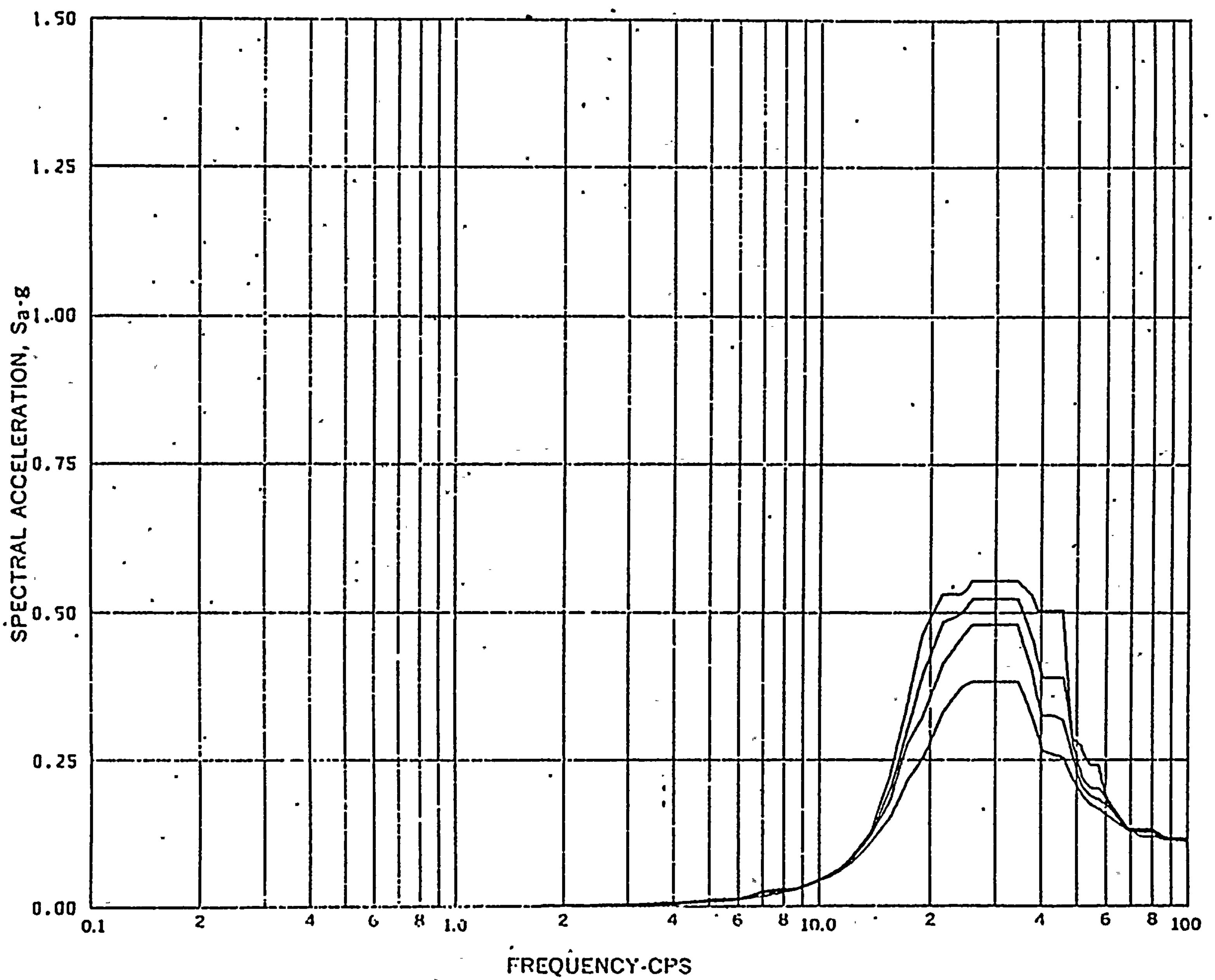

Acceleration Spectra for CONTAINMENT SHELL

Load Case: Susquehanna KWU-SRV #76 ASYMM.

Node 135, Direction Y, Elev 672'-0"

Damping: 0.005, 0.01, 0.02, 0.05

REV. 6, 4/82

SUSQUEHANNA STEAM ELECTRIC STATION
UNITS 1 AND 2
DESIGN ASSESSMENT REPORT

SSES CONTAINMENT RESPONSE
SPECTRA KWU SRV #76
ASYMMETRIC - DIRECTION
HORIZONTAL

FIGURE 10-22

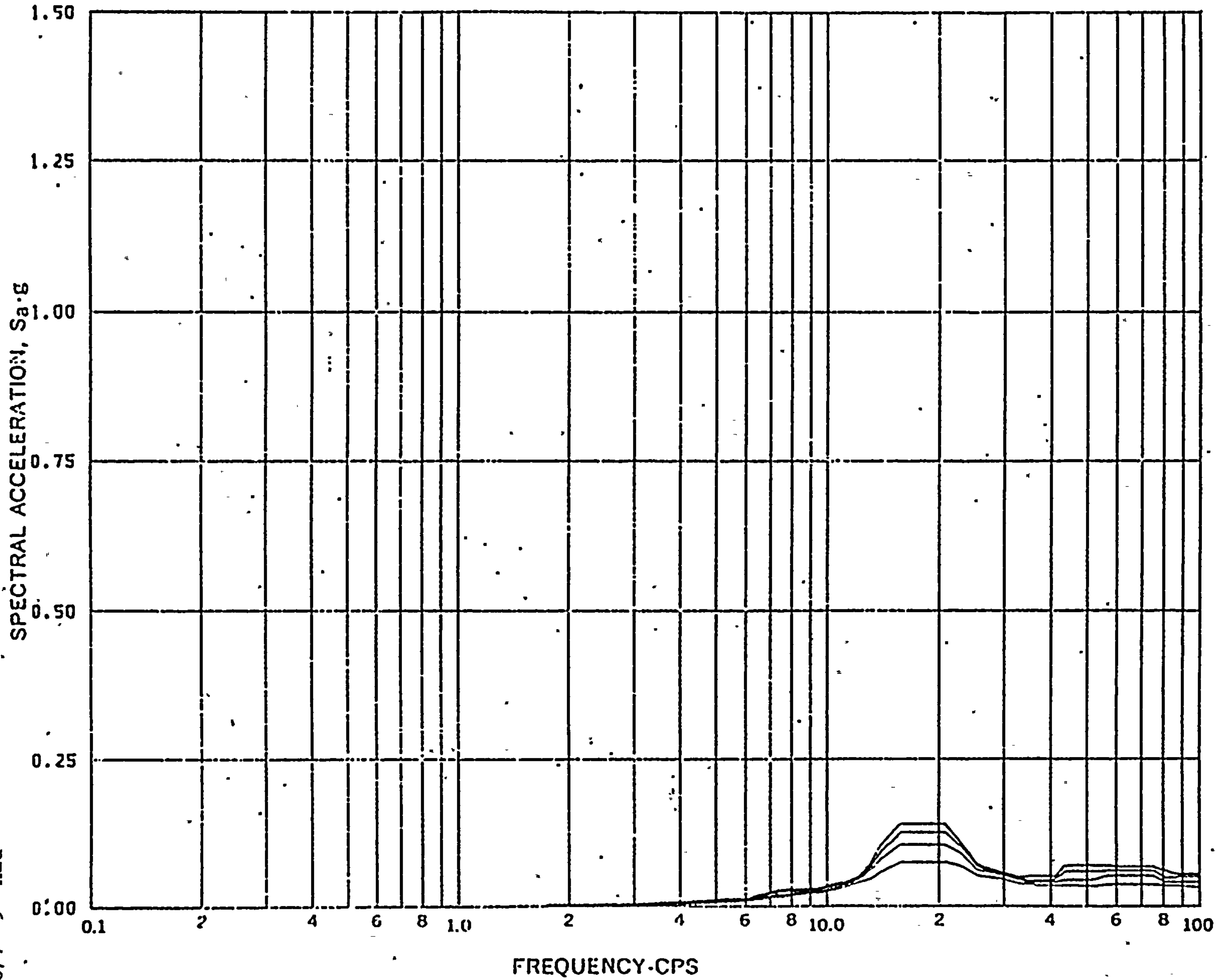

Acceleration Spectra for CONTAINMENT SHELL

Load Case: Susquehanna KWU-SRV #76 ASYMM.

Node 135, Direction Z, Elev 672'-0"

Damping: 0.005, 0.01, 0.02, 0.05

REV. 6, 4/82

SUSQUEHANNA STEAM ELECTRIC STATION
UNITS 1 AND 2
DESIGN ASSESSMENT REPORT

SSES CONTAINMENT RESPONSE
SPECTRA KWU SRV #76
ASYMMETRIC - DIRECTION
VERTICAL

FIGURE 10-23

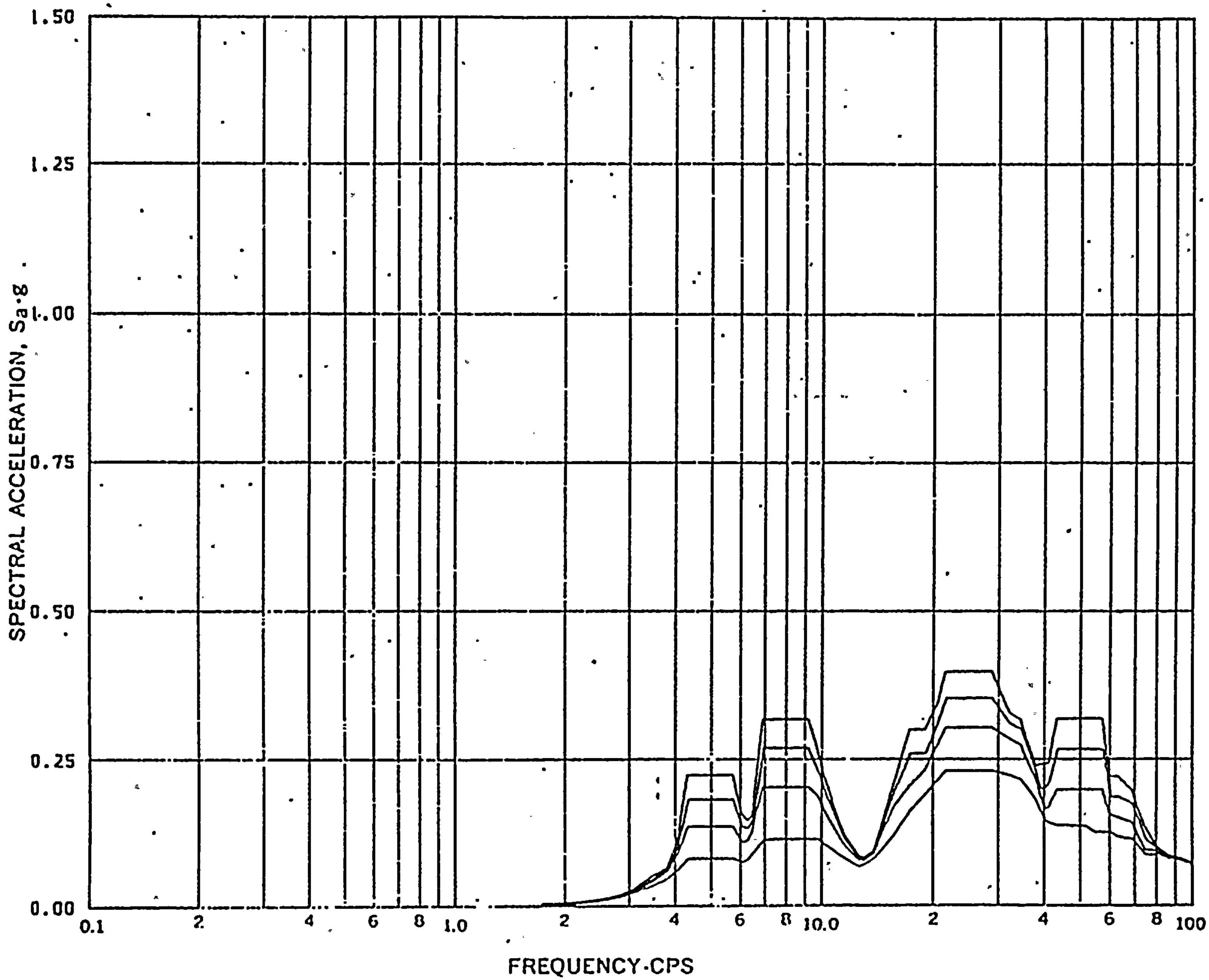

Acceleration Spectra for PEDESTAL

Load Case: Susquehanna KWU-SRV #76 ASYMM.

Node 211, Direction X, Elev 702'-3"

Damping: 0.005, 0.01, 0.02, 0.05

REV. 6, 4/82

SUSQUEHANNA STEAM ELECTRIC STATION
UNITS 1 AND 2
DESIGN ASSESSMENT REPORT

SSES CONTAINMENT RESPONSE SPECTRA KWU SRV # 76 ASYMMETRIC - DIRECTION HORIZONTAL

FIGURE 10-24

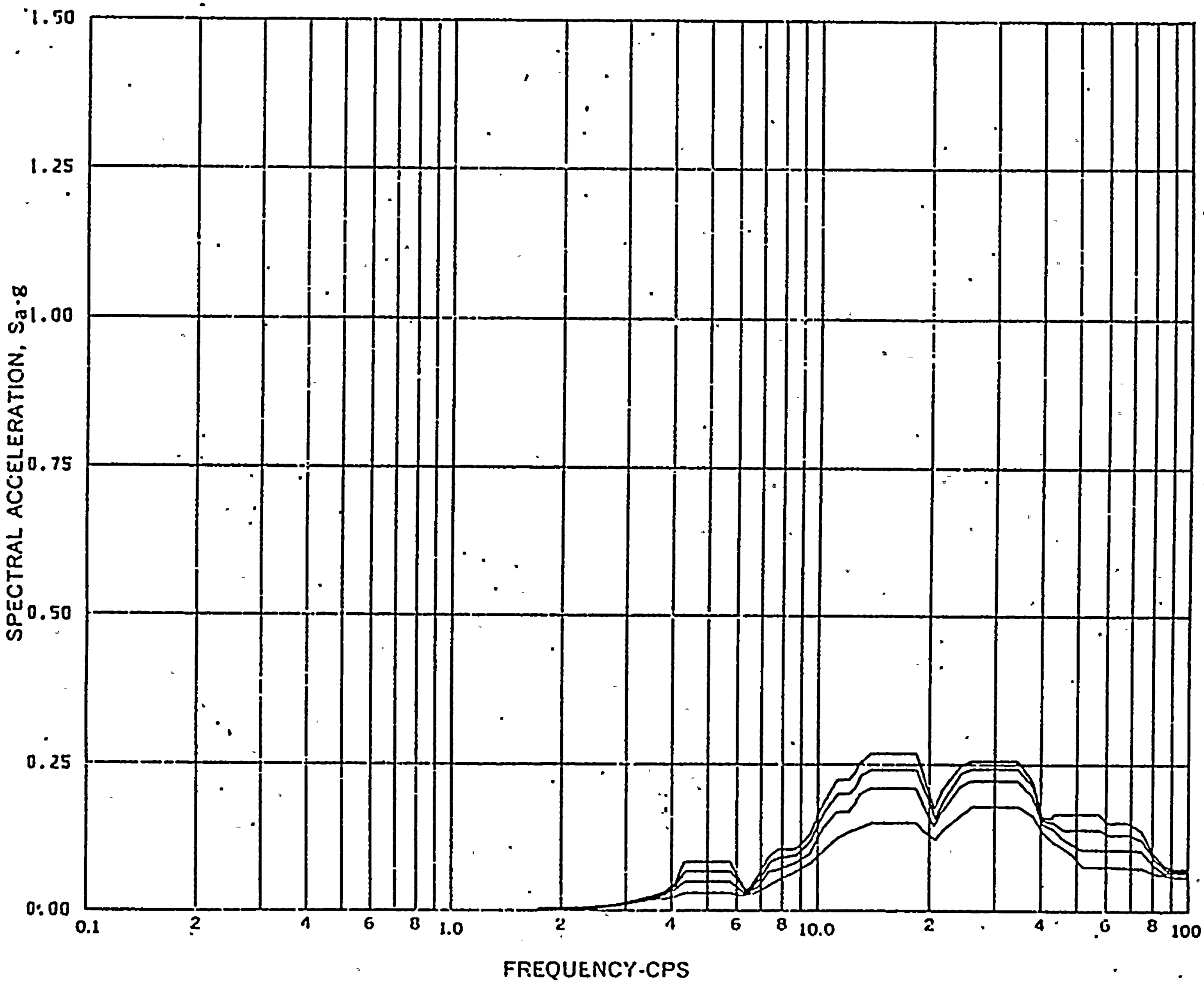

Acceleration Spectra for PEDESTAL

Load Case: Susquehanna KWU-SRV #76 ASYMM.

Node 211, Direction Z, Elev 702'-3"

Damping: 0.005, 0.01, 0.02, 0.05

REV. 6, 4/82

SUSQUEHANNA STEAM ELECTRIC STATION
UNITS 1 AND 2
DESIGN ASSESSMENT REPORT

SSES CONTAINMENT RESPONSE
SPECTRA KWU SRV #76
ASYMMETRIC - DIRECTION
VERTICAL

FIGURE 10-25

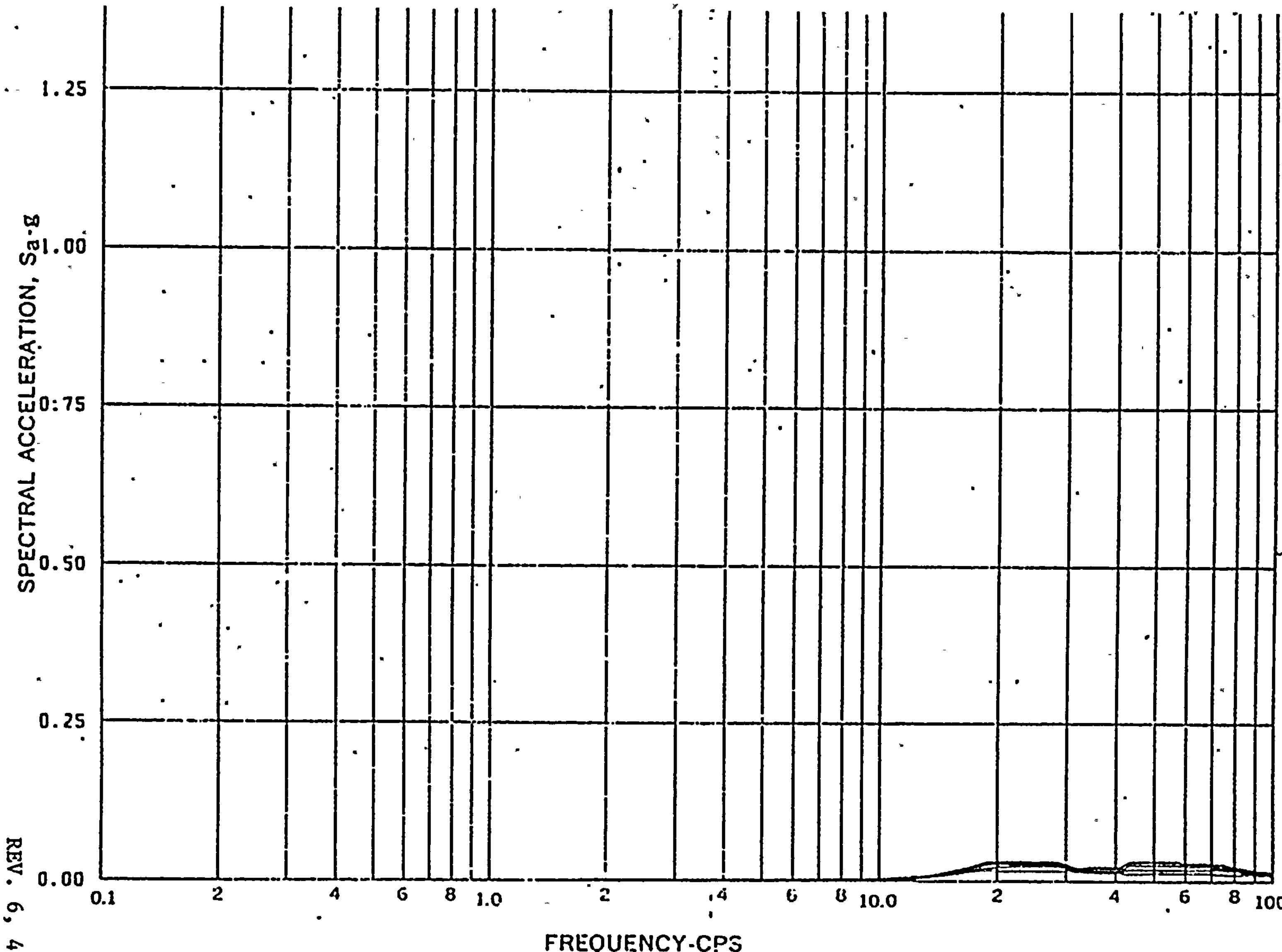

Acceleration Spectra for PEDESTAL

Load Case: Susquehanna KWU-SRV #76 ASYMM.

Node 215, Direction Y, Elev 702'-3"

Damping: 0.005, 0.01, 0.02, 0.05

REV. 6, 4/82

SUSQUEHANNA STEAM ELECTRIC STATION
UNITS 1 AND 2
DESIGN ASSESSMENT REPORT

SSES CONTAINMENT RESPONSE SPECTRA - KWU SRV #76 ASYMMETRIC - DIRECTION HORIZONTAL

FIGURE 10-26

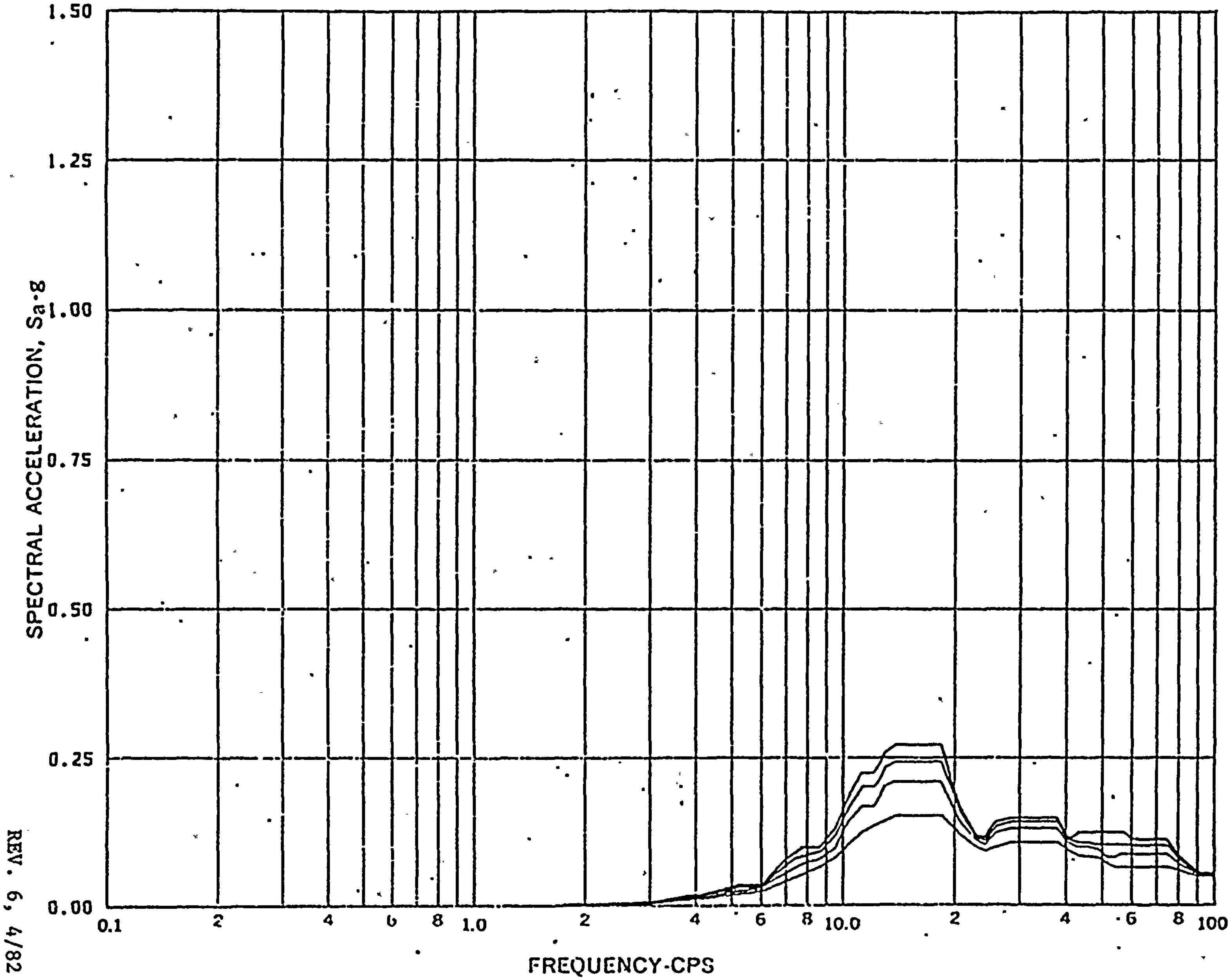

Acceleration Spectra for PEDESTAL

Load Case: Susquehanna KWU-SRV #76 ASYMM.

Node 215, Direction Z, Elev 702'-3"

Damping: 0.005, 0.01, 0.02, 0.05

REV. 6, 4/82

SUSQUEHANNA STEAM ELECTRIC STATION
UNITS 1 AND 2
DESIGN ASSESSMENT REPORT

SSES CONTAINMENT RESPONSE
SPECTRA KWU SRV #76
ASYMMETRIC - DIRECTION
VERTICAL

FIGURE 10-27

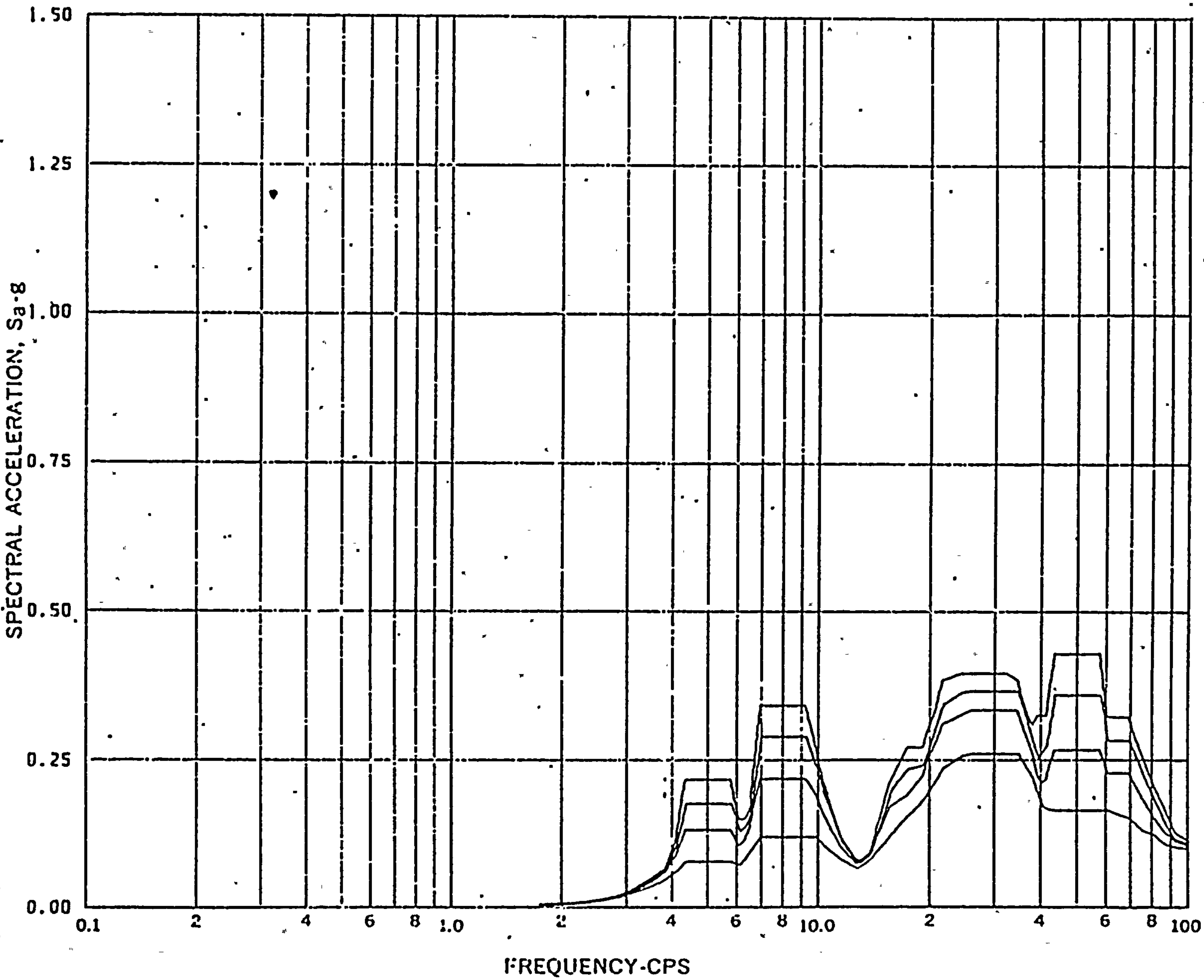

Acceleration Spectra for CONTAINMENT SHELL

Load Case: Susquehanna KWU-SRV #76 ASYMM.

Node 291, Direction X, Elev 702'-3"

Damping: 0.005, 0.01, 0.02, 0.05

REV. 6, 4/82

SUSQUEHANNA STEAM ELECTRIC STATION
UNITS 1 AND 2
DESIGN ASSESSMENT REPORT

SSES CONTAINMENT RESPONSE
SPECTRA -KWU SRV #76
ASYMMETRIC - DIRECTION
· HORIZONTAL

FIGURE 10-28

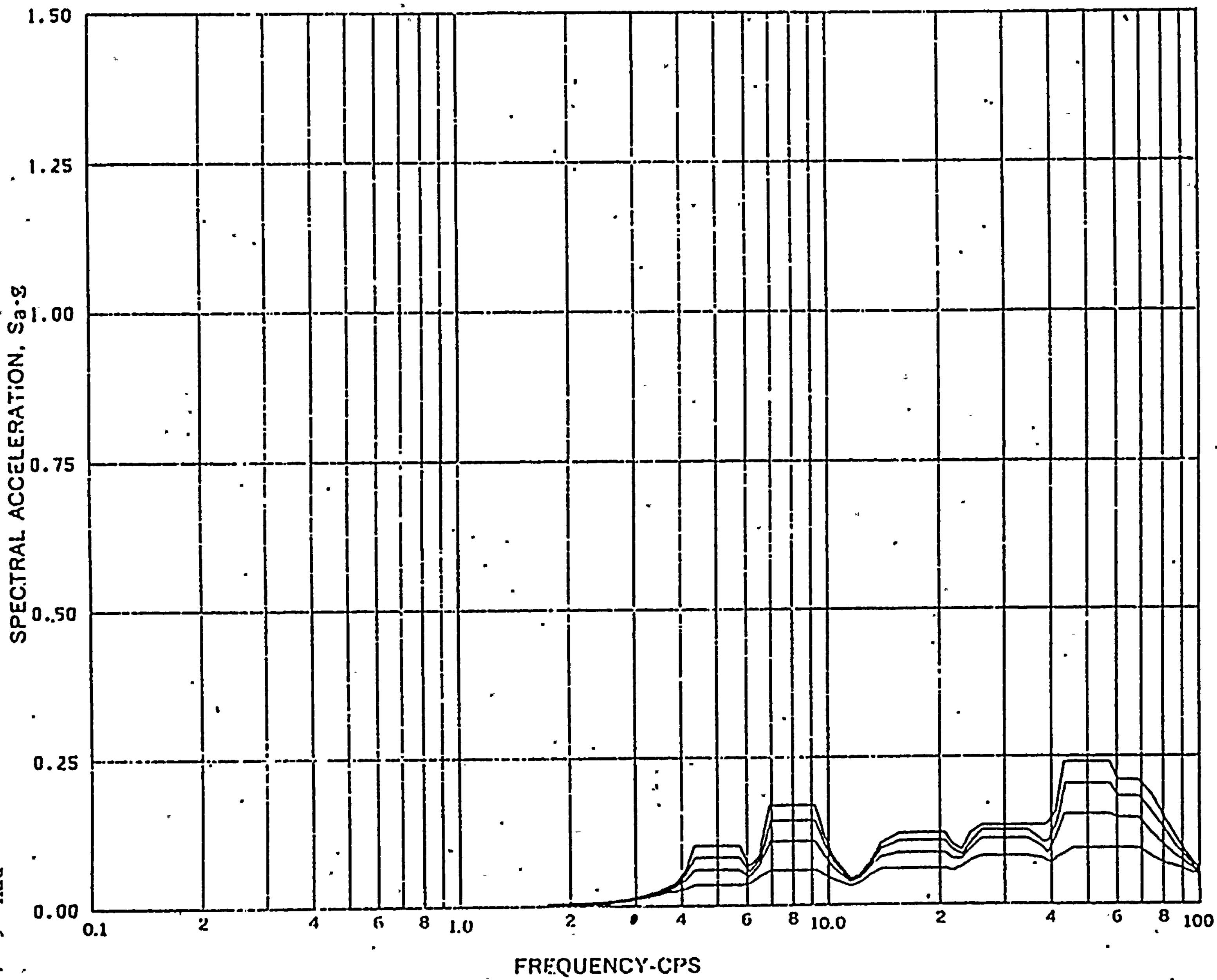

Acceleration Spectra for CONTAINMENT SHELL

Load Case: Susqushanna KWU-SRV #76 ASYMM.

Node 291, Direction Z, Elev 702'-3"

Damping: 0.005, 0.01, 0.02, 0.05

REV. 6, 4/82

SUSQUEHANNA STEAM ELECTRIC STATION
UNITS 1 AND 2
DESIGN ASSESSMENT REPORT

SSES CONTAINMENT RESPONSE SPECTRA - KWU SRV #76 ASYMMETRIC -DIRECTION VERTICAL

FIGURE 10-29

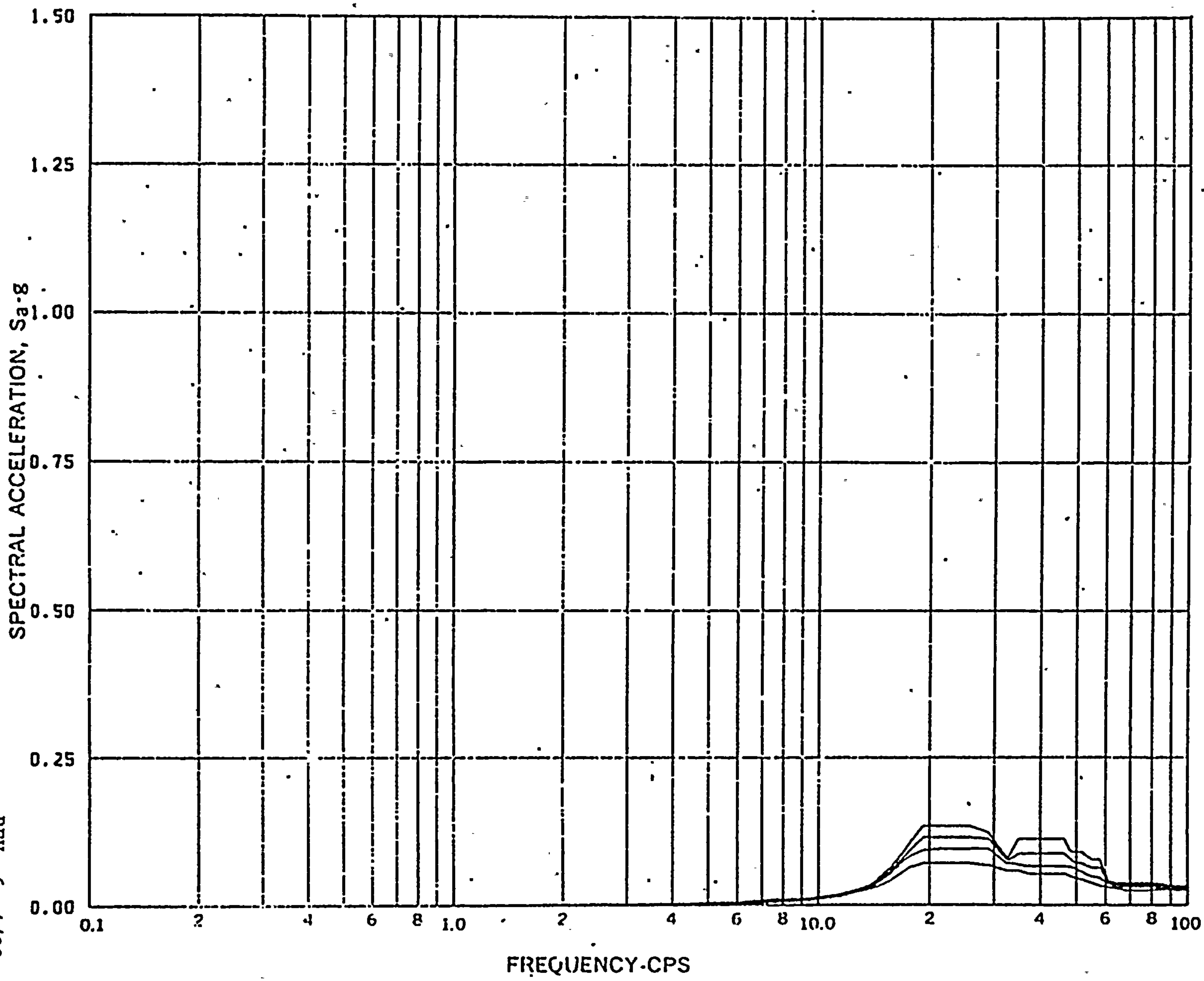

Acceleration Spectra for CONTAINMENT SHELL

Load Case: Susquehanna KWU-SRV #76 ASYMM.

Node 295, Direction Y, Elev 702'-3"

Damping: 0.005, 0.01, 0.02, 0.05

REV. 6, 4/82

SUSQUEHANNA STEAM ELECTRIC STATION
UNITS 1 AND 2
DESIGN ASSESSMENT REPORT

SSES CONTAINMENT RESPONSE SPECTRA- KWU SRV #76 ASYMMETRIC - DIRECTION HORIZONTAL

FIGURE 10-30

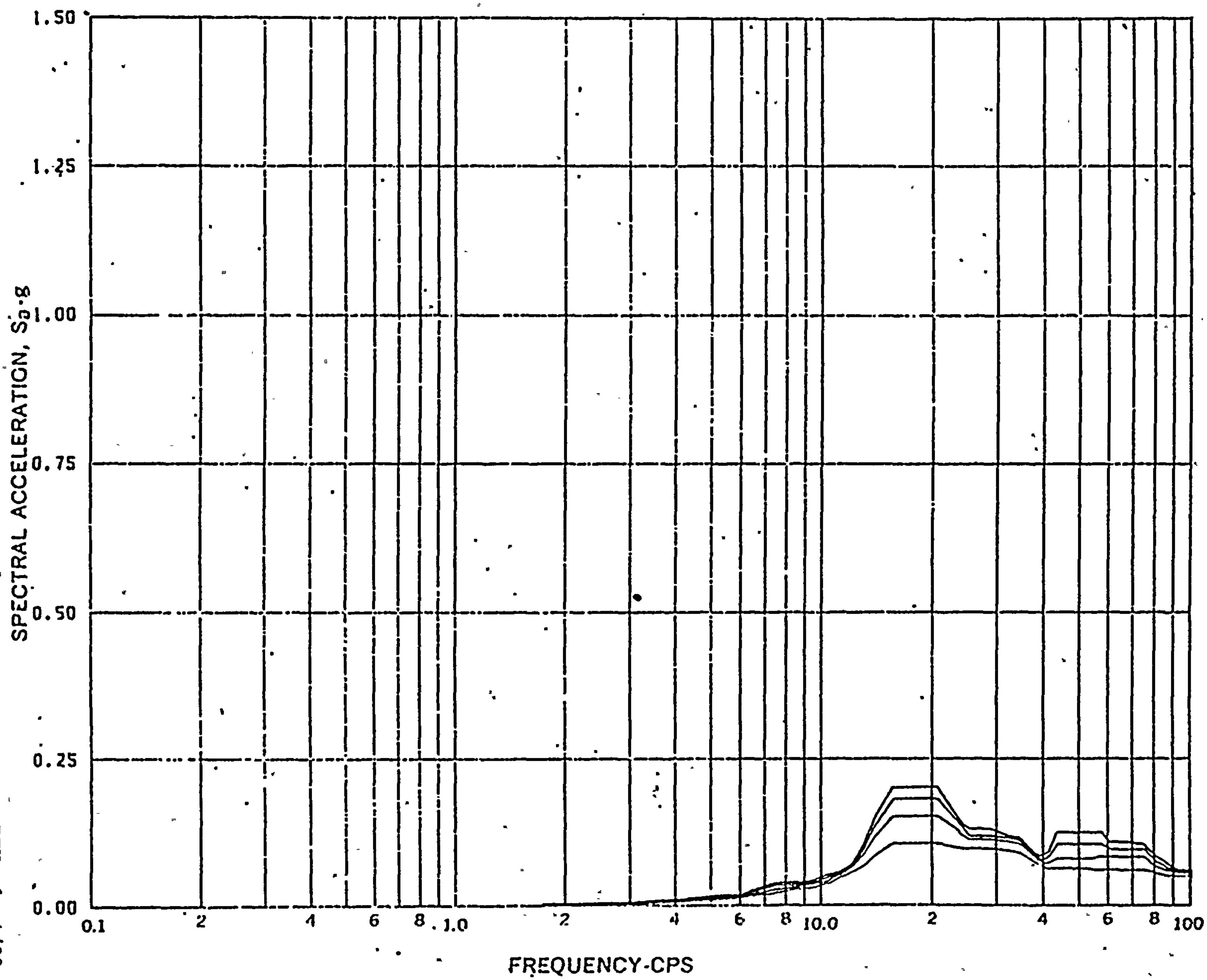

Acceleration Spectra for CONTAINMENT SHELL

Load Case: Susquehanna KWU-SRV #76 ASYMM.

Node 295, Direction Z, Elev 702'-3"

Damping: 0.005, 0.01, 0.02, 0.05

REV. 6, 4/82

SUSQUEHANNA STEAM ELECTRIC STATION
UNITS 1 AND 2
DESIGN ASSESSMENT REPORT

SSES CONTAINMENT RESPONSE
SPECTRA - KWU SRV #76
ASYMMETRIC - DIRECTION
VERTICAL

FIGURE 10-31

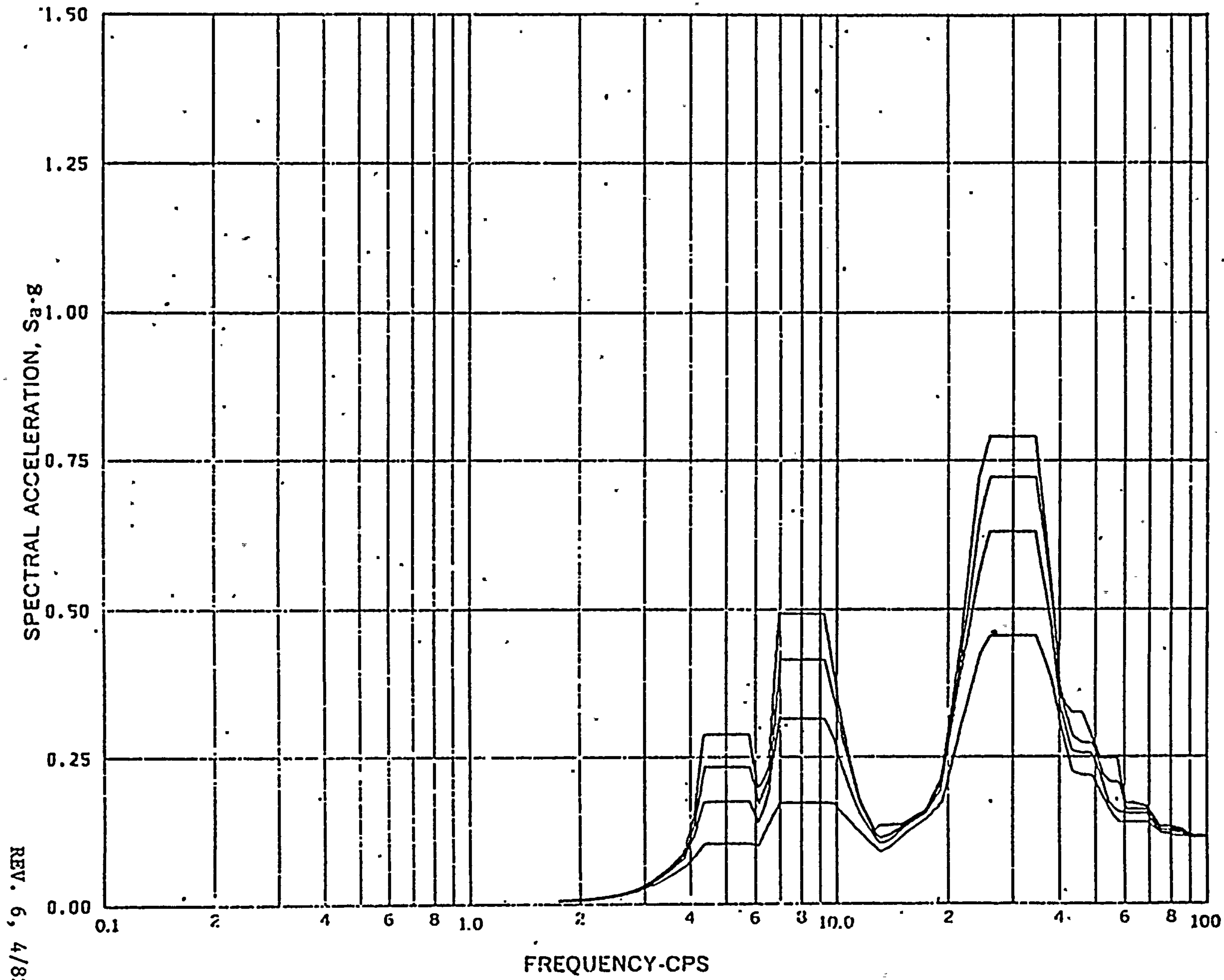

Acceleration Spectra for CONTAINMENT SHELL

Load Case: SusquehannaKWU-SRV #76 ASYMM.

Node 331, Direction X, Elev 730'-8-1/2"

Damping: 0.005, 0.01, 0.02, 0.05

REV. 6, 4/82

SUSQUEHANNA STEAM ELECTRIC STATION
UNITS 1 AND 2
DESIGN ASSESSMENT REPORT

SSES CONTAINMENT RESPONSE
SPECTRA - KWU SRV #76
ASYMMETRIC - DIRECTION
HORIZONTAL

FIGURE 10-32

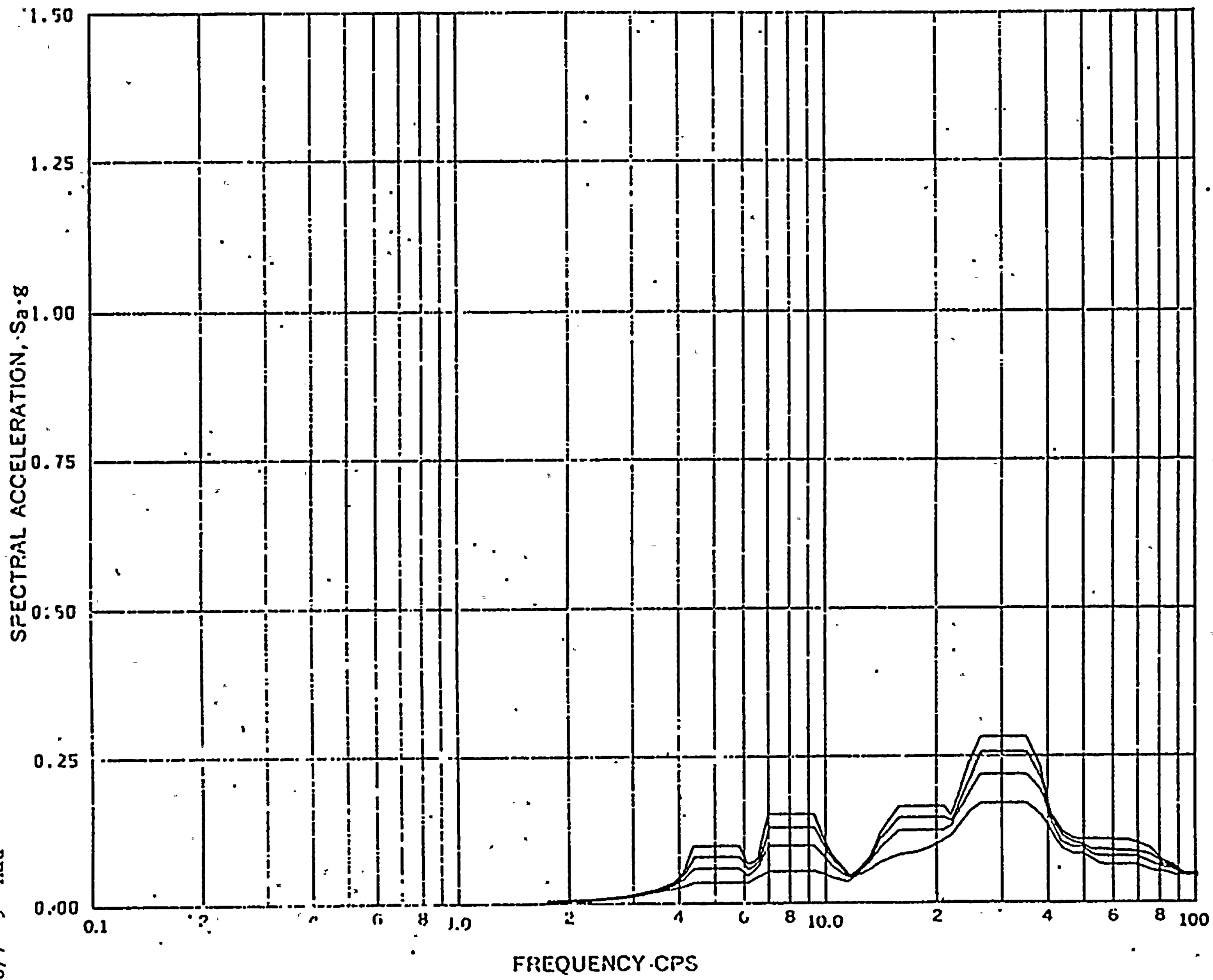

Acceleration Spectra for CONTAINMENT SHELL

Load Case: Susquehanna KWU-SRV #76 ASYMM.

Node 331, Direction Z, Elev 730'-8-1/2"

Damping: 0.005, 0.01, 0.02, 0.05

REV. 6, 4/82

SUSQUEHANNA STEAM ELECTRIC STATION
UNITS 1 AND 2
DESIGN ASSESSMENT REPORT

SSES CONTAINMENT RESPONSE SPECTRA - KWU SRV #76 ASYMMETRIC - DIRECTION VERTICAL

FIGURE 10-33

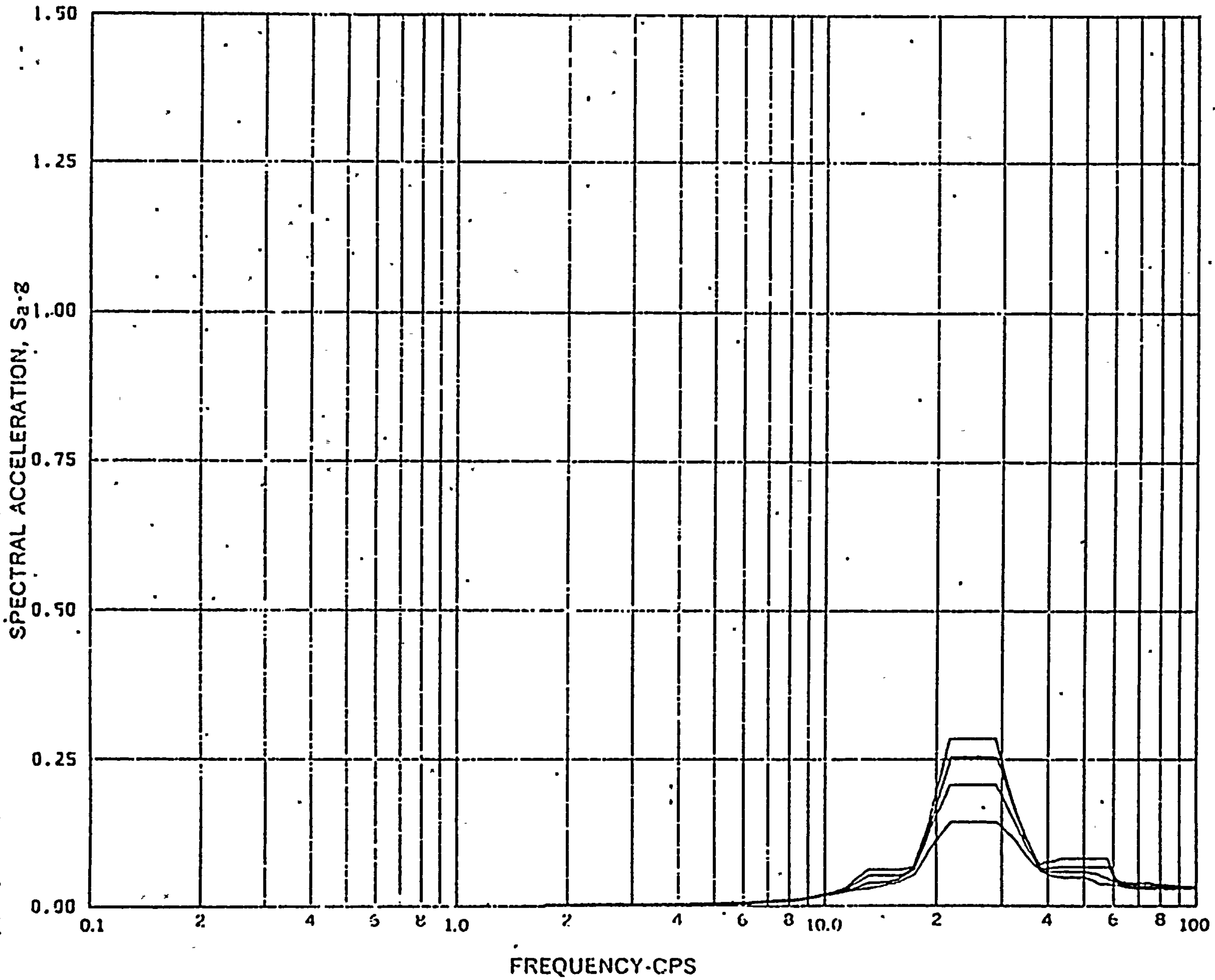

Acceleration Spectra for CONTAINMENT SHELL

Load Case: Susquehanna KWU-SRV #76 ASYMM.

Node 335, Direction Y, Elev 730'-8-1/2"

Damping: 0.005, 0.01, 0.02, 0.05

REV. 6, 4/82

SUSQUEHANNA STEAM ELECTRIC STATION
UNITS 1 AND 2
DESIGN ASSESSMENT REPORT

SSES CONTAINMENT RESPONSE
SPECTRA - KWU SRV #76
ASYMMETRIC - DIRECTION
HORIZONTAL

FIGURE 10-34

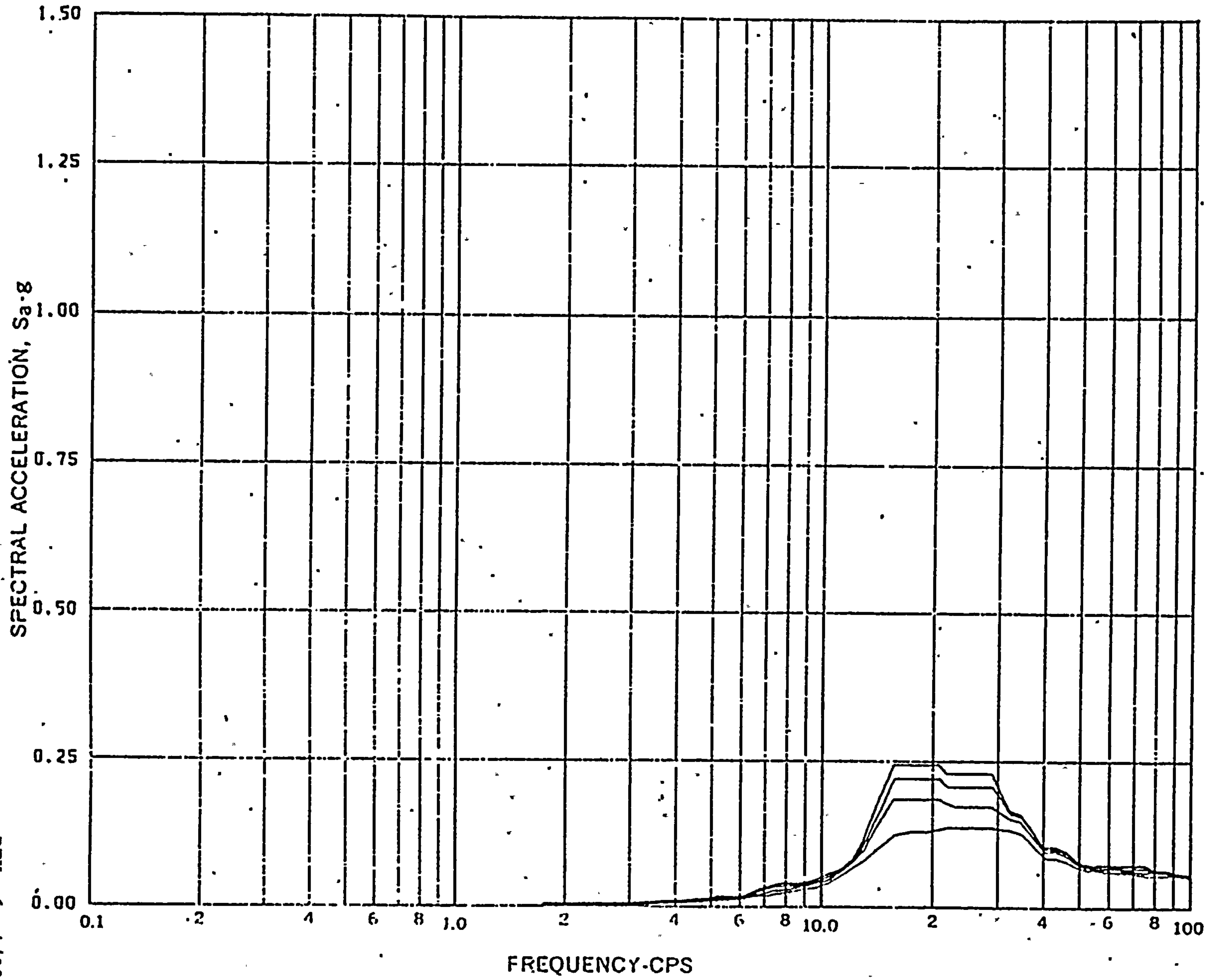

Acceleration Spectra for CONTAINMENT SHELL

Load Case: Susquehanna KWU-SRV #76 ASYMM.

Node 335, Direction Z, Elev 740'-8-1/2"

Damping: 0.005, 0.01, 0.02, 0.05

REV. 6, 4/82

SUSQUEHANNA STEAM ELECTRIC STATION
UNITS 1 AND 2
DESIGN ASSESSMENT REPORT

SSES CONTAINMENT RESPONSE SPECTRA - KWU SRV #76 ASYMMETRIC - DIRECTION VERTICAL

FIGURE 10-35

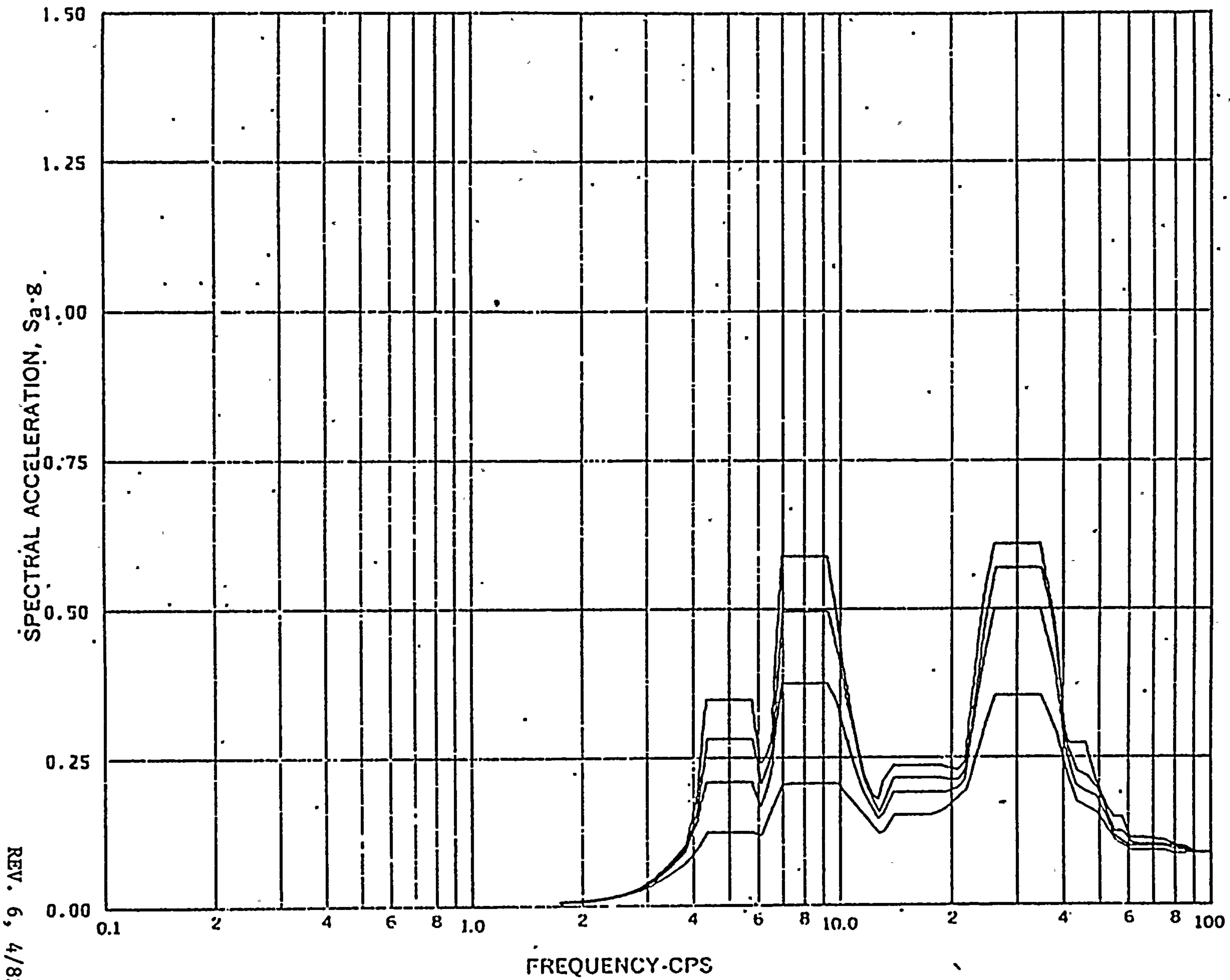

Acceleration Spectra for CONTAINMENT SHELL

Load Case: Susquehanna KWU-SRV #76 ASYMM.

Node 371, Direction X, Elev 750'-1-1/2"

Damping: 0.005, 0.01, 0.02, 0.05

REV. 6, 4/82

SUSQUEHANNA STEAM ELECTRIC STATION
UNITS 1 AND 2
DESIGN ASSESSMENT REPORT

SSES CONTAINMENT RESPONSE
SPECTRA KWU SRV #76
ASYMMETRIC - DIRECTION
HORIZONTAL

FIGURE 10-36

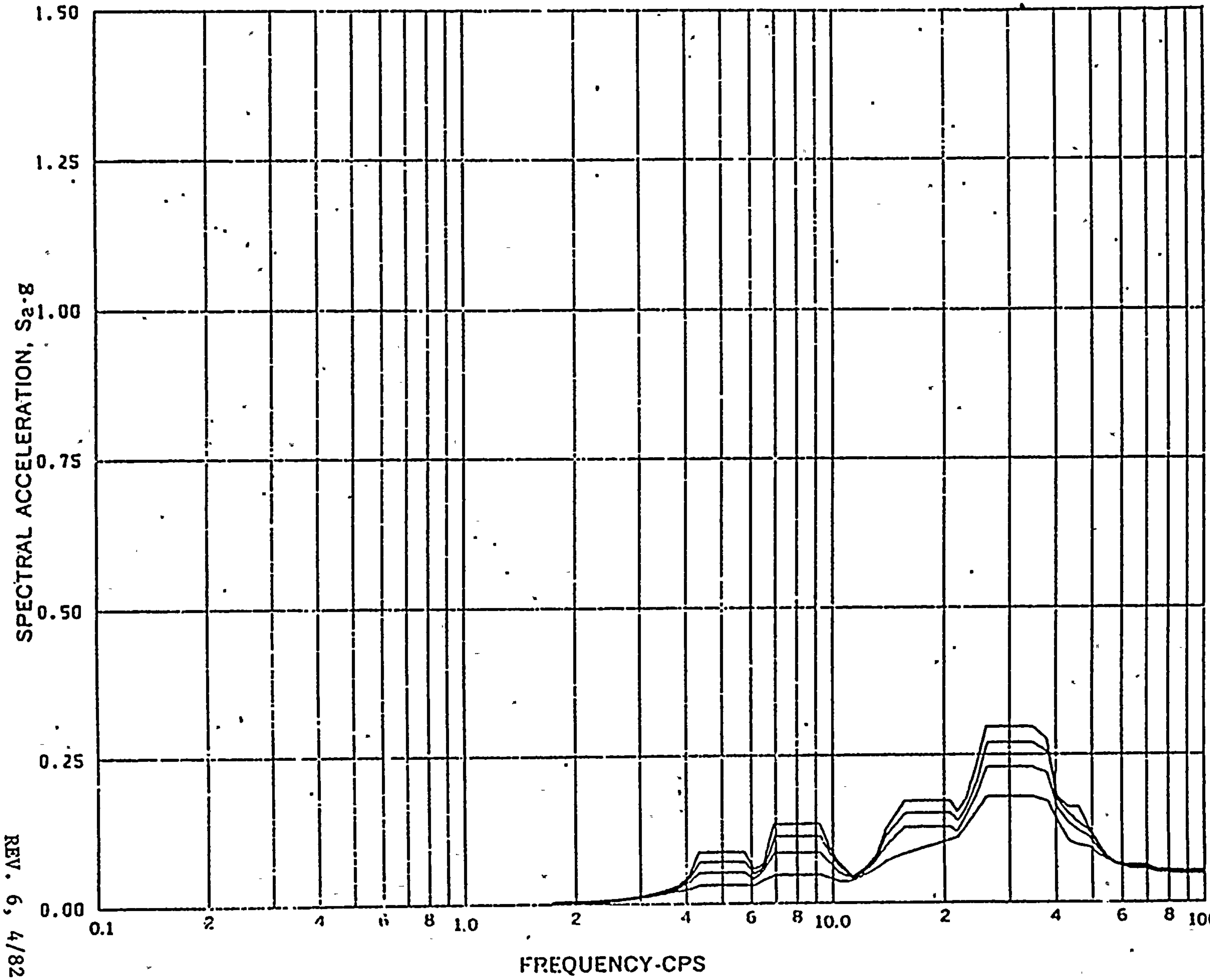

Acceleration Spectra for CONTAINMENT SHELL

Load Case: Susquehanna KWU-SRV #76 ASYMM.

Node 371, Direction Z, Elev 750'-1-1/2"

Damping: 0.005, 0.01, 0.02, 0.05

REV. 6, 4/82

SUSQUEHANNA STEAM ELECTRIC STATION
UNITS 1 AND 2
DESIGN ASSESSMENT REPORT

SSES CONTAINMENT RESPONSE
SPECTRA KWU SRV #76
ASYMMETRIC - DIRECTION
VERTICAL

FIGURE 10-37

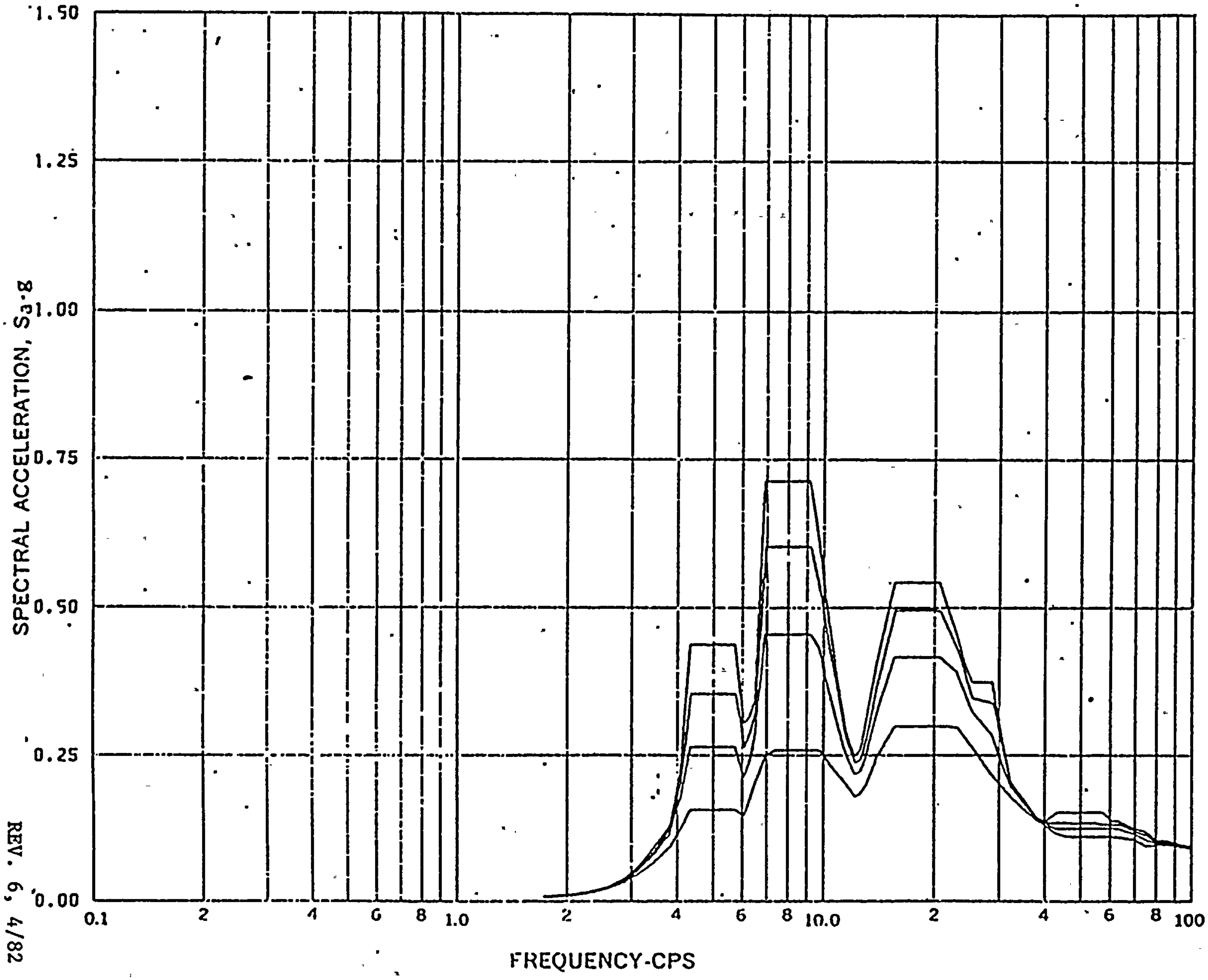

Acceleration Spectra for CONTAINMENT SHELL

Load Case: Susquehanna KWU-SRV #76 ASYMM.

Node 411, Direction X, Elev 778'-9-3/4"

Damping: 0.005, 0.01, 0.02, 0.05

REV. 6, 4/82

SUSQUEHANNA STEAM ELECTRIC STATION
UNITS 1 AND 2
DESIGN ASSESSMENT REPORT

SSES CONTAINMENT RESPONSE SPECTRA KWU SRV #76
ASYMMETRIC - DIRECTION HORIZONTAL

FIGURE 10-38

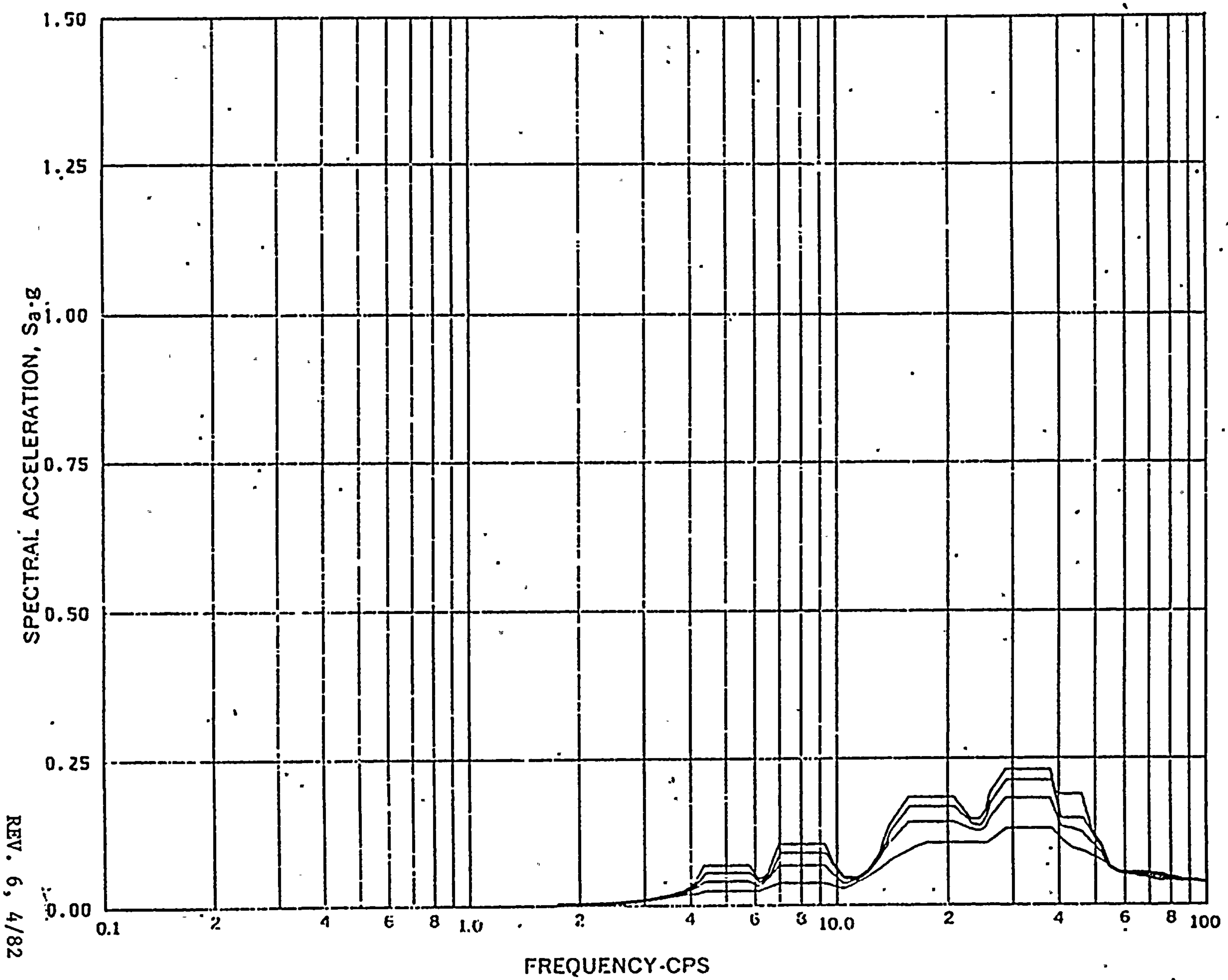

Acceleration Spectra for CONTAINMENT SHELL

Load Case: Susquehanna KWU-SRV #76 ASYMM.

Node 411, Direction Z, Elev 778'-9-3/4"

Damping: 0.005, 0.01, 0.02, 0.05

REV. 6, 4/82

SUSQUEHANNA STEAM ELECTRIC STATION
UNITS 1 AND 2
DESIGN ASSESSMENT REPORT

SSES CONTAINMENT RESPONSE
SPECTRA - KWU SRV # 76
ASYMMETRIC - DIRECTION
VERTICAL

FIGURE 10-39

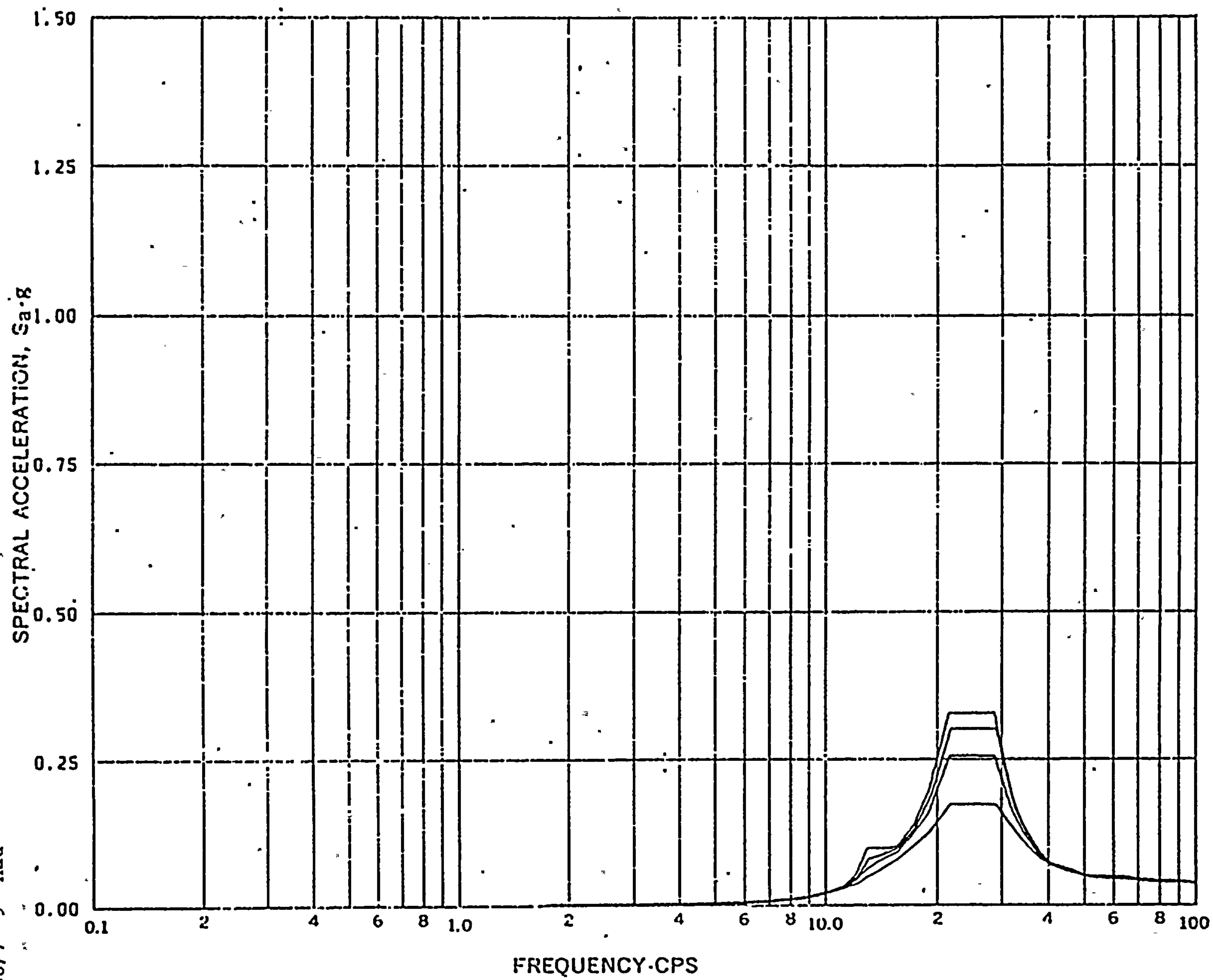

Acceleration Spectra for CONTAINMENT SHELL

Load Case: Susquehanna KWU-SRV #76 ASYMM.

Node 415, Direction Y, Elev 778'-9-3/4"

Damping: 0.005, 0.01, 0.02, 0.05

REV. 6, 4/82

SUSQUEHANNA STEAM ELECTRIC STATION
UNITS 1 AND 2
DESIGN ASSESSMENT REPORT

SSES CONTAINMENT RESPONSE
SPECTRA KWU SRV #76
ASYMMETRIC - DIRECTION
HORIZONTAL

FIGURE 10-40

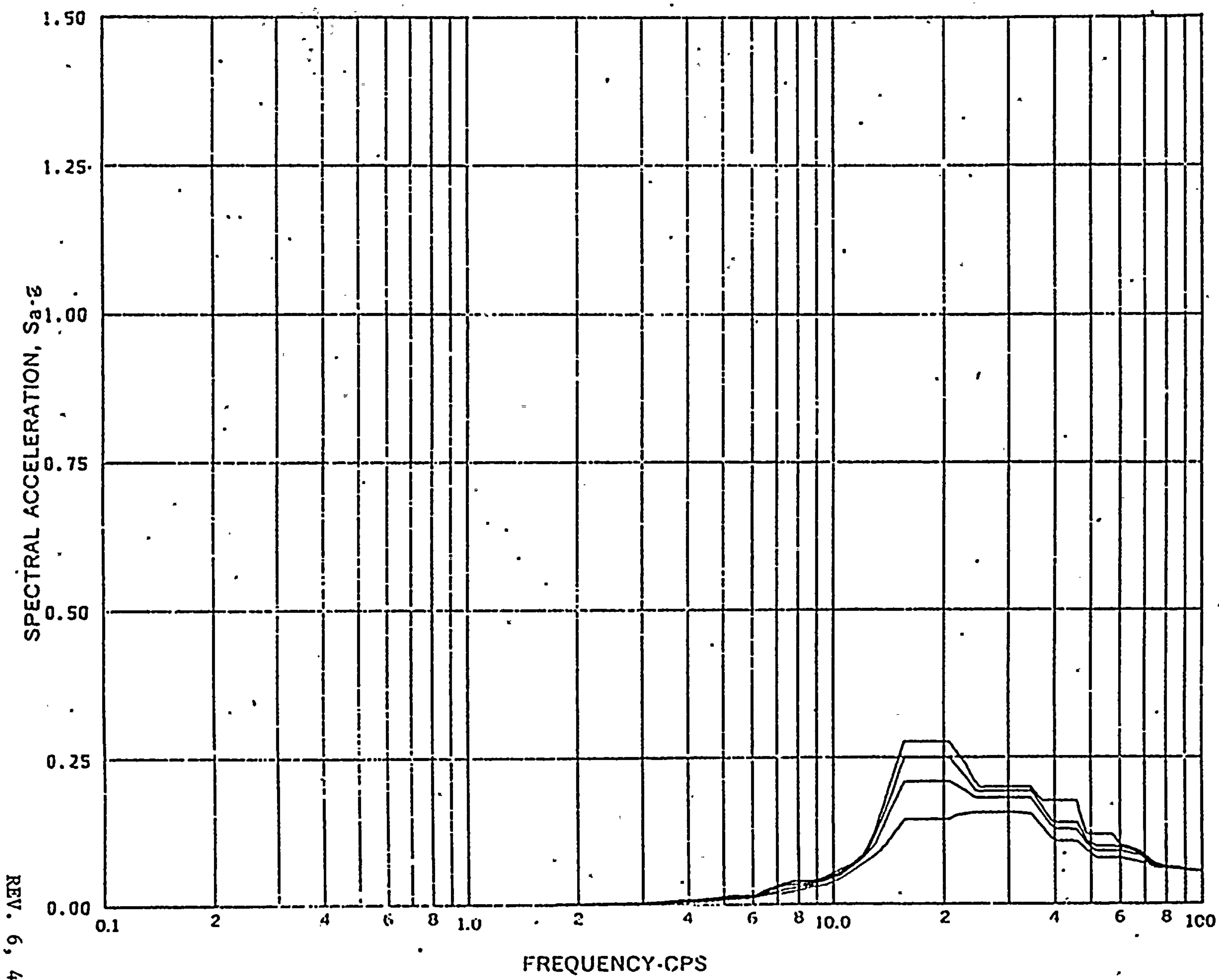

Acceleration Spectra for CONTAINMENT SHELL

Load Case: Susquehanna KWU-SRV #76 ASYMM.

Node 415, Direction Z, Elev 778'-9-3/4"

Damping: 0.005, 0.01, 0.02, 0.05

REV. 6, 4/82

SUSQUEHANNA STEAM ELECTRIC STATION
UNITS 1 AND 2
DESIGN ASSESSMENT REPORT

SSES CONTAINMENT RESPONSE SPECTRA KWU SRV #76 ASYMMETRIC - DIRECTION VERTICAL

FIGURE 10-41

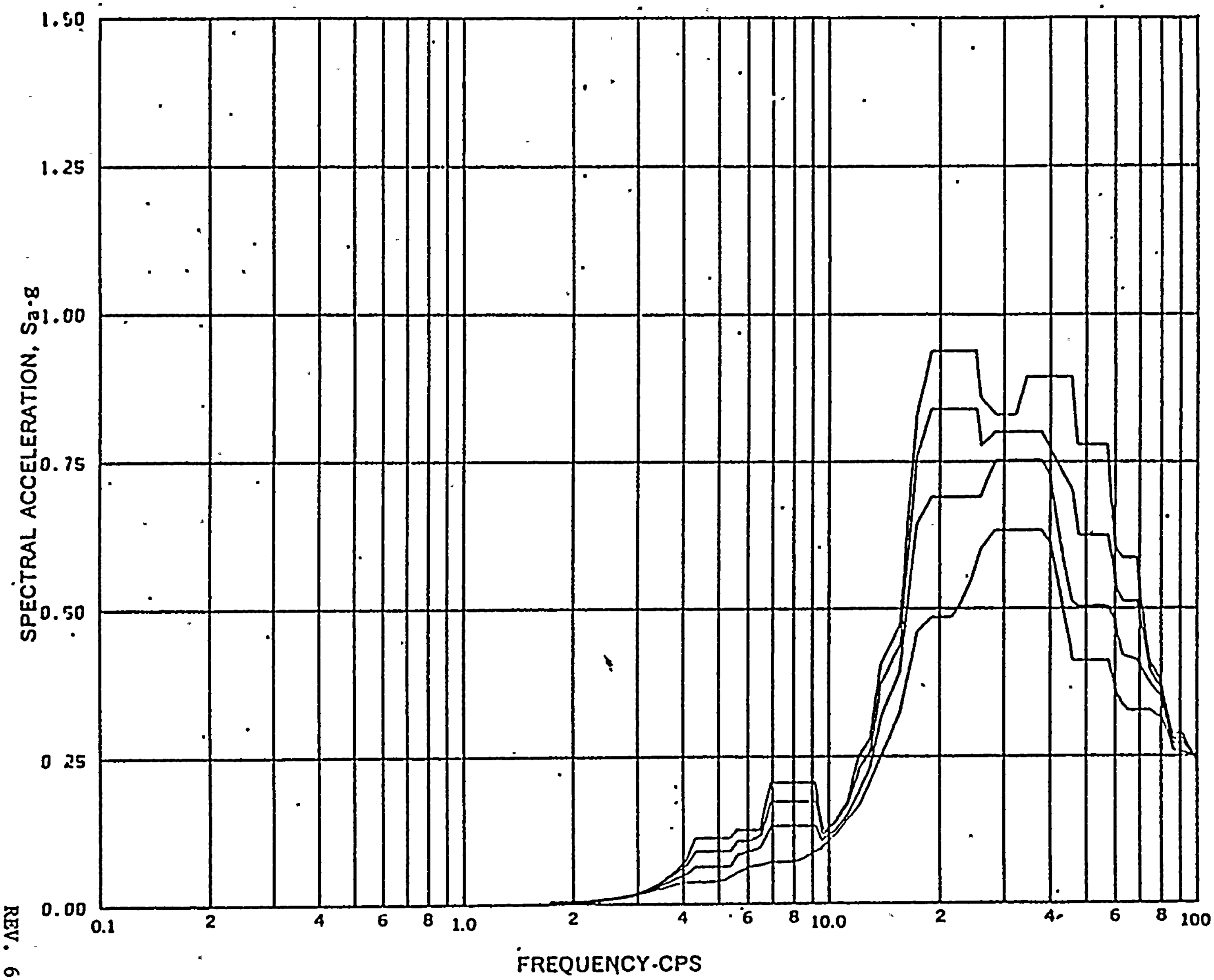

Limerick Generation Station, Acceleration Spectra for WETWELL

Load Case: SRV - ASYMMETRIC - TRACE 76

Node: 131 Direction: HORIZ Elev: 205'-11" Angle: 0°

Damping: 0.005,0.01,0.02,0.05 By: PC Date: 5-5-80 Check: Kw Date: 5/6/80

REV. 6, 4/82

SUSQUEHANNA STEAM ELECTRIC STATION
UNITS 1 AND 2
DESIGN ASSESSMENT REPORT

LGS CONTAINMENT RESPONSE
SPECTRA-KEWU SRV #76
ASYMMETRIC - DIRECTION
HORIZONTAL

FIGURE 10-42

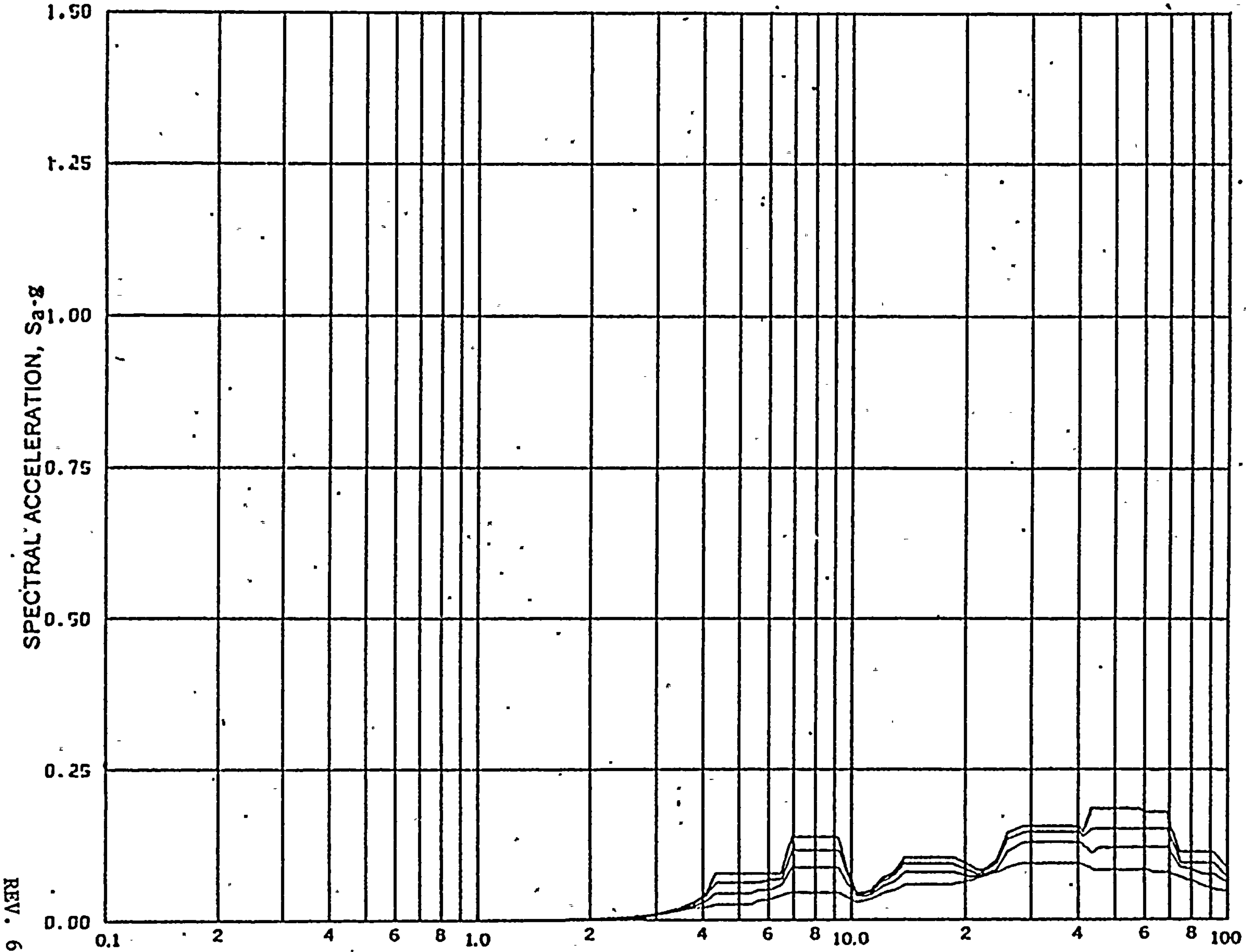

Limerick Generation Station, Acceleration Spectra for WETWELL

Load Case: SRV - ASYMMETRIC - TRACE 76

Node: 131 Direction: VERT Elev: 205'-11" Angle: 0°

Damping: 0.005,0.01,0.02,0.05 By: PL Date: 5-5-80 Check: Kw Date: 5/6/80

REV. 6, 4/82

SUSQUEHANNA STEAM ELECTRIC STATION
UNITS 1 AND 2
DESIGN ASSESSMENT REPORT

LGS CONTAINMENT RESPONSE
SPECTRA-KWU SRV #76
ASYMMETRIC - DIRECTION
VERTICAL

FIGURE 10-43

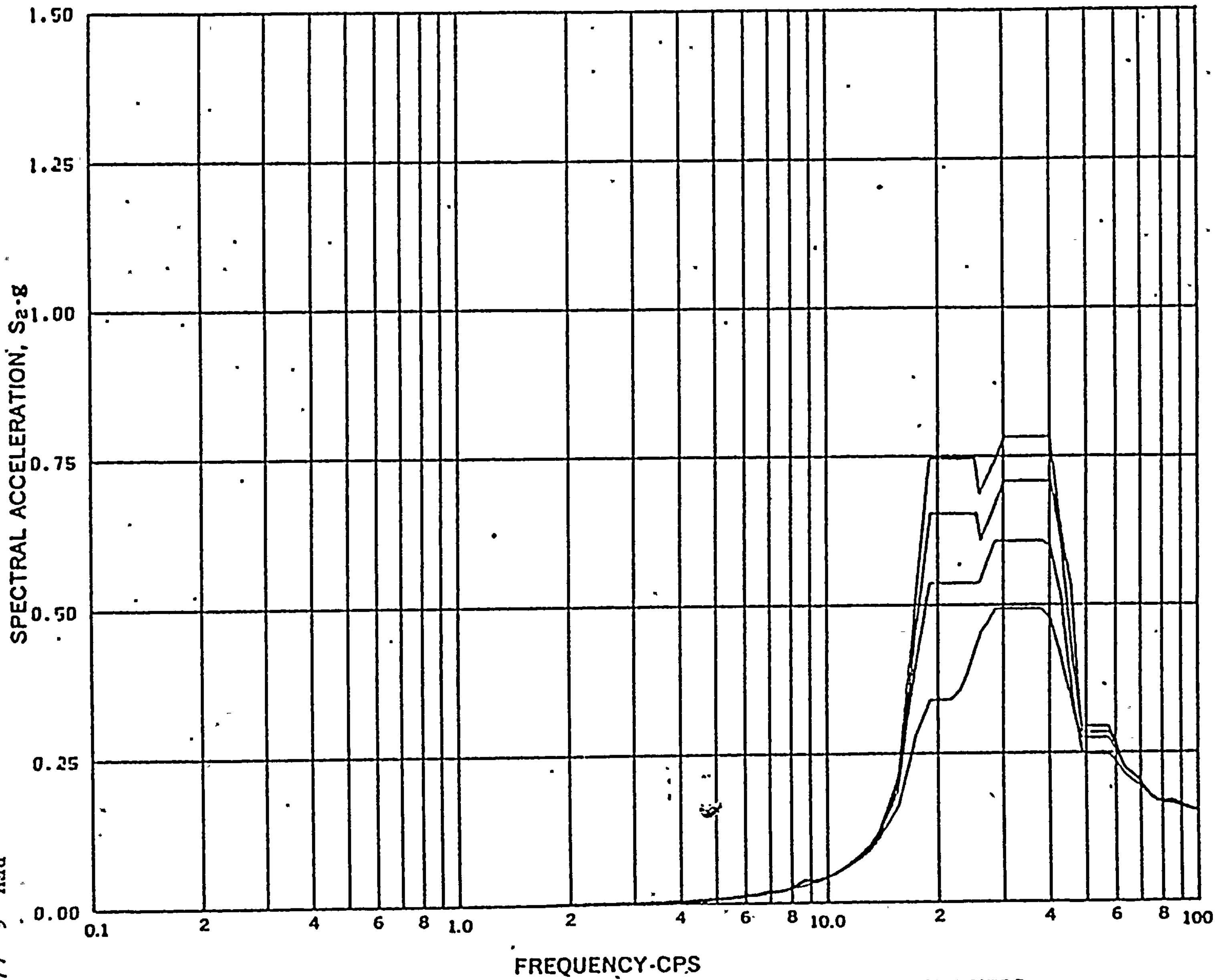

Limerick Generation Station, Acceleration Spectra for WETWELL

Load Case: SRV - ASYMMETRIC - TRACE 76

Node: 135 Direction: HORIZ Elev: 205'-11" Angle: 90°

Damping: 0.005,0.01,0.02,0.05 By: PC Date: 5-5-80 Check: Km Date: 5/6/80

REV. 6, 4/82

SUSQUEHANNA STEAM ELECTRIC STATION
UNITS 1 AND 2
DESIGN ASSESSMENT REPORT

LGS CONTAINMENT RESPONSE SPECTRA - KWU SRV #76 ASYMMETRIC - DIRECTION HORIZONTAL

FIGURE 10-44

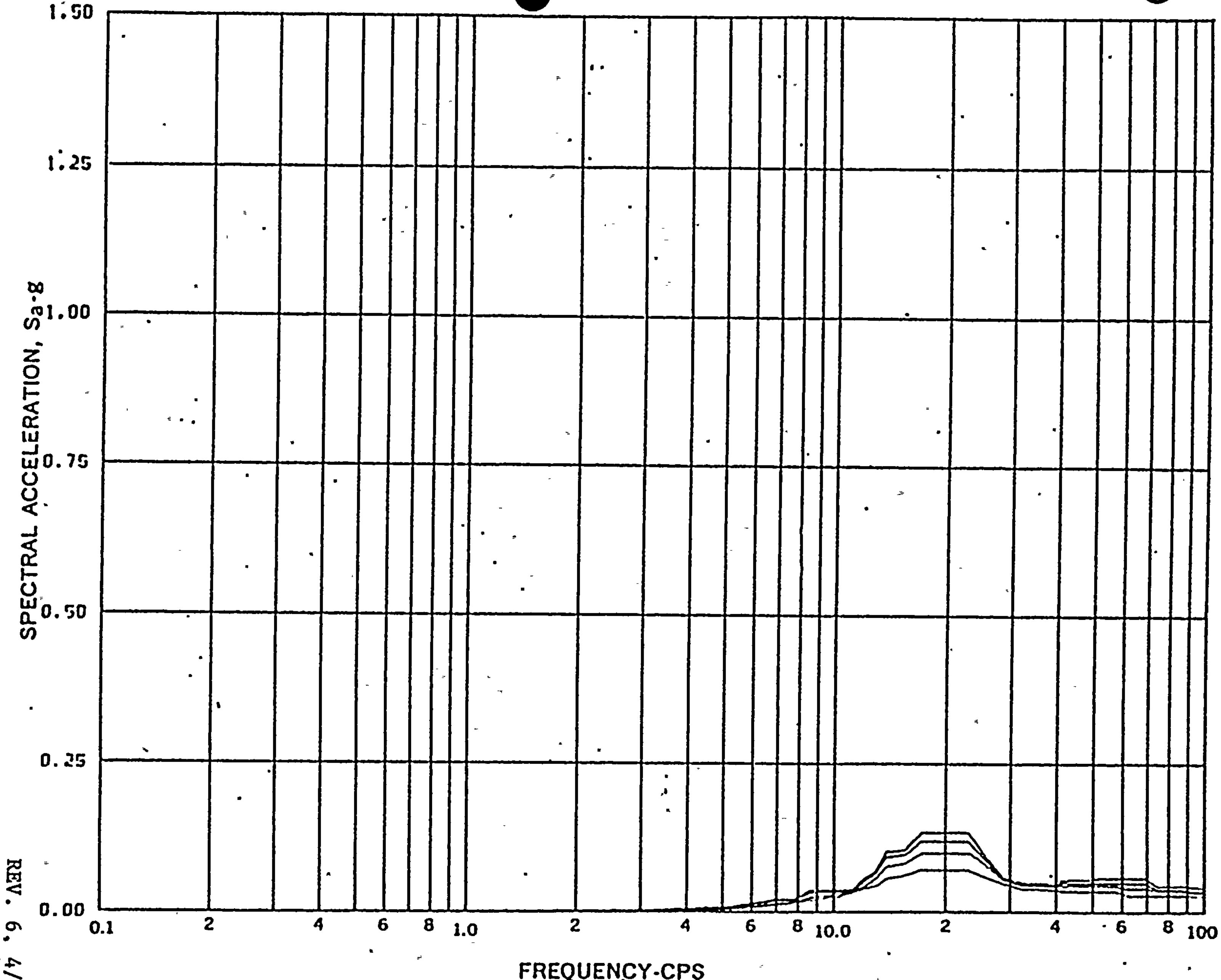

Limerick Generation Station, Acceleration Spectra for WETWELL

Load Case: SRV - ASYMMETRIC - TRACE 76

Node: 135 Direction: VERT Elev: 205'-11" Angle: 90°

Damping: 0.005,0.01,0.02,0.05 By: PC Date: 5-5-80 Check: KW Date: 5/6/80

REV. 6, 4/82

SUSQUEHANNA STEAM ELECTRIC STATION
UNITS 1 AND 2
DESIGN ASSESSMENT REPORT

LGS CONTAINMENT RESPONSE
SPECTRA - KWU SRV #76
ASYMMETRIC - DIRECTION
VERTICAL.

FIGURE 10-45

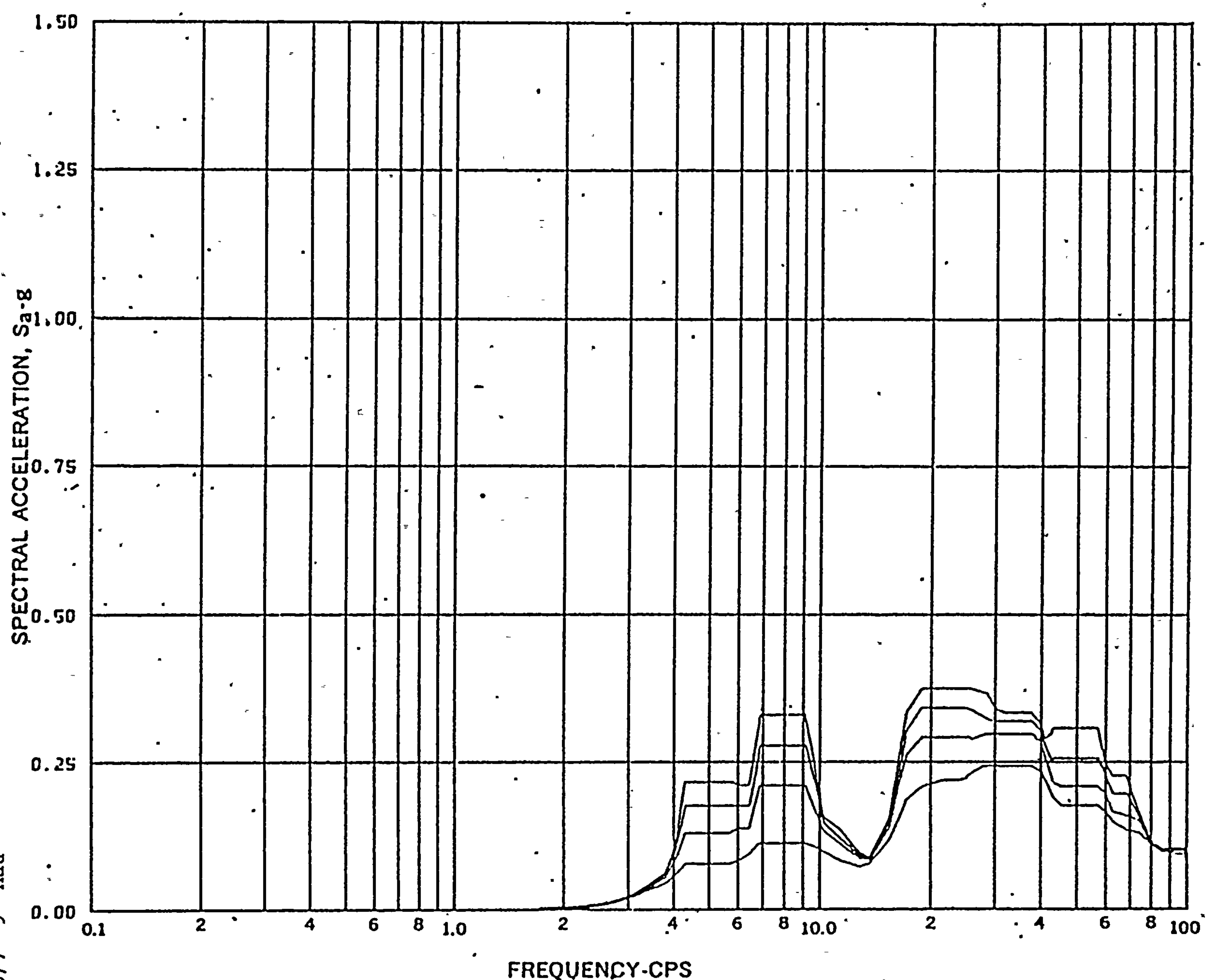

Limerick Generation Station, Acceleration Spectra for PEDESTAL

Load Case: SRV - ASYMMETRIC - TRACE 76

Node: 211 Direction: HORIZ Elev: 236'-2" Angle: 0°

Damping: 0.005,0.01,0.02,0.05 By: PC Date: 5-5-80 Check: Kw Date: 5/6/80

REV. 6, 4/82

SUSQUEHANNA STEAM ELECTRIC STATION
UNITS 1 AND 2
DESIGN ASSESSMENT REPORT

LGS CONTAINMENT RESPONSE SPECTRA - KWU SRV #76 ASYMMETRIC - DIRECTION HORIZONTAL

FIGURE 10-46

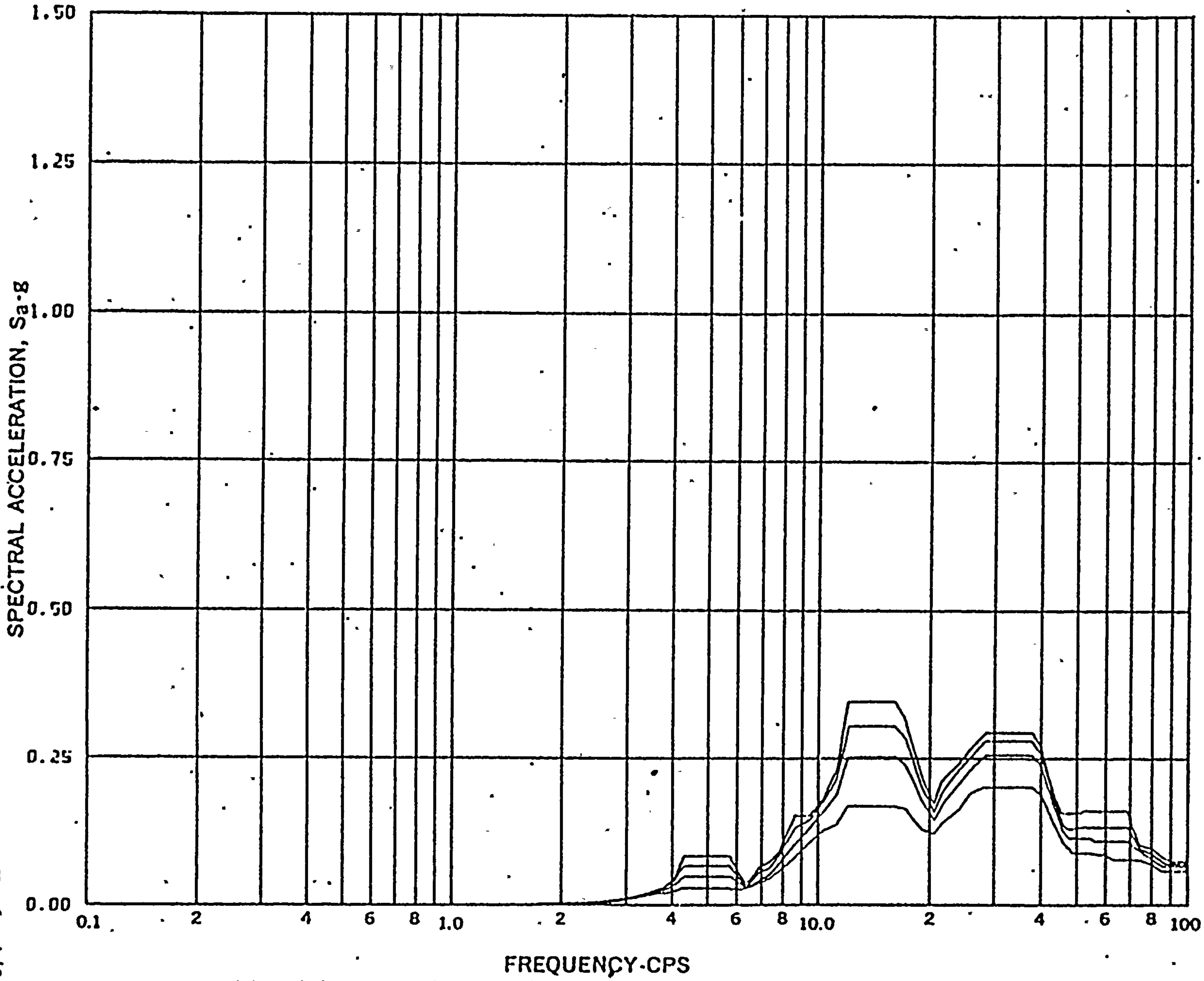

Limerick Generation Station, Acceleration Spectra for PEDESTAL

Load Case: SRV - ASYMMETRIC - TRACE 76

Node: 211 Direction: VERT Elev: 236'-2" Angle: 0°

Damping: 0.005,0.01,0.02,0.05 By: PC Date: 5-5-80 Check: KW Date: 5/6/80

REV. 6, 4/82

SUSQUEHANNA STEAM ELECTRIC STATION
UNITS 1 AND 2
DESIGN ASSESSMENT REPORT

LGS CONTAINMENT RESPONSE SPECTRA - KWU SRV #76 ASYMMETRIC - DIRECTION VERTICAL

FIGURE 10-47

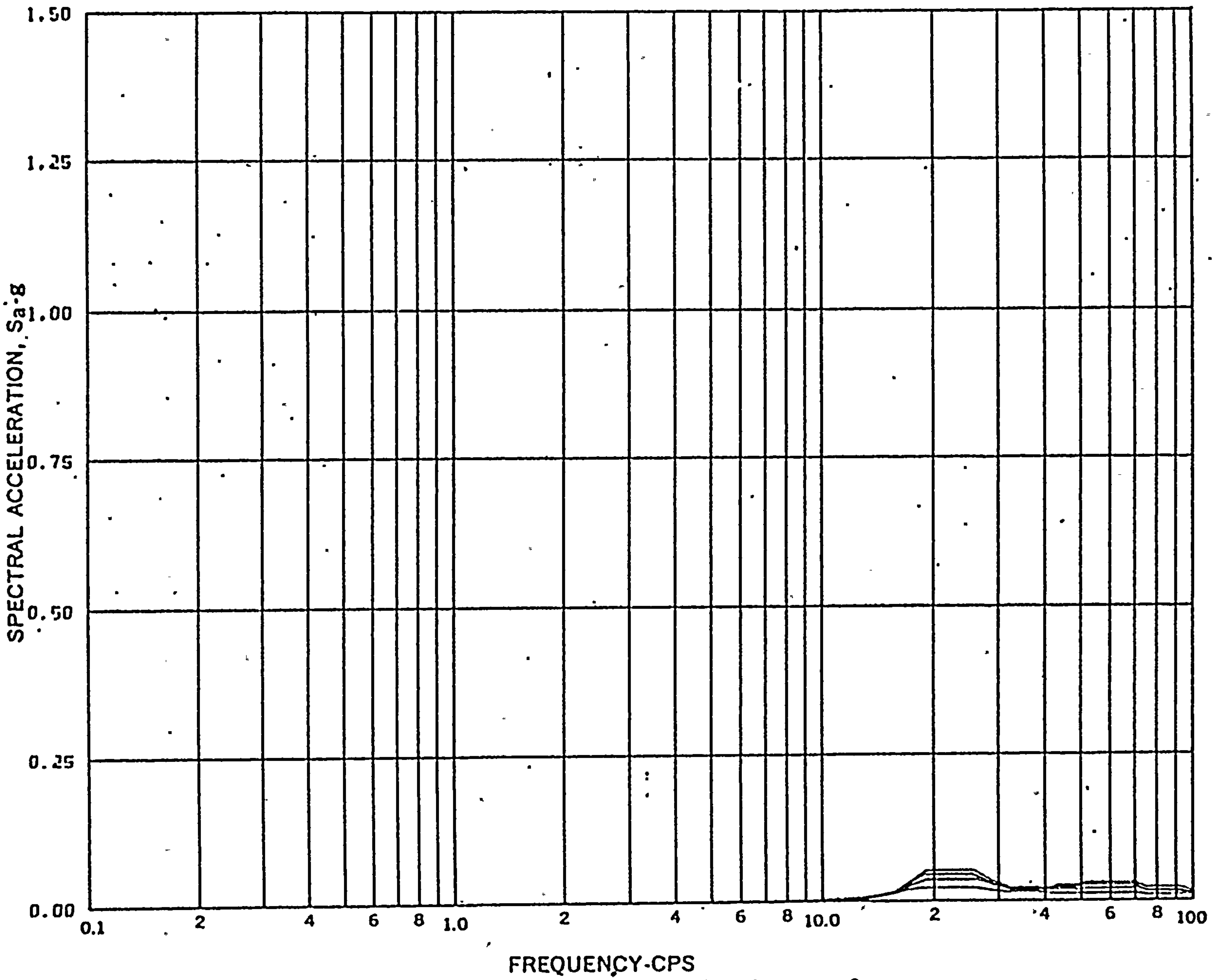

Limerick Generation Station, Acceleration Spectra for PEDESTAL

Load Case: SRV - ASYMMETRIC - TRACE 76

Node: 215 Direction: HORIZ Elev: 236'-2" Angle: 90°

Damping: 0.005,0.01,0.02,0.05 By: PC Date: 5-5-80 Check: KW Date: 5/6/80

REV. 6, 4/82

SUSQUEHANNA STEAM ELECTRIC STATION
UNITS 1 AND 2
DESIGN ASSESSMENT REPORT

LGS CONTAINMENT RESPONSE SPECTRA - KWU SRV #76 ASYMMETRIC - DIRECTION HORIZONTAL

FIGURE 10-48

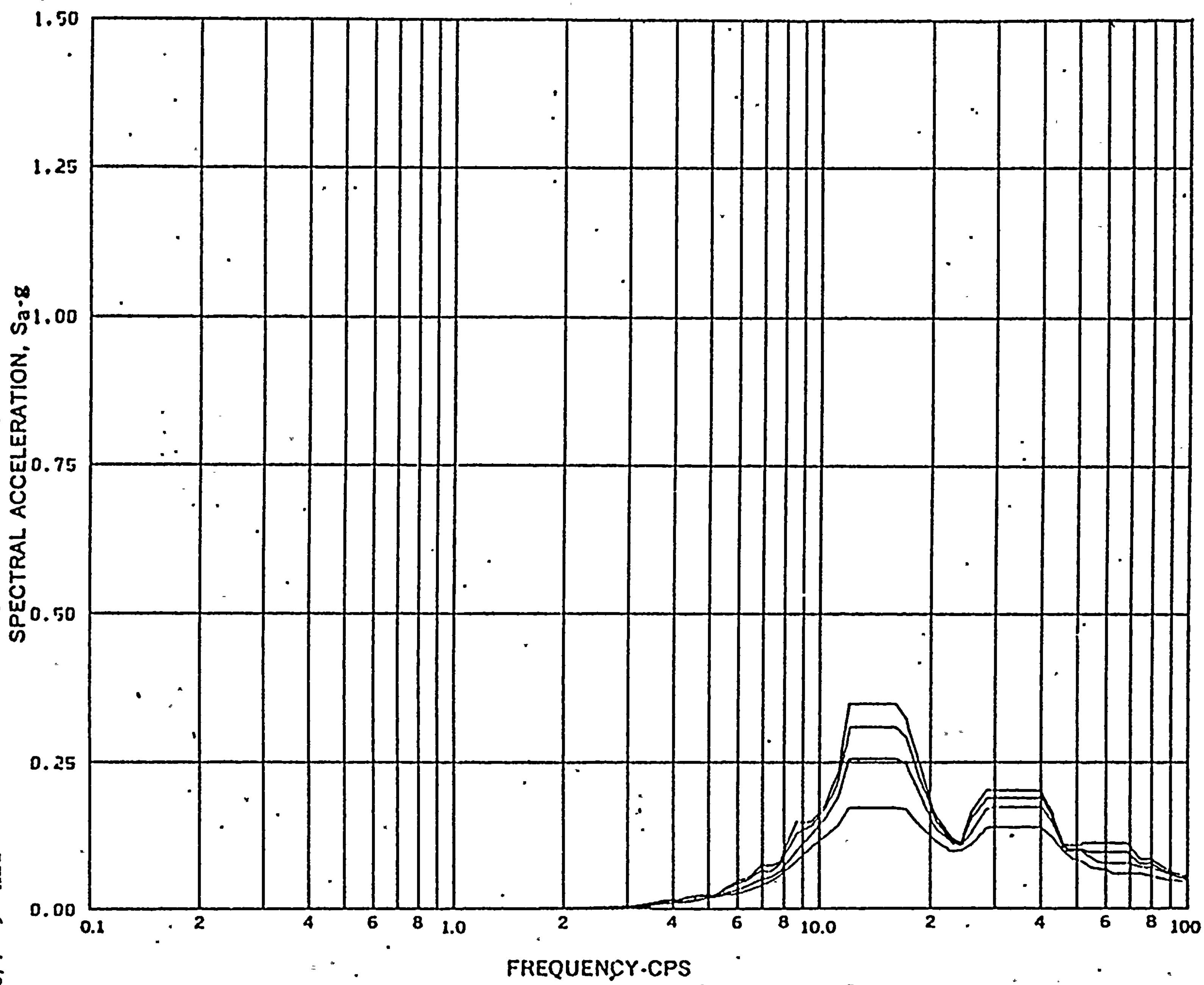

Limerick Generation Station, Acceleration Spectra for PEDESTAL

Load Case: SRV - ASYMMETRIC - TRACE 76

Node: 215 Direction: VERT Elev: 236'-2" Angle: 90°

Damping: 0.005,0.01,0.02,0.05 By: PC Date: 5-5-80 Check: KW Date: 5/6/80

REV. 6, 4/82

SUSQUEHANNA STEAM ELECTRIC STATION
UNITS 1 AND 2
DESIGN ASSESSMENT REPORT

LGS CONTAINMENT RESPONSE
SPECTRA - KWU SRV #76
ASYMMETRIC - DIRECTION
VERTICAL

FIGURE 10-49

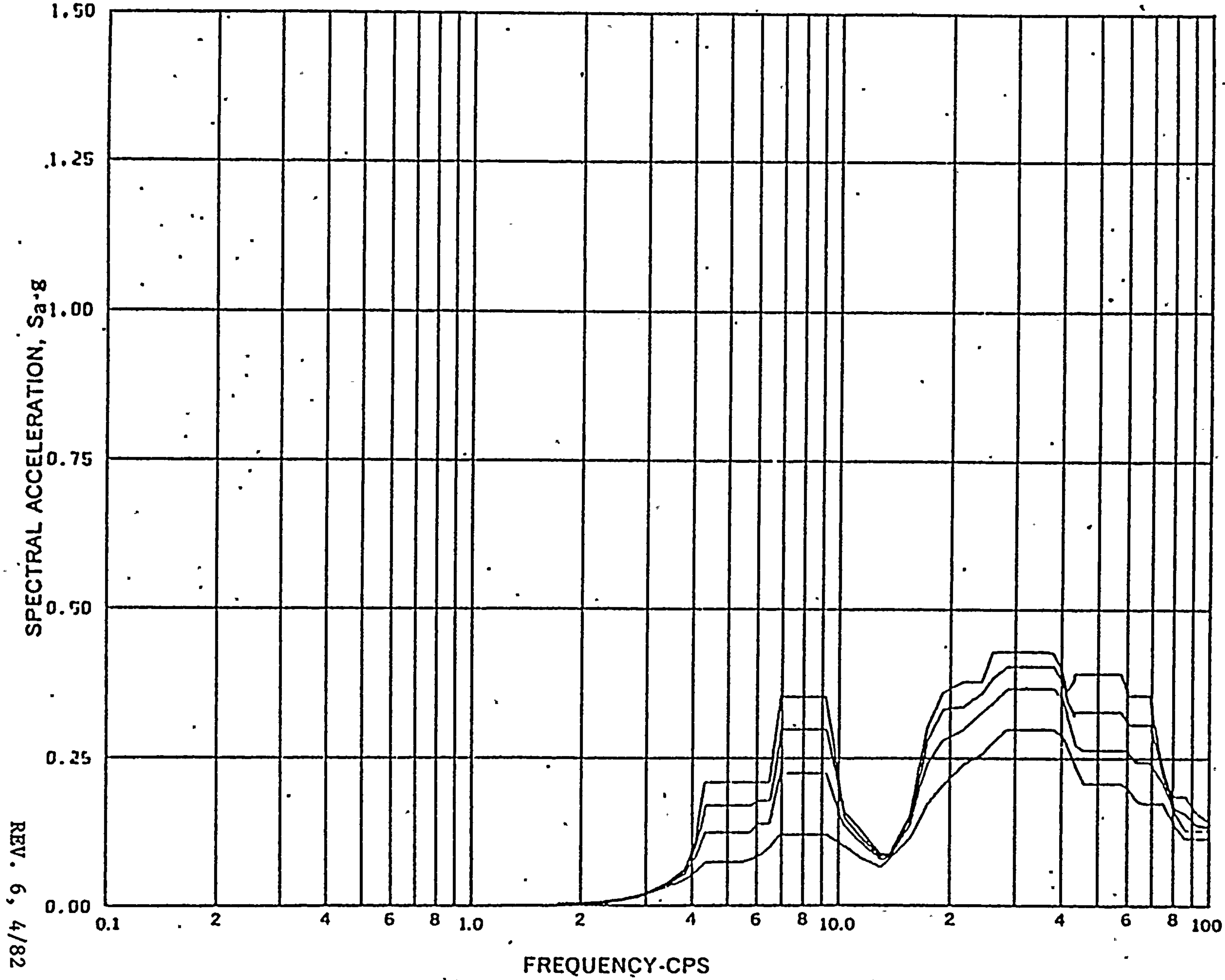

Limerick Generation Station, Acceleration Spectra for WETWELL

Load Case: SRV - ASYMMETRIC - TRACE 76

Node: 291 Direction: HORIZ Elev: 236'-2" Angle: 0°

Damping: 0.005,0.01,0.02,0.05 By: PC Date: 5-5-80 Check: Kw Date: 5/6/80

REV. 6, 4/82

SUSQUEHANNA STEAM ELECTRIC STATION
UNITS 1 AND 2
DESIGN ASSESSMENT REPORT

LGS CONTAINMENT RESPONSE SPECTRA - KWU SRV #76 ASYMMETRIC - DIRECTION HORIZONTAL

FIGURE 10-50

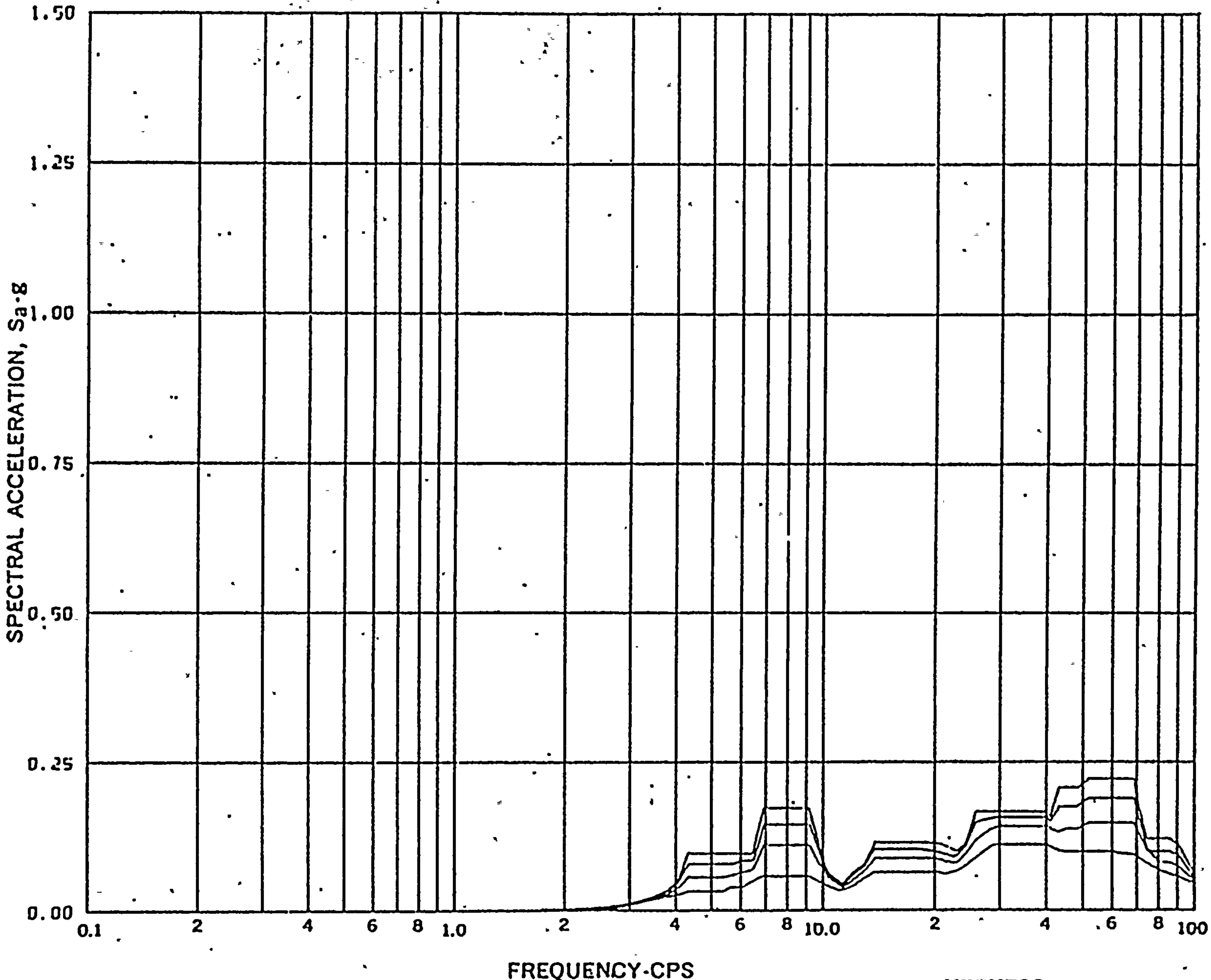

Limerick Generation Station, Acceleration Spectra for WETWELL

Load Case: SRV - ASYMMETRIC - TRACE 76

Node: 291 Direction: VERT Elev: 236'-2" Angle: 0°

Damping: 0.005,0.01,0.02,0.05 By: PC Date: 5-5-80 Check: KW Date: 5/6/80

REV. 6, 4/82

SUSQUEHANNA STEAM ELECTRIC STATION
UNITS 1 AND 2
DESIGN ASSESSMENT REPORT

LGS CONTAINMENT RESPONSE SPECTRA - KWU SRV #76 ASYMMETRIC - DIRECTION VERTICAL

FIGURE 10-51

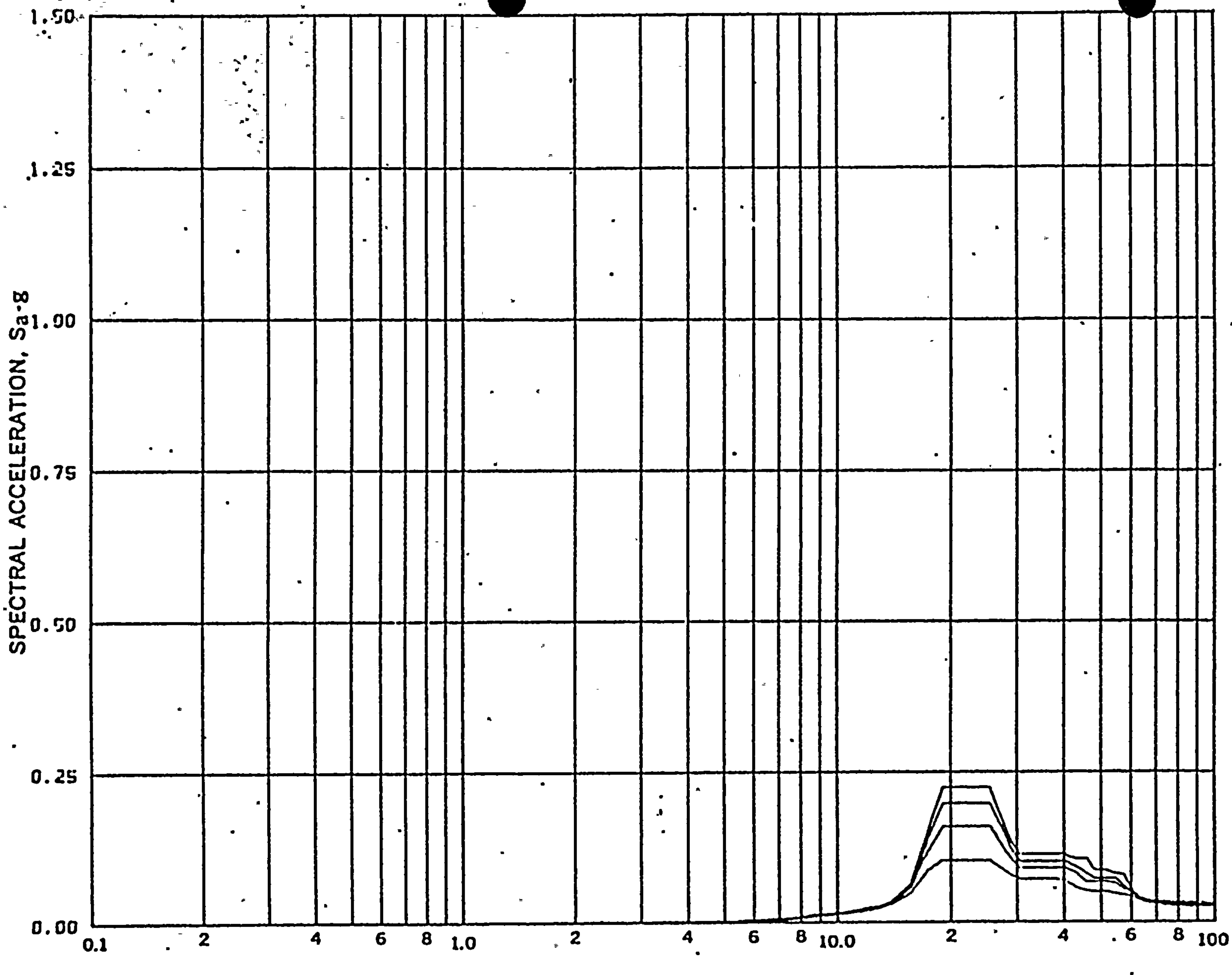

Limerick Generation Station, Acceleration Spectra for WETWELL

Load Case: SRV - ASYMMETRIC - TRACE 76

Node: 295 Direction: HORIZ Elev: 236'-2" Angle: 90°

Damping: 0.005,0.01,0.02,0.05 By: PC Date: 5-5-80 Check: KW Date: 5/6/80

REV. 6, 4/82

SUSQUEHANNA STEAM ELECTRIC STATION
UNITS 1 AND 2
DESIGN ASSESSMENT REPORT

LGS CONTAINMENT RESPONSE
SPECTRA - KWU SRV #76
ASYMMETRIC - DIRECTION
HORIZONTAL

FIGURE 10-52

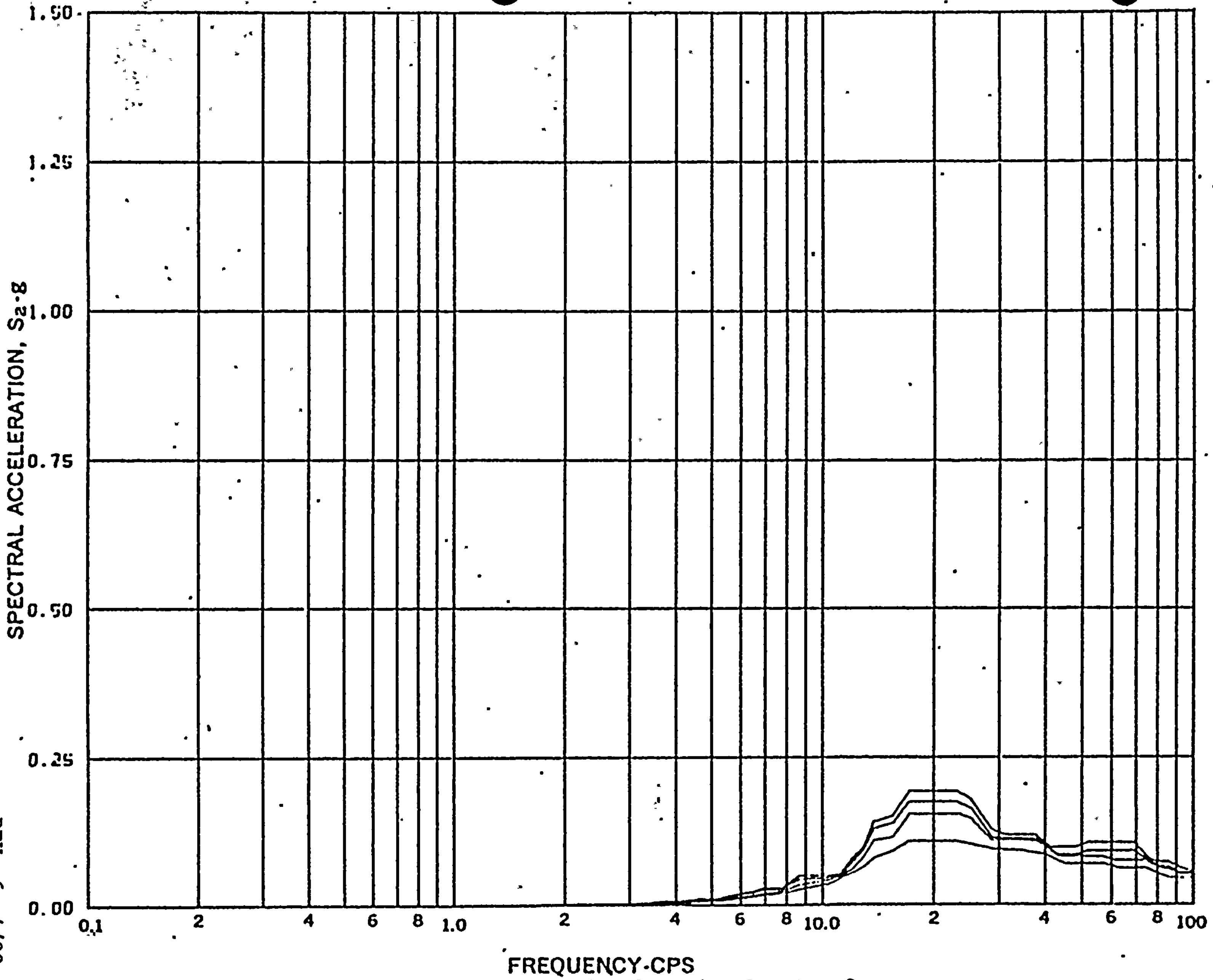

Limerick Generation Station, Acceleration Spectra for WETWELL

Load Case: SRV - ASYMMETRIC - TRACE 76

Node: 295 Direction: VERT Elev: 236'-2" Angle: 90°

Damping: 0.005,0.01,0.02,0.05 By: PC Date: 5-5-80 Check: KW Date: 5/6/80

REV. 6, 4/82

SUSQUEHANNA STEAM ELECTRIC STATION
UNITS 1 AND 2
DESIGN ASSESSMENT REPORT

LGS CONTAINMENT RESPONSE
SPECTRA - KWU SRV #76
ASYMMETRIC - DIRECTION
VERTICAL

FIGURE 10-53

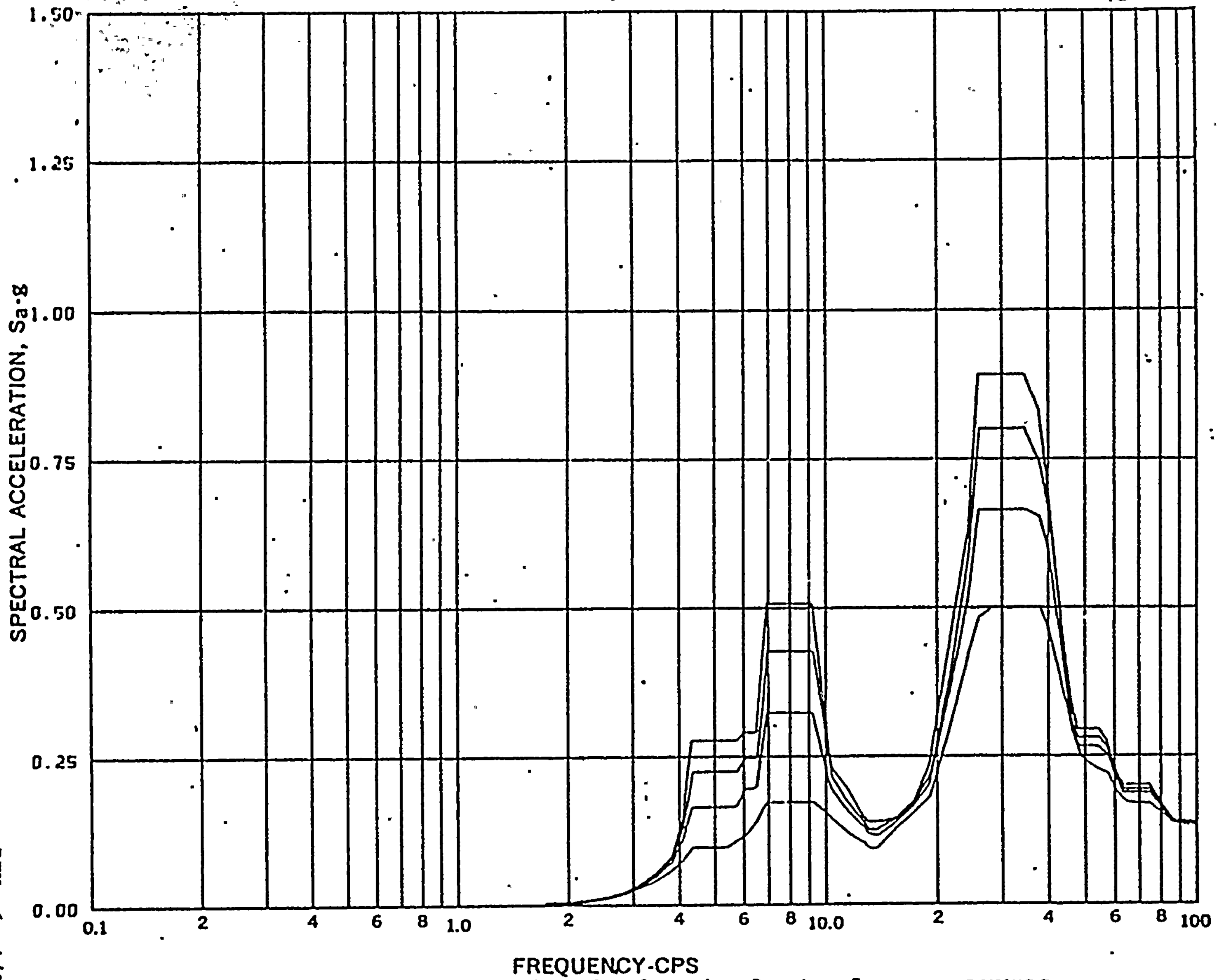

Limerick Generation Station, Acceleration Spectra for DRYWELL

Load Case: SRV - ASYMMETRIC - TRACE 76

Node: 331 Direction: HORIZ Elev: 264'-6" Angle: 0°

Damping: 0.005,0.01,0.02,0.05 By: PC Date: 5-5-80 Check: Kw Date: 5/6/80

REV. 6, 4/82

SUSQUEHANNA STEAM ELECTRIC STATION
UNITS 1 AND 2
DESIGN ASSESSMENT REPORT

LGS CONTAINMENT RESPONSE SPECTRA - KWU SRV # 76
ASYMMETRIC - DIRECTION HORIZONTAL

FIGURE 10-54

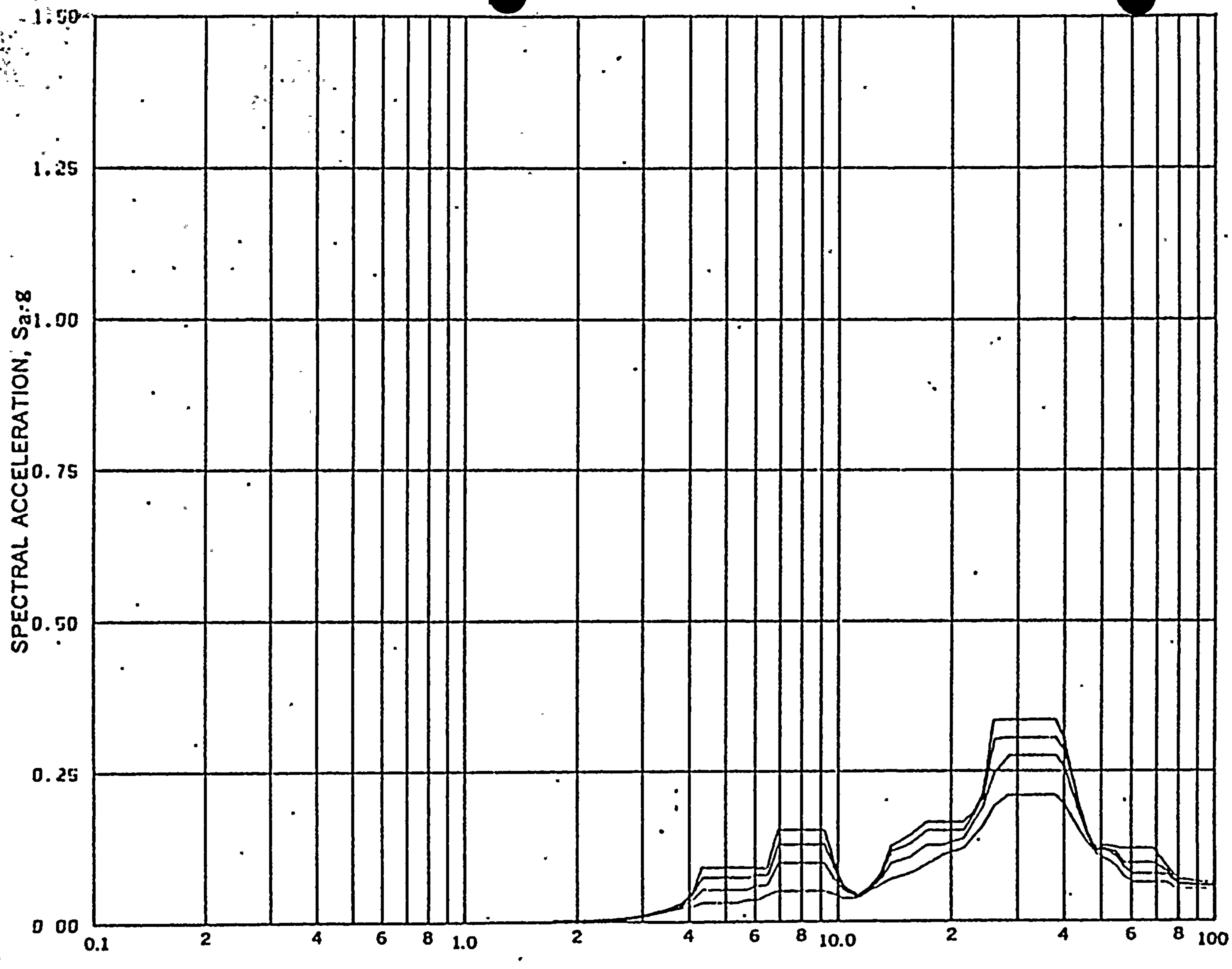

Limerick Generation Station, Acceleration Spectra for DRYWELL

Load Case: SRV - ASYMMETRIC - TRACE 76

Node: 331 Direction: VERT Elev: 264'-6" Angle: 0°

Damping: 0.005,0.01,0.02,0.05 By: PC Date: 5-5-80 Check: Kw Date: 5/6/80

REV. 6, 4/82

SUSQUEHANNA STEAM ELECTRIC STATION
UNITS 1 AND 2
DESIGN ASSESSMENT REPORT

LGS CONTAINMENT RESPONSE
SPECTRA - KWU SRV #76
ASYMMETRIC - DIRECTION
VERTICAL

FIGURE 10-55

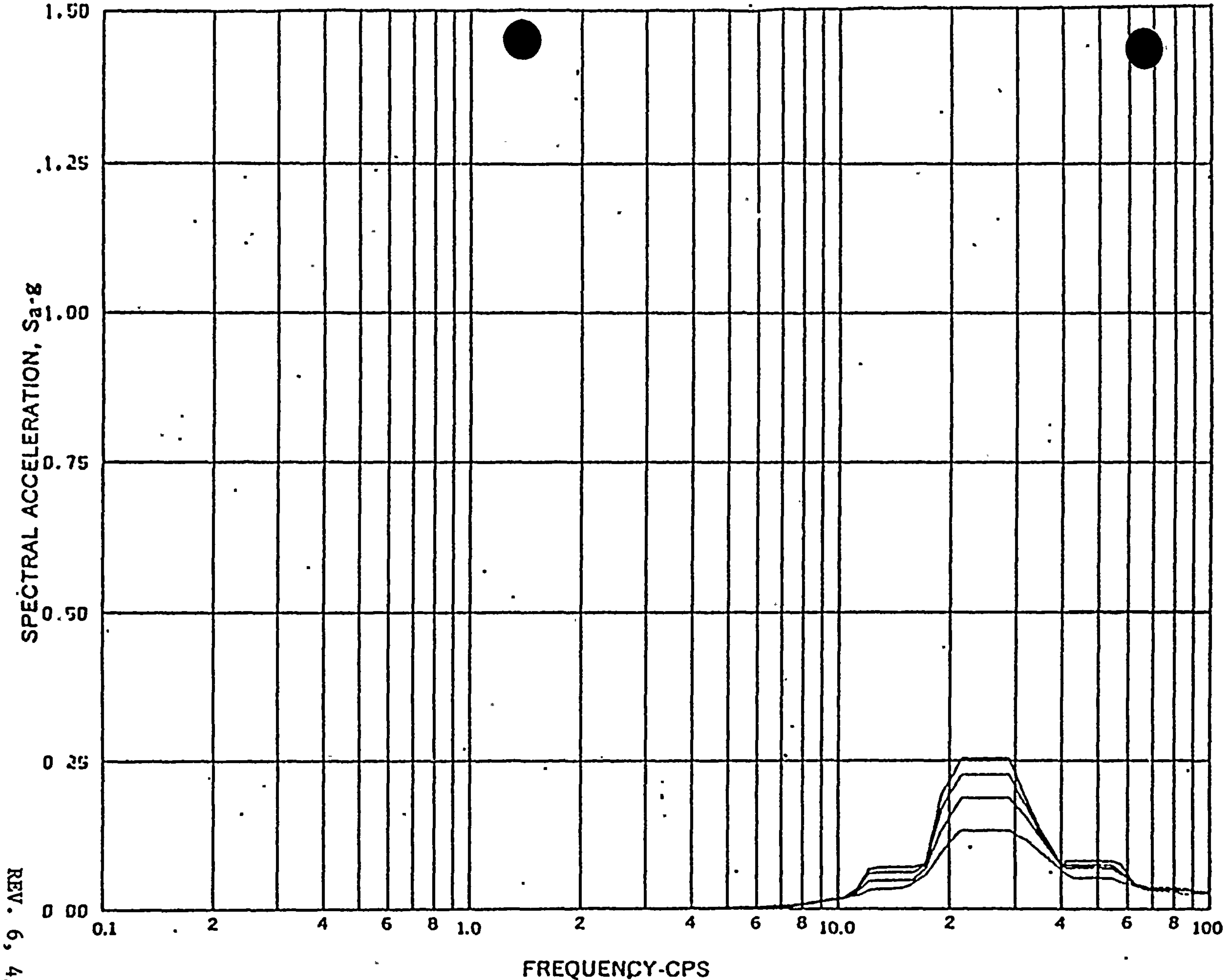

Limerick Generation Station, Acceleration Spectra for DRYWELL

Load Case: SRV - ASYMMETRIC - TRACE 76

Node: 335 Direction: HORIZ Elev: 264'-6" Angle: 90°

Damping: 0.005,0.01,0.02,0.05 By: PC Date: 5-5-80 Check: KW Date: 5/6/80

REV. 6, 4/82

SUSQUEHANNA STEAM ELECTRIC STATION
UNITS 1 AND 2
DESIGN ASSESSMENT REPORT

LGS CONTAINMENT RESPONSE
SPECTRA - KWU SRV #76
ASYMMETRIC - DIRECTION
HORIZONTAL

FIGURE 10-56

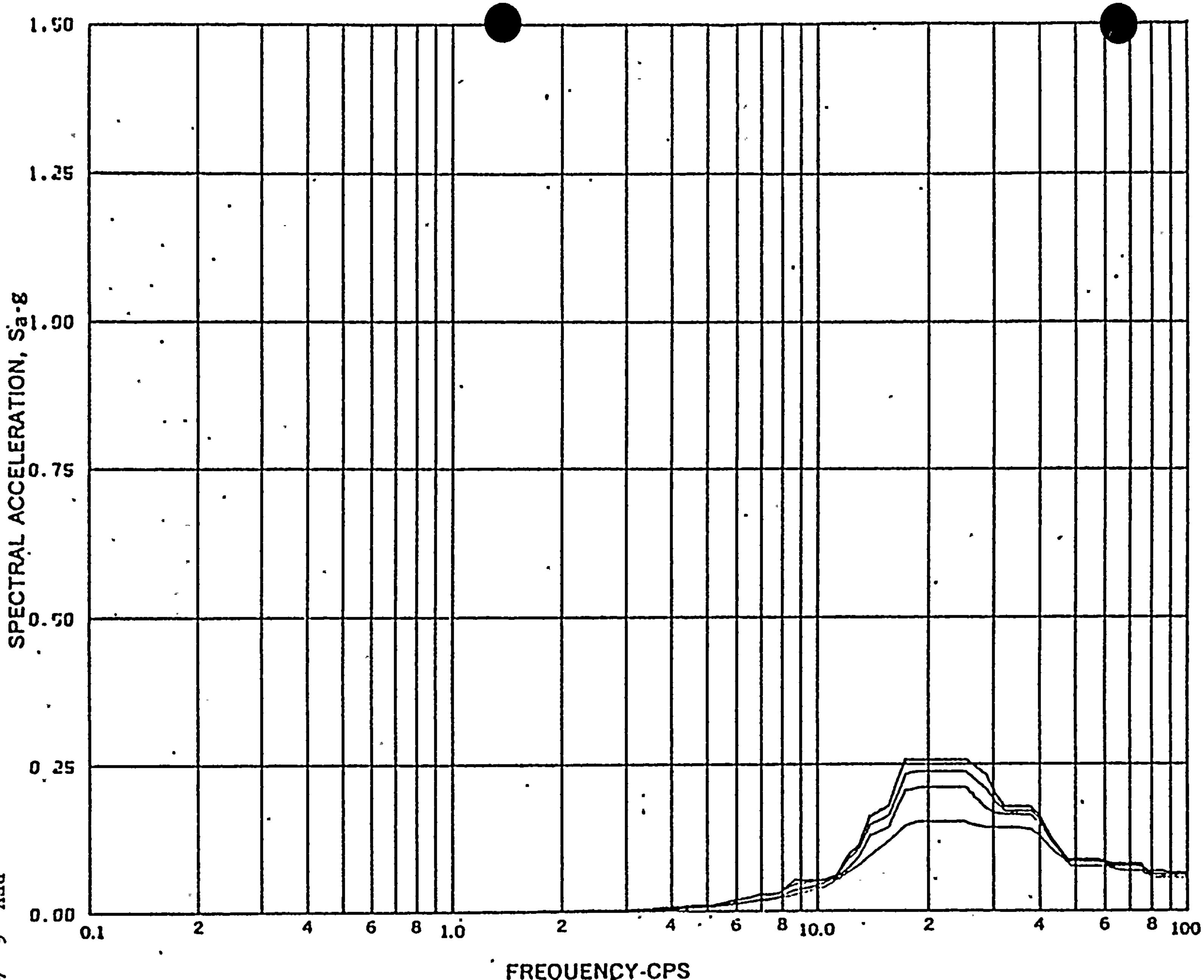

Limerick Generation Station, Acceleration Spectra for DRYWELL

Load Case: SRV - ASYMMETRIC - TRACE 76

Node: 335 Direction: VERT Elev: 264'-6" Angle: 90°

Damping: 0.005,0.01,0.02,0.05 By: PC Date: 5-5-80 Check: KW Date: 5/6/80

REV. 6, 4/82

SUSQUEHANNA STEAM ELECTRIC STATION
UNITS 1 AND 2
DESIGN ASSESSMENT REPORT

LGS CONTAINMENT RESPONSE
SPECTRA - KWU SRV # 76
ASYMMETRIC - DIRECTION
VERTICAL

FIGURE 10-57

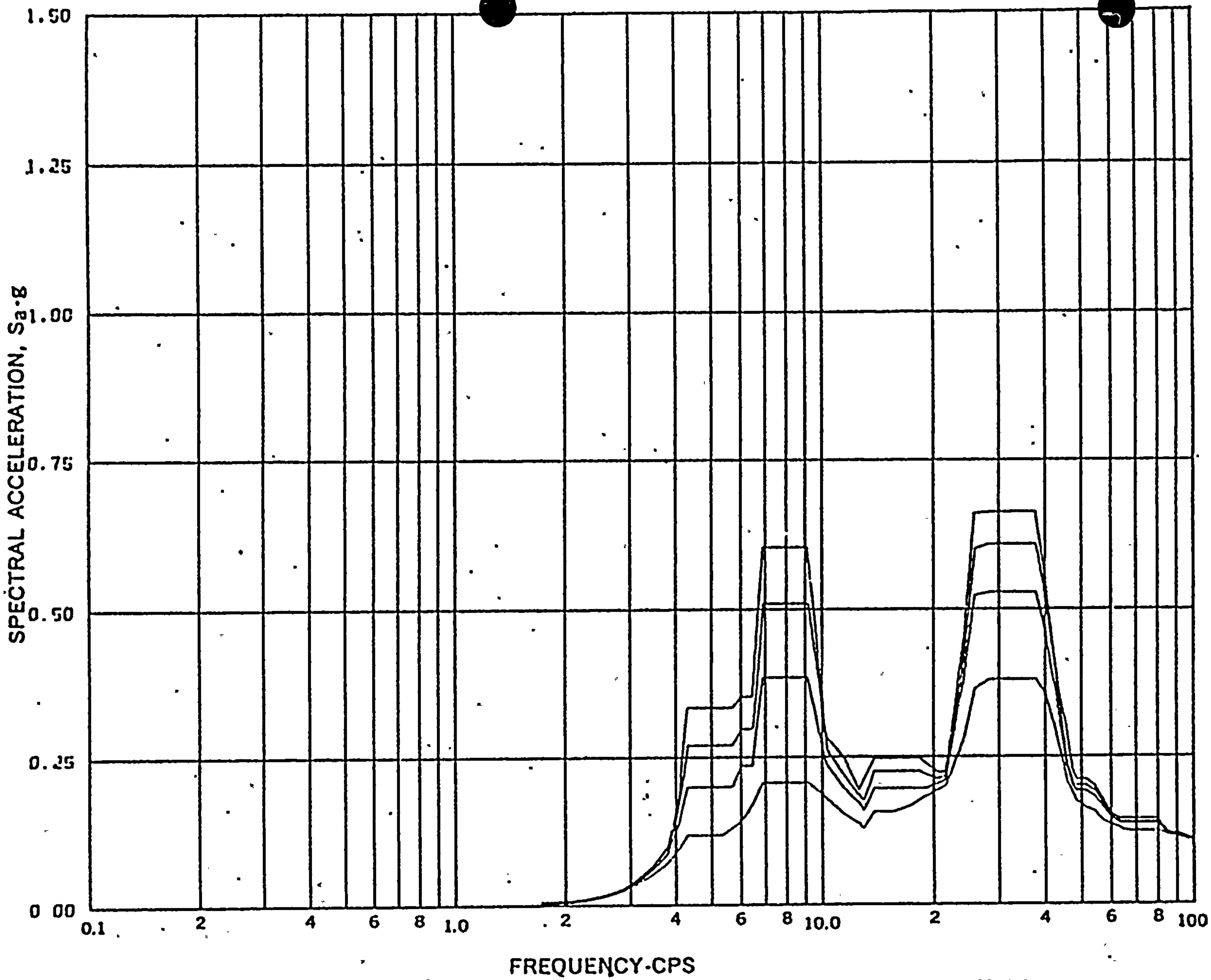

Limerick Generation Station, Acceleration Spectra for DRYWELL

Load Case: SRV - ASYMMETRIC - TRACE 76

Node: 371 Direction: HORIZ Elev: 283'-11" Angle: 0°

Damping: 0.005,0.01,0.02,0.05 By: PC Date: 5-5-80 Check: KW Date: 5/6/80

REV. 6, 4/82

SUSQUEHANNA STEAM ELECTRIC STATION
UNITS 1 AND 2
DESIGN ASSESSMENT REPORT

LGS CONTAINMENT RESPONSE SPECTRA - KWU SRV #76
ASYMMETRIC - DIRECTION
HORIZONTAL

FIGURE 10-58

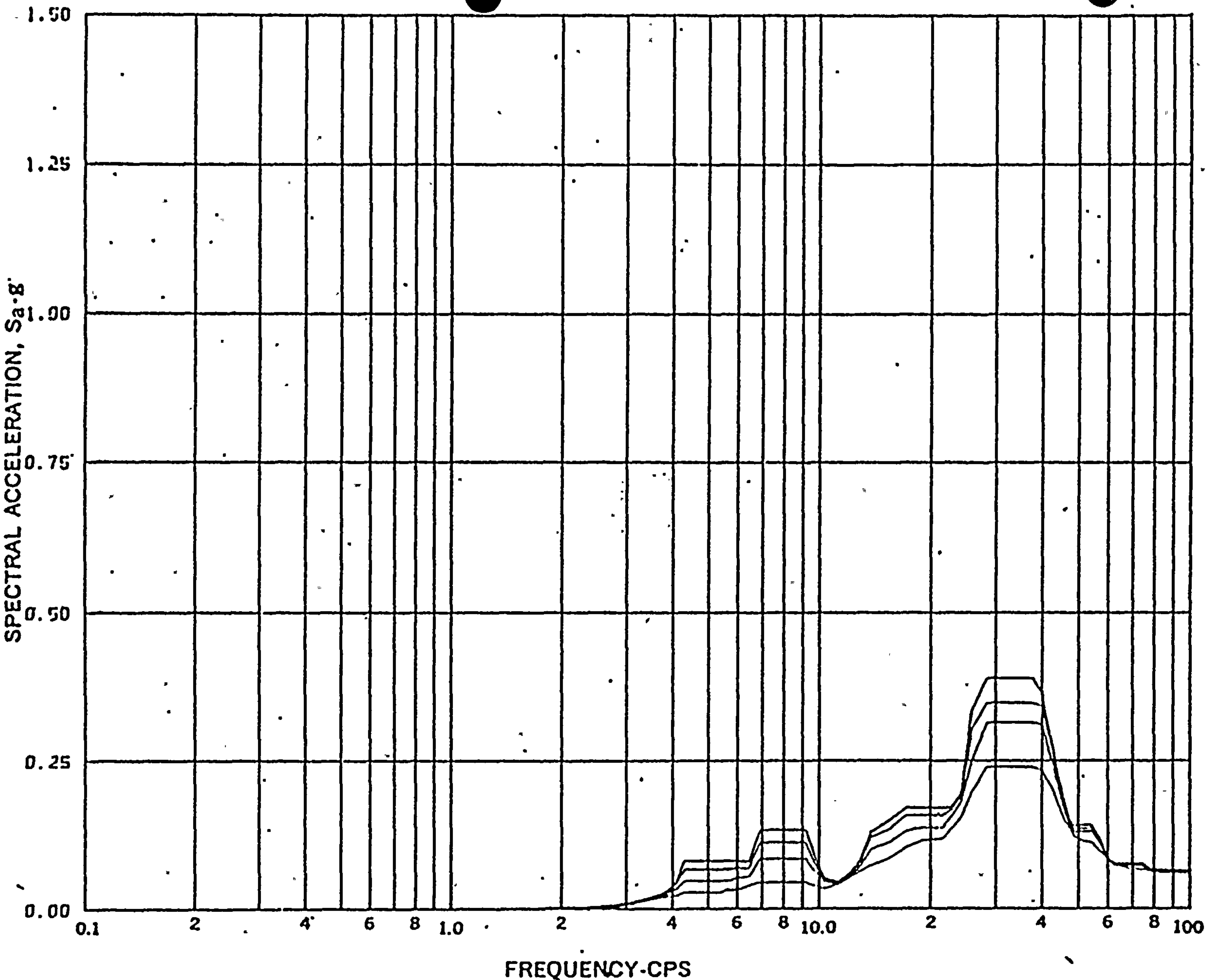

Limerick Generation Station, Acceleration Spectra for DRYWELL

Load Case: SRV - ASYMMETRIC - TRACE 76

Node: 371 Direction: VERT Elev: 283'-11" Angle: 0°

Damping: 0.005,0.01,0.02,0.05 By: PC Date: 5-5-80 Check: Kw Date: 5/6/80

REV. 6, 4/82

SUSQUEHANNA STEAM ELECTRIC STATION
UNITS 1 AND 2
DESIGN ASSESSMENT REPORT

LGS CONTAINMENT RESPONSE SPECTRA - KWU SRV #76 ASYMMETRIC - DIRECTION VERTICAL

FIGURE 10-59

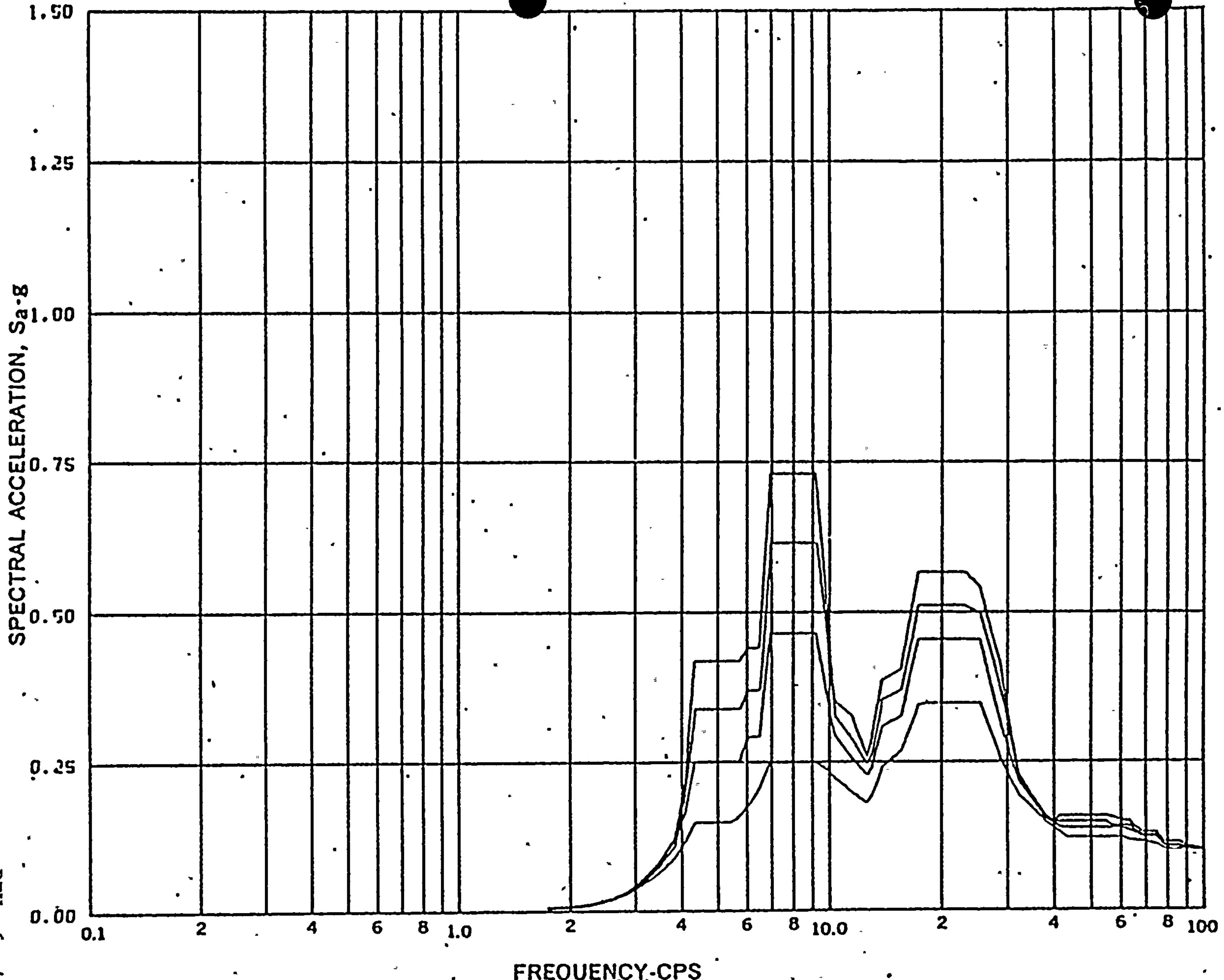

Limerick Generation Station, Acceleration Spectra for DRYWELL

Load Case: SRV - ASYMMETRIC - TRACE 76

Node: 411 Direction: HORIZ Elev: 312'-7" Angle: 0°

Damping: 0.005,0.01,0.02,0.05 By: RC Date: 5-5-80 Check: Kw Date: 5/6/80

REV. 6, 4/82

SUSQUEHANNA STEAM ELECTRIC STATION
UNITS 1 AND 2
DESIGN ASSESSMENT REPORT

LGS CONTAINMENT RESPONSE SPECTRA - KWU SRV # 76 ASYMMETRIC - DIRECTION HORIZONTAL

FIGURE 10-60

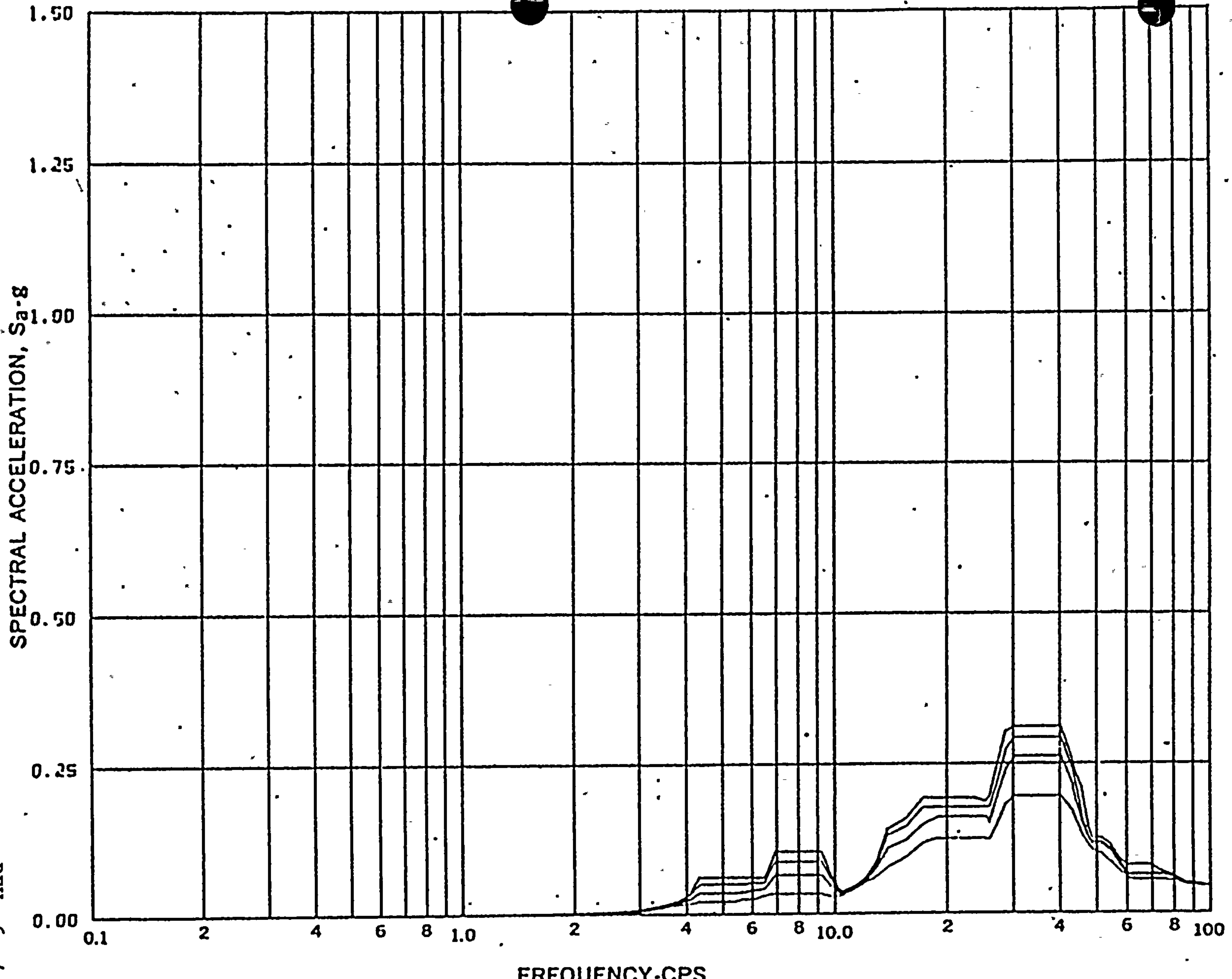

Limerick Generation Station, Acceleration Spectra for DRYWELL

Load Case: SRV - ASYMMETRIC - TRACE 76

Node: 411 Direction: VERT Elev: 312'-7" Angle: 0°

Damping: 0.005,0.01,0.02,0.05 By: PC Date: 5-5-80 Check: Kw Date: 5/6/80

REV. 6, 4/82

SUSQUEHANNA STEAM ELECTRIC STATION
UNITS 1 AND 2
DESIGN ASSESSMENT REPORT

LGS CONTAINMENT RESPONSE SPECTRA - KWU SRV # 76
ASYMMETRIC - DIRECTION VERTICAL

FIGURE 10-61

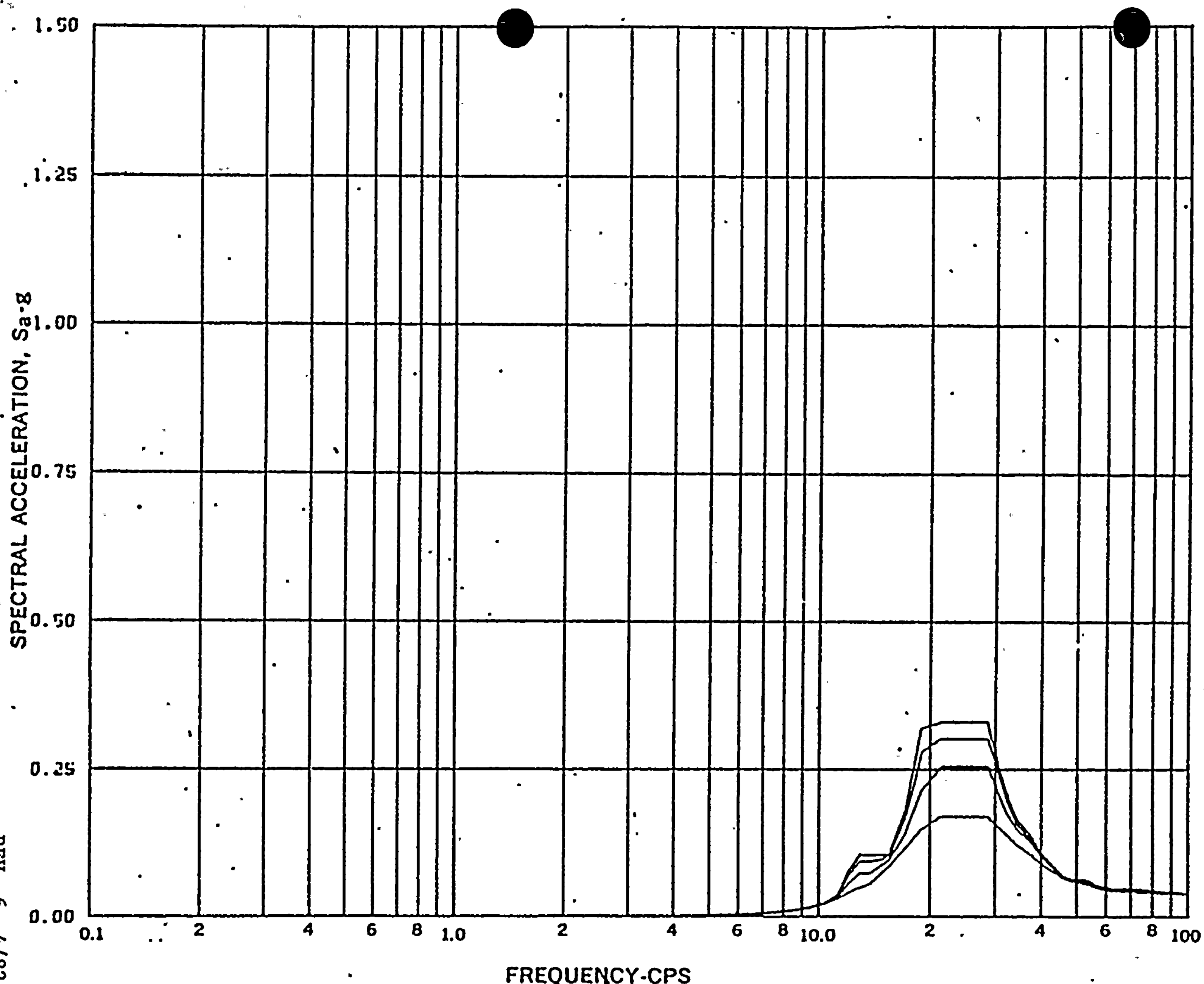

Limerick Generation Station, Acceleration Spectra for DRYWELL

Load Case: SRV - ASYMMETRIC - TRACE 76

Node: 415 Direction: HORIZ Elev: 312'-7" Angle: 90°

Damping: 0.005,0.01,0.02,0.05 By: ft Date: 5-5-80 Check: Kw Date: 5/6/80

REV. 6, 4/82

SUSQUEHANNA STEAM ELECTRIC STATION
UNITS 1 AND 2
DESIGN ASSESSMENT REPORT

LGS CONTAINMENT RESPONSE
SPECTRA - KWU SRV # 76
ASYMMETRIC - DIRECTION
HORIZONTAL

FIGURE 10-62

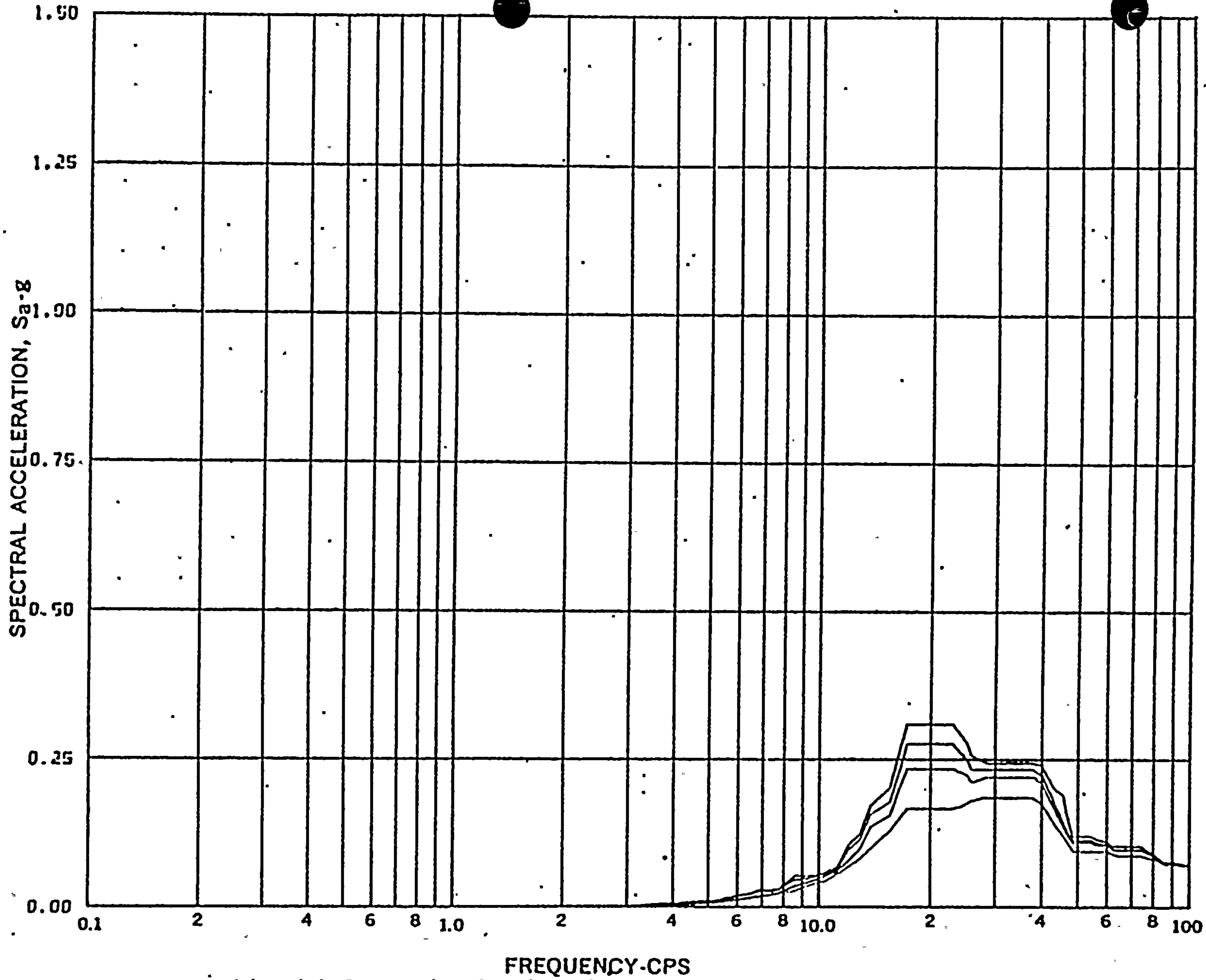

Limerick Generation Station, Acceleration Spectra for DRYWELL

Load Case: SRV - ASYMMETRIC - TRACE 76

Node: 415 Direction: VERT Elev: 312'-7" Angle: 90°

Damping: 0.005,0.01,0.02,0.05 By: pc Date: 5-5-80 Check: Klu Date: 5/6/80

SUSQUEHANNA STEAM ELECTRIC STATION
UNITS 1 AND 2
DESIGN ASSESSMENT REPORT

LGS CONTAINMENT RESPONSE SPECTRA - KWU SRV #76 ASYMMETRIC - DIRECTION VERTICAL

FIGURE 10 - 63

REV. 6, 4/82

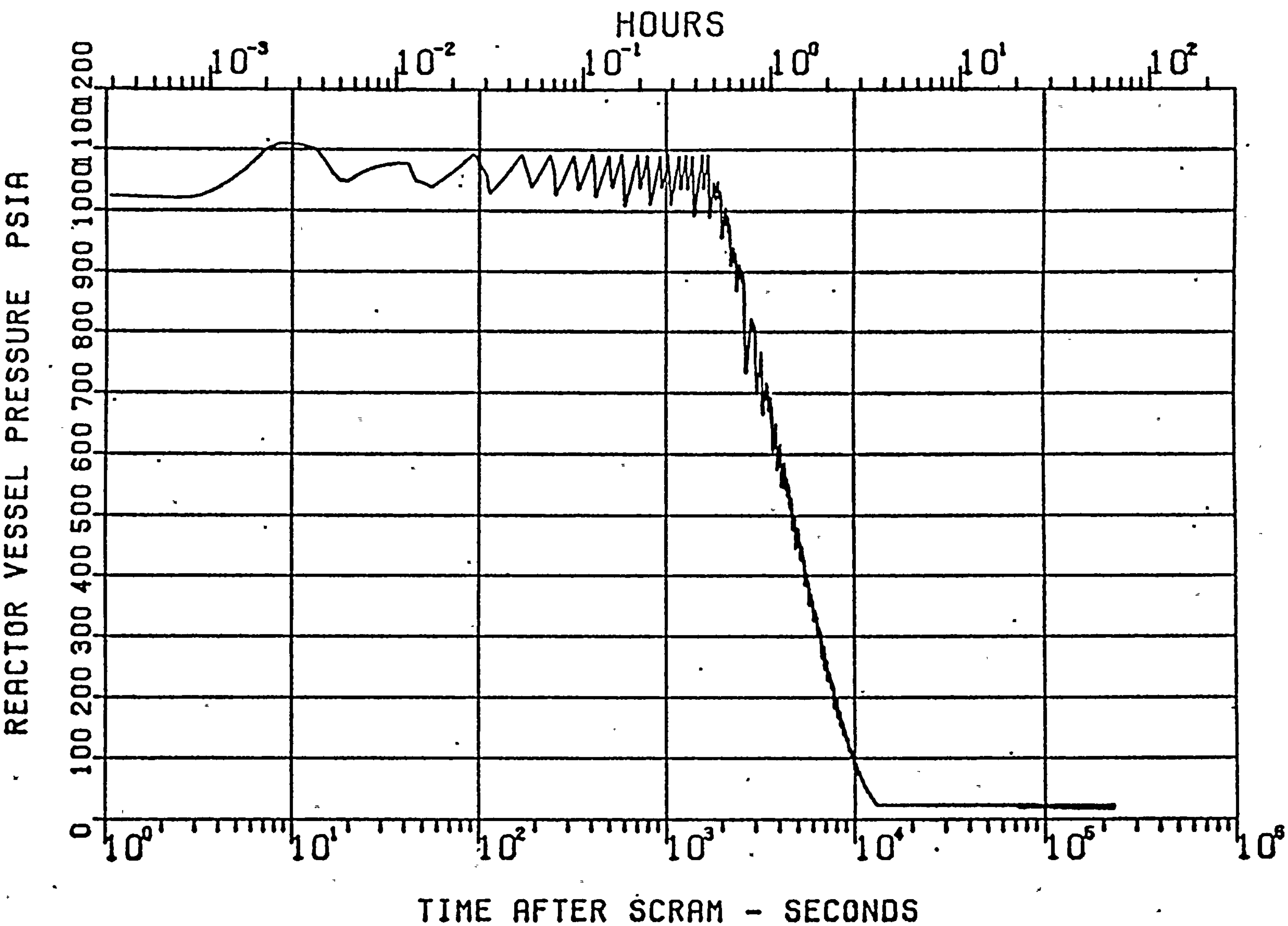

REV. 6, 4/82

SUSQUEHANNA STEAM ELECTRIC STATION
UNITS 1 AND 2
DESIGN ASSESSMENT REPORT

REACTOR PRESSURE
TRANSIENT - CASE 2.A
WITHOUT SHUTDOWN COOLING

FIGURE 10-64

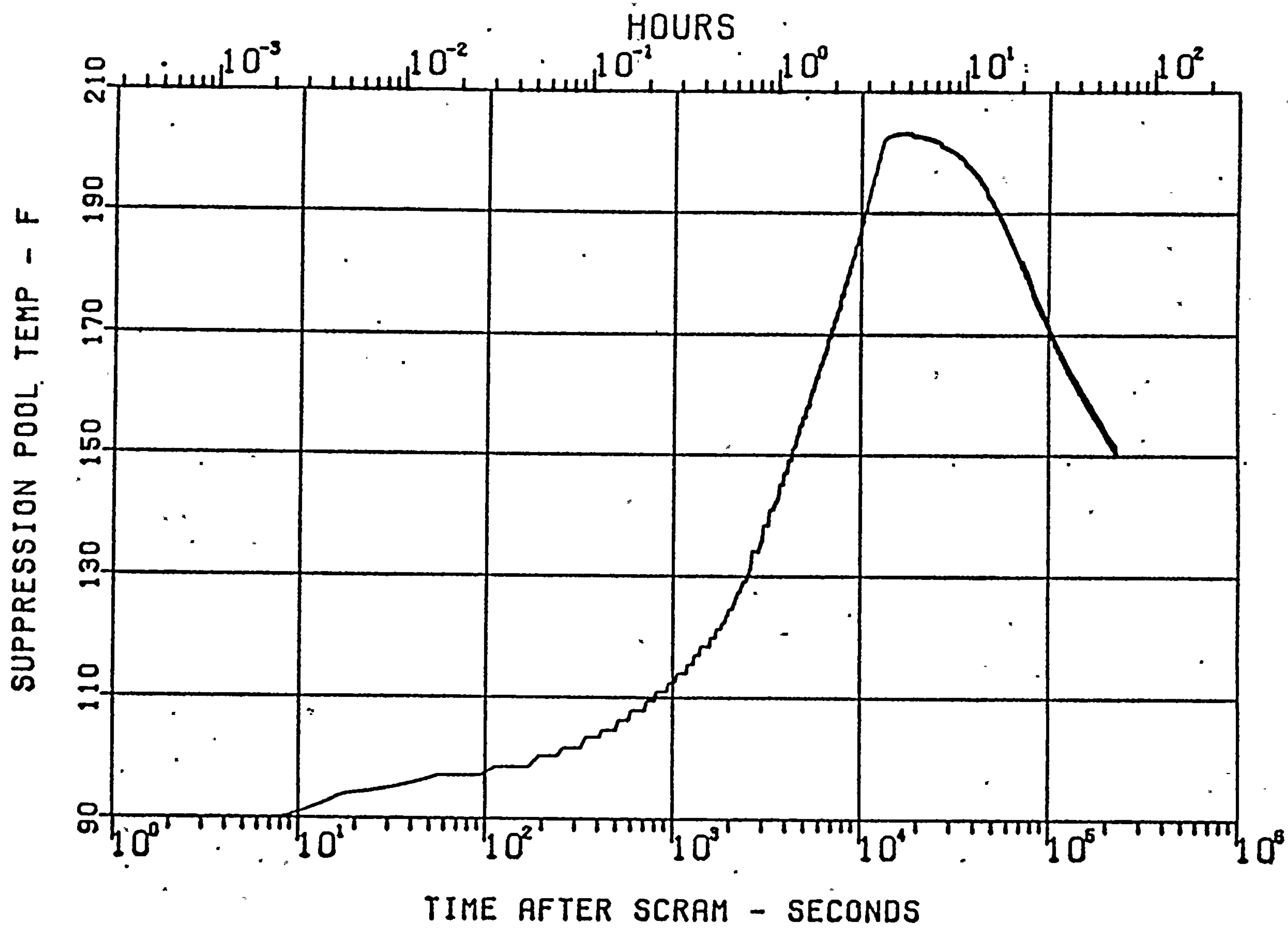

REV. 6, 4/82

SUSQUEHANNA STEAM ELECTRIC STATION
UNITS 1 AND 2
DESIGN ASSESSMENT REPORT

REACTOR PRESSURE
TEMPERATURE TRANSIENT-CASE
2.A WITHOUT SHUTDOWN COOLING

FIGURE 10-65

TABLE 10-1
JAERI DATA

JAERI TEST	CHUG START TIME (sec)	NORMALIZED RMS VENT STATIC PRESSURE VENT 1	VENT 2	VENT 3	VENT 4	VENT 5	VAR. σ^2
0002	58.65	–	0.88	–	1.13	0.99	.015
	62.37	–	0.87	–	1.38	0.75	.114
	66.35	–	1.17	–	1.03	0.81	.033
	72.65	–	0.99	–	1.29	0.72	.083
	74.65	–	0.72	–	1.29	0.98	.080
	76.75	–	0.85	–	1.06	1.09	.018
	78.80	–	0.85	–	1.09	1.06	.016
	80.25	–	0.90	–	1.03	1.07	.007
0003	82.27	–	1.10	–	1.01	0.89	.011
	84.10	–	0.83	–	1.07	1.10	.021
	85.98	–	0.61	–	1.36	1.04	.141
	87.85	–	1.16	–	1.13	0.71	.064
	89.90	–	0.64	–	1.05	1.31	.144
	91.45	–	0.54	–	1.50	0.97	.232
	96.85	–	1.12	–	1.01	0.83	.014
0004	39.50	–	0.95	–	1.44	0.61	.173
	40.65	–	0.86	–	1.34	0.79	.089
	43.00	–	0.47	–	1.77	0.76	.461
	45.20	–	0.41	–	1.35	1.23	.264
	49.00	–	0.44	–	1.75	0.81	.453
	53.05	–	0.68	–	1.29	1.03	.094
1101	40.40	0.81	0.86	–	1.36	0.97	.061
	42.02	0.91	0.78	–	1.21	1.10	.036
	44.20	1.34	0.68	–	1.01	0.96	.075
	46.25	0.77	0.49	–	1.24	1.50	.207
	48.80	0.89	0.54	–	1.42	1.14	.140
1201	47.60	0.86	1.00	–	1.15	1.00	.013
	49.40	1.11	1.35	–	0.72	0.82	.081
	51.20	1.08	0.93	–	1.23	0.75	.042
	53.00	1.31	0.65	–	1.15	0.90	.084
	54.90	1.22	0.60	–	1.27	0.91	.097
2101	85.80	1.14	0.84	0.84	0.90	1.28	.040
	89.75	1.13	1.17	0.89	0.99	0.82	.023
	92.00	1.07	0.67	0.98	0.89	1.40	.071
	93.85	0.89	1.07	1.23	1.22	0.60	.072
	96.10	2.08	0.56	0.29	1.20	0.88	.478
	98.15	0.87	0.82	1.10	1.30	0.90	.039
	100.10	0.96	0.71	0.93	1.18	1.21	.041

TABLE 10-2
JAERI/GKMIIM COMPARISON

DATA BASE	NORMALIZED MEAN VARIANCE
JAERI DATA	0.108
GKMIIM MSL DATA (0.5-13 Hz)	0.107
GKMIIM 1/3 MSL DATA (0.5-13 Hz)	0.083
GKMIIM 1/6 MSL DATA (0.5-13Hz)	0.064

11.0 REFERENCES

1. Dr. M. Becker and Dr. E. Koch, "KKB-Vent Clearing with the Perforated-Pipe Quencher" (translated by Ad-Ex, Watertown, Massachusetts), KWU/E3-2796, Kraftwerk Union, October 1973.

2. Dr. M. Becker and Dr. E. Koch, "Construction and Design of the Relief System with Perforated-Pipe Quencher" (translated by Ad-Ex), E3/E2-2703, Kraftwerk Union, July 1973.

3. Dr. M. Becker, "Results of the Non-Nuclear Hot Tests with the Relief System in the Brunsbuttel Nuclear Power Plant" (translated by Ad-Ex), KWU/R113-3267, Kraftwerk Union, December 1974.

4. Dr. H. Weisshaupl, "Formation and Oscillations of a Spherical Gas Bubble Under Water" (translated by Ad-Ex), AEG-Telefunken Report No. 2241, Kraftwerk Union, December 1972.

5. Dr. H. Weisshaupl and Schall, "Calculation Model to Clarify the Pressure Oscillations in the Suppression Chamber After Vent Clearing" (translated by Ad-Ex), AEG-Telefunken Report No. 2208, Kraftwerk Union, March 1972.

6. Dr. M. Becker, Feist and M. Burro, "Analysis of the Loads Measured on the Relief System During the Non-Nuclear Hot Test in KKB" (translated by Ad-Ex), R 113/R 213/R 314/R 521-3346, Kraftwerk Union, April 1975.

7. Letter, J. W. Millard to M. J. Lidl, "Susquehanna 1 & 2: Mass and Energy Release for Suppression Pool Temperature Analysis during Safety Relief Valve and LOCA Transients," GB-77-65, March 14, 1977.

8. R. J. Ernst and M. G. Ward, "Mark II Pressure Suppression Containment Systems: An Analytical Model of the Pool Swell Phenomenon," NEDE-21544P, General Electric Co., December 1976.

9. Letter, F. C. Rally to Mark II Technical Steering Committee Members, "Pool Swell Model Test Cases," MKII-301-E, August 22, 1977.

10. "Dynamic Forcing Functions Information report (DFFR)," Rev. 2, NEDO-21061, General Electric Co. and Sargent and Lundy Engineers, September 1976.

10a. "Dynamic Forcing function Information Report (DFFR)," Rev. 3, NEDO-21061, General Electric Co. and Sargent and Lundy Engineers, June, 1978.

11. T. Y. Fukushima, et al., "Test Results Employed by GE for BWR Containment and Vertical Vent Loads," NEDE-21078-P, Table 3-4, General Electric Co., October 1975.

12. F. J. Moody, Analytical Model for Liquid Jet Properties for Predicting Forces on Rigid Submerged Structures, NEDE-21472, General Electric Co., September 1977.

13. R. J. Ernst, et al., Mark II Pressure Suppression Containment Systems: Loads on Submerged Structures - An Application Memorandum, NEDE-21730, General Electric Co., September 1977.

14. F. J. Moody, Analytical Model for Estimating Drag Forces on Rigid Submerged Structures Caused by LOCA and Safety Relief Valve Ramshead Air Discharges, NEDE-21471, General Electric Co., (to be published).

15. Mark II - Phase I, 4T Tests Applications Memorandum, Letter and Report to W. R. Butler (NRC) from J. F. Quirk (GE), June 14, 1976.

16. W. J. Bilanin, et. al., Mark II Lead Plant Topical Report: Pool Boundary and Main Vent Chugging Loads Justification, NEDE-23617P, July 1977.

17. Warmeatlas (Heat Transfer Data), VDI (Society of German Engineers), Dusseldorf, 1974.

18. T. E. Johnson, et al., "Containment Building Liner Plate Design Report," BC-TOP-1, Bechtel Corporation, San Francisco, December 1972.

19. "Seismic Analysis of Piping Systems," BP-TOP-1, Rev 2, Bechtel Power Corporation, San Francisco, January 1975.

20. Letter, F. C. Rally to Mark II Technical Stearing Committee Members, August 22, 1977, MK II-301-E, Subject: Pool Swell Mode Test Cases.

21. Letter, J. R. Martin to Mark II Owners Group and TSC, MK II-250-E, Subject: Condensation Oscillation Excerpts to Applications Memorandum, July 1, 1977.

22. D. Hoffman and E. Schmid, "Brunsbuttel Nuclear Power Plant List of Test Parameters and Most Important Measurement Results of the Non-Nuclear Hot Tests with the Pressure Relief System" (translated by Ad-Ex), R 521/40/77, Kraftwerk Union, August 1977.

23. D. Gobel, "Results of the Non-Nuclear Hot Tests with the Relief System in the Philippsburg Nuclear Power plant" (translated by Ad-Ex), R 142-38/77, Kraftwerk Union, March 1977.

24. D. Hoffman and E. Schmid, "Philippsburg I Nuclear Power Plant List of Test Parameters and Most Important Measurement Results of the Non-Nuclear Hot Tests with the Pressure Relief System" (translated by Ad-Ex), R 521/41/77, Kraftwerk Union, August 1977.

25. Klans-D. Werner, "Experimental Studies of Vent Clearing in the Model Test Stand" (translated by Ad-Ex), KWU/R 521-3129, Kraftwerk Union, July 1975.

26. D. Gobel, "KKB - Nuclear Start-Up Results of the Tests with the Pressure Relief System" (translated by Ad-Ex), R 142-136/76, Kraftwerk Union, September 1976.

27. D. Hoffman and Dr. K. Melchior, "Condensation and Vent Clearing Tests in GKM with Perforated Pipes" (translated by Ad-Ex), KWU/E3-2594, Kraftwerk Union, May 1973.

28. GE Drawing 761E579, Bechtel No. 8856-M1-B11-89

29. ASME Boiler and Pressure Vessel Code, Section III, Division 1, 1974.

30. ASME Boiler and Pressure Vessel Code, Section III, Division 2, 1974.

31. ACI 318-71.

32. R.L.Kiang and B.J. Grossi, "Dynamic Modelling of a Mark II Pressure Suppression System," EPRI-NP-441, Palo Alto, April 1977.

33. "Seismic Analyses of Structures and Equipment for Nuclear Power Plants," BC-TOP-4A, Bechtel Power Corporation, November 1974.

34. MARC-CDC User Information Manual Control Data Corporation, 1975

35. Morse, P.M. and H. Feshbach Methods of theoretical physics I McGraw Hill, New York, Toronto, London, 1953

36. E. Kamcke Differentialgleichungen Losungsmethoden und Losungen (Differential Equations Solution Methods and Solutions) Volume I Akademische Verlagsgesellschaft, Leipzig, 1967.

37. Properties of Water and Steam in SI-Units Springer-Verlag, Berlin, 1969

38. Gobel, KKB hot test results Loads on internals in the pool of he suppression chamber during pressure relief processes 13 Nov. 1974; KWU-R 113/203

39. Prandtl Stromungslehre (Hydrodynamics) Vieweg & Sohn, Braunschweig, 1965

40. Werner Tests of mixed condensation with model quenchers KWU-E 3-2593, May 1973

41. T. Potna Dehnungsmessstreifentechnik (Foil Strain Guage Technology) Philipps-Taschenbucher T11, 1968

42. McCandlers Methods Guide for Reactor Internal Structure Vibrations Analysis GE Memo SAR -2A July 1966

43. Dubbels Taschenbuch fur den Maschinenbau (Dubbels Pocketbook for Machine Construction) Springer, Berlin 1963

44. J. M. Biggs Introduction to Structural Dynamics, McGraw Hill, 1964

45. Becker, Gobel, et al. Analysis of the loads measured on the relief system during the KKB non-nuclear hot test KWU-R11-R31-3346, April 1975

46. "Mark II Containment Lead Plant Load Evaluation and Acceptance Criteria", Rev. 0, NUREG-0487, U.S. Nuclear Regulatory Commission, October 1978

47. "Dynamic Lateral Loads on a Main Vent Downcomer-Mark II Containment," NEDE-24106-P, General Electric Co., March 1978

48. Davis, W. M., MK II Main Vent Lateral Loads Summary Report, NEDE-23806-P, General Electric Co., October 1978.

49. Kenleqn, G. H. and Carpenter, L. H. "Forces on Cylinders and Plates in an Oscillating Fluid," NBS J. of Research, Vol. 60, pp. 423-44D, 1958.

50. Sarpkaya, T., "Forces on Cylinders and Spheres in a Sinusoidally Oscillating Fluid," Trans. ASME, J. of Applied Mech., pp. 32-37, 1975.

51. Chandra, V., Donashovetz, I. and Hsieh, J. S., "Response to NUREG-0487 Criteria for Computing Loads on Submerged Structures," SAI-161-79-PA March 1980.

52. Pankhurst, R. C. and Holder, D. W., "Wind Tunnel Technique," Chapter 8, Pitman and Sons, Ltd., London, 1952.

53. Wilson, E. L, "A Computer Program for the Dynamic Stress Analysis of Underground Structures," USAEWES, Control Report No. 1-175, January, 1968.

54. Desai and Abel, "Introduction to the Finite Element Method," Van Nostroid Reinold Co., 1972.

55. "IEEE Recommended Practices for Seismic Qualification of Class 1E Equipment For Nuclear Power Generating Stations," IEEE Std. 344-1975.

56. A. J. James, "The General Electric Pressure Suppression Containment Analytical Model," GE, July 1971.

57. Letter MFN-080-79, L. J. Sobon (GE) to J. F. Stolz (NRC), Subject: Vent Clearing Pool Boundary Loads for Mark II Plants, 3/20/79.

58. P. W. Huber, A. A. Sonin, W. G. Anderson, "Considerations in Small-scale Modeling of Poolswell in BWR Containments," NUREG-CR-1143, July 1979, Contract No. NRC-04-77-011.

59. C. K. Chun, "Suppression Pool Dynamics," NUREG-0264, Contract No. AT (49-24)-0342.

60. R. L. Kiang and P. R. Jeuck, "A Study of Pool Swell Dynamics In a Mark II Single Cell Model," EPRI, Draft Report. 2

61. Conrant, R. and Hilbert, D., "Methoden der Mathematischen Physik I (Methods of Mathematical Physics I)," Springer-Verlag, Berlin, Heidelberg, New York, 1968.

62. Antony-Spies, P., "Theory of the Excitation of Eigenmodes of a Water-Filled Tank by a Callapsing Steam Bubble" (translated by Ad-Ex), Technical Report KWU/R14/77, September, 1977.

63. MARC-CDC, User Information Manual, Control Data Corporation, 1976.

64. Koch, E. and Sobottka, H., "KKP 1/KKI - Estimate of the Miting Values of the Dynamic Loads on the Pressure Suppression System During Air-Free Condensation at the Vent Pipes", Technical Report KKU/R113/3593, December 1975.

65. "Mark II Improved Chugging Methodology", NEDE-24822-P, General Electric Company, May 1980.

66. "Single and Multivent Chugging Final Report", NEDE-24300-P, General Electric Company, May 1980.

67. Mark II Owners Group, "Assumptions for use in Analyzing Mark II BWR Suppression Pool Temperature Transients Involving Safety/Relief Valve Discharge," Revision 1, December 1980. 5

68. Everstine, G. C., "A Nastran Implementation of the Doubly Asymptotic Approximation for Underwater Schock Response", Nastran Users's Experiences, NASA TMX 3428, pp 207-228, October 1976.

69. MacNeal, R. H., Citerley, R., and Chaigin, M., "A New Method for Analyzing Fluid-Structure Interaction using
5 M.S.C/Nastran", Trans. 5th Int. Conf. on Structural Mechanics in Reactor Technology, Paper B4/9, August 1979.

70. Mach II Generic Condensation Oscillation Load Definition Report, NEDE-24288-P, General Electric Company, November 1980.

71. C. W. Hirt, B. D. Nichols, N.C. Romero, "SOLA: A Numerical Solution Algorithm for Transient Fluid Flows, "LA-5852, April 1975.

72. B. D. Nichols, C. W. Hirt, R. S. Hotchkiss, "SOLA-VOF: A Solution Algorithm for Transient Fluid Flow with Multiple Free Boundaries," LA-8355, August 1980.

73. C. W. Hirt, B. D. Nichols, L. R. Stein, "Multidimensional Analysis for Pressure Suppression Systems," LA-UR-79-1305, April 1979.

74. Zimmer Nuclear Power Station - Unit, Attachment 1.k, Amendment 99, Submittal of Revision 61 to the FSAR, September 28, 1979.

6

75. "ANSYS Engineering Analysis System Theoretical Manual," November 1, 1977 by Swanson Analysis Systems, Inc.

76. "ANSYS Engineering Analysis Systems Users Manual" August 1, 1978 by Swanson Analysis Systems, Inc.

77. A. Kalmins "Analysis of Shells of Revolution Subjected to Symmetrical and Non-Symmetrical Loads", Journal of Applied Mechanics, September 1964.

78. Abrahamson, G. R., and Hashemi, A., "SSES In-Plant Tests to Measure Submerged Structure Loads and Pool Frequencies," SRI Report to PP&L, April 1980.

79. "Mark II Containment Lead Plant Program Load Evaluation and Acceptance Criteria," NUREG-0487 Supplement No. 1, USNRC, September 1980.

80. General Electric report NEDO-24310, "Technical Bases for the Use of the Square Root of the Sum of the Squares (SRSS) Method of Combining Dynamic Loads for Mark II Plants," July 1977.

81. Letter from Roger J. Mateson, Office of Nuclear Reactor
7 Regulations, to Dr. H. Chau, Chairman of the Mark II Owners Group, dated February 25, 1982.

82. Letter from G. D. Bouchey to A. Schwencer, "Desynchronization Methodology in the Chugging Load Specification," dated March 15, 1982, Letter No. G02-82-324.

83. Letter from G. D. Bouchey to A. Schwencer," Comparison of Structural Response to Symmetric and Asymmetric Chugging and Seismic Loads," dated April 5, 1982, Letter No. G02-82-362.

84. G. K. Ashley II and N. M. Howard, "Understanding Poolswell in a Mark II Type BWR," ANS Topical Meeting on Thermal Reactor Safety, July 31-August 4, 1977, Sun Valley, Idaho.

85. B. R. Patel, F. X. Dolan and J. A. Block, Creare TN-307 Report (NEDE-24781-1-P), January, 1980.